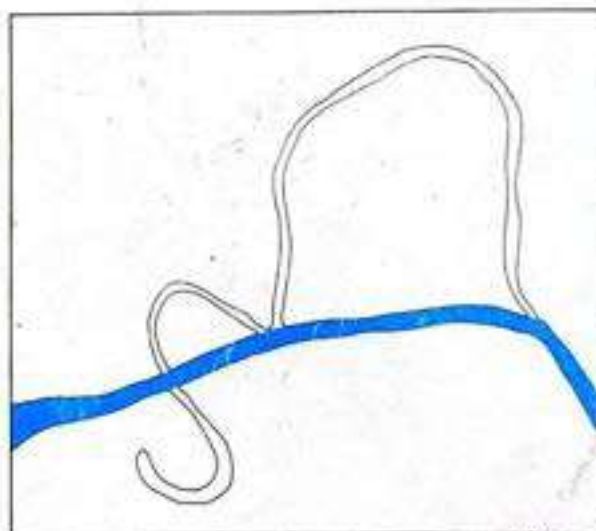
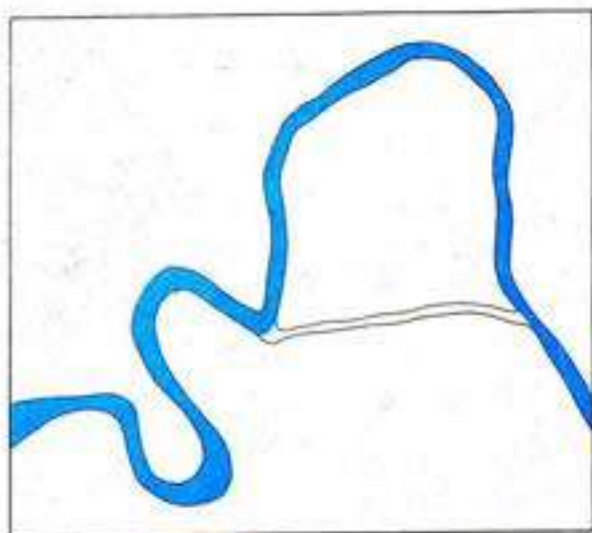


PROPERTY OF MYAN WA
FOR INSPECTION ONLY !!!

River Plan-form Movement in an Alluvial Plain



DONATION TO WRIC MYANMAR LIBRARY
FROM DR. IR. KHIN NI NI THEIN

RIVER PLAN-FORM MOVEMENT IN AN ALLUVIAL PLAIN

River Plan-form Movement in an Alluvial Plain

A thesis

Presented to the International Institute for Infrastructural,
Hydraulic and Environmental Engineering, Delft,
in Partial Fulfilment of the Requirements for the Degree of
Doctor of Philosophy,
to be defended in public, in front of an Awarding Committee,
on Monday, 30 May 1994 at 15:00 h

by

KHIN NI NI THEIN

*born in Rangoon, Myanmar
Hydraulic Engineer*

W R T C
Water, Research and Training Centre
RESOURCE LIBRARY
Dr. Ir. Khin NI NI Thein
Founder and President



- 5 AUG 2004



A.A. BALKEMA / ROTTERDAM / BROOKFIELD / 1994

This thesis is approved by the promoter
Prof. dr M. B. Abbott
Department of Hydraulic and Hydrological Engineering, IHE Delft

and the co-promoter
Prof. dr J. Fredsøe
Department of Hydrodynamic and Hydraulic Engineering
Technical University, Lyngby, Denmark

Authorization to photocopy items for internal or personal use, or the internal or personal use of specific clients, is granted by A. A. Balkema, Rotterdam, provided that the base fee of US\$1.50 per copy, plus US\$0.10 per page is paid directly to Copyright Clearance Center, 27 Congress Street, Salem, MA 01970, USA. For those organizations that have been granted a photocopy license by CCC, a separate system of payment has been arranged. The fee code for users of the Transactional Reporting Service is: 90 5410 401 5/94 US\$1.50 + US\$0.10.

Published by
A. A. Balkema, P.O. Box 1675, 3000 BR Rotterdam, Netherlands
A. A. Balkema Publishers, Old Post Road, Brookfield, VT 05036, USA

ISBN 90 5410 401 5

© 1994 A. A. Balkema, Rotterdam
Printed in the Netherlands

CURRICULUM VITAE

Khin Ni Ni Thein, born 9 April 1955 at Yangon (Rangoon), Myanmar (Burma), passed her Matriculation examination at Yangon with Distinction, receiving the Gold Medal of the graduate year in Physics. She studied civil engineering at Yangon Institute of Technology (YIT), from which she received her Bachelor of Engineering degree (Civil) with Distinction in 1977. During this period she participated actively in student affairs, being at various times Editor, General Secretary, Treasurer and Representative of the Students Association of YIT. After graduation she worked for two years supervising water supply and waste water maintenance and new installations at Gyogone, Insein, with special responsibility for a low-cost housing project. From there she proceeded in 1980 to the Irrigation Department of Myanmar as project engineer at the Ngalaik Dam Project, where she worked alongside the San Yu consulting company of Japan. In 1981 she transferred to the Sittang Project as a design engineer of the Planning and Design Office. She there participated in preparing proposals for control structures, both for the Sittang and an adjacent project, calculating alternative and detail designs for a variety of hydraulic structures, carrying out work-site inspections and exercising quality control functions. Alongside this she carried out calculations of crop-water requirements and water balances for project appraisal reports. She then transferred to Yangon Institute of Technology as an Instructor, where, from 1983 to 1984, she worked on her Master of Science Thesis, entitled *Optimum Use of Water Resources and an Economic Analysis of the Ngalaik Dam Project*. Alongside this work she conducted tutorials in Hydraulics and Hydrology subjects and instructed in experimental and survey practices. In 1984 she carried out her compulsory national service, proceeding first to platoon and subsequently to company commander. Returning to YIT she gave undergraduate lectures on Fluid Mechanics and post-graduate lectures in Hydraulic Engineering and instructed in the one-month undergraduate field trip in surveying and cartographic mapping. She was also responsible for the operation of the Hydraulic Laboratory of YIT. From 1987 onwards she held the position of Assistant Lecturer at YIT. She left YIT at the end of 1987 to study at IHE, where she received her Diploma with Distinction in the Computational Hydraulics Branch of the Hydraulic Engineering Course, with a group work on the modelling of supercritical flow. On this basis she continued to her second Master of Science studies, which were carried out at Delft Hydraulic in de Voorst, receiving her degree for a thesis entitled *One Dimensional Morphological Modelling of Graded Sediments*. In 1989 she was appointed Lecturer in the Civil Engineering Department at YIT, but she continued, in this position, to conduct the work presented in this thesis for the Ph.D degree of IHE. The first part was conducted over two years at the Danish Hydraulic Institute and, after a short period back at YIT, it has been concluded over another two-year period at IHE.

*My lord,
until I attain enlightenment,
I will not violate sacred precepts,
I will not be arrogant before people regardless of age, sex, race, position, belief and
wealth. I will cherish love in my heart and be a good example for all.*

PREFACE

Having been brought up among engineers, medical doctors and other professionals, it was always my dream to attain to knowledge, and this dream led me forward into adulthood. However, I now find that my dream has come true in an extraordinary way. My educational background was that of a Civil Engineer, which subsequently turned into the direction of Water-resources Engineering. It was on this basis that I came to IHE, in order to acquire advancement in this Hydraulic Engineering field of study. I saw the many possibilities which IHE could offer, but I felt that my best choice was Computational Hydraulics. Being a very obedient student, trained in a very Eastern culture and having never been out of my country, I came into a new world with a completely different educational system and an almost completely different life-style and way of thinking. My struggle started, alongside my study, to come to terms with this different life-style, the different cultural background, and the different demands made from the educational system. This storm struck me more strongly than did any other in my life. In this respect I should like to mention my sincere thanks to the person who I met as my first teacher abroad, *ir. Tony Minns*. It was he who helped me in this first period when I stood in much need because of the sudden changes in environment. From then on I could say that my study period resembled a sailing into an intellectual ocean. Sometimes I sailed with the wind, often I sailed in various states of struggling against the wind, and between times I just rowed, without any wind at all! And yet, at all times, in every difficulty and specifically at every critical moment, help came to me. It came from the staff of IHE, who worked hard to keep me on track and on schedule, it came from my fellow participants, who explained, encouraged and corrected me, and it came from the several warm-hearted friends who I made in the Netherlands. Of these last, a very special thanks is due here to *dr. Urs Eichenberger and drs. Susi Schultz*. Throughout this time, and increasingly as the work progressed beyond this period, *Prof. dr. M.B. Abbott* has been a **constant source of help**. It was a tempestuous journey, but I always received assistance, and by these means this became also a *spiritual journey*. Now is the time to express my gratitude, not only for the knowledge acquired but also for the accompanying spiritual development. This first, very demanding passage prepared me for my further studies on my M.Sc degree, carried out at Delft Hydraulics (DH), and the present Ph.D degree, carried out at the Danish Hydraulic Institute (DHI), and completed at IHE. The work continued to be very demanding, but once again help constantly appeared, and it was always there at the critical moments. In this respect I owe a special debt of gratitude to *dr. ir. Kim Wium Olesen* of DHI, who carried me all the way through the period of difficulty, and to *Prof. dr. J. Fredsøe*, who was a guiding light throughout my study. By virtue of so much help which came from so many sides and **in so many forms** from teachers, colleagues and friends, I not only acquired knowledge, but something more, which I would dare to call *wisdom*. The knowledge acquired has prepared me to take my place in terms of influencing the world in its own worldly terms, for *knowledge is power*, but the very process of acquiring this knowledge has formed me in another way as well, for it has taught me the profound truth of the ancient adage, that even though *knowledge is power*, **WISDOM IS FREEDOM**.

ခင်နီနီသိန်း

ကစီက

Delft, April 1994
Khin Ni Ni Thein

မြို့ပြအင်ဂျင်နီယာဌာန
ရန်ကုန် ဝက်ပူ တက္ကသိုလ်

CONTENTS

I	PREFACE	5
II	CONTENTS	7
III	SUMMARY	15
1.	INTRODUCTION	17
1.1	Aim and emphasis	17
1.2	Alluvial plain classification	18
1.3	Scope of the study	18
	1.3-1 Previous work	19
	1.3-2 Present study	21
1.4	Outline of the thesis	23
2.	REVIEW OF THE EXISTING THEORIES	25
2.1	Introduction	25
2.2	Selection of the theories and ideas	25
2.3	Division of the subject matter	25
2.4	Part A	26
	2.4-1 Flow and bed topography in meandering rivers	26
	2.4-1.1 The secondary flow	26
	2.4-1.2 Sediment transport in general and sand transport in particular	29
	2.4-2 Mathematical model in a 2D-bend; the extent to which mathematical models have been developed, applied and extended	29
2.5	Part B	30
	2.5-1 The stability of self-formed alluvial rivers	30
	2.5-2 Stable-width criteria	31

2.6	Part C	32
2.6-1	Bank erosion mechanism of self-formed alluvial rivers	32
2.6-2	The overall history of meandering rivers: river channel patterns and their evolution	33
2.6-2.1	Time scales of alluvial rivers	33
2.6-2.2	Theories of meandering	34
2.6-2.3	Sediment transport in meandering rivers	38
3.	DEVELOPMENT OF A BED TOPOGRAPHY MODEL IN A MEANDERING RIVER	41
3.1	Introduction	41
3.2	Description of the model	42
3.2-1	Co-ordinate system	42
3.2-2	Grid mapping	43
3.3	Flow computation	47
3.3-1	Governing differential equations of the flow model	48
3.3-2	The vertical distribution of the flow	51
3.3-3	The longitudinal flow velocity	52
3.3-4	The transverse flow velocity	53
3.3-5	Bed shear stresses and directions	60
3.3-6	The vertical flow velocity	63
3.3-7	The stream-line curvature	64
3.4	The depth-averaged flow model	64
3.5	The integration procedure of the flow model	68
3.6	Verification of the flow model	72
3.7	Bed-topography computation	74
3.7-1	Governing differential equations of the bed-topography model	74
3.7-2	Bed shear stress in the case of a mobile bed	76
3.7-3	Bed shear stress direction in an alluvial river bend	76
3.7-4	Sediment transport capacity	76
3.7-4.1	Bed load	79
3.7-4.2	Suspended load	79

3.7-4.3	Total load	79
3.7-5	Sediment transport direction	80
3.7-5.1	The bed-slope effect	80
3.7-5.2	The transverse-slope effect	82
3.7-5.3	Non-uniform sediment	82
3.7-6	Variable roughness	84
3.8	The depth-averaged bed topography model	85
3.9	The integration procedure of the model	86
3.10	Analysis of the morphological model	87
3.10-1	Olesen solution	87
3.10-2	Talmon solution	90
3.10-3	Discussion	90
3.11	Verification of the morphological model	91
3.11-1	The basic data needed for the model	91
3.11-2	Flume experiments	91
3.11-3	The natural river situation	94
3.12	Performance of the model	96
3.12-1	Case 1: Ishikari River, Hokkaido, Japan	97
3.12-2	Case 2: Hypothetical river with parabolic cross-section	98
3.13	Conclusions	101
3.14	Discussion	102
3.15	Continuation	104
4.	A HEURISTIC APPROACH TO THE DETERMINATION OF OPTIMUM RIVER WIDTH	105
4.1	Theoretical background of self-formed alluvial rivers	105
4.2	Present study	105
4.3	Maximum transport capacity (MTC) channel width	107

4.3.1	Problems in previous studies	107
4.3.2	Possible solution to these problems	107
4.4	Flow resistance in alluvial rivers	107
4.4.1	Friction conditions in a straight alluvial river	108
4.4.2	Friction conditions in a meandering river	109
4.5	Shape and dimensions of stationary dunes in alluvial rivers	110
4.6	Development of the roughness predictor model	111
4.7	Theoretical considerations for the roughness factor	113
4.8	Connection to the bed topography simulation model	119
4.9	Calculation of an MTC channel width for a straight river	128
4.10	Calculation of an MTC channel width for a meandering river	132
4.11	The meander arc length and the MTC channel width	137
4.12	Width-over-depth ratio	139
4.13	The determination of friction in a meandering river	140
4.13-1	Shear stresses in channel bends	140
4.13-2	Updating the sediment transport capacity	141
4.14	The role of discharge	141
4.15	Analytical model for transverse bed slope in a river bend	141
4.16	Conclusions	145
4.16-1	Suggestions for further study	147
4.16-2	Relationship between this specific chapter and the river plan form movement simulation model	147
5.	RIVER PLAN-FORM MOVEMENT	149
5.1	Introduction	149
5.2	River parameters	153

5.3	Bank erosion mechanisms	154
	5.3-1 Fluvial entrainment	154
	5.3-2 Mass failure	156
	5.3-3 Feedback processes	157
5.4	Bank erosion rates	157
	5.4-1 Theoretical derivation of the present study	158
	5.4-2 The hypothesis of near-bank velocity excess	161
	5.4-3 Empirical relationships	162
5.5	Verification	168
	5.5-1 Case 1: verification with empirical formulae	168
	5.5-2 Case 2: verification with field data from Rillito Creek	168
5.6	Modular structure developments of the bank erosion modules	175
5.7	Tentative Grouping of sites for different erosion types	179
5.8	The selection of the bank erosion rate module	179
5.9	R P M model	180
	5.9-1 Some discrepancies between physical sense and modelling workability	182
5.10	Grid generation	184
	5.10-1 Grid map setting by differential geometry	184
	5.10-2 Coordinate transformation	187
5.11	Simulations	190
5.12	Conclusions	192
5.13	Discussion	193
5.14	Suggestions	194
	5.14-1 Discharge-induced river bank erosion	195
	5.14-2 The need for care in the choice of a representative discharge	195

5.14-3	An introduction to Magnitude Frequency Analysis	196
6.	CONCLUSIONS AND DISCUSSION	199
6.1	Conclusions	199
6.1-1	Summary	199
6.1-2	Part A (Chapter 3)	200
6.1-3	Part B (Chapter 4)	201
6.1-4	Part C (Chapter 5)	202
6.2	Discussion	203
6.2-1	The physics of natural rivers	203
6.2-2	The mathematical formulation	203
6.2-2.1	Path of the sediment particle travelling along the river bend	203
6.2-2.2	The secondary convection factor	204
6.2-3	The computational method	204
6.3	Suggestions for the further study	204
6.3-1	Suggestions for part A	204
6.3-2	Suggestions for part B	205
6.3-3	Suggestions for part C	206
	REFERENCES	209
	LIST OF SYMBOLS	223
	APPENDICES	227
	APPENDIX-A	229
A.1	Overview of the study	229
A.2	Accuracy of the grid mapping	230
A.3	Derivation for bank-shear-stress value in a meandering river	232
A.4	Einstein (1934) side wall correction	238
A.5	Program listing	241

APPENDIX-B	277
B.1 Roughness predictor model: Dune size calculation	277
B.2 Input data example for the dune size and roughness predictor model	289
APPENDIX-C	293
C.1 River Plan-form Movement Model	293
C.1-1 Main program	293
C.1-2 Grid generation program	295
C.1-3 Graphical presentation program	302
C.2 Variety of bank erosion models	311
C.2-1 Bank erosion rate calculation for cohesive material	312
C.2-2 Bank erosion rate calculation using force balance theory	314
C.2-3 Bank erosion rate calculation using near bank excess-velocity theory	317

SUMMARY

Rivers are a dynamic and increasingly important part of our physical environment. Their behaviour is of interest in a wide variety of contexts, ranging from disaster prevention, such as by flood control, to water resources development for navigation and recreation. At the present moment certain additional man-made effect of previous river-training works, such as the straightening of meandering channels, are also involved. For these reasons, studies of river morphology and associated river plan-form movements are urgently needed. Indeed today many scientists and engineers are aware of this and are actively working on it from various directions. We may mention here the geographers, geologists, geo-morphologists and hydraulic engineers who are attracted to such studies. The last of these has a handy tool, which is composed of computational methods and mathematical models. The present study is one of this kind. Although it is not possible to tackle the river plan-form movement study in a completely holistic way, the present study is based firmly upon mathematical modelling as a core, even as it tries to consider the possibilities of obtaining assistance from the neighbouring sciences mentioned above.

In order to study the river plan-form movement, the first step in this study is that of developing an own mathematical model. First of all straight rivers are seldom, and indeed rivers flow nearly always have sinuous plan-forms, so that the 'natural' co-ordinate systems of their models are curvilinear co-ordinate systems. Since the river evolution and its movement cannot be studied with a purely one-dimensional approach, the model must be at least two dimensional. Moreover the complex system of secondary flow which is provided by the flow circulation across the river, in a direction perpendicular to the longitudinal direction of flow, is so important in the channel bends that the vertical profile of this velocity has to be studied and introduced in such a way that its effect is included in the model. By this means the model becomes in effect even more than two dimensional. These studies are presented in chapter 3. The model is developed, tested and verified with flume experiments and also with two well-documented natural river situations, these being the river Waal in the Netherlands and the river Ishikari in Hokkaido, Japan. The results are presented also in chapter 3.

After this foundational work, the present study continues to consider the stability of rivers, as described in chapter 4. The river stability problem is an elusive problem. This problem is influenced by the strength of the flow and the resistance of the container which is the river bed and banks. Up to this point it is very clear that the river will be the more stable as the flow is weaker or the resistance of the ground to erosion is stronger. Unfortunately, the problem involves much more than that, and its complexity is described in chapter 4. The many interrelated effects of the flow and sediment transport in the first place and the bed topography of the river and flow in the second place are shown to lead to temporal changes of bed forms in the river bed and meso-scale bed features such as bars and pools along the river reach, all of which add their own complexity. This problem is studied and eventually a maximum (sediment) transport capacity (MTC) channel width is chosen as a deciding criterion for straight-channel stability. A rather detailed explanation of the MTC channel width concept is provided in chapter 4. At this point the present study

necessitated that a test be made to verify whether an MTC channel width could exist for a meandering channel. Also the present study was concerned with preparing this test after developing a bed topography model for meandering rivers. Therefore the model which is developed in chapter 3 is used to test for the existence of an MTC channel width in meandering rivers. The conclusion made from this test is that the concept of an MTC channel width can also be introduced in meandering rivers. During the process of investigating the MTC channel width in meandering rivers, however, some rather difficult computational problems arose. A detailed presentation is given in chapter 4. The problem was experienced as one that could not be resolved with the numerical methods so far employed; it appears for the moment at least as a 'missing link' between the physics and the corresponding mathematical expressions which have to be adapted to the numerical simulation model in a synchronized manner. Eventually the problem was circumvented in the simulations and these simulations then provide a very useful tool despite the still small 'missing link'. After completing the description of this work, the study continues to the problem of bank erosion.

If and when rivers lose their stability, the river channel alignment starts to change. In fact no river has stability-as-such, but only a relative temporal equilibrium. The river channel alignment changes because its banks are eroded on one side. Clearly the rate of the plan-form movement depends on the rate of the bank erosion. The various bank erosion mechanisms are discussed in chapter 5. Bank-erosion-rate modules are then constructed according to existing theories and empirical formulae which have been found from field observations and experiments. Once the rate of bank erosion is calculated with sufficient accuracy, the river bank shifting can be simulated. In the present study this involved making a grid mapping to the new channel alignment and the corresponding computational domain. This work is described in chapter 5. After implementing this, the model was connected to the bed-topography model as already described in chapter 3. The resulting model is called a River Plan-form Movement model and the abbreviation **RPM** is used. The conclusions and discussion are presented in chapter 5. In summary, it is found that the RPM model developed here can simulate a reasonable range of regular-channel plan-form movements, but for certain particular cases, such as that of a movement obliquely downstream, it is still not satisfactory at the present stage of its development. It is concluded none the less that the RPM model introduced here is very promising and deserving of further development.

".....counted as the small dust of the balance."

Isaiah XI., 15. A.V.

1. INTRODUCTION

1.1 Aim and emphasis

River plains are the great centres of population, industry, commerce and transportation, and for a number of reasons. The flat surfaces of plains are most easily cultivated and generally contain the most productive soil. They became some of the principal areas of population growth relatively early in human history. Their level surfaces offer fewer obstacles to land transportation than do hills, mountains or plateaus, and the rivers of plains are generally much easier to navigate than are those of rougher terrain.

Movement of the earth's crust is considered to be an important geologic agent causing modern river instability. Major shifts of many miles in the position of the Brahmaputra River toward the west are attributed by Coleman (1969) to tectonic movements. However, it is probable that, during a period of several years, neither neotectonics nor a progressive climate change will have a detectable influence on river character and behaviour. Then the instability of a river is a result of *the slow but implacable shift of a river channel through erosion and deposition at bends*. Such activities as the cutoffs of meander bends cause a new channel alignment to develop, leaving behind oxbow lakes. This implacable shift of rivers generally is a rather slow phenomenon but it often has a great influence on man's use of rivers and valleys.

Since the dawn of civilization, mankind has faced problems associated with rivers, and solved them to the best of its ability. Increased understanding of the mechanism of morphological changes and effects of river training works call for the utmost care and better physical insight, which extends from a state of descriptive empirical knowledge to the gradual build-up of rational models. River bank erosion, and river meandering in general, is one of the most important problems to be solved for economic reasons as well as for the prevention of disasters.

The observation of a phenomenon is in general incomplete unless it results in quantitative information (Alonso, 1967). Mathematical models are applied in order to assess morphological changes quantitatively (Olesen, 1987). Therefore *the aim of the present investigation* is to understand the physics of bank erosion in alluvial rivers, as one of the major factors affecting the formation of river patterns, to formulate the physical

phenomena in mathematical expressions so as to obtain quantitative information, and to develop a two-dimensional mathematical model for a river's plan-form movement in alluvial plains. *The ultimate objective is to predict the future plan-form of the river.* The present study is primarily concerned with river bank erosion and stability problems of non-tidal meandering rivers in alluvial plains.

Each chapter cited here is arranged by topic in order to compose a study which is centred on the bank erosion processes and river bank stability. Like a mosaic, this study is made up of separate chapters that relate to each other so as to form a meaningful pattern. Each chapter could in its term be greatly enlarged and detailed by experimental and field results.

1.2 Alluvial plain classification

Alluvial plains have been classified by Melton (1936) into three basic types. These are *meander plains*, built up largely of meander scrolls, *covered plains*, which are built up mainly of over-bank deposits and are generally characterized by the presence of levees and an absence of meander scrolls, and *bar plains*, which have braided river channels and no levees or meander scrolls. The present study concentrates on the first type, *the meander plain*.

1.3 Scope of the study

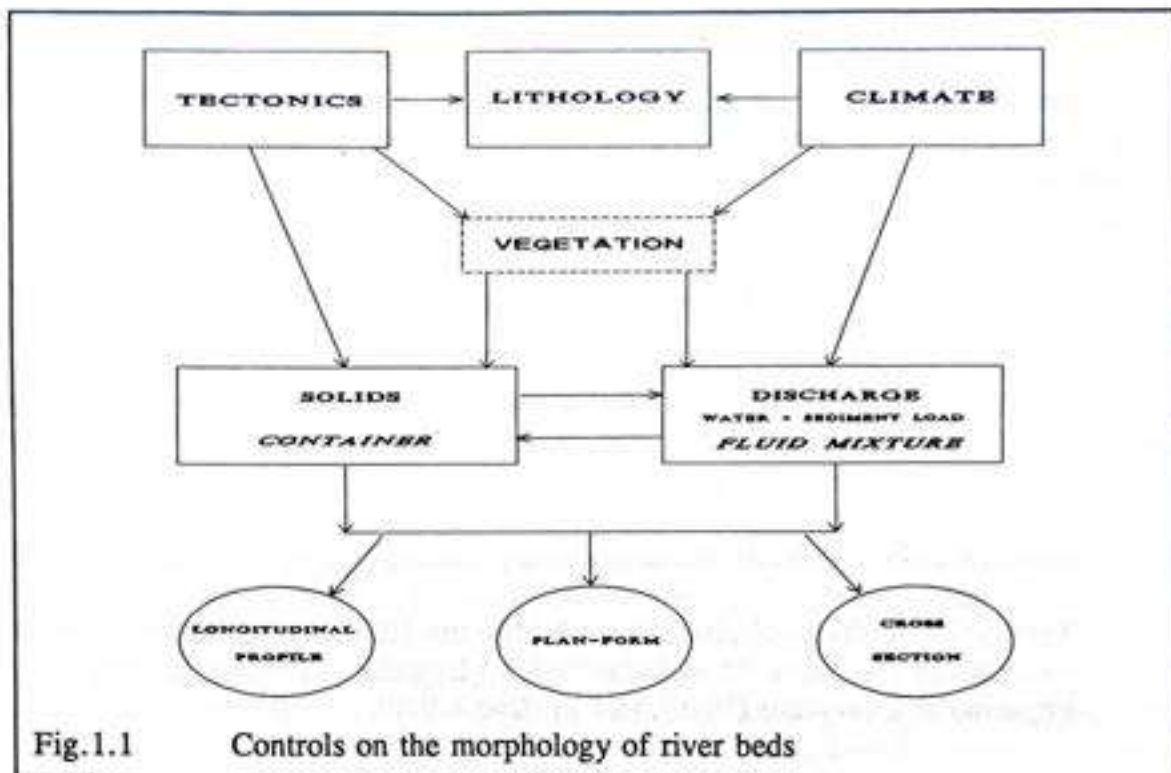
In order to achieve the aim as mentioned above, the scope of the study is divided into three fields of study as follows:-

1. Flow and bed topography in a meandering river
2. Fluvial processes and geomorphology of the river basin
3. Morphological computations in mathematical modelling.

In nature there are no geometrically straight rivers. Alluvial rivers have been classified into many classes. An important class of rivers exhibits a relatively stable meandering plan-form on the basis of differences in their curvilinearity. Next to this class we observe some kinds of migration of meander bends. Bed deformation in bends and at crossings in alluvial rivers is an intriguing feature in geomorphology since it governs, to a high degree, the plan-form of a river. Every river has then in principle to be seen as a three-dimensional body. In order to gain an insight into the laws of river bed evolution, plan-form, longitudinal profile and cross-section are considered as parts of the whole. They are also parts of *an interconnected system* which is furthermore controlled by the discharge and sediment load.

Rivers on loose earth can be considered as conveyers, which consist of two parts : a loose-boundary container, and a fluid mixture. These two are naturally interrelated. Therefore, starting out from the natural bases of the formative processes of river bends (ie. tectonics, the lithology, the climate, and vegetation) and proceeding through the two

important transportation processes (ie. run-off of water and the transportation of sediments), an interconnected system can be developed as shown in Fig. 1.1. The directions of influences are shown by arrows.



As mathematical models are becoming increasingly important in these fields, the mathematical formulation of the relevant physical phenomena is a keystone to further development. After this, it is necessary through the numerical integration procedure to maintain a balance between computational time and accuracy of computational results. Thus morphological *computations* in mathematical modelling become an essential part of the present study as a basis for obtaining practically-applicable results.

1.3-1 Previous work

Earlier work has of course to be studied as extensively as possible before an own beginning can be made. Relevant theories are discussed in Chapter 2 and specific contributions to these theories are introduced further in Chapters 3,4 and 5. In this section only a general classification and overview of previous work is given.

Theoretical and experimental investigations of flow characteristics in bends with flat beds were made by Rozovskii (1961) and Yen (1965).

In the case of a fixed bed topography in a river bend, many mathematical models

have been developed to study flow characteristics in bends, e.g. two-dimensional models of Huang et al. (1967), and De Vriend (1976). Interactions between flow and bed topography in movable-beds have been investigated in considerable detail. Some important results of works in this area are: Yen (1967, 1970), Engelund (1974), Kikkawa et al. (1976), Onishi et al. (1976), Zimmermann and Kennedy (1978), Falcon (1979), and Odgaard (1981), Struiksma et al. (1985), Blondeaux and Seminara (1985), Ikeda and Nishimura (1986), Odgaard (1986a,1986b), Ikeda et al. (1987). However, until now, the temporal evolution of bed topography has been only a little studied by comparison with this areas. Among the studies are these of Olesen (1987), Yen et al. (1990), Shimizu et al. (1990) {3 -dimensional model}.

Based on the available knowledge, the present study falls into this last category, and an own mathematical model is developed in Chapter 3.

Stability theories of fluvial meandering have been produced by many investigators: Adachi (1967), Hayashi (1970), Sukegawa (1970), Engelund & Skovgaard (1976), Fredsøe (1978), Ikeda et. al. (1981) and Olesen (1983).

From these investigations, three instability mechanisms can be identified : -

1. The bar instability mechanism found by Hansen (1976) and Callander (1969) and included in the work of Adachi (1976), Hayashi (1970), Sukegawa (1970), Engelund & Skovgaard (1976), and Fredsøe (1978).
2. The bend instability mechanism found by Ikeda et. al. (1981): a stability analysis of a sinuous channel with erodible banks allows for the delineation of a bend instability that does not occur in straight channels, and differs from the alternate-bar instability.
3. An idea that the development of meanders is caused by a stationary wave, as proposed by Olesen (1983). A steady-state analysis of the linearized mathematical model in the case of generally low erodibility of the banks gave an adequate explanation.

These earlier studies are used as a foundation for the present study of stability and migration of alluvial river banks. Over recent years a major research effort has been made to develop grid- generation methods which can adequately discretise complex geometrical regions, together with adaptive techniques which can ensure that the grid reflects the features in the flow-field. Some of these methods are, for example, structured meshes from partial differential equations, conformal and orthogonal mapping, algebraic mesh generation, automatic generation of unstructured meshes, mesh adaptivity techniques, geometry modelling and surface grids.

In fact, the above mentioned are merely nomenclatures for various forms of numerical grid generation. The essence of this is that, instead of considering and calculating all points in the continuous domain, one selects a subset of points within a

domain at which flow quantities can be calculated. The combination of points and connections between points defines a mesh or grid on which numerical methods for the solution of the flow equations can be constructed. The assumption is then made that the information at these points is sufficient to describe the complete flow-field. The idea follows simply from a demand for accurate solutions of ever more realistic problems. Obviously, there are many aspects which must be considered if accurate computer simulations are to be achieved.

One writer on numerical grid generation, Weatherill (1990), said, "some success in this area has been reported although there is still some way to go before complete adaptation is routine in computational fluid dynamics". Therefore, in the present study, after much analysis of economic and accuracy requirement in the light of the particular objects of the present study, it is shown that the negative factors outweigh the positive ones in existing approaches; hence the decision to propose a new method see Section 5.10.

1.3-2 Present study

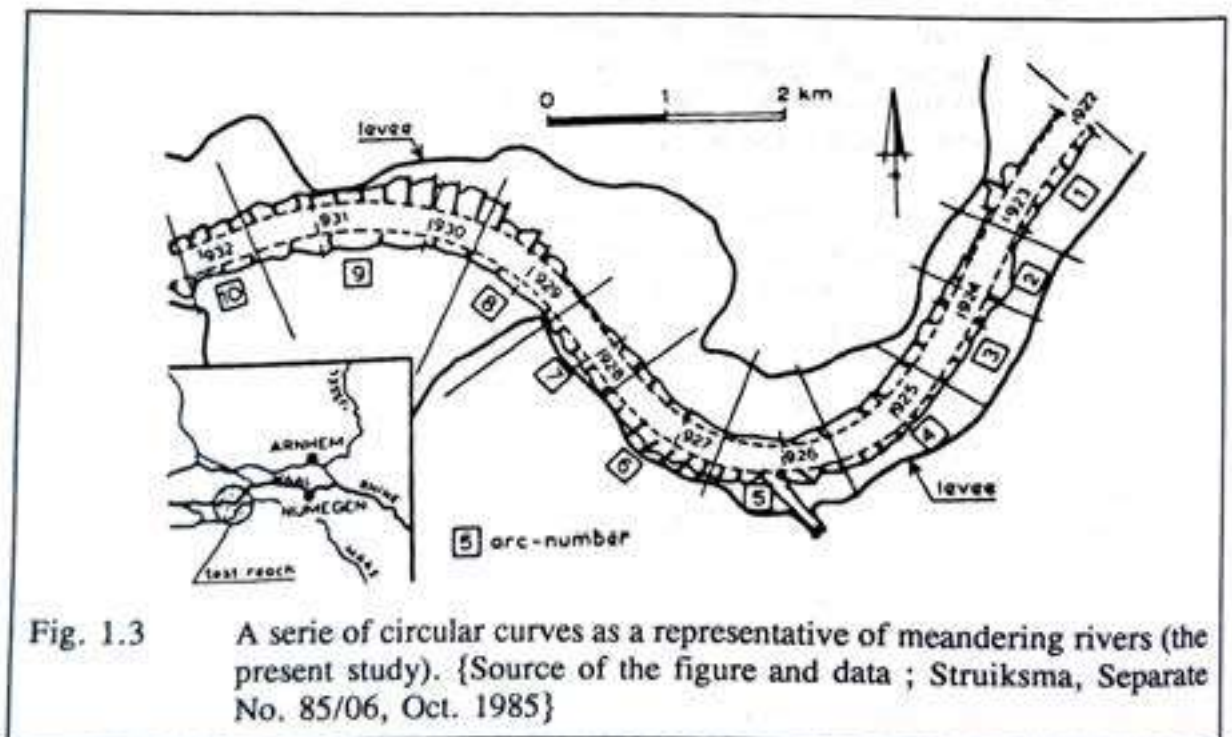
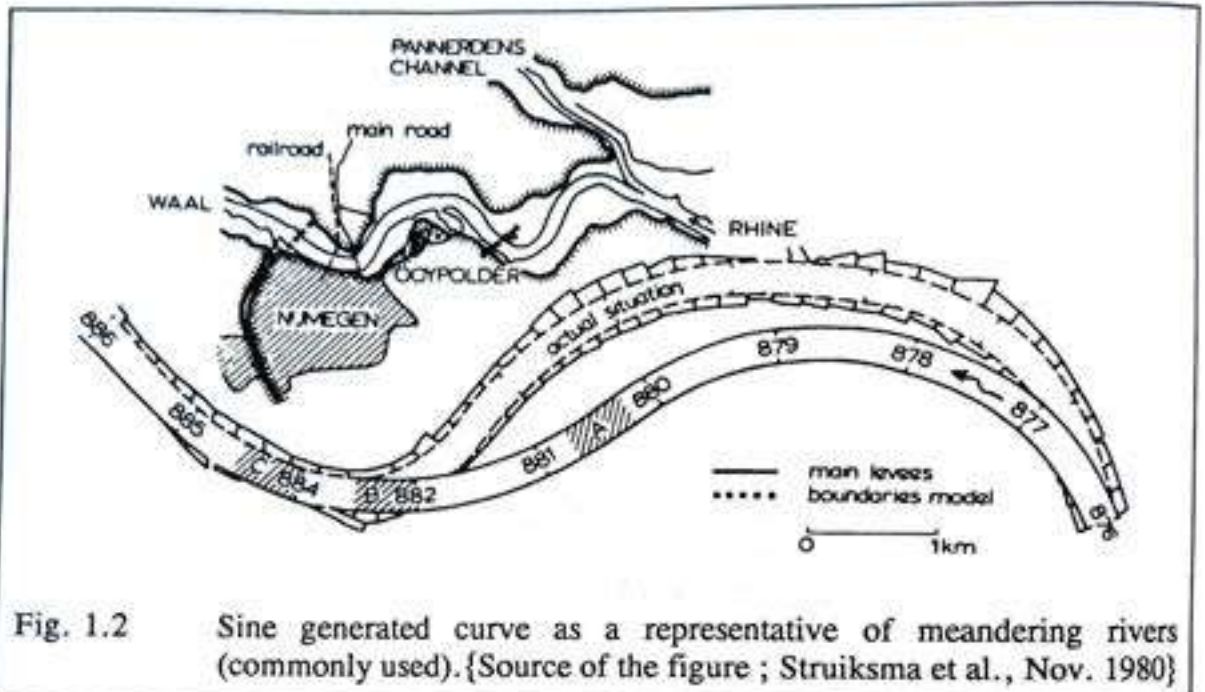
The present study consists of four major parts. In the first part, a two dimensional mathematical model for a meandering river is developed in a curvilinear co-ordinate system. Grid mapping for the computational domain of the entire area (a complete meander wave length or a succession of bend trains of long-lasting meander length) is developed. This type of grid mapping can offer a more acceptable representation of the plan-form of a river which is to be simulated. The difference between a representation by a sine-generated curve (which is the most commonly used) and that of a series of circular curves with different radii of curvature are shown in Figures 1.2 and 1.3. Details are explained in Chapter 3 and derivations are presented in Appendix A. The model is verified in both cases using flume experiments and results obtained from a natural river, the Waal river in the Netherlands. The agreement is found to be good. The second natural-river case of verification is performed on the river Ishikari in Hokkaido, Japan. The agreement is also good and it confirms that the present model is reliable.

In the second part of this study the (intermediate) goal of the investigation is to define a relationship between depth, discharge, slope and sediment properties that can be used in a wide range of situations where uniform flow conditions are present and which can also be adapted for use in the mathematical model of the first part of the present study.

In the third part, which is based on previous knowledge, a heuristic approach to determine the optimum river width is attempted. From this part of the study, one can deduce whether river migration or a relative stability of the bank will occur.

In the last part, a simple geometric construction of a new grid mapping together with a curve-fitting method is proposed. Bank erosion modules are developed and a mathematical model leading to a plan-form movement is also developed. Finally, the hydrodynamic model and bed topography model of Chapter 3 are added in front of the bank erosion model, followed by a plan-form movement model. In this study, every part

is made separately as a modular construction. By so doing, the model becomes more flexible and reconstructable while modules can be changed (or others added) so as to describe a whole series of different geomorphological properties along the bank line of the entire study area.



The present study tries to put together three aspects of river evolution (ie. geomorphology, fluvial hydraulics and hydrodynamics) into a simulation model called *RPM* which stands for *River Plan-form Movement* model. In order to verify the *RPM* model, physical evidence for lateral erosion of natural rivers as well as flume experiments are studied. However, the input data needed for the *RPM* model are rather specific and are not fully available from field data as derived from the literature survey. In fact, field data for such bank-line movements were traditionally documented in such a way that only the most interested variables are measured and listed in the light of geomorphological aspects, geological aspects, and geographical aspects. Nothing specifically new is done from a hydrodynamic point of view.

Accordingly, the verification of the model cannot be carried out for a bank line displacement of a natural river but only for bank erosion rates. However many of these can be used as some guide lines. For example, the Mississippi river (width about 790 m ; depth in flood, 36 m ; sine of gradient, 0.000066 ; mean annual discharge, 17000 m³/s) has provided some reliable estimates along a total water distance of 1355 km by a Lieut. Ross in 1765, the United States Land Office survey of 1820 to 1830, the Mississippi River Commission surveys of 1881 to 1893, and 1930 to 1932, and subsequent surveys. From these, forty selected meanders, with an average lateral amplitude of 12.8 km, radius of curvature 3 km and, channel width 0.8 km, have migrated an average of 2.24 km laterally in 167 years, or 13.44 m a year. Such information can be used as a guide line for the present model. Besides, this model is developed for study purposes and it functions under its hypothesis to fulfil the main study objectives. After this, the conclusions are summarized and some discussions are added by way of a closing of the present study.

1.4 Outline of the thesis

The present study is presented in six chapters. After the introduction, Chapter 2 reviews the relevant theories. The main parts of the whole investigation are reported in Chapters 3,4 and 5. A summary of conclusions and recommendations resulting from Chapters 3 to 5 are presented in Chapter 6.

In *Chapter 2*, the flow and bed topography in a meandering river are studied and are presented. In order to complete the scope of the present study, the stability of self-formed alluvial rivers, their bank erosion mechanism and finally their river channel patterns and evolutions are studied. Some key points are reviewed.

In *Chapter 3*, a two dimensional mathematical model for a meandering river is developed in a curvilinear coordinate system. The essential parts of the model are described. The model is verified by comparing its results with measured data from flume experiments, as well as by comparing computational results with measured data from the Waal river in The Netherlands and the Ishikari river in Japan. The performance of the

model is evaluated. Thus Chapter 3 facilitates the selection of the various types of graded¹ meandering rivers that are used in Chapters 4 and 5. The codes produced for this Chapter are given in Appendix-A.

In *Chapter 4*, the stability of meandering rivers is studied in connection with the friction condition and the sediment transport capacity. A mathematical model is then developed for the shape and the dimensions of the stationary dunes based upon a theory of Fredsøe, (1982) together with an alluvial roughness-predictor model. The corresponding code is given in Appendix-B. An attempt is made to determine the optimum river width. A heuristic approach is used and while it is proceeding a new shear-velocity relationship between plane bed and dune-covered bed is found for a constant discharge condition. This is new and the reason that it cannot be experienced when using physical models is explained. It is essentially only through computation that this relation has been found. This velocity relationship facilitates the morphological modelling of a more acceptable friction condition for a proposed regime in alluvial rivers. From this study, one can deduce whether river migration or a certain stability will occur in a given meandering river. Thus, when the river width is not optimum (stable), then the model developed in the next chapter must be used to predict the changes that will occur.

In *Chapter 5*, the bank erosion mechanism in alluvial rivers is studied. Mathematical expressions for various bank erosion rates are derived. After the verifications of computed bank erosion rates, a mathematical model leading to a river plan-form movement is developed and a new position of the river is simulated. An automatic grid-generation procedure is proposed. This technique may bring out the simulation of river plan-form movement in an alluvial plain which actually is a meander migration model. Some numerical experiments are carried out. This part of the study provides a tool to predict river migration in alluvial plains.

Finally, in *Chapter 6*, the most important conclusions are summarized and discussed, and suggestions for further research are given.

The derivations, detailed explanations and equations of the models are listed in appendixes A, B and C which follow, respectively, chapters 3, 4 and 5.

¹ For the definition of graded rivers; see Garde and Raju, 1985, 'Mechanics of sediment transportation and alluvial stream problems'.

".....for tolerance, for reasons, for the adventure of ideas, and for the search for truth."

Jawaharlal Nehru

2. REVIEW OF THE EXISTING THEORIES

2.1 Introduction

This chapter presents a review of alluvial river form and processes, and attempts to integrate the distinct but related approaches of geomorphologists, geologists, geographers and, hydraulic engineers. From which physically based numerical model will be developed in the following chapters. Thus mathematical models of flow and bed topography in meandering rivers are also reviewed.

2.2 Selection of the theories and ideas

A researcher who is working in the field of science gathers many experiences, including confusion and contradiction. For example, the idea of Lord Kelvin, *"when you can measure what you are speaking about and express it in numbers you know something about it; but when you cannot measure it, when you can not express it in numbers, your knowledge is of a meagre and unsatisfactory kind"*, has often been quoted by scientists and researchers. On the contrary, two professors of Statistics, Yule, G.U. and Kendall, M.G., say, *"This remark has often been quoted with an approval which it does not altogether deserve - it does not, for example, do justice to the work of Darwin and Pasteur, to name only two of Kelvin's contemporaries. But there can be no denying that it expresses a point of view which many people will endorse."* Therefore it should be mentioned here that this study only follows the selected ideas which selections are made both intuitively and deductively by the author. In this context, relevant but distinctly opposed theories are also discussed in the corresponding sections and chapters.

2.3 Division of the subject matter

Such a complex subject as this has to be divided clearly if only in order to provide a properly organized presentation. This thesis covers a very wide range whereby it introduces material from various different areas of science and technology, such as hydraulics, geomorphology, continuum mathematics, computational methods in general and mathematical modelling in particular. Accordingly, the subject is divided here into three main parts referred to as Part A, Part B and Part C, as already introduced in the list of contents of this chapter.

2.4 Part A

2.4-1 Flow and bed topography in meandering rivers

2.4-1.1 The secondary flow

A secondary flow or spiral (helical) flow that occurs in curved channels was first observed and described systematically by Thomson in 1876. This phenomenon is due mainly to

1. friction on the channel walls, which causes higher filamental velocities near the centre of the channel than near the walls.
2. centrifugal force, which deflects the particles of water from a rectilinear, or straight-line motion.
3. a vertical velocity distribution which exists in the approach channel and thus initiates a spiral motion in the flow.

In curved channels, friction is greater than it is in the straight channel and this is naturally associated with the spiral flow that leads to local bed and bank scour. The relation between the spiral flow and the radius-to-width ratio has been investigated experimentally by (Shukry, 1950) using a bend in a rectangular steel flume. In this and many subsequent studies this is called the secondary flow. The "strength" of the secondary flow, S_{yz} is defined as the ratio of the mean kinetic energy of the lateral motion to the total energy of the flow at a given cross-section. Since the kinetic energy of flow depends on the square of the velocity, this provides a relation of the form

$$S_{yz} = \frac{v^2}{U^2} \quad (2.1)$$

in which

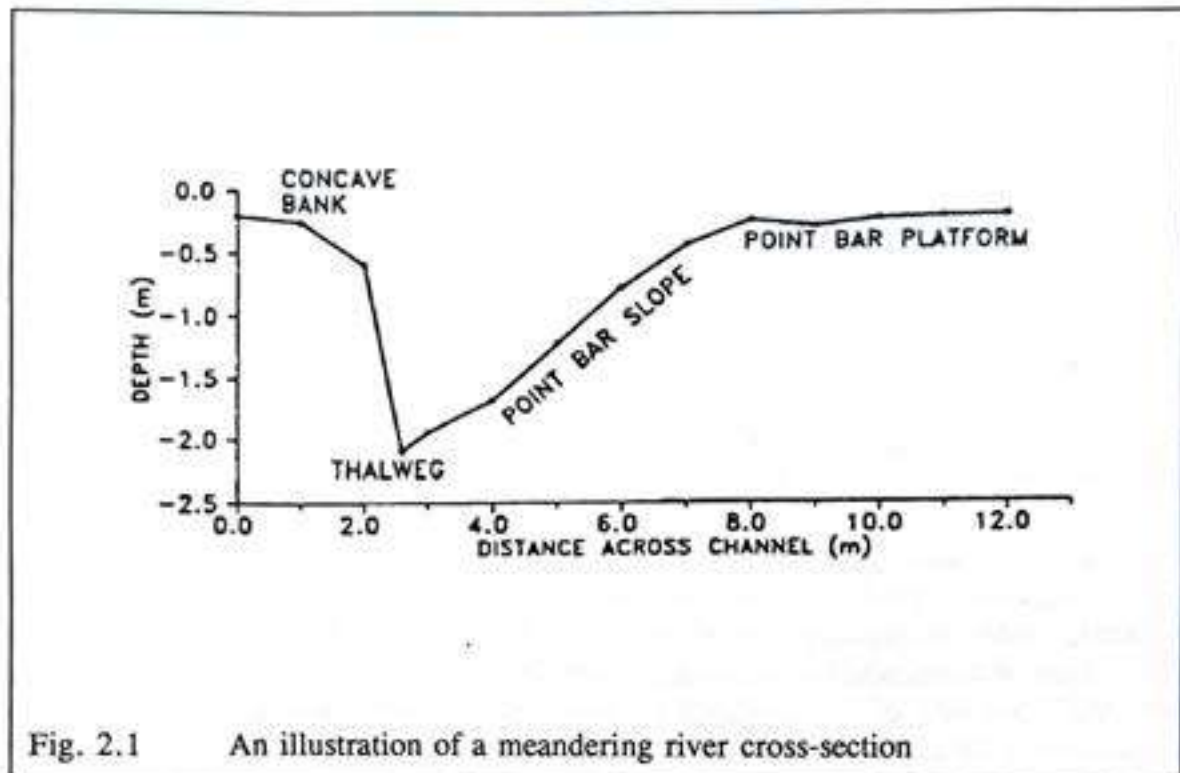
v	=	magnitude of the mean-velocity vector projected on the yz plane
U	=	mean-velocity over the section
S_{yz}	=	strength of the secondary flow

The strength of the secondary flow decreases considerably with increasing Re , the Reynold's number. It also decreases gradually due to the increase of radius to width ratio, R_c/W . (We observe, following (Shukry, 1950) that a value of approximately $R_c/W = 3$ gives a minimum value of S_{yz} , i.e., the curvature effect approaches a minimum. It similarly decreases when the width to depth ratio decreases, which in turn implies that this strength increases in shallow-water flows. Again the strength increases when the deviation angle of the bend becomes larger. More specifically, from $\theta/180^\circ = 0$ to $\theta/180^\circ = 0.5$, the increase in the strength is nearly double that obtaining for the range from 0.5 to 1.0.

Flow characteristics and sediment movement are much more complex in channel bends than in straight channels. Theoretical and experimental investigations of flow characteristics in bends with flat beds have been made by Rozovskii (1961) and Yen (1965).

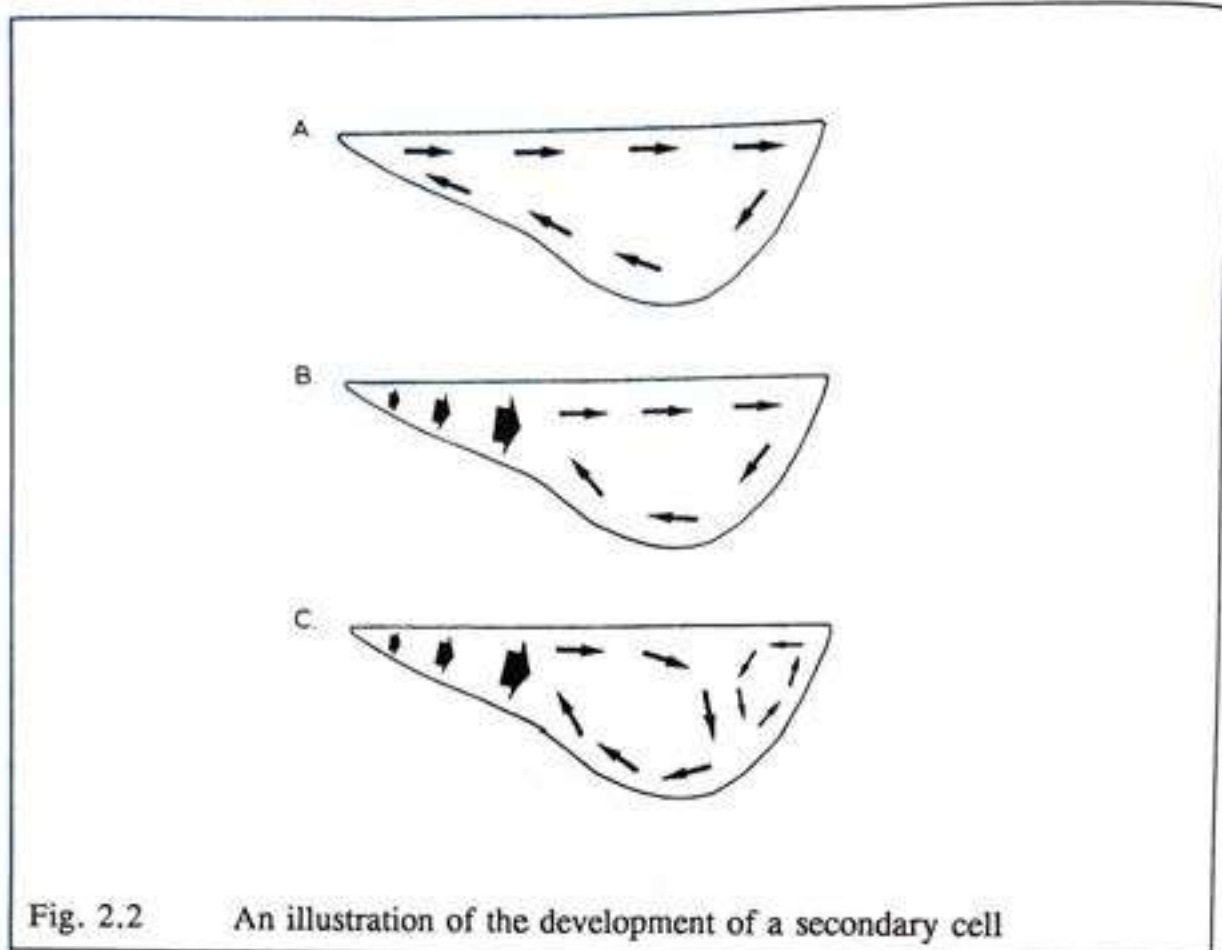
A typical channel cross-section topography in a meandering channel is characterized by three zones (fig. 2.1): a relatively deep thalweg located along the outer

concave cut bank; a point bar top or platform along the inner bank; and the point-bar slope, which connects the two, making up the central portion of the channel. One of the primary characteristics of flow through a meander is the helical- or secondary-flow cell (Leopold and Wolman, 1960; Rozovskii, 1961). The combination of centrifugal force, resultant super-elevation and cross-stream pressure differential create a small transverse current. When coupled with the primary longitudinal flow, this creates a helical-flow cell in the bend (Fig. 2.2-A). The longitudinal velocity field differs from that in a straight channel because the position of maximum velocity varies through the bend, shifting from near the inner bank at the bend entrance to the outer bank near the bend apex, where it stays until the bend exit (Leopold and Wolman, 1960; Dietrich and Smith, 1983, 1984; Johannesson and Parker, 1989).



Dietrich and Smith (1983) and Thorne et al. (1985) noted that the helical cell was present only in the deeper part of bend cross-sections, while all transverse flow over the point bar platform was directed towards the outer bank (Fig. 2.2-B). In addition, smaller transverse cells of opposite rotation to the main helical cell have been measured near the water surface adjacent to the outer, concave bank of several rivers (Fig. 2.2-C: see Bridge and Jarvis, 1982; Thorne et al. 1985) and near banks and at sudden depth changes in flumes (Tominaga and Nezu, 1991).

The mathematical modelling of such flows and their related channel characteristics has proved to be difficult. Most such models are based on simplifications of the equations



of continuity for water and sediment and on the Reynolds' (or St. Venant's) equations of motion (Rozovskii, 1961; Yen and Yen, 1971; Engelund, 1974; Smith and McLean, 1984; Odgaard, 1986). As noted by several researchers (Odgaard and Bergs, 1988; Yen and Ho, 1990), most of these models simulate bend flow and channel topography only in the "fully developed" portions of the bend, i.e., where velocity and thalweg depth do not vary longitudinally. Other models predict these characteristics throughout the bend, even when velocity and depth change downstream (Dietrich and Smith, 1983; Engelund, 1974; De Vriend and Geldof, 1983; Odgaard, 1986; Yen and Ho, 1990). In addition, considerable disagreement exists over the simplifications and eliminations that have been used to solve these equations (Dietrich and Smith, 1983).

Most of the mathematical models have been tested or verified in flumes, some of which had fixed beds (Yen and Yen, 1971) or constant radius of curvature segments connected to straight segments (Yen and Yen, 1971; Odgaard and Bergs, 1988). Even when model testing is done on rivers with constantly-varying radii of curvature and mobile bed materials, problems with measurement accuracy of the various model components often dominate the final result (Dietrich and Smith, 1983).

2.4-1.2 Sediment transport in general and sand transport in particular

The mechanisms of transport of uniform and graded sand have both similarities and differences. The movement of sand and gravel in streams is usually classified under the two headings of bed load and suspended load (i.e. wash load is usually neglected). The movement process of bed load and suspended load are different and the size of the material are also different. The difference in movement processes of uniform and non-uniform grains are considered only for the bed load since gravels cannot be suspended in a gentle flow. The formulae used to estimate the bed load discharge are numerous, from the well-known Einstein's function (1950) to recent time by many researchers. Although the sediment discharge is usually expressed as a function of the flow intensity, the movement mechanism of sand grains is not completely clarified yet and these formulae are dynamically insufficient. The present situation is that a universal theory of sand movement has not been established. In order to clarify the mechanics of such a complex sand movement in a stream, methods of measuring the movement of a single sand particle in a flow and researching the characteristics of sand movement as a group must be considered. Such an investigation was carried out by Yano et al., 1969, who investigated the mechanics of sand movement as a group phenomenon. From their attempt it was reported that: "sand grains start to move by hydrodynamic drag forces acting on a sand grain caused by mean velocity and turbulence of flow and collision of moving sand grains with bed ones, but they usually rest after moving a certain distance. The movement is a repeated phenomenon of irregular and intermittent motion".

The average travelling velocity of large sand grains in graded sediments is larger than that of uniform sediments due to the accelerating effects of the grains, and, on the other hand, the velocity of small sand grains is smaller than that of uniform ones due to the hiding effects of the grains. It was found that such a phenomenon also intrudes when measuring the rate of transport of sand grains in graded sediments.

2.4-2 Mathematical model in a 2D- bend; the extent to which mathematical Models have been developed, applied and extended.

In the case of a fixed bed topography in a river bend, many mathematical models have been developed to study flow characteristics in bends. (Eg. two-dimensional models of Huang et al. (1967), De Vriend (1976), Smith and McLean (1984), Ali (1985) and Olesen (1987).)

Interactions between flow and bed topography in movable-beds have been investigated in great detail. Some important results of those works are as follows:

- Yen (1967, 1970) investigated the equilibrium bed topography and its effects on flow in a channel bend with fixed walls.
- Engelund (1974) analyzed the movement of sediment in bends, and employed sediment continuity and transport formulas to predict the equilibrium bed topography.
- Kikkawa et al. (1976) showed that the bed evolution in the fully developed region of channel bends can be simulated by an uncoupled scheme.

- Onishi et al. (1976) suggested that bed topography enhances the nonuniformity of the water discharge, resulting in a greater sediment transport.
- Zimmermann and Kennedy (1978), Falcon (1979), and Odgaard (1981) analyzed the transverse bed slope in the fully developed region of the bend, and concluded that the weight of sediment particles and the shear force are the dominant factors influencing the transverse movement of sediment.
- Struiksma et al. (1985) investigated the wavelength and the amplitude of the bend deformation, and also derived a form for the transverse bed profile in the fully developed region of the bend.
- Blondeaux and Seminara (1985) studied the mechanisms of meander initiation and its growth, and found that alternate-bar formation and bend amplification are due to different mechanisms.
- Ikeda and Nishimura (1986) showed that the inclusion of a suspended load can increase the maximum scour depth by as much as 8% and that the secondary flow in a sinuous bend has a phase lag relative to the bend's plan form.
- Odgaard (1986a,1986b) considered the transverse mass shift to be due to the secondary flow and the bed topography, and employed a mass-flux balance to link the equation for equilibrium bed profile in a bend to the momentum equations.
- Ikeda et al. (1987) found that the sorting of bed material can reduce the maximum equilibrium scour depth by as much as 30-40% in the fully developed region of uniformly curved bends.

However, in comparison with the preceding, until now, the temporal evolution of the bed topography has received few studies. Some of studies published are those of Olesen (1987) and Yen et al. (1990). The present study follows this last category and later looks into the process of bank erosion as well.

2.5 Part B

2.5-1 The stability of self-formed alluvial rivers

One of the main difficulties of our subject is that the bed configuration depends on the discharge. Moreover, the hydraulic resistance is a complicated function of the bed configuration, so that we are faced with a very intricate problem of mutual interaction. As the problem of sand wave formation depends on hydrodynamic stability, we even find that changes in bed formation may have a nearly discontinuous character at a certain stage (corresponding to a shift from the 'lower' to the 'upper' flow regime).

The minimum width of an essential straight alluvial channel capable of transporting a given quantity of water, with or without a mobile bed material or a wash load, is related to the tractive strength and the sliding strength of the bank soils, either alluvial or residual. In addition, the variation of the bed level at the banks due to bed forms, alternate bars, and other three-dimensional flow effects is an important factor. This variation can be defined in terms of the ratio of the maximum depth along the bank to the average depth over the bed. The use of bank soil properties to determine stable channel widths indicates

that more than one width and slope are possible to carry a given water discharge with or without bed-material load. For design purposes, the minimum allowable width is usually the best choice (Stevens, 1989).

Historically, there have been three approaches to determining the stable (noneroding and nondepositing) width of such a channel. The earliest was the Lindley (1919) regime width, followed in the next forty years by numerous other width predictors of the same type. In 1955, Lane presented the tractive force theory developed by many persons at the U.S. Bureau of Reclamation. More recently, concepts of minimum stream power (Chang 1980) and maximum sediment transporting capacity (White et al., 1982) have been put forth as suitable width indicators. From a theoretical point of view, it is the interplay of the properties of the fluid and the soil at the banks that determines the minimum and maximum stable width of erodible channels which are essentially straight. The minimum stream power method underpredicts appreciably the widths of Punjab and Sind canals wider than 150 ft (46m) but fits smaller canal data much better. The maximum sediment transport carrying capacity method was similarly found to underpredict the width of large canals (widths greater than 33 ft or 100m) by significant amounts on the average. Agreement was found to be much better for smaller canals, with widths of 10 to 30 ft (3 to 10 m)(Steven, 1989).

2.5-2 Stable-width criteria

In order for the banks to be stable, two criteria must be satisfied. In the first place, the shear stress on the banks must be such that the suspended sediment is not deposited on the banks and no particles are eroded from the banks. Some deposition and erosion might of course in practice occur, but it should remain on the average insignificant. Secondly, the banks must remain free from sliding failures or other types of geotechnical failures under adverse conditions in the soil. In this work, the first is labelled the "tractive strength" criterion and is directly related to the tractive force; the second is called the "sliding strength" criterion and is only indirectly related to the tractive force. The sliding strength concerned with subaerial/subaqueous weakening and weathering which are associated directly with soil moisture conditions.

If we consider the tractive strength of cohesive soils, we observe immediately that fine particles of suspended sediment, such as clays, are carried in greater concentration than are larger particles at and near the surface of the flow. Clay particles have electrical charges, on their edges as well as on the flat sides of their lamella, where there are some unshared electrons from oxygen molecules in the silicon-oxygen layering common in most clays. The attraction or repulsion forces between charged particles of clay can be much greater than the gravity force acting to settle all the particles. The gravity force is of course proportional to the submerged weight of the particle, while, as illustrated by Lane (1955), the allowable shear stress for clays is unrelated to the particle size. In wide prismatic channels, the shear stress on the banks near the surface is low, especially for sloping banks (Ghosh and Roy, 1970) so that clay particles moving near the bank can become deposited even on a vertical face if the shear stress at the surface is very small. Thus a number of clay particles are deposited when the shear stress is low, but as

the bank builds-up into the flow, the slope steepens and the shear stress increases. Thus a criterion for mathematical (and physical) stability is present and this already indicates that, as the phenomenon of bank deposition develops, its rate of development decreases.

The same is true for erosion: when particles are plucked from the top of the bank by the shear stress of the flowing water, the slope decreases, which in turn decreases the shear stress.

In the case of non-cohesive soils, the tractive strength which the soil possesses to resist the dislodging of particles is directly related to the easily-measured properties of the individual particles. By neglecting the lift forces on the particles on the bank (see Graf, 1984), Lane's (1955) value for tractive strength for sand is:

$$C_t = \theta_c (S_s - 1) \gamma D_{50} \cos \theta_s \left(1 - \frac{\tan^2 \theta_s}{\tan^2 \phi}\right)^{0.5} \quad (2.2)$$

in which

- θ_c = critical Shield's parameter
- S_s = specific gravity of the solid particles
- θ_s = side-slope angle measured from the horizontal.
- D_{50} = median sieve size (by weight) of the particles on the side slope
- ϕ = angle of repose for the particles

When the flow at the banks is hydraulically rough, $\theta_c = .047$ (Gessler, 1971) but for small particles and high viscosity θ_c can be as low as (0.030). The tractive strength of a cohesive soil is not so easily related to the other soil properties: the electrochemical forces which dominate in cohesive soil are only partially understood (Partheniades 1962, 1971) and vary for the most part with changing moisture content and with dissolved solids in the water.

2.6 Part C

2.6-1 Bank erosion mechanism of self-formed alluvial rivers

There is a considerable divergence of conclusions concerning the dominant mechanisms of bank retreat, as shown below:

"The major controls on bank erosion remain unclear at present" (Hasegawa, 1989),

The bank retreated primarily by mass failures of overheightened and oversteepened banks.

(Little, Thorne and Murphey, 1982)

The shearing of bank material by hydraulic action at high discharges is a most effective process, especially on non-cohesive banks and against bank projections.
(Knighton, 1984)

The erosion of a (river) bank is not the result of erosion by high-velocity water, whether in a concave bank on a curve or in a straight section. Rather, for effective erosion to occur, the material must be loosened-which in this stream, is done by the formation of ice crystals in winter.

(Leopold, 1973)

There are many authors who believe that it is combinations of processes that are important (e.g. Hooke, 1979; Thorne, 1982; Lawler, 1987). Perhaps, in view of the wide range of alluvial materials, riverine forms and hydroclimatic environments encountered, a variety of conclusion is to be expected. However some hypotheses are selected to be followed in this study and they are reviewed here in order to try to disentangle competing hypotheses of process-dominance in river bank erosion systems.

2.6-2 The overall history of meandering rivers: river channel patterns and their evolution

2.6-2.1 Time scales of alluvial rivers

There are several possible space and time scales for considering morphological changes in alluvial rivers, each valid for its own specific purpose. At the *micro scale*, studies have been carried out on the mechanics of entrainment and transport of an individual particle within a uniform bed material. From flume experiments, the drag and the lift forces can be calculated but these cannot be transferred directly to models of transport and morphological changes of natural channels over larger space and time scales and associated variability.

At the *meso-scale*, physically-based equations which model general reach processes have been developed for flow resistance and sediment transport. These apply to average channel conditions and are general. Normally total transport rates are predicted without regard for sediment grain size or calibre, although equations are now being developed for routing different size fractions. Morphological models to predict scour and fill, using these equations in conjunction with continuity principles, enable spatial and temporal changes in channel depth, slope and velocity to be simulated. A fixed width and plan shape have to be assumed and, given knowledge of flow and sediment inputs, the spatial and temporal response of the river can be modelled. In reality the input conditions can also change in response to erosion and deposition, which further limits the application of this type of mathematical model. Even downstream from dams, where feedback mechanisms are precluded, problems arise because of difficulties in predicting the rate at which the bed becomes armoured. When considering larger-scale development of river systems over longer time periods, *macro-scale* approaches can be adopted. Instead of routing every flow

which transports material through a series of reaches, the average bankfull dimensions of the river can be modelled over time and space based on systematic changes that occur in the dominant, channel-forming flow and its associated sediment load. Although process-based, it uses a simpler transport function to simulate channel change.

Finally *mega-scale* approaches, which consider the sequence of runoff, sediment supply and sediment transport, are being developed by geomorphologists to investigate the more dynamic and discontinuous aspects of channel development at the drainage basin scale. Sections located between zones of sediment supply and transfer, where temporary storage occurs, have a considerable tendency to lead to very rapid changes in channel geometry. In such sediment-balance models, based on long-term average sediment loads throughout the river system, only general conclusions can be drawn about the nature of the channel, zones of high deposition being characterized by braided channels or alluvial fans. These black box models provide no direct physical insight into the processes controlling sediment transport and channel adjustment.

To manage a river system effectively, particularly with regard to river engineering schemes, it is necessary to have due regard for its natural stability (Hey, 1987). Channel response to any natural or man-made induced changes will depend on the degree of change and the prevailing stability of the channel. Consequently it is very important to identify the controls on natural erosion and deposition and channel response to such activity. This can be achieved by considering the interaction between channel form, flow regime and sediment transport. All these factors are interrelated during periods of dynamic change through the operation of a number of process equations. A simple macro-scale model enables the nature of this interaction to be outlined in general terms and, although it is essentially concerned with the longer-term evolution of river channels, it is suggested that the principles apply equally well to changes over shorter, engineering time scales (Hey, 1987).

2.6-2.2 Theories of meandering

The process of initiation of meandering and the mechanism of meander development have been studied historically by many researchers. Since the present study is concerned primarily with the migration of meandering rivers, it is naturally also concerned, at least on part, with the meander-development-mechanism. Therefore a brief review has been made of some of the theories that have been advanced to explain this process, as follows:

(a) **Earth's rotation theory:** An object moving over the Earth's surface is effected by a transverse force (i.e. Coriolis force) normal to its path. This force represents the inertial reluctance of a moving body to participate in the rotational motion of the Earth. According to Baer (1860) and Gilbert (1884), the force produced by the Earth's rotation is sufficient to deflect the stream. The tendency of the Mississippi river and some rivers in Alaska (U.S.A) to deflect towards the right is still sometimes quoted in support of the above argument. However, Quraishy (1943) already objected that the tendency of a stream to deflect either to the right or to the left is merely a matter of chance, and the force due

to the Earth's rotation is usually very small: the erodibility of the bank material certainly plays a much more important role in this environment.

On the other hand, Neu (1967) again demonstrated how a secondary circulation may be developed in a stream because of the Earth's rotation. The relative intensity of this secondary circulation depends on the latitude of the place and the depth-to-velocity ratio for the stream: for values of depth-to-velocity exceeding 20, the flow may deviate from its axis by as much as 20° . Deviations of the order of 10° to 15° were observed on the St. Lawrence river (Canada) but even Neu concluded that at least a part of this deviation might be due to the secondary circulation naturally present in the river and not induced by Earth's rotation.

The older geographic literature pays much attention to the question of the influence of the earth's rotation on the movements on its surface. Up to the mid-19th century the standpoints of Hadley (mentioned in Henkel, 1922, Mangelsdorf *et al.*, 1980) prevailed, ascribing the direction of the trade winds to the rotation of the earth, using the difference in velocity at different latitudes as an explanation. It was then gradually recognized that every movement of a body on the earth is deflected to the right on the northern and to the left on the southern hemisphere. However, it was assumed that the theoretically postulated deflection was too weak to exert any notable influence on *flowing water*.

In 1860 the Baltic scientist K. E. von Baer published a report in the Annals of the St. Petersburg Academy of Sciences under the title: *On a general law of formation of river beds*. He attempted to prove that the steep nature of the right and the flat shape of the left bank of most major rivers, could be explained through the rotation of the earth. This long and hotly-debated theory has since become known as Baer's law (mentioned in Mangelsdorf *et al.*, 1980). The introductory statements of Baer himself are: "The flowing water, coming from the equator to the poles, will have a rotational velocity greater than that of the higher latitudes and thus will press against the eastern bank, as the rotation is directed east and with it also this little surplus brought along by the water flowing from lower to higher latitudes. On the other hand, water flowing from more or less polar regions to the equator will arrive there with lower rotational velocities and thus press against the western banks. In the northern hemisphere for rivers flowing north, the east bank is the right one". As proof, this author described his observation of a number of rivers and especially of the Volga, the right bank of which in Russian is called the "hill bank" and the left bank the "meadow bank". The high hill bank is the preferred area for settlements, whereas in the swampy flats on the left bank only few villages are found. The hill bank is subjected to continuous erosion which results in the collapse of enormous masses of rock from time to time. Olearius described in his *Persian Travel Notes (1666)*, that this process led to the burial of an entire ship and its crew which had been lying in the shelter of the bank above Astrachan.

Baer collected reports not only on the Russian rivers but also on the other rivers of the earth such as the Rhine, Nile, Mississippi, la Plata, etc. With only a few exceptions, such as that of the left-hand turn of the Euphrates near Aleppo, he found support for his law of dextral deflection. He stated that this law would become more

pronounced with a more north-south orientated course of the river. To support his theory he even suggested evaluating statistically whether derailments of trains travelling exactly north or south were more frequent to the right or to the left. He eventually tried to develop his law purely from physical factors. He was only partly successful - being himself a biologist - and he had to accept that the forces of deflection are very small indeed. It was held against him that the real reasons for the undeniable asymmetry of river beds should be sought rather in the prevailing wind directions and the condition of the bed rock. Nevertheless, the author adhered to his convictions with his characteristic intuition.

In the following decades Baer's law was repeatedly attacked. The protagonist of this opposition was Zöppritz (in Henkel 1922 and Wegener 1925), who criticized Baer severely by stating that in a straight river course the deflection force of the earth's rotation would lead only to a gradient of the water level at right angles to the direction of flow. The difference in height between the right and left water levels would be so small that it could not exert any notable influence. He added: "For the situation on the Siberian rivers which Baer without doubt described correctly, different explanations have to be found. They must be sought with certainty in the westerly winds prevailing there throughout the year".

Fabre (1903) devoted a detailed discussion to the reasons for or against the validity of Baer's law. Based on a 1789 article of the French hydrographer Lambardie, the *Morphology of the Earth's Surface* of Penck (1894), and his own observations, especially in the Gascogne area of France, he concluded that Baer's proposals on the influence of the terrestrial rotation on the development of the cross-section of rivers could not be upheld. For an explanation of this situation, meteorological and geological factors should be preferred. Fabre's ideas culminated in the statement that the asymmetry of valleys and the deflection of the thalweg are caused by geological and geographical factors, and mainly those of torrential erosion and wind deflection.

During the 1920's, the discussion of Baer's law was revived. Reference must be made here primarily to Henkel (1922, 1928), who submitted cogent arguments for its applicability. Wegener (1925) also arrived at a positive verdict, attacking Zöppritz for an insufficient consideration of the dynamics of transport of solids in rivers. Eventually, Exner (1927) found some basic proof for the applicability of Baer's law when allowing water in a test model to flow over a sandy surface on a rotating disc. As was to be expected, the right bank of the channels showed bulges when the disc rotated counterclockwise. Exner mentioned that these tests were also carried out specifically to disperse the doubts on the validity of Baer's law voiced previously by Schmidt (1942). Finally, in 1942, Dantscher verified this by calculating the forces acting in a river according to these mechanical principles.

(b) Disturbance theories: A disturbance in a straight channel travelling downstream causes change in the flow pattern that result in meanders. The initial disturbance could be caused by various circumstances. For example, an overloaded stream could deposit some of its load behind an obstacle and thus cause an asymmetry in the flow which might lead to meandering. According to Hjølstrom (1957) the irregular disturbances

of turbulent flow may cause a transverse oscillation of the water surface which travels downstream and causes a regular oscillation of the fluid mass, which leads to meandering. Also an experiment has been documented which obtained meander patterns by allowing water to enter a straight channel at an angle. Werner (1951) postulated that meanders are initiated by some disturbance which, by inducing transverse oscillations from one bank to the other, starts erosion and the first bend forms. This bend often constitutes a sufficient disturbance to continue the process of meandering.

(c) Helicoidal-flow theories: The currently dominant theory is that meandering is the result of helicoidal or secondary flow. The ideas developed in this regards have been supported by experiments; for example, different types of secondary flow could be obtained in successive downstream bends by causing artificial secondary flow at the entrance to the first bend. Apparently any disturbance which produces secondary circulation can lead to meandering. Since secondary flow is present even in a straight channel, one may suppose that the secondary flow pattern must become unsymmetrical before it can produce meandering. On the other hand a symmetrical secondary flow pattern will induce meandering if the erodibility of the bank material varies along the length of the stream. According to the Japanese researcher Fujiyoshi, a simple harmonic motion is set up in the flow when the pattern of secondary flow in the channel becomes unsymmetrical. From this concept, an empirical equation for the meander length M_L is given as follows:

$$M_L = A_1 \sqrt{RS} \quad (2.3)$$

in which R = radius of the meander bend

S = sinuosity

A_1 = meandering coefficient ; f(Chézy coeff., flow characteristics)

A_1 was found to vary from 75 to 125 for small streams, from 125 to 200 for medium streams and from 200 to 300 for large streams.

(d) Excess-energy theory: The idea behind this theory is that the process of meandering is related to the energy content of the stream. Schoklitsch observed that the meander formation might be due to the fact that the slope in such stretches is too great and is not in equilibrium with the size of bed sediment grains. The similar statement by Inglis is that meandering is nature's way of damping out excess energy during a wide range of varying flow conditions: the pattern depending on the grade of material, the relation between water discharge and sediment transport and rate of change of water discharge and sediment transport. This means that a channel having an excess energy tries to increase its length by meandering, thereby decreasing its slope. It has been found that generally in meandering streams, the ratio of radius of curvature to width lies between 2 and 3, and indeed Bagnold (1960) has shown that the bend loss becomes a minimum around this range of radius-to-width ratios. From this, Leopold and Wolman came to believe that some principle related to minimum energy is associated with meander formation. Although the above-mentioned researchers agree about this theory, an objection exists, as usual: Joglekar contends that the primary cause of meandering is an excess of sediment load

during floods. He argues that a river tends to build a steeper slope by depositing sediment load on the bed when the load is in excess of that required for equilibrium. This increase in slope leads to a decrease in depth and this tends to increase the width of the channel if the banks are not resistant. As soon as a slight deviation from a uniform axial flow appears, it causes more flow towards one bank than the other. Additional flow is attracted towards one bank, leading to a shoaling along the other bank, introducing the curvature of flow and resulting in a meander pattern. Although Joglekar objects to the excess energy theory, his idea too has been subjected to objections arising from cases which do not fit in with the excess sediment load idea, such as the incised meanders that appear on a glacier surface.

(e) **Instability theory:** Stability analysis is a well-known and useful means for treating plan-forms in alluvial streams analytically. The analyses are based on the condition that a straight channel with a mobile bed is only slightly deformed by a double harmonic disturbance, so that flow relations obtaining for a steady uniform flow can be used with minor modifications. A linearized formulation of the flow is employed, essentially, in such analyses. Using a suitable sediment transport law, the resulting equations are solved to obtain expressions for the variation of the bed profile with time. The stability analysis is invariably carried out using the equations of motion and the continuity equations for water and sediment. Depending on whether the analysis is one-dimensional, two-dimensional or three-dimensional, one, two or three equations of motion have been used. All these models assume steady, uniform flow and a rectangular channel cross-section. The two-dimensional models usually assume additionally a constant velocity over the vertical and a linear distribution of shear stress and pressure over the vertical.

2.6-2.3 Sediment transport in meandering rivers

The main sources of sediment in natural rivers are erosion by overland flow, river-channel erosion, bank cutting and supply from small erosion channels formed in unconsolidated soil. The term *alluvial* is usually applied to rivers in which the moving sediment and the sediment in the underlying bed is of the same character. However, even the rivers which flow in alluvial plains, the sediment transportation is not a simple process. The bed configuration of the river depends on the strength of the flow and the strength of the flow depends on the hydraulic resistance and the hydraulic resistance is a complicated function of the bed configuration. Therefore the sediment transport process is a very intricate problem of mutual interaction. Moreover, the sand wave formation depends on hydrodynamic stability, the changes in bed formation may have a nearly discontinuous character at a certain stage (shift from lower to upper flow regime). As the sand wave formation depends on hydrodynamic stability, the cross-sectional form of the river depends on the unequal distribution of the hydrodynamic forces which induced by curvature of the river bend. In meandering rivers the cross-sectional forms of the most parts of the river are asymmetric and the most common bed-feature is dune-covered bed. The meandering river reach consists of the series of pools and bars. Consequently, the transport process is different from that of sediment transport in straight rivers. As discussed extensively elsewhere, the shoaling of the flow over the bar forces near-bed flow (secondary flow) and, consequently, bed load transport across the top of the bar (Dietrich

et al. 1989). In the pool it is well known that the near-bed flow (the transverse direction flow) is strongly inward. From the field observations of (Dietrich et al., 1979; Dietrich and Smith, 1984; Dietrich, 1987), at the edge of the bar top, the coarse sediment travels against this inward component of the secondary circulation by rolling, avalanching obliquely down from the crests of migrating dunes on the side or face of the point bar, and by being transported by trough-wise currents of obliquely oriented dunes. The finer sediment crosses the coarse sediment as it is carried inward from the deeper water and up onto the downstream end of the bar by the inward direction secondary circulation. This is very important and well observed sorting process in the channel bends. Sorting occurs because grain weight, which opposes the transverse direction near-bed flow. Thus the net sediment transport in the meandering rivers results in a dynamic balance of longitudinal direction sediment transport and transverse direction sediment transport including above mentioned sorting effect controlling the equilibrium bed topography.

".....what can be checked, what can be simulated, and at what price."

3. DEVELOPMENT OF A BED TOPOGRAPHY MODEL IN A MEANDERING RIVER

3.1 Introduction

A mathematical model for two-dimensional morphological computations in alluvial river bends is developed. In this model, a curvilinear co-ordinate system is used to define a grid of computational points along the river, while two equations of motion, for the main flow direction and the transverse direction, are used, but extended so as to account for the vertical flow profile in the transverse direction (ie. secondary flow). Sediment transport is then calculated in these two directions. The model is primarily intended for research purposes. There were two main reasons for building such a simulation model. The first reason was to study the morphological changes occurring in alluvial river bends, while the second was to generate a set of simulated river morphologies sufficient to provide a basis for the study of river plan-form movements. It is very well known that studies of alluvial river bank erosion and its associated river plan-form movement are essential to the understanding of the development of a bed topography. However there are many aspects to be considered in the study of alluvial river bank erosion and plan-form movement (see also Chapter 5), if only because no two rivers are identical and it is nearly impossible to derive overall descriptions of river behaviour in a sufficiently generalised form. In the following chapters, the river width stability problem and the closely related problem of river plan-form movement will be studied. Although the results of many flume experiments and observed field data are introduced, the hypothetical examples of river behaviour are still necessary. Hence, this chapter serves as a study of river morphology in alluvial river bends and as means of producing working examples of river behaviour.

Although the present model follows the same main principles as were used by Kalkwijk and De Vriend (1980) and Olesen (1987), as just outlined in Chapter 2, the present study introduces some further developments. In particular, the system to construct the grid mapping for the computational domain is different and the manner in which the bed shear stress in the transverse direction is used is also somewhat novel. Moreover, in the following chapter the alluvial roughness is predicted in terms of the dimensions of dunes, and representative roughness coefficients distributed over the entire computational domain are introduced (see further Chapter 4). The model is then extended to provide a series of bank erosion models which simulate the river plan-form movement. Consequently, a method to regenerate the grid over time is required and one approach to this is proposed in Chapter 5.

3.2 Description of the model

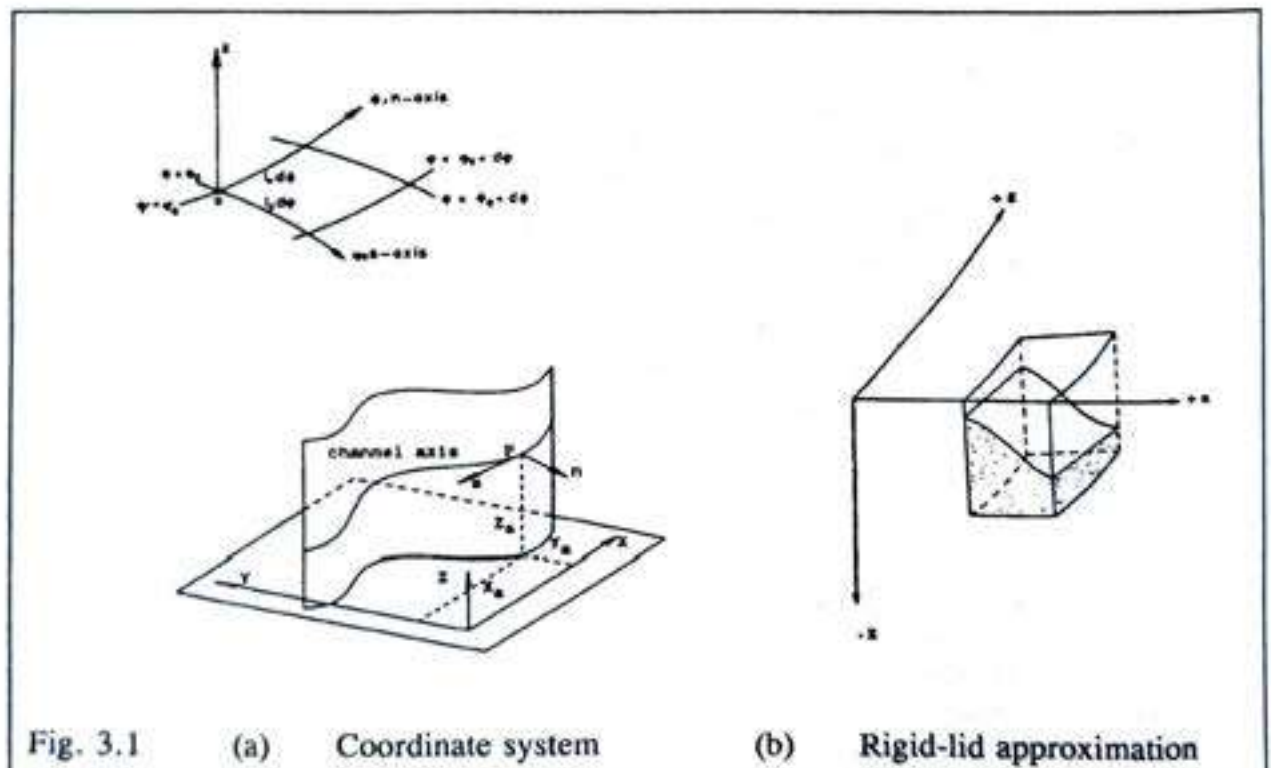
The bed topography model consists of two parts. These provide the depth-averaged flow simulation and the bed topography simulation.

3.2-1 Co-ordinate system

Since the alignment of the river sections that are considered here are usually themselves sinuous, or curvilinear, it is realistic and convenient to use a curvilinear co-ordinate system which follows at least to some degree the alignment of the river. The differential equations describing the conservation of mass and momentum must then be formulated using a co-ordinate system (ψ, ϑ, z) , where ψ and ϑ are orthogonal curvilinear coordinates in the horizontal plane and where the z -axis is vertical and positive in the upward direction.

The distance, taken along the co-ordinate curves $\psi = \text{constant}$ and $\vartheta = \text{constant}$, is indicated by s and n , respectively, in which the s -axis coincides with the channel axis and, the n -axis is horizontal and perpendicular to the s -axis see Fig. (3.4). The co-ordinate system is shown in fig. 3.1. The length of the infinitesimal arcs ds and dn can be written as follow (Pipes, 1958, p.395):

$$\begin{aligned} ds &= l_s d\psi, & \text{with } l_s &= l_s(\psi, \vartheta); \\ dn &= l_n d\vartheta, & \text{with } l_n &= l_n(\psi, \vartheta). \end{aligned} \tag{3.1}$$



The corresponding spatial derivatives of any function $f(\psi, \sigma, z)$ are then:

$$\partial f / \partial s = 1/l_s \cdot \partial f / \partial \psi \quad ; \quad \partial f / \partial n = 1/l_n \cdot \partial f / \partial \sigma \quad ; \quad \partial f / \partial z = \partial f / \partial z \quad (3.2)$$

The local curvature of the s-line is taken as positive when the positive n-lines diverge, and inversely.

$$\frac{1}{R_s} = \frac{1}{(l_s \cdot l_n)} \cdot \frac{\partial l_s}{\partial \phi} \quad (3.3)$$

$$\frac{1}{R_n} = \frac{1}{(l_s \cdot l_n)} \cdot \frac{\partial l_n}{\partial \psi} \quad (3.4)$$

in which R_s = radius of curvature of ψ -axis
 R_n = radius of curvature of σ -axis

This type of co-ordinate system can describe the three dimensional flow pattern very well. However, according to Olesen (1987), it can be considerably simplified if only rivers of constant width are considered. In this case any local n-axis can be taken as a straight line. As a consequence of this simplification, a number of small inertia and friction terms vanish in the mathematical model. It does not qualitatively or quantitatively influence the result of the depth-integrated flow model: detailed derivations are given in Olesen, (1987). Kalkwijk *et al.*, (1980) gave a three-dimensional mathematical description of the flow in a curvilinear co-ordinate system in which both horizontal co-ordinate axes are curved, but they avoided the comprehensive description of the friction terms. In this case little or no advantage is gained from using the curvilinear n-axis for this particular type of problem and, on the contrary the computational time will usually be longer. Hence the n-axis is taken as a straight line in the present investigation, i.e. $R_n \rightarrow \infty$ in Eqn. (3.4). The river then presents the aspect of a sequence of circular arcs each of which has a constant radius but in which the radius can change from the one segment to the next. Since the circumference of a circle is orthogonal to its radius, the coincidence of radial lines guarantees the local continuity in the first derivative of the corresponding adjacent arcs (see Figs. 4 and 5 later).

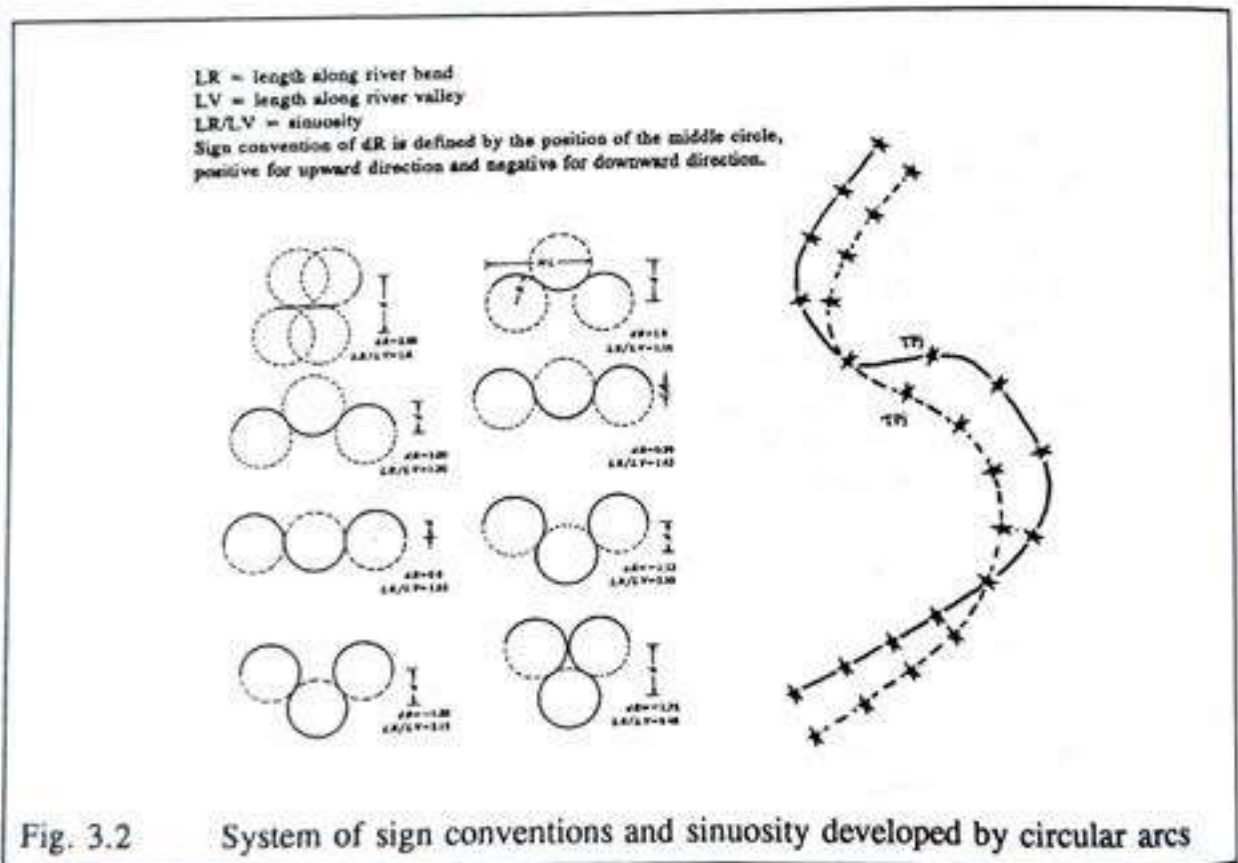
3.2-2 Grid mapping

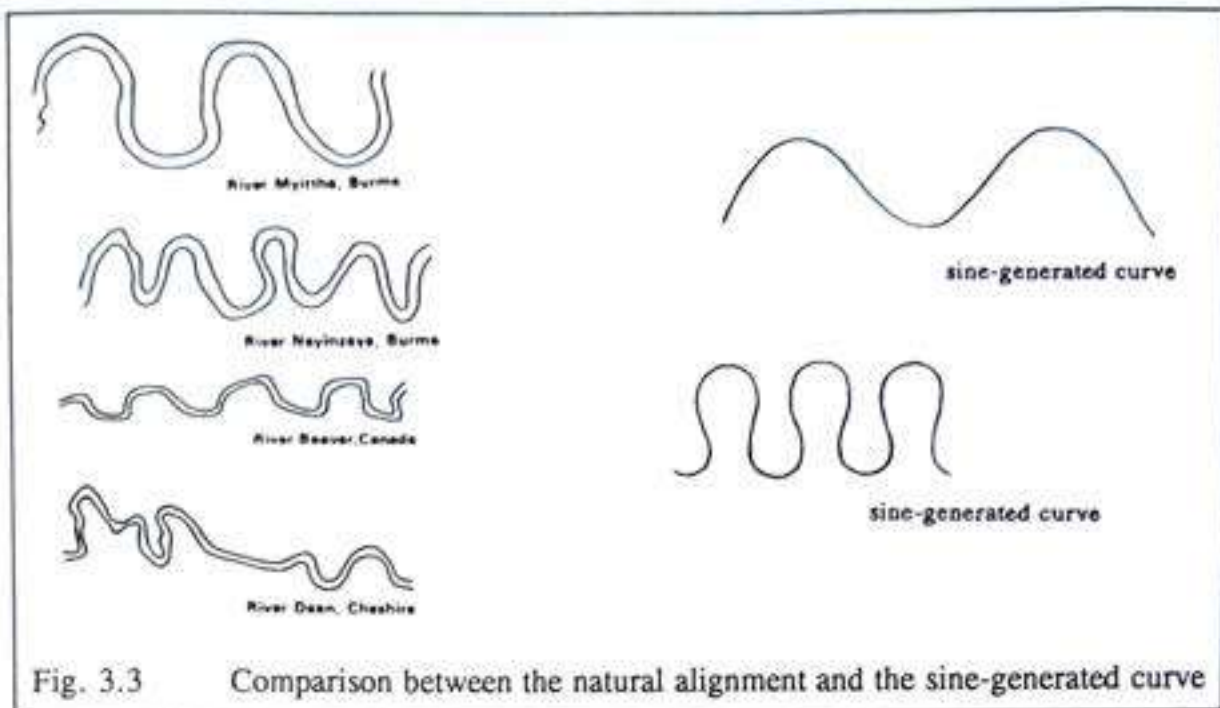
The first step in the grid mapping is the selection of a shape of the path along which rivers flow (or a plan-form of meandering rivers) and its mathematical (geometrical) expression. Between any two points on the valley floor, a variety of paths are possible, including a straight path. Historically, the plan-forms of meandering rivers have been represented by four different types of curves, as listed below. A path of greatest probability formulation of the problem of river meanders was derived by Langbein and Leopold (1966). This is based on the original theory of a class of random-walk problems developed by Von Schelling (1951, 1964). According to Langbein and Leopold (1966), the best way to represent the meandering pattern is to have a minimum variance of the reciprocal of the

radius of curvature along the mean down-stream direction (ie. mean square of deviations in direction from the mean down-stream direction). In mathematical expression, this means that $\Sigma (\Delta\theta^2/\Delta s) = a$ minimum, in which Δs is a unit distance along the path and $\Delta\theta$ is the angle by which direction is changed in distance Δs and also is the reciprocal of the radius of curvature of the path in that unit distance Δs . From this point of view, the following four kinds of curves can be ranked in order of ascending minimum variances as follows:

1. sine-generated curve
2. circular curve
3. sine curve
4. parabolic curve

It can be seen that the sine-generated curve is the first in rank and the circular curve is second. On the other hand, the fitness of the alignment produced by sine-generated curve is poor for the non-regular meander paths, especially in the case of successive bends in nature, where the amplitude and the wave length of each bend is different. This nature cannot be successfully represented by a sine-generated curve. Therefore, if we take the other aspects into account (such as flexibility, the mathematical formulation, exactness of the natural alignment) the entire river reach can best be represented by a series of circular segments with different radii of curvature. The illustrations are shown in Figs. 3.2 to 3.5.





The location of the turning points (TP) are marked with heavy stars in the figure and between two adjacent turning points an adequate number of computational points are placed in order to obtain the desired solution. The advantages of this type of representation are three fold; firstly, it provides a curve flexible enough to trace a river plan-form that is adequately close to the natural river plan-form (as can be seen in the comparison between Fig. 1.2 and Fig. 1.3); secondly, its mathematical formulation is both simple and sufficiently accurate; thirdly, the river alignment can be started from an arbitrary origin in the (s, n, z) co-ordinate system. Moreover, using the arcs of circles as the basic building blocks and by locating the centre of circular curves of radii R_i at various distances d_i , a channel meander having sinuosity ratios varying from 1.0 to 5.5 can be easily generated. In the physical sense, a sinuosity ratio of 1 implies a straight river, while a value of 5.5 appears to be the limiting value when consecutive bends cut into one another. In nature, meander cutoffs occur before the value of sinuosity of 5.5 is reached. This approach can also be used to describe a complicated plan-form like that of the skew bends shown in Figs. 3.2 and 3.5. Therefore this method is versatile enough to describe practically all meander plan-forms. The procedure for this type of mapping has only one fundamental rule, which is that a common tangent between two consecutive segments has to be used. The example of such a grid mapping is shown in Fig. 3.4. The equation of the curve (s -line) is expressed in term of the direction angle α_i between an arbitrary horizontal line and arc/chord of the segment (see Eqn. 3.5 & Fig. 3.5). The relevant derivations are presented in Appendix A.

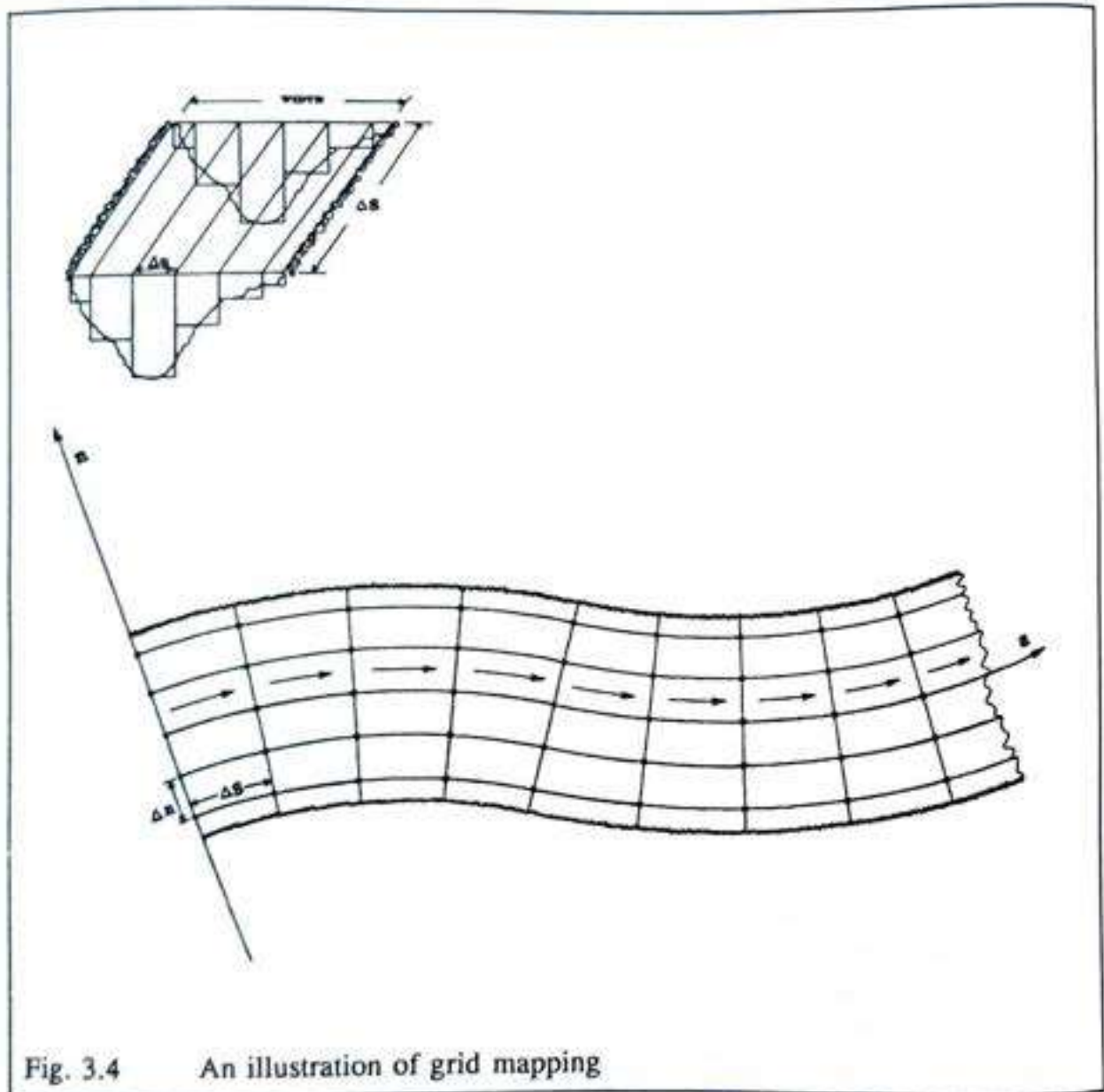
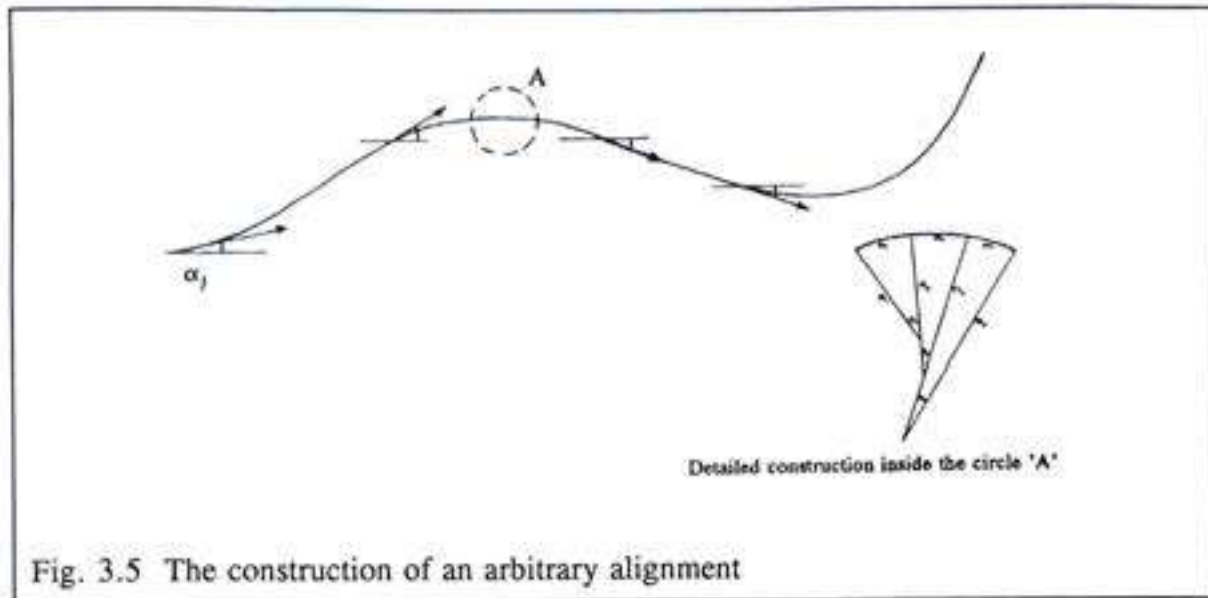


Fig. 3.4 An illustration of grid mapping

$$\alpha_j = \frac{(\pi - |\theta_j|)}{2} - \sum_{j=1}^j \theta_j \quad (3.5)$$

$$\theta_j = \frac{\Delta s_j}{R_j} \quad (3.6)$$

θ_j = an angle subtend at the centre of each segment or of each distance step Δs_j .



3.3 Flow computation

The flow pattern in river bends is known to be fairly complex and three-dimensional. In the river bend the magnitude and direction of the bed shear stress and the friction between the water particles (strictly speaking, the particles of the fluid mixture) become very important. For each particle in a vertical, the dynamic equilibrium ($F = m a$) has to be observed both in the radial and the tangential directions. Since all the particles are influenced by the radial water-level slope, but the centripetal acceleration (U^2/R) is larger at the water surface than near the bed, because of the logarithmic distribution of U in a tangential direction over the vertical, these forces will never be in equilibrium. Due to the shear stresses between the respective fluid particles, however equilibrium is established. Since these shear stresses can only be caused by asymmetric velocity distributions, the fluid particles near the water surface will move in the direction of the outer bend, whilst those near the bed will move toward the inner bend. To maintain continuity, a vertical velocity component is present near the river banks. Thus the flow pattern is three dimensional as shown in Fig. 3.6.

The computation of this three dimensional flow comprises a computational procedure for steady flow in curved channels with two main components. These are the procedures based on the integration of the depth-averaged main flow equations including the convective influence of the secondary flow, and the procedures based on the integration of the complete three-dimensional flow equations. The predictions of the second group yields better result than the first group in critical cases; however for the many rivers that are shallow and have bends of moderate curvature, the first method is more computationally efficient. Therefore, in this study, the first procedure is used for rivers of which:

- the depth is small compared with the width;
- the width is small compared with the radius of curvature;

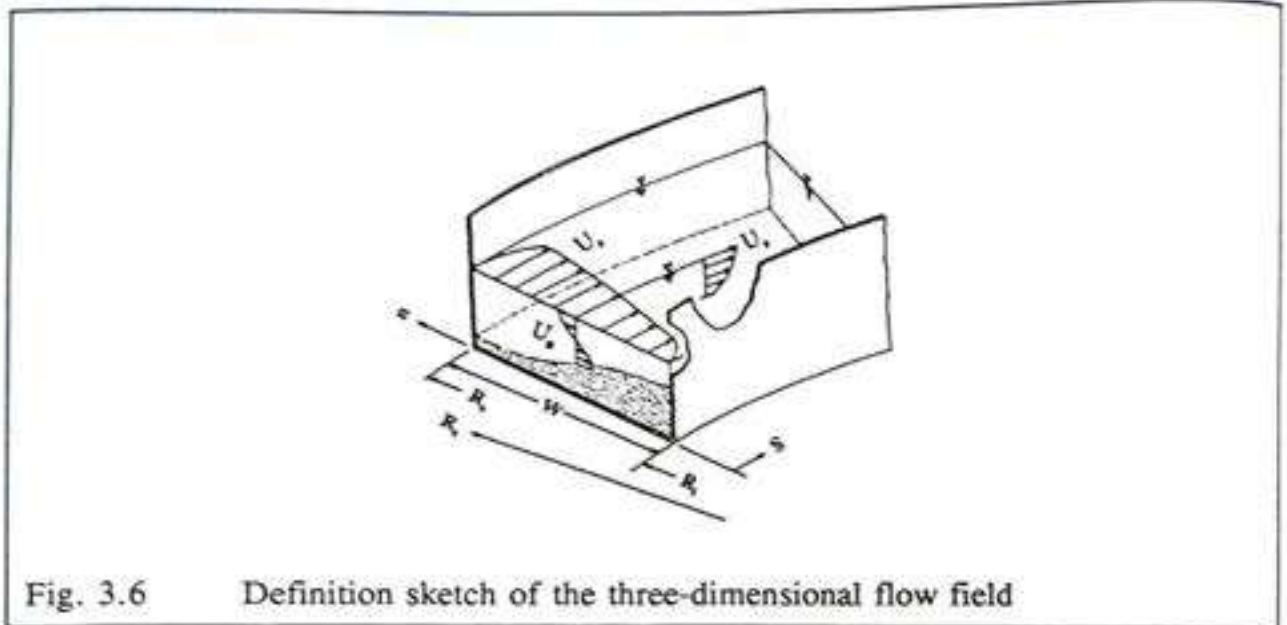


Fig. 3.6 Definition sketch of the three-dimensional flow field

- the horizontal length scale of the bottom variation is of the order of magnitude of the width;
- the flow is mainly friction controlled, although inertial forces can also be significant;
- the longitudinal component of the velocity dominates the other velocity components;
- the Froude number is small.

3.3-1 Governing differential equations of the flow model

Without yet relating the horizontal coordinates to the channel geometry, the equation of continuity for steady incompressible flow reads

$$\frac{1}{(l_s \cdot l_n)} \frac{\partial(U_s \cdot l_n)}{\partial \psi} + \frac{1}{(l_s \cdot l_n)} \frac{\partial(U_n \cdot l_s)}{\partial \phi} + \frac{\partial U_z}{\partial z} = 0 \quad (3.7)$$

using Eqns. (3.2), (3.3) and (3.4), Eqn. (3.7) can be written as

$$\frac{\partial U_s}{\partial s} + \frac{U_s}{R_n} + \frac{\partial U_n}{\partial n} + \frac{U_n}{R_s} + \frac{\partial U_z}{\partial z} = 0 \quad (3.8)$$

The momentum equations can be written as

$$\frac{\partial U_s^2}{\partial s} + \frac{\partial U_n U_s}{\partial n} + \frac{\partial U_z U_s}{\partial z} + 2 \frac{U_n U_s}{R_s} + \frac{U_s^2 - U_n^2}{R_n} + \frac{1}{\rho} \frac{\partial P}{\partial s} + F_s = 0 \quad (3.9)$$

$$\frac{\partial U_s U_n}{\partial s} + \frac{\partial U_n^2}{\partial n} + \frac{\partial U_z U_n}{\partial z} + 2 \frac{U_s U_n}{R_n} + \frac{U_n^2 - U_s^2}{R_s} + \frac{1}{\rho} \frac{\partial P}{\partial n} + F_n = 0 \quad (3.10)$$

$$\frac{\partial U_s U_z}{\partial s} + \frac{\partial U_n U_z}{\partial n} + \frac{\partial U_z^2}{\partial z} + \frac{1}{\rho} \frac{\partial P}{\partial z} + F_z = -g \quad (3.11)$$

in which

P = pressure

ρ = mass density of the fluid

g = acceleration due to gravity

U_s, U_n, U_z = velocity components in s -, n - and z - directions respectively

F_s, F_n, F_z = friction terms in s -, n - and z - directions respectively

Here we neglect wall effects and assume a scalar eddy viscosity coefficient together with the assumption that $O \left[\frac{h}{R} \right]^2$ can be omitted in natural rivers on the basis that the depth-to-radius ratio (h/R) is small. 'Radius' means here the radius of curvature of the river. In this case, the friction terms F_s and F_n can be approximated by

$$F_s = \frac{1}{\rho} \frac{\partial \tau_{sz}}{\partial z} \quad (3.12)$$

$$F_n = \frac{1}{\rho} \frac{\partial \tau_{nz}}{\partial z} \quad (3.13)$$

where τ_{sz} and τ_{nz} are shear stresses in the s - z plane and n - z plane respectively, which hereafter will be called τ_s and τ_n . Actually, the above-mentioned approximations consist of a shallow water approximation in which all lateral exchange of momentum due to friction in the fluid can be neglected.

The friction terms can be expressed in terms of velocities in their respective directions by introducing the Reynold's stress concept and the Prandtl mixing length hypothesis. Therefore the following equations can be written.

$$\frac{\tau_s}{\rho} = A \frac{\partial U_s}{\partial z} \quad (3.14)$$

$$\frac{\tau_n}{\rho} = A \frac{\partial U_n}{\partial z} \quad (3.15)$$

$$A = L^2 \frac{\partial \sqrt{U_s^2 + U_n^2 + U_z^2}}{\partial z} \approx L^2 \frac{\partial U_s}{\partial z} \quad (3.16)$$

in which A is the turbulent coefficient of viscosity or the eddy-viscosity coefficient and L is the mixing length, which is a function of z . When the viscosity of water is concerned, the applied formulation implies two assumptions: the first is that the laminar sub-layer is much smaller than fully developed boundary layer, which is considered as the prevailing condition, while the other is that the eddy viscosity is assumed isotropic.

The solution of the mathematical model is facilitated by introducing the rigid lid approximation for the water-surface boundary condition. The rigid lid approximation means that the water surface is considered as a rigid, impermeable and shear-stress-free plate with only normal stresses (pressures). This also means that *an average water surface elevation* (i.e. the elevation of the rigid lid) is used instead of the local water surface elevation. The error introduced by this approximation is justified in the case when the Froude number and the depth-to-radius ratio (h/R) are small. Further, Rozovskii (1957) simplified the equation of motion in the z -direction to

$$g + \frac{1}{\rho} \frac{\partial P}{\partial z} = 0 \quad (3.17)$$

which provides a hydrostatic pressure. An error will appear close to the side walls which will be of the order of magnitude (h/R). In the central regions of the flow, the error is much smaller. The pressure at any local point in the vertical can be written by integration of this equation, assuming $z = 0$ at the channel bed and applying the rigid lid approximation. Thus,

$$P = P_r + \rho g (h-z) \quad (3.18)$$

where P_r is the pressure at the rigid lid and $(h-z)$ is the position of any local point measured from the rigid lid.

Finally Eqns. (3.9) and (3.10) can be written in terms of the simplified Eqns. (3.10) through (3.18) as follow:

$$\frac{\partial U_s^2}{\partial s} + \frac{\partial U_n U_s}{\partial n} + \frac{\partial U_z U_s}{\partial z} + 2 \frac{U_n U_s}{R_s} + \frac{U_s^2 - U_n^2}{R_n} + \frac{1}{\rho} \frac{\partial P}{\partial s} = \frac{\partial}{\partial z} \left(A \frac{\partial U_s}{\partial z} \right) \quad (3.19)$$

$$\frac{\partial U_s U_n}{\partial s} + \frac{\partial U_n^2}{\partial n} + \frac{\partial U_z U_n}{\partial z} + 2 \frac{U_s U_n}{R_n} + \frac{U_n^2 - U_s^2}{R_s} + \frac{1}{\rho} \frac{\partial P}{\partial n} = \frac{\partial}{\partial z} \left(A \frac{\partial U_n}{\partial z} \right) \quad (3.20)$$

The flow computation follows the governing equations presented in this section.

3.3-2 The vertical distribution of the flow

The vertical distribution of the flow velocities can be obtained by the technique of asymptotic expansion. In brief, the zero-order approximation of the longitudinal-flow velocity is obtained from Eqn. (3.19) assuming that U_n and U_z are equal to zero and $\partial U_s / \partial s = 0$. Then the transverse velocity is computed from Eqn. (3.20) with the zero-order longitudinal velocity inserted and terms of the order of magnitude $(h/R)^2$ are neglected. These terms are $U_n \partial U_n / \partial n$ and $U_z \partial U_n / \partial z$. The vertical flow velocity is obtained directly from Eqn. (3.8).

After this a first order approximation of the longitudinal flow velocity can be obtained by introducing the (first-order) secondary flow velocities into Eqn. (3.19). This was done by De Vriend (1981a) and De Vriend & Struiksma (1983). They showed that the form of the first-order solution only differs a little from the zero-order solution. In order to solve the flow model, a choice of the mixing length is important, as the mixing length is used in defining the eddy viscosity coefficient, as in Eqn. (3.16). Three different mixing length models are applied here, viz:

$$L = \kappa z \sqrt{1-z} h \quad (3.21)$$

$$L = \kappa z^{1-1/m} \sqrt{1-z} h \quad (3.22)$$

$$L = 2 \kappa (1 - \sqrt{1-z}) \sqrt{1-z} h \quad (3.23)$$

where κ is the Von Kàrmàn constant, and m is a factor depending on the bed roughness. In rectilinear, uniform flow, the mixing length given by Eqn. (3.21) results in the well known logarithmic velocity profiles, Eqn. (3.22) results in a power profile and Eqn. (3.23) in the Von Kàrmàn velocity profile (cf. Jansen, 1979). The logarithmic velocity profile and the

power profile are the two most frequently used velocity profiles for river flows. Verifications of the mixing length models are mostly based on uniform shear flow: it is known that the models predict nearly the same velocity distribution (cf. Olesen, 1987). Consequently, no significant distinction can be made between these. However, it is physically reasonable to assume that the mixing length close to the bottom grows linear with the distance to the bottom (Olesen, 1987). This implies that the most realistic shear stress and flow distribution can be derived from Eqns. (3.21) and (3.23). Thus, for the sake of balancing reasonableness and simplicity, Eqns. (3.21), (3.23) and a power profile, i.e. Eqn. (3.22), are used respectively in the following sections.

3.3-3 The longitudinal flow velocity

The longitudinal flow velocity is the major component of the three-dimensional flow velocity field. Its behaviour is described by the longitudinal momentum equation, Eqn. (3.9), which later becomes Eqn. (3.19). The right hand side of the Eqn. (3.19) is the eddy viscosity term. The zero-order version of Eqn. (3.9) reads as follows:

$$\frac{\partial}{\partial \tilde{z}} \left[\left(\frac{L}{h} \right)^2 \left(\frac{\partial \mathcal{L}u_s}{\partial \tilde{z}} \right) \right]^2 = - \frac{g}{C^2} \quad (3.24)$$

where \tilde{z} is the dimensionless depth and $\mathcal{L}u_s$ is the 'shape function' of the longitudinal flow velocity, or mathematically $\mathcal{L}u_s = U_s/U_{s,avg}$, where $U_{s,avg}$ is the depth-averaged longitudinal flow velocity, and C is the Chézy roughness coefficient. The boundary conditions for this differential equation are vanishing shear stress at the water surface and no slip at the border plane between the laminar sub-layer and the turbulent boundary layer (ie. at \tilde{z}_0), where $\tilde{z}_0 = e^{(-1-xC/4\beta)}$, $\tilde{z}_0 = 0$ and $\tilde{z}_0 = e^{(-1.14-xC/4\beta)}$ for Eqns. (3.21), (3.22) and (3.23) in that order. Then the shape of the longitudinal flow velocity reads:

$$\mathcal{L}u_s = \int_{\tilde{z}_0}^{\tilde{z}} \left[\int_1^{\tilde{z}} -\frac{\sqrt{g}}{C} \partial \tilde{z} \right] \frac{h}{L} \partial \tilde{z} \quad (3.25)$$

The velocity profiles can be obtained by inserting the models for the mixing length, Eqns. (3.21), (3.22) and (3.23), giving in the same order, and after integration,

$$\mathcal{L}u_s = \alpha \ln \frac{\tilde{z}}{\tilde{z}_0} = 1 + \alpha (1 + \ln \tilde{z}) \quad (3.26)$$

$$\mathcal{L}u_s = \alpha m \tilde{z}^{1/m} \quad (3.27)$$

$$\mathcal{L}u_z = \alpha \left[\sqrt{1-z} - \sqrt{1-z_0} + \ln \frac{1-\sqrt{1-z}}{1-\sqrt{1-z_0}} \right] \quad (3.28)$$

in which $\alpha [= \sqrt{g} / (\kappa C)]$ is a dimensionless roughness coefficient. In Eqn. (3.26), m is a coefficient already introduced in 3.2-2, the depth-averaged value of which can be derived by integrating Eqn. (3.26). Therefore

$$\alpha = \frac{m+1}{m} \quad (3.29)$$

According to its definition, the depth-averaged value of $\mathcal{L}u_z$ is equal to unity. This equation is given by Jansen (1979). There are different definitions of m , such as those given by Zimmermann & Kennedy (1978) and Nunner (1956). These differences come from the different definitions of the mixing length. Nevertheless, these different values of m allow one and the same definition of $\mathcal{L}u_z$.

The zero-order viscosity coefficient for the logarithmic model, the power model and Von Kàrmàn models can be obtained by substituting the pairs of Eqns. (3.21)(3.25), (3.22)(3.26) and (3.23)(3.27) into Eqn(3.16). The eddy viscosity distributions are as follow:

$$A = \kappa^2 \alpha z (1-z) h \bar{u} \quad (3.30)$$

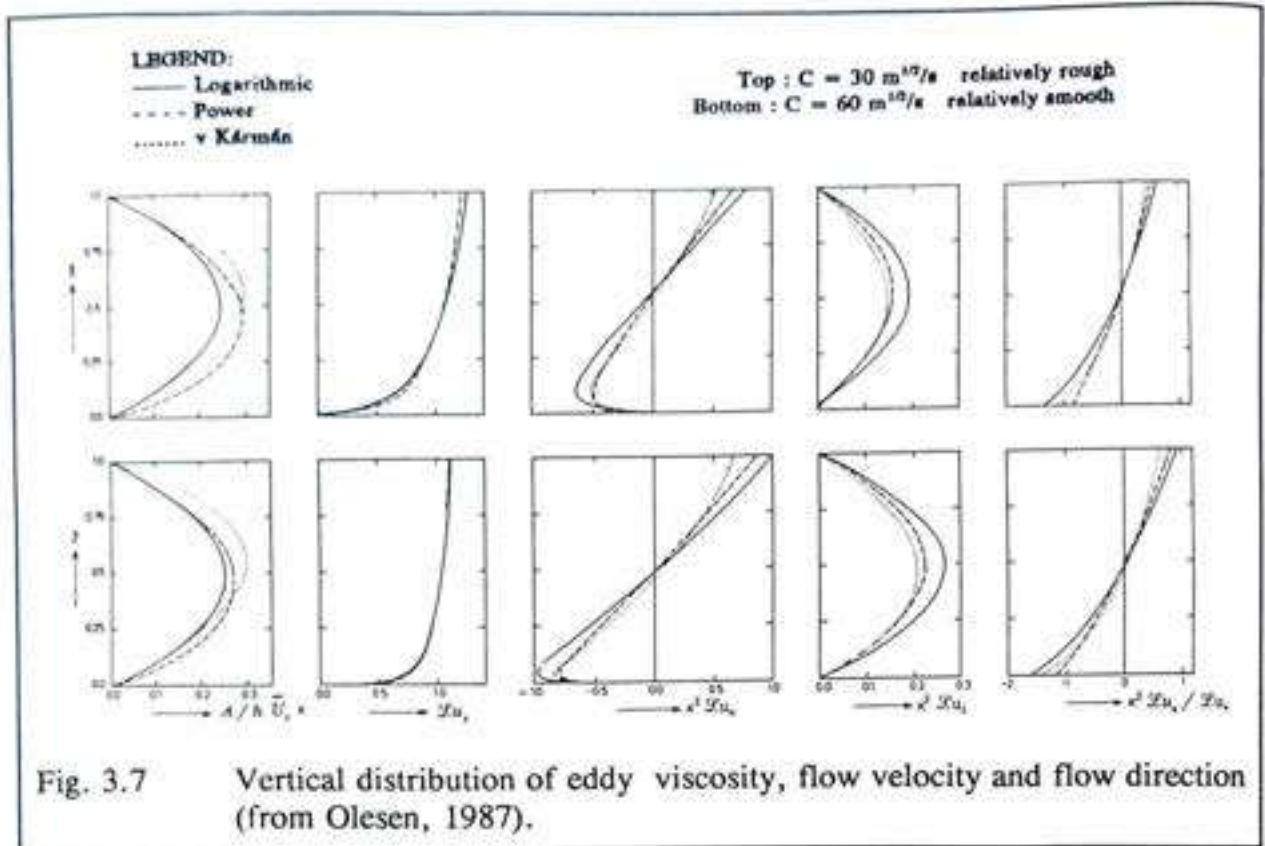
$$A = \kappa^2 \alpha z^{1-\frac{1}{m}} (1-z) h \bar{u} \quad (3.31)$$

$$A = 2 \kappa^2 \alpha (1-\sqrt{1-z}) (1-z) h \bar{u} \quad (3.32)$$

The profiles are shown in Fig. (3.7).

3.3-4 The transverse flow velocity

The transverse flow velocity is an important feature of the alluvial river bend flow, which is an essential component in the formation of a flow pattern, being three-dimensional in the river bends. Moreover, this three-dimensional flow pattern varies from section to section depending on the location of the cross-section along the reach. If and when the bend is continuous and long enough, the fully-developed bend flow is established after some distance from the entrance of the bend. A fully-developed bend flow is a flow in which the mean flow characteristics do not change from section to section along the main flow direction. It means the derivatives of the flow parameters along the main flow direction are equal to zero. Before this (fully-developed bed topography) region, the developing bend flow occurs. If the bend ends after a certain length, the transitional flow which will adjust to the bed topography of the following reach occurs just before and just after the exit of the bend.



Therefore when we consider flows in the river bends, there are two types of bed topography, namely fully-developed bed topography and the developing bed topography. In terms of mathematical expression, the fully-developed bed topography can be expressed by zero-order solution and the latter can be expressed by the first-order solution.

Around the entrance of the bend the transverse water surface slope will grow rapidly from zero until its final value in the bend. Therefore, along the convex bank the longitudinal water surface slope will increase rapidly and cause an acceleration of the flow there. Along the concave bank the slope decreases and the flow decelerates. In turn this ensures a gradual growth of the streamline curvature around the entrance. The secondary flow will also grow gradually and it will establish a transverse bed slope (see section 3.3). The main flow will adapt to the changing bed topography and to the influence of secondary flow convection. Consequently the main flow velocity will increase along the concave bank. Moreover, main flow will also adapt the new friction condition according to the new flow field. On the other hand due to the inertia of the main flow the adaptation of increasing main flow velocity along the concave bank will take place gradually. In other words changing of the flow distribution will lag the changing of the bed topography. Therefore the magnitude and process of adaptation are discussed as following. The transverse flow velocity is expressed by Eqn. (3.10), the transverse flow momentum equation. The total strength of the transverse velocity in river bends is the combination of transverse flow velocity due to flow curvature (secondary flow) and transverse flow velocity due to the redistribution of the longitudinal flow. Hence, mathematically,

$$U_n = \bar{U}_n \mathcal{L}u_l + i_s \mathcal{L}u_n \quad (3.33)$$

in which

U_n = transverse velocity

$\mathcal{L}u_l$ = shape of the longitudinal flow velocity

$\mathcal{L}u_n$ = shape of the secondary flow velocity

i_s = the secondary flow intensity which is given as follows:

$$i_s = \bar{u} \frac{h}{R} \quad (3.34)$$

(cf. De Vriend, 1981a)

We recall Eqn. (2.1) from section 2.4-1.1, which gives the strength of the secondary flow, S_{yz} , as derived by Shükry, 1950, and we now compare this with the more comprehensive Eqn.(3.34). The relationship can be written as follows:

$$S_{yz}^{1/2} = \frac{\bar{U}_n}{i_s} \frac{h}{R} \quad (3.35)$$

The strength of the secondary flow in Eqn.(2.1) is, in turn, the square of the tangent of the angle $\alpha_{s,avg}$ in which $\alpha_{s,avg}$ is the angle of the mean flow velocity deviation from the xz-plane. On the other hand, this is the depth-averaged value of the skew angle, which can be taken as the deviation angle between the local point velocity and the depth-averaged velocity, as illustrated in Fig. (3.8).

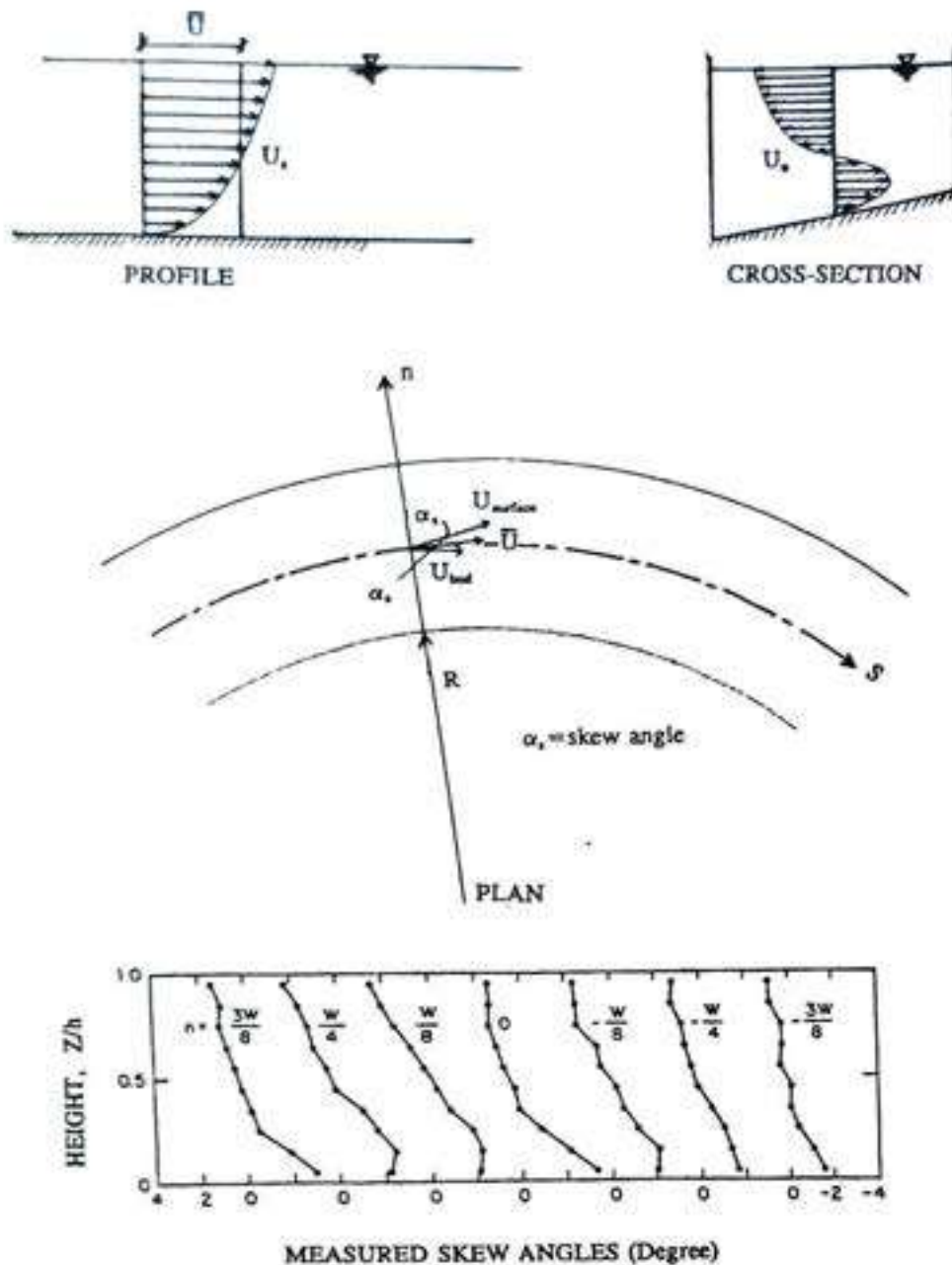


Fig.3.8 Illustration of skew angle as the strength of the secondary flow

Thus over the whole \mathcal{L}_{u_n} , the shape of the secondary flow velocity is the theoretical representation of the measured skew angles in Fig. 3.8 and i_s is the secondary flow intensity which we utilized in the computation. The complete secondary flow that is associated with the transverse velocity is schematised in Fig.3.9.

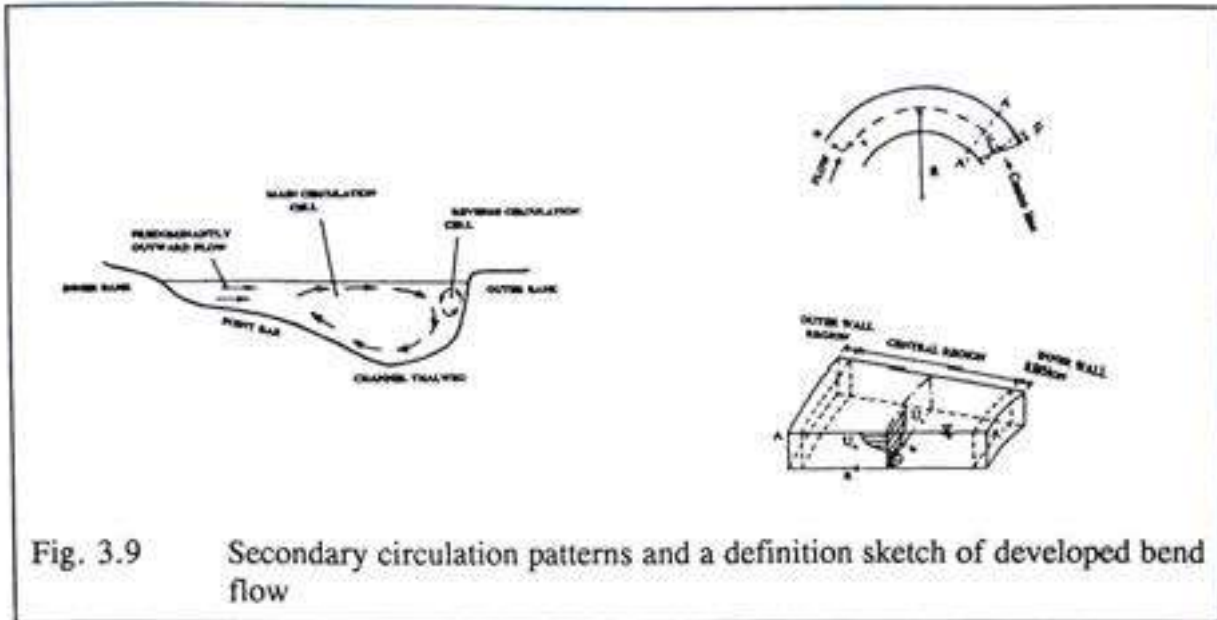


Fig. 3.9 Secondary circulation patterns and a definition sketch of developed bend flow

The inertia of the secondary flow has been investigated analytically (using a similarity hypothesis) by among others Rozovskii (1957) and Noh & Townsend (1979). Numerical investigations of this have been carried out by De Vriend (1981a), Booij & Kalkwijk (1982) and Kalkwijk & Booij (1986). A widely applied procedure to determine the magnitude of the secondary flow is to solve the momentum equation in the n -direction, disregarding all lateral friction terms and all inertia terms except the centrifugal one. Introducing the eddy viscosity concept for the vertical friction terms, this equation reads the same as eqn.(3.37).

When the secondary flow is considered in the numerical models, it is not sufficient when only the strength of it is taken into account but it is also necessary to take account of the way it adapts to the main flow. In regions of changing curvature, the secondary flow will adapt gradually. The function describing the adaptation of the secondary flow can be considered in its simplest form: a straight river, at $s = 0$, entering a long bend with constant curvature. The following approximations can be used to characterise the properties of an 'adaptation length'.

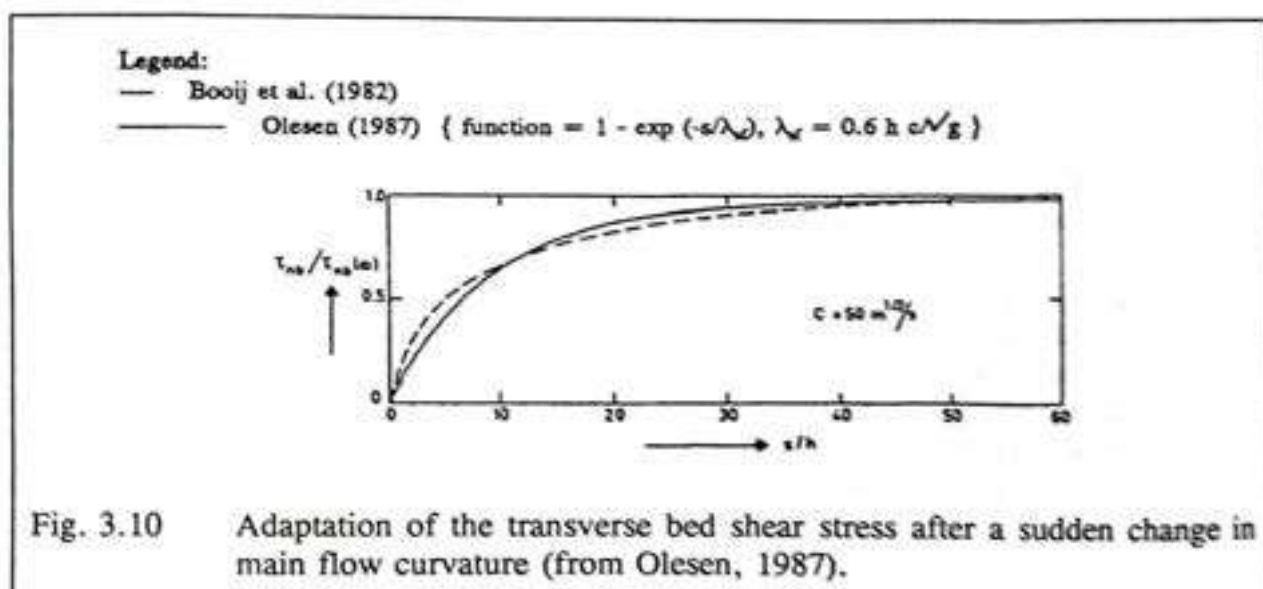
$$U_{n,s} = i_s \mathcal{L}u_n g(s) \quad (g(0) = 0, g(\infty) = 1) \quad (3.36)$$

$$\frac{\partial P}{\partial n} = \frac{\partial P_1}{\partial n} + g(s) \frac{\partial P_2}{\partial n} \quad (3.37)$$

In Eqn. (3.36), $U_{n,s}$ = transverse velocity component due to secondary flow, i_s and $\mathcal{L}u_n$ are as mentioned before and $g(s)$ is a function describing the adaptation of the secondary flow. In Eqn. (3.37) the transverse water surface slope is split up into a part (P_1) balancing the centrifugal force and a part (P_2) generated by the bed shear stress. Conceptually, $g(s)$ provides a function form but not a definite quantity. Consequently the appropriateness of a similarity hypothesis is investigated and it is concluded by Olesen, 1987 that "...an analytical approach based on similarity is not likely to provide an accurate description of the gradual

adaptation of the secondary flow". Therefore the way of numerical investigations initiated of De Vriend (1982), Booij *et al.* (1983) and Kalkwijk *et al.* (1986) seems to be the best approach.

According to the numerical results, the process of adaptation cannot be characterised by one length scale only. The process involves at least two length scales; namely the adaptation length of the secondary flow and the length scale associated with the bed shear stress due to the secondary flow. However, the latter type of characteristic length scale is obtained from the numerical computations of De Vriend (1982), Booij *et al.* (1983), and Kalkwijk and Booij (1986). Later, Olesen (1987) proposed a purely exponential adaptation with a length scale of $\lambda_{sr} = 0.6 h C / \sqrt{g}$, as a means of representing the influence of the bed shear stress. The functional form reads $\{1 - \exp(-s/\lambda_{sr})\}$, in which λ_{sr} is the adaptation length of the secondary flow. The results of Booij *et al.* (1983) and Kalkwijk and Booij (1986) are quite similar. Therefore the result of Booij *et al.* and Olesen (1987) are depicted in Fig. 3.9 as two different adaptation lengths of the transverse bed shear stress after a sudden change in the main flow curvature. The applicability of the purely exponential function proposed by Olesen (1987) gives sufficiently accurate results compared with Booij *et al.* (1983) and therefore an adaptation length of "0.6 hC/√g" is use in the mathematical model.



Since the shape of the secondary flow velocity is a function, $\mathcal{L}u_x$, of the transverse flow velocity itself (i.e. eqn.(3.33)), it is necessary to solve the depth-averaged value of U_x from the truncated (first-order) version of the transverse momentum equation by integrating over the depth. The truncated momentum equation is

$$\frac{1}{\rho} \frac{\partial P}{\partial n} - \frac{U_s^2}{R} = \frac{\partial}{\partial z} \left[A \frac{\partial U_n}{\partial z} \right] \quad (3.38)$$

and the appropriate dimensionless form is as follows:

$$\frac{\partial}{\partial \tilde{z}} \left[\frac{A}{hU\kappa^2\alpha} \frac{\partial \mathcal{L}u_n}{\partial \tilde{z}} \right] + \frac{1}{\kappa^2} \mathcal{L}u_n^2 = c \quad (3.39)$$

in which \tilde{z} is still the dimensionless depth and c is a constant (independent of \tilde{z}) which is proportional to the transverse water surface slope. The different solutions of the eqn. (3.39) can be obtained by integrating it using different shape functions of the longitudinal velocity profile, $\mathcal{L}u_n$, and the different eddy viscosity models (i.e. definition of A). Olesen, 1987 used the boundary conditions of vanishing velocity and shear stress at $\tilde{z} = \tilde{z}_0$ and $\tilde{z} = 1$ respectively, in which $\tilde{z} = \tilde{z}_0$ is used instead of $\tilde{z} = 0$, thus automatically disregarding the 'tail' of the logarithm. This makes an analytical solution of the logarithmic and the Von Kàrmàn model laborious, but the numerical approach becomes much easier and safer when $\mathcal{L}u_n \rightarrow \infty$ and $\partial \mathcal{L}u_n / \partial \tilde{z} \rightarrow \infty$ at the bottom. For the determination of the right hand side (i.e. the transverse water surface slope), the auxiliary condition,

$$\int_0^1 \mathcal{L}u_n \, d\tilde{z} = 0 \quad , \quad (3.40)$$

is used. It implies that there is no net flow in the transverse direction.

Let us take an example, one of the possible solutions of eqn. (3.39) can be as follows in case of the power model. The dimensionless vertical shear stress variation can be obtained by integrating through eqn. (3.39), combined with eqn. (3.27) and $\tau'_s = 0$ at $\tilde{z} = 1$, viz:

$$\tau'_s = \frac{A}{h U_s \kappa^2 \alpha} \frac{\partial \mathcal{L}u_n}{\partial \tilde{z}} = \frac{(m+1)^2}{m(m+2)} \left[1 - \tilde{z}^{\frac{2}{(m+1)}} + c(\tilde{z}-1) \right] \quad (3.41)$$

in which c is an integration constant which still has to be determined (Olesen, 1987). κ and α are already mentioned in 3.3-3. From eqns. (3.40) and (3.31), the horizontal secondary flow component can be obtained by an integration, in which it has been already assumed that \tilde{z} is small. Then the equation reads as follows:

$$\mathcal{L}u_n = \frac{1}{\kappa^2} \frac{m(m+1)}{m+2} \int_0^{\tilde{z}} \left[\frac{\tilde{z}^{\frac{1}{(m-1)}} - \tilde{z}^{\frac{3}{m}}}{1-\tilde{z}} - c\tilde{z}^{\frac{1}{(m-1)}} \right] d\tilde{z} \quad (3.42)$$

Thus eqn. (3.42) is the solution of eqn. (3.39) when main flow distribution is represented by the power model.

If the logarithmic tail is not omitted, the analytical solution of Eqn. (3.39) reads (cf. Rozovskii, 1957 and De Vriend, 1981a):

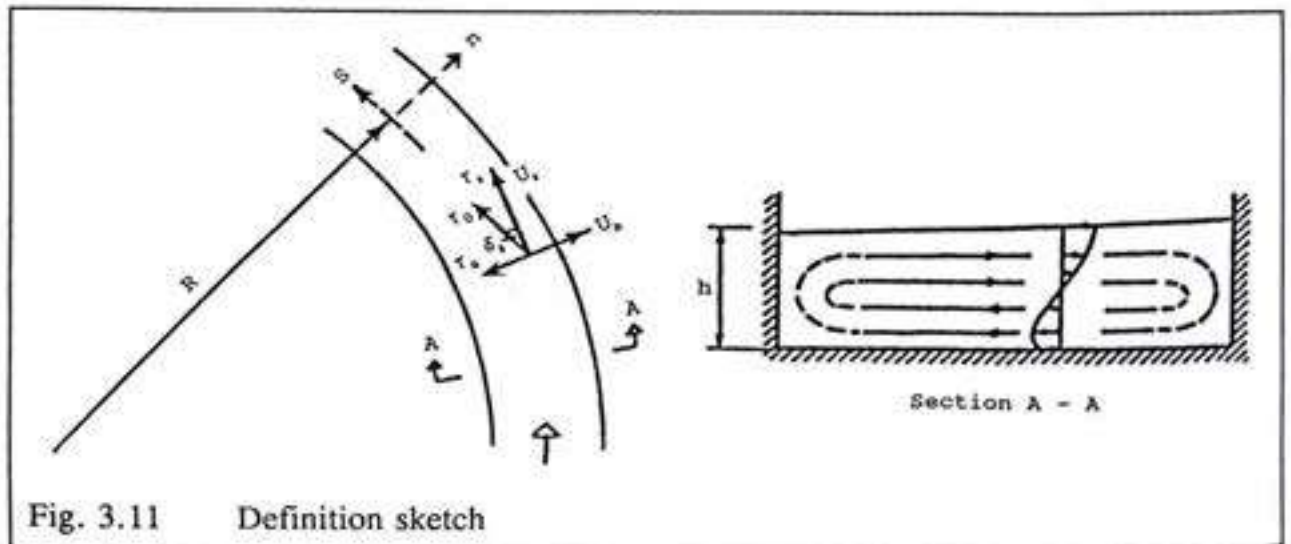
$$\mathcal{L}u_n = \frac{1}{\kappa^2} [2F_1(\xi) + \alpha F_2(\xi) - 2(1-\alpha)\mathcal{L}u_s] \quad (3.43)$$

in which

$$F_p = \int_0^\xi \frac{\ln P_\xi}{1-\xi} d\xi \quad (p = 1,2) \quad (3.44)$$

As mentioned earlier, transverse velocity profile function, $\mathcal{L}u_n$ or the solution of the eqn. (3.39) can be as many as possible combinations of main flow velocity profile function, $\mathcal{L}u_s$, models and A, eddy viscosity models. However there are no significant differences between the flow profiles of the different mixing-length models. In Fig. (3.7) the shapes of the secondary flow are also depicted. Finally, by eqn.(3.33) through eqn.(3.44), the total strength of the transverse velocity in river bends, which is the combination of transverse flow velocity due to flow curvature (secondary flow) and transverse flow velocity due to redistribution of the longitudinal flow, is obtained. The consequences of the formation of this transverse velocity as bed shear stresses and their directions are discussed in the following section.

3.3-5 Bed shear stresses and directions



As the result of the helical motion in bends, the bed shear stress forms an angle with the mean flow direction; see Fig. (3.11). The model for the bed shear stress direction in a

curved flow plays a vital role in the bed topography model for river bends. The bed shear stresses in the s and n directions, still called τ_s and τ_n respectively, and their magnitudes can be estimated by Eqns. (3.14), (3.15) and (3.16) together with mixing-length model results. The direction angle is known as δ_s given by $\{\tan(\delta_s) = \tau_n / \tau_s\}$. According to Engelund, (1974),

$$\tan \delta_s = \frac{\dot{U}_n + \ddot{U}_n}{U_s} \quad (3.45)$$

in which

\dot{U}_n = velocity component along the bed (transverse direction)

\ddot{U}_n = velocity component along the bed (secondary flow)

U_s = longitudinal flow velocity

and

$$\dot{U}_n = -7 \frac{h}{R_s} \dot{U}_s f_o \quad (3.46)$$

in which

h = water depth

R_s = s-line curvature

\dot{U}_s = mean flow velocity in the longitudinal direction

f_o = a function to take account of the influence of the side walls, which can be calculated from the experimental results. The logarithmic model of Rozovskii (1957) yields a bed shear stress direction in river bends as follows:

$$\tan \delta_s = -\beta \frac{h}{R_s} \quad (3.47)$$

in which $\beta = \beta(c)$ is a coefficient which weighs the influence of the spiral motion, depending on the eddy viscosity model applied. In the case of a logarithmic vertical velocity profile:

$$\beta = \frac{2}{\kappa^2} (1-\alpha) \quad (3.48)$$

The power model of van Bendegom (1947) yields

$$\beta = \frac{2}{\kappa^2} \frac{m^2}{(m+2)(m+3)} \quad (3.49)$$

in which m is a coefficient. As a consequence, the direction of the bed shear stress in case of a continuously-varying curvature can be calculated by

$$\lambda_{sf} \frac{\partial \tan \delta_s}{\partial s} + \tan \delta_s = -\beta \frac{h}{R_s} \quad (3.50)$$

in which δ_s is the angle between the stream-line and the bed shear stress principal direction, s is the distance along the stream-line and λ_{sf} is an adaptation length for the secondary flow intensity see section (3.3-4); where β , R_s and h have the same definitions as given earlier. The quantity β of Rozovskii may vary between 10 to 12. However Engelund obtained a value of 7 for this coefficient in eqn. (3.46). Engelund applied a parabolic distribution of main flow velocity and a finite slip velocity near the bed whilst Rozovskii assumed a logarithmic distribution of the main flow velocity. Engelund's distribution appears to be more accurate for the greater part of the flow but is less accurate close to the bed. In 1981, Knudsen, calculated this coefficient using Deigaard's (1980) eddy viscosity distribution (ie. the velocity distribution in the main flow direction consisting of a logarithmic distribution in the lower 20% of the depth and a parabolic distribution in the remaining part). This combined velocity distribution describes the condition better than a purely logarithmic velocity distribution or a purely parabolic distribution. The resulting β value is approximately constant, varying between 10 to 11.

Moreover the quantity β is a function of the Chézy coefficient, as given by the four different models, as shown in Fig. (3.11), and is to be used in the model for the direction of the bed shear stress. Olesen, (1987; see Fig. 3.11) also pointed out that the differences concerning bed shear stress direction between the models are surprisingly large in view of the close similarity of the vertical distribution of eddy viscosity and transverse as well as longitudinal flow velocities. Consequently, the bed shear stress direction is extremely sensitive to the mixing length model applied.

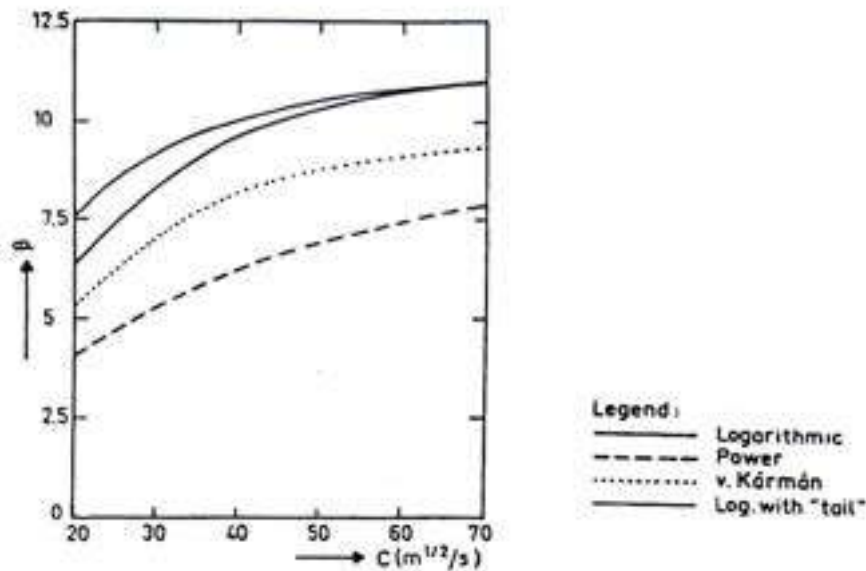


Fig. 3.12 The coefficient β in the model for the direction of the bed shear stress in a curved flow (from Olesen, 1987)

3.3-6 The vertical flow velocity

The present model is established as a two-dimensional depth-integrated model. Therefore the nature of the vertical flow velocity is only briefly outlined here. The vertical secondary flow velocity component is written as follows:

$$U_z = - \int_{\xi}^z \left(\frac{\partial i_s}{\partial n} + \frac{i_s}{R_s} \right) \mathcal{L}u_n dz \quad (3.51)$$

The 'shape' of the vertical velocity, $\mathcal{L}u_z$, is given by

$$\mathcal{L}u_z = \int_{\xi}^z \mathcal{L}u_n dz \quad (3.52)$$

which can be seen in Fig. 3.6. The notations are as mentioned earlier and from now on we shall simply write z again in place of ξ .

3.3-7 The stream-line curvature

The stream line curvature is introduced in order to improve the computation for developing flow regions. If the flow is not fully developed (i.e. fully developed means that all derivatives in s-direction other than $\partial P/\partial s$ equal to zero), the stream lines will either diverge or converge, so developing flow cannot be described using a natural curvilinear coordinate system without curvature of the normal axis. This type of flow occurs at entrances and exits of bends and at other places where larger longitudinal gradients in the transverse depth-averaged velocity arise. If the streamline curvature is approximated by the local curvature of the channel instead of being calculated from the flow field, it implies that the divergence or convergence of the streamline curvature is neglected and this causes an error in the transverse water surface configuration and the prediction of the secondary flow based on the main flow field. Therefore the path of the stream line is calculated and is introduced using an iterative method.

The exact mathematical expression for the streamline curvature is (De Vriend, 1978)

$$\frac{1}{R_n} = \frac{-1}{(\bar{U}_s^2 - \bar{U}_n^2)^{3/2}} \left[\bar{U}_s \left(\bar{U}_s \frac{\partial \bar{U}_n}{\partial s} + \bar{U}_n \frac{\partial \bar{U}_s}{\partial n} - \frac{\bar{U}_s^2}{R_s} \right) - \bar{U}_n \left(\bar{U}_s \frac{\partial \bar{U}_s}{\partial s} + \bar{U}_n \frac{\partial \bar{U}_n}{\partial n} + \frac{\bar{U}_s \bar{U}_n}{R_s} \right) \right] \quad (3.53)$$

in which R_n is the radius of curvature of the streamline and the rest are as mentioned earlier. However, regarding the derivation of the longitudinal and transverse direction momentum equations, it does not make sense to apply such an extensive expression (Olesen, 1982). Applying the same rule for the truncation of the above expression as for the equations of momentum, a simplified expression for the streamline curvature reads

$$\frac{1}{R_n} = \frac{1}{R_s} - \frac{1}{\bar{U}_s} \frac{\partial \bar{U}_n}{\partial s} \quad (3.54)$$

3.4 The depth-averaged flow model

For small Froude numbers the water surface can be considered as if it were a rigid frictionless plate at $z = 0$. At the fixed boundaries the usual conditions of impermeability and no-slip apply (Kalkwijk, et al., 1980). For the shallow flow which occurs in large-scale variations of the bed level with gently sloping banks, the water depth decreases gradually to zero at the banks. Therefore the shear stress in the vertical planes will be negligible as compared with the shear stress (friction) in the horizontal planes. The pressure can be assumed to be hydrostatic. Integrating Eqns. (3.8) through (3.10) from the bottom at $z = -h(s,n)$ to the surface at $z = 0$ yields

$$\frac{\partial h \bar{U}_s}{\partial s} + \frac{h \bar{U}_s}{R_n} + \frac{\partial h \bar{U}_n}{\partial n} + \frac{h \bar{U}_n}{R_s} = 0 \quad (3.55)$$

$$\frac{\partial h \bar{U}_s^2}{\partial s} + \frac{\partial h \bar{U}_s \bar{U}_n}{\partial n} + 2 \frac{h \bar{U}_s \bar{U}_n}{R_s} + \frac{h (\bar{U}_s^2 - \bar{U}_n^2)}{R_n} + \frac{h}{\rho} \frac{\partial P}{\partial n} + \frac{\tau_s}{\rho} = 0 \quad (3.56)$$

$$\frac{\partial h \bar{U}_s \bar{U}_n}{\partial s} + \frac{\partial h \bar{U}_n^2}{\partial n} + 2 \frac{h \bar{U}_s \bar{U}_n}{R_n} + \frac{h (\bar{U}_n^2 - \bar{U}_s^2)}{R_s} + \frac{h}{\rho} \frac{\partial P}{\partial n} + \frac{\tau_n}{\rho} = 0 \quad (3.57)$$

in which over-bars denote depth-averaging ; τ_s and τ_n are s- and n- direction components of the bed shear stress and $P = \text{total pressure}, = p + \rho g z$.

In the region of developing flow, the transverse velocity averaged over the depth may differ from zero. The transverse flow velocity expressed by eqn. (3.33) is solved together with eqns. (3.56) and (3.57). For the sake of simplicity, the stream-lines are assumed to follow the co-ordinate system in the mathematical model (i.e. $U_{n,avg} / U_{s,avg}$ is assumed small, which almost always applies in alluvial channels) and later it is introduced gradually, numerically. In addition, the water-depth to radius-of-curvature ratio is assumed small. These assumptions lead to the conclusion that the quadratic terms of the transverse flow velocity can be neglected (i.e. $U_{n,avg}^2$, i_s^2 and $U_{n,avg} \cdot i_s$ are very small) and the secondary flow components in the longitudinal direction can be omitted. Thus eqns. (3.56) and (3.57) can be elaborated into (see also Kalkwijk et al. 1980) :

$$\begin{aligned} \frac{1}{\rho} \frac{\partial P}{\partial s} + k_{uv} \left[\bar{U}_s \frac{\partial \bar{U}_s}{\partial s} + \bar{U}_n \frac{\partial \bar{U}_n}{\partial n} + \frac{\bar{U}_n \bar{U}_s}{R} \right] \\ + \frac{\tau_s}{h} + \frac{k_{vn}}{h} \left[\frac{\partial}{\partial n} (\bar{U}_s i_s h) + 2 \frac{\bar{U}_s i_s h}{R} \right] = 0 \end{aligned} \quad (3.58)$$

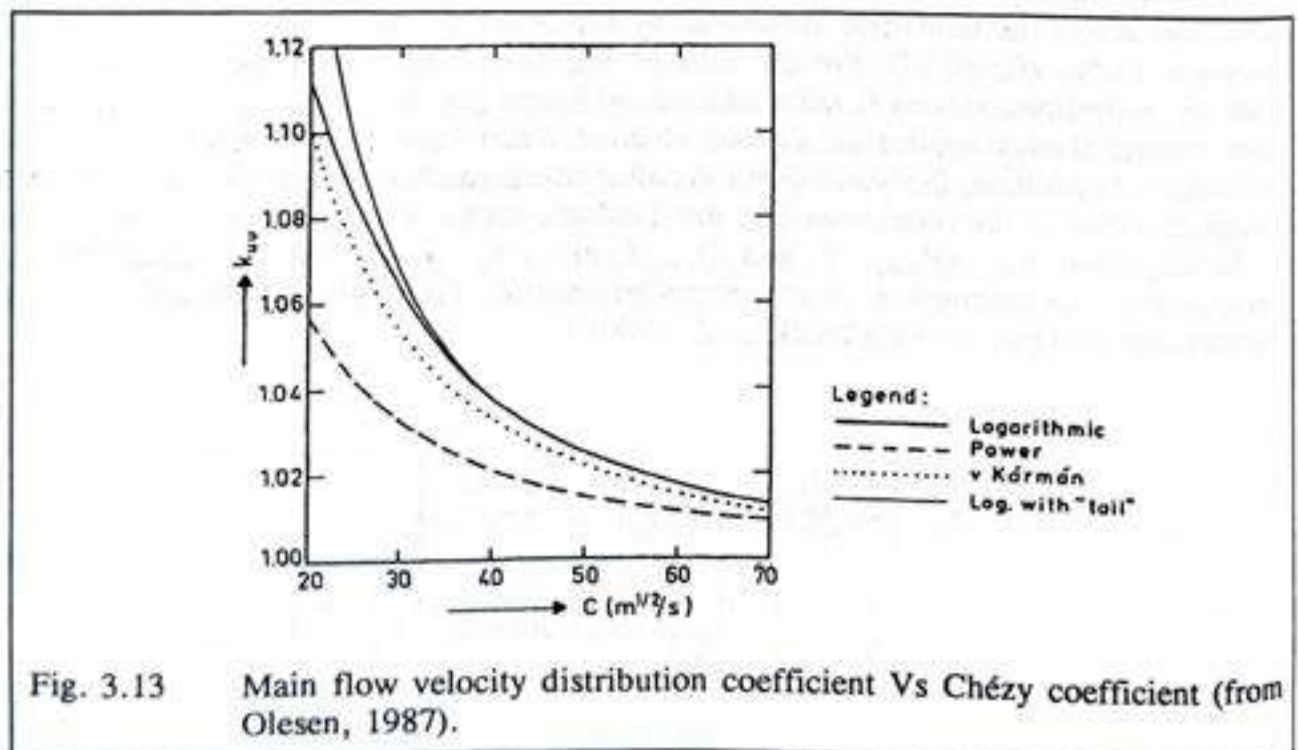
$$\frac{1}{\rho} \frac{\partial P}{\partial n} + k_{uv} \left[\bar{U}_s \frac{\partial \bar{U}_n}{\partial s} - \frac{\bar{U}_s^2}{R} \right] + \frac{k_{sn}}{h} \frac{\partial \bar{U}_s}{\partial s} i_s h + \frac{\tau_n}{h} = 0 \quad (3.59)$$

in which

$$k_{uv} = \int_{z_b}^1 (\mathcal{L}u_s)^2 dz \quad (3.60)$$

$$k_{sn} = \int_{z_b}^1 \mathcal{L}u_s \mathcal{L}u_n dz \quad (3.61)$$

In eqn. (3.59), the second order terms have been neglected and in eqn. (3.33) the vertical velocity component has been eliminated by partial integration and application of the continuity equation (3.8) in order to facilitate the depth integration.



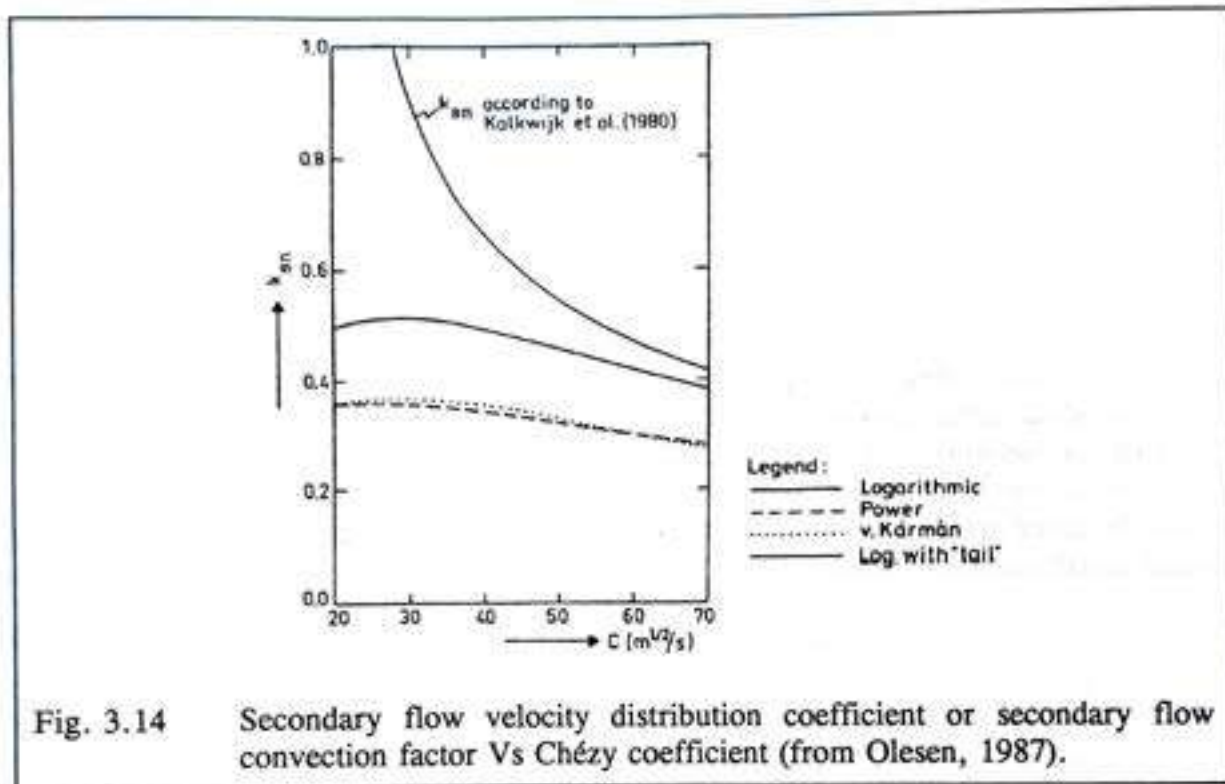


Fig. 3.14 Secondary flow velocity distribution coefficient or secondary flow convection factor Vs Chézy coefficient (from Olesen, 1987).

k_{uu} and k_{nn} are velocity distribution coefficients. They have been obtained with the numerical model for the three different mixing length models (as shown in Figs. 3.12 and 3.13, from Olesen, 1987) and in case of the power model also analytically. In case of the logarithmic model with the logarithmic tail included, the variation of k_{nn} has been obtained from Kalkwijk et al. (1980) and that of k_{uu} by direct integration of eqn. (3.26), viz:

$$k_{uu} = 1 + \alpha^2 \quad (3.62)$$

According to Olesen (1987), setting $k_{uu} = 1$ will be sufficiently accurate in most cases. The velocity distribution coefficient k_{nn} , which is related to the convection of momentum by the secondary flow, is very sensitive to the logarithmic tail in the case of a rough bed. The k_{nn} values vary considerably with the mixing-length model applied. The secondary flow convection term in the depth-integrated transverse momentum equation is very small compared to the dominant inertia term (U_*^2/R), and as a consequence this may be disregarded.

The depth-averaged equations for bed shear stress in the s- and n- directions are as follows:-

$$\tau_s = (\rho g U_s \sqrt{U_s^2 + U_n^2}) / C^2 \quad (3.63)$$

$$\tau_n = (\rho g U_n \sqrt{U_s^2 + U_n^2}) / C^2 \quad (3.64)$$

in which C is the Chézy coefficient. According to the eqns. (3.63) and (3.64), the direction of the bed shear stress coincides with the direction of the depth-averaged velocity, which is only true for non-curved flow. However, it is assumed that, for curved flow, the influence of this deviation on the main flow is negligible even though it is accepted that the influence of this deviation on the sediment motion is not negligible. Thereafter, the bed shear stress (s- and n- components) and the direction can be approximated by

$$\tau_s = (\rho g \bar{U}_s \sqrt{\bar{U}_s^2 + \bar{U}_n^2}) / C^2 \quad (3.65)$$

$$\tau_n = \rho \frac{g}{C^2} \bar{U}_s (\bar{U}_n + \bar{U}_s \tan \delta) \quad (3.66)$$

$$\tan \delta = \frac{\bar{U}_n}{\bar{U}_s} + \tan \delta_s \quad (3.67)$$

in which $\tan \delta_s$ must be obtained from eqn.(3.50).

3.5 The integration procedure of the flow model

This efficient integration procedure is in principle based on the method suggested by Kalkwijk & de Vriend (1980). In their model, however, the streamline curvature is approximated by the local curvature of the coordinate lines, resulting in a model with a purely hyperbolic mathematical character. This permits a straight-forward marching integration procedure with an implicit finite difference scheme, but Kalkwijk & de Vriend suggested an iterative procedure with an explicit scheme, which appears to be far more economical. The basic principle in this solution procedure is that terms containing the transverse main velocity are supposed to be known. With a first guess for the transverse flow velocity (e.g. $U_{n,avg} = 0$), the longitudinal flow velocity can be obtained from eqns. (3.9) and (3.10) with a constant discharge as boundary condition. Next, the continuity eqn. (3.8) can be applied to obtain an improved estimate for the transverse flow velocity, after which $U_{s,avg}$ can be recomputed with this U_n value and as many iterations can be made as accuracy

requires. In this step, the continuity equation can be applied after each ray is or after sweeping through the whole field. A ray is defined as a strip across the river cross-section which has the unit width Δs . This integration procedure appears to be unconditionally stable.

Later Olesen (1982 b) extended this model with an improved approximation for the streamline curvature, whereby eqn. (3.54) and is introduced gradually, by iterations, as follows:-

$$\left(\frac{1}{R_{st}}\right)^p = \Omega \left[\frac{1}{R_s} - \frac{1}{U_s} \frac{\partial \bar{U}_s}{\partial s} \right]^{p-1} + (1-\Omega) \left(\frac{1}{R_{st}}\right)^{p-1} \quad (3.68)$$

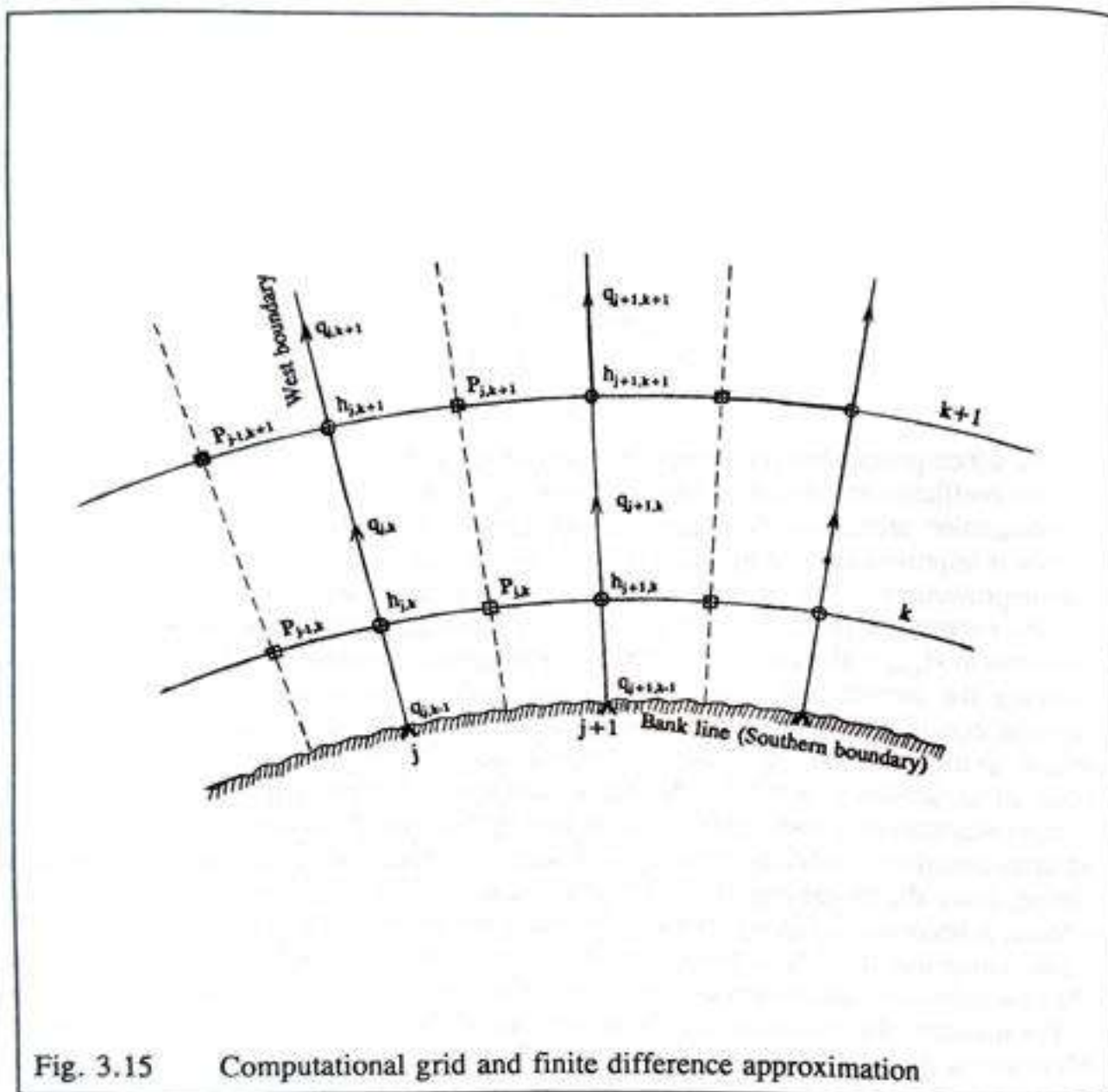
In which p represents the number of iterations and Ω is a relaxation coefficient. The relaxation coefficient is defined as that necessary to maintain stability and is explained below. In the integration procedure, the same basic principle is applied, but now also the streamline curvature is improved in each iteration step. In fact the procedure is very attractive not only for the improvement of the estimate of $U_{n,avg}$ in each iteration step, but also for updating the streamline curvature eqn. (3.68). An obvious first guess for the streamline curvature, which corresponds to $U_{n,avg} = 0$, is the curvature of the longitudinal coordinate line, (i.e. R_s). After introducing the stream line curvature, the characteristic direction of the set of partial differential equations has acquired a mixed hyperbolic- elliptic character. The change of character, as a consequence of the introduction of the streamline curvature, implies that the solution in an arbitrary point of the considered area changes from dependence on the upstream conditions only into dependence on both upstream and downstream conditions, such as an extra boundary condition at the outflow section, which can be a prescribed streamline curvature. Since the mixed hyperbolic-elliptic character does not allow a forward marching procedure, it becomes necessary to sweep through the whole field in each iteration step. In this case, numerical stability is assured by using an underrelaxation, viz only a certain part of the new calculated streamline curvature is taken into account in the following iteration step. For instance, the streamline curvature applied in iteration number p is given by eqn. (3.68) in which Ω is a relaxation coefficient. A relaxation coefficient which ensures stability is observed as

$$\Omega \leq 8 \left(\frac{\Delta\theta_s}{W/R_c} \right)^2 \quad (3.69)$$

Experience with the present model has shown that the most efficient value is given approximately by

$$\max \Omega = \left[4 \left(\frac{\Delta\theta_s}{W/R_c} \right)^2 ; 8 \left(\frac{\Delta\theta_s}{W/R_c} \right)^2 \right] \quad (3.70)$$

while for simplicity, the range of value $\{ 1/6 \leq \Omega \leq 2/9 \}$ is experienced to be a safe one. In this equation, (3.70) $\Delta\theta_s$ is the angle subtend to the arc length of the segment, Δs .



A staggered computational grid is applied as shown in Fig. (3.15). This grid allows a discretization of the equations, with central differences and relatively short space steps, which is not generating oscillations. Eqns. (3.9) and (3.10) are transformed in such a way that flux instead of velocities are reformulated. That is, ($p = U_x \cdot h$) and ($q = U_y \cdot h$) are used instead of U_x and U_y . Moreover the function ($f = p^2/h$) is used in the integration, which has the advantage that non-linear terms like $(U_x)^2$ and $(U_y)^2$ become linear in integration. Therefore, the final version of the momentum equations before the discretization is the following:

$$\begin{aligned} \frac{1}{h} \frac{\partial f}{\partial s} + \frac{1}{h} \frac{f}{R_n} + \frac{1}{\rho} \frac{\partial P_r}{\partial s} + f \frac{1}{h^2} \left[\frac{g}{C^2} \sqrt{1+q^2/p^2} + K_m \frac{\partial}{\partial n} \left(\frac{i_s h^2}{p} \right) \right] \\ = - \frac{1}{h} \frac{\partial}{\partial n} \left(\frac{pq}{h} \right) - \frac{2pq}{h^2 R_n} + \frac{q^2}{h^2 R_n} \end{aligned} \quad (3.71)$$

$$\begin{aligned} \frac{1}{h} \frac{\partial}{\partial n} \left(\frac{q^2}{h} \right) - \frac{1}{h} \frac{f}{R_n} + \frac{1}{\rho} \frac{\partial P_r}{\partial n} + \frac{g}{C^2 h^3} q^2 \sqrt{1+q^2/p^2} \\ = - \frac{1}{h} \frac{\partial}{\partial s} \left(\frac{pq}{h} \right) - \frac{2pq}{h^2 R_n} - \frac{q^2}{h^2 R_n} \end{aligned} \quad (3.72)$$

Referring to Fig. (3.15), it is seen that equation (3.71) is discretized into (k) and (k+1) points and eqn. (3.72) is discretized into (j-1) and (j) points. The four discretized equations centred at k, k+1, j-1, j are subtracted in the way of {k-(k+1)} - {(j-1)-j} and the pressure term is eliminated. The pressure can also be eliminated directly from equations (3.71) and (3.72) by cross differentiation but the order of differentiation is important and the elaboration of the corresponding differences is somewhat more complicated. Therefore, after testing both methods, the first has been selected in preference. Thus, after the pressure term is eliminated, the resultant equation reads in the form of a function of f as follows:

$$\begin{aligned} \text{Unknown} * A_1 + \text{Assumption} * A_2 + A_3 = \text{Known} \\ f_{j,k+1} * A_1 + f_{j,k} * A_2 + A_3 = f(p,q)_{\text{at } k, j-1, j, k+1, k, j, k+1} \\ + \text{other parameters} \end{aligned} \quad (3.73)$$

With a known inflow distribution, this equation is solved explicitly and $f_{j,k+1}$ is calculated; from this and the assumed value $f_{j,k}$, $p_{j,k+1}$ and $p_{j,k}$ are recalculated by the equation $f = p^2/h$ as already mentioned earlier. In fact, p is previously set as a function of the longitudinal velocity, $p = U_s h$; therefore $U_{s,j,k+1}$ and $U_{s,j,k}$ are then recalculated. After having completed this procedure from the k=1 point to the k=kk point which is the point at the other side of the river, the jth ray of the computational domain or, in physical sense, the jth section of the considered river-reach longitudinal flow velocity at each and every point over the cross-section is calculated. After that the integral condition of continuity equation (3.74) is used as an auxiliary condition to check the computed longitudinal velocity values.

$$\int_w h \bar{U}_s \, dn = Q \quad (3.74)$$

in which W is the width and Q is the total discharge. In this way, Eqn. (3.73) is iterated by improving the assumed value until eqn. (3.74) is sufficiently accurately fulfilled. Hence the longitudinal flow velocities of the entire river reach are calculated. Until this point, the transverse flow velocity component has been assumed to be zero ($U_{n,avg} = 0$). Therefore from there on the term which concerned with the transverse flow velocity U_n and U_n itself are calculated and put back into the eqns. (3.71) and (3.72) and recalculated all over again in order to get the true value of U_n , p and f under the condition of the existence of the U_n component and q . The calculation is repeated as before and it is completed when Eqn. (3.74) is sufficiently accurately fulfilled after the eqn. (3.73) is iterated by all necessary components of p , q and f which have been improved. Thus the complete two-dimensional flow field of the entire river reach is calculated.

3.6 Verification of the flow model

The flow model is tested with the experimental results of a moderately-curved flume with mildly sloping banks. The flume is a large curved flume consisting of a 38 m long straight reach, with a symmetric parabolic cross-section, followed by a 90° bend with a radius of curvature of 50 m in which the deepest point of the bed gradually shifts from the middle of the flume towards the outer banks. Therefore the bed-topography of the flume is a fixed uneven bed, as if it were a typical equilibrium bed-topography of a classical river bend. This type of experiment is an intermediate step before going into the morphological changes in the movable bed models. Therefore it also is a sensible check point for the flow model which has been developed so far in this chapter. A complete description and results of the experiments are given by De Vriend and Koch (1978). The plan-form, bed topography and dimensions of the flume (DHL flume; which is from Delft Hydraulics) are shown in Fig. 3.16, in which dimensions are in meters.

Measurements of the flow distribution and the water surface level performed with a discharge of 0.463 m³/s are selected to be used in the verification. The Chézy coefficient in this experiment was about 60 m^{1/2}/s. The curved part of the flume had a longitudinal slope of about 10⁻³ in order to compensate for friction losses; however, back-water effects were noticed in the measured water level data, so only the transverse distribution of the water surface is suitable for comparison with the theoretical results. The flow distributions are compared with the measured data in Fig. 3.17. Figure 3.17 shows that the flow distribution simulated by the numerical model agrees with the experimental results except for the region near the concave bank. Therefore the simulation results are satisfactory on the ground of the following explanation. Since the difference between the experimental data and the computational results seem systematic, it is concluded that the model has experienced the phenomena described by Kalkwijk *et al.* (1980) and Olesen (1987). They suggested that the possible causes of this type of discrepancy could be that the magnitude of the secondary flow is underestimated by the theory, or the omission of the effect due to the net outwards transport of momentum by the horizontal component of the secondary flow or, finally, the secondary flow intensity close to the concave bank cannot be described by local parameters only, due to a rather steep transverse slope of about (1:3). In this case, the difference which is found here is inevitable unless the flow model is reformulated as a complete three-

dimensional model, which has already been discussed in section 3.3, and so it was decided here to accept this discrepancy and carry on to the bed-topography computation.

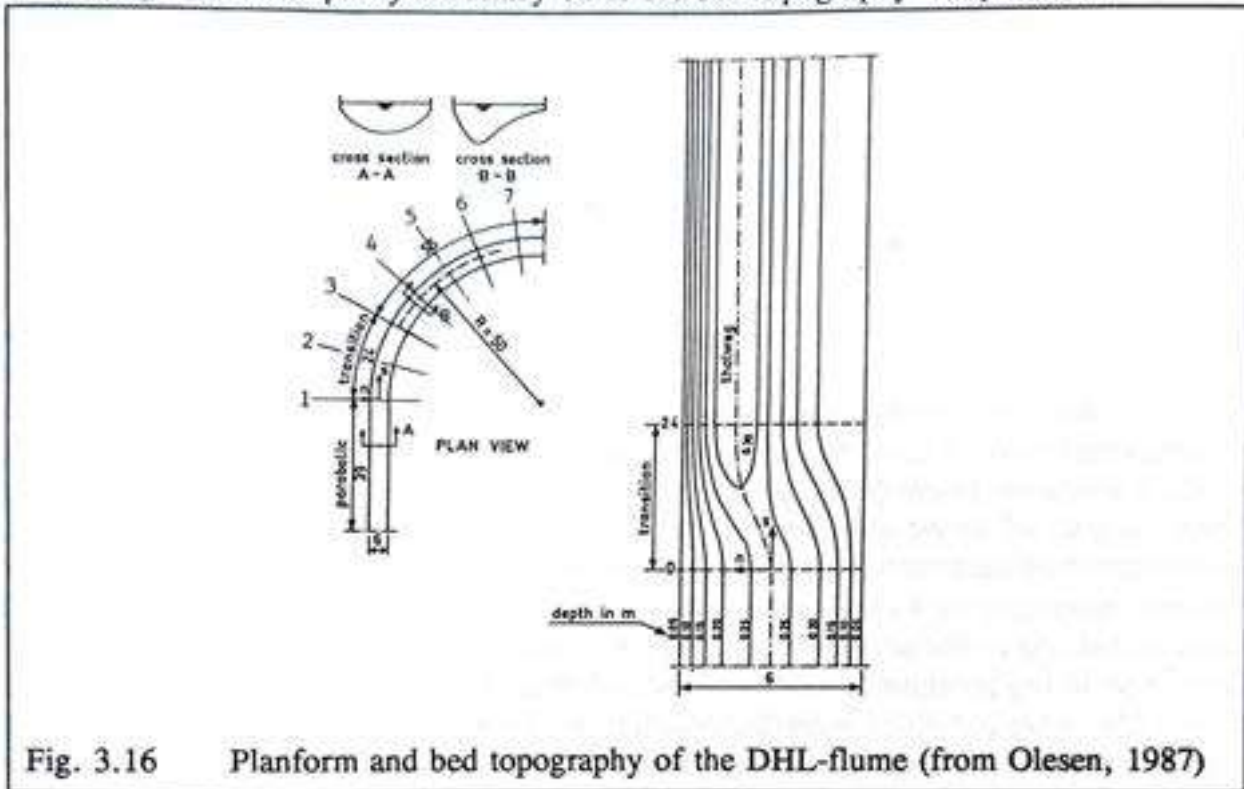


Fig. 3.16 Planform and bed topography of the DHL-flume (from Olesen, 1987)

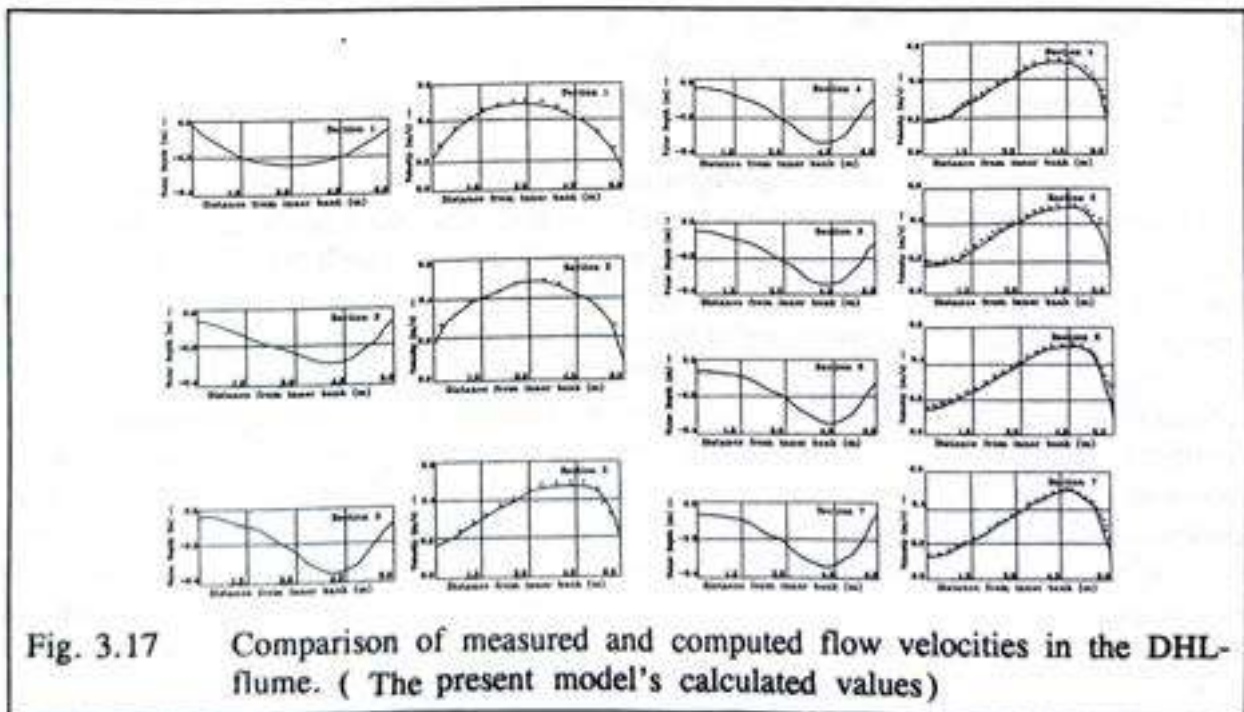


Fig. 3.17 Comparison of measured and computed flow velocities in the DHL-flume. (The present model's calculated values)

3.7 Bed-topography computation

Alluvial rivers possess channels that are self-formed by the flow of water and sediment mixture. This fluid mixture also has to flow under the prevailing geometry of the cross-section and the shape of the river bend together with other bed features. Consequently the presence of a circulating flow exerts an influence on the flow structures, the sediment transport capacity and the sediment distribution of a meandering river reach. It causes a transverse transport of sediment and directly brings about the scour and deposition of the material of the river bed. In this way, the morphology of a bend is gradually formed. On the other hand, the position of the main flow current and its variation, as determined by the morphology of the bend, it is again the evolution of the secondary flow. Depending on the strength of main flow and the secondary flow, the overall flow field has been changed and the other changes, such as the sediment transport capacity and the sediment distribution of a meandering river, follow. Hence the new bed topography and its corresponding flow field of the entire river reach develop together. The bed topography computation of the present study consists of above-mentioned steps. However, the intrinsic connection between the longitudinal and transverse variation of a meandering river reach as well as the evolution of the bed topography of a meandering river could only be revealed after the structures of the longitudinal and secondary flows have been simulated. In this case, the flow computation is completed in the previous sections and the bed shear stresses, sediment transport rates and the directions are computed hereafter including the bed slope and the transverse slope effects. The computation of the sediment transport rates and the directions of the sediment transport is very important in order to simulate the bed-topography of the river bend. Both the sediment transport rates and directions depend on the bed slopes in the two directions (ie. the longitudinal and the transverse directions) and on the magnitude and the directions of the bed shear stresses.

3.7-1 Governing differential equations of the bed-topography model

The development of the bed-topography model follows a principal assumption that disturbances of the flow travel at a much higher celerity than do disturbances of the bed. The bed level computation is therefore divided into small steps in which the bed is kept fixed and the flow considered as quasi-steady. At each time step a steady flow field is computed and from this the sediment transport rate is calculated and the bed configuration at the following time level is computed using an iterative explicit finite difference approximation (i.e. the replacement of implicit finite difference scheme) for the equation of continuity of the sediment. The governing differential equations are the sediment continuity equation and the sediment motion equation as shown below in eqns. (3.75) and (3.77). In principle, any of the equations available can be used to compute the sediment motion. In this study, however, the sediment motion equations are used selectively. The major components of the bed topography model are sediment transport rate and direction, bed shear stresses in magnitude and direction, the roughness factor and the integration procedure.

$$\frac{\partial Z_b}{\partial t} + \frac{\partial S_s}{\partial s} + \frac{\partial S_n}{\partial n} + \frac{S_s}{R_s} + \frac{S_n}{R_n} = 0 \quad (3.75)$$

where the components of the volumetric sediment transport (including pores, i.e. the bulk transport) per unit length in the s- and n- directions are given by

$$S_s = S_e \cos\psi \quad ; \quad S_n = S_e \sin\psi \quad (3.76)$$

in which

- S_e = total effective volumetric sediment transport including pores, taken per unit length, or the volumetric sediment transport flux.
- ψ = sediment transport direction angle, i.e. the angle between the direction of the sediment transport and the local stream line, which, however, only becomes coincident with the s coordinate through the iteration procedure discussed earlier in section 3.5.

$$S_e = mU^b \quad ; \quad S_e = \frac{8}{1-e_v} (\mu\theta - \theta_c)^{1.5} \quad (3.77)$$

or any transport equation, which is suitable; in the first part of eqn. (3.77), S_e is the transport rate, U is the mean flow velocity and m , and b are constants; in the second part of it, e_v is the void ratio, approximately 0.4, μ is the ripple factor, which is the ratio of the dimensionless shear stress due to skin friction and the total dimensionless bed shear stress, and θ_c is the critical shear stress.

Again, S_n can be calculated as follows:-

$$S_n = S_s \tan\psi \quad (3.78)$$

Using the rigid-lid approximation for the bed level, eqn. (3.75) becomes

$$\frac{\partial h}{\partial t} = \frac{\partial S_s}{\partial s} + \frac{\partial(S_s \tan\psi)}{\partial n} + \frac{S_s \tan\psi}{R_s} + \frac{S_s}{R_n} \quad (3.79)$$

Thus the bed topography computation is based on eqns. (3.76), (3.77), (3.78) and (3.79).

3.7-2 Bed shear stress in the case of a mobile bed

The bed shear stress in mobile-bed-river-bends is controlled by the forces which arise from topographically induced spatial acceleration in longitudinal and transverse directions. In fact there are two relationships to be considered and calculated hereafter. These are a relationship between the bed shear stress field and the channel topography and, a relationship between the bed shear stress field and the sediment transport field. The first relationship can be considered in three components. The curvature of the river, spatial variation in bed topography and the corresponding bed shear stress field. Actually, the key effect of the downstream changes of the bed topography induced by the first two components on flow is modest on the magnitude of the boundary shear stress at any point on the river bed, but rather on the direction of the bed shear stress vector. In a sequence of bends, the effects of changing curvature alone on the growth and strength of secondary flow will cause a zone of maximum bed shear stress to shift from near the upstream convex bank to the downstream concave bank. More over the effect of the variation in bed topography is added. Due to the fact that the bed and bank materials are erodible and thus the boundary of the flow is mobile, bed shear stress magnitude and direction are time dependent. The magnitude of the bed shear stress components in s- and n- directions are calculated by eqns. (3.63) and (3.64).

3.7-3 Bed shear stress direction in an alluvial river bend

The bed shear stress direction in curved flow is described in sections 3.3-4 and 3.3-5 without going into the level of mobile bed condition, concerning alluvial bed roughness coefficient in the manner of time dependent factor. Most frequently the deviation angle for the direction of flow and the direction of bed shear stress are described in two statements. The first is the direction of the bed shear stress deviates from the direction of the depth-averaged velocity. The second is the direction of the depth-averaged velocity deviates from the local point velocity. However the magnitude of the deviation angle must be the same, because bed shear stress follows the direction of local flow or in other words the direction of the resultant velocity. It is illustrated in fig. 3.18. The deviation angle δ_s is related to the secondary flow intensity and so as to the longitudinal and transverse flow velocities, which are conditioned by the prevailing condition of the flow and alluvial bed roughness. In this section and the following section the roughness factor (in the form of Chézy coefficient) is of the kind which varies with time, space and the property of bed material. Therefore bed shear stress direction here is closely related to the time dependent evolution process of the bed configuration. This essence is put into practise when the numerical model is integrated. In the mathematical model the equations used are the same as in section 3.3-4 and 3.3-5.

3.7-4 Sediment transport capacity

The main interest in this section is concentrated on the prediction of the amount of sediment carried by the flow. The capacity mainly depends on the strength of the flow, not on the supply from the upstream. It is reasonable to suppose that the transport capacity can be considered from two aspects: from the point of view of magnitude (as scalar quantity) and from the point of view of the direction (as vector quantity). From the first point of view, the

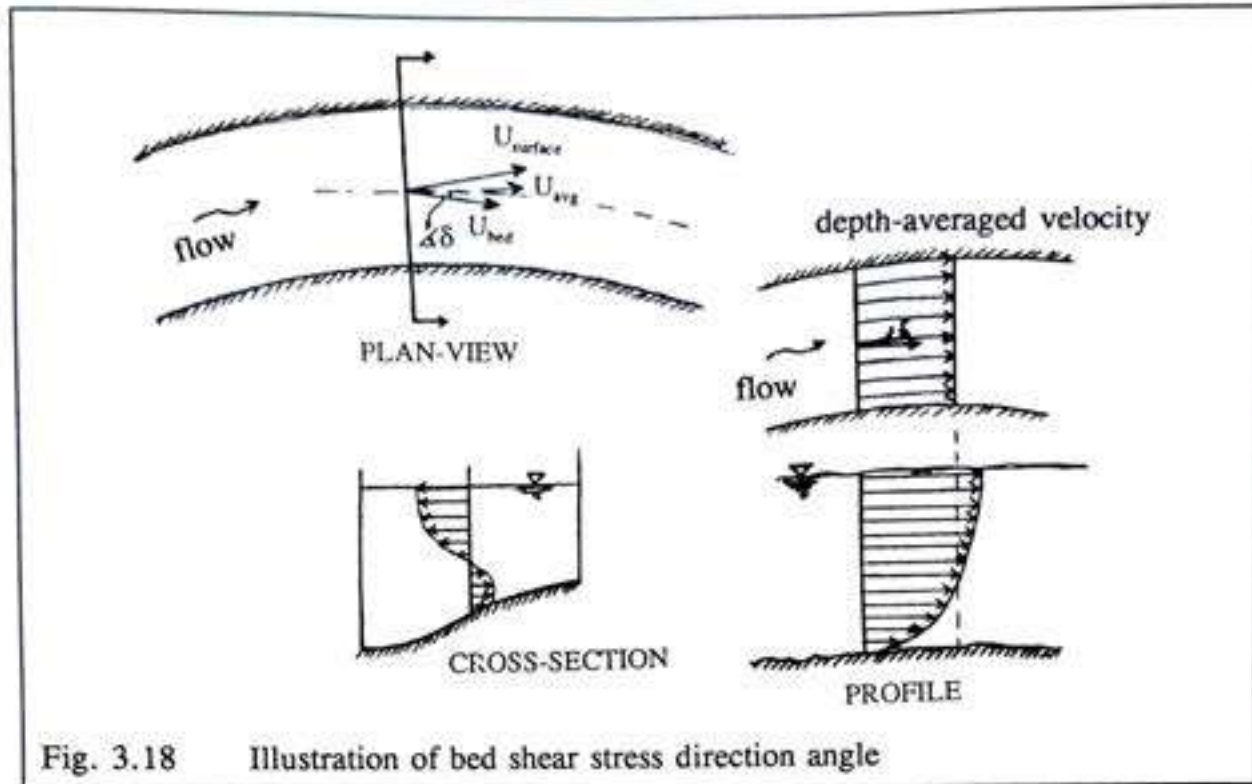


Fig. 3.18 Illustration of bed shear stress direction angle

sediment transport capacity here is the total load of the alluvial river. From the second point of view, it is supposed that the sediment transport capacity is the sum of the longitudinal transport- which is determined by the direction of the flow at bottom and the bed slope in the longitudinal direction- and the transverse direction transport- which is determined by the direction of the flow at bottom and the bed slope in the transverse direction. Here both are calculated so far as possible given the limitations of the knowledge of sediment transport in this theoretical field. Yalin (1972) explains that given the number of variables involved, transport relationships require a family of surfaces, or a family of families of curves, for adequate graphical representation. He notes that this is strictly true only for the case of uniform two-dimensional flow: Yalin avoids the case of non-uniform three-dimensional river flow as presumably too complex to be worth discussing in theoretical terms. However here a start is made to calculate sediment transport rate in uniform shear flow. The available sediment transport relationships in this type of flow mainly give a relation between a sediment transport rate and the dimensionless excess shear stress. The excess shear stress means the shear stress which can be used to move a sediment particle against its own contact resistance. The shear stress which has to be used to get the threshold point of a sediment particle is called the critical shear stress. Therefore the excess shear stress can be calculated by subtracting the critical shear stress from the bed shear stress which is induced by the flow. Each grain has its own capacity to resist being washed away by the flow. Therefore the critical shear stress can never be the same anyway. However, a uniform grain size is considered just to reduce the complexity, or to help in overcoming the difficulty. The calculation of the sediment transport rate, and the bed shear stress is mostly represented in a dimensionless form in terms of Shields parameter, defined as

$$\theta = \frac{\tau_b}{\rho g \Delta D} \quad (3.80)$$

in which τ_b is the bed shear stress in the dimensions given in Section 3.3-3, ρ is the density of the water (strictly speaking, the density of the fluid), g is the acceleration due to gravity, Δ is the specific gravity of the sediment ($\Delta \approx 1.65$ for normal sand), and D is a characteristic grain size. The characteristic grain size differs from model to model, such as D_{50} , D_{65} , D_m . The critical shear stress is denoted by θ_c and the value varies from about 0.033 to 0.06. There are numerous formulae to estimate the sediment transport rate but they mainly fall under only two categories. The first category considers the sediment transport rate as the function of the strength of the flow. The second category considers the sediment transport rate as a function of the excess shear stress. The first relationship is in the form of

$$S_e = m U^b \quad (3.81)$$

in which S_e is the transport rate, U is the mean flow velocity and m , and b are constants. The second relationship is in the form of

$$S_e = m (\mu\theta - \theta_c)^b \quad (3.82)$$

in which m and b are coefficients, μ is the ripple factor, which is the ratio of the dimensionless shear stress due to skin friction and the total dimensionless bed shear stress, and θ_c is the critical shear stress. Here it should be noted that the relevance of the two-dimensional flow condition to the dimensionless bed shear stress can be expressed as follows:

$$\theta = \sqrt{\frac{\tau_{bs}^2 + \tau_{bn}^2}{g\rho\Delta D}} \quad (3.83)$$

These are the general expressions of the magnitude of the sediment transport rate and the specific formulae which are used in the present study are discussed in section 3.7-4.1, 3.7-4.2, and 3.7-4.3. Moreover the selection of an appropriate sediment transport equation has puzzled at least a generation of river engineers and computer modellers. Although an attempt is made by Williams and Julien, (1989), to give an applicability index for sand transport equations they selected only four equations, which are those of Ackers and White, (1973), Shen and Hung, (1971), Toffaleti, (1968) and Yang, (1973). In the connection to this present study, Williams et al. attempt only contribute to stop choosing appropriate equation. Because the applicability of these four equations are very sensitive to sediment size. The experiments were made under different flow condition and if there any more variety of flow conditions are added, more scattered results are expected.

3.7-4.1 Bed load

Bed load is the part of the sediment transport which is sliding, rolling, jumping or saltating over the bed. Bed load transport generally occurs when the bed is experiencing lower flow regime, such as a dune-, a ripple-, or a mixed-covered bed. A large amount of literature is available elsewhere; therefore the detail will not be mentioned here. In this study, the bed load is calculated from the bed load equations formulated by Mayer Peter and Müller, Engelund and Hansen and the power law. Engelund and Hansen formula is also used frequently in this study to calculate the bed load transport. In principal, the Engelund and Hansen formula was derived for a total load calculation but it is justified to use it as a bed load formula when the Shields parameter is low. The power law is the principally-used equation when the mathematical model was derived. However, any available and reasonably reliable formulae for the bed-load equation can be used here.

3.7-4.2 Suspended load

Grains set in motion and dispersed into the flow are supported either by upward diffusion of turbulence from the bed boundary (i.e., the weight of the grain is balanced by the upward component of fluid momentum transferred to it) or by the vertical component of forces arising from transfer of momentum from grain to grain and grain to bed (or, in principle at least, by rotational lift). The suspended load is the part of the sediment transport which is carried in suspension under a particular flow and particle-interaction situation. The suspended sediment transport capacity is closely related to the energy of the turbulent motion available to keep particles in suspension. For the calculation of this suspended sediment load the concentration fields have to be computed in the first place. There are many equations available, from Einstein, (1950) to van Rijn (1981, 1984) and, in between, many others. In the present study the suspended load is calculated using Diegaard's (1980) model and the concentration profile is also taken from Diegaard (1980). The suspended load calculation is essential when the dune formation is simulated. In the bed topography model the suspended load is often included, although not always. When this load is included, the wave length and the damping of the point bar and pool configuration are significantly affected by the suspended sediment transport process.

3.7-4.3 Total load

The total sediment load in nature is the sum of the bed load, the suspended load and the wash load. In laboratory studies, the wash load is almost invariably absent and frequently the total load amounts to bed load only. In this study, predictions of bed load and the suspended load are summed to provide the total load. Engelund and Fredsøe (1976) formula is used to calculate the total load. This formula which partly is based on ideas originally introduced by Bagnold (1954) has the advantage that the sediment load is split up into bed load and suspended load. Since all the formulae which are used here are entirely based on laboratory data, the wash load is not included.

3.7-5 Sediment transport direction

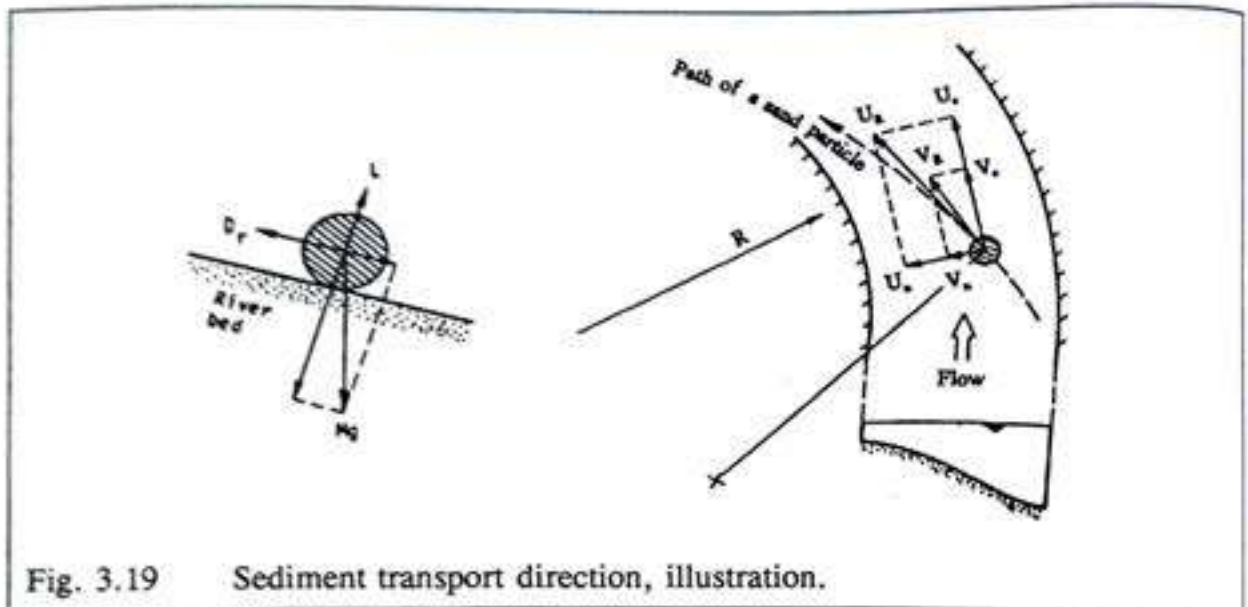


Fig. 3.19 Sediment transport direction, illustration.

The forces acting on the grain which is moving on a sloping alluvial bed are: (1) drag, (2) lift, (3) gravitational, (4) normal and (5) friction forces. These five are intrinsic forces and, according to the type of computation, such as one-, two- or three- dimensional, the directions of drag, gravitational and friction forces are accounted for in their corresponding directions. In this study, these forces are accounted for in two-dimensions. A common approach is to divide the governing phenomena into two components: (1) the influence of the secondary current due to curved flow and (2) the influence of the sloping bed. The direction of the sediment transport is derived from the path of a grain which is moving with the flow or lying on the bed of the river. When the formulation is based on the moving grain, the drag force is calculated from the relative flow velocity (i.e. the flow velocity related to the velocity of the sediment particle); this is known as "dynamical approach". When formulation is based on the resting grain, the forces acting on the grain are equate in such a way that the velocity of the sediment particle is negligible as compared to the flow velocity near the bed. Here the present study follows the dynamical approach. A review of this subject is given by Odgaard (1981).

3.7-5.1 The bed-slope effect

The influence of the bed slope on the transport rate is calculated in such a way that the magnitude of the bed shear stress is modified according to the bed slope. Therefore the bed shear stress for horizontal bed is calculated in the first place and added the bed slope effect as following:

$$\theta_0 = \theta_{0h} \frac{\sin(\phi - I)}{\sin\phi} \quad (3.84)$$

in which ϕ is the dynamic friction angle, where $\phi = \tan^{-1} \beta_r$ and β_r is the dynamic friction coefficient; I is the longitudinal bed slope, θ_0 is the bed shear stress for horizontally sloping bed and θ_{0h} is the bed shear stress value for horizontal bed. The influence of the bed slope on the transport rate in river bends is very modest; which is declared by Olesen (1987), he continues: however, the slope dependence of the sediment transport rate is maintained because it appears convenient in the numerical integration procedure. The same is experienced in this model, therefore it is maintained in the present study for the same reason. Moreover, in order to integrate this bed-slope effect with the type of sediment transport relation, as shown in eqn. (3.81), which does not calculate the bed shear stress, the bed-slope effect can be introduced using the relation:

$$S_e = m \bar{U}^b \left(1 + e \frac{\partial h}{\partial s}\right) \quad (3.85)$$

in which e is a coefficient which is proposed by Olesen, 1987, whereby

$$e = \frac{b}{2} \frac{\theta_c}{\mu\theta} \quad (3.86)$$

and variation of b and e are depicted as a function of $\mu\theta/\theta_c$ as shown in Fig (3.20).

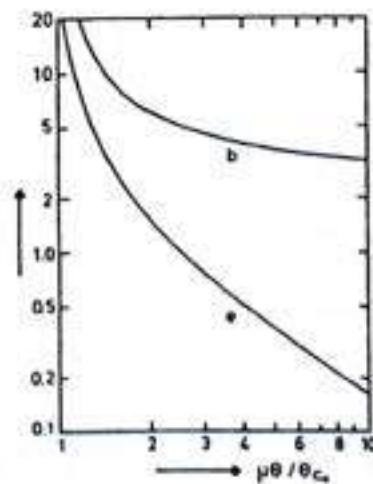


Fig. 3.20 Variation of the coefficients b and e in the linearized Meyer-Peter and Müller formula; (from Olesen, 1987).

3.7-5.2 The transverse-slope effect

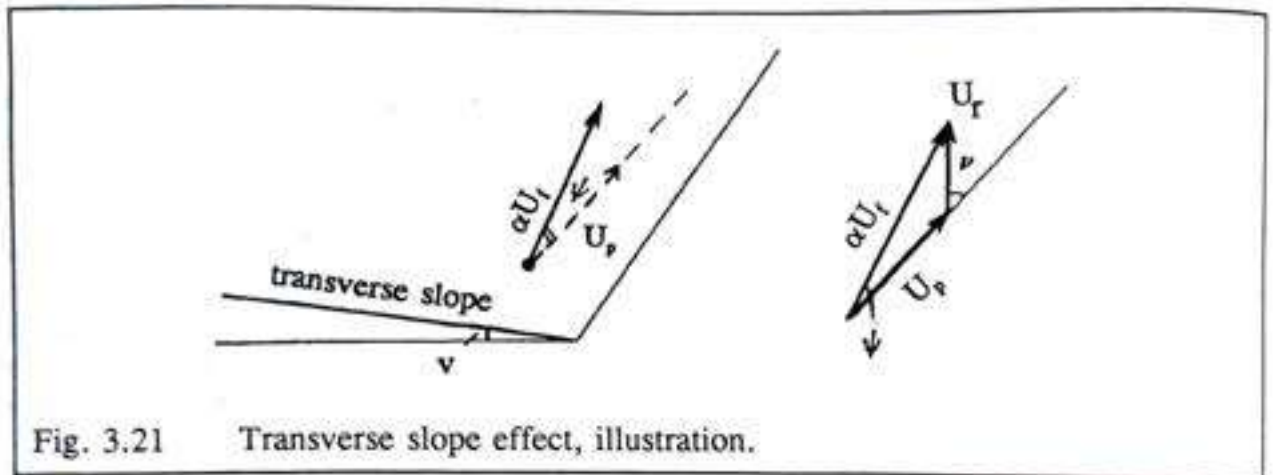


Fig. 3.21 Transverse slope effect, illustration.

The transverse bed slope is much steeper than the overall longitudinal bed slope. Thus the component along the transverse bed of the gravitational force cannot be neglected with respect to the other forces acting upon the bed. Therefore this effect is introduced as following. The path of a moving grain on a transverse slope will form an angle ψ with the direction of the flow. The flow velocity at particle level is taken as αU_l as shown in Fig. 3.21, while U_p denotes the mean particle velocity, ν is the angle between the particle path and the drag. The direction angle ψ can be found by the following equation of Engelund, (1981).

$$\tan \psi = \frac{\beta_f}{\kappa_1 \kappa_2} \frac{\tan \nu}{\left(\frac{\theta'}{\theta_0}\right)^{0.5}} \quad (3.87)$$

slope, θ' and θ_0 are shear stress due to skin friction and initial bed shear stress respectively.

3.7-5.3 Non-uniform sediment

The relationship between the bed load transport and the boundary shear stress fields in river meanders varies with the size and the heterogeneity of the bed material. The expression for the rate of bed load transport can be derived from knowledge of the mean particle velocity. It is assumed that the bed load is the transport of a certain fraction p (i.e. probability) of the particle located in a single layer. One of the distinct characteristics of the river bend topography is that the grain size distribution of the bed material varies considerably in the transverse as well as in the longitudinal direction. Therefore instead of a certain fraction, a number of discrete size fractions are considered by several researchers. This means that the sediment mixture is divided into a number of discrete size fractions. For each size fraction a sediment transport formula and continuity equation are applied. Several

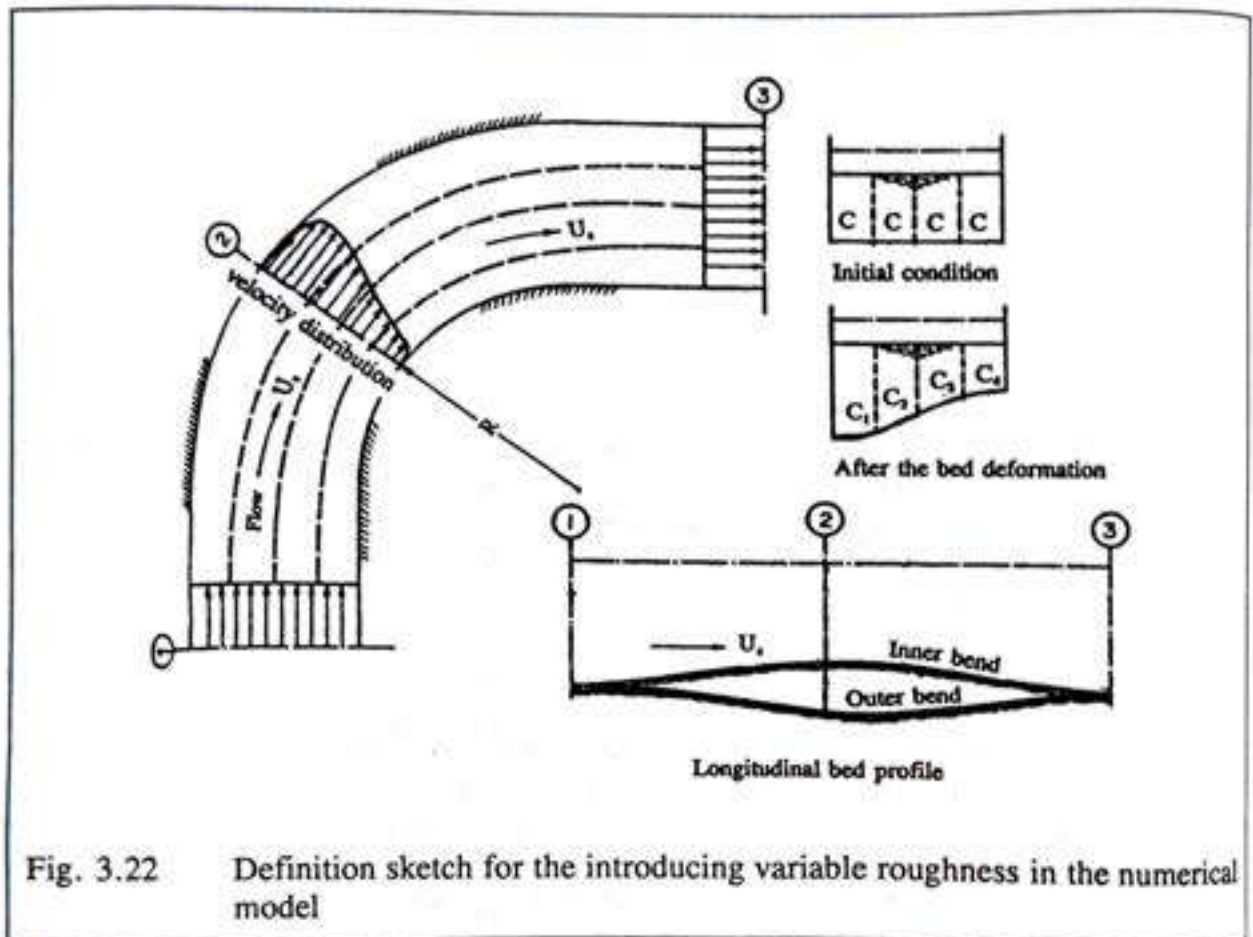
investigations have been made, but the most common type of model used for this purpose is one-dimensional. Among the more important models are those of Thomas (1979), Ribberink (1980), Deigaard (1980), Odgaard & Kennedy (1982) and Olesen (1987). Olesen's (1987) model is a two-dimensional extension of the Ribberink (1980) model. Deigaard (1980) and Odgaard and Kennedy (1982) have developed models for the grain size distribution in river bends. Non-uniformity of the bed material is also an important factor when the accuracy is concerned. The total transport capacity prediction will be different if we calculate the sediment transport in fractions: this will make a big difference in the bed level configuration and consequently the bed forms and the bar formation in the bend.

However the ultimate goal of the study is to be able to predict the plan-form movement and thus a non-uniform sediment transport calculation is here considered from two points of view. The first involves including the non-uniform sediment transport and the second restricts itself by omitting this step for the time being. Positive and negative points on both sides are considered. The most important reasons and positive points that give support to the first approach have already been mentioned in the previous paragraph. There are also reasons that support the second approach, as follow. A methodology for the modelling of non-uniform sediment transport was developed by Ribberink (1980). The main principal is that the alluvial bed can be divided into an active and a passive layer. The interface between the two layers is poorly defined. Although the definition of the interface does not appear to have any excessively negative influence on the final computed equilibrium bed topography or grain size distribution, Olesen (1987) has reported that *it may have a large influence on the simulation time needed to obtain equilibrium*. In the size-fraction transport formulae, the equations for the sediment transport rate which have been developed for uniform sediment have long been used because there appeared to be no practical alternatives. Therefore the ideology of predicting-correcting has been introduced for the non-uniform sediment transport calculation. The essence of this approach is that the transport rate is predicted by the simplified equations and the corrections that follow can be reasonably accurate for certain specific phenomena such as these in which the smaller grains 'take refuge' behind the larger grains. These corrections are known by the name of the 'exposure corrections', and the 'sheltering or hiding corrections' and are expressed in terms of coefficients. The following physical phenomena are generally supposed to determine the sheltering coefficients:

- (1) *sheltering or hiding of the smaller sizes behind or below or underneath of the larger sizes.*
- (2) *an increased exposure to the flow of the larger sizes.*

In many transport formulae, the transport is calculated in terms of the excess shear stress ($\tau - \tau_c$). It is clear that a constant τ_c value apply for all size fractions. Therefore a correction factor (sheltering coefficient) for the critical bed shear stress is used. This correction has a similar effect, viz. a reduction of the transport rate of the smaller sizes and an increase of the transport rate of the larger sizes. Moreover, from the accuracy point of view it has earlier been concluded (Thein, 1989) that *using more size fractions in numerical simulations results in more accurate answers but at the same time the accuracy decreases significantly when the Courant number is very small*. Therefore, the second point of view is adopted in such a way as to omit the non-uniform sediment transport computation in this study.

3.7-6 Variable roughness



The important role of the roughness coefficient is considered here. The roughness coefficient is commonly used as a calibration factor to allow for all the other uncertainties in an application, (eg. phenomena which are not accounted for). Therefore the Chézy value used in the numerical model may sometimes vary much from the value which represents only the frictional resistance of the channel boundary. *Nevertheless, it is important that the coefficients should retain a physically realistic value since the predictive capability of the calibrated model may otherwise be endangered (Cunge et al., 1980, pp381).* In the present study, the local actual coefficient of friction is simulated and investigated (see Fig. 3.22) in order to be able to distinguish between two representations, as the frictional resistance and as a calibration factor. The local alluvial roughness is simulated from the formation and dissipation of dunes, from which grain-resistance and form-resistance are calculated. The roughness predictor is used twice, firstly explicitly in the hydrodynamic equations as the hydraulic friction term and secondly, implicitly, in the transport prediction.

3.8 The depth-averaged bed topography model

The depth-averaged bed topography model based on the depth-averaged form of following equations; (1) continuity of sediment, (2) angle between the depth-averaged velocity and the bed shear stress, (3) direction of bed shear stress, (4) direction of sediment transport and (5) transport models. These equations which are used in the present model are listed below.

$$S_s = S_r \cos\psi \quad (3.88)$$

$$S_n = S_r \tan\psi \quad (3.89)$$

$$\frac{\partial h}{\partial t} = \frac{\partial S_s}{\partial s} + \frac{\partial(S_r \tan\psi)}{\partial n} + \frac{S_r \tan\psi}{R_s} + \frac{S_r}{R_n} \quad (3.90)$$

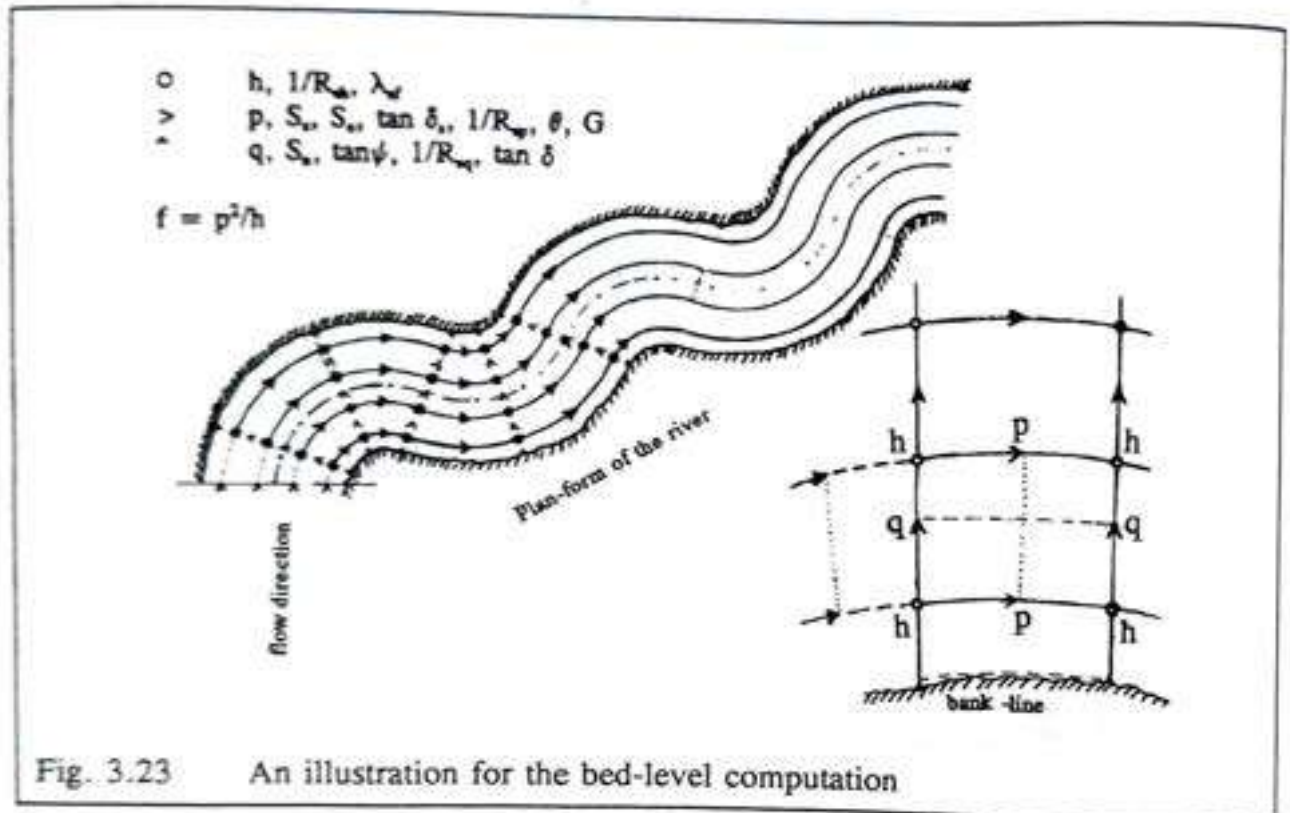
$$\lambda_d \frac{\partial \tan\delta_s}{\partial s} + \tan\delta_s = -\beta \frac{h}{R_s} \quad (3.91)$$

$$\frac{\tau_{br}}{\tau_{bn}} = \tan\delta = \frac{\bar{U}_s}{\bar{U}_n} + \tan\delta_s \quad (3.92)$$

$$\tan\psi = \tan\delta + G \left[\frac{\partial}{\partial \theta} \right]^p \frac{\partial h}{\partial n} \quad (3.93)$$

$$S_r = m \bar{U}_s^b \left(1 + e \frac{\partial h}{\partial s} \right) \quad (3.94)$$

3.9 The integration procedure of the model



There are fifteen variables to be calculated in order to complete the bed topography simulation. These are $h, p, q, S_a, S_b, S_c, \lambda_{st}, \delta, \delta_s, \iota, R_{ab}, R_{sp}, R_{sq}, \theta$ and G . The meaning of symbols are explained in their corresponding equations. The computational points for these variables are shown in their corresponding places in Fig. 3.23.

The bed elevation is calculated in the manner, that rate of change of elevation over an area which is discretised in a unit computational grid times that reference area is equal to the total change of mass balance in that particular computational grid. Each grid is considered in this way and calculated one by one from the convex bank to the concave bank through the whole width. After the whole width is through with one time calculation, it is called one ray. In this way the entire river reach is calculated from the upstream entrance to the downstream end ray by ray. Therefore the calculation procedure consists double sweep algorithm in the sense of the first and second sweep crosses each other perpendicularly. The direction of the first sweep is across the river width from the convex bank to the concave bank and the direction of the second sweep is along the longitudinal direction from the upstream of the river reach to the downstream of the river reach.

3.10 Analysis of the morphological model

Here some analytical solutions of the morphological model are described as a basis for the later discussion of the behaviour of the numerical model in the verification and calibration phases, which will follow after this section. Analytical (model) solutions provide rough estimates as well as certain fundamental insights into the interactions between various parameters. A simple analytical solution has the advantage of acting as a guide for solving practical problems and for the verification of numerical models that have been developed to handle more complex situations. The analytical solutions for two dimensional morphological model in case of depth-averaged equations are derived previously amongst other by two authors Olesen (1987) and Talmon (1990). The present model has many differences in comparison with Olesen (1987) model; yet the basic depth-averaged equations can be analyzed in the same way. Therefore the following solutions are described and discussed.

3.10-1 Olesen solution

The analytical solution of the flow and bed topography in the river bend is initiated by Struiksmā, 1983 with strongly simplified model. The flow is simplified by dividing the channel into two adjacent straight channels, both of uniform depth. In stream-wise direction sinusoidal perturbations, with amplitudes being a function of the stream-wise co-ordinate, for the flow and the bed topography are assumed. In the analysis adaptation lengths for the flow and bed topography are introduced.

λ_w adaptation length of flow is given by the equation:

$$\lambda_w = h \frac{C^2}{2g} \quad (3.95)$$

λ_b adaptation length of bed topography is given by the equation

$$\lambda_b = \frac{1}{\pi^2} \left(\frac{W}{h}\right)^a \frac{h}{G_0} \quad (3.96)$$

The solution of the problem is given by the following equation

$$(k\lambda_w)^2 + i(k\lambda_w) \left(\frac{b-3}{2} - \frac{\lambda_w}{\lambda_b}\right) - \frac{\lambda_w}{\lambda_b} = 0 \quad (3.97)$$

in which k is the wave number of the bed deformation, i for imaginary part, and b is the power of the sediment transport equation. The solution mainly depends on the ratio of the adaptation length of the flow to that of the bed topography. In fact the solution can be interpreted as saying that bed disturbances in the alluvial river bend will either grow or decay in the flow direction according to the ratio of λ_w/λ_b . In equation (3.89), the wave number k is dominating influence on the deformation of bed disturbances. The wave number k itself consists however two parts, namely a real part and an imaginary part: k can be written as $k_j = \pm k_r + k_i$ where $i = \sqrt{-1}$ as usual and subscripts r and i represent the real and

the imaginary parts respectively. Once again, as a dominant factor, k is directly related to the ratio λ_s/λ_w .

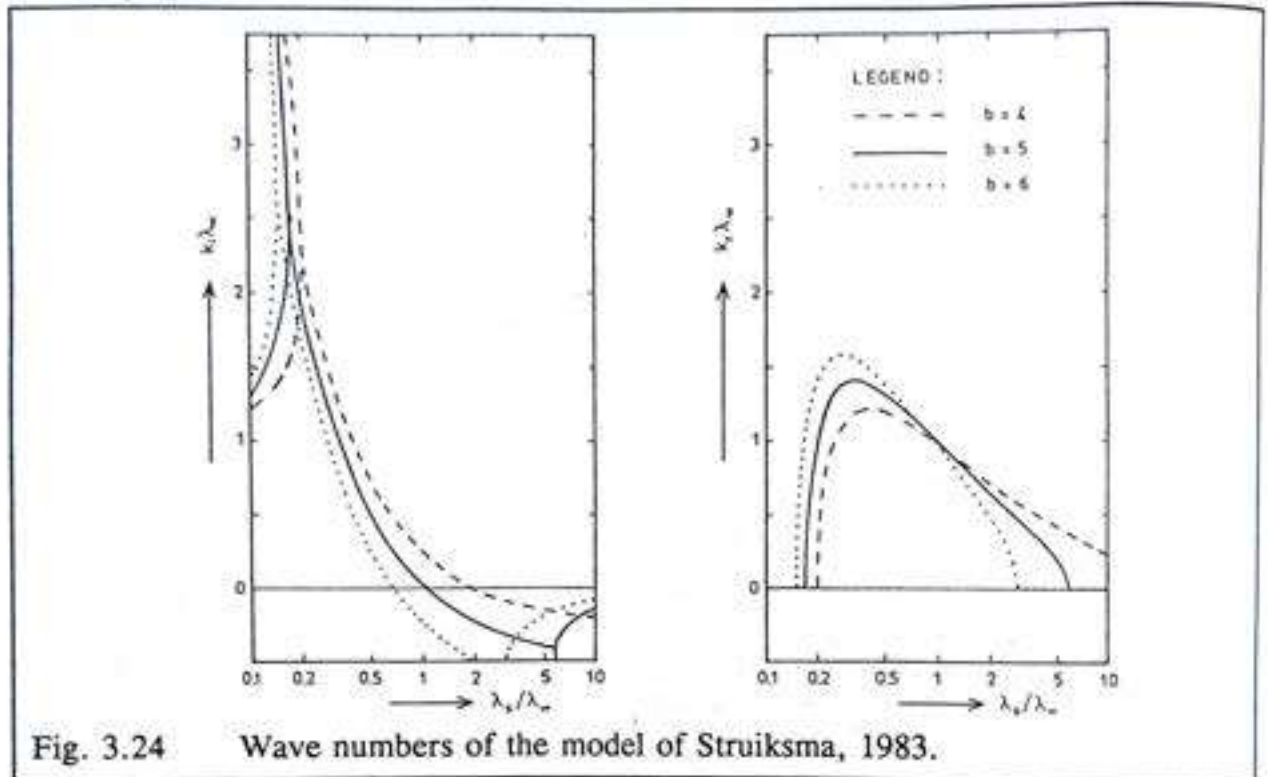


Fig. 3.24 Wave numbers of the model of Struikma, 1983.

In Fig. 3.24, $k_r \lambda_w$ and $k_i \lambda_w$ are depicted as a function of λ_s/λ_w . Eqn. (3.97) suggests that an increasing alluvial roughness provides less damping and shorter wave lengths. For comparison with numerical simulations a somewhat more quantitatively accurate analysis is called for. Therefore Olesen, 1987 has contributed the extended analysis. The flow model of the analytical solution is based on the depth-averaged flow model. Curvature of the coordinate system and secondary flow convection, however are neglected (i.e. $1/R = 0$, $k_{\theta} = 0$). The depth-averaged set of flow equations is linearized by superposition of perturbations on the leading variables, such as U_s , U_n , h and R_s . For instance, $\bar{U}_s = \bar{U}_{s0} + \bar{U}'_s$. With \bar{U}_{s0} the value in the unperturbed situation and \bar{U}'_s the perturbation. For U_n , h and $1/R_s$ similar expressions are substituted. After this manipulation, the governing set of equations for the analytical model becomes a set of the first-order perturbation equations. From there the fluctuating pressure is eliminated by cross differentiations for longitudinal- and transverse-momentum equations. The fluctuating components of the variables at coordinate s and n are modelled by harmonic perturbations.

For this purpose, additional dimensionless wave numbers, k and k_B is introduced, such that k is the wave number in the longitudinal direction and k_B is the wave number in the transverse direction. The boundary condition of impermeable side walls constraints the transverse wave number as follows:

$$k_B = \pi \frac{h_0}{W} m \quad (m = 1, 2, 3, \dots) \tag{3.98}$$

At this point the solution of the analytical model appears in a sixth order polynomial form as follows:

$$\begin{aligned} & l^6[\lambda_y \epsilon k_B^2] + l^5 i [b \lambda_y k_B^2 - \epsilon k_B^2 - \lambda_y \epsilon k_B^2] \\ & + l^4 [b k_B + \lambda_y (G+e) k_B^2 + b \lambda_y \epsilon k_B^2 - \epsilon \epsilon k_B^2] \\ & + l^3 i [\beta k_B^2 - \lambda_y k_B^2 + (G+e) k_B^2 - 2 \lambda_y \epsilon k_B^2 - b \epsilon k_B^2 - G \lambda_y \epsilon k_B^2] \\ & + l^2 [k_B + (3-b) \lambda_y \epsilon \lambda_B^2 + 3 \beta \epsilon k_B^2 + G \lambda_y k_B^2 - 2 \epsilon \epsilon k_B^2] \\ & + l i [(b-3) \epsilon k_B - G k_B^2 - 2 G \lambda_y \epsilon k_B^2] + [2 G \epsilon k_B^2] = 0 \end{aligned} \tag{3.99}$$

in which $l = k/k_B$, $\epsilon = g/C^2/k_B$, the other variable being the same as those introduced earlier.

The solution is depicted in Fig. 3.25 this is a typical standard guide for the simulation of two-dimensional bed topography model. That is why it is used as a standard guide for the present model.

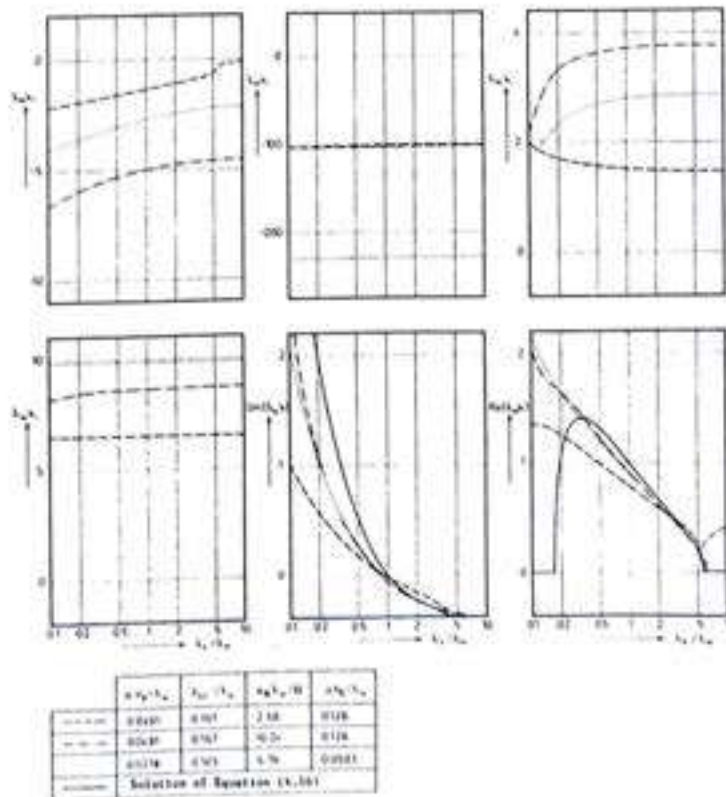


Fig. 3.25 Solution of the extended model of Olesen.

3.10-2 Talmon solution

Talmon, 1988 has recalculated the analytical model of Olesen, by adding the bed shear stress direction angle δ into the flow model equations. Detail explanation is referred to Talmon, 1988. Hence the solution of the analytical model reads:

$$\begin{aligned}
 & l^6 [ek_B^3 \frac{\lambda_{sf}}{h_0}] + i l^5 [-ek_B^2 - ek_B^3 \epsilon \frac{\lambda_{sf}}{h_0} + bk_B^2 \frac{\lambda_{sf}}{h_0}] \\
 & + l^4 [bk_B + b\epsilon k_B^2 \frac{\lambda_{sf}}{h_0} - \epsilon \epsilon k_B^2 + ek_B^3 \frac{\lambda_{sf}}{h_0} + Gk_B^3 \frac{\lambda_{sf}}{h_0}] \\
 & + i l^3 [-b\epsilon k_B - ek_B^2 - ek_B^3 \frac{\lambda_{sf}}{h_0} 2\epsilon + k_B^2 \beta + k_B^2 \frac{\lambda_{sf}}{h_0} - Gk_B^2 - Gk_B^3 \epsilon \frac{\lambda_{sf}}{h_0}] \quad (3.100) \\
 & + l^2 [-b\epsilon k_B^2 \frac{\lambda_{sf}}{h_0} - 2\epsilon \epsilon k_B^2 + k_B + 3\epsilon k_B^2 \frac{\lambda_{sf}}{h_0} + 3\epsilon k_B^2 \beta - G\epsilon k_B^2 + Gk_B^3 \frac{\lambda_{sf}}{h_0}] \\
 & + i l [b\epsilon k_B - 3\epsilon k_B - Gk_B^2 - 2G\epsilon k_B^3 \frac{\lambda_{sf}}{h_0}] - 2G\epsilon k_B^2 = 0
 \end{aligned}$$

in which all symbols are transformed to same notations as Olesen's symbols in order to compare easily.

3.10-3 Discussion

The analytical solutions presented in Sections 3.10-1 and 3.10-2 has the only one difference that is the way of applying the angle δ ; δ is an angle between the direction of bed shear stress and the direction of the depth averaged velocity. Talmon, 1988 claimed that this angle has been incorporated in both the flow model and the sediment model while Olesen, 1987 has omitted this angle for the flow model but incorporated in the sediment model. Talmon model gives a resultant equation which is different from Olesen's resultant equation. However, at that stage it has not been investigated in how far results deviate from each other. In this study, this effect is investigated by means of numerical model. In one version of the numerical model, the angle is omitted in the flow equation and in another version of the flow model, the angle is incorporated in both flow and sediment models. Any significant differences have not been noticed by studying the bed topography configuration of the simulated results. For the second test, in the first version, this angle is omitted in both flow and sediment models; in the second version, this angle is incorporated in both flow and sediment models. Of cause, as expected the bed topography changes significantly. Therefore it can be concluded that the effect of this angle is more important in sediment transport model than in the flow model.

Besides above mentioned way, the two analytical solutions are almost identical. Thus these two are regarded as one analytical solution, and it is used as a guide to discuss the behaviour of simulated bed topography of the present numerical model, in terms of wave numbers and adaptation lengths.

3.11 Verification of the morphological model

For the verification of the numerical model, the flume experiment T4 (Olesen, 1985b) and the natural river situation described in section 3.11-3 are used. The model is tuned by means of measurements until the best agreement between calculated and measured results is obtained.

3.11-1 The basic data needed for the model

The basic data needed for the model are as shown in Fig. 3.26.

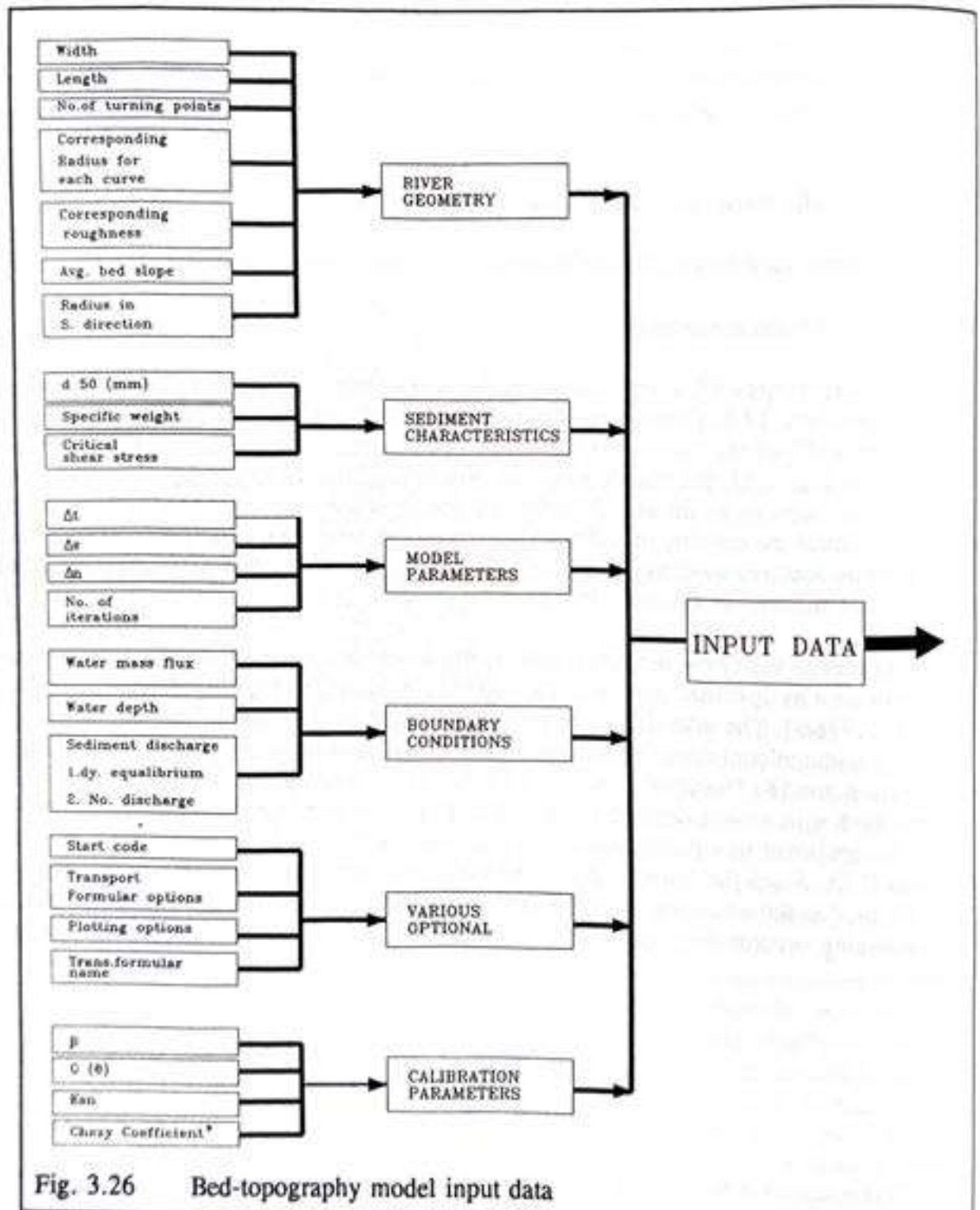
3.11-2 Flume experiments

The experiment T4 which characteristics listed below is used to verify the present model. Experiment T4 has been carried out in the DHL (Delft Hydraulics) flume by Olesen, 1985b). The width of the flume is 2m, the radius of curvature of the centre line of the flume is 11.75m. In Fig. 3.25, the plan form of the flow is depicted. In experiment T4 most of the straight inflow section, as far as 1 meter before the bend entrance, was filled with gravel in order to minimize the quantity of sediment require and to promote a homogeneous flow field. The sediment was released to the flume at the end of the gravel layer. The measuring procedure are referred to Olesen, (1985b).

In order to verify the numerical model, the set-up of the numerical model follows the experiment such as upstream portion of the bed is kept fixed also 1 meter before the entrance (precisely 0.926m). The grid size is the s-direction $\Delta s = 0.925\text{m}$ and in the n-direction, $\Delta n = 0.5\text{m}$. Computational nodes across the flume width are 4 numbers and number of nodes in s-direction are 58. Therefore entire area of the flume is covered by 236 numbers of unit surfaces, each unit area is defined as $\Delta s * \Delta n$. Engelund and Hansen transport formula is applied for sediment transport calculation. The coefficient for the secondary flow intensity is used as 0.75. Since the flume is in rectangular cross-section and the governing equations which are used in the numerical model is only suited for the mildly sloping banks, the artifice for the adapting vertical steep side wall is necessary. Equation (3.101) is used to achieve this purpose.

$$\frac{i_s h}{U} = \frac{h_0^2}{R_c} \left[1 - \left| \frac{2n}{W} \right|^q \right] \quad (3.101)$$

This equation is somehow added to the flow model from the early stage and controlled by 'q' value to decide whether this effect to be included or omitted. For this experiment q equal to 2, was suitable. The time step $\Delta t = 600$ sec and about 300 time steps are needed to reach the equilibrium condition. The result is found to be very good and it is presented in Fig. 3.28. This particular simulation has been selected here because it was found by Olesen, 1987 to be a particularly critical and difficult one to perform.



* This over-rides the input of the corresponding roughness used when setting up the river geometry if it is necessary.

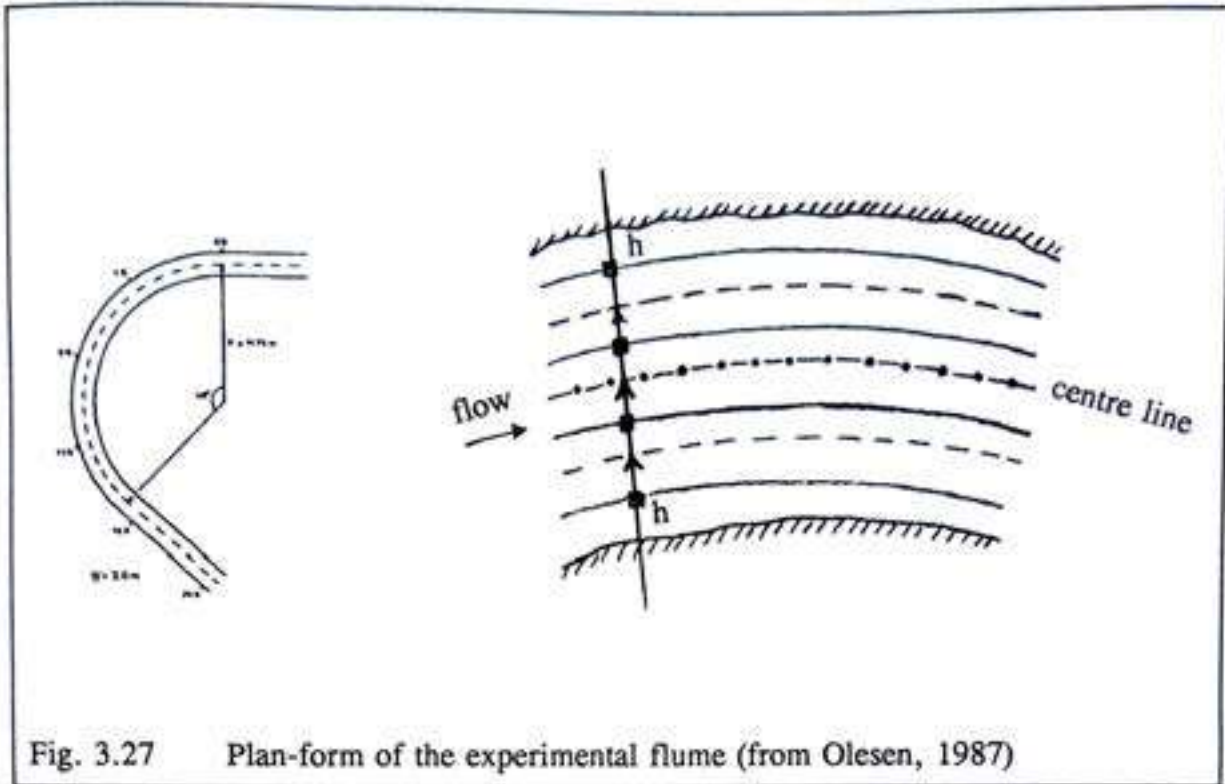


Fig. 3.27 Plan-form of the experimental flume (from Olesen, 1987)

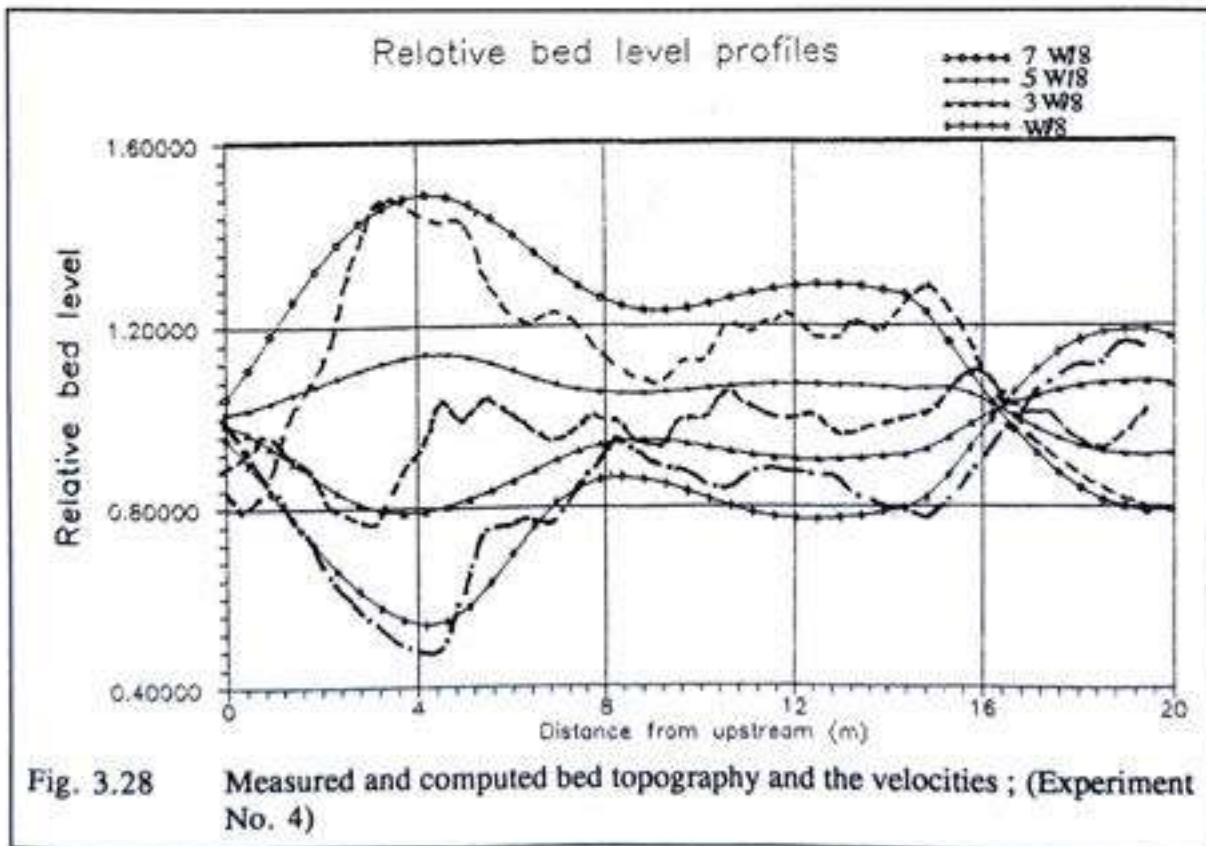


Fig. 3.28 Measured and computed bed topography and the velocities ; (Experiment No. 4)

3.11-3 The natural river situation

The application of the model to the natural river situation is very much different from the flume experiments. The main differences are as follow:

1. The steady flow condition is not well defined. Consequently, it demands a choice of a dominant discharge and water surface level. It is especially important to choose a representative width-to-depth ratio, as this has a large influence on the predicted bed topography. The discharge, in the sense of overall mean-flow velocity, has an influence only on the equilibrium bed topography through the term $f(\theta_0)$. On the other hand, the term $f(\theta_0)$ is used as a calibration parameter, and it influences the time scale at which bed level changes take place (through the sediment transport model, eqn.; $dh/dt = dS_1/ds + dS_2/dn + S_2/R$).

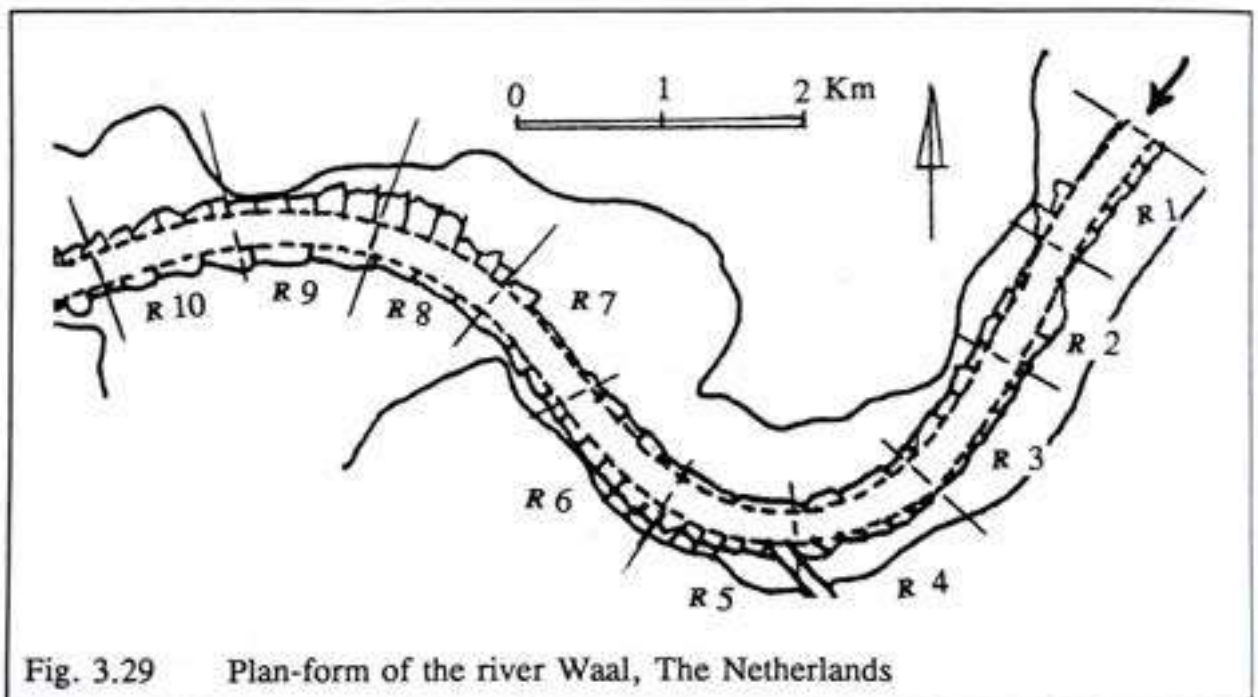
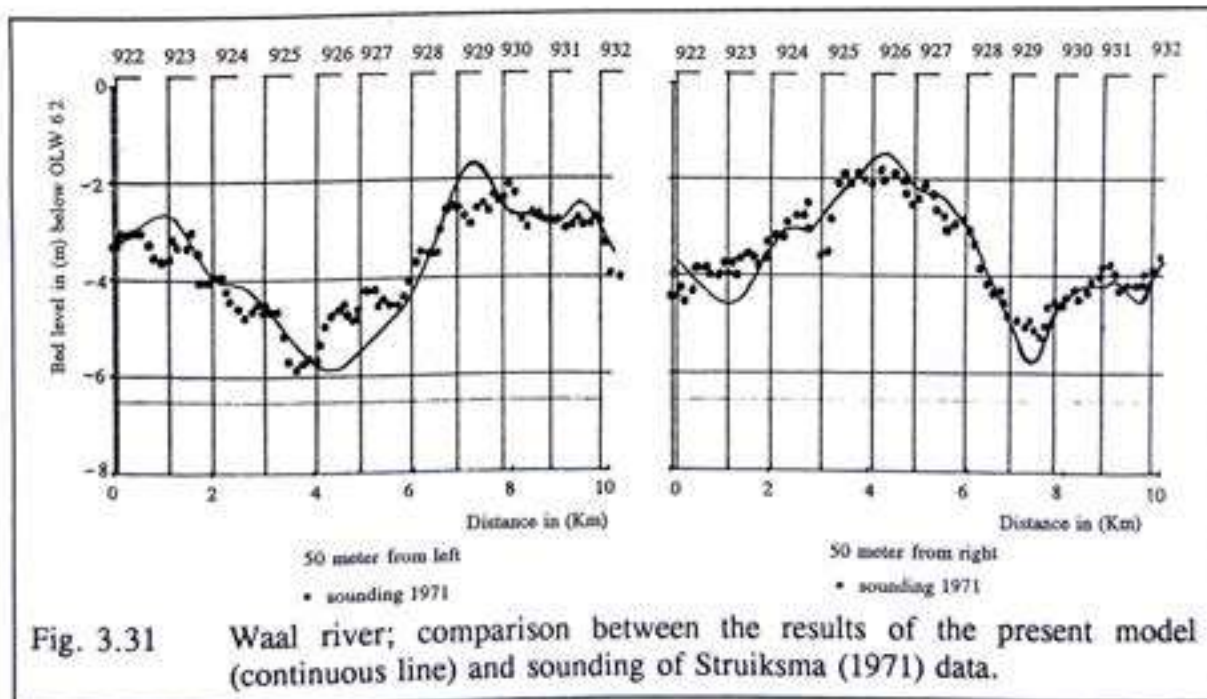
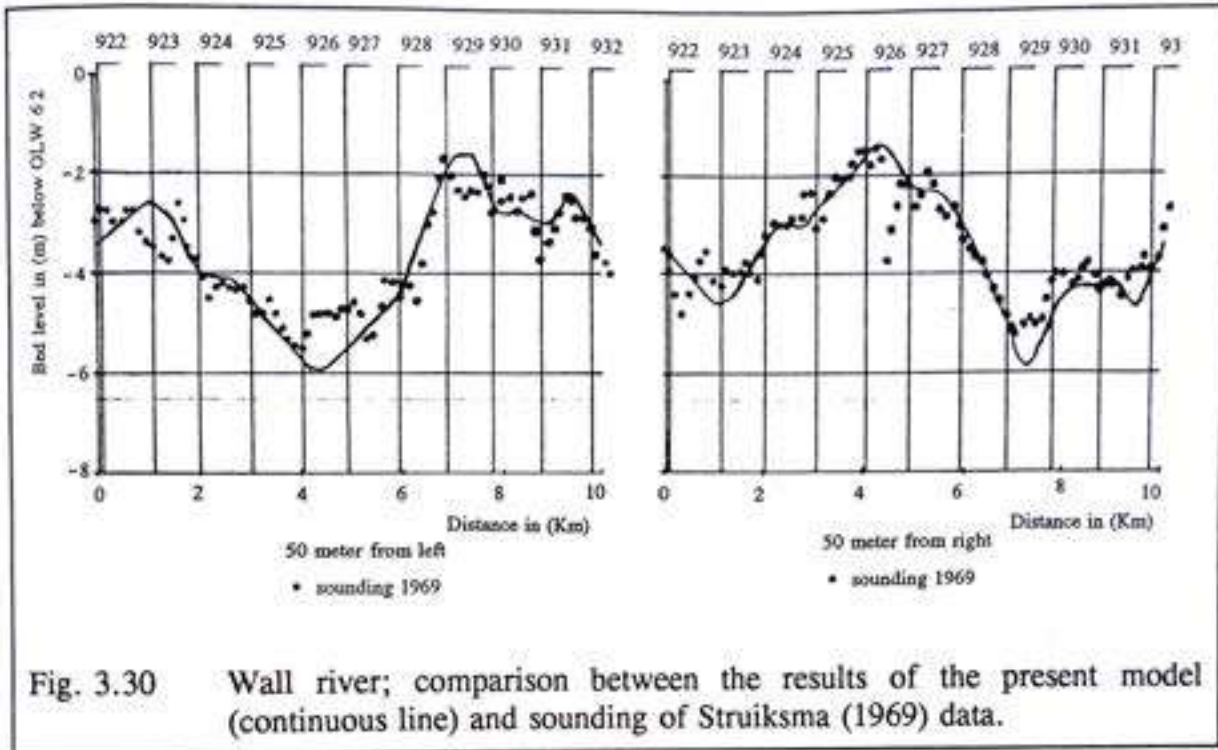


Fig. 3.29 Plan-form of the river Waal, The Netherlands

2. The plan-form of the river is not the shape of an alluvial container; instead is the alignment along the centre line of the thalweg. Therefore the plan-form varies with the width of the thalweg and the width varies along the river and with the water surface level. In the case of bank-full flow, it is rather easier compare to the form at low flow. In the case of low flow, the situation in which the survey took place, the point bars are not submerged. This implies that the curvature of the river axis is poorly defined.

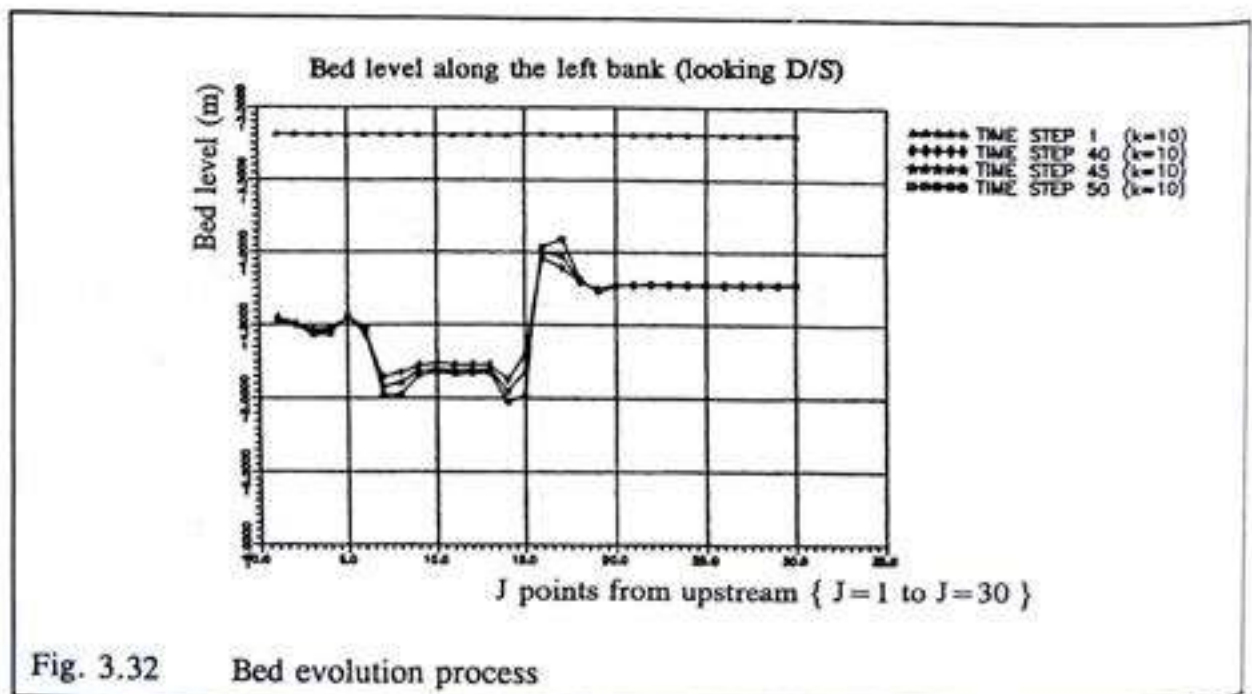


3. The river banks can very rarely be seen as vertical side walls. The vegetation cover both on the bed and the bank produces an extra friction factor, which corresponds to a non-alluvial roughness, influencing the flow distribution and consequently the sediment structure.
4. The grading of the sediment of the river bed influences the estimate of the roughness coefficient which has to be used in the simulations, and thus the total and local sediment transport rates. It thus has an influence the shape of the equilibrium bed topography.

3.12 Performance of the model

The application of the proposed model is tested in two cases. Case number one is using field observations in the Ishikari river in Hokkaido, Japan and case number two is tested on the trapezoidal cross-sectional shape of an arbitrary river. These can be considered as a calibration phase.

The temporal evolution of the bed topography has been simulated by the numerical model. The numerical routine repeats the calculations until the rate of bed level profile evolution becomes 'negligible'. The correct definition of the term 'negligible' is not obvious and may vary depending on the purpose of the simulation. Thus the convergence criterion will not be specified further until specific numerical experiments are discussed. Some example test runs which illustrate the general trend of the convergence criteria have been performed.



3.12-1 Case 1: Ishikari River, Hokkaido, Japan

The model is tested using field observations in the Ishikari river in Hokkaido, Japan, to be considered as a calibration phase. The river characteristics used for the computation are summarized in Table 3.2. The bed material and the sediment transported by the river flow are relatively coarse. Consequently, the bed topography is formed under a sediment transport regime which can be classified as being dominated by bed load.

Table 3.2 Hydraulic condition of test reach in Hokkaido, Japan.

Name of the river	Ishikari
Range of calculation (Km)	30 - 34
Average bed slope	1/4900
Flow rate (m ³ /s)	7200.
Manning's roughness coefficient	0.027
Average channel width (m)	150 - 250
Characteristic grain size (mm)	1.5
Regime criteria of meso-scale bed configuration	no bars

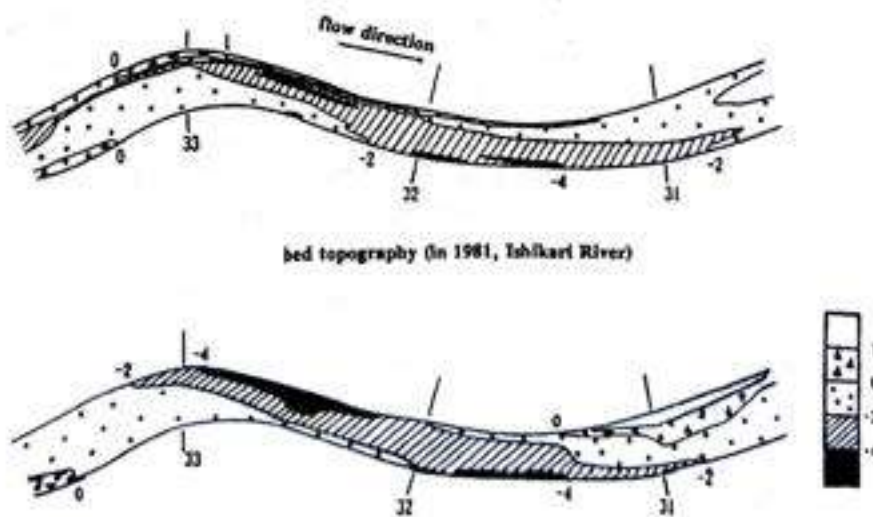


Fig. 3.33 The Ishikari river; the measured data of Shimizu, et al., 1987 (fig. above) and the simulated bed topography by the present model with avg. width of 200m (fig. below).

Fig. 3.33 shows a comparison of the bed configurations between the observed and the present model's calculated values, using the averaged width of 200 meter. For the comparison, the sounding data of Shimizu, et al., 1987 is used and it is seen that the performance of the present model is good.

3.12-2 Case 2: Hypothetical river with parabolic cross-section

Case number two deals with a 20 m wide hypothetical river with a straight leading part which is followed by a series of 175° bend and 275° loop as shown in Fig. 3.34. This experiment is carried out to test the model response to the shape of the channel. The philosophy of the self-formed alluvial rivers could be explained in a way that the flow exerts a shear stress upon the bed and banks, one 'adjusted' or stable form which the channel can assume is one in which the shear stress at every point on the perimeter of the channel is just balanced by the resisting stress of the bed or bank at each point. Consider, for example, a channel in uniform noncohesive sand at a constant discharge. In this ideal sand channel, at each point on the perimeter the resisting force due to the weight of the particle is just balanced by the applied stress. The maximum angle of the bank will approach the angle of repose, near the surface, where the shear stress provided by the flow approaches zero. As shear stress increases toward the centre or deeper part of the channel, the inclination of the side slope must decline. In the stable or equilibrium sand channel, the channel must be able to transmit the flow, the shear stress associated with the flow must equal that required for stability of the bed and banks. By equating expressions for these two stresses and expressing the tangent of the side slope as a differential or change of height with change in lateral distance, the resultant cross section has a shape close to that of a parabola. The essential point of this theoretically ideal cross section in the simplest stable channel with mobile bed and banks, two conditions must be satisfied simultaneously - the transmission of the flow and the stability of the banks. In this hypothetical condition a channel could not transport sediment because the required increase in stress would cause erosion of the banks. In actuality a natural channel not only carries sediment but migrates laterally by erosion of one bank, migrating on the average a constant channel cross section by deposition at the opposite bank. In this case the condition of no bank erosion is replaced by an equilibrium between erosion and deposition. The form of the cross section is 'stable', meaning constant, but position of the channel is not. This can be called dynamic equilibrium of the channel cross section in straight channels. In the case of meandering rivers, channel cross sections are asymmetric at bends. The appearance of the asymmetric cross section is expected to be double harmonic perturbation and channel width can still be constant and position of the channel is not. This hypothetical river is tested by the present model and the results are shown in Figs. 3.35, 3.36, and 3.37. As we have seen, the results are very satisfactory indeed while they have reproduced the expected behaviour as mentioned above.

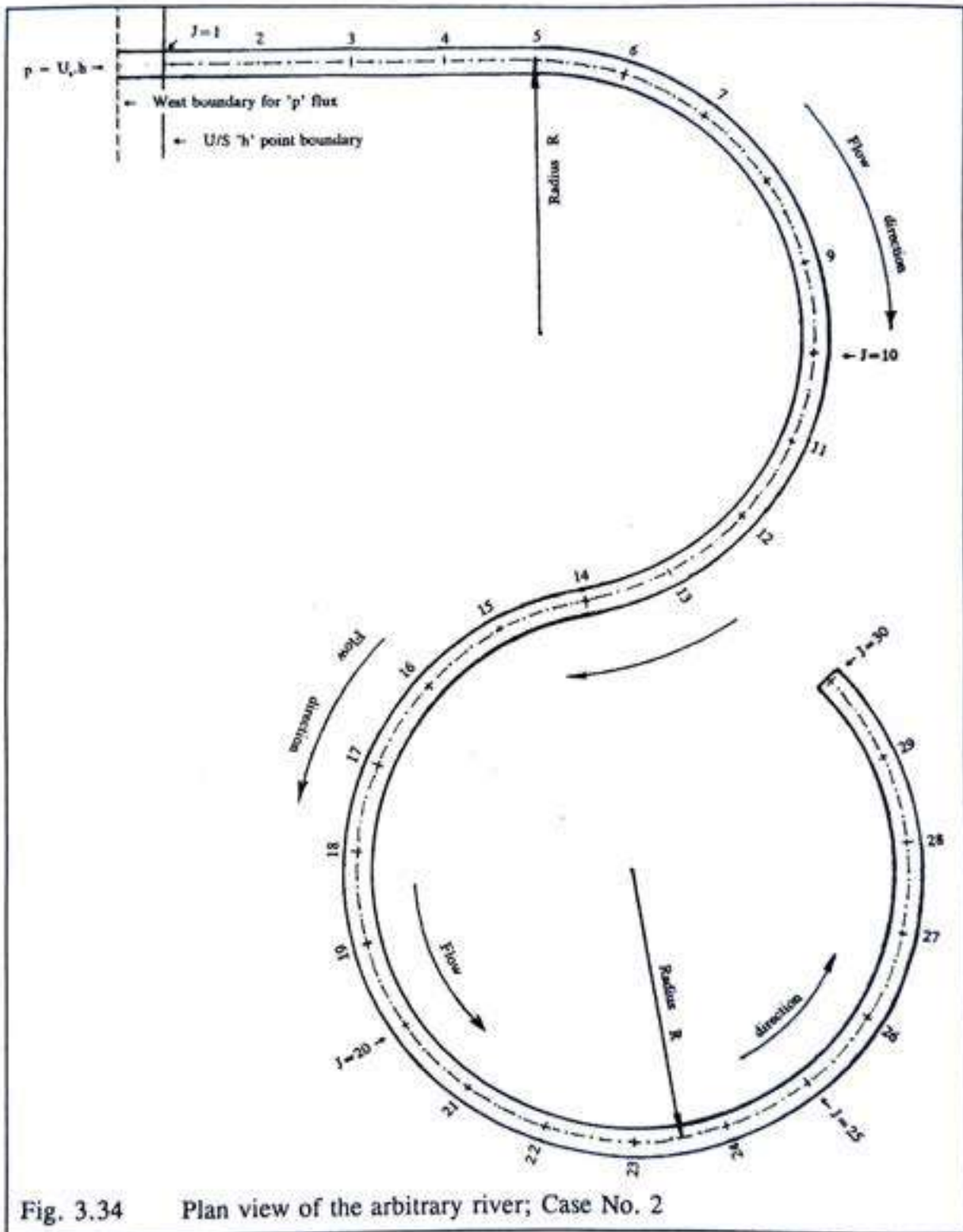
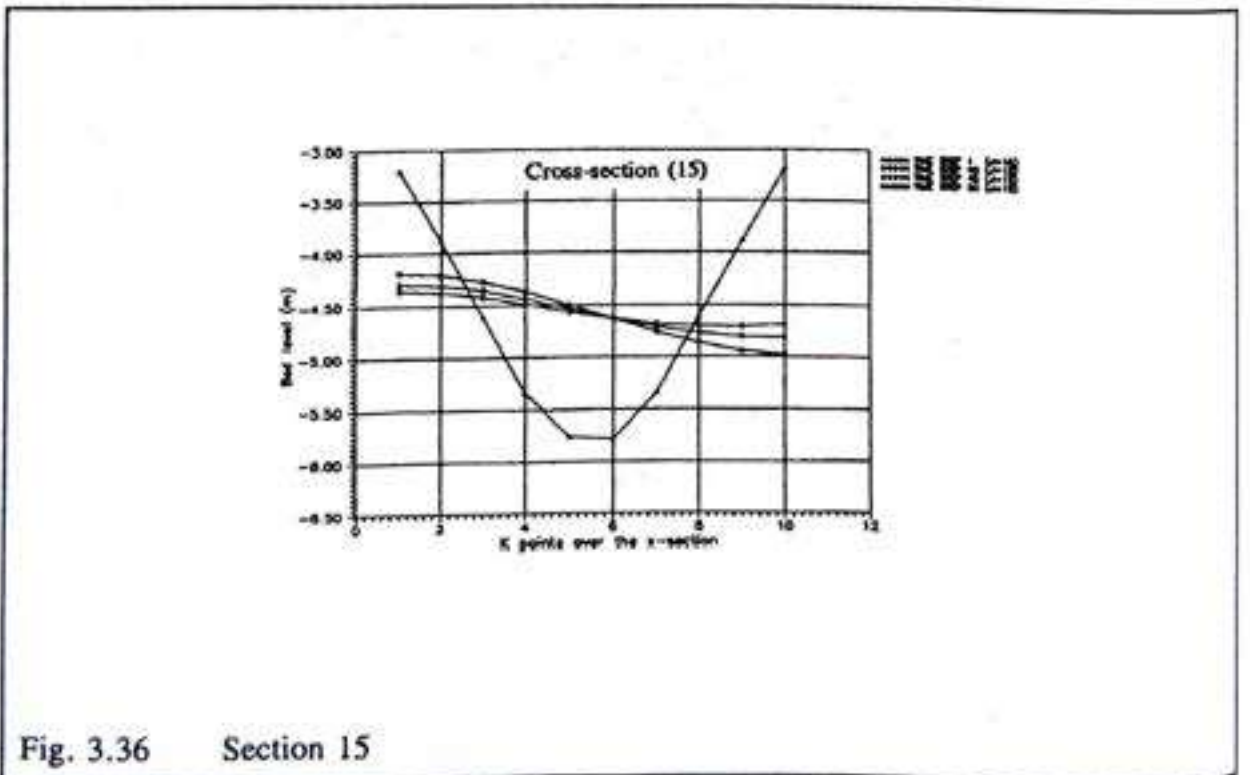
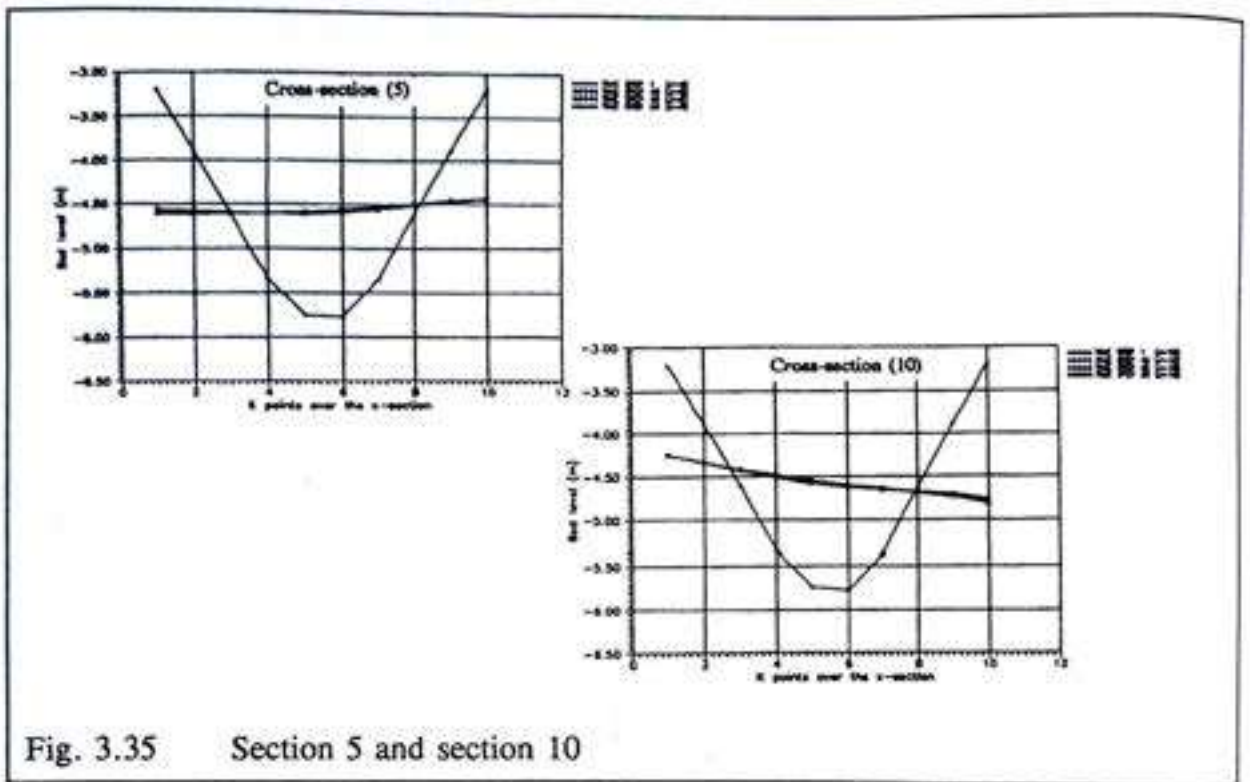


Fig. 3.34 Plan view of the arbitrary river; Case No. 2



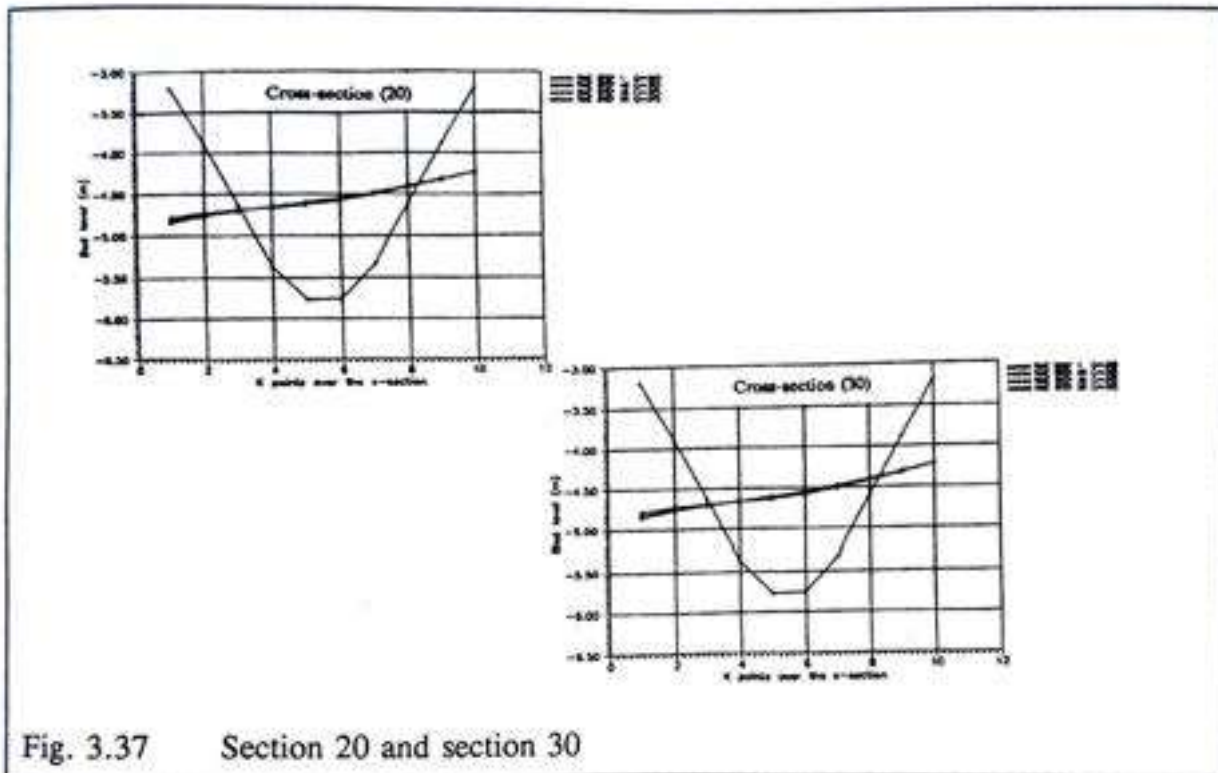


Fig. 3.37 Section 20 and section 30

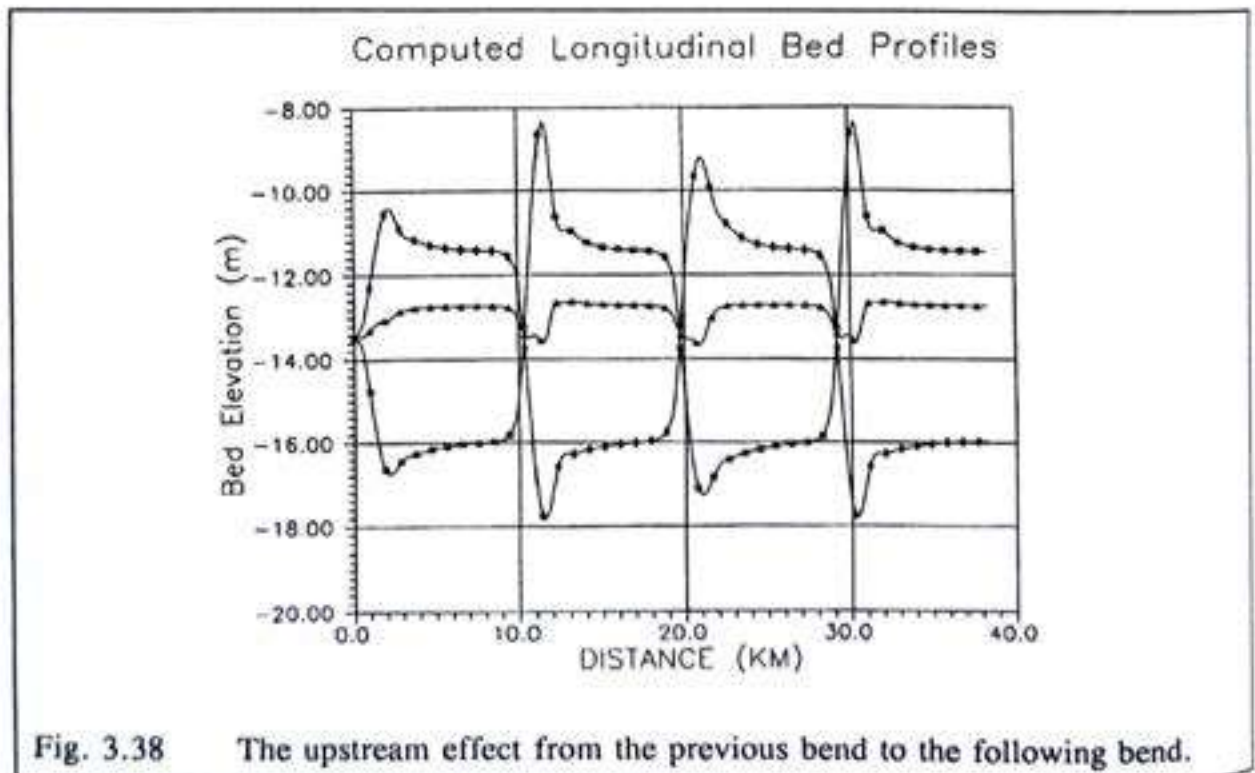
3.13 Conclusions

The model has been verified with flume experiments and natural river situations. It has been proven to be reasonably accurate with regard to the depth-averaged flow field and the resulting bed topography.

Concerning the bed evolution process in river bends, it can be concluded that the point bar and pool configuration of the equilibrium bed in curved alluvial rivers have to be attributed to a transition in channel curvature. This fact is proven in the verification of the model in the critical regions such as downstream of the entrance, the exit of a bend, and the region of the sudden change of the curvature or inflection points in the successive bend train. Only in a very long bend of constant curvature (eg. Fig. 3.34; Case 2), there will be a region (the fully developed zone) where transitional effects have damped out and the *classical* theory of river bend morphology holds good agreement with simulated bed configuration. i.e. the transverse shear force due to the secondary flow is balanced by the downstream gravitational force, whence the main flow and the sediment transport are parallel to the channel axis.

3.14 Discussion

Path of the sediment transport:: An attempt is made to trace the path of the sediment transport along the single stream line. There are two possible paths to form a point bar which is located at the inner bend, downstream of the bend apex. The first one is material entrained from the concave bank is caught in the transverse component and carried toward the middle of the channel near the bed. The vigorous crosscurrents near the bed in a bend can transport a considerable amount of bed material toward the convex bank. This is a part of the mechanism of point-bar building. If the location from which the bed material was derived is far enough downstream in the bend, such material is not carried across the bed to the other side of the channel but moves into the crossover without having crossed the channel. Once into the reversed curve, it is drawn toward the same bank from which is started. To trace this phenomenon, the single bend and a series of bends are simulated with the same hydraulic characteristics and the same bed material properties. Unfortunately, it has not been possible to explain the path of the sediment movement cannot be clearly explained from the results of the simulations. However, the cyclic order of curvature effect from the previous bend to the following bend is clearly noticed, see Fig. (3.38).



The secondary flow convection factor:: The model shows that simulation results using the fixed secondary flow convection factor across the width of the river agree with the measurements along the outer wall while it is somewhat underestimated along the inner wall. On the other hand, if the simulated results fits with the measurements along the inner wall, it will differ from the measurements along the outer wall. The last and the most laborious trial is introducing the theoretical value of the secondary flow convection factor at the convex bank while introducing the double magnitude of the factor at the concave bank; it was introduced gradually over the river width from first value to the second.

The choice of grid size:: The choice of grid size depends partly upon the amount of local geometry detail that is to be included, and partly upon the computing cost; often a compromise has to be made between these two factors.

Some sources of discrepancies and proposed treatments:: Since the nature of the present model is physical-based numerical model, sources of discrepancies are both physical and mathematical. In addition, the existence of numerical effects are unavoidable. The numerical scheme and the integration method are chosen in favour of efficiency and economy, the consequent-short-comings are accepted without any further investigations. To improve the quality of the model the proper mathematical expressions which can represent the physical phenomena as precise as possible is necessary. For this purpose the following issues are considered and the corresponding treatments are applied in the present model.

1. The channel width used in this study is an average of many repeated measurements (or at least it is being considered in this way) made from the topographic maps from which the centre-line is defined as the middle of two bank lines. Therefore, the width used to normalize the other variables is generally somewhat smaller than the bank-full value.
2. Inaccuracies in transport predictors and roughness predictors cause inaccuracies in the numerical model. These predictors are based on a steady uniform flow. There is already a potential source of errors in applying these predictors in a model with (unsteady) and non-uniform flow. (Note. The present model has an assumption of quasi-steady water motion.)
3. Boundary shear stress and sediment transport
Many scales of resistance contribute to the total boundary shear stress.
4. The present model yields satisfactory results in cases of bed configurations deviating from a flat bed. However, the influence of the side walls must be taken into account. The description of the flow field near the sidewalls raises many problems, both physical and mathematical. The physical problems can be named as those of turbulence modelling and the others can be mentioned as the computations of laminar, axisymmetric flows.

3.15 Continuation

So far the simulation of the bed topography in an alluvial river bend gives satisfactory predictions and other information about the various sizes of river bend, including an infinitely long bend train. At this point, however, an important question arises. That is, on what basis one can say definitely that a river will change its plan-form. If it will change, in what way will it shift, and with which pattern; (eg. lateral movement, downward movement, or a combination of these). Of course, since we are concerned about the instability of the river, the inseparable phenomena is the stability of the river. Strictly speaking no flowing river is completely stable, but it does have an equilibrium condition, which is the result of a balance between different processes involving both erosion and deposition within the meso-scale time-span. This equilibrium condition can last momentary, or some years. If it may in certain singular cases endure for a couple of decades, it implies the river is not actively changing its plan-form for a certain time-span. Therefore to be able to distinguish between these two is prime important for the continuation of the present study.

"Genuine observation shows plainly that river flow seeks the greatest inefficiency that still permits action"

Crickmay, 1974.

4. A HEURISTIC APPROACH TO THE DETERMINATION OF AN OPTIMUM RIVER WIDTH

4.1 Theoretical background of self-formed alluvial rivers

The general and elusive problem of river regime or alluvial channel stability is the prediction of the self-formed active bed and banks of an alluvial river. A common formulation (Henderson, 1966) is reached by ignoring plan geometry and through attempting to resolve relationships between six variables, i. e. water discharge, sediment discharge, sediment size, channel width, depth, and slope. Of these, three are specified, and three governing relationships are therefore required for a solution.

One main approach to the problem employs equations to describe the dominant processes, notably sediment transport, flow resistance, and bank stability. Some attempts to characterise bank stability have been made (Parker, 1978; Fredsøe, 1978; Ackers, 1980), sometimes assuming the constancy of total sediment concentration in a stable channel.

The other main approach that associated with the various Extremal Hypotheses. There are in fact five extremal hypotheses that have been applied to sand and gravel bed rivers. Theoretical justifications for the hypotheses, where they exist, are discussed elsewhere (see, for instance, Davies and Sutherland, 1983 and Griffiths, 1984) and remain a subject of continuing debate. In this paper, attention is restricted to one of the five Extremal Hypotheses which is that of the Maximum Sediment Transport Capacity (MTC).

4.2 Present study

The present study aims to extend the present knowledge concerning an MTC channel width for meandering rivers. The main objective of this study is to discover whether an MTC solution exists in meandering rivers, and, if it does exist, whether the width of a meandering river can define an arc length as a unique function of channel width, which in turn is a means of characterising the bank stability.

Based upon studies of these three existing theories, namely,

- (1) the principle of maximizing the sediment transport capacity (or) the hypothesis of maximum transport capacity (MTC) channel width (see 4.3);

- (2) flow resistance in alluvial rivers, considering friction conditions in both straight and meandering rivers (see 4.4);
- (3) shape and dimensions of the stationary dunes in a straight river (see 4.5);

the following further elaborations and developments have been carried out:

- (4) Development of a mathematical model providing the shape and dimensions of the dunes and roughness predictor model for an alluvial river.
- (5) The advancement of theoretical consideration concerning the calculation of roughness factors for three sets of specified variables i.e. discharge, slope and the characteristic properties of the bed materials.
- (6) Coupling the roughness predictor model to the numerical model which simulates the flow and bed topography in a meandering river.
- (7) Analysis of the improvements in total sediment transport capacity due to the modification of roughness after the first and second improvements in the numerical model simulations.
- (8) Development of an analytical model to predict the equilibrium transverse bed slope of a meandering channel for the purpose of completing the study range of width-to-depth ratio between 0.1 and 15.
- (9) Calculation of a maximum transport capacity channel width for both straight and meandering rivers; the width to depth ratio studied ranges from 0.1 to 200.

Particularly in item (5), new theoretical relationships are proposed.

Some insight into the main objective and a method for coupling the numerical simulation model, which simulates the bed topography in a meandering river, are gained. The maximum transport capacity (MTC) channel width can be predicted from the function of slope for a given representative diameter of bed material (see fig. 4.18), or from the function of representative grain diameter of bed material for a given slope (see figs. 4.19 and 4.20).

Finally the existence of the MTC solution in meandering rivers is found. It can be concluded that the width of a meandering river may define an arc length as a unique function of channel width for three specified sets of variables namely of discharge, slope and the properties of the bed materials.

4.3 Maximum transport capacity (MTC) channel width

The notion that sediment load attains a maximum at some particular width for three specified variables i.e. discharge, slope, and the properties of the bed material, is not at all new. It was first proposed by Gilbert (1914) on the basis of results from his flume experiments. Chang(1979, 1980) and White et al. (1982) discovered the same phenomenon by iterative computer analysis. Ramette(1979), Chang(1979,1980a,1980b) and White et al.(1982) have proved the existence of the MTC state in their analyses. Carson et al.(1987) confirmed the existence of the MTC solution from four analyses.

WRTC

Water, Research and
Training Centre

4.3-1 Problems in previous studies

Previous studies were based on three assumptions specifying channel shape, a sediment transport law, and a resistance law that allows the elimination of the unknown depth term in the transport law. Recently Ferguson (1986) commented that an MTC solution fails to emerge when the Einstein-Brown transport formula is combined with the Manning-Strickler resistance equation. Carson et al.(1987) found as a limitation of the MTC solution that an optimum width will not occur when $c < m$, in which c is a power of flow depth in Manning's formula and m is a power of effective shear stress in the transport formula.

4.3-2 Possible solution to these problems

Taking into account these previous studies, it is clear that the key to solving the problem is to obtain a unique water depth for a certain (flow and bed) condition. Consequently, a determinate solution of channel roughness is essential.

4.4 Flow resistance in alluvial rivers

There are three types of resistance in alluvial rivers. The first type is skin friction, caused by the roughness that is, in turn, determined by the size and character of the material in the bed and banks. For a given roughness, the amount of resistance varies with the square of the flow velocity. The second type is an internal distortion resistance, caused by discrete boundary features such as bank protuberances, bends, bars, individual boulders, and dunes that set up eddies and secondary circulations. Resistance from these features is also proportional to the square of the mean flow velocity. The third type is spill resistance, where energy is dissipated by local waves, and by turbulence caused when a sudden reduction in velocity is imposed. Spill resistance is associated with local high velocities, as when water backs up behind an obstruction and spills into lower velocity flow. Blocks of bank material slumped into a channel cause such spills, as do some channel bends of tight curvature. In a natural stream these individual resistance types cannot be measured. The total dissipation, however, is indicated by the longitudinal profile of the stream.

The variables determining the resistance to flow are numerous. Major variables can be categorised into four groups, as follows:

- (1) flow variables such as velocity, depth and energy slope of the flow, and seepage forces in the bed of the channel
- (2) physical properties of water, such as density, and apparent dynamic viscosity
- (3) physical properties of the sediment, such as density, representative diameter of bed material, standard deviation of the size distribution of bed material and the shape factor of the particles
- (4) geographic parameters such as the shape factor of the channel reach, the shape factor of the channel cross section, the gravitational accelerations which are introduced through the flow resistance at the reach-averaged level as an integrated resistance.

Previous attempts to predict the flow resistance can be broadly divided into two categories: (a) those which deal with *the integrated resistance* offered to the flow using either a logarithmic or power type relationship for the mean velocity and (b) those in which the total resistance is separated into *the grain roughness* and *the form roughness*. The latter is meant for the small scale or one-station geometry resistance excluding shape factor of the channel reach and the cross-section. After Yalin (1964), an analytical expression for the roughness factor in terms of the geometry of the bed undulations and the sediment size is proposed. The expression was derived by summing the grain roughness with the form roughness obtained by treating the flow in the lee of the undulations as a case of sudden expansion. The practical utility of this approach mainly depends on the geometry of the bed undulations. The total resistance of the flow and the roughness factor can be predicted by various formulae. There are at least 37 of these which have been proposed by various authors from Chézy (1769) to Şentürk (1973).

4.4-1 Friction conditions in a straight alluvial river

The friction condition in a straight river is mainly a function of skin friction and the form friction of the bed forms. Low water discharges produce very rugged arrays of ripples and dunes on the bed, which give rise to large friction factors. High river flows, on the other hand, obliterate the bed forms and move over flat beds whose roughness approaches the irreducible minimum. There is also a considerable range of experiments which shows that the bed-form roughness responds in much the same way to sediment discharge or concentration.

The river channel roughness, far from being constant, varies widely with both water and sediment discharge. The friction factors of many natural streams vary by factors of two or more (in terms of Chézy's coefficient), and are more variable than depth or velocity. This is because forms and dimensions of bed roughness, the sediment concentration and the flow

condition are all interrelated. Correspondingly, this interaction poses great obstacles to the mathematical formulation of natural streams.

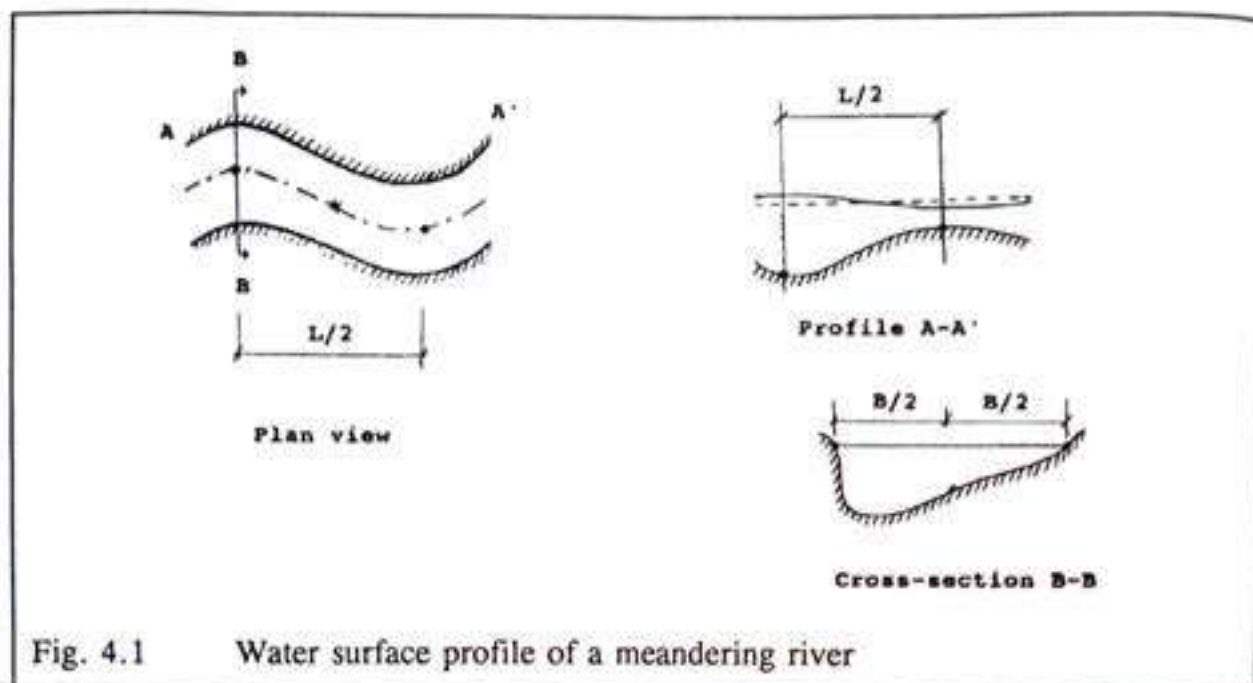
4.4-2 Friction conditions in a meandering river

The friction condition in a meandering river is determined by the skin friction, the form friction of bed forms and the plan geometry. Plan geometry produces extra boundary features which also govern the friction conditions of the meander. The meandering river consists of a series of deep pools in the outer part of the bends associated with point bars in the inner part of the bends and shallow crossings in the short straight reaches connecting the bends. The pools tend to be somewhat triangular in section with point bars located on the inside of the bend. Secondary currents occur in this section. In the crossing, the channel tends to be more rectangular, widths are greater and depths are relatively shallow. Therefore the velocity distribution is different from that occasioned by straight flows. Point bars and pools are additional boundary features and, in addition, dunes and ripples occur at the lower flow regime.

Skin friction is mainly calculated as being of the order of magnitude of the representative diameter of the bed material. In the bend, both longitudinal and transverse sorting occurs. Therefore, the composition is different on the inner side of the bend compared to the outer side. The dominant grain diameter at the pool is always greater than that of the point bar.

Another factor which affects the friction factor variation in the transverse direction is the water surface slope. The slope of the water surface is a direct measure of the energy exchange when there is no velocity change at a point (steady flow) and when there is no change in velocity with distance along the channel (uniform flow). For a certain location of the river reach, the water surface slope is more or less constant over the cross-section in a straight river, but this is not the case for a meander (See fig. 4.1). The slope of the water surface in a meandering channel varies in the transverse direction even if the flow is assumed to be steady and uniform. The slope is steeper on the inside of the bend and is milder on the opposite side. Moreover, it also changes in the longitudinal direction when water passes through the series of pools and point bars.

In summary, water depth, water surface slope and velocity distribution vary in both the transverse and longitudinal directions. Bed material composition and dominant grain size vary similarly. Moreover, the width of the active channel along the thalweg varies in the longitudinal direction. Therefore the friction factor is a variable parameter over the entire reach of the meandering river. Thus it seems inappropriate to use a constant value or a cross-sectional average value for those cases which require accuracy.



4.5 Shape and dimensions of stationary dunes in alluvial rivers

A deterministic solution for the roughness/friction factor is possible, because resistance to flow in alluvial channels depends on the geometry of the bed patterns that are formed by the flow, the properties of the sediment, and the transport rate of sediment. Suspended load and its concentration is of major importance due to the fact that bed forms are very significant for values of the dimensionless bed shear stress between about 0.04 and 0.8. In that region the amount of suspended sediment is much larger when the bottom is covered by ripples and dunes than when the same flow conditions influence a smoothed bottom, which incidentally after some time will be changed into a stable bed form. To be able to determine the roughness factor in an alluvial river, knowledge of these parameters is of decisive importance.

Fredsøe's (1982, 1985) method (see appendix B) provides the geometry of the bed patterns from a knowledge of the flow parameters, the suspended sediment load and the bed load. Details of the method can be found in Fredsøe, (1982) and lecture notes by Fredsøe, (1985). The accent is on the mass flux ($q = U \cdot h \text{ m}^2/\text{s}$) as this determines the sediment transport. The total load is split up into a bed load and a suspended load. The calculated bed load, suspended load and their gradients with respect to the dimensionless shear stress are introduced into the dune dimension formula and the dune dimension is calculated. The shear stress due to the form friction is then calculated.

Finally, the total shear stress is calculated and converted to an actual water depth corresponding to the prevailing situation. There is only one depth corresponding to a given situation and another cannot be assumed. As mentioned above, obtaining a unique water depth makes it possible to predict a channel roughness. This method determines automatically

the regime of the flow according to the knowledge of the dune's dimension (eg. for a plane bed situation the dune height to length ratio tends to zero). The Reynold's number is used as a guide to distinguish between ripples and dunes.

4.6 Development of the roughness predictor model

The shape and dimensions (length, height) of sand dunes in rivers are calculated by use of the bed shear stress distribution downstream of a rearward-facing step. The transport of sediment is split up into bed load and suspended load, which makes it possible to explain the transition to a plane bed. The model can predict flow-resistance in alluvial streams (Fredsoe, 1982). In order to transform the theory into a mathematical model, the following operations have been carried out.

For the first step of the calculation, the river bed is assumed to be plane, i.e. no sand wave is present at the bottom. In this case the bed roughness K_p is approximately (2.5 times d_{50}) in which d_{50} is mean grain diameter. The flow equation, the resistance equation (Colebrook-White) and the bed shear stress equation can be solved simultaneously by using three specified variables i.e. discharge, slope and roughness K_p . Thus water depth, shear parameter, and bed shear stress are calculated for the plane bed situation. According to the Engelund (1967) similarity theory, "In the particular case, where the stream bed is covered by dunes, only a certain part of the total shear is effective in the sediment transport process". That is, only the shear stress due to the skin friction, the magnitude of which is the same as bed shear stress in the plane bed situation, is effective. It is because of this that the sediment transport can be calculated.

Further, the sediment transport is split up into two parts and calculated as bed load and suspended load. Engelund and Fredsoe's equation is used for the bed load transport. For suspended sediment transport, it is rather difficult to apply an integration procedure because of the integral form which consists of vertical velocity profile and eddy viscosity distribution over the vertical plane. The basic principle of Einstein's (1950) graphs are adopted (see Appendix B). The evaluation of the integral of suspended sediment load equation is greatly facilitated by these graphs, but these are of course of little or no help in computer calculations (Deigaard, 1980). Therefore, in addition, Deigaard's models (see appendix B) for the vertical velocity profile and eddy viscosity distribution over the vertical plane are adopted in this computer model. Since the two-dimensional model in curvilinear coordinate system has been developed in such a way that the width of the river is split into many strips (sub-channels), forming a compound channel composed of many sub-channels, Deigaard's models are applied at each strip across the river. The suspended sediment load is calculated in this way.

Also the rate of change of bed load with respect to the bed shear stress and the rate of change of suspended load with respect to the bed shear stress are calculated. The dimension of the dune is calculated by the use of a bed shear stress distribution downstream of a rearward-facing step. As shown in section B-1 appendix B, the length and height of the dune are functions of the bed load, the suspended load, and the gradients of the loads.

After obtaining the dune dimensions, the dimensionless shear stress due to the expansion loss can be calculated through the ratio between it and the dimensionless shear stress of the plane bed. This ratio is a function of the dune height, the dune length, and the ratio of the mean velocity to the friction velocity due to the skin friction.

It should be mentioned that the ratio of mean velocity to the friction velocity due to the skin friction is taken from the plane-bed condition. To be more precise, U_d/U_{fp} should be determined by the equation:

$$\frac{U_d}{U_{fp}} = 6. + 2.5 \ln \left(\frac{h_p}{K_d} \right) \quad (4.1)$$

$$U_{fp} = \sqrt{gh_p I} \quad (4.2)$$

in which

U_d	=	mean velocity of the prevailing condition (dune-covered bed)
U_{fp}	=	friction velocity due to the skin friction
h_p	=	water depth corresponding to the plane bed situation
K_d	=	total roughness (dune-covered bed)
g	=	acceleration due to gravity
I	=	water surface slope

but because U_d and h_d are unknown this requires a complicated iteration procedures and the introduction of a further assumption. The assumption is that, instead of the ratio U_d/U_{fp} , the ratio of plane bed U_p/U_{fp} can be used because small deviations in water depth do not change the value of U_d/U_{fp} . However it is not justified in the case of a constant discharge accompanied with given slope and grain size diameter, the difference between these two ratios are presented in Fig. 4.2. Therefore further improvements are made in following section 4.7.

Besides this particular assumption, which has been improved in section 4.7, the total dimensionless shear stress is calculated as the sum of the dimensionless shear stress due to the expansion loss and the dimensionless shear stress of the plane bed. After obtaining the total shear stress, the water depth is deduced. Then the new water depth and the corresponding water discharge for the prevailing situation are updated. In this process, the total roughness can be found from the Colebrook and White resistance equation.

The necessary physical parameters for the model are the unit discharge, the width of the river, the water surface slope, the mean grain diameter, the fall velocity, and the grain size distribution curve.

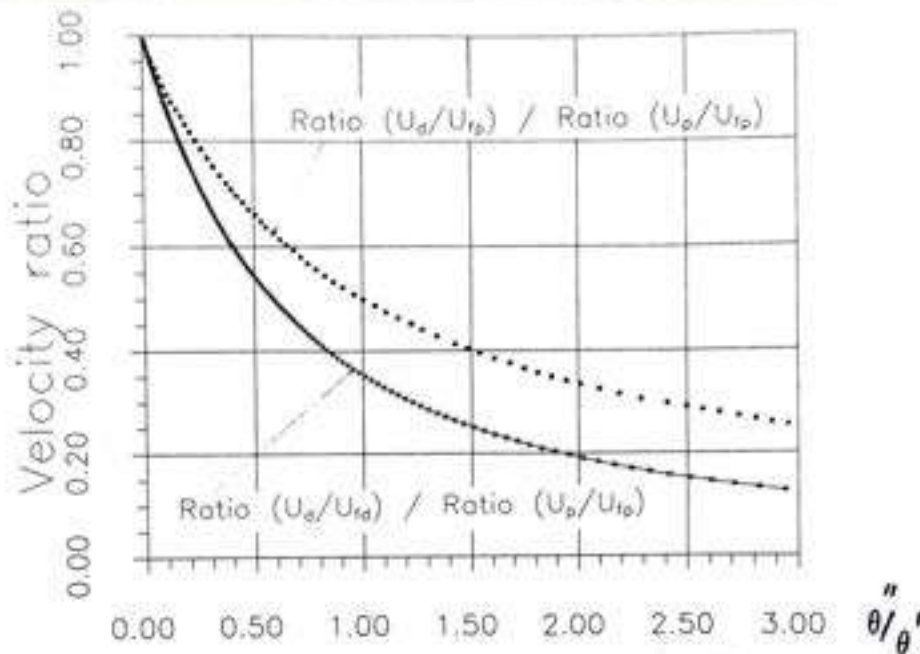


Fig. 4.2 The differences between velocity ratios involved in the calculation of the roughness factor in an alluvial-river bed

4.7 Theoretical considerations for the roughness factor

The development of the mathematical model for the shape and the dimensions of the dunes and the roughness predictor model is described in section 4.6. Here theoretical considerations for the calculation of the roughness factor for the three specified variables of unit discharge, slope, and the properties of the bed materials are made. The assumption that leads to the use the velocity ratio (U_p/U_{fp}) for the plane bed instead of U_d/U_{fp} is not justified for the case of constant discharge accompanied with a given slope and sediment grain diameter - which is exactly the situation holding in the bed topography model of meandering rivers (see Chapter 3). Consequently, two features are introduced that do not enter into the existing theories.

- (1) The existing theories allow the discharge to be varied from a plane bed to a dune phase due to the fact that most theories were verified with experiments. It is impracticable to make experiments with different regimes under the same magnitude of discharge and slope. Therefore experiments are made for the plane bed and the dune-covered bed separately, but in order to investigate an interrelating phenomenon between the two different regimes, the mean flow velocity is kept constant for the corresponding experiments. The result is the change in hydraulic radius. Thus the discharge is varied. However in the corresponding calculations, some have used an assumption as described in 4.6 that the ratio of mean velocity U_d and the friction velocity due to the skin friction U_{fp} is taken from the plane bed condition. Instead of the ratio U_d/U_{fp} , the ratio U_p/U_{fp} of plane bed is used as an approximation. To be correct,

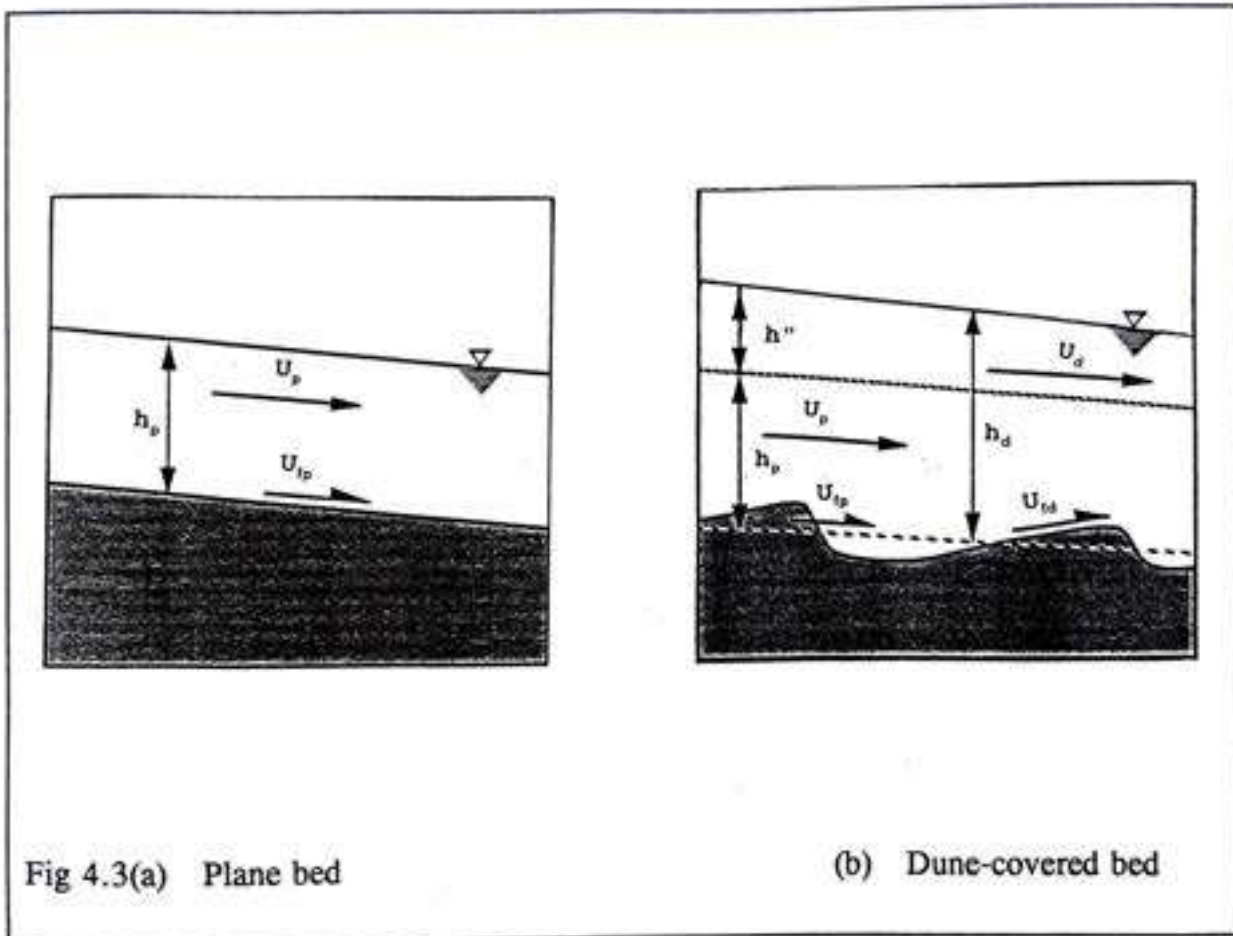
U_d/U_{fp} should actually be determined by the equation (4.1). However, since U_d is unknown, this has required complicated iteration procedures. The resulting calculation was previously nearly impossible to carry out without a computer utility.

- (2) Consequently the calculations start with the discharge under plane bed condition and, after water depth has been calculated for dune phase condition, the corresponding discharge for the dune phase condition is always found to be 2 to 3 times greater than it was under the plane bed condition for a given flume. The calculation cannot be done reciprocally starting from a prevailing discharge of a dune covered bed. Therefore, according to the existing methods, the calculations are always made in one direction only, namely from the plane bed to the dune phase.

The existing methods are applicable as far as plane bed and dune phase situations are calculated with different corresponding discharges in a one-way direction, because small deviations in water depth do not change the value of U_d/U_{fp} since the mean velocity is kept constant.

However, the roughness predictor model which must be calculated at the same computational points and with the same initial and boundary conditions as the numerical simulation model (see Chapter 3) which simulates the flow and bed topography in a meandering river, has to be developed under two constraints. In the first place the water discharge should be the same both before and after the roughness has been updated. In the second place, the discharge which is present in the current simulation time step should be representative of the prevailing condition. Consequently, the approximation of the velocity ratio $U_d/U_{fp} = U_p/U_{fp}$ of plane bed cannot be used and the calculation procedure has to be reciprocal. This means that the calculation of the real roughness predictor should be able to start from both conditions, namely the dune-covered bed and the plane bed.

Initially during the process of development, attempts were made to approximate U_d/U_{fp} in many ways and each value was introduced into the computation by iteration methods the two water discharges, corresponding to before and after the roughness update, converged. After many trials and errors with different numerical filters, it was found that the implementation could not be achieved by computer iteration methods only. For example, to achieve convergence by using different filters for a specified discharge, the more powerful the numerical filter, the greater are the errors in the physics. This is because it is so vital to keep an accurate value of the definition of U_d/U_{fp} . Consequently the following theoretical considerations and calculations are introduced.



$$\begin{array}{ll}
 U_p \neq U_d & Q_p = Q_d \\
 U_{bp} \neq U_{bd} & l_p = l_d \\
 h_p \neq h_d & d_{50} = d_{50}
 \end{array}$$

The condition between case (a) and (b)

The important parameters such as the mean velocity, the friction velocity, the water surface slope (or strictly speaking the energy slope), and the friction factor are each split into two parts. For example, the water surface slope is implicitly composed of the two parts of the river surface slope, namely (1) the grain-influenced slope and (2) the form-influenced slope, as shown in Figs. 4.3(a) and (b).

The integrated roughness factor is simulated by the computer program for both plane bed and dune-covered bed conditions as shown in figures 4.3(a) and (b). The results are presented as a family of curves. One family of curves serves as a graphical solution for a given discharge, slope and, the properties of bed material for the maximum range of water depths, for example those of Fig. (4.4). For several slopes and different grain sizes a large number of families of curves are produced. These are family of paraboloids the focal lengths of which vary with the discharges.

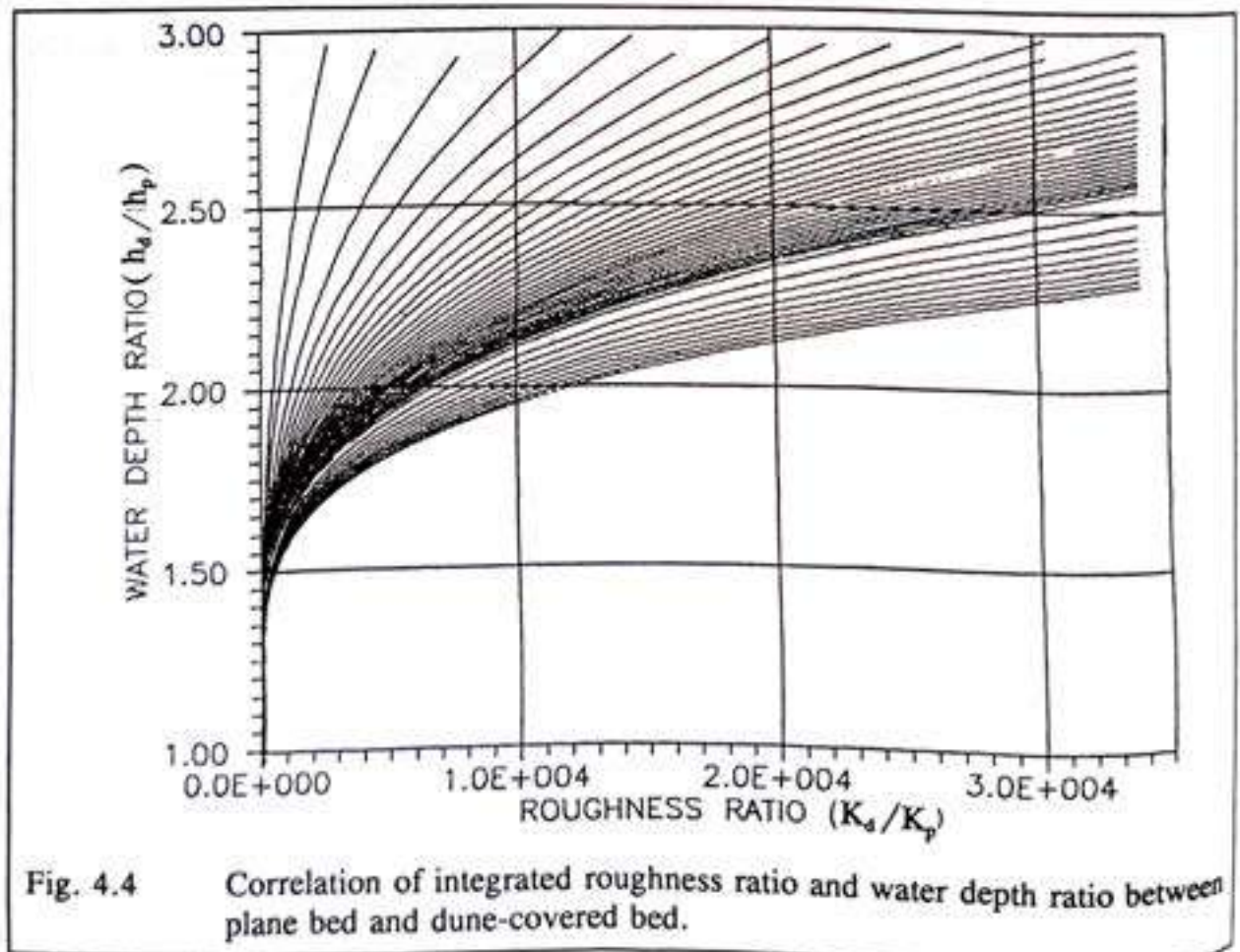


Fig. 4.4 Correlation of integrated roughness ratio and water depth ratio between plane bed and dune-covered bed.

The other parameters such as the total dimensionless shear stress, the dimensionless shear stress due to the skin friction, the friction factor, and the friction velocity are simulated similarly. Therefore the relationships between each parameter mentioned above and the shear parameter are found for both conditions. To find the dimensionless ratios of the parameters for two different conditions, the corresponding value of each parameter in the dune-covered bed case is divided by the corresponding value of each parameter in the plane-bed case (see figs. 4.5 and 4.6). These dimensionless ratios of the parameters are used to draw up the general relationship shown in Fig. 4.7.

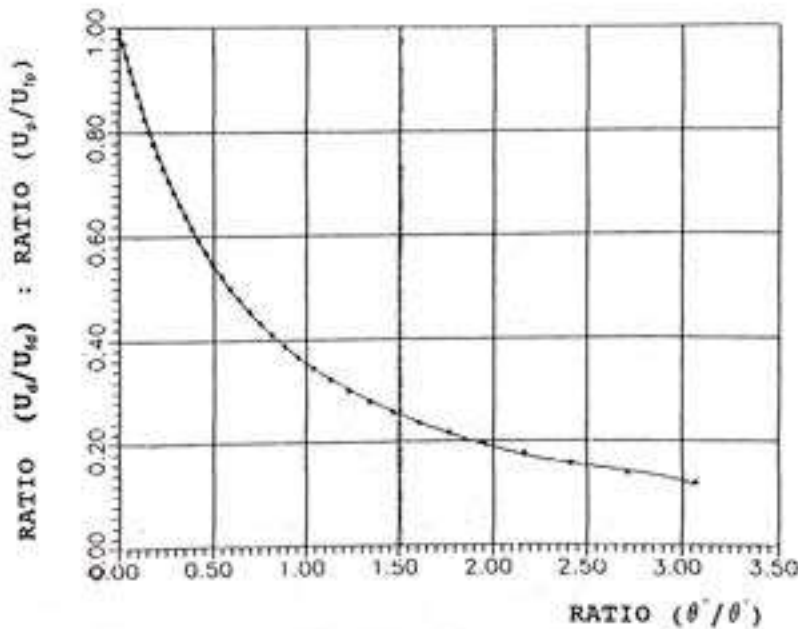


Fig. 4.5 Correlation of dimensionless shear stress ratio and mean velocity to friction velocity ratio in dune-covered bed and plane-bed condition

From the over all picture of the simulation results, a general relationship between the plane bed and the dune-covered bed is found for a constant discharge and energy slope combination (see fig. 4.7). Fig. 4.7 gives the U_d/U_{fd} ratio in terms of the U_d/U_{fd} and U_s/U_{fp} ratios. The U_d/U_{fd} ratio is very important, not only for the development of the computer model, but also for the physical expression. U_d is the mean velocity of the river and U_{fp} represents a variation of the fluctuation of turbulence around a point near the boundary of a channel excluding the bed forms.

Thus a general relationship between the ratio of mean and friction velocities of a dune-covered bed and of a plane bed can be written as follow :

$$\left(\frac{U_d}{U_{fp}}\right) = \left(\frac{U_p}{U_{fp}}\right)^{1/3} * \left(\frac{U_d}{U_{fd}}\right)^{2/3} \quad (4.3)$$

if the set of three specified variables - discharge, slope, and bed material properties - is the same in both conditions.

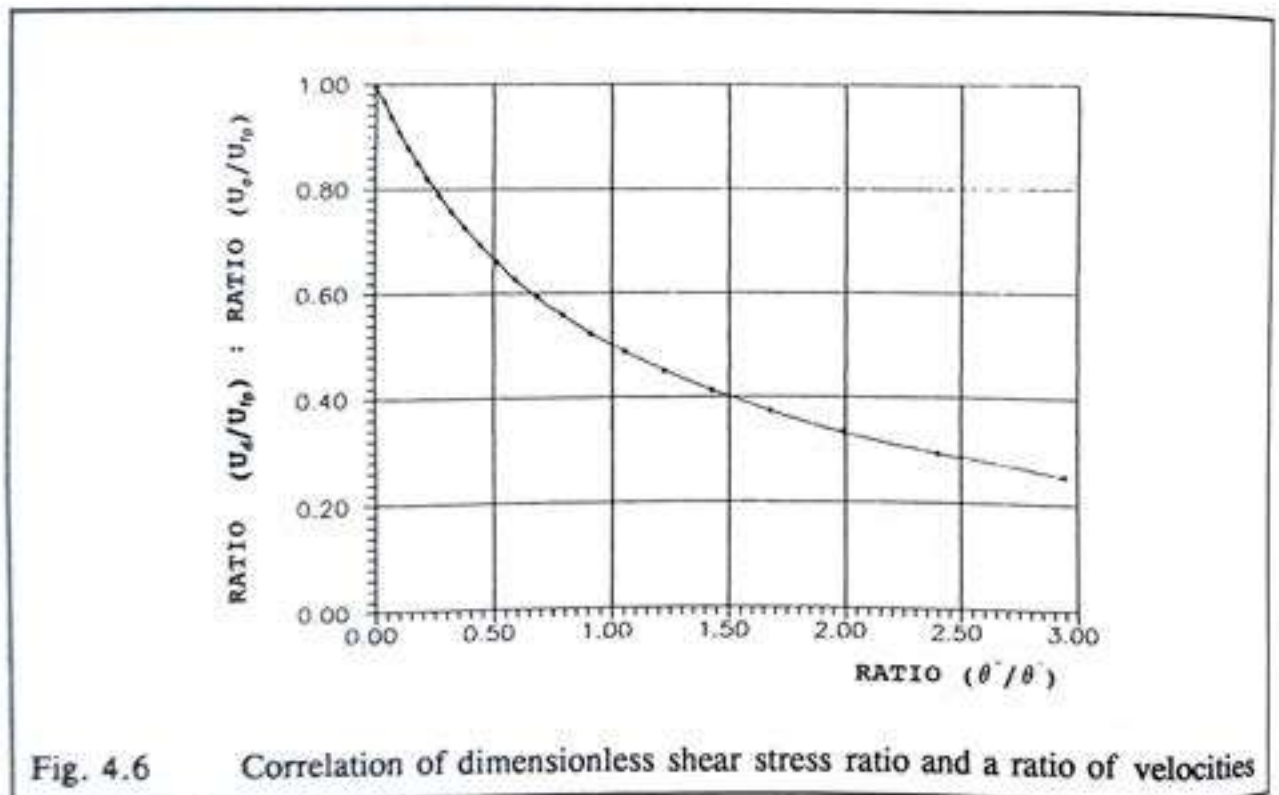
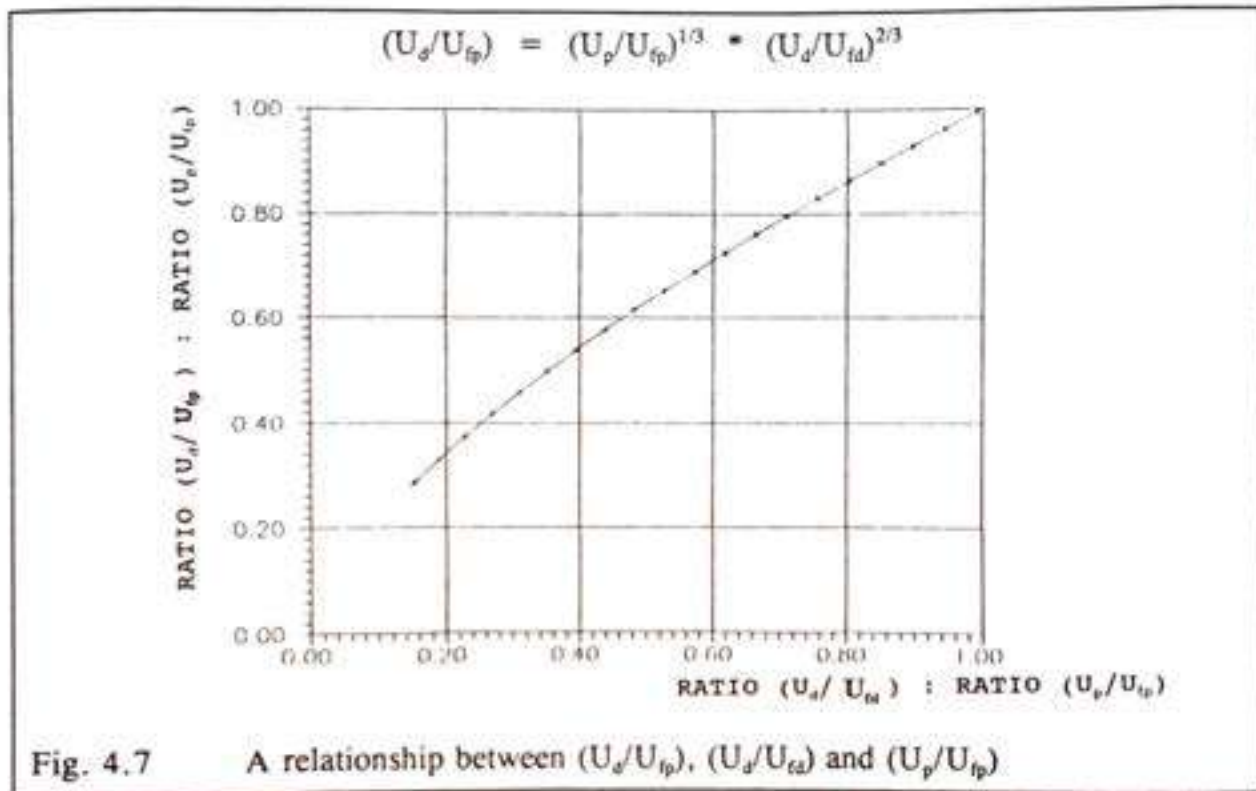


Fig. 4.6 Correlation of dimensionless shear stress ratio and a ratio of velocities

It can be stated as a general relationship which can be applied within a wide range of validity. The range of the validity of the velocity relationship is limited by three variables : (1) water discharge Q from $130 \text{ m}^3/\text{s}$ to $88136.0 \text{ m}^3/\text{s}$; (2) energy slope I from 10^{-6} to $51 * 10^{-6}$ see Fig. (4.4); (3) mean grain diameter d_{50} from 0.47 mm to 1.25 mm . Finally the roughness coefficient and the dune dimensions are satisfactorily predicted and the model is compatible to the bed topography simulation model's specifications. The frequency with which the model can be applied to a bed topography computation is only a question of computer time and related economics.



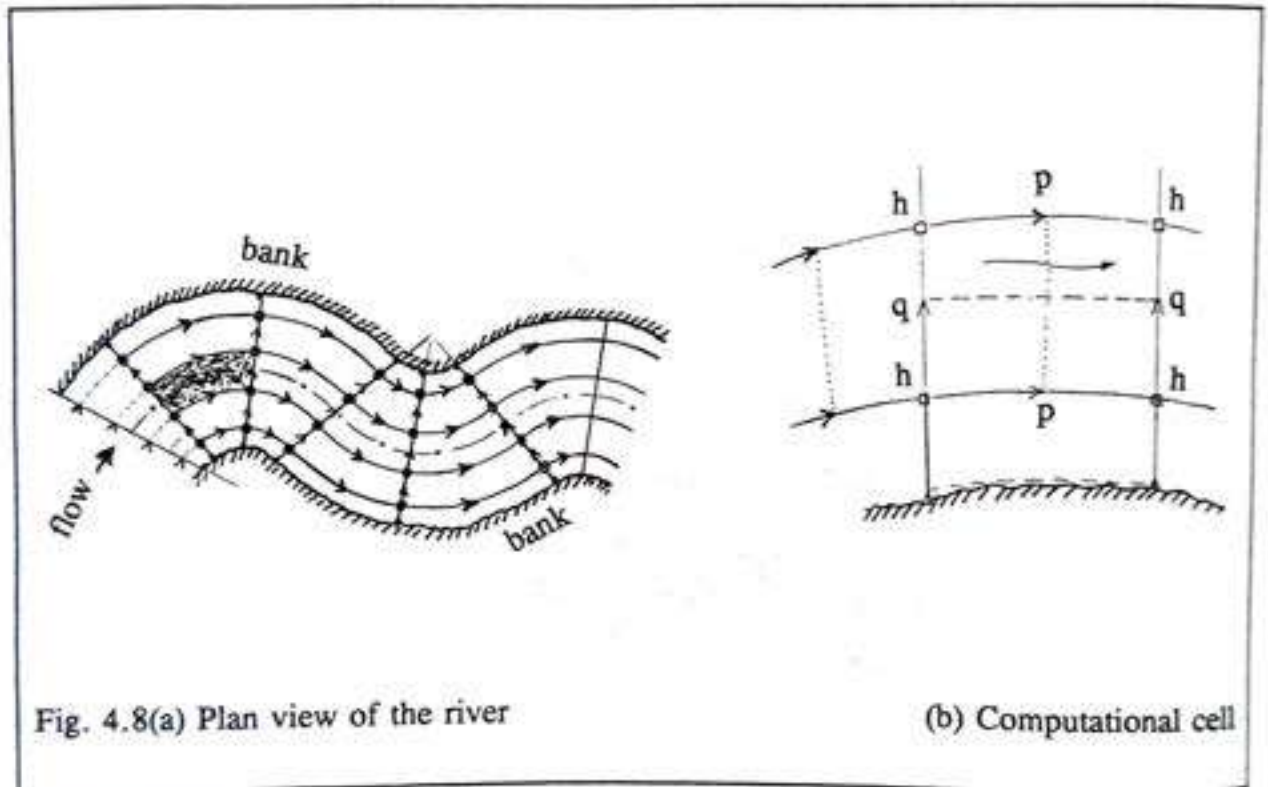
4.8 Connection to the bed topography simulation model

The roughness predictor model is added to the bed topography simulation model and a verification for the consistency of the discharge is made. The deviation of water discharge before and after the roughness has been updated is proved to be only 0.35%. Therefore, the discharge which is present in the current simulation time step is hardly affected by the updated procedure of the roughness and is still representative of the prevailing condition. Thus the calculation can proceed from a plane-bed to dune-covered bed and vice versa.

The computational domain of the bed topography simulation model consists of single cells in both downstream and cross-stream direction over the entire area of the river bend as shown below (see Fig. 4.8). Each individual cell has its own water discharge, velocity, water depth, sediment discharge, and bed shear stress. However, the roughness coefficient is the same for all cells. Before the roughness is updated, a constant Chézy's coefficient is used. After the adaptation of the roughness predictor model each cell has received its own roughness coefficient.

However, after the roughness is updated in each computational cell (see Fig. 4.9), the bed topography model can become unstable. The explanation for this instability is the following. The present model based on the set of two-dimensional shallow-flow equations. The sediment is eroded and is deposited along the each strip of the river cross-section, for water depth, velocity and water surface slope are calculated separately in each strip. This implies that each strip of the river cross-section behaves as a separate channel and each abides by both mass and momentum conservation laws. Since the roughness coefficient varies

from upstream to downstream in the simulation model, the water level along the specific strip becomes undulated. Hence it comes into conflict with rigid lid assumption of the bed topography model (see details in Chapter 3 and appendix A) and this results in instability. On the other hand, the simulation model works very well if a variable roughness is introduced in the transverse direction only. In fact, the variation of the roughness coefficient in both directions is a little bit exaggerated and this is not really necessary in the case of simulations of the bed-topography and the meander evolution since the necessary and sufficient solution is obtained by applying the variable roughness in the transverse direction only (see Fig. 4.15(b)).



Next to the above-mentioned investigation, the following calculations are made to achieve the main objective of determining the optimum channel width in a meandering river:

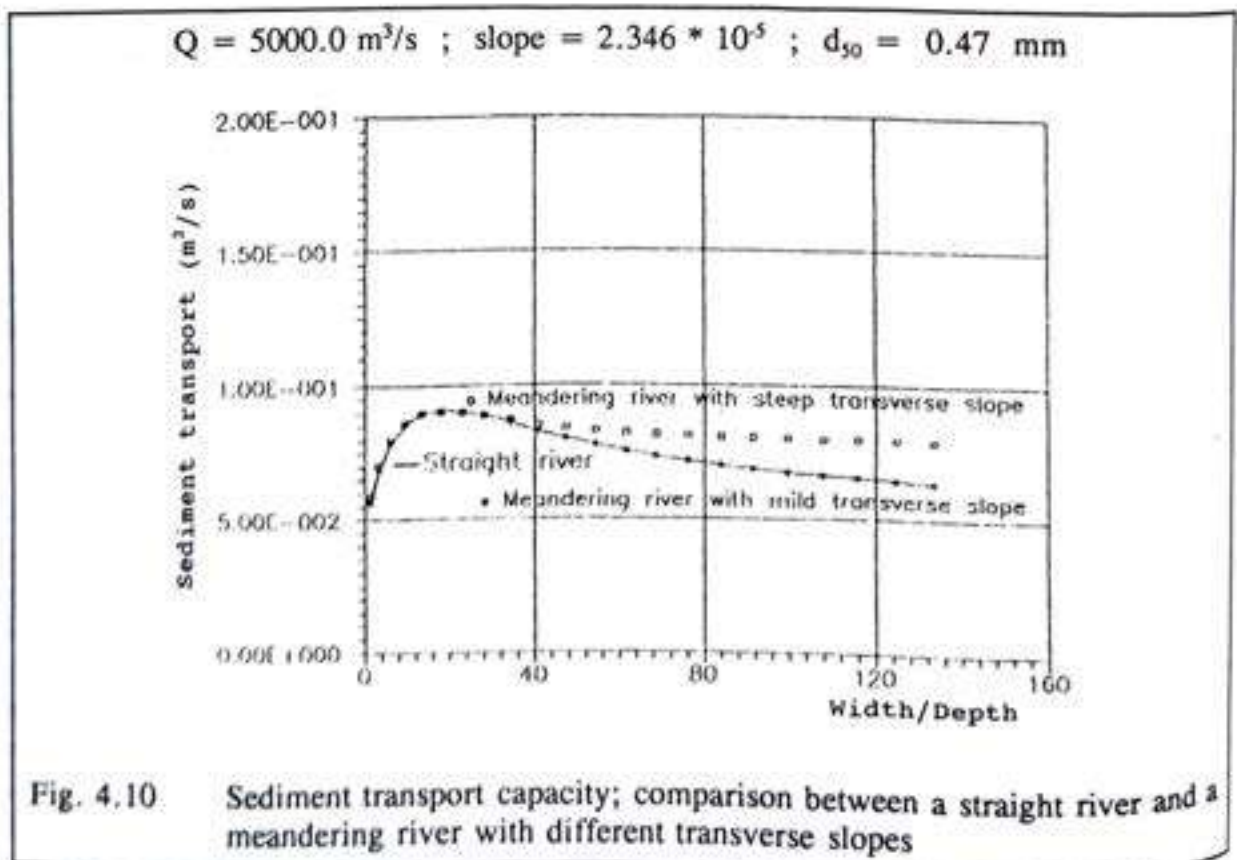
- (1) Three variables - the unit discharge, the slope, and the mean grain diameter - which are to be used in the simulation model are specified and the corresponding roughness coefficient for the initial condition is predicted. It should be mentioned that the grain size distribution of the bed materials has to be specified.
- (2) The predicted roughness coefficient is used for the entire area of the river until an equilibrium bed topography is reached. Therefore it is constant over the entire reach but the accent is on presentation in the context of the bed material properties and the flow.

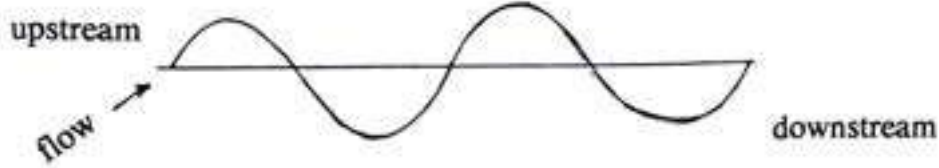
discharge and slope and the use of a roughness factor determined independently from the bed material property, the Chézy coefficient is found to be $30 \text{ m}^{0.5}/\text{s}$. The sediment transport capacity for various widths of the rivers calculated using this value is shown by the full line.

The first improvement in the estimate of the roughness is obtained by taking more account of bed material properties and the flow. The cross-sectional averaged value is used for the sediment transport calculation. The sediment transport capacity calculated by this roughness is shown by squares in the figure.

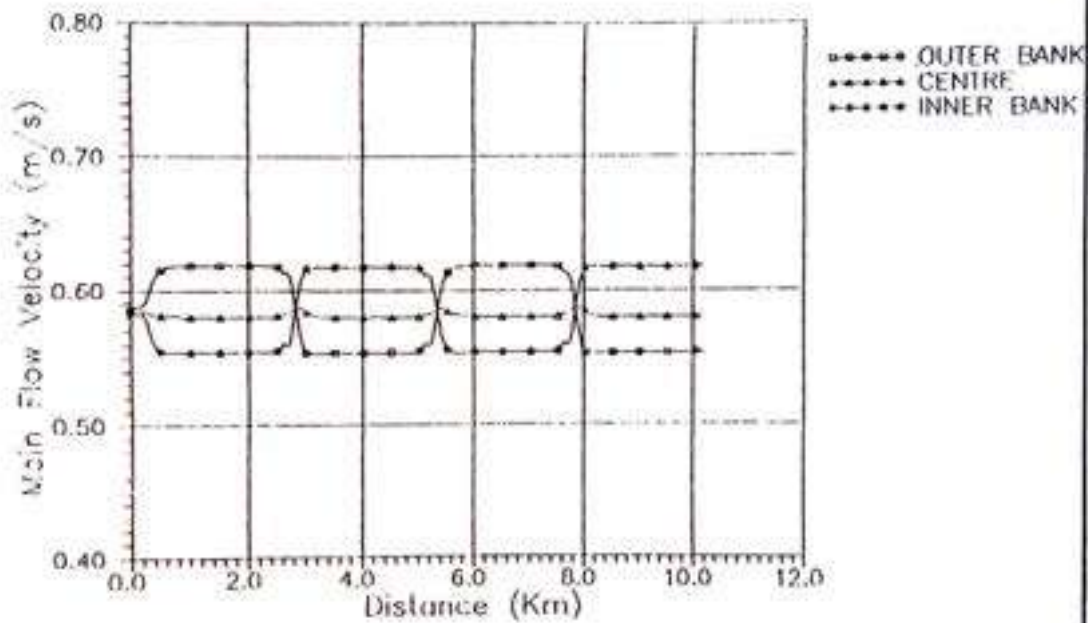
The second improvement in the roughness estimate is obtained by taking more account of the bed material properties and the *local flow conditions*. The sediment transport capacity is calculated by varying the roughness along the transverse direction. The result is indicated by triangles in the figure.

Figure 4.15(b) suggests that using a mean value of alluvial roughness in the simulation is justified and attractive in the case that only the total sediment rate is of interest and if the calculation of the roughness factor is based on the flow, the bed material properties, and the corresponding regime.





Main flow velocity profiles



Computed Longitudinal Bed Profiles

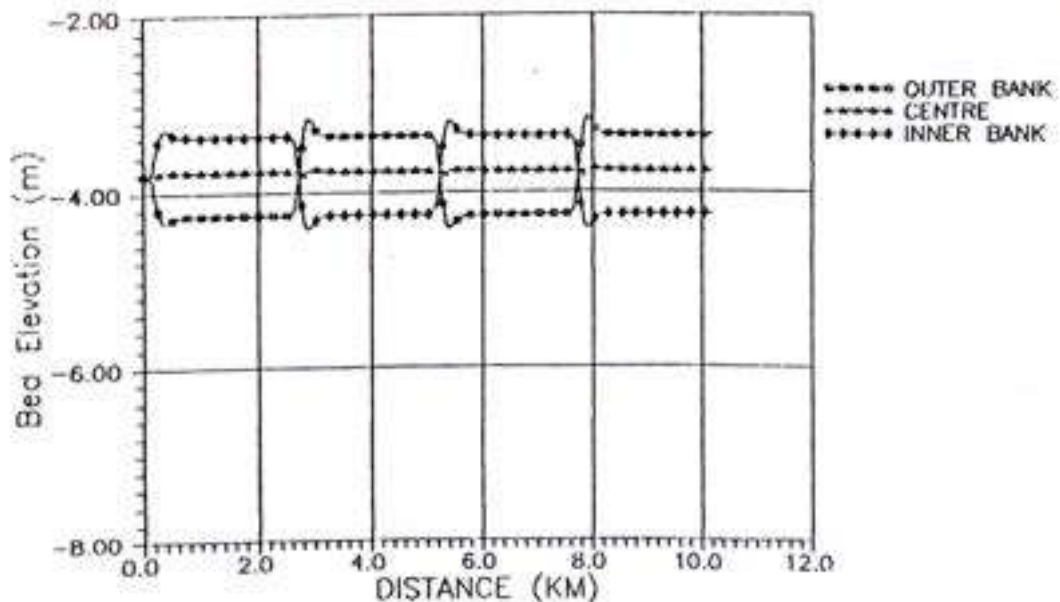


Fig. 4.11 An example of simulated bed-level profiles, near-bank velocities and transverse bed slopes

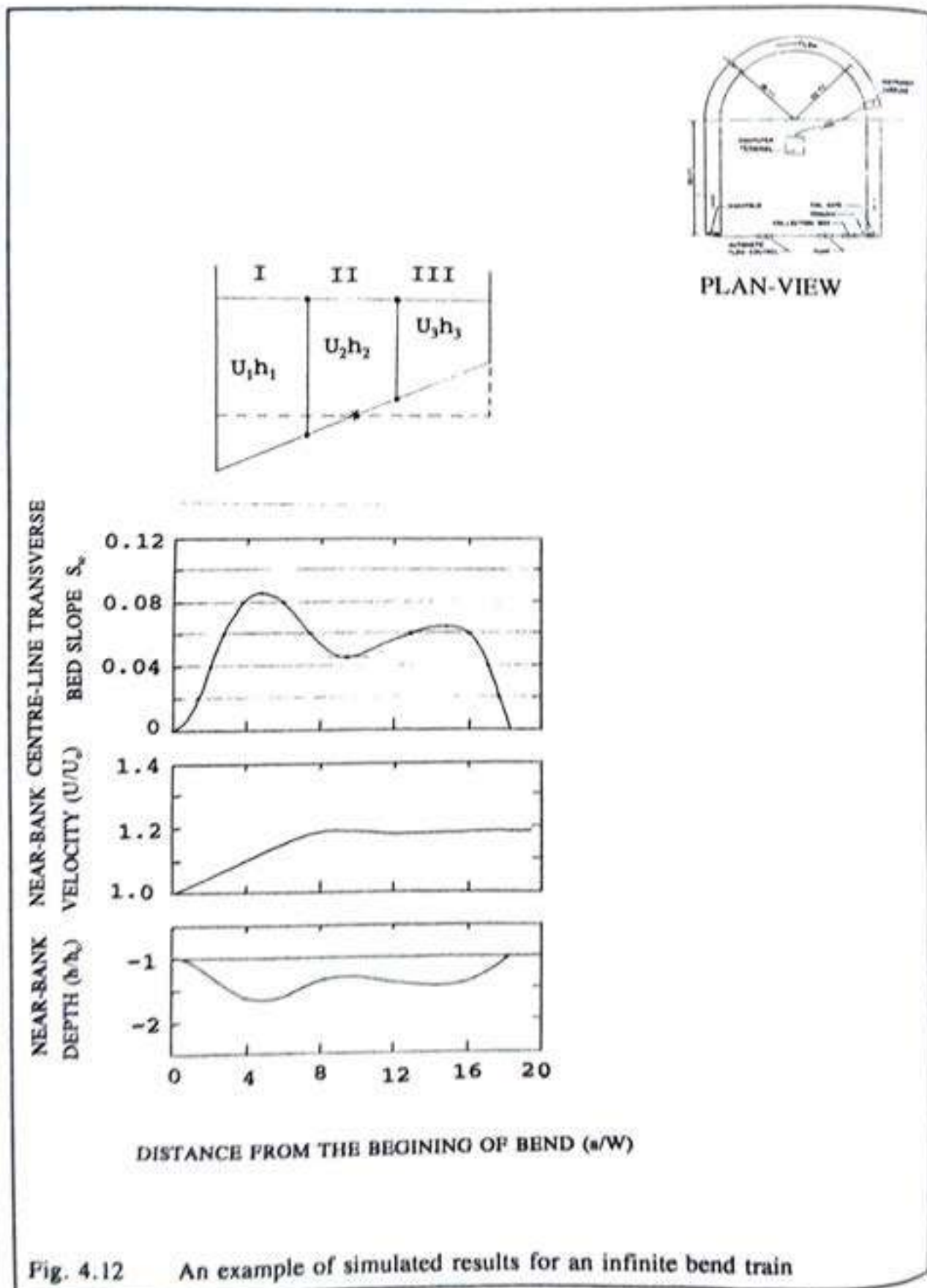


Fig. 4.12 An example of simulated results for an infinite bend train

Note. Figure (a) shows the resultant (deeper) water-depth and (smaller) radius of curvature than figs. (b) and (c). Figure (b) and (c) have the same physical parameters but different calibration parameters. Therefore these two figures illustrate the effect of calibration parameters.

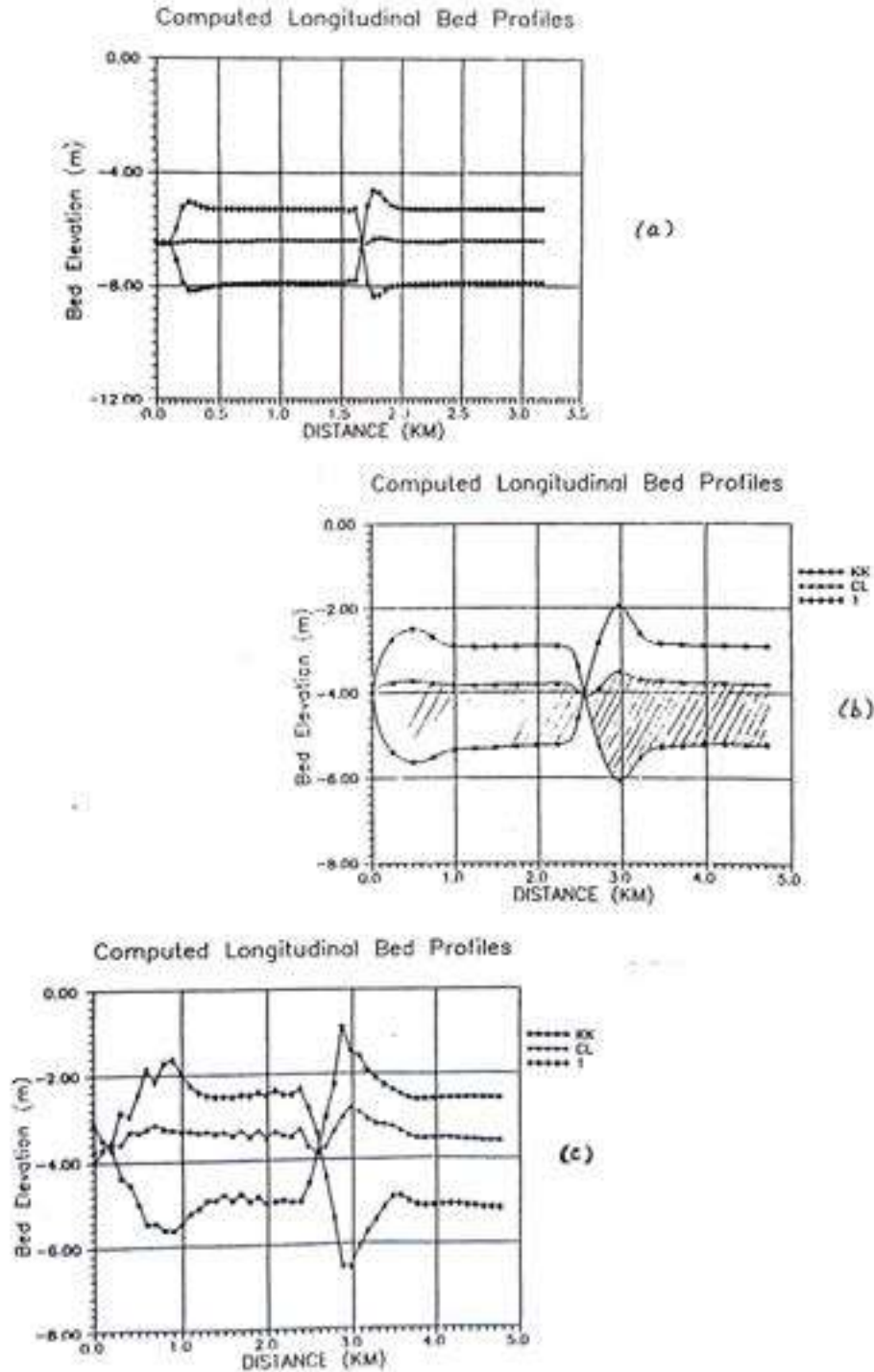
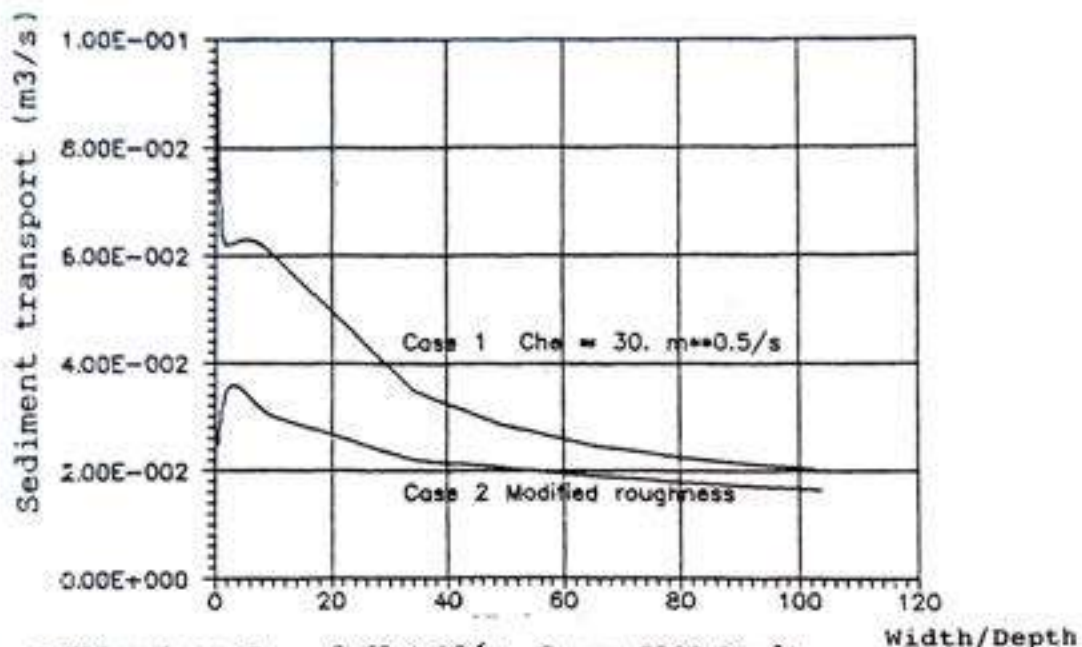
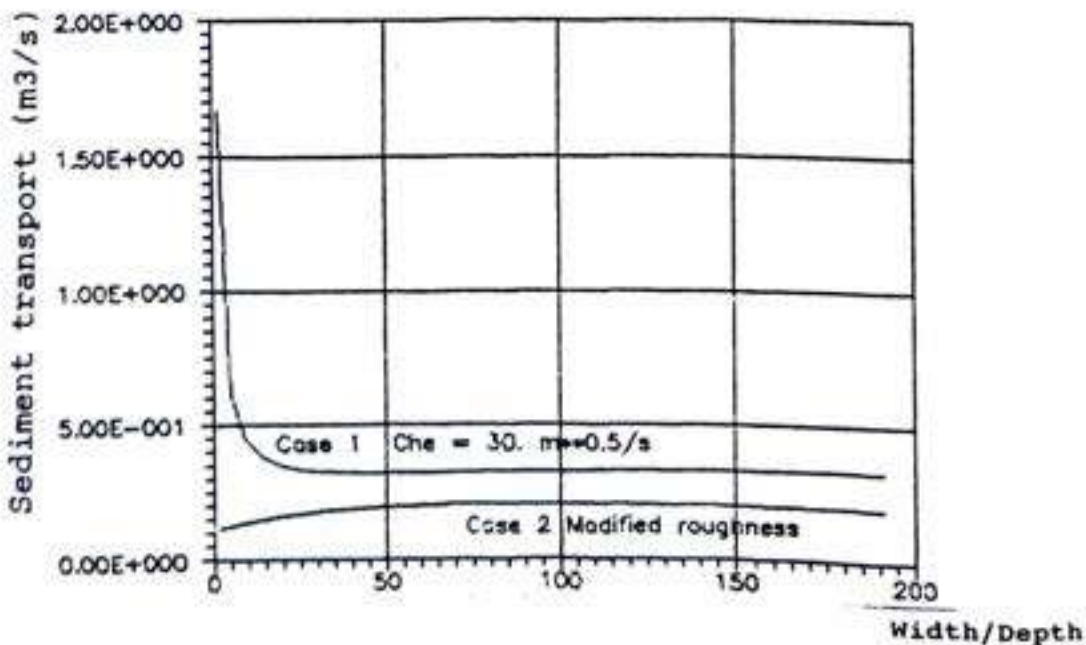


Fig. 4.13 The effect of calibration parameters

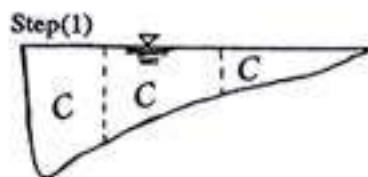


(a) Milder slope $S = 9.69 \times 10^{-6}$; $Q = 5000.0 \text{ m}^3/\text{s}$

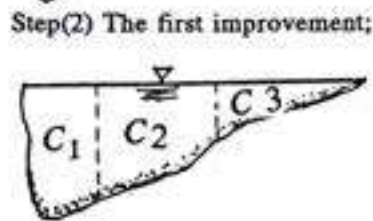


(b) Steeper slope $S = .51 \times 10^{-4}$; $Q = 5000.0 \text{ m}^3/\text{s}$

Fig. 4.14 Sediment transport capacity ; comparison between results obtained with a constant Chézy coefficient and with modified roughness.



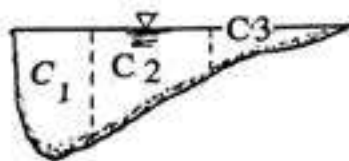
Step(1) The roughness factor is calculated from the flow condition only. E.g. Chézy's coefficient is calculated from $C = U/(RI)^{0.5}$



Step(2) The first improvement;

The roughness factor is predicted by the flow, the bed material properties and the corresponding regime. The averaged value over the cross-section is used in the flow simulation model. $C_{avg} = (C_1 + C_2 + C_3)/3$

Step(3) The second improvement;



The roughness factor is predicted by the flow, the bed material properties and the corresponding regime. The local roughness factors C_1 , C_2 and C_3 are used as variable roughness factors over the entire reach.

Fig. 4.15(a) An illustration of the step-by-step improvement in the roughness factor employed

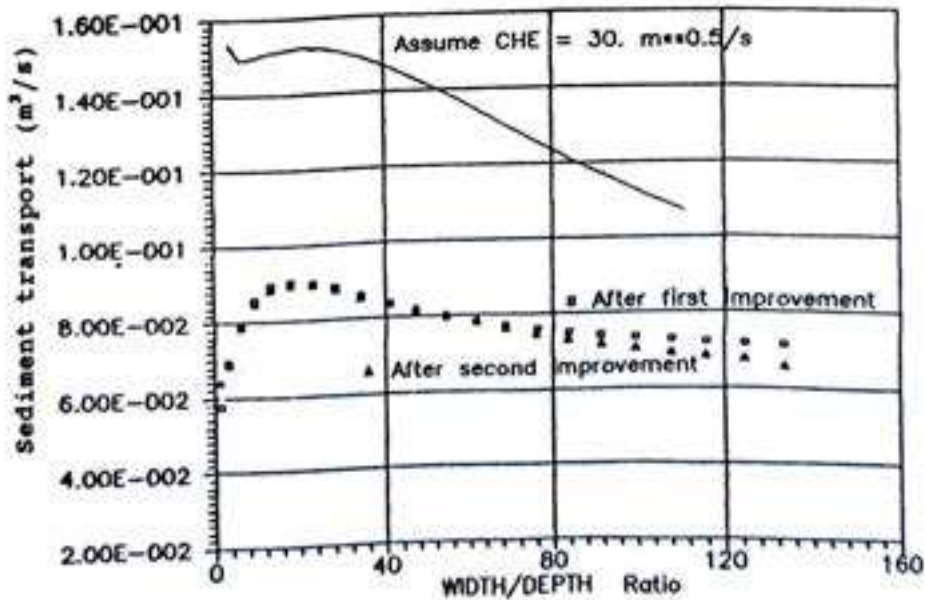


Fig. 4.15(b) Sediment transport capacity corresponding to the improvement of the roughness factor

4.9 Calculation of an MTC channel width for a straight river

The calculation of a maximum transport capacity (MTC) channel width for a straight river over the range of width-to-depth ratios from 0.1 to 200 has been made. The numerical model is used in a range of width-to-depth ratio from 15 to 200. For a width-to-depth ratio between 0.1 and 15, the analytical model described in section 4.14 is used (see Fig. 4.16).

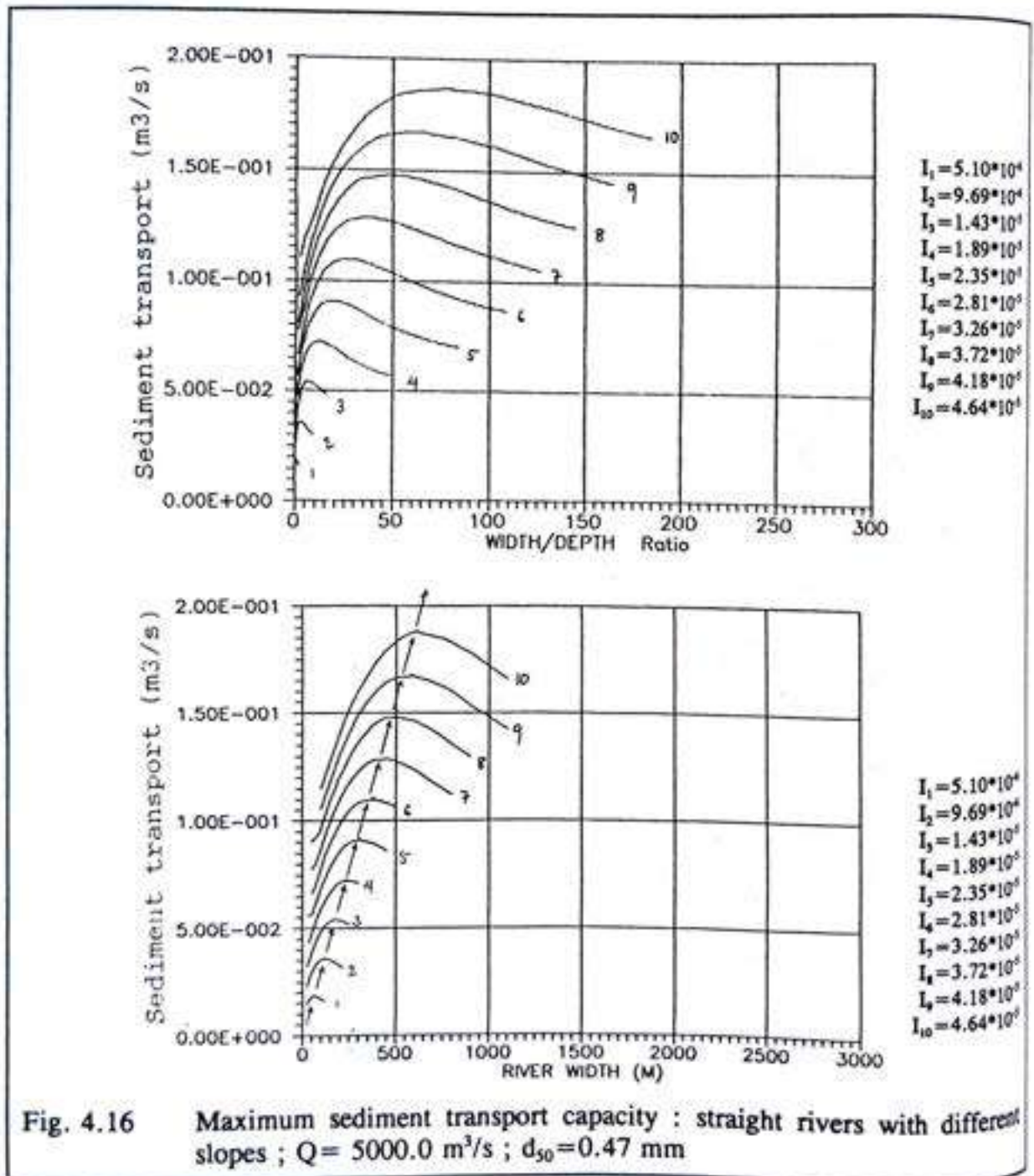


Fig. 4.16 Maximum sediment transport capacity : straight rivers with different slopes ; $Q = 5000.0 \text{ m}^3/\text{s}$; $d_{50} = 0.47 \text{ mm}$

After obtaining the roughness factor for a certain condition, it is then quite straightforward to calculate the sediment transport capacity of the river. For this calculation, Fredsøe's formula is used to obtain the total load in a straight river. For a given set of slopes (I) and representative diameters (d_{50}), the sediment transport is calculated for variable widths.

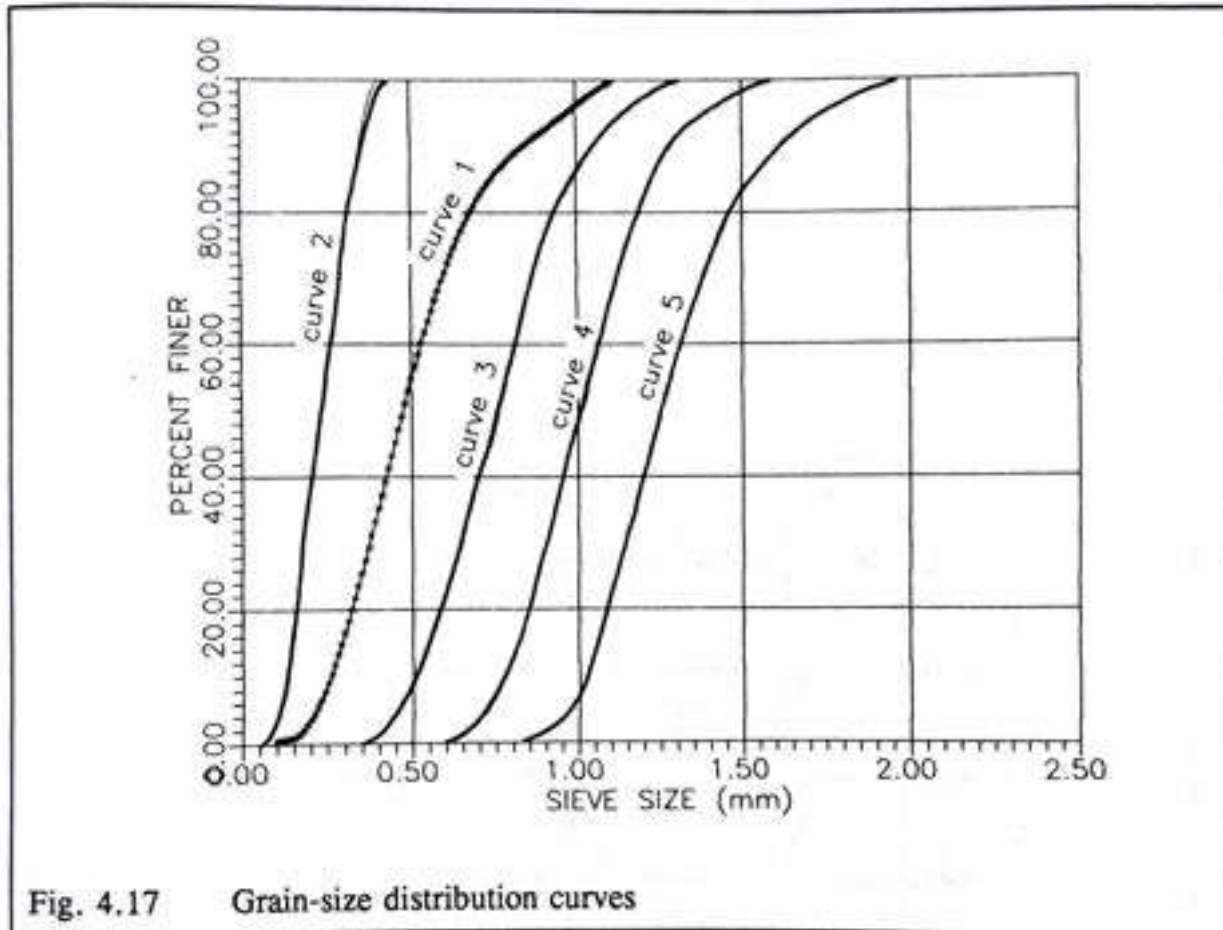
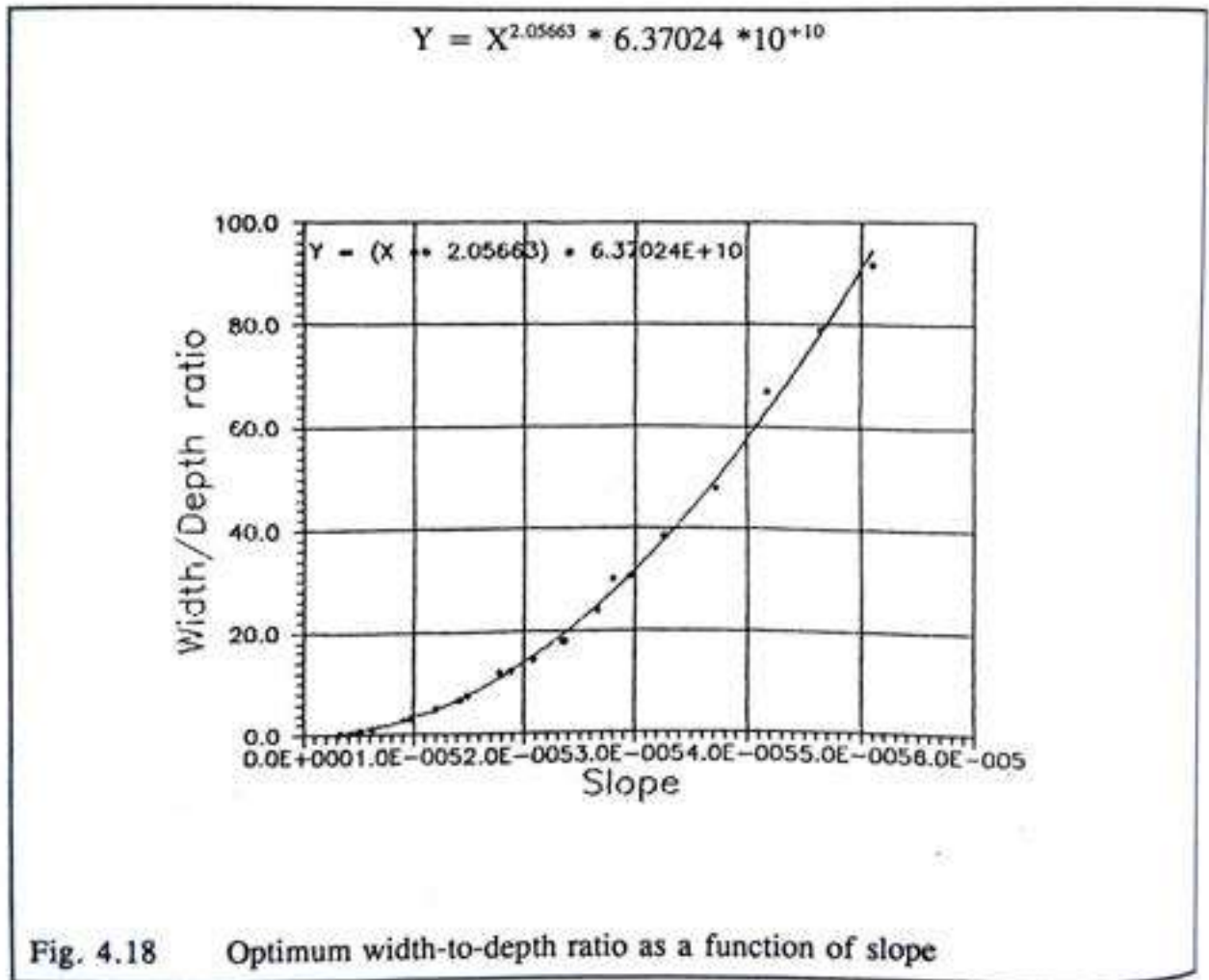


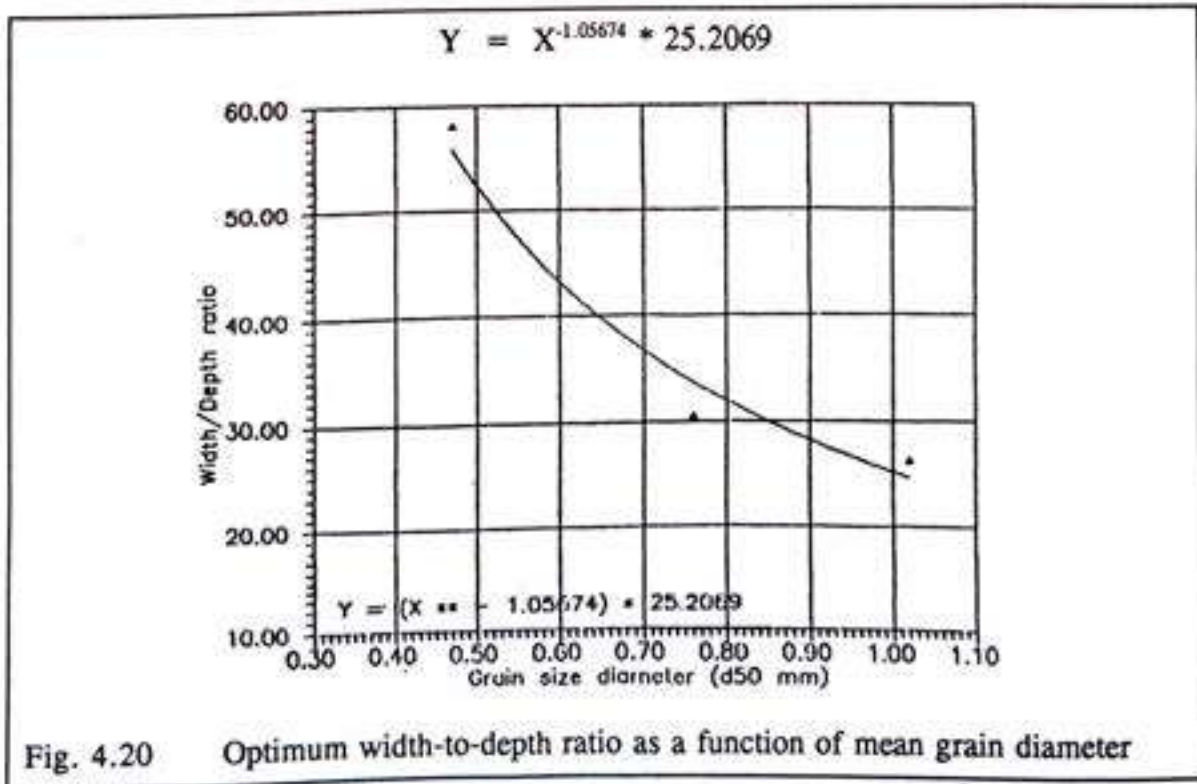
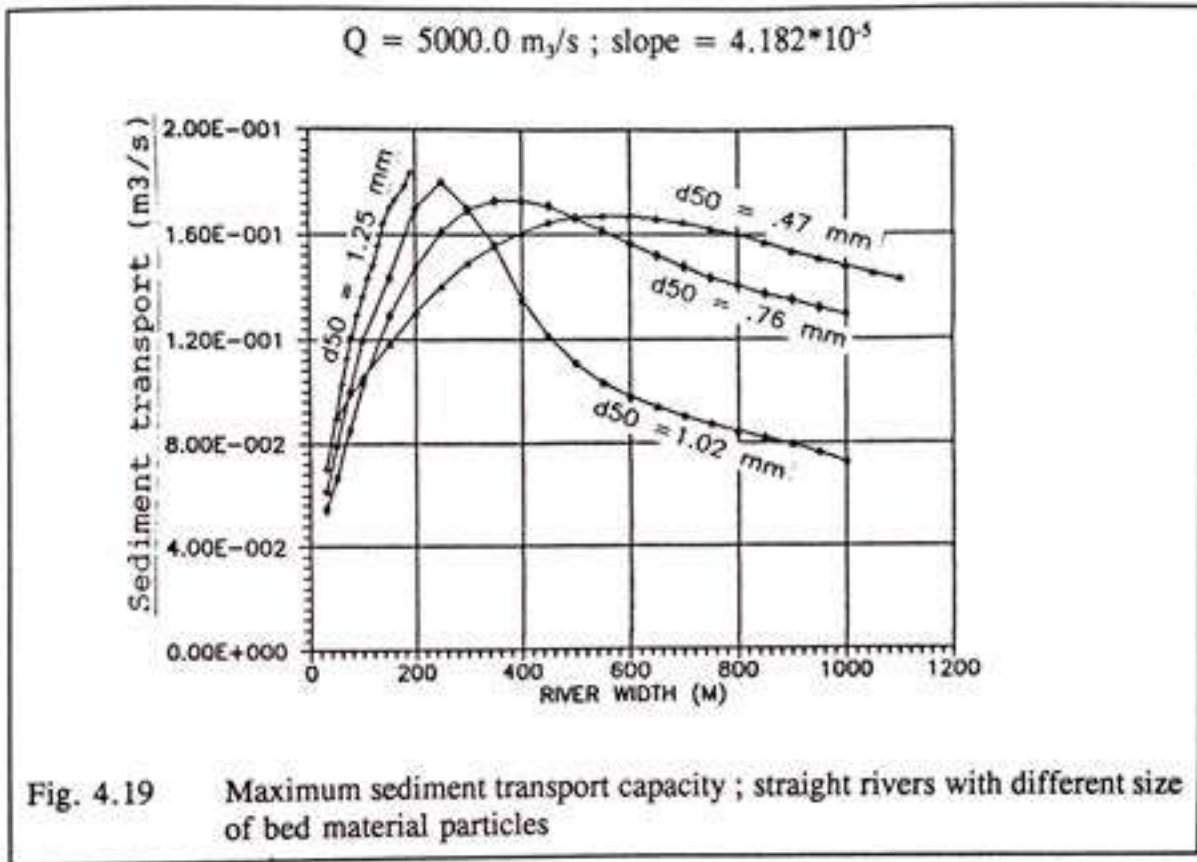
Fig. 4.17 Grain-size distribution curves

While computing sediment transport capacities for different grain diameters, some effects of sediment distribution is noticed. In the computations, five different bed materials are used. The grain size distribution curves of these different bed materials are shown in fig. (4.17). The geometric standard deviations of the grain size distribution for all curves are the same; the value is 1.59. If the river bed consist of the bed material shown in curve No. 5, with mean diameter 1.25 mm, there is a deficit in fine sediments. The critical shear stress then appears before the maximum sediment transport capacity has been reached. At another extreme, curve No. 2 corresponds to a very fine sand and lack of coarse materials; therefore the bed shear stress is very high and the grains are not able to form a dune covered bed. Therefore the regime is that of a plane bed under the strength of the flow which is specified by the given discharge and slope. It is noteworthy that, for such a condition, the maximum sediment transport capacity appears for a width-to-depth ratio 3.0. This means that comparatively, the inertia of the flow is very much effective than the resistance.

Taking into account the above mentioned calculations, the resulting experience can also be connected to the physics. One of the factors which affects the resistance of alluvial rivers is the presence of sediment in suspension. From the laboratory experiments, leaving all other parameters unchanged, the mean velocity of water charged with silt is greater than that for clear water. Similarly, for a given stage and slope, the Nile river, for example, has a greater mean velocity on the rising stage than on the falling stage. The appreciable reduction in Manning's roughness factor was believed to be due to the increase in suspended load which damps the turbulence near the bed. The experimental results of Vanoni and Nomicos show that the presence of fine sediment in suspension decreases the resistance to flow; the decrease is more in the case of a plane bed. With a plane bed, a reduction in friction factor due to suspended sediment, from 5 to 28 per cent, was observed.



The MTC solution emerges for different slopes and different width combinations. Finally the maximum transport capacity, MTC channel width can be predicted from the function of slope for a given representative diameter of bed material (See figs. 4.16 and 4.18), or from the function of representative grain diameters of bed material for a given slope (see figs. 4.19 and 4.20).



4.10 Calculation of an MTC channel width for a meandering river

The calculation of a maximum transport capacity MTC channel width for a meandering river ranges from width-to-depth ratio 0.1 to 200. The numerical model is used in the range of width-to-depth ratios from 15 to 200. For width-to-depth ratios between 0.1 and 15, the analytical model described in section 4.14 is used (see figs. 4.21, 4.22, 4.23 and 4.24).

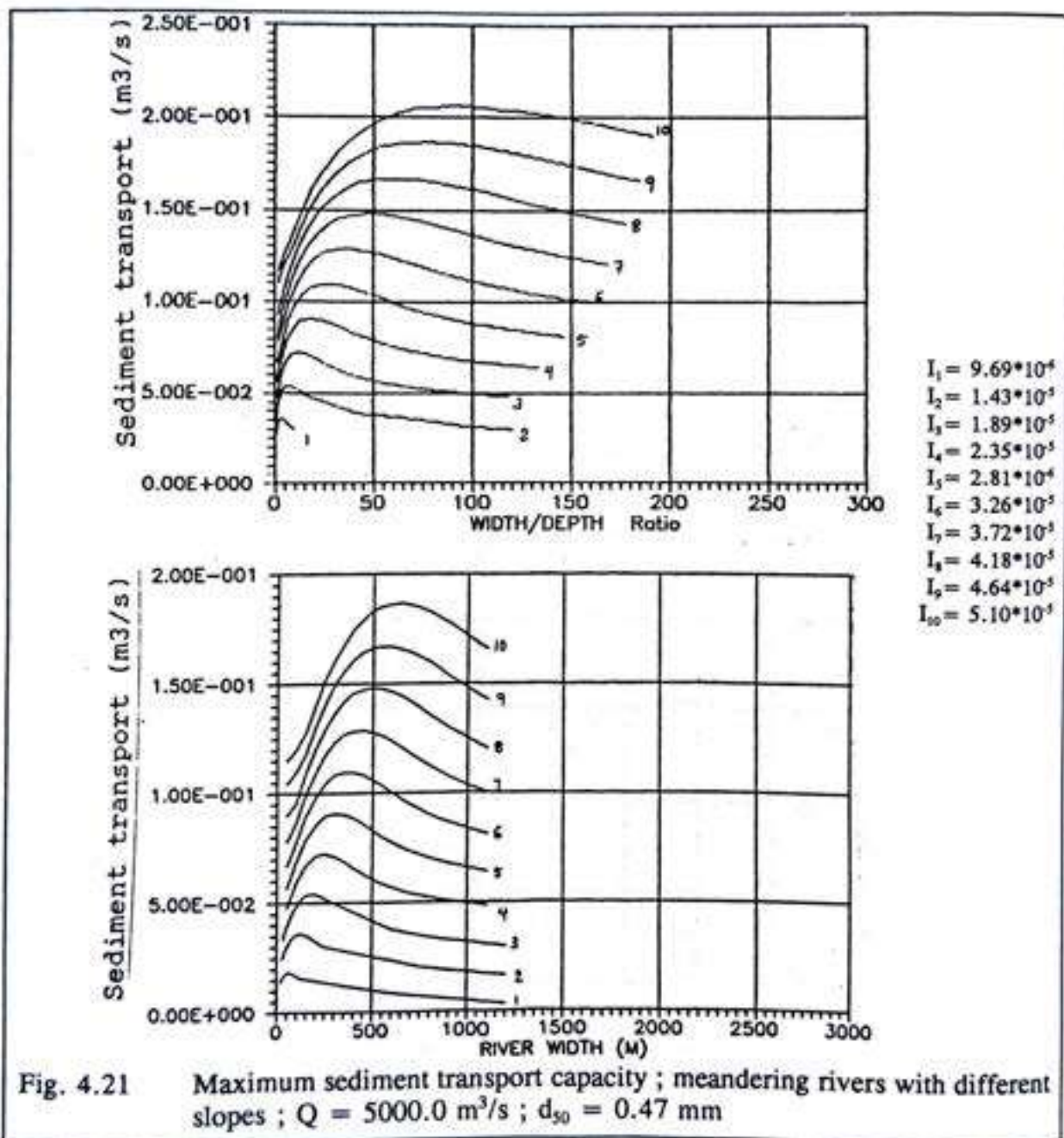
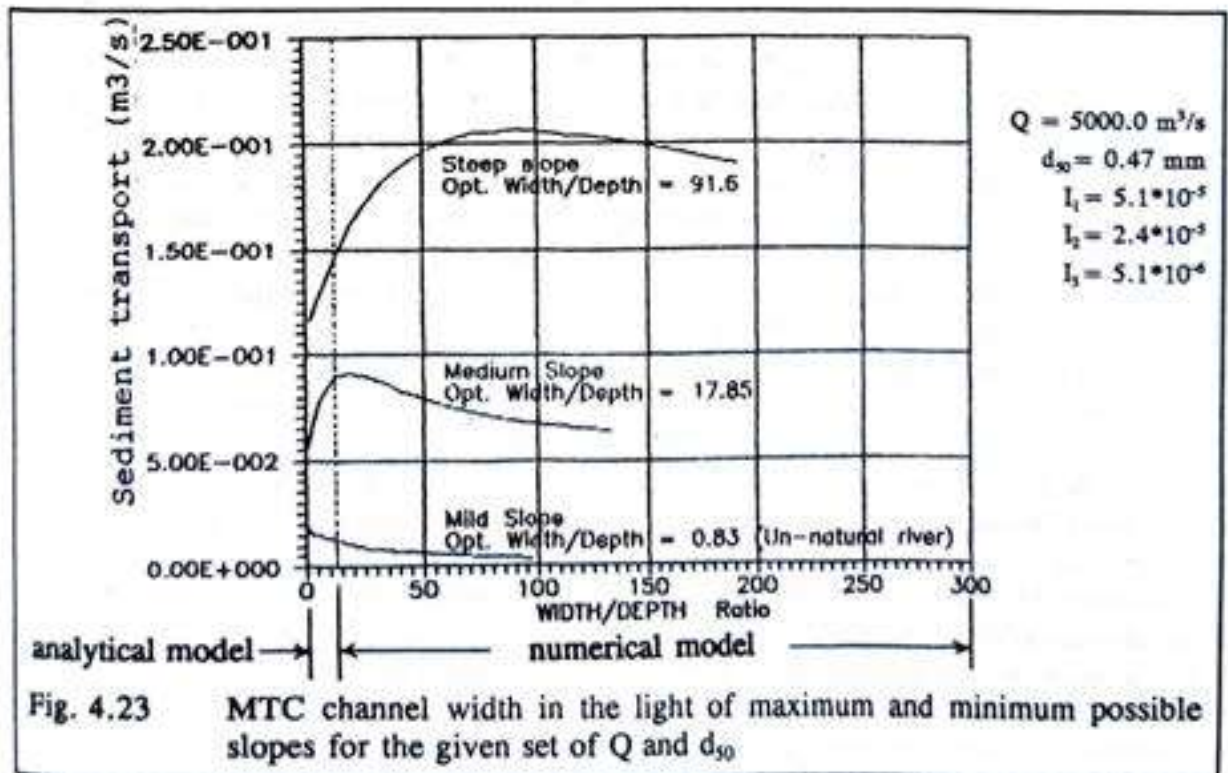
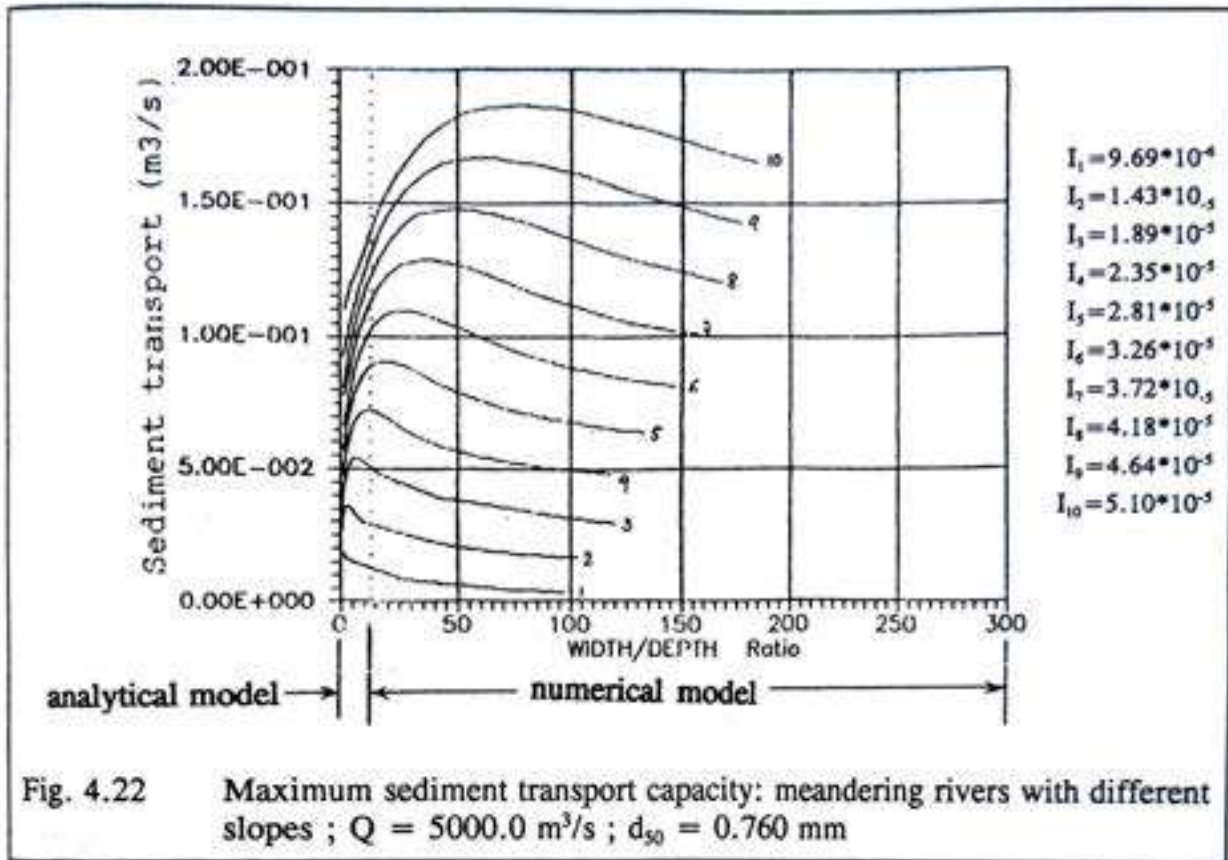
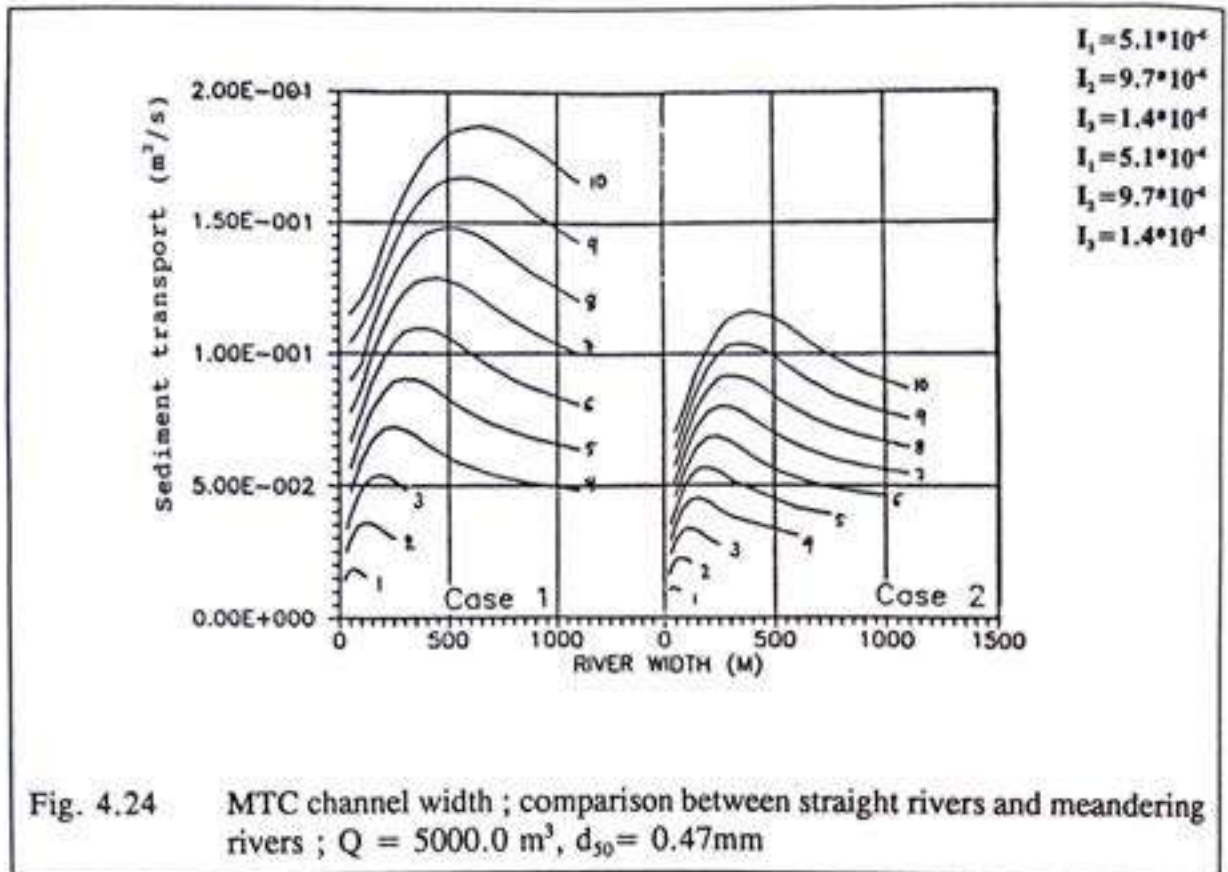


Fig. 4.21 Maximum sediment transport capacity ; meandering rivers with different slopes ; $Q = 5000.0 \text{ m}^3/\text{s}$; $d_{50} = 0.47 \text{ mm}$





For a meandering river, the maximum transport capacity is calculated for a certain dynamic equilibrium condition. The procedure consists of four steps. In the first step, the roughness factor is predicted as for a straight river for a given discharge, slope and properties of bed materials. Secondly, the equilibrium bed topography for a meander is simulated from a constant roughness factor determined from the first step (see figs. 4.11, and 4.12). Thirdly, the equilibrium transverse bed slope and local downstream water surface slope for each strip across the width are taken into account to predict the corresponding roughness factors for corresponding positions and the corresponding roughness factors are calculated (see fig. 4.15(a) and (b)). The shear stress is then calculated for the prevailing condition. Finally, the sediment transport can be calculated for variable widths.

The MTC solution emerges for different slopes and different width combinations. Thus the maximum transport capacity, MTC channel width can be predicted as a function of slope for a given representative diameter of bed material (see figs. 4.23 and 4.24). A comparison between the straight river and the meandering river is shown in fig. 4.24. A comparison between two MTC solutions for meandering rivers that were calculated from the downstream channel thalweg slope and down-valley slope is shown in figure 4.25. From these figures, it can be concluded that the river develops into a meander rather than a very wide straight reach (see figs. 4.26 and 4.27). This is achieved by adjusting the slope from an upstream point to a downstream point controlled by the same energy

Case1 : river axis slope = I_1 to I_{10}

Case2 : river axis slope = I_1 to I_{10}

$$I_1 = 5.10 \cdot 10^{-6}$$

$$I_2 = 9.69 \cdot 10^{-6}$$

$$I_3 = 1.43 \cdot 10^{-5}$$

$$I_4 = 1.89 \cdot 10^{-5}$$

$$I_5 = 2.35 \cdot 10^{-5}$$

$$I_6 = 2.81 \cdot 10^{-5}$$

$$I_7 = 3.26 \cdot 10^{-5}$$

$$I_8 = 3.72 \cdot 10^{-5}$$

$$I_9 = 4.18 \cdot 10^{-5}$$

$$I_{10} = 4.64 \cdot 10^{-5}$$

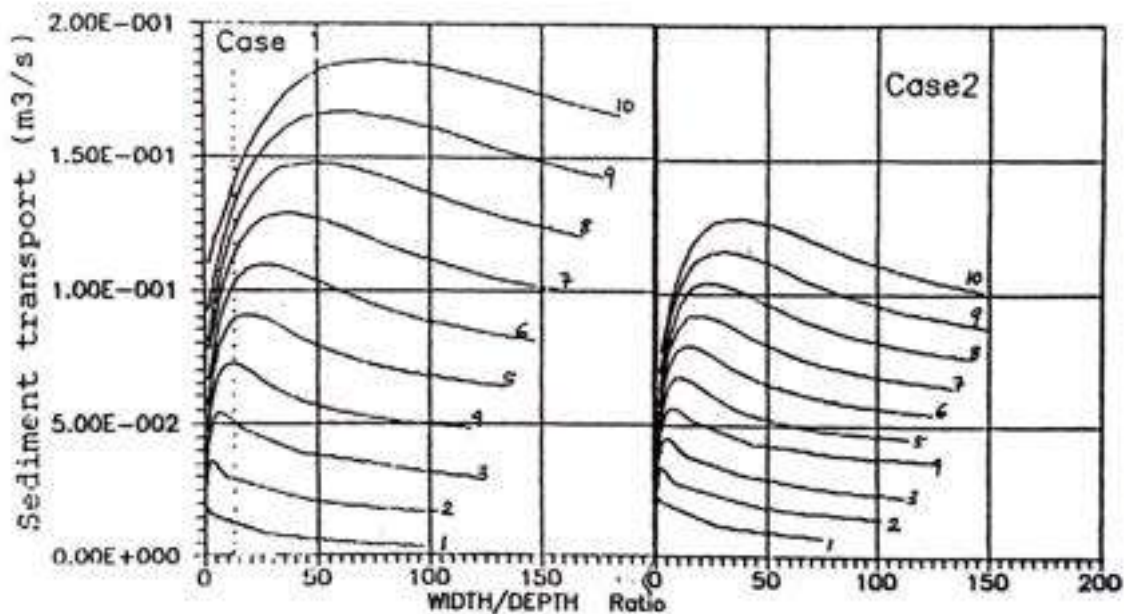
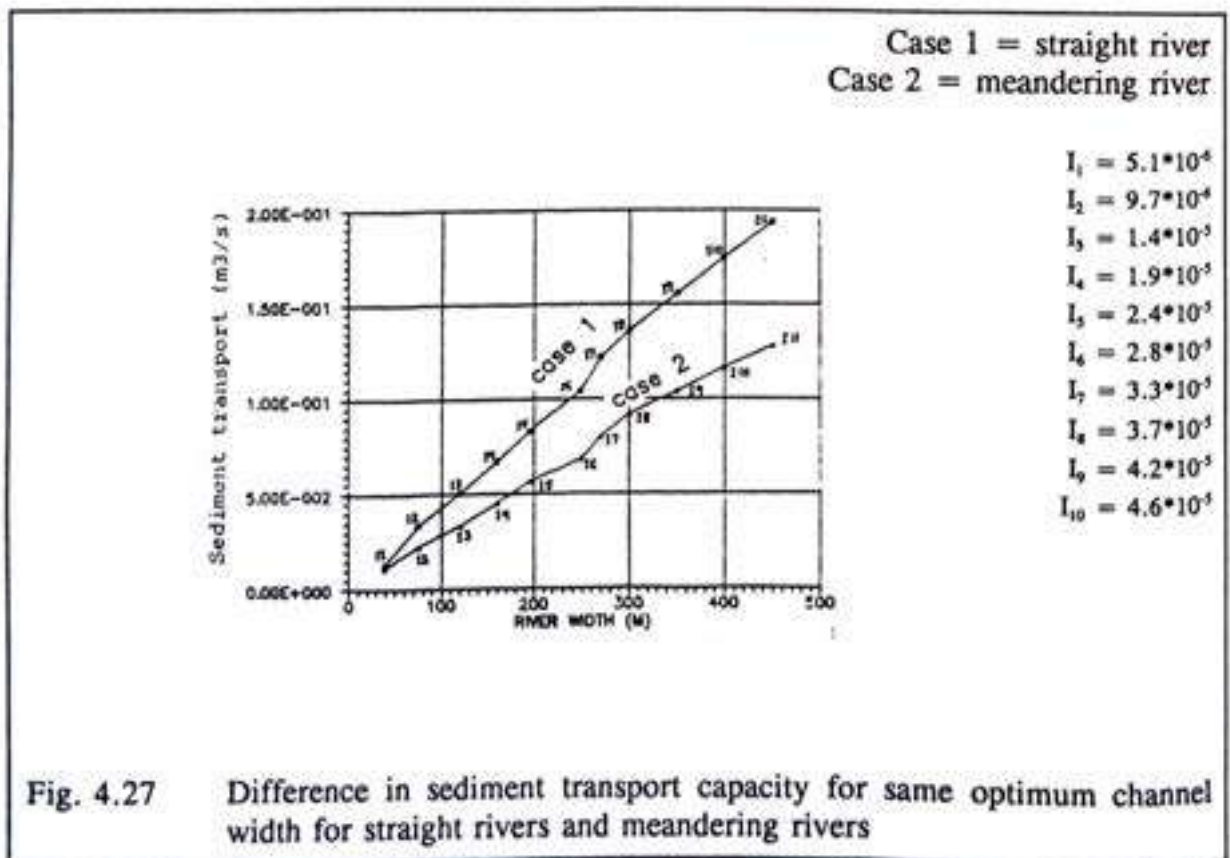
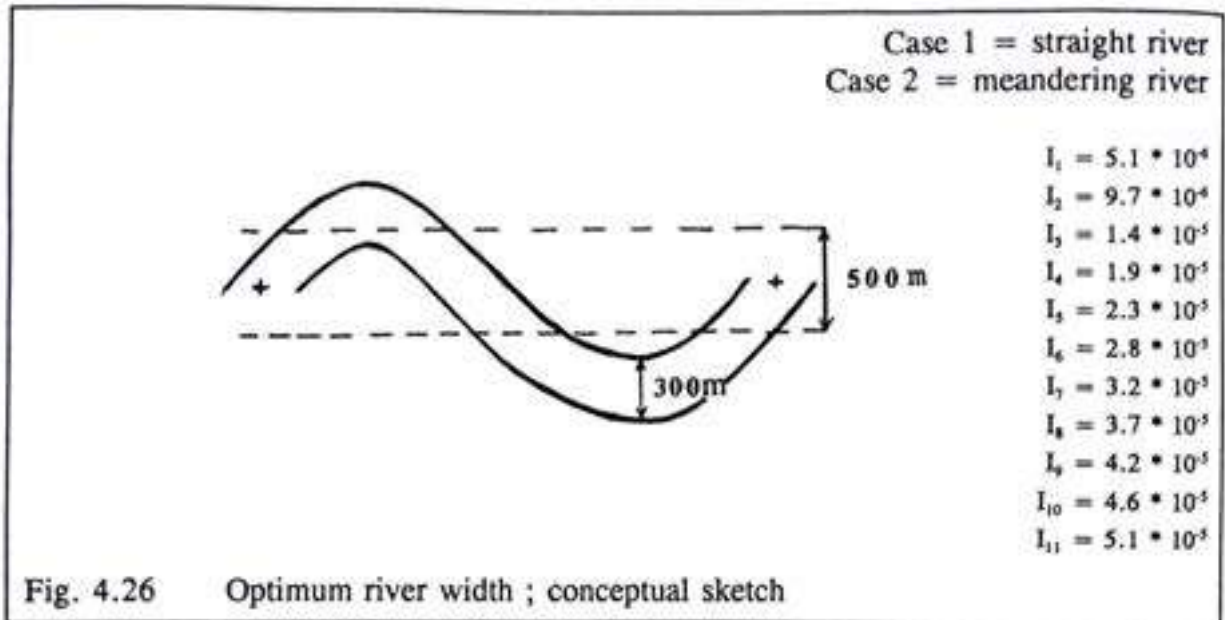


Fig. 4.25 Maximum sediment transport capacity ; meandering rivers with different slopes ; $Q = 5000.0 \text{ m}^3/\text{s}$; $d_{50} = 0.47 \text{ mm}$

expenditure. By doing so, the river attempts to reduce its destructive potential, as expressed in terms of the bank erosion. In other words, a kind of stable condition develops.

The last calculation is made in order to include the effect of grain sorting on the meandering river. The sediment transport rates for the cases with and without grain sorting are calculated and compared. Grain sorting provides a natural prevention to the river bed against being scoured too deeply at its outer bend. Grain sorting causes a variation in roughness factor from the outer bend to the inner bend. The water surface slope along the

river bend is not the same for each strip across the width, since the outer bend water surface slope is milder than it is at the inner bend, because of the different distances over



which the flow has to be conveyed. The sorting effects counterbalance the effects of the velocity being so different from inner bend to the outer bend and the sediment transport rate increases by only one or a few percent.

The two possible reasons for this are now seen to be as follows :

- (1) the representative diameter is changed but not the composition. Therefore the sediment transport rate is not properly treated as a graded sediment transport rate calculation.
- (2) dune sizes are predicted and taken into account in some particular way (ie. different dune dimensions distributed over the entire area). Therefore the friction due to the size of the individual grains does not contribute the major part of the roughness factor, but only a part of it.

It can be concluded that if only the total sediment transport is of interest and when the changes of water surface slope and total roughness factor are taken into account, the grain sorting can be neglected.

Figure 4.14 suggests that most of the error comes from the use, or rather misuse of the roughness factor. The accent is on the calculation of the roughness factor and if the roughness factor is correctly calculated it will result in no serious harm to use the mean value of the alluvial roughness over the cross-section. This appears from the effects of the first and second improvements introduced earlier.

4.11 The meander arc length and the MTC channel width

Existing theories indicate a general relationship between meander arc length and channel width whereby it is possible to define the relationships between the wavelength, the radius of curvature and the channel width for different circular-arc angles (Table 4.1). This explains why empirical equations are specific to a given set of data unless the meander arc length is invariant. Sinuosity is probably the best measure because it is related to the meander processes. Any change in channel slope due to a value defined by the sediment transport capacity results in a new width (see figs 4.18, 4.19 and 4.20). It can be considered as a constant valley slope with various arc lengths (see fig. 4.28). For a single value of sinuosity, an almost infinite number of patterns are possible. If the meander geometry is to be specified accurately, then it is necessary to determine the size of each meander arc, since arc length is a unique function of channel width, (e.g. fig. 4.29) which in turn is a function of the bank stability equation.

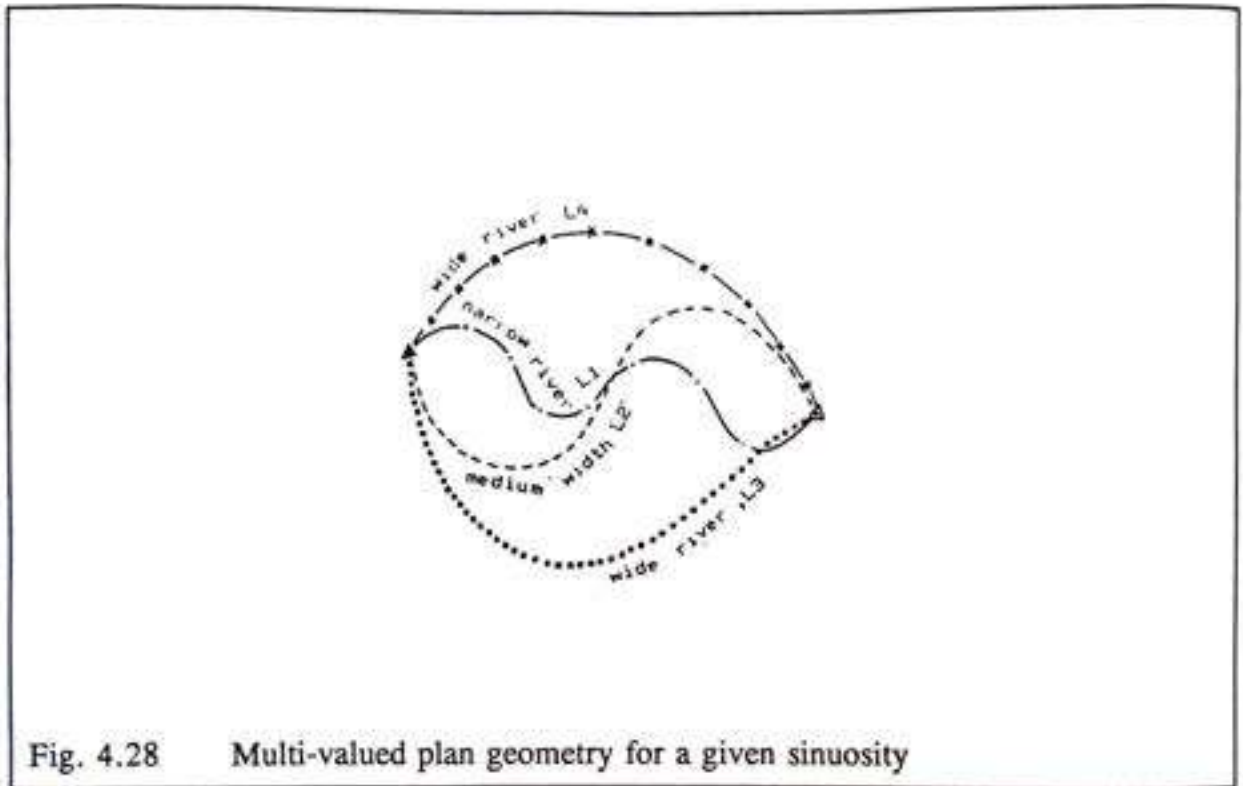


Fig. 4.28 Multi-valued plan geometry for a given sinuosity

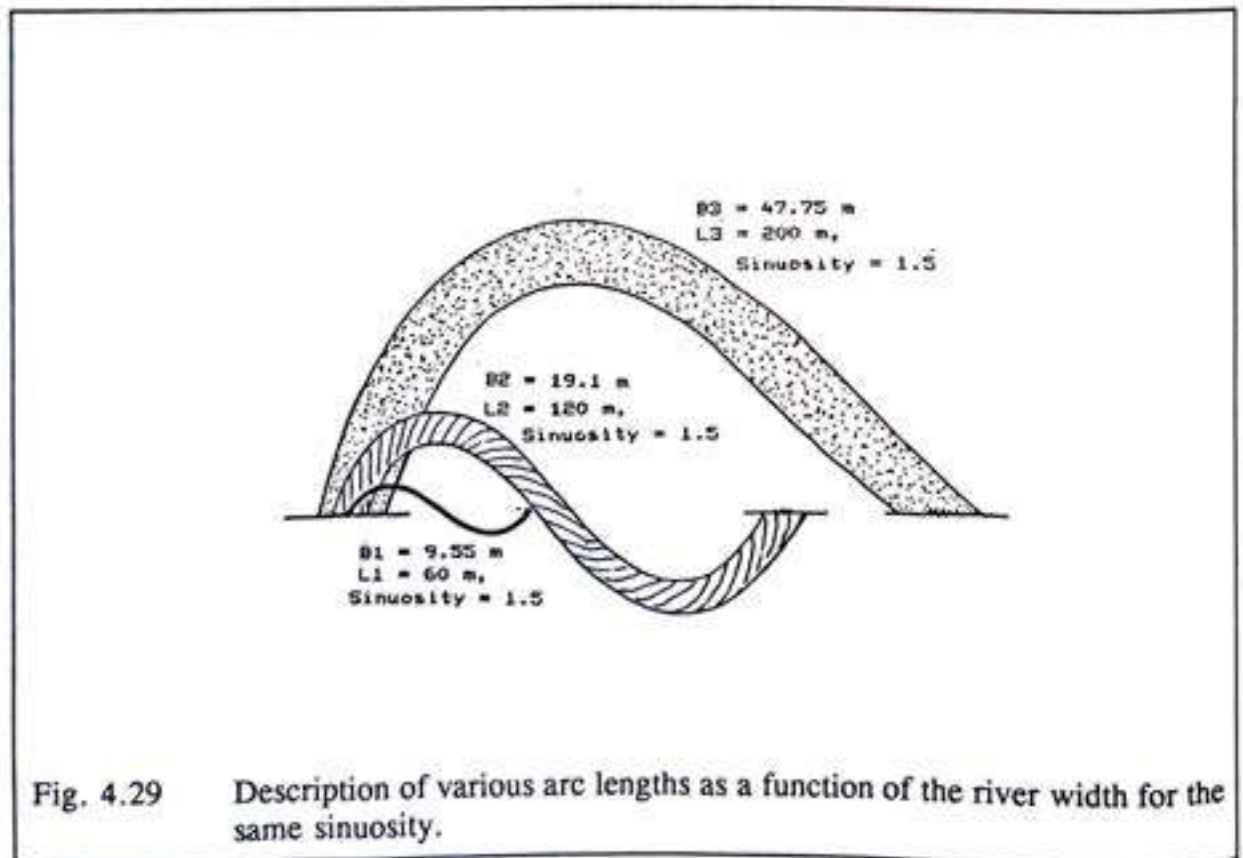


Fig. 4.29 Description of various arc lengths as a function of the river width for the same sinuosity.

Table 4.1 Relationship between wavelength (λ), radius of curvature (R) and bank-full channel width (W) for various arc angles (θ)

Arc angle (θ°)	Value of k in ($R = k.W$)	Value of m in ($\lambda = m.R$)	Value of n ($\lambda = n.W$)
270	1.33	2.83	3.77
225	1.60	3.70	5.91
180	2.00	4.00	8.00
150	2.40	3.86	9.27
135	2.67	3.70	9.85
120	3.00	3.46	10.39
90	4.00	2.83	11.31
60	6.00	2.00	12.00
45	8.00	1.53	12.25
30	12.00	1.04	12.42
15	24.00	0.52	12.53
10	36.00	0.35	12.55
5	72.00	0.17	12.56
1	360.0	0.04	12.57

in which $k = 360/\theta$; $m = 4 \sin (\theta/2)$; $n = (1.440/\theta) \cdot \sin (\theta/2)$

(Source ; Nature Vol. 262 August.5.1976)

4.12 Width-over-depth ratio

In natural fluvial channels, width-over-depth is a fundamental parameter, the reciprocal of which Gilbert (1914) used and called a form ratio, as depth-over-width, in his studies. Every stream has a characteristic width in each section. Almost all natural river beds are considerably wider than they are deep. In a larger river, if the width-over-depth ratio is less than 14, a special, possibly erosive condition prevails. Small mountain streams and narrow, canyon-bound rivers, in which the width-over-depth is less than 12 are erosive and have three peculiarities: prevalent bed-rock in the channel and along the banks, steep gradients, and coarse, scanty alluvia. In a large river running full, the value of this ratio is

usually between 14 to 26. If the river is large and lies entirely in stream-brought alluvium, and that alluvium is fine, the value may be close to 20. In such rivers, there is also a correlation between the size of grain and the cross-sectional outline. Where much of the alluvium is coarse and therefore carried close to (and on) the bottom, the bed is flat and broad. Where most or all of the alluvium is fine and carried well off the bottom, the bed is gently concave across, and the depth somewhat greater in proportion.

Large ratios, that is, over 30, usually indicate a slowly progressive failure in the carrying of sediments. Natural alluvial rivers in the normal high-flood condition in which they generate their channel morphology have width-over-depth ratios of between 14 and 28. A river that has fallen to a low-water stage may have however, through decrease of depth, a width-over-depth ratio of 40 or more. Thus there is a problem to find some central region of balance, among width-over-depth values, between increasing and decreasing alluvial conveyance.

For meandering rivers width-to-depth ratio is somewhat more complex because of the asymmetric cross-sectional shape. Moreover, within a selected reach, series of asymmetric and nearly symmetric cross-sections having different degrees of asymmetry can be expected. The cross-sectional shape depend on their corresponding locations in the plan-form. Therefore, width-to-depth ratio varies not only according with the width, but also varies with the averaged-depth of the cross-section.

4.13 The determination of friction in a meandering river

The determination of friction in alluvial rivers to a meandering river is possible from a knowledge of the similarities and differences between straight rivers and meanders (see sub-sections 4.4-1 and 4.4-2). In this case dunes are assumed to be in local equilibrium. From the calculations, if the bed material is assumed to have the same composition (ie. ignoring the grain sorting which takes place in nature) and the same representative diameter is used in the transport formula, the sediment transport capacities of a straight river and a meandering river are the same for the case that water surface slope in the meander is measured along the downstream thalweg direction. It is, of course, different when the valley slope is used as a measure for comparison. From this knowledge, the transverse bed slope in a meandering rivers has a different cross-sectional shape than that of a straight river, but application of the friction analysis in alluvial rivers to a meandering river is justified when the slope is measured along the downstream thalweg direction and mass flux is taken as the responsible driver for the sediment transport of each strip across the width of a meander.

4.13-1 Shear stresses in channel bends

Secondary currents and curved flows cause shear stress distributions to differ from those occasioned by straight flows. Sinuous channel flow is not uniform. The magnitude of the shear stress is related to the geometric and flow variables for the channel. The loss of energy and the stability of banks in open channels is also related to the distribution and magnitude of the shear stress generated by the flow in the bend. In steady uniform flow, the bottom shear stress is calculated by a very simple formula ($\tau = \rho \cdot g \cdot R \cdot I$). However the

correct value of the bed shear stress cannot be obtained unless the correct hydraulic radius is used. In other words, the definite water depth for a certain condition is essential. In this study, the local water depth, which is a function of space and time, can be predicted by the simulation model starting with a constant Chézy roughness coefficient. Later, the actual roughness coefficient is calculated by the procedure mentioned in sections 4.5 and 4.6. After the roughness is updated, the flow field is automatically updated and the new bed shear stress is found.

4.13-2 Updating the sediment transport capacity

It is obvious that all transport formulae are based on an effective shear stress. Therefore an updated shear stress will give a more accurate transport rate, and thereby bed level changes can also be updated. In order to be able to simulate the bed topography in a meandering river more accurately closer to nature, the shear stress values should be updated.

Figure 4.14 illustrates how the sediment transport rate would differ in both amount and trend from the value that it would take if the roughness coefficient were determined independently from the bed material property. The plane bed assumption, which makes the calculation so much easier, is also not recommended. Using an averaged value of roughness over the cross-section in the simulation is justified if the calculation of the roughness factor is based on flow and bed material conditions and only the total sediment transport rate is of interest.

However the use of a variable roughness is preferred for two-dimensional sediment transport calculations. It is also preferred for the calibration of the model. In all simulations it was necessary to tune the lateral flow distribution. This need is most probably related to lateral variation of the alluvial roughness and secondary flow condition (Olesen, 1987). For this purpose, the second improvement of the roughness factor is necessary (see Fig. 4.15(a) and (b)).

4.14 The role of discharge

The discharge regime of the catchment upstream from a river cross-section itself provides a fundamental independent control of the channel cross-sectional morphology. As the discharge varies at an individual cross-section, changes occur in the water surface width, mean flow depth and velocity and in other variables such as the water surface gradient, the friction factor, and bed shear stress. Although all the calculations have been based on a constant discharge so far, a variable discharge conditions can be simulated by using a discharge hydrograph as input.

4.15 Analytical model for transverse bed slope in a river bend

A bed topography simulation model for a meandering river has been developed in Chapter 3. As usual, a numerical model has its limitations, such as those of shallow water, mildly sloping bank, mildly curved plan-form, etc. However, in this chapter the wider area

of alluvial rivers, both straight and meandering is investigated with the least possible number of constraints. In order to be able to do this, an analytical model is applied to calculate the equilibrium transverse bed slope of a meandering river. Width-to-depth ratios of between 15 (ie. deep water rivers) and 0.1 (ie. unnatural rivers, just for study purpose) are calculated using this analytical model.

The transverse distribution of depth can be obtained by either assuming a constant transverse bed slope (an assumption, supported by field data, by among others De Vriend and Geldof 1983 ; Dietrich and Smith 1983 ; Odgaard and Kennedy 1982 ; and Thorne et al. 1983) such that the depth is given by

$$\frac{h}{h_c} = 1 + S_{tc} \frac{R_c}{h_c} \left(\frac{R}{R_c} - 1 \right) \quad (4.4)$$

in which

- h = local water depth
- h_c = water depth at the river axis
- R = local radius of curvature
- R_c = radius of curvature at the river axis
- S_{tc} = transverse bed slope at the river axis

or by allowing for the transverse bed slope's dependence on R (Odgaard 1986a), in which case the depth variation is given by

$$\frac{h}{h_c} = \left(\frac{R}{R_c} \right)^\beta \quad (4.5)$$

in which, $\beta = S_{tc} (R_c/h_c)$

In order to calculate the transverse distribution of depth, the transverse bed slope has to be known in advance. The transverse bed slope in a curved alluvial river (Zimmermann & Kennedy, 1978) is given by:

$$S_{tc} = \alpha \frac{(n+1)}{2n(n+2)} \frac{h}{R_c} \frac{U^2}{(s-1)gd} \quad (4.6)$$

$$S_{tc} = \alpha \frac{(n+1)}{2n(n+2)} \frac{h}{R_c} F_d^2 \quad (4.7)$$

in which

α = shape factor of the particle

F_d = the particle densimetric Froude No.

$$F_d = \frac{U}{\sqrt{(s-1)gd}}$$

- n = a dimensionless exponent which is derived from the vertical distribution of tangential velocity, v
 U = mean velocity
 g = acceleration due to gravity
 h = local water depth
 R_c = radius of curvature at the river axis
 S_{tc} = transverse bed slope at the river axis

The quantity n can be estimated from the Darcy-Weisbach friction factor, f . The equation (4.7) becomes

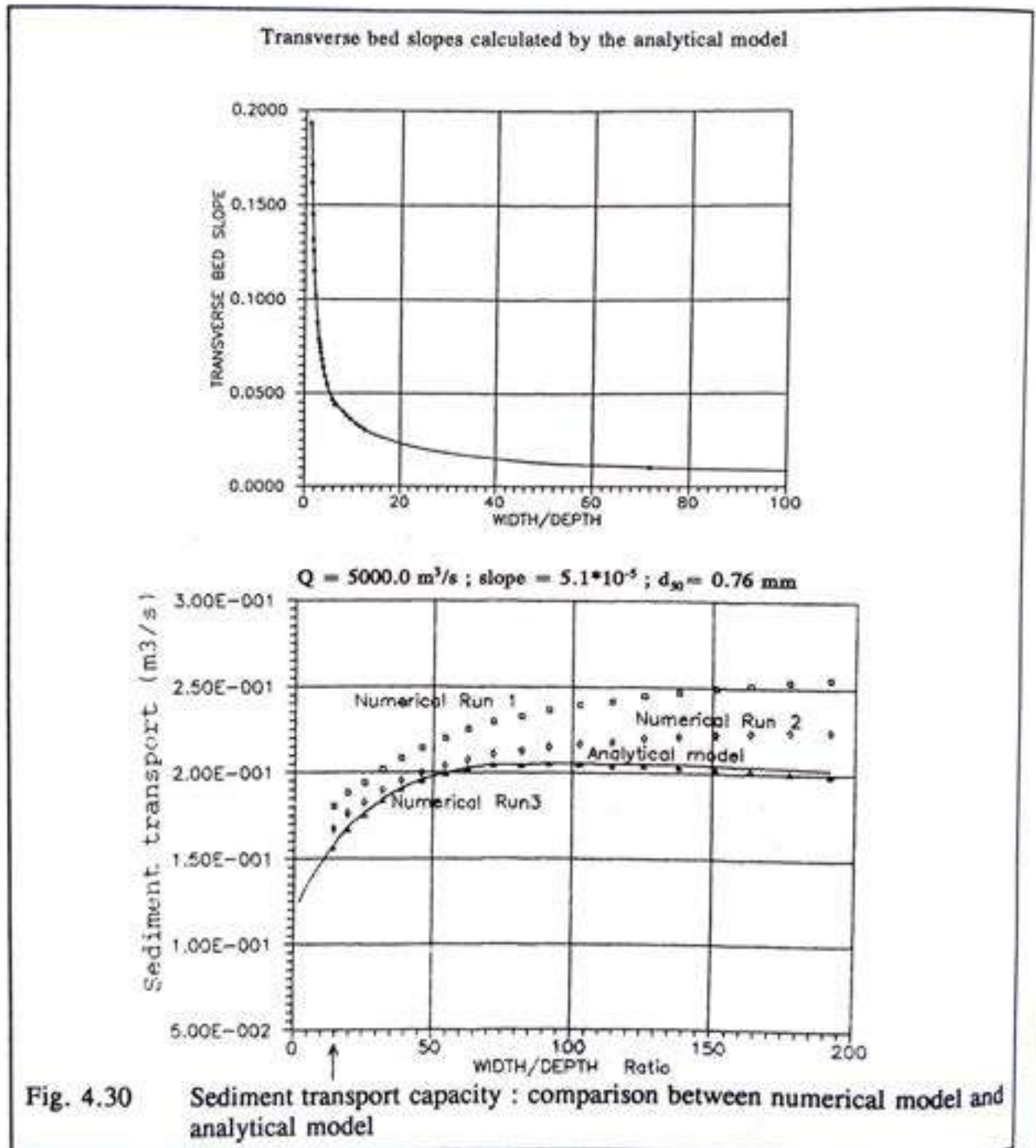
$$S_{tc} = \alpha \frac{(f + \sqrt{f})}{2(1 + 2\sqrt{f})} \frac{h}{R_c} F_d^2 \quad (4.8)$$

The model of Odgaard, (1984) for the steady-state transverse bed slope in a fully-developed alluvial channel bend can be described by the equation

$$S_t = 4.8 \theta^{0.5} F_d d \frac{h}{R} \quad (4.9)$$

- where S_t = local transverse bed slope
 θ = Shield's parameter
 F_d = densimetric particle Froude number
 d = representative grain diameter
 h = local water depth
 R = local radius of curvature

The analytical model mentioned above does not include the effects of flow and channel non-uniformities in the stream-wise direction, and is applicable only to fully-developed flow in channels with constant curvature. However, it is reasonable to expect that it will yield acceptable estimates of the local transverse bed slope in channels that change alignment gradually enough for the flow to be treated as quasi-uniform. The calculated transverse bed slope and the ratio of river width-to-depth are shown in Fig. 4.30.



4.16 Conclusions

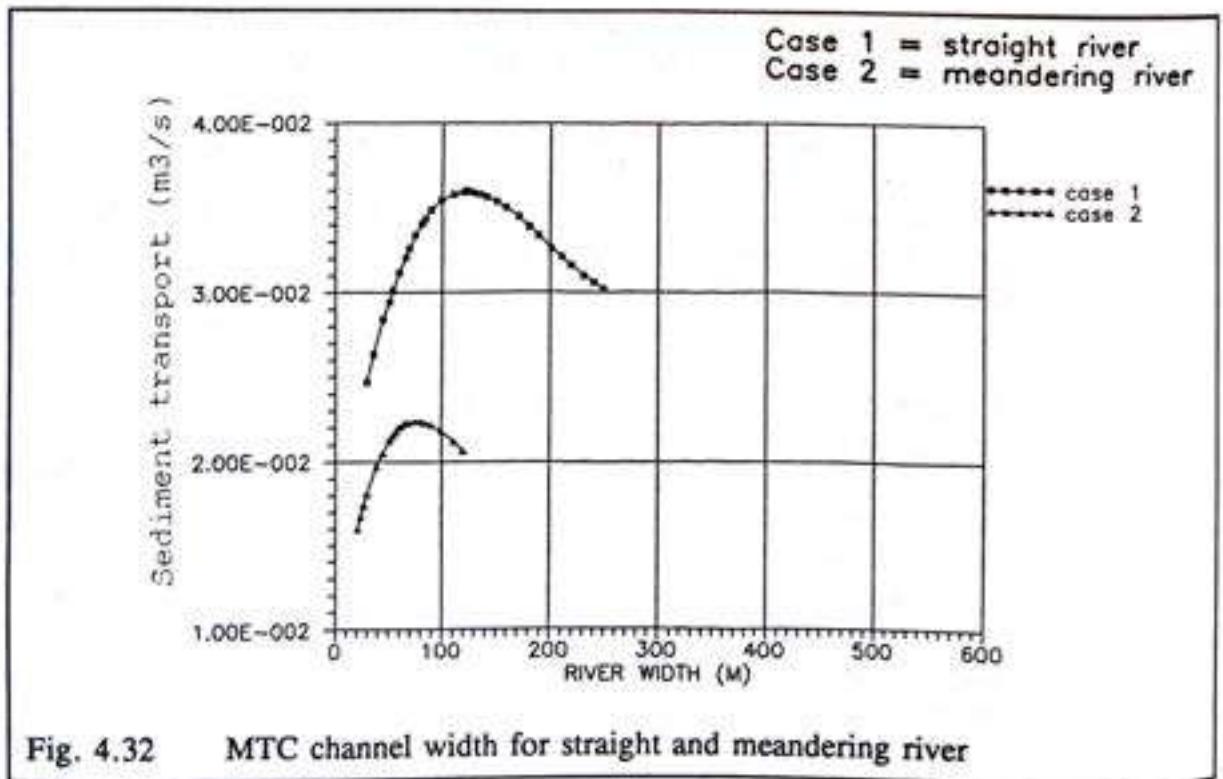
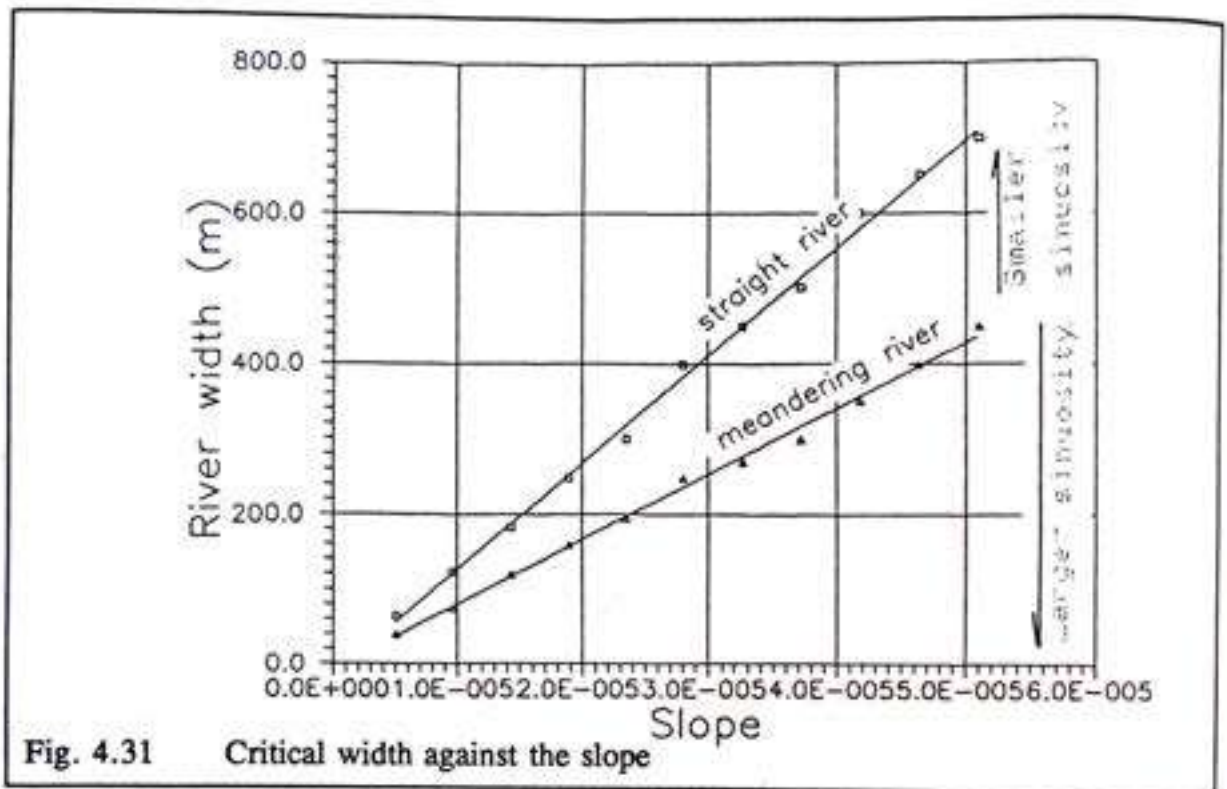
The principle of maximizing the sediment transport capacity for straight and meandering rivers is studied. This hypothesis is stated as follows : "for a particular water discharge and slope, the width of the channel adjusts to maximise the sediment transport rate " (White *et al.*, 1982). Here, in this study, the principle is applied to the problem of determining the plan shape of a river. A deterministic solution for channel roughness is applied and the unique water depth for a certain condition is calculated. The maximum transport capacity (MTC) channel width for both straight and meandering rivers is then calculated. Thereby the existence of the MTC state in meandering rivers is proven.

The following is a discussion of the principle of maximizing the sediment transport capacity. This principle is involved in determining the plan shape of a river. Onishi *et al.* (1976) claim that "a meandering channel can be more efficient than a straight one, in the sense that a given water discharge can transport a larger sediment load and, for some channel configurations and flow conditions, can require a similar energy gradient." Thus they postulate that the plan geometry of a river presents an attempt to maximize the transport rate.

This postulate that the plan geometry of a river presents an attempt to maximize the transport rate, is however not complete. In fact the plan geometry of a river presents an attempt to maximize the transport rate with an optimum river width. (See fig. 4.24) The sediment transport rate increases as the width increases until the optimum width is reached and, thereafter, the sediment transport rate decreases with increasing width. This can be interpreted as an attempt by the river to transport its own maximum possible load under the control of a given discharge, slope and the properties of bed materials.

Since discharge, slope and the properties of bed materials are fixed, the stable channel width must be adjusted in order to achieve a stable condition in which a certain amount of water and sediment can be transported. As shown in figs. 4.31 and 4.32, a meandering channel can be stable with a narrower width than a straight river for any given slope. This implies that a river tends to meander in order to stabilise and to reduce its destructive potential, including the bank erosion potential, which is a de-stabilising potential.

Therefore it does not follow that "a meandering channel can be more efficient than a straight one, in the sense that a given water discharge can transport a larger sediment load and, for some channel configurations and flow conditions, can require a similar energy gradient". It can also be seen from the calculations that a straight river can transport a larger sediment load than a meandering one for two cases. The first case is the sediment transport rate for different slopes when the width of the straight and the meandering rivers are the same (see Fig. 4.27). The second case is the sediment transport rate for different widths when the valley slope for the straight and the meandering rivers are the same (see Fig. 4.32). In this case the optimum river widths can be seen.



4.16-1 Suggestions for further study

This study has assessed and applied existing theories and has assembled them in an appropriate manner into specific problem areas in order to get nearer to a solution. Some interesting points for further study are suggested here:-

- (1) general conclusions should be defined for meandering rivers for various sinuosity values, various bend angles, and various discharges. Some have been done already and can serve as working examples for the remaining areas of study.
- (2) the grain sorting effect is also attractive for further study. Sediment transport per size fraction can be calculated by size fraction formulae and the composition of the bed material can be changed as in nature. It will be interesting to see the interaction between local roughness and the bed material composition.

4.16-2 The relationship between this specific chapter and the river plan form movement simulation model

- (1) The major deficiencies of the present mathematical model of river flow have been its failure to represent the dependence of friction factor on sediment discharge or concentration and to include temperature and channel-curvature effects. Natural rivers adjust their hydraulic roughness in their own ways. Getting more insight into the physics and the ability to add more appropriate friction factors will help the simulation one step nearer to a reasonable prediction.
- (2) The shear stress is calculated from local flow and roughness conditions. Local shear stress is also calculated by dividing the river cross-section into a number of strips. Therefore, the local bank shear stresses of the inner and outer banks can be calculated from the two outer-most strips correspondingly. However, this is not really important for the case where the width-to-depth ratio is greater than 15. Moreover, although the local shear stresses are estimated, the critical bank shear stress is still unknown and indeed known not better than an empirical relationship, such as 0.75 times the bed shear stress. Therefore further research should be concentrated on both local and critical bank shear stresses.

"Rivers as models of each other."

5. RIVER PLAN-FORM MOVEMENT

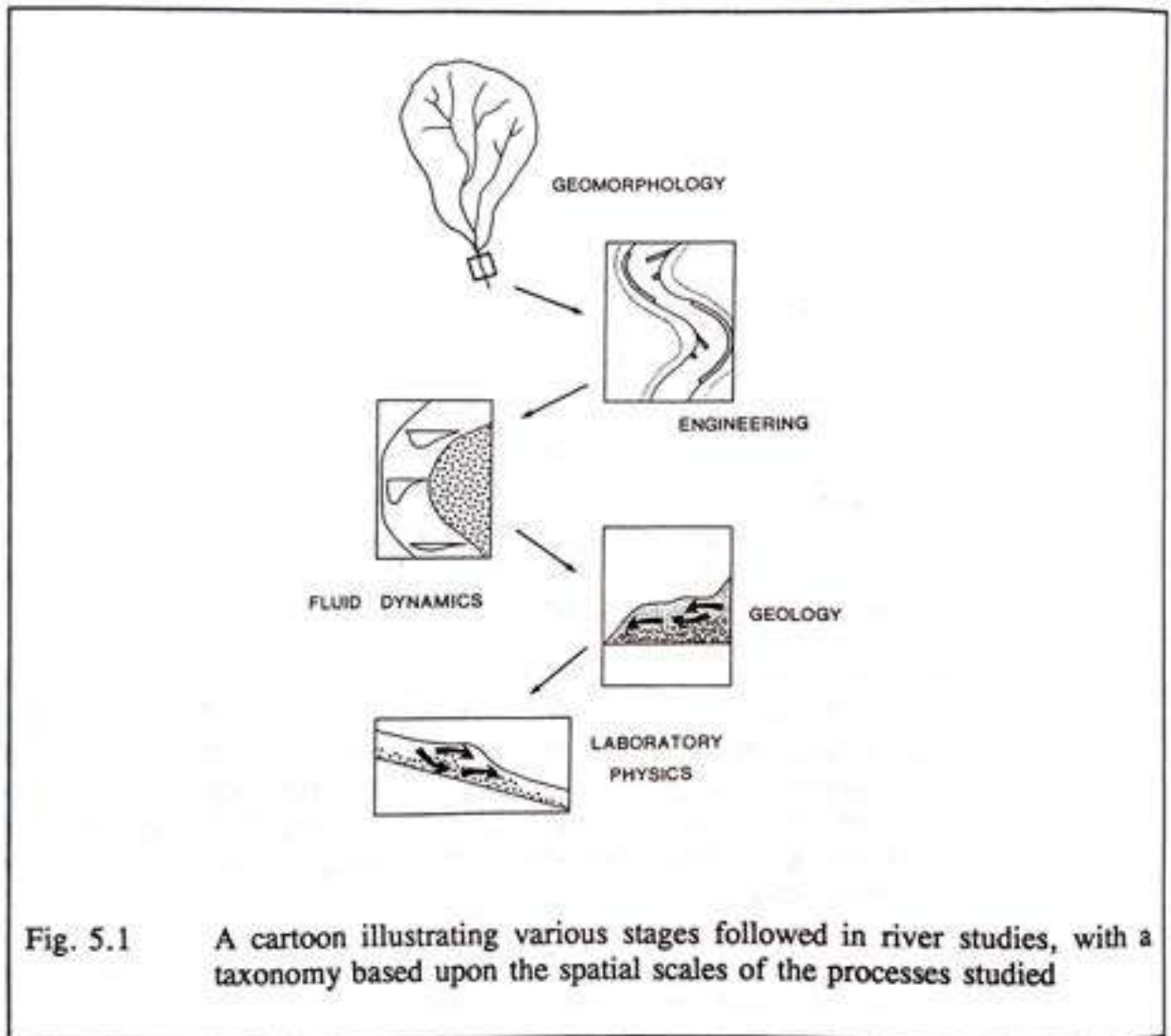
5.1 Introduction

Observations show that meanders tend to migrate. Their migration proceeds through a shifting of the loops in the downstream direction and an enlarging of the looped form. At low sinuosities, bends that have a moderate rate of migration tend to have a relatively regular shape. At high sinuosities, bends that are actively migrating downstream tend to show a marked asymmetry in shape. In both cases the river plan-form is changing over time. The factors affecting the river plan-form movement are numerous, but can be grouped under three major headings, as the nature of water and sediment-mixed flow, the nature of the flexible-boundary alluvial container and the interaction processes of these two major items. Consequently, it is clear that the study of river plan-form movement should start out from the geomorphology and be followed by the engineering fluviology, fluid dynamics, geology, and sedimentology together with their supporting laboratory physics.

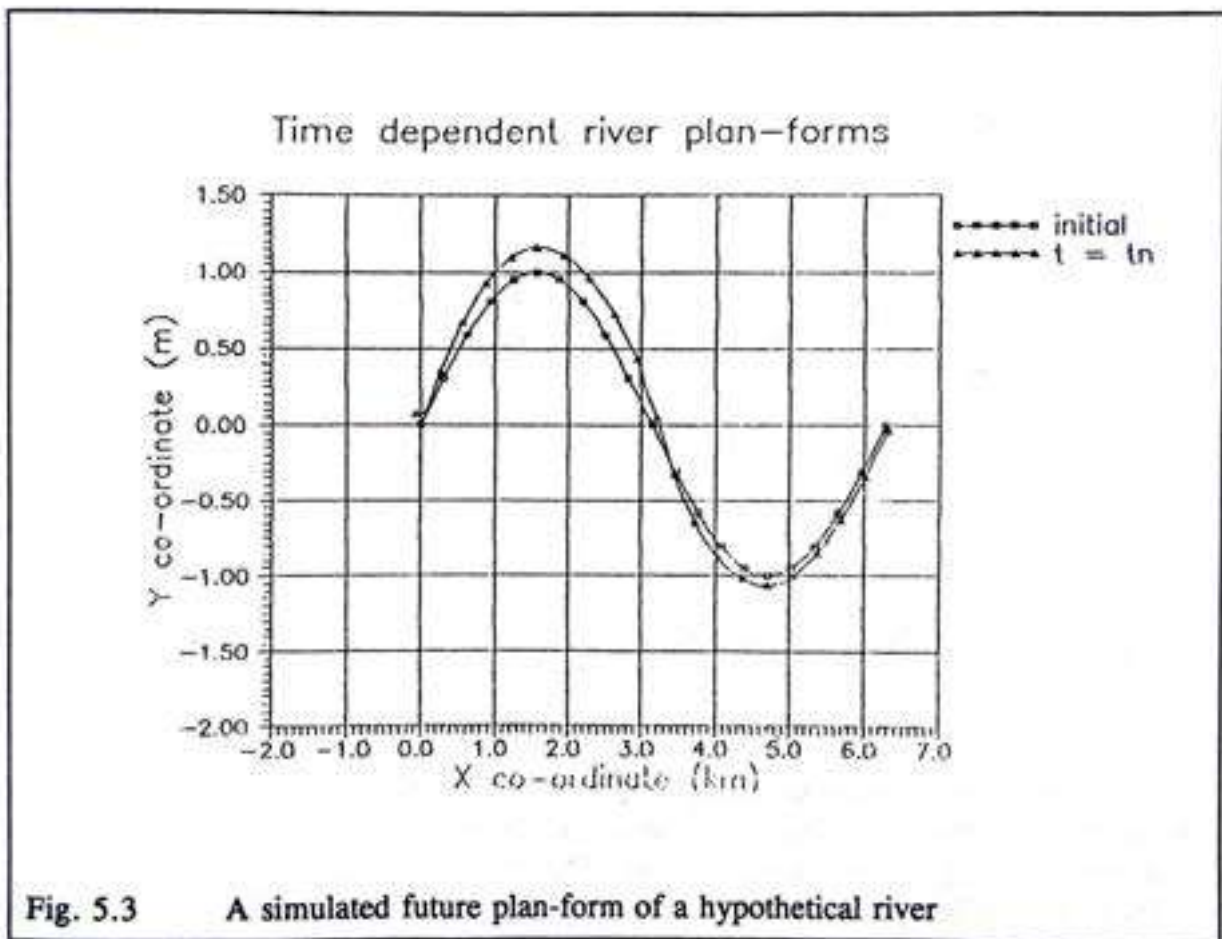
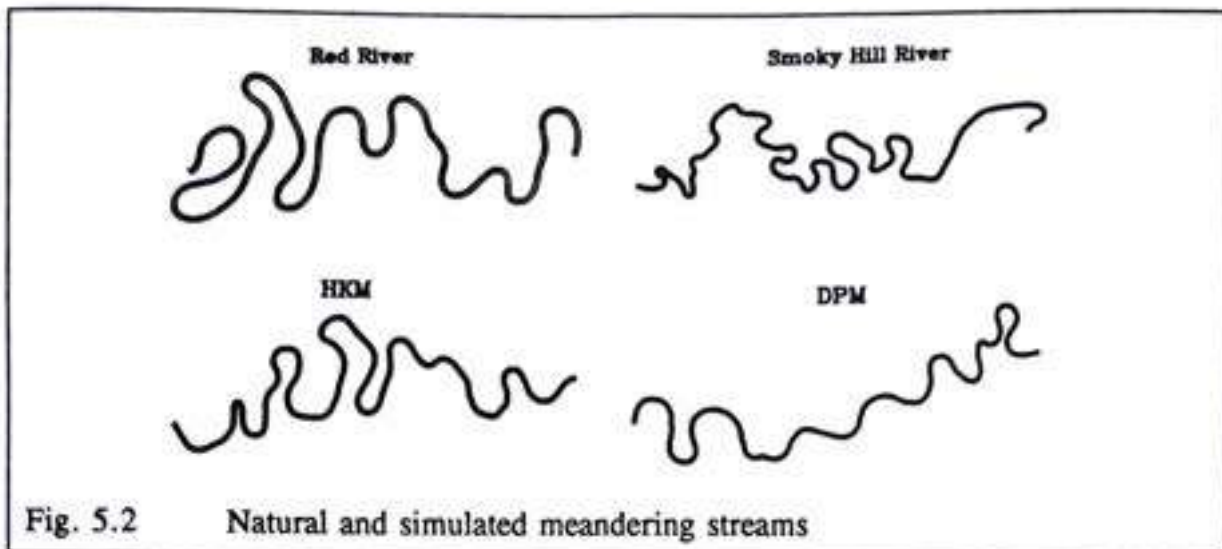
River studies are studies of variations in space and time which involve numerous spatial and time scales. Because of the complexity of the phenomena, changes have to be explained both inductively and deductively. Historically many scientists from different fields, such as Hydraulic Engineers, Geographers, Geologists and Hydrologists, studied river dynamics from different angles using different approaches. In Fig. 5.1, a cartoon due to (Newson, M.D. and Leeks, G.J., 1987) illustrates the various approaches to river studies and their corresponding spatial scales.

However, the results of the various approaches mentioned call for a new approach which can explain the river plan-form movement observed by monitoring systems. For example, the geomorphological approach of (Ferguson, 1976, 1979: abbreviated DPM, standing for Disturbed Periodic Model for river meander) and (Howard and Knutson, 1984: abbreviated as the HKM simulation model). In general, even with a variable bank resistance introduced into the HKM model and a disturbance parameter introduced into the DPM model, simulated streams show too great a regularity in meander size and shape (Howard and Hemberger, 1991). Fig. 5.2 shows portions of the Red River, Minnesota, and a comparative HKM simulation. The figure also shows the Smoky Hill River, Kansas, as compared to a DPM stream. Similarly, as can be seen in Fig 5.3 that the predicted bank line of a hypothetical river which is supposed to have an isotropic and homogeneous bed and bank material, can be simulated by the present model. It can represent the growth of the plan-form for an individual river bend. However the predictability of the model is still far from

describing the real river situation. For taking the traditional reached-average approach, the mathematical model is developed under the corresponding simplifications. These are just three examples of the general shortcomings; the other approaches experience similar difficulties. In general, the limitations of mathematical models are many and the range of validity of the models is limited. Therefore a reasonable forecast of the future plan-form of the river has not yet been realised successfully and is and remains a challenging topic.



One of the basic reasons for these shortcomings may be that an insufficient attention is given to the multiple scales of the processes involved in river morphology. Geologists and geomorphologists approach the system from the larger scale down to the smaller scale in time. Meteorologists approach the system using a global scale in space but a meso-scale in time. Hydraulic engineers approach the system starting from a micro scale in time (e.g. turbulence, eddy viscosity, etc.) and space, and from there proceed to larger scales. Accordingly, the system is studied by many specialists from many directions, and these



frequently intercross. When the system is approached from the larger scales and solved downward in the space scale, the **initial smoothing effects** cause errors. If the approach is made from the opposite direction, the **residual smoothing effects** cause errors. As Mosselman (1992) expressed this matter: *The problem can only partly be ascribed to limitations of data acquisition and computer capacity. Parts of the problem are of a more*

fundamental nature, refuting Laplace's (1814) idea that a powerful intelligence knowing all fundamental laws of nature and all initial conditions would be able to compute predictions for an arbitrarily long period.

Despite all these difficulties, the present study is an attempt to make a predictive system by putting together three aspects of river evolution (ie. geomorphology, fluvial hydraulics and hydrodynamics) into a simulation model with the assistance of laboratory physics, field observations and numerical methods. The present investigation starts from the micro scale and proceeds to the larger scales by a process of integrating. The effects of climate, lithology and geological activities are considered as given premises. Moreover, the chaotic behaviour and some exceptional events are excluded.

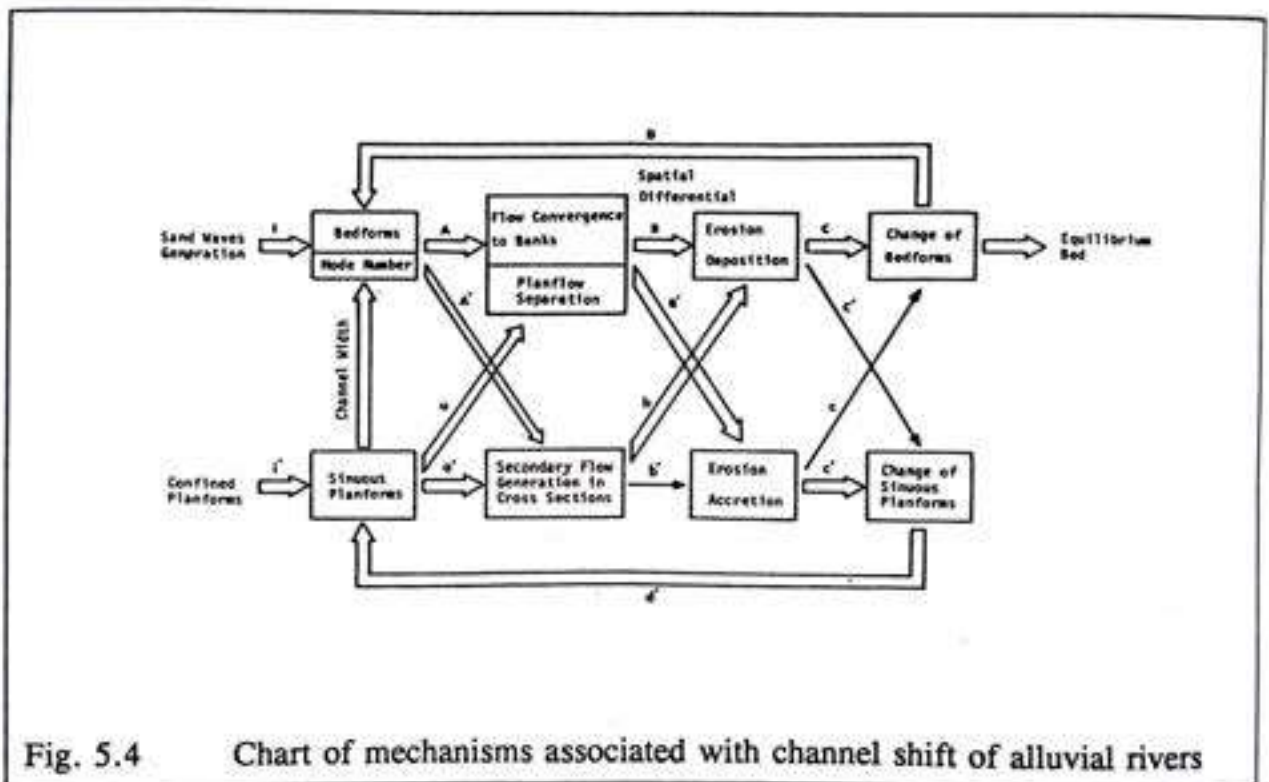


Fig. 5.4 Chart of mechanisms associated with channel shift of alluvial rivers

In Fig 5.4 a chart due to (Hasegawa, 1983) illustrates the interrelationships obtaining among factors governing channel changes in alluvial rivers. The arrows indicate the influences operating among various factors. The degree of association is expressed by the thickness of the arrow. This is a fluvial-hydraulic approach and the present study is concerned with identifying interrelationship orders among the factors, as related to the intensities of the influences. The hydrodynamic standpoint for the present investigation has been described in detail in Chapter 3.

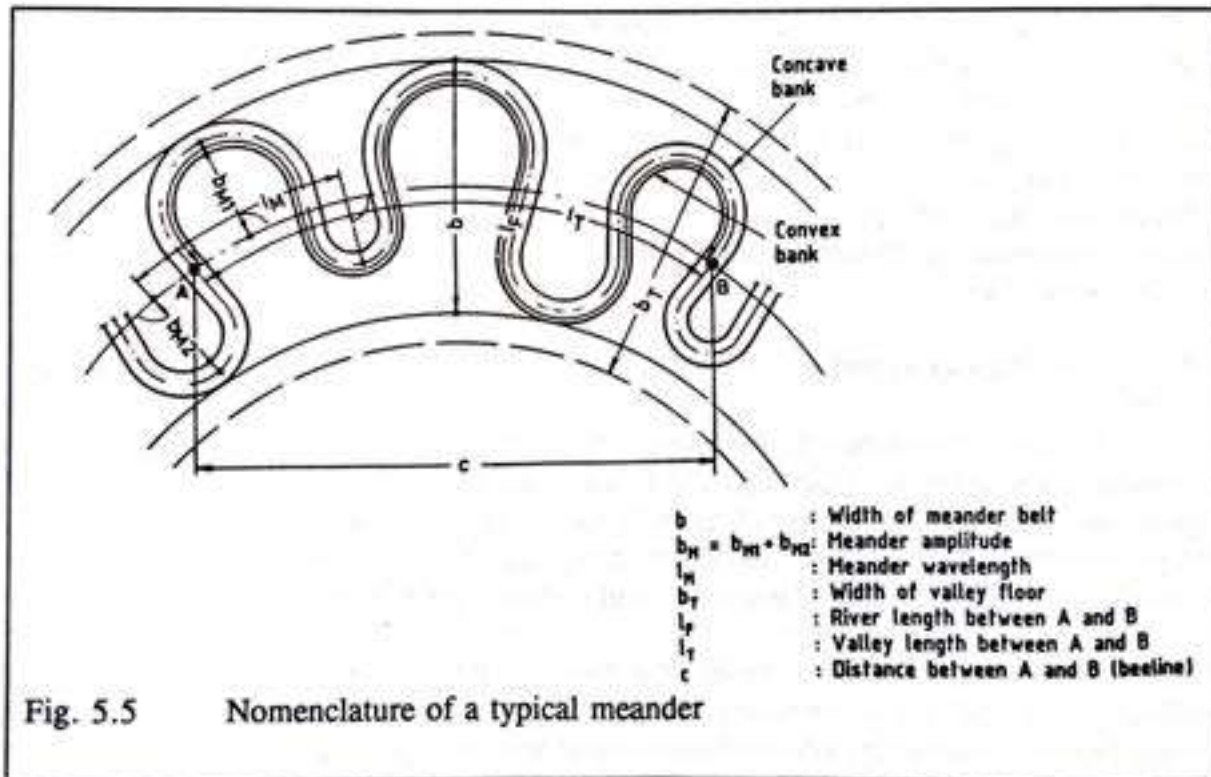
Finally, a mathematical model is developed on the basis of the mechanisms associated with the channel shift of alluvial rivers. The geomorphology of the river bank which is considered in the present study, the bank erosion mechanisms and their derivations are

presented in sections 5.3 and 5.4. The computational methods applied and proposed are presented in sections 5.6, 5.7 and 5.10. The results are also discussed in section 5.12.

5.2 River parameters

The geometrical configuration of a river is defined by its cross-sectional geometry, plan view, and longitudinal profile. The documented river distances usually take account of the river regulation and start from a point at the mouth and proceed from there upstream. The length scale of the river is usually introduced through river parameters and their ratios.

The cross-sectional dimensions and the asymmetries are mostly correlated with representative dimensions in meandering alluvial rivers. The scatter of the (weak) relationships between width and depth has been found to be at least partly related to the asymmetry of the cross-sectional shape. On the average, the distance through which the cross section is essentially symmetrical is only about one-tenth of the wave length. Nevertheless, the width-to-depth ratio is an essential parameter in the present investigation. Therefore the average width-to-depth ratio for an asymmetric cross-section is presented in Appendix-C.



The river evolution (sinuosity) is expressed in terms of the ratio between the straight line 'C' from source to mouth, as deduced from the length of the river ' l_p ' and divided by 'C' (Fig. 5.5). It should be noted that some natural meandering streams appear to have short meanders superimposed upon longer meanders, often generating the compound or cumuliform

meander forms noted by (Brice, 1974) and (Hickin, 1974). Therefore river evolution is defined at three levels, such as course evolution, valley evolution and river evolution. The sinuosity of the plan-form shape at the reach level is defined as the ratio of the distance along the channel to the distance joining the ends of the path. Occasionally the straight line distance may not coincide with down-valley direction and gradient, especially if the plan-form is confined within valley bends. Often it is justified to assume that at the within-reach level the valley is straight. Fig.5.5 depicts the river parameters which are used in the present study.

The longitudinal profile of the river system is mostly, and certainly on average, concave. The slope of the profile is steeper at the source and milder towards the mouth. On a reach basis, however, the slope can be considered constant.

5.3 Bank erosion mechanisms

River bank erosion is a complex phenomenon. The bank erosion mechanism can be divided into two categories (Thorne, 1982; Osman, 1985). One is the entrainment of the individual particles (hereafter called fluvial entrainment) and the other is the mass failure, such as sliding failures or other types of geotechnical failures that occur under adverse condition in soil. These two cases are considered individually for convenience, but the strength of the interaction that can occur between these two erosion processes is fully appreciated. Fluvial processes appear to be the most important in the case of non-cohesive banks, but it is particular combinations of processes that prove to be most effective in the case of cohesive banks (Hasegawa, 1989). The balance between the rate of supply of bank sediment into the bank toe, and the rate of removal of the same material from the toe by fluvial entrainment, is the dominating factor in controlling the rate of retreat of banks of all types (Thorne, 1982).

5.3-1 Fluvial entrainment

This is a time-dependent erosion, proceeding with a rate that is decreasing or increasing accorded to the flow regulation conditions for a specific bank. The erosion rate depends on a number of factors, such as shear stress, velocities, secondary flow, composition and properties of the soil, dispersion of the soil, water quality, bank geometry, presence of vegetation cover and density of big trees, and (other) natural and man-made effects.

Shear stress variations along the banks are very important factors. Spatially oscillating flow and bed deformation provide the shear stress variation. There are several concepts for the shear stress which controls the erosion process. The effective stress concept appears to be the most popular one. The bed shear stress resultant direction neither coincides with the water flow direction nor the sediment transport direction in the river bends. The mathematical expression for the bed shear stress resultant direction and sediment transport direction has been discussed earlier, in Chapter 3. A very important problem is the definition of a critical shear stress for river banks consisting of cohesive soils. When the bank material properties are concerned, the critical shear stress of the bank is further affected by such variables as the sodium adsorption ratio, the pore fluid salt concentration, and the dielectric dispersion.

Velocities near the bank and secondary flow velocities play a vital role in the process of bank erosion, because the flow velocity and acceleration provide the drag force and flow mass which carry the sediment products. Their importance is also very obvious in all the sediment transport formulae. The near bank excess velocity is used as a direct measurement of the rate of fluvial entrainment, a practice initiated by Ikeda *et al.* 1981. In the river bends, **the secondary flow** is generated by channel curvature (sinuosity). The vertical distribution of the main flow takes on the form of a spiral, which in its turn induces a pronounced bed slope perpendicular to the main flow direction. The pronounced bed topography and flow variations cause spatial variations of the grain size of the river bed and near-bank bed deformation; it thus produces bank erosion and a changing of the curvature.

The stability of the bank depends on **the type of the soil** and its **composition** and **compaction**. Because of the compaction or composition, there may be variations in the soil shear strength. Soil shear strength is proportional to the cohesion and the angle of friction. Dispersion of the soil is a major concern in the case of cohesive soil, while most river banks are predominantly cohesive. Usually, three types of sediment structures are defined in cohesive soil, depending on the forces of attraction and repulsion occurring during sedimentation: these are known as the salt flocculation structure, the non-salt flocculation structure, and the disperse structure (Lambe and Whittman, 1969; Hough, 1957; Taylor, 1948). The cohesive property is determined mainly by physio-chemical interparticle forces that result from residual electrical charges at the surfaces of clay mineral sheets. These forces depend on temperature and the electro-chemical properties of the bank soils.

For non-cohesive soils, the properties having the greatest significance for soil erosion are the dispersion ratio, the ratio of colloid to moisture equivalent, and the silica-sesquioxide ratio (Middleton, 1930).

The **grain size distribution** of the fluvial sediment also controls the fluvial entrainment. Extensive particle size analyses of bed and bank material samples from perennial streams of the Missouri River basin (Osterkamp and Wiseman, 1980) suggested that the formation of a stable alluvial bank is dependent on the availability and sorting of specific size ranges of sediment. They concluded that relatively stable banks are deficient in 0.35 to 1.3 mm diameter sand grains, regardless of channel gradient or basin characteristics. This implies that, if the total sediment load of a river is predominantly medium- to coarse-grained sand, a wide, unstable channel will result because the fine (less than 0.35 mm) and coarse (greater than 1.3 mm) sizes required for bank stability are not available. It can be noted that the grain size distribution of the bed and bank material affect the stability of the river in two ways. The first one has already been discussed in chapter 4, as it concerned the relation between total sediment transport and channel width. The second is the particular combination of grain sizes which reinforce the bank stability.

Water quality is related to the type of bank soil. As cohesive materials are affected by the electrochemical properties of the eroding fluid, water quality strongly influences the erodibility of the banks. Most of the flume experiments use distilled water to find the erodibility and then check with river water ; researchers have concluded that the influence

of the water quality is significant (Arulanandan, *et al.*, 1980). On the other hand, the water quality is heavily affected by vegetation.

The effect of **vegetation and intensity of cover of big trees** can be taken into some account through a coefficient defined in (Pizzuto and Meckelnburg, 1989). Grass and shrubs almost always increase the stability of the bank. The existence of trees can both increase and decrease the bank erosion rate. Detailed study of this factor and a thorough qualitative description of how type, age, health, and density of trees influence bank stability is given by (Thorne and Osman, 1988). The lateral migration of the Genesee river, New York, was studied by (Beck, S. *et al.*, 1980). The lateral migration rate in farmland was found to be 130% faster than that in forested areas. In this case, the existence of trees decreases the bank erosion rate.

5.3-2 Mass failure

As mentioned above, this type of failure is constituted by sliding failures or other types of geotechnical failures that occur under adverse condition in soils. It depends on the balance of forces on the most critical potential failure surfaces. The factors and forces which cause mass failure are well recognized. These factors are bulk ground-water flow, ground-water seepage, bank soil structure, stratigraphy of the bank, near-bank bed degradation, and sudden drawdown of the water level in the river. Most of the work done in this area treats the phenomenon as a soil mechanics problem. The principles used in the stability and analysis of earth embankments and structures are thereby used to analyze bank stability and erosion.

One of the main causes is the removal of particles at the toe, which makes the bank behaves as a cantilever. Later the cantilever will collapse under gravity. But there are also other causes, such as the development of tension cracks and their filling with water (Springer *et. al.*, 1985). Actually, failure may also start from a temperature effect: when a bank-surface is exposed to a considerable daily range of temperature, as in arid and semi-arid regions the expansion which occurs during the day and the contraction at night, constantly repeated, may results in the opening of many small cracks. The decomposition of the bank soil and its disintegration occur when water enters into these cracks. This may be very important for regions where high day and low night temperatures are prevalent.

The failures of river bank of the move massive type takes the form of slope failures (ranging from progressive, continuous failure by creep to almost-instantaneous, or catastrophic shear failure) of the bank.

5.3-3 Feedback processes

The bank erosion mechanism is also a circular process. The causes affect the bank erosion and bank erosion products affect the variation of the intensity of the causes. This can be seen as follows. Flow exerts shear stresses that remove particles from the banks and the bed: it shapes the near-bank bed topography. The near-bank bed topography affects bank erosion in two ways, namely, directly and indirectly. The first case arises because the total bank height is itself an important parameter for bank stability: an increase in bank height decreases stability. The second indirect way arises because the topography influences flow velocities in the bank region and hence the shear stresses. For example, let us suppose that the river banks are being eroded and bank erosion products are being released into the flow. The bank-erosion products participate in the sediment transport process. The sediment imbalance, defined as the difference between sediment transport capacity and the actual sediment flux, is a distinct factor affecting the channel migration rate. A correlation between migration rates and sediment imbalance was determined by Murphey Rohrer (1983). Neil (1987) estimates the limits of channel migration from sediment transport rates. A case study described by (Neil, 1983) of a bend migration in the Tanana River (Alaska) is there given in evidence: in this case there was a more-or-less complete exchange of bed load, all incoming bed load being deposited on the inner point-bar and being replaced by material derived from outer-bank erosion. This mechanism results in an extremely high migration rate, of about 50 m/year. Humphrey (1978) also reported some enhancement of migration rates downstream of meander cutoffs, which is ascribed to a local increase in sediment supply. Therefore these circular influences cause river bank erosion to proceed in a faster and more complicated manner. Thus this can be supposed to provide a positive feedback to the erosion system.

The other circular process can be regarded as one that provides a negative feed-back system, arising from the bank surface conditions. Erosion is a surface phenomenon which refers to the area exposed to erosive water flow. Two surface conditions are relevant. The first condition, involving as it does the interaction between bank materials and the eroding fluid, may alter the bank erosion resistance by an order of magnitude. The instantaneous physicochemical composition of the surface material is uniquely related to stability (Lambermont and Lebon, 1978). The second surface condition involves the physical configuration of the material surface: cohesive materials have rigid boundaries and the roughness of the boundary material may induce sufficient form roughness to affect near-surface conditions. This aspect of the stability of bank soil materials has not been fully explored because of the extreme difficulty of quantifying and interpreting turbulent velocity fluctuations in close proximity to rough surfaces.

5.4 Bank erosion rate

The bank erosion rate can be estimated qualitatively from the hydrodynamic forces, bank characteristics (such as geometry and vegetation cover), bank material type (such as silt and clay contents, organic matter content, bank soil stratigraphy and chemical characteristics), and erodibility of the soil. However, mathematical formulae account for only some of the parameters quantitatively, and not all. The completion of the set of mathematical

expressions involves the selection of dominant factors, while neglecting minor factors, and the introduction of simplifications due to the inadequate state of knowledge of interaction effects, and by no means are these neglected parameters negligible. Theoretical derivations of bank erosion rates are presented in section 5.4-1.

On the other hand there are many empirical relationships which can be used to estimate the bank erosion rate. These relationships, proposed by many authors, give again the impression that the bank erosion rate is estimated primarily on a basis of personal experience, as this is influenced by an own specialization, such as may be geomorphologically biased or hydrodynamically biased. A summary of these bank erosion rate relationships leads one to think about their relevant utilities. For this reason, the most empirical relationships which are used in this study are presented under four categories corresponding to their governing parameters, as shown in section 5.4-2.

5.4-1 Theoretical derivation of the present study

A derivation has been made of linearised bank erosion equation, and some simple computer programs have been made as listed in Appendix-C and tested in order to check whether their formulations were consistent with measured values given in the standard references. Empirical relationships of bank erosion rate were used in order to check the quantity of bank erosion rate so provided. Very few field data are available and only some of these have been compared with calculated values. The verifications are presented in section 5.5.

On the side of the theoretical formulation there are two possibilities to estimate the bank erosion rate. The first considers the balance of forces on the moving grain. The derivation and the mathematical expression can be found in the reference (Hirano, 1973). The second considers the net sediment balance in a certain cross-section as an amount of lateral bank erosion volume. The hypothesis is originated by Hasegawa, 1987. This type of calculation emphasized on unit length of the cross-section and sediment volume balance is made along the transverse direction. Therefore this formulation is appropriate only when the river reach has attained certain equilibrium. The mathematical expression for the bank erosion rate appears as following.

We use the form

$$\bar{\xi} = \frac{1}{(1-\lambda)(H_0 + \eta n_i + h_f)} \left[\int_{n_0}^{n_s} \frac{\partial q_s}{\partial s} dn - q_s(n_s) \right] \quad (5.1)$$

for the second term

$$\left[n_s \int_{n_s}^{n_b} \frac{\partial q_s}{\partial s} dn - q_n(n_s) \right] = \left[\frac{\partial q_s}{\partial s} (n_b - n_s) - q_n(n_s) \right] \quad (5.2)$$

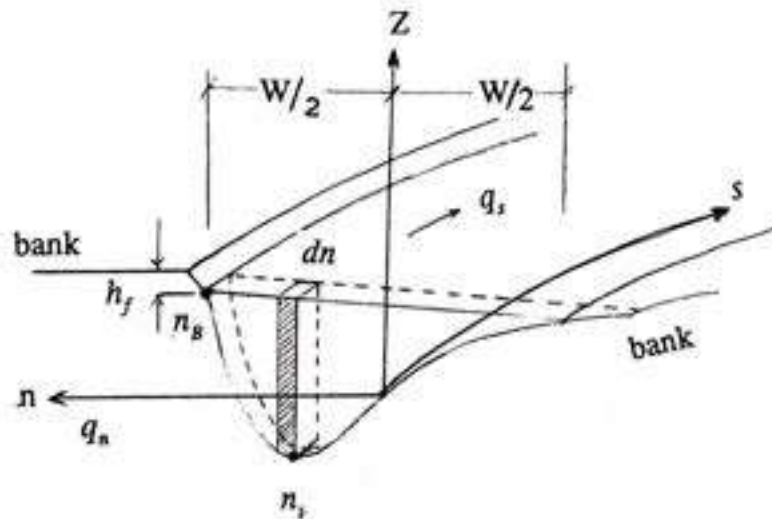


Fig. 5.6 Definition sketch

and this becomes

$$2^{nd} term = \frac{\partial}{\partial s} \left[K \sqrt{\left(\frac{\rho_s}{\rho} - 1 \right) g d^3 (\tau_s - \tau_{s,c})^{1.5}} \right] (n_b - n_s) - q_s \left(\frac{U_s}{U_0} + \tan \psi + T \frac{\partial \eta}{\partial n} \right) \quad (5.3)$$

Here τ_* is expressed as follows:

$$\tau_* = \left[\frac{1}{\left(\frac{\rho_s}{\rho} - 1\right)gd} C_{f_0} U_0^2 + \frac{1}{\left(\frac{\rho_s}{\rho} - 1\right)gd} C_{f_0}^2 U_0 U_B \right. \\ \left. + \frac{1}{\left(\frac{\rho_s}{\rho} - 1\right)gd} C_{f_0} U_B^2 \right] \left(1 + \frac{\eta}{H_0}\right)^{-\frac{1}{3}} \quad (5.4)$$

Using binomial series and neglecting higher order terms provides:

$$\left(1 + \frac{\eta}{H_0}\right)^{-\frac{1}{3}} = 1 - \frac{1}{3} \frac{\eta}{H_0} + \frac{2}{9} \frac{\eta^2}{H_0^2} \quad (5.5)$$

Therefore equation (5.1) can be written in the form of

$$\bar{\xi} = C_1 T_1 \quad (5.6)$$

in which

$$C_1 = \frac{q_{s0}}{(1-\lambda)} \quad (5.7)$$

and

$$T_1 = \frac{\partial}{\partial s} \left[K \sqrt{\left(\frac{\rho_s}{\rho} - 1\right)gd^3} \left(\tau_{*0} - \frac{\eta\tau_{*0}}{3H_0} - \tau_{*c}\right)^{1.5} \right] (n_b - n_i) \\ - \left[K \sqrt{\left(\frac{\rho_s}{\rho} - 1\right)gd^3} \left(\tau_{*0} - \frac{\eta\tau_{*0}}{3H_0} - \tau_{*c}\right)^{1.5} \right] \left(\frac{U_a}{U_0} + \tan\psi + T \frac{\partial\eta}{\partial n}\right) \quad (5.8)$$

where

$$\tau_{*0} = \frac{1}{\left(\frac{\rho_s}{\rho} - 1\right)gd} C_r U_0^2 \quad (5.9)$$

in which

- ξ = bank erosion rate
- C_r = local resistance coefficient
- H, H_0 = local mean water depth
- τ_* = critical shear stress parameter
- λ = void ratio
- q_s = sediment discharge/ unit width in the s s direction
- q_n = sediment discharge/ unit width in the n direction
- h_r = bank height
- n = transverse direction coordinate
- s = longitudinal direction coordinate ; see Fig. (5.6).

5.4-2 The hypothesis of near-bank velocity excess

Ikeda *et al.*, 1981 have suggested the following equation:

$$\bar{\xi} = E (U_b - U) \quad (5.10)$$

in which

- ξ = the rate of bank migration m/s
- U_b = the velocity near the bank m/s
- U = reach-averaged velocity m/s
- E = a dimensionless erosion coefficient

Alongside this, a scour parameter A has been related to the local bed geometry through the following equation, also presented by Ikeda *et al.* (1981).

$$m = - A H C n \quad (5.11)$$

where

- m = local bed elevation
- C = local bend curvature
- H = reach-averaged depth
- n = the cross-channel coordinate (n is orthogonal to s)

The cross channel coordinate 'n' is zero at the channel centre and the datum for 'm' is the bed elevation at the channel centre.

In this connection, reference should be made to the models of Parker (1981, 1983) and Odgaard (1987).

5.4-3 Empirical relationships

The bank erosion rate models which are used in the present study can be categorised in four groups which are base on the differentiation between the governing parameters used to express the rate. In the first group, the bank erosion rate is mainly determined by the plan geometry and cross-sectional geometry of the river. In the second group, it is mainly concerned with the bank and bed material properties of the river. In the third group, it is calculated as a function of the catchment area. In the last group, the bank erosion rate can be estimated as a function of flow velocity. Various models are described briefly and bank erosion rate models are developed as individual modules. These modules can be attached to the main simulation program in accordance with the specific requirement of the simulation and can be shifted around as needed. Each module should be chosen with a concern for the physical balance.

- **Bank erosion rate equations group (1)**

This is mainly concerned with the plan geometry and cross-sectional geometry of the river. We then have the following formulations:

- Brice, 1982 model:

Rate of bank erosion increases with increasing channel width.
The relationships are as follow:

- (1) 0.1 m/yrfor a 10 meter wide channel
- (2) 9.0 m/yrfor a 600 meter wide channel

- Hicken and Nanson, 1975 ; Nanson and Hicken, 1983, model:

These suggest that

$$\xi = 2.0 * \frac{B}{R_c} \tag{5.12}$$

when $\{B/R_c \leq 0.32\}$

$$\xi = 0.2 * \left(\frac{R_c}{B}\right) \quad (5.13)$$

when $\{B/R_c\} > 0.32\}$

in which

ξ = erosion rate (m/yr)

B = channel width (m)

R_c = radius of curvature of the channel centre line



• Bank erosion rate equations group (2)

This group is mainly concerned with the bank and bed material properties of the river. We next consider the formulation of Ariathurai and Arulanandan (1978) which was applied to a cohesive soil with 30% illite. In this case,

$$\xi = 0 \quad \text{for } \theta > \theta_c \quad (5.14)$$

$$\xi = M \left(\frac{\tau}{\tau_c} - 1\right) \quad \text{for } \theta \leq \theta_c \quad (5.15)$$

where

$M = (0.003 < M < 0.03)$ gm/cm²/min; an erosion rate constant

Modification of the unit of ξ to suit the unit which is expected in the simulation model ξ can be determined as follows:

$$\xi = \frac{M}{s} * \frac{5}{3} * \left(\frac{\tau}{\tau_c} - 1\right) \quad (5.16)$$

(or)

$$\xi = \frac{M * e}{s} * \frac{5}{3} * \left(\frac{\tau}{\tau_c} - 1\right) \quad (5.17)$$

in which

- s = relative density of the soil
- e = voids ratio of the material
- ξ = m/s

Therefore equation (5.16) is taken excluding voids in the material and equation (5.17) is taken including voids in the material.

- Partheniades, (1963) model

Erosion rate for mud, generally, expressed as

$$\xi = \frac{dm}{dt} = M \frac{\tau_b - \tau_c}{\tau_c} \quad \text{for } \tau_b > \tau_c \quad (5.18)$$

in which M, a coefficient (in mass per unit area and time), is a material 'constant' depending on mineral composition, organic material content, salinity etc. Reported values are in the range of $M = 0.00001$ to $0.0005 \text{ Kg/m}^2.\text{s}$ for soft natural muds.

- Parchure and Mehta (1985) model:

Their model is expressed by a relationship of the form:

$$\xi = E_0 e^{\alpha(\tau_b - \tau_c)^{0.5}} \quad \text{for } \tau_b > \tau_c \quad (5.19)$$

in which the E_0 value (in $\text{Kg/m}^2.\text{s}$) is defined as the value for $\tau_b = \tau_c$ (at the surface $z = 0$) and can be determined by extrapolation from a plot of E against τ_b . The E_0 values are in the range of 0.00001 to $0.001 \text{ (Kg/m}^2.\text{s)}$ for kaolinite and natural mud in saline water. The α coefficient is in the range of 5 to $20 \text{ (m/N}^{0.5}\text{)}$.

- **Bank erosion rate equation group(3)**

This is calculated as a function of the catchment area.

- Hook (1980) model:

$$\bar{\xi} = 0.0245 A^{0.45} \quad (5.20)$$

in which, ξ = Mean erosion rate m/yr
 A = Catchment area Km²

The range of the data started from 0.05 m/year for a drainage area of 3 Km² and continued up to 800 m/yr for a drainage area of 1000,000 Km². Hooke, (1980) obtained a regression relation between the migration rate of a meander loop and the catchment area by using her own data as well as those of others. An approximate relation that was obtained of bank erosion rate ξ to the square root of the catchment area A implies that ξ should increase in proportion to the channel width W , because the square root of A can be expected to be in proportion to W . This suggests that bank erosion rates are similar for basins of all sizes if normalized in terms of increase in channel width per year.

- **Bank erosion rate equations group (4)**

In this last group bank erosion rate can be estimated from the function of flow velocity.

- Wiggert and Contrator (1969) model:

$$\xi = 0.25 U^{3.8} \quad (5.21)$$

in which ξ = erosion rate (ton/ft/day)
 U = mean velocity (ft/s)
 Note that no bank soil properties are considered.

• Pizzuto and Meckelnburg (1989) model:

This model was based on the hypothesis that erosion rates are controlled primarily by the near-bank velocity. This near-bank velocity was measured at nine survey sites and a statistical analysis of the relationship between bank erosion rate and near-bank velocity was made over a two years period. For a long-term analysis, which considered the period from 1937 to 1980, no velocity measurements were available for the bend; the model of Parker et al. (1983) was consequently used here in order to estimate the near-bank velocities and the model of Ikeda et al. (1981) was used in order to estimate the scour parameter A.

The result of the study was a linear bank erosion equation which read:

$$\xi = 2.62 (10^{-10}) + 2.15 (10^{-8}) U'_b \quad (5.22)$$

with again

- ξ = bank erosion rate m/s
- $U'_b = U_b - U$
- U_b = near-bank velocity m/s
- U = reach averaged velocity m/s

In addition, the rates of bank migration were reduced where the density of (silver maple) trees was high: it was observed that the size and position of the trees tended to protect the bank from erosion. The equation for areal density of the trees along the bend was expressed as:

$$T = \frac{N \frac{\pi}{4}}{4.5 L} d_i^2 \quad (5.23)$$

where

- L = length of the bank segment
- d = diameter of the tree, i
- N = total number of trees in the segment

When the effect of large trees near the river bank was included, equation (5.22) took the form

$$\ln(\xi) = 3.25 + 3.06 U'_b - 44.6 T \quad (5.24)$$

Therefore for the river which has no tree along the bank, then T becomes zero and eqn. (5.24) will be equal to eqn.(5.22). Nevertheless, eqns. (5.22) and (5.24) obviously cannot be applied casually to other rivers. The excellent correlation obtained between near-bank velocity and bank erosion rate was partly a result of a fact that the bank sediments were relatively uniform and cohesive all the way down to the bed. The main characteristics of the study reach are shown in table (5.1).

Table 5.1 Characteristics of the river

Variable	Value	Dimension
Mean annual discharge	11.1	m ³ /s
Bank-full discharge	151.1	m ³ /s
Recurrence interval of bank-full discharge	2.4	year
Bank-full width	42.0	m
Bank-full average depth	2.6	m
Bank-full mean velocity	1.37	m/s
Bank-full friction factor	0.0135	-
Bed sediment D_{94}	69.0	mm
Bed sediment D_{50}	30.0	mm
Bed sediment D_{16}	7.6	mm
Sinuosity	1.15	-
Slope	0.0010	-

It then appears that this model can be applied for cohesive bank and gravel bed rivers, which could have similar characteristics to these shown in Table (5.1).

- Dickinson and Scott, (1979) model:

Stream bank erosion rate in cm/yr

$$\xi = 2 (10^{-10}) (I_e^{2.5} I_a^{7.2}) + 1.75 \left(\frac{0.50}{T}\right) \quad (5.25)$$

in which

- I = 0.0097 (S)^{-0.60}; hydraulic stability index
- S = energy slope of the river
- I_e = soil erodibility factor
- I_a = agricultural intensity index

5.5 Verification

5.5-1 Case 1: verification with empirical formulae

Why should we attempt to verify our model with empirical formulae at all, since an empirical formula is only valid for the circumstances under which it has been developed. Certainly such 'validation' can only constitute what may be called isolated approaches. However, to the extent that we have constructed a unified theory and corresponding model, it should be possible to compare the predictions of this model with those of the empirical models for the particular circumstances concerned. Our model then gives us a number of 'answers' to the questions posed and solved by the empirical models. This can be done on a module-by-module basis but not by relating certain combinations of modules. Limitations and applicability of the model is that the model is applicable but limited essentially to alluvial rivers of the homogeneous and isotropic material type.

5.5-2 Case 2: verification with field data from Rillito Creek

Rillito creek is a stream representative of water courses throughout the Basin and Range Province of the interior southwestern United States and northwest Mexico. The Rillito flows 18.4 Km (11.5 mile) through an alluvium filled fault-block valley to its junction with the region's major stream, the Santa Cruz River, at an elevation of 670 m.

At its mouth the Rillito drains an area of approximately 2378 Km² that is dominated by porous soils. The vegetation cover consists primarily of Arizona upland subdivision vegetation, mostly saguaro cactus, palo verde trees, and creosote bushes. The annual rainfall over most of the basin is 20-40 cm (8-16 inches), according to data from Graf, 1984. The annual flood series for Rillito Creek is shown in Fig. 5.8.

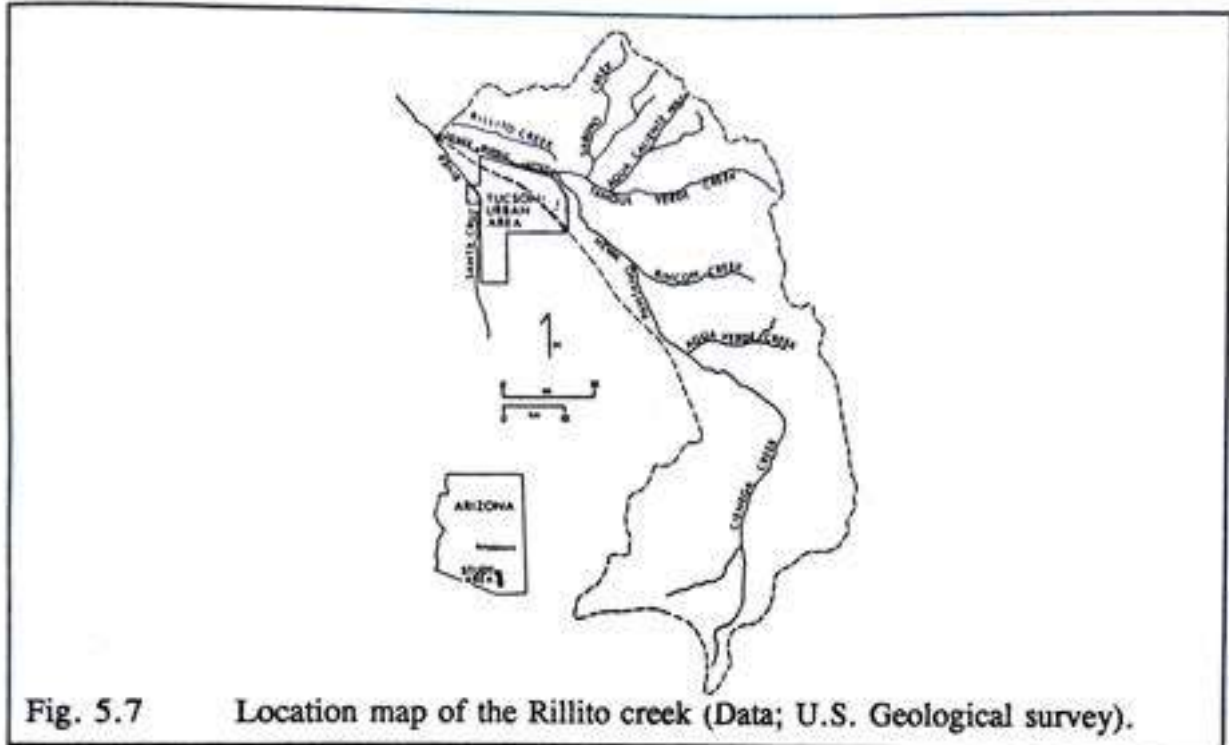


Fig. 5.7 Location map of the Rillito creek (Data; U.S. Geological survey).

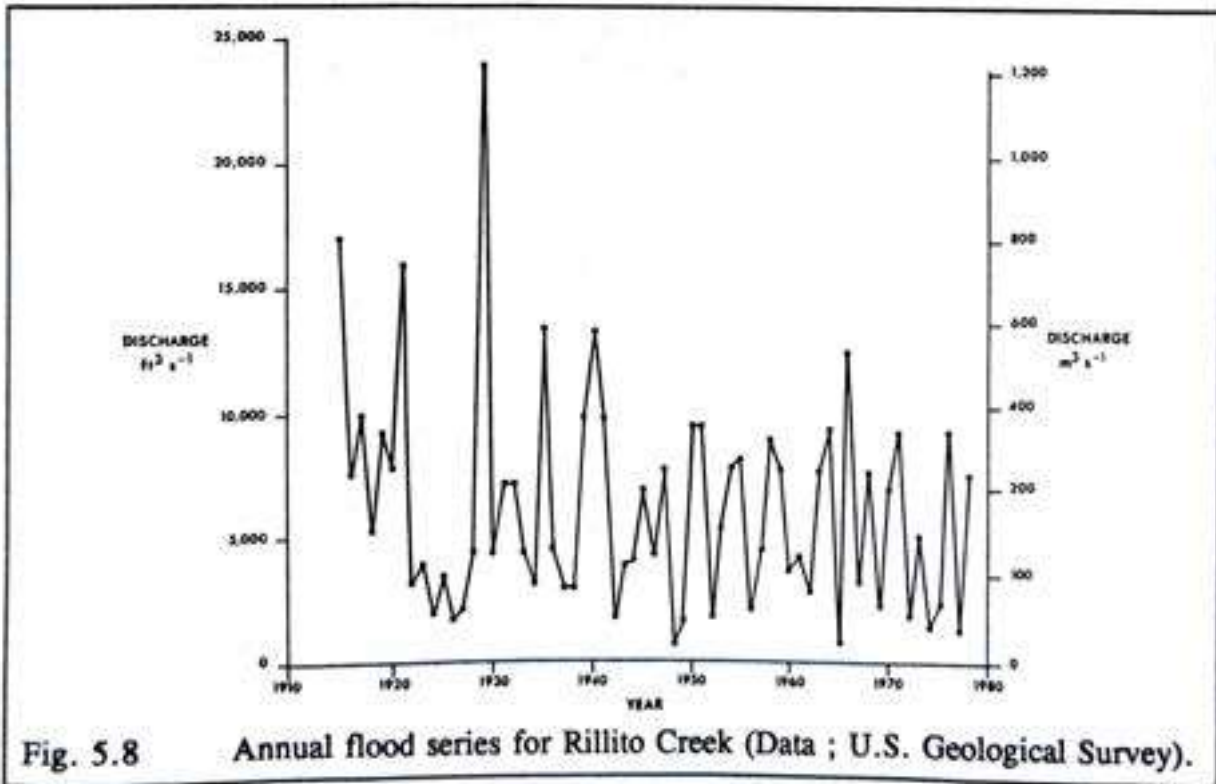


Fig. 5.8 Annual flood series for Rillito Creek (Data ; U.S. Geological Survey).

A review of historical channel locations along the Rillito Creek indicates that an unstable period extended from 1871 (and probably earlier) to about 1937. Instability has not been constant through time or space; see figs 5.9 and 5.10. Prior to 1890 the channel was flowing on an upper surface of alluvial fill, but in the period after 1890 the Santa Cruz River became entrenched through a series of floods (Hastings, 1958). Headward erosion of the arroyo from the major stream resulted in the entrenchment of Rillito Creek in several reaches, converting it from a shallow marshy stream to an arroyo. Once this conversion was completed (by about 1937) instability was manifested primarily by bank erosion (Graf, 1984). Smith, 1910, attributed the entrenchment of Rillito Creek to overgrazing and haymaking associated with an army post established at the junction of Pantano Wash and Tanque Verde Creek in 1872. He reported a major flood in 1881 but no channel instability until the 1890's. The significance of these events is that after entrenchment (especially in the lower reach) the arroyo is so large that it can contain even the 500-year flood (U.S. Army Corps of Engineers, Los Angeles District Office, unpublished overflow calculations, 1983; requoted from Graf, 1984). Generally the 1871-1937 maps reveal more instability than the 1937-1978 maps. Lower Rillito Creek has consistently been more unstable than the upper and middle reaches. Extensive bank protection efforts have been successful in stabilizing the middle and upper reaches since 1960. All three reaches have shown decreasing instability over the 107-year period, probably in response to generally smaller annual floods since 1941 as shown in fig. 5.8. Floods in 1983 interrupted the general trend.

The upper and middle reaches have modest degrees of locational instability (Figs. 5.9 and 5.10), while the lower reach migrated over substantial areas (Fig. 5.11). A comparison of Figs. 5.9, 5.10 and 5.11 shows the spatial variation in instability among the reaches.

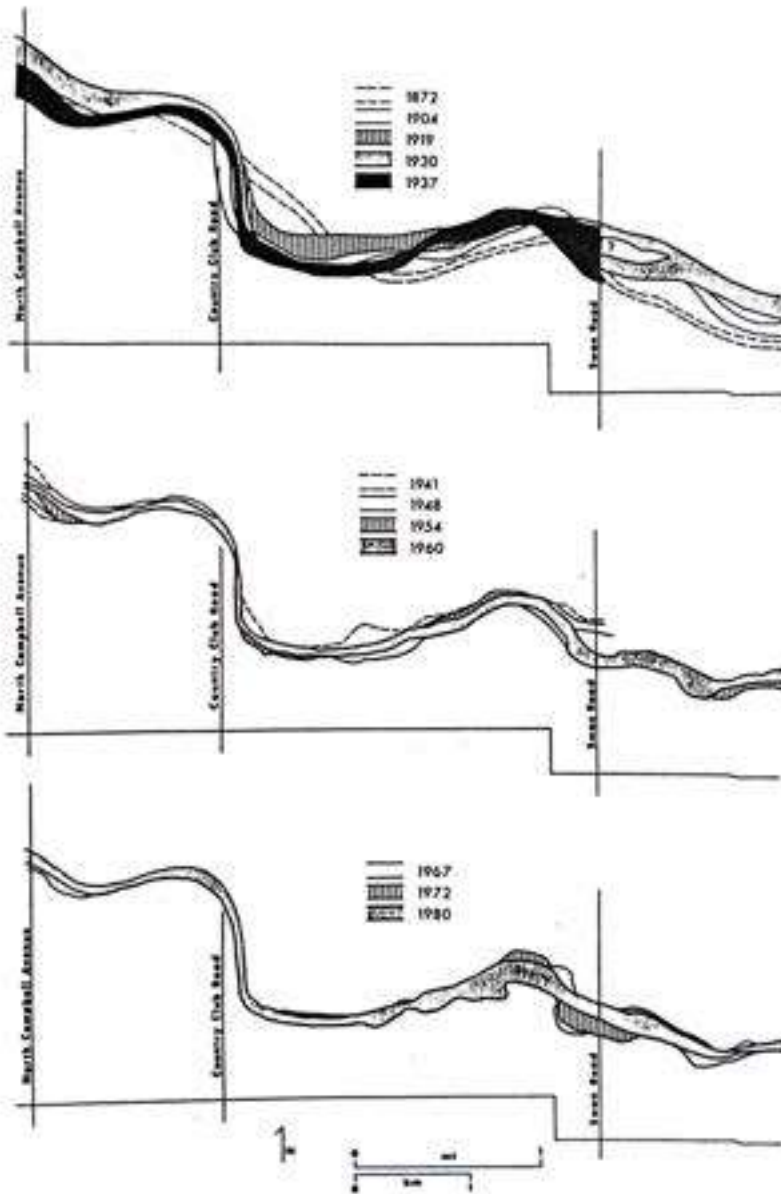


Fig. 5.9 Historical channel locations along upper Rillito creek (Data; Graf, 1984).

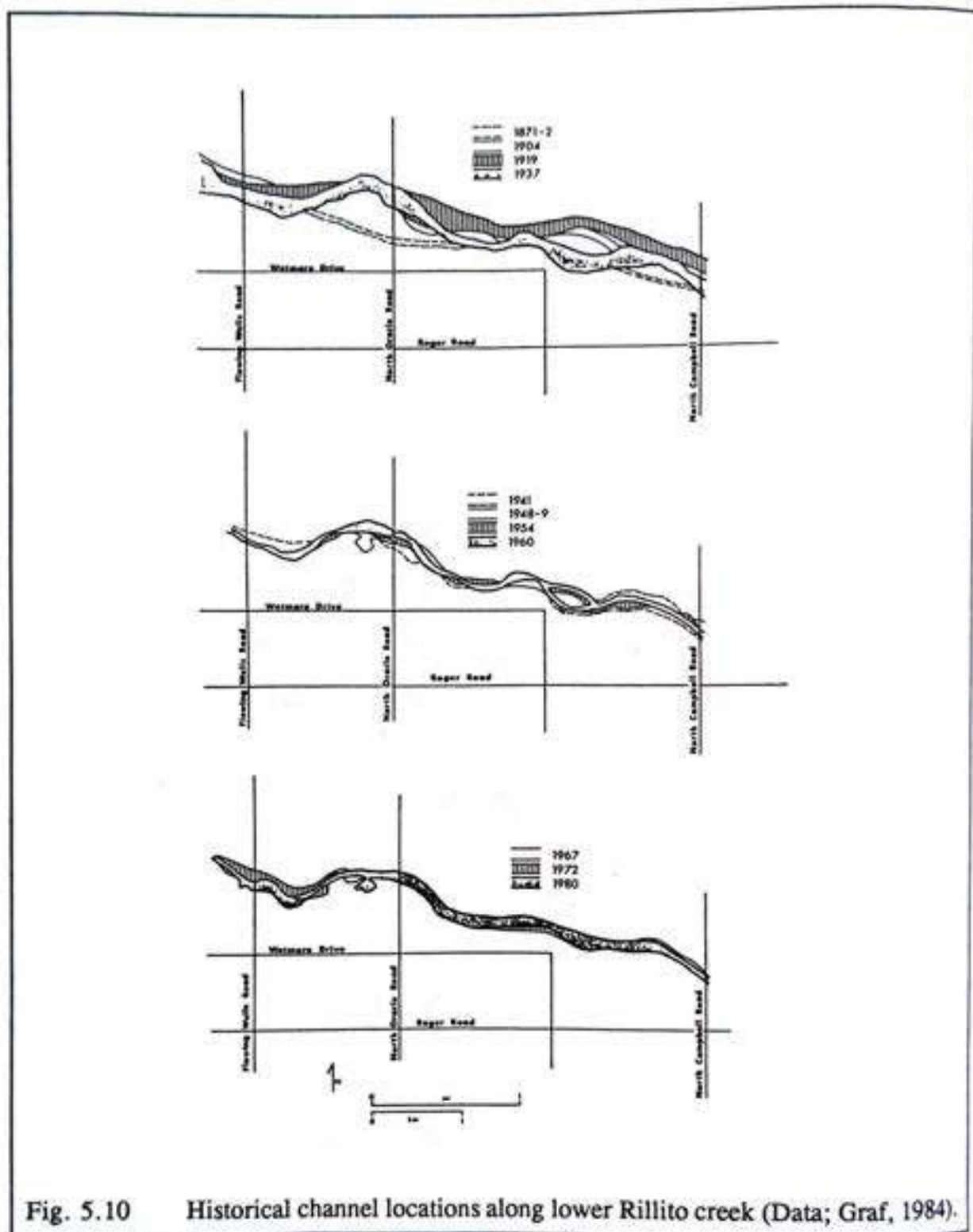


Fig. 5.10 Historical channel locations along lower Rillito creek (Data; Graf, 1984).

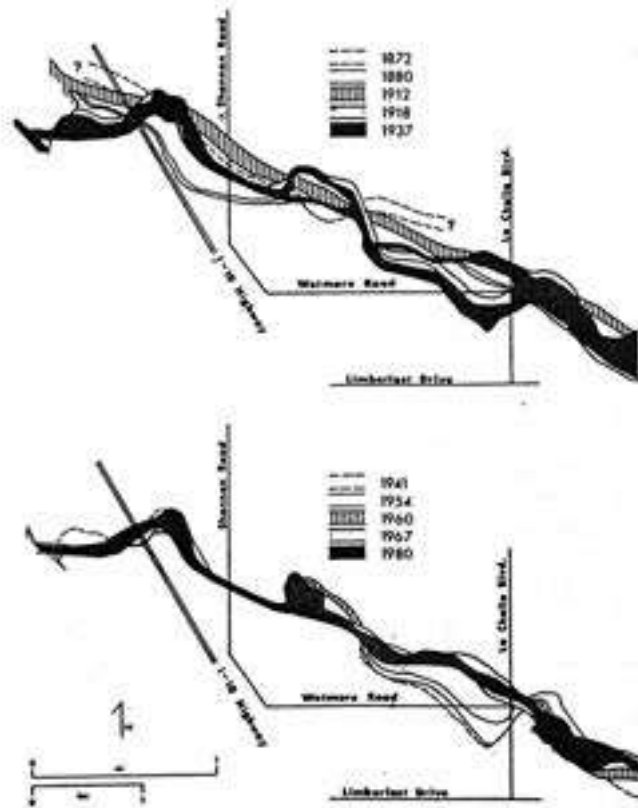


Fig. 5.11 Historical channel locations along lower Rillito creek (Data; Graf, 1984).

As we see in figures (5.8) to (5.11), the channel shift of Rillito creek as shown in Fig (5.11) is nearly impossible to tackle. Therefore the upper Rillito creek as shown in Fig 5.9 is chosen to test the bank erosion rate for the period of 1954 to 1960. However the observed channel shift from the figure and the simulated channel shift are not compatible. Because the simulated channel shift is too regular for the natural river shift. It can be concluded here that the present model give the result of shift no where near from the actual situation. On the other hand, the bank erosion rate of the river on a-station-geometry is satisfactory. The results are shown in Table 5.2.

Table 5.2 Verification of the bank erosion rate model

J	U_B (m/s)	$\xi^- = E_0^{-1}U_B$ (m/s)	$\Delta B(m)/4days$	$\Delta B(m)/11days$
4	0.1385133	$8.006 * 10^8$	+0.02767	+13.834
5	0.1862911	$10.767 * 10^8$	+0.03721	+18.605
6	0.22166	$1.28119 * 10^7$	+0.04428	+22.139
7	0.24678	$1.42638 * 10^7$	+0.04930	+24.648
8	0.26615	$1.53835 * 10^7$	+0.053165	+26.583
9	0.2799	$1.6178 * 10^7$	+0.05591	+27.956
10	0.2914	$1.68429 * 10^7$	+0.05821	+29.1045
11	0.29983	$1.7330 * 10^7$	+0.059892	+29.946
12	0.30625	$1.77012 * 10^7$	+0.061175	+30.588
13	0.31245	$1.80596 * 10^7$	+0.062414	+31.207
14	0.31584	$1.82555 * 10^7$	+0.06309	+31.546
15	0.31164	$1.80127 * 10^7$	+0.06225	+31.126
16	0.34569	$1.99809 * 10^7$	+0.06905	+34.527
17	0.19171	$1.10808 * 10^7$	+0.03830	+19.148
18	0.044167	$2.55285 * 10^8$	+0.008823	+4.4113
19	0.0406	$2.34668 * 10^8$	+0.008110	+4.055
20	-0.02074	$-1.1988 * 10^8$	-0.004143	-2.071
21	-0.059805	$-3.4567 * 10^8$	-0.011946	-5.973
22	-0.07755	$-4.4824 * 10^8$	-0.01549	-7.746
23	-0.09433	$-5.4523 * 10^8$	-0.018843	-9.422
24	-0.11632	$-6.723 * 10^8$	-0.02323	-11.617
25	-0.1273197	$-7.3591 * 10^8$	-0.02543	-12.716
26	-0.128748	$-7.4416 * 10^8$	-0.02572	-12.859
27	-0.123868	$-7.1596 * 10^8$	-0.02474	-12.372
28	-0.11740	$-6.78572 * 10^8$	-0.02345	-11.726
29	-0.112664	$-6.51198 * 10^8$	-0.022505	-11.253
30	-0.108916	$-6.2953 * 10^8$	-0.02176	-10.878

$E_0 = \sqrt{C_r X^3 I_0 E}$; The mathematical model is simulated for the river width of 66 m, Δt time step 4 days is used, the number of time steps needed for the equilibrium is 254 time steps. From field data $E = 5.78 * 10^{-7}$ m/s is observed. Therefore it can be seen from column 3 that the rate is not very much differ from the observed rate and the calculation is acceptable although it is not identical.

5.6 Modular structure developments of the bank erosion modules

The reason for developing various modules is that rivers are very dynamic and each river has its own characteristics, so that if at all possible the best way to calculate the bank erosion rate is to consider each river individually. This is most conveniently done by dividing the description of the river-bank system into a number of independent parts. The modules are as following.

1. BANK1.FOR ; Ariathurai and Arulanandan Model, 1978.
Based on the flume studies.
Cohesive material with 30% illite.
2. BANK2.FOR ; Hirano Model, 1973.
Based on hydrodynamic forces.
Derivation has been made by myself and adding some different linearizations than the original paper.
Please see derivations.
3. BANK3.FOR ; Hasegawa Model, 1987.
Based on hydrodynamic forces.
Derivation has been made by myself and adding some different linearizations than the original paper.
Please see derivations. Shear stress ratio has been changed.
4. BANK4.FOR ; Wiggert and Contrator Model, 1969.
Either cohesive or non-cohesive material.

$$\xi = 0.25 U^{3.8} \quad (5.26)$$

in which ξ = bank erosion rate (ton/ft-day)
 U = mean flow velocity (m/s)

5. BANK5.FOR ; Hicken and Nanson Model, 1975.
Nanson and Hicken Model, 1983.

in which W = channel width

$$\begin{aligned} \xi &= 2.0 \frac{W}{R_c} & \frac{W}{R_c} &\leq 0.32 \\ \xi &= 0.2 \frac{R_c}{W} & \frac{W}{R_c} &\geq 0.32 \end{aligned} \quad (5.27)$$

R_c = the radius of curvature of the channel centre line
 ξ = bank erosion rate (m/year)

6. BANK6.FOR ; Hooke Model, 1980.

Based on the field observations.

$$\xi = 0.05 \sqrt{A} \quad (5.28)$$

in which A = Catchment area in km^2

ξ = bank erosion rate (m/year)

Note : Range of the bank erosion rate 0.05 to 800 (m/yr) for the range of drainage area 3 to 1000,000 km^2

7. BANK7.FOR ; Dickinson and Scott Model, 1979

$$\xi = 2 * 10^{-10} (I_s^{2.5} I_a^{7.2}) + 1.75^{0.5II} \quad (5.29)$$

in which

$$I = 0.0097 * S^{-0.6} \quad (5.30)$$

I = hydraulic stability index

S = river bed slope

I_s = soil erodibility factor

I_a = agricultural intensity index

ξ = bank erosion rate (cm/year)

8. BANK8.FOR ; Brice Model, 1982

Empirical relationship only.

$$\begin{aligned} \xi &= 0.1 \text{ m/yr} & \text{when} & \text{width} = 10 \text{ meter} \\ \xi &= 9.0 \text{ m/yr} & \text{when} & \text{width} = 600 \text{ meter} \end{aligned}$$

in which

ξ = bank erosion rate (m/year)

9. BANK9.FOR ; Ikeda et. al Model, 1981

$$\xi = E * (U_b - U) \quad (5.31)$$

in which

E = erosion constant

U_b = near-bank depth average mean velocity (m/s)

U = reach-averaged mean velocity at bank-full discharge (m/s)

ξ = bank erosion rate (m/s)

This model is directly attached to the subroutine of the bank line displacement.

10. BANK10.FOR ; Parker Model, 1983

$$\xi = E_0 [1+e(X - 1)]U_b \quad (5.32)$$

in which

E_0 = primary coefficient of bank erosion

e = secondary coefficient of bank erosion

$(X-1)$ = the reduction in reach-average velocity with increasing sinuosity

U_b = near bank excess velocity

ξ = bank erosion rate (m/s)

In the dimensionless form the equation is reduced to

$$\frac{\xi}{U_b} = E_0 A \frac{W}{R_c} \quad (3.33)$$

in which

E_0 = coefficient of bank erosion

A = an order-one scour factor parameterizing the role of secondary currents

U_b = near bank excess velocity (m/s)

W = width of the river

R_c = radius of curvature of the channel centre line

ξ = bank erosion rate (m/s)

This model is also directly attached to the subroutine of the bank line displacement.

11. The conceptual models ;

- (a) Middleton Model, 1930: Bank erosion rate is a function of dispersion ratio, the ratio of colloid to moisture equivalent, and silica-sesquioxide ratio. However mathematical expression is not available. The concept is drawn from the study of three types each of cohesive and non-cohesive soils.
- (b) Schumm Model, 1960: Bank erosion rate is a function of the percentage of silt and clay in the parameter of stable river cross-section. The concept is drawn from the study of 60 rivers. Mathematical expression is not available.
- (c) Partheniades, 1965: Based on the flume experiments with two different clay beds. On the contrary of many other theories that bank erosion rate is independent of the suspended sediment concentration. In his flume experiments, 60% of the eroded material from the bank is going to be suspended sediment load. Mathematical expression is not available.
- (d) Arulanandon, Gillogley and Tully, 1980
A quantitative method to predict the critical shear stress and the rate of bank erosion was based on the flume experiments for the cohesive material. 42 numbers of soil samples and river water samples from all over the U.S.A.

$$SAR = \frac{N_a}{\sqrt{0.5(C_a + M_g)}} \quad (5.34)$$

in which SAR = Sodium adsorption ratio
 Na = measure of Sodium ion
 Ca = measure of Calcium ion
 Mg = measure of Magnesium ion

Bank erosion rate = f(SAR, dielectric dispersion of the soil)

Although this is a quantitative method, it is still hard to get the accurate analysis for both soil and water qualities. Therefore no further development is made for mathematical model.

5.7 Tentative Grouping of sites for different erosion types

The analysis and observations have shown that there is considerable variation in the types of erosion and the factors which influence the processes, even within a reach experiencing similar rainfall, discharge and temperature conditions. It is likely that sediment composition is a major factor affecting the spatial distribution of erosion and its relationship to the erosion processes, although, in general, banks with higher clay composition appear to be more resistant and experience less slumping. The sites may nevertheless be divided into four types on the basis of Hooke's (1979) analyses and observations, as follows:

- (1) Sites where erosion is driven mostly by corrosion at high flow and the magnitude of the peak discharge is of primary importance.
- (2) Sites possibly of coarser, sandy material, where soil moisture conditions are of greatest significance and erosion is usually initiated by a collapse of material.
- (3) Sites where again soil moisture conditions are important but the amount of erosion is low, the material being highly resistant, so that high flows are also necessary for erosion to occur.
- (4) Sites where erosion is infrequent and takes place by a sudden excavation of lobes at high flows.

Hence these aspects also should be introduced together with those of section 5.4-1 when the mathematical model is presented in section 5.9.

5.8 The selection of the bank erosion rate module

Bank materials are considered that are composed of both cohesive and granular material. Corresponding partly to this, it is assumed that, after being eroded, some part of the cohesive material will be transported as wash load and the rest will be bed load transport driven by the flow. The sediment continuity equation is expressed in one-dimensional and two-dimensional forms so as to account for the mass which has been eroded from the bank.

The physical processes which are the result of river bank erosion are presented. Since sediment transport is directly influenced by bank erosion products, it is the fine particles that will be transported as wash load after being eroded with the rest being transported as bed load. If a distinction is not made between wash load and bed load, the sediment transport due to bank erosion may easily be wrongly estimated. The noticeable manner of bank erosion is when particles are plucked from the top of the bank by the shear stress of the flowing water, causing the slope to decrease, which in turn decreases the shear stress (Stevens, 1989).

In the process of simulating the river bank-line position, the hypothesis of near-bank velocity excess, i.e. a hydrodynamic aspect is considered initially. However, bank erosion is not only dependent on the flow conditions, but also on the geomorphology of the river banks. Therefore the selection of the most appropriate module, corresponding to the specific situation of the river from the geomorphological point of view, is most important. On the other hand, if the geomorphological data concerning the selection of the appropriate module is not available, there are three more modules to be selected which are based on the theoretical derivations of the bank-erosion-rate equations.

5.9 R P M model

A simulation model to predict the river plan-form movement has been developed (abbreviated *RPM*). The model consists of three major stages. These are a hydrodynamic simulation stage, a bed topography simulation with fixed-banks condition stage, and a bank erosion and plan-form shifting stage. The first two stages have already been described in Chapter 3. The last stage is presented in this section. It is possible, and indeed most usual, for vertical and horizontal erosion to be active in the same place at the same time. This concurrence will come about in all curved parts of those channels that are being eroded vertically, however small the vertical component may be. The resultant cutting of the ground over which the stream runs is '*obliquely downward*', that is, both downward and toward the concave bank (Crickmay, 1974). Here the simulation result of the numerical model comes to resemble this behaviour as mentioned by Crickmay, (1974). Moreover he recommended this mode as '*Much of the erosion of all rivers is of this sort: it is the most general mode*'; see Fig. 5.24. The structure of the model is presented in Fig. 5.12.

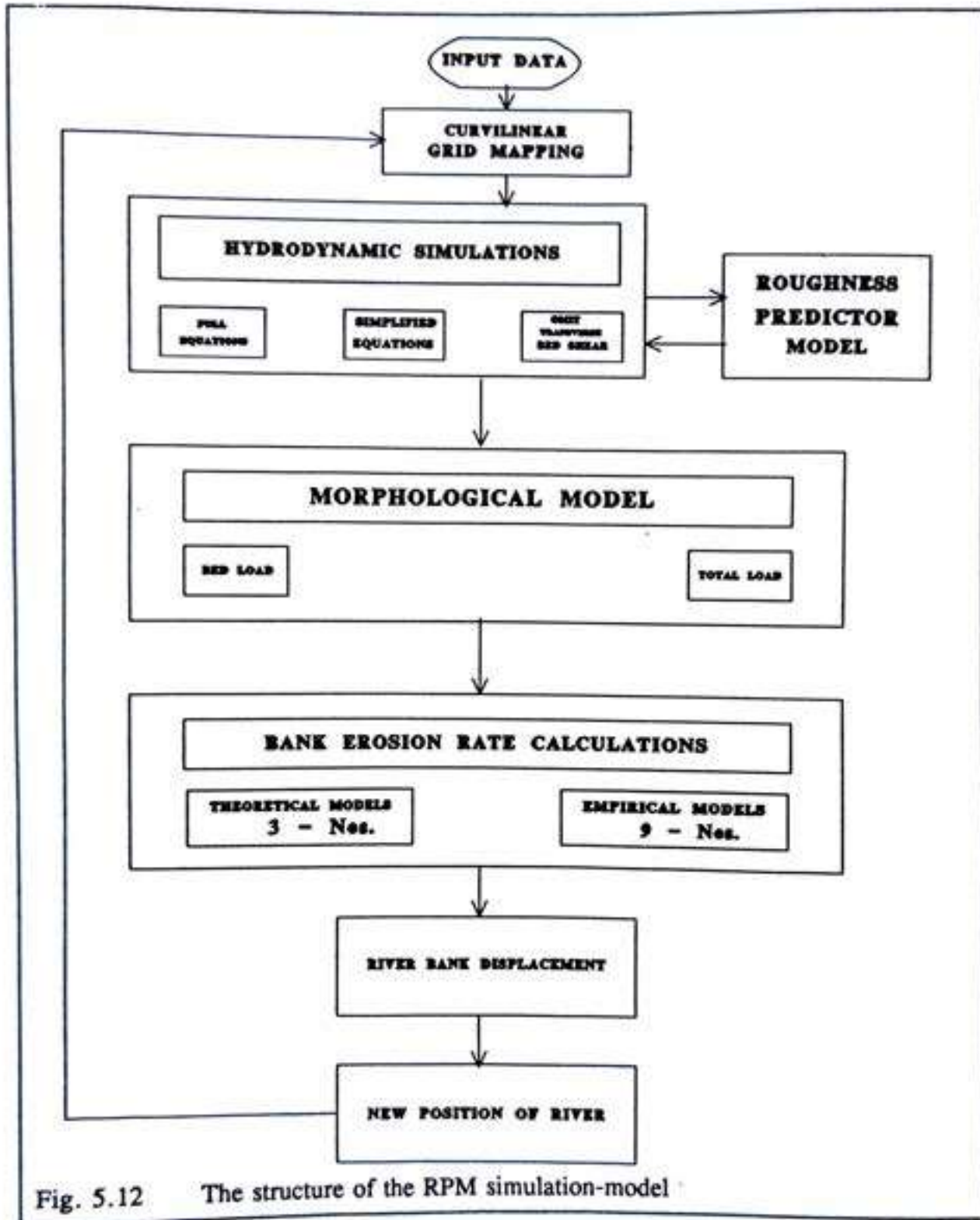
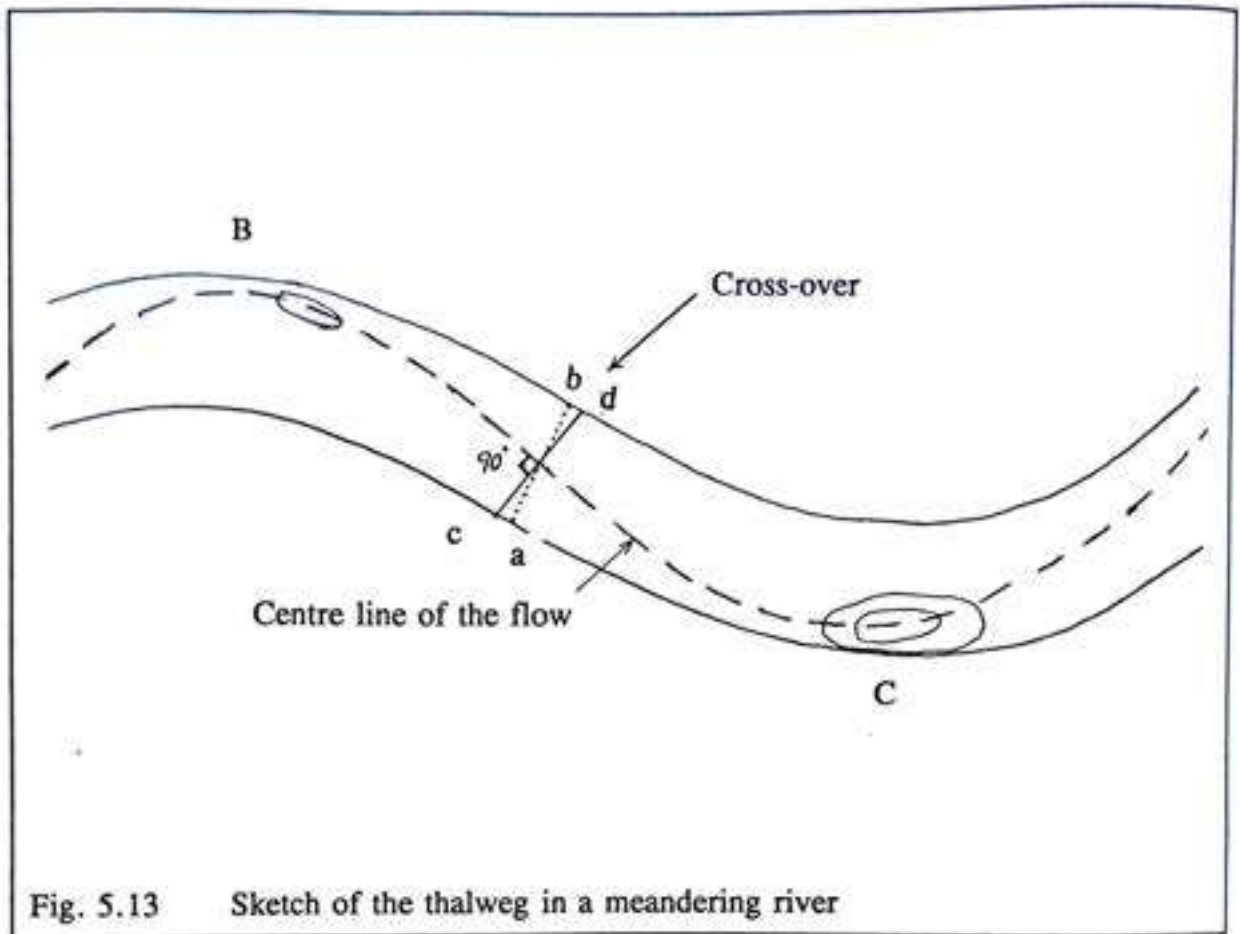
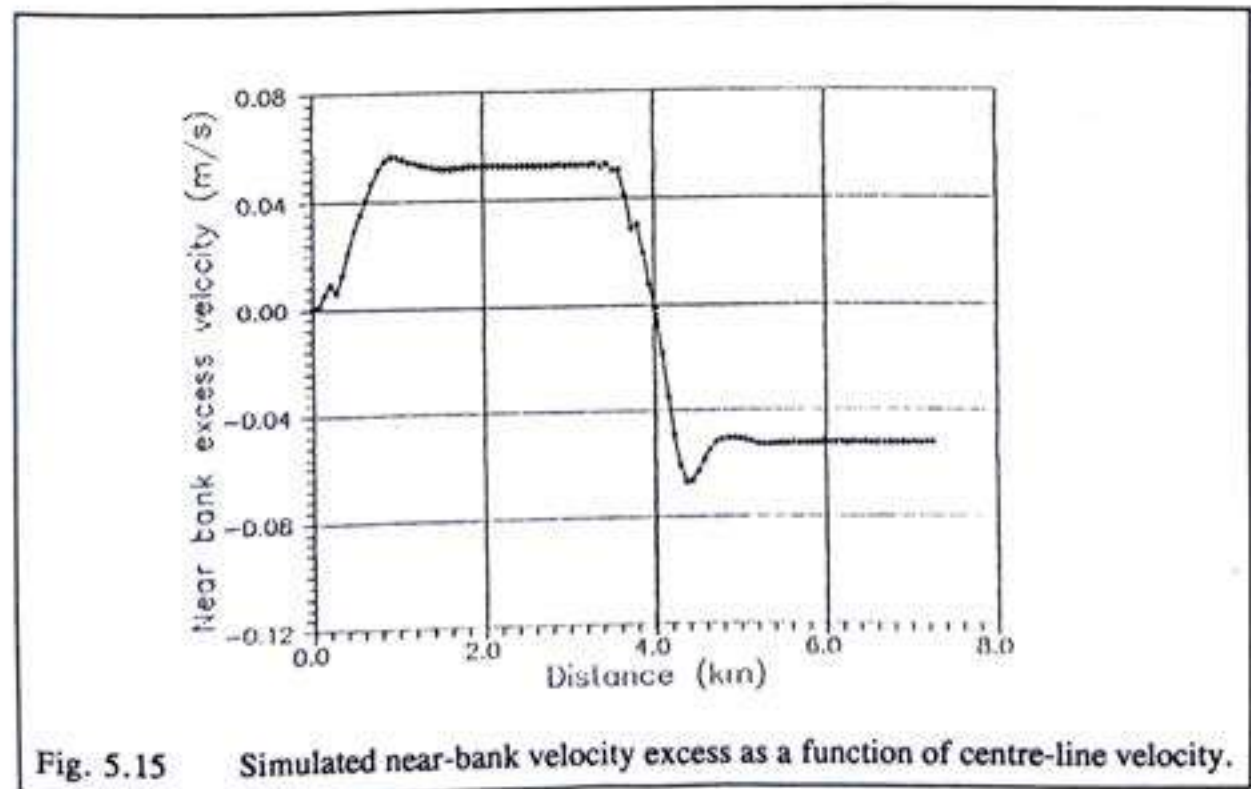
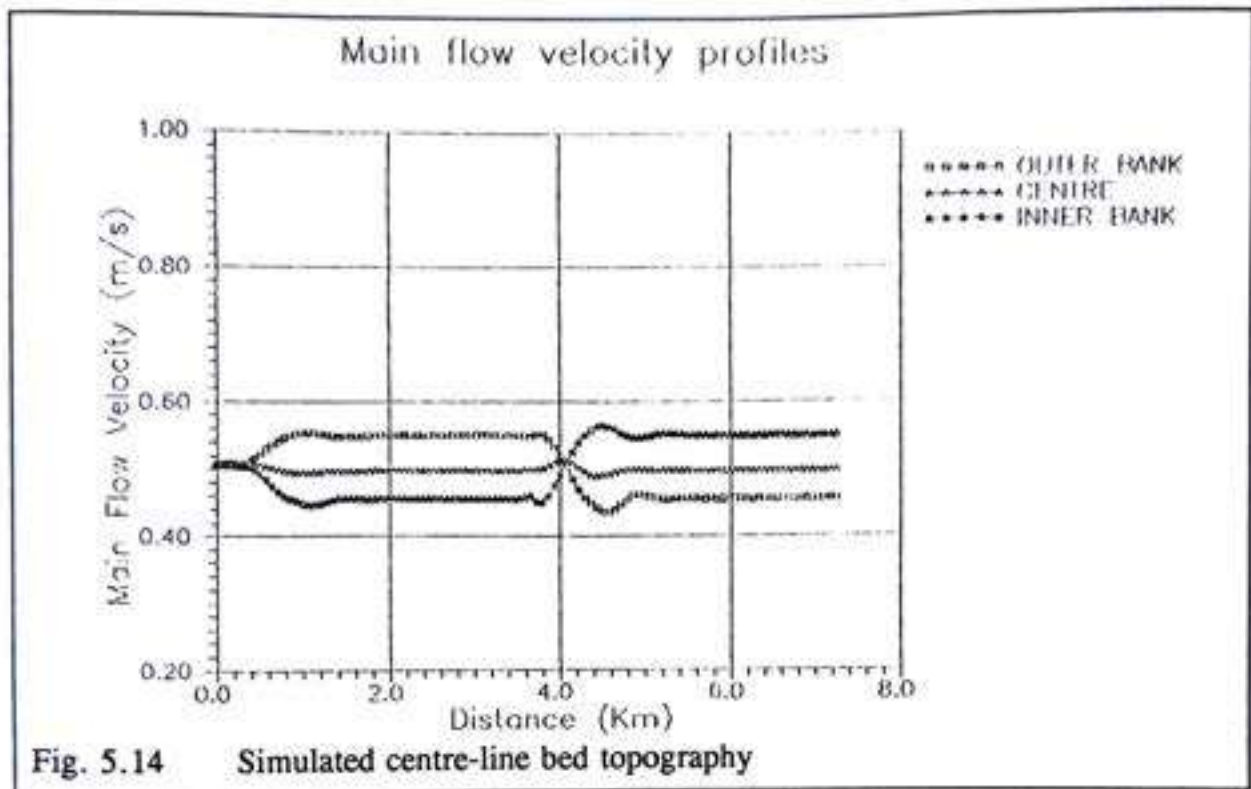


Fig. 5.12 The structure of the RPM simulation-model

5.9-1 Some discrepancies between physical sense and modelling workability



Since the area of waterways measured along the line 'cd' in Fig. (5.13) is much larger than that along 'ab', it follows that the velocity at the inflection point is far less than in the curve, and this explains in part the formation of the shoal, for, as the velocity drops, the sediment carried by the current is deposited. A decrease of the bottom slope at the approach to the point of inflection contributes further to reduce the velocity and consequently to increase the amount of the deposited sediment. The present model display this phenomenon and when the river width is split into many strips across the stream it shows more detailed patterns of flow and bed topography. For example, if there are five computational points across the river width, five stream lines will be simulated and five separate but continuous bed topography paths will represent the river bed topography. In this case, the centre-line bed topography will be deformed a little because of the lateral flow from one stream line to the adjacent stream line. Consequently, the sand-bed will erode and a scour hole will be formed. This phenomenon is depicted in Fig. (5.14).



The study by Ikeda *et al.* (1981) which provides the analytical basis for the theory is based on the assumption that the bank erosion rate at any point is proportional to the near-bank perturbation of the depth-averaged flow velocity (*i.e.*, the difference between the near-bank and the centre-line value), *i.e.* $U_b' = U_b - U_c$ where U is the reach-averaged velocity and U_c is the local centre-line velocity of the reach.

However, because of the phenomenon mentioned above, the near bank velocity excess in the longitudinal direction fluctuates and likely to result in a saw-tooth-like bank displacement; see Fig. 5.15. These fluctuations cause difficulties at the new grid generation stage. Although this can be smoothed out by using a cubic spline function, it is preferable to derive a smooth development from the start since the model grows larger and more complicated after the joining together of the many individual modules.

Hence $U_b' = U_b - U$ is used instead of $U_b' = U_b - U_c$ where U is the reach-averaged velocity and U_c is the local centre-line velocity of the reach. This modification is probably justified in the sense of its analytical basis to the extent that it is applied to the near-bank perturbation of the depth-averaged flow velocity when the width of the river is considered as a whole.

5.10 Grid generation

Basically, techniques for numerical grid generation can be divided into two classes, viz. techniques which themselves involve solving partial differential equations, and algebraic interpolation techniques (Gilding, B.H. 1988). In general, the techniques involving the numerical solution of a partial differential equation appear to generate a smoother grid in which the propagation of boundary slope discontinuities is attenuated. On the other hand, algebraic techniques provide a more explicit grid control and, in comparison to the other class of techniques, require relatively few computations. Subsequently, in calculation, they have the advantage of speed and simplicity. In this study, the time dependent shifting of the river plan-form mapping is invented by using a simple geometrical method, see Fig. (5.13).

5.10-1 Grid map setting by differential geometry

The first step of the grid mapping is the construction of the river reach discretization with various curvilinear surface-blocks the boundaries of which are made up of circular segments as shown in Fig. 5.16.

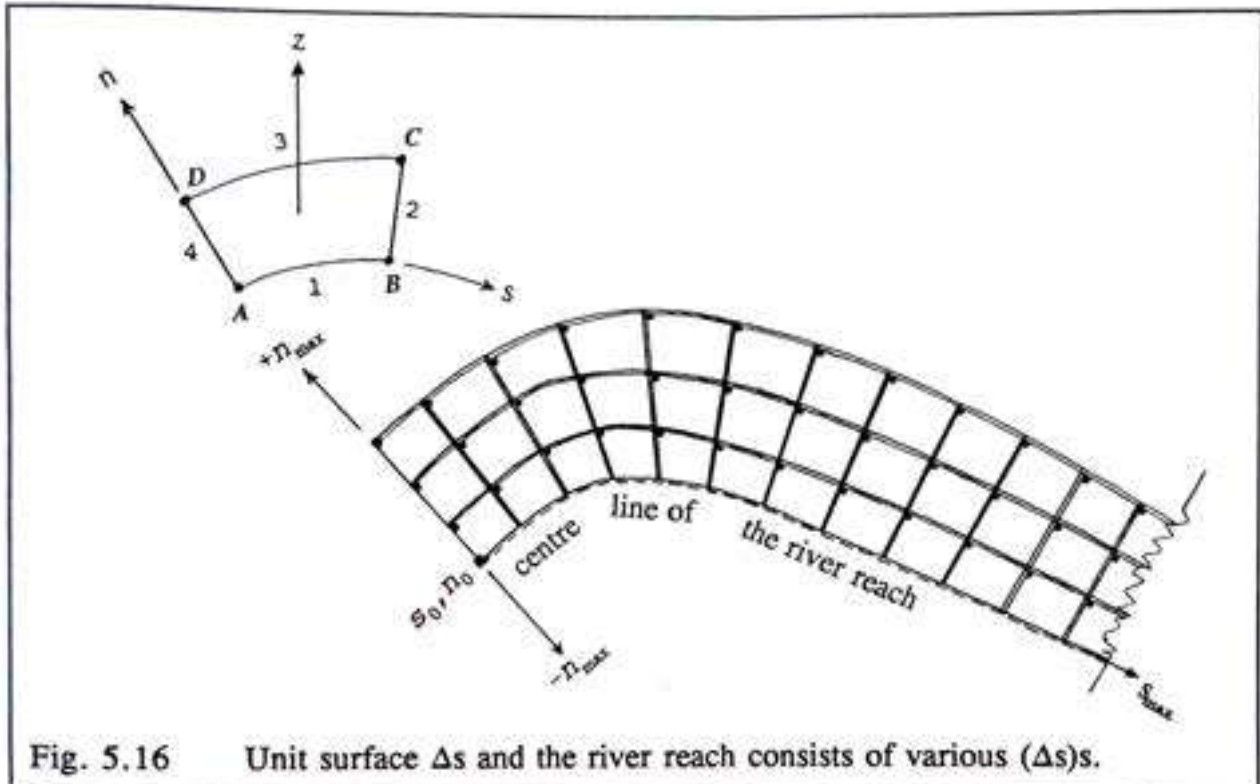


Fig. 5.16 Unit surface Δs and the river reach consists of various (Δs) s.

Consider the surface of the river reach as a continuous surface S represented by $S = S(s, n)$ consisting of a number of blocks called Δs . Any block Δs on the surface is bounded by 4 lines, see Fig. 5.16; lines 1 and 3 are curved and 2 and 4 supposed to be straight; and four corners called (A), (B), (C) and (D). The location and size of each independent block is defined by the curvature value taken at the corner (D) and the arc length of the line (3). The surface area of $\Delta s = \Delta s(s, n) \in [s_j, s_{j+1}] * [n_k, n_{k+1}]$. A local orthogonal panel coordinate system is then introduced, with its origin at any arbitrary point called (s_0, n_0) ; in the case of even nodes in n -direction (s_0, n_0) can be written as

$$(s_0, n_0) = \left[\left(s_j, \frac{(n_k + n_{k+1})}{2} \right) \right] \quad (5.35)$$

and in the case of odd nodes in n -direction (s_0, n_0) can be written as

$$(s_0, n_0) = (s_j, n_k).$$

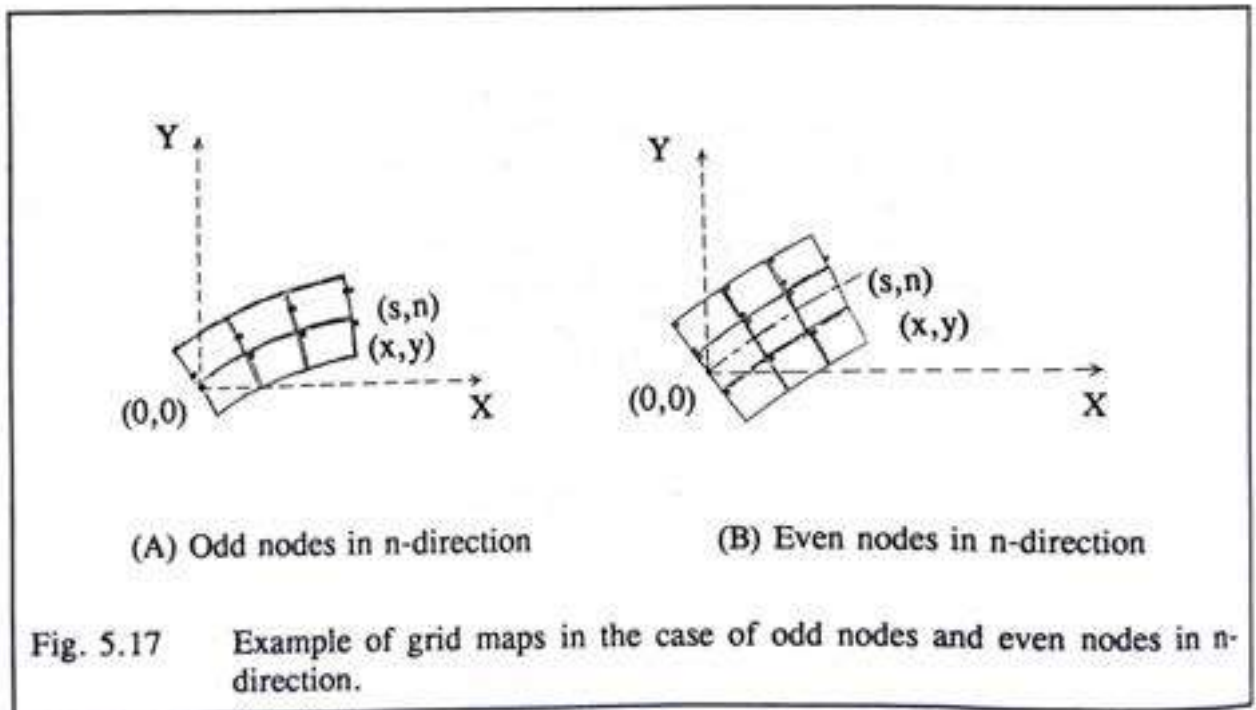
The width of the domain is from $-n_{\max}$ to $+n_{\max}$ and the length of the domain is from s_0 to s_{\max} , where

$$-n_{\max} = -\sum_{k=1}^{k=C_2} \Delta n ; +n_{\max} = \sum_{k=C_2}^{k=kk} \Delta n \quad (5.36)$$

$$s_{\max} = \sum_{j=1}^{j-1} \Delta s \quad (5.37)$$

Therefore the domain reads

$$[s_0, s_{\max}] * [-n_{\max}, +n_{\max}] \quad (5.38)$$



The hydrodynamic and bed topography computations take place on this domain and let us assume that now we arrive at the stage of bank-line shifting. The displacement of the bank line is calculated and the value of the displacement is known. Therefore the outermost layer of the computation domain which is according to Fig. 5.13 the series of surface blocks from (s_0, n_{\max}) to (s_{\max}, n_{\max}) should be shifted in the positive n direction and the value of each shift can be represented, for instance, by Δb_j . Since the left-top corner point of each surface identifies its location, the shift is executed at that corner. However, in this study, the river width is kept constant although the bank lines are shifting as mentioned earlier. This implies that the series of surface blocks from the centre line of the river reach, from (s_0, n_0) to (s_{\max}, n_0) will move towards positive n direction and the value of each shift will also be the value of Δb_j . Therefore instead of the series of surface blocks from (s_0, n_{\max}) to (s_{\max}, n_{\max}) , the series from (s_0, n_0) to (s_{\max}, n_0) is shifted. In this stage, we have a new centre line of the river reach and the entire grid mesh is calculated in the same was as previous one. The superimposing feature of new mapping over the previous mapping is illustrated in Fig. (5.18).

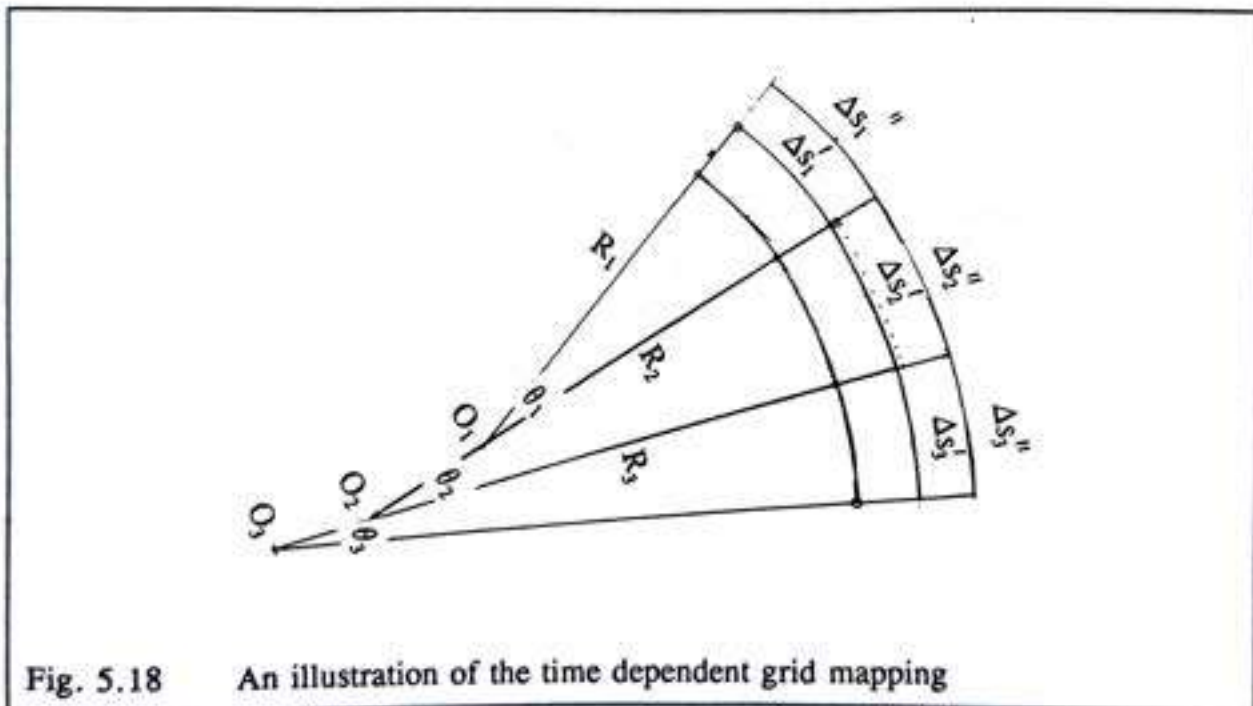
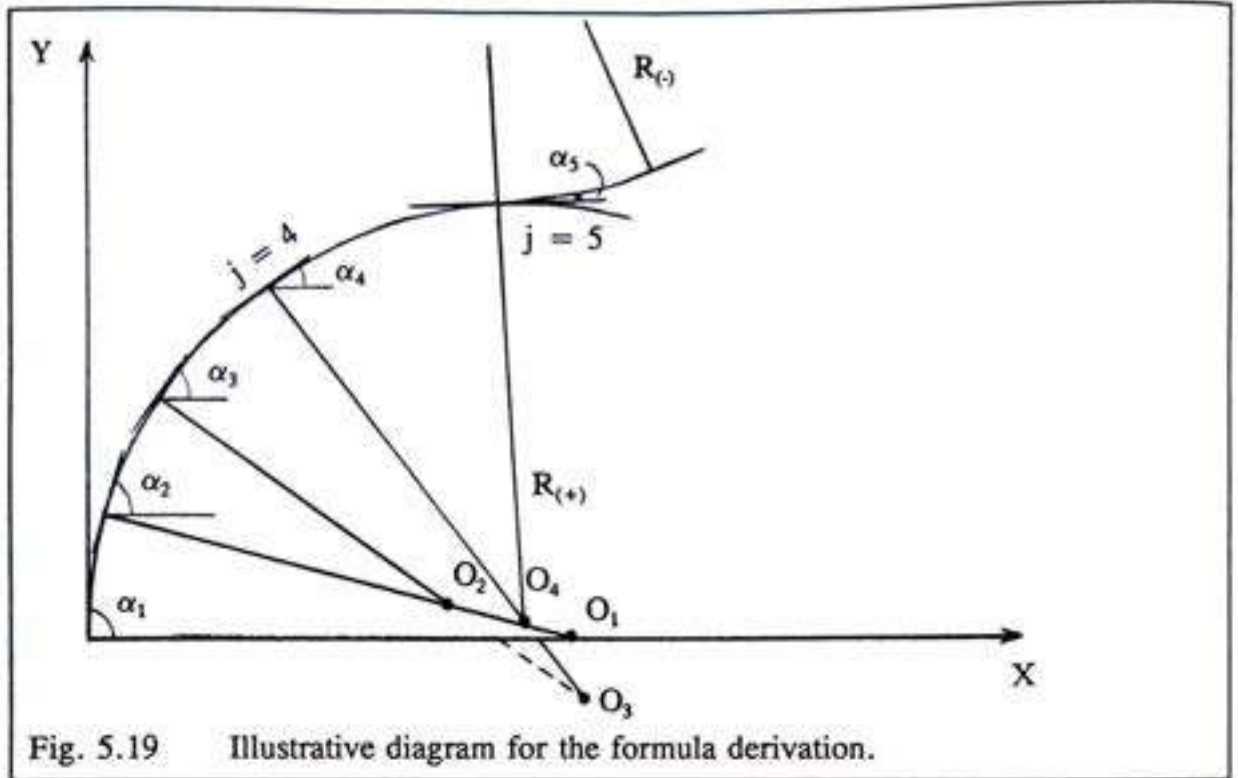


Fig. 5.18 An illustration of the time dependent grid mapping

5.10-2 Coordinate transformation

After the completion of the plan-form movement simulation it is necessary to present the results in the graphical form. Since all the graphic softwares work with cartesian coordinate system, the coordinate transformation from curvilinear coordinate to the cartesian coordinate is derived. The curvilinear coordinate is constructed by series of circular segments, depicted in Fig. 5.19. The direction angle α_j defines the path and the first segment



of the river alignment has angle α_1 which is written as

$$\Delta\alpha = \frac{(\pi - \theta)}{2} = \left(\frac{\pi}{2} - \frac{\Delta s}{2R}\right) \quad (5.39)$$

General formula of angle α_j for any j point on the curve along the path except the origin where $j=s_0$ can be written as

$$\Delta\alpha_j = \frac{(\pi - \theta_j)}{2} - \sum_{j=s_0}^j \theta_j \quad (5.40)$$

in which the sign convention of the angle θ_j is consistent with that of n-axis. Therefore θ_j is negative when the curvature is negative. Therefore the entire river reach can be plotted in the cartesian coordinate system for every (s_j, n_j) points in terms of (x, y) points using following equations

$$x_j = x_{(j-1)} + \Delta x \quad ; \quad y_j = y_{(j-1)} + \Delta y \quad (5.41)$$

$$\Delta x_j = \Delta s_j \cos\alpha_j \quad ; \quad \Delta y_j = \Delta s_j \sin\alpha_j \quad (5.42)$$

It should be mentioned here that each segment 'j' is an independent segment and obtaining its own identity such as Δs_j and radius of curvature R_j . More over inflection point or turning point can be at any 'j' point of the entire curve. Nevertheless there is only one rule which is two adjacent segments should have a common tangent. If and when this rule is fulfilled, there is only one general equation to be used in the complete computation.

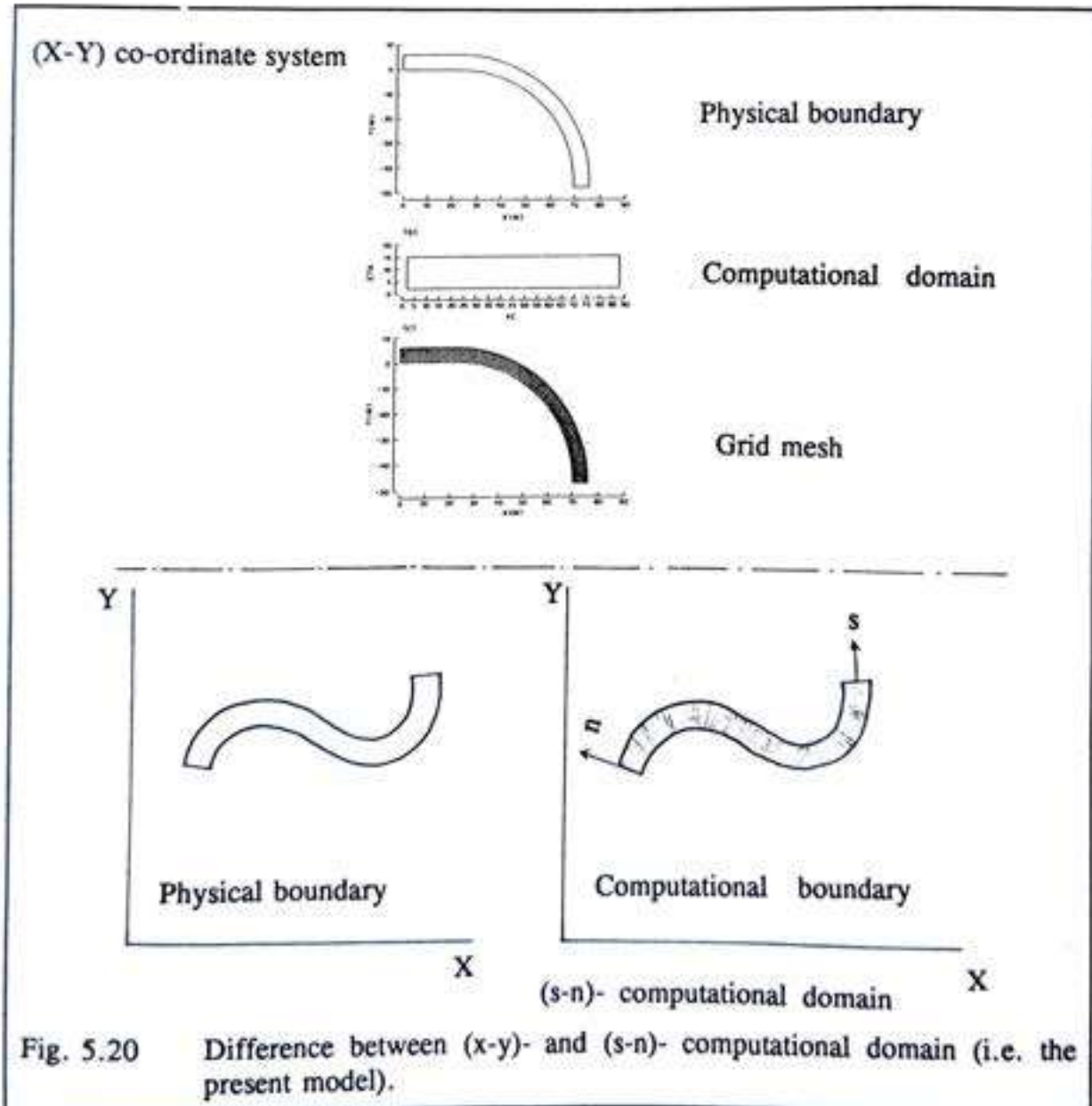
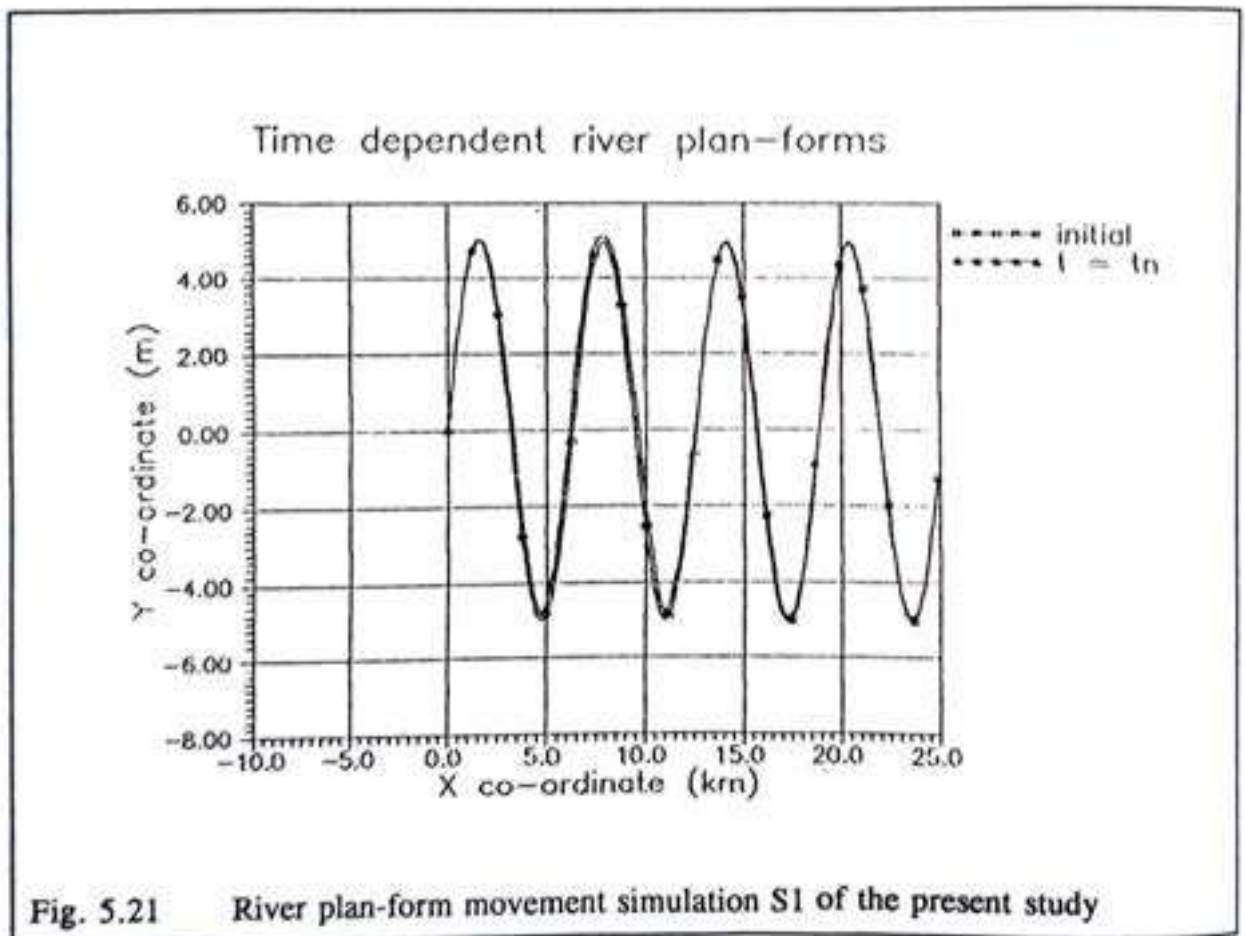
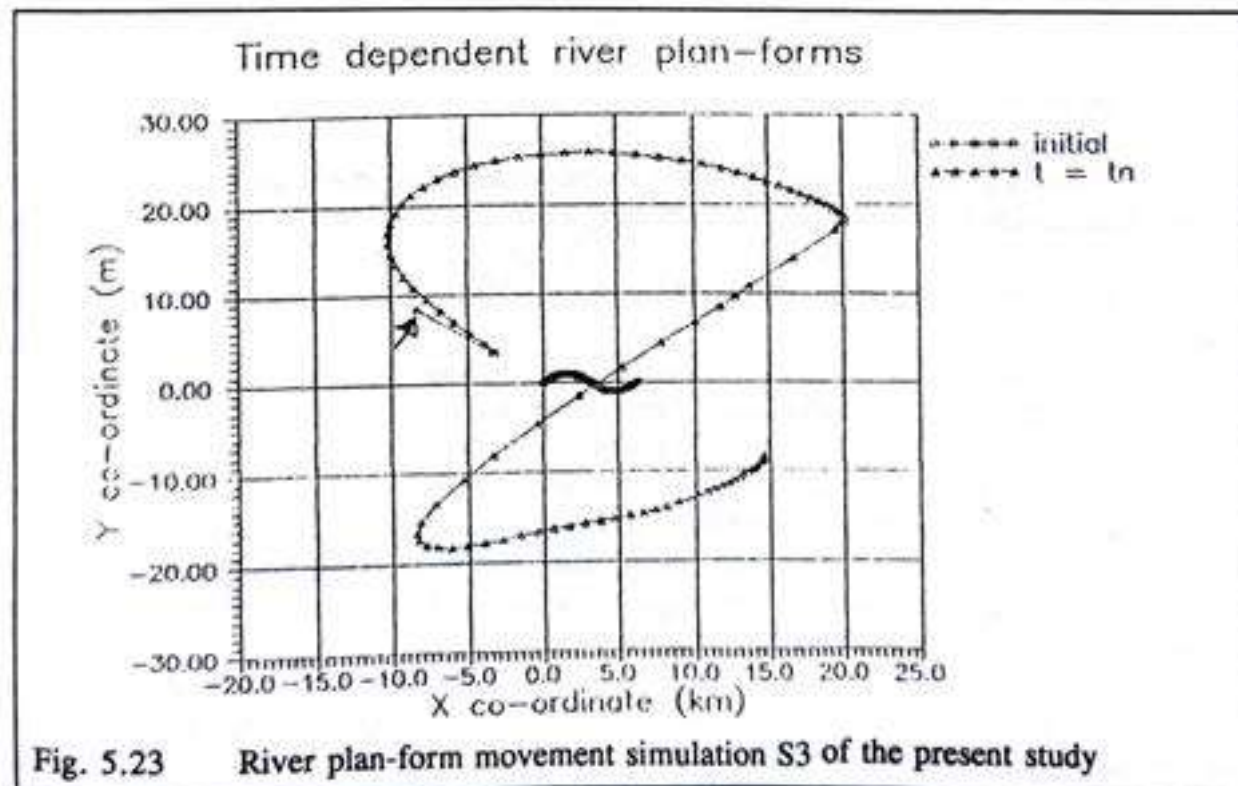
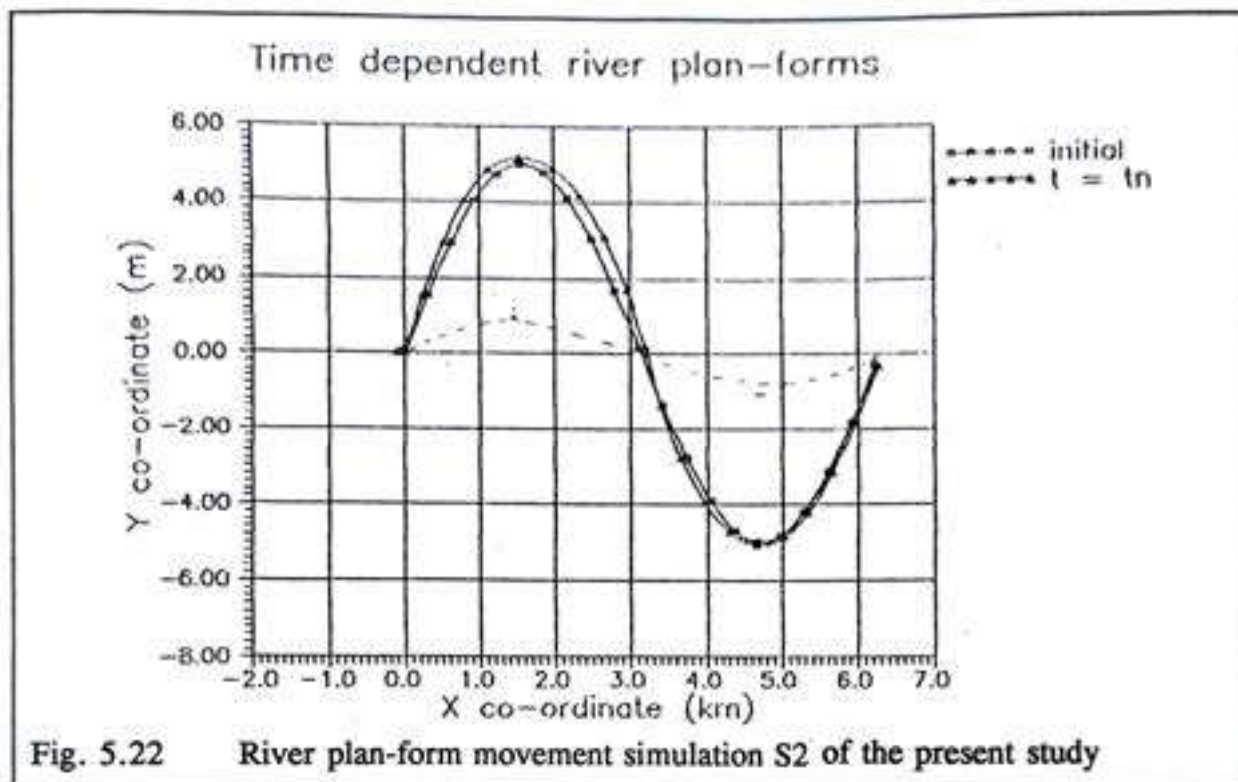


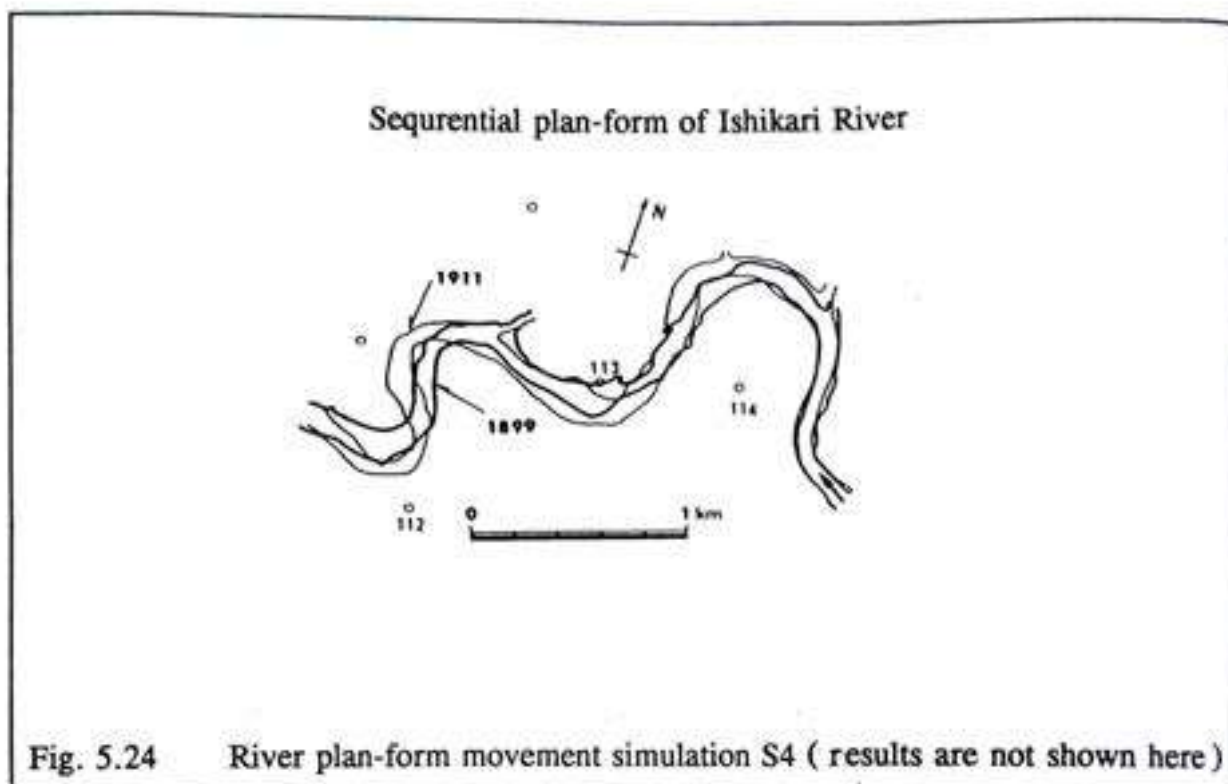
Fig. 5.20 Difference between (x-y)- and (s-n)- computational domain (i.e. the present model).

5.11 Simulations

The simulation results of RPM model are presented in Figs. 5.21 to 5.24. The results are satisfactory although it cannot be verified by the field measurements. For the regular curves as shown in Figs. 5.21, 5.22, and 5.24 are satisfactory. For the particular type of skew channel shift, which is called *obliquely downward*, as shown in Fig. 5.24, could not be simulated more than one to two times shifting. The maximum two times shifting is possible but still more work has to be done on this simulation.







5.12 Conclusions

Actually equilibrium does not exist in the sense that there is no one discharge of a certain magnitude, or frequency of occurrence, with which the channel is in equilibrium.

The factors affecting the temporal variation of bank erosion can be divided into five groups:

- (1) parameters of the flow condition and hydrographic characteristics
- (2) the rain-fall characteristics of the storm
- (3) the duration between peak flows
- (4) the soil moisture conditions, and
- (5) the temperature conditions, primarily the incidence of frost.

The first three factors can be taken into account through a consideration of the effective discharge. In particular, the temporal variation of the bank erosion can be related to the reformation of the shape of the river cross-section.

There are two different situations that we have to confront. The first situation is dealing with rivers in which geological, hydrological and morphological data are well documented. The present model could simulate these kinds of rivers conveniently and the calibration of the model is relatively easy because of the facilities of well documented data. The other situation arises when dealing with rivers for which only geographical data is

available. These rivers can be considered as hypothetical cases by specifying them using dimensionless characteristic parameters, such as width-to-depth ratios, radius-to-width ratios, and sediment sizes. In this case, the sediment properties can be simplified by considering them as sand-bed and sand-bank rivers.

This study strongly proposes the idea of "Rivers as models of their own", through the RPM simulation model. The river models have the advantages that the discharge can be regulated at will and the bed can be inspected in detail anywhere. It is also liable to exaggerate the relative importance of factors that are relatively unimportant in the prototype—as we shall call the fully-natural river. The word 'model' always implies a comparison with something else which is then called the prototype; either partner may be called 'the model', and the other is then the prototype. In this study, rivers are treated as models of their own implies each river is unique and through the process of simulation each river obtains its own design. Therefore RPM model simulation actually is not merely a mathematical modelling, rather compounding process of unique rivers.

It can be concluded that bank erosion rate modules represent the field measurements and the RPM model is capable of simulating alluvial-river plan-form movement.

5.13 Discussion

Almost every theoretical study in the history of this subject has pointed out the vital role of width-to-depth ratio and radius-to-width ratio. However, each theory has proposed another weight of how these ratios contribute to the equilibrium bed topography and the bank erosion. In this study, the bank erosion rate (m/yr) and these two ratios are studied for some hypothetical rivers (simulated) and the interrelationships have been further considered. However, as this work remains inconclusive, it will not be reported.

It has been mentioned earlier that this work is based on the assumption of constant width while channel alignment is shifting. The constant width assumption can be justified in the real river case. The following case has been described in detail (Neil, 1983) and will only be summarized briefly. Over a ten year period, the progressive shift and accentuation of a sharp bend in the Tanana River, Alaska, was documented (Fig. 5.25a) and over a five year period careful measurements of bed load were made at a section just upstream (Burrows *et al.*, 1981; Burrows and Harrold, 1983). Comparison of quantities showed that the average annual bed load transport rate balanced very closely the average annual rate of bank erosion, implying a complete exchange of material whereby incoming bed load was deposited on the accreting point bar and replaced by material derived from bank erosion (Fig. 5.25b). Since a single severe bend of changing geometry is involved rather than a succession of bends as previously assumed, it cannot be generalized for all kinds of meandering rivers. However, it is an evident to prove the justification of the assumption used in this study.

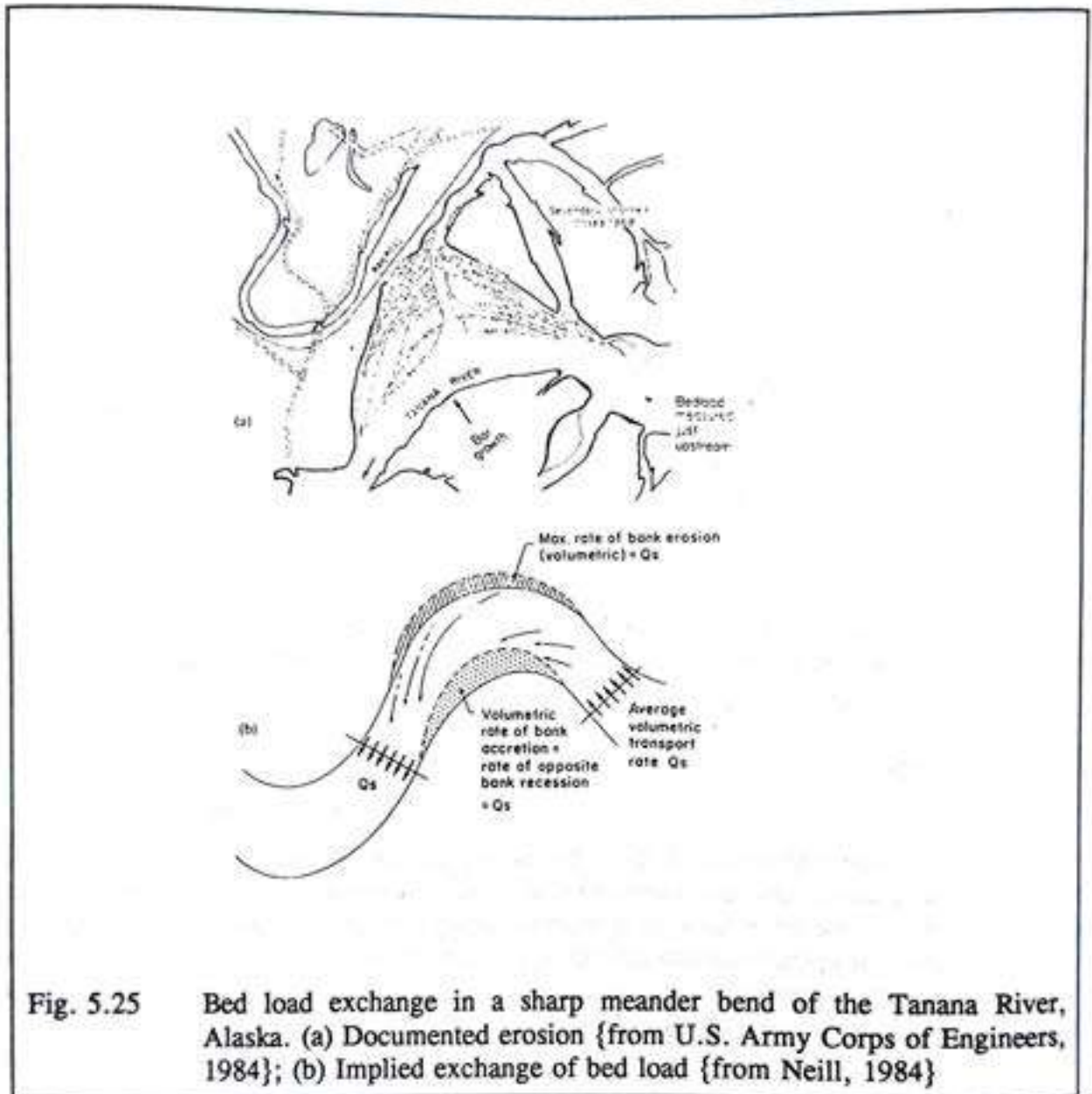


Fig. 5.25 Bed load exchange in a sharp meander bend of the Tanana River, Alaska. (a) Documented erosion {from U.S. Army Corps of Engineers, 1984}; (b) Implied exchange of bed load {from Neill, 1984}

5.14 Suggestions

There are some important elements related very much close to this area of study should be mentioned in this section. The suggestion is made to incorporate for the future studies.

5.14-1 Discharge-induced river-bank erosion

From an analysis of the characteristics of the one-dimensional model it is concluded that generally river widths cannot be stabilized by protecting certain carefully chosen bank sections only, and that computations of river planimetry can be decoupled from the computations of flow and bed topography (Mosselman, 1989). Several indices of stream-flow have been employed, including dominant discharge and bank-full discharge, but in a study based upon several rivers of the United States, Carlston (1965) concluded that the discharge controlled the meander wavelength over a range of flows, possibly falling stage flows, between the mean annual discharge and the mean discharge of the month of maximum discharge, and that meander migration took place during these stages. The size of meanders has been related to the catchment area, and this also reflects the fact that the meander geometry should be related to some parameter of stream discharge. The peak discharge can be used as a direct measure of the maximum force exerted on the bank by the flow during a storm event.

5.14-2 The need for care in the choice of a representative discharge.

When considering the variation of the discharge which is possible between the probable minimum discharge and maximum (bank-full) discharge, Beck *et al.* (1980) showed that for more than 50% of the time the actual discharge in the river is less than 20% of the bank-full discharge. We refer to Fig. 5.15 (pg. 514 of their River Meandering). During 50% of the time, however, only 10% of the bank-full flow is possible. According to this consideration, lateral bank erosion should be calculated from the effective flow rates, which are usually less than the bank-full discharges. For cutoff and mass failure of the river bank, the calculation should be made for the bank-full flow condition or some probable maximum flood of a definite return period.

The discharge regime of the catchment upstream from a river cross-section forms a fundamental independent control of channel cross-sectional morphology. As discharge varies at an individual cross-section, changes occur in the water surface width, mean flow depth and velocity and in other variables such as water surface gradient, the friction factor, and the bed shear stress.

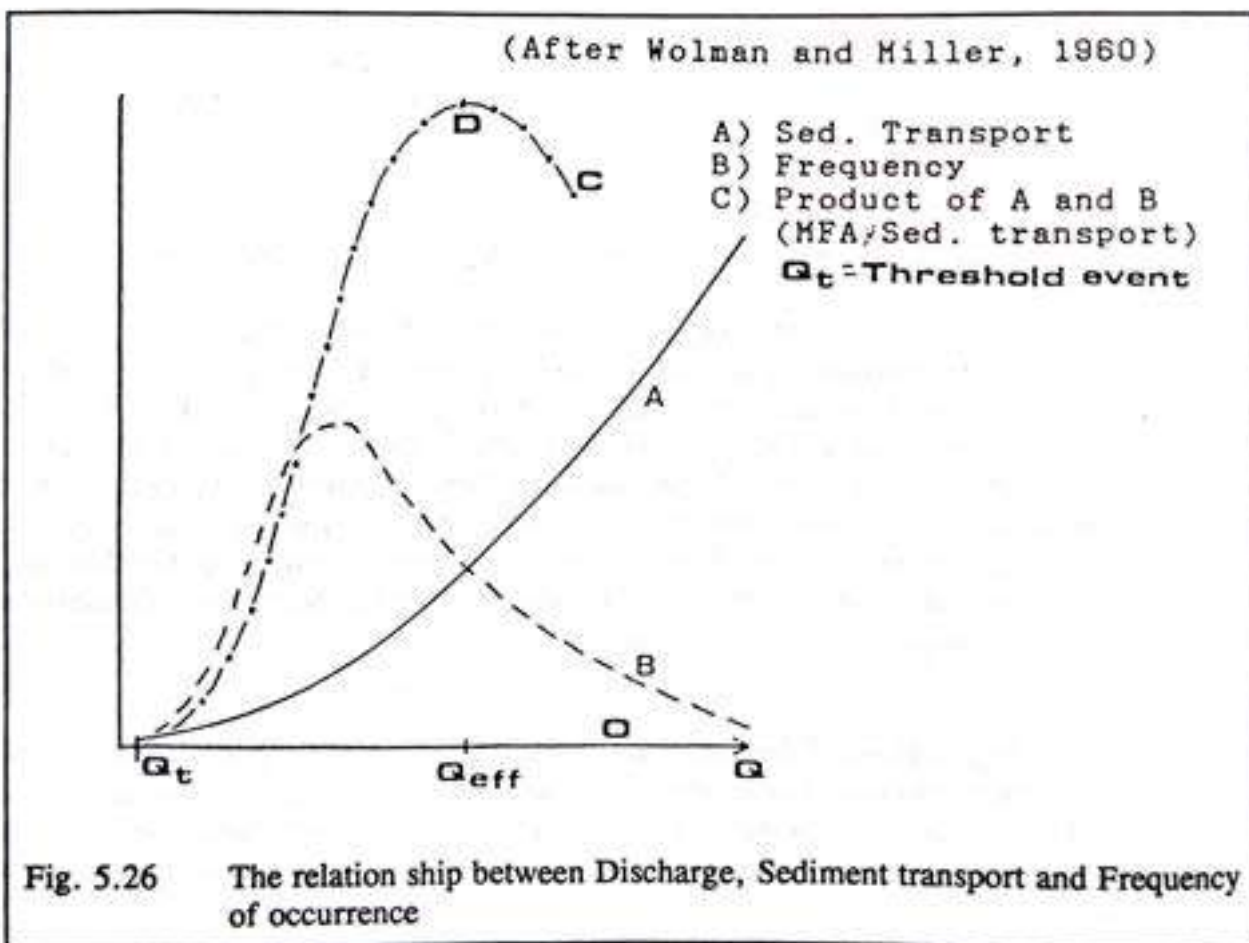
The fluctuating discharge of a natural river is unlikely to be represented by a single dominant discharge. It is important to select the effective discharge or the representative discharge of the specific river which has to be used in the simulation.

5.14-3 An introduction to Magnitude Frequency Analysis

Although studies concerning the magnitude of the effective discharge have been contributed by many authors, the main exponents of these are Pickup and Warner (1976), Benson et al. (1966), and Andrew(1980).

A definition of effective discharge is given by Benson (1966) as:

'The discharge that, over a long period of time, transports the most sediment'.



In this point it is clear that the effective discharge is associated with the moderate, high-frequency discharges, and not with the rare catastrophic events (see point D in fig. 5.26). The effectiveness with respect to sediment transport of a given discharge is studied in Chapter 4 within the context of the stable channel width of the meandering river (see Chapter 4). However in the case of selecting an appropriate representative discharge, the effectiveness of a given discharge is governed not only by its magnitude, but also by its

frequency. As shown in fig. 5.26, even though the sediment transport curve (A) rises with the magnitude of the discharge, the high sediment transport rates associated with high discharges occur so infrequently as to have little effect on the channel properties. The relative effectiveness of a given discharge as defined by the magnitude frequency analysis transport curve (C), is the product of the sediment transport rate and the frequency of its occurrence.

On the other hand, Richards (1985) stated that, in humid environments, extreme events may modify the channel form by as much as 40% .

It is still a useful exercise to set these apparently contrary views into the context of this study. One can use the first idea, that is a definition by Benson (1966) for the lateral bank erosion process, and use the second idea for a mass failure of the river bank and for a bend neck cutoff, since most probably lateral bank erosion may occur over a long period of time and the mass failure may be associated more with extreme events. Wolman and Miller, (1960) noted that, in many instances, land features were formed by relatively frequent geomorphic forces, and not by the rare flood events. To be specific, they suggested that the meander wave length and the channel geometry were governed by the effective discharge.

In fact, the situation is likely to be much more complicated in nature than that mentioned above. For example, after a certain flood, subsequent lower flows will allow the stable 'regime' form to recover. (This may take a considerable period, say 10-15 years). However, firstly, the recovery period may exceed the return period of the flood causing the channel modification, and, secondly, Newson (1980) suggests a case, where, after prolonged above-normal discharges, sediment may be washed through the system, and the river will become 'supply limited', causing severe erosion problems.

The concept of '*magnitude and frequency*' of geomorphic forces, developed by Wolman and Miller could be use as a tool for the selection of the effective discharge. Two principles of quantitative geomorphology are invoked in this approach. The first is that effective geomorphologic forces occur relatively frequently. The second principle concerns the relationship between land form and discharge. Two methods for calculating the effective discharge exist. The effective discharge model can be developed and this separate module can be joined as an assistant to the river plan-form movement model. However it must be stressed that such details can be introduced into a further study. Naturally these details have been borne in mind although the present study, but could not be included here. Therefore, details of the method are not mentioned here and only the references are given (Benson, *et al.*, 1966, Andrew, 1980, and Pickup, *et al.*, 1976).

"And don't we all sin by basing our judgements on too short periods of time?"

Sigmund Freud

6. CONCLUSIONS AND DISCUSSIONS

6.1 Conclusions

To avoid too many complications arising at any one time, the present study concatenates the long story of mathematical modelling, starting from the flow in the meandering river and proceeding to the prediction of channel shifting. Consequently, the conclusions are arranged chapterwise. Therefore there are three main parts, called part A, B and C, that must conclude this study, which in the main work are presented as the three corresponding main chapters, namely chapters 3, 4 and 5. The summary is presented first, in section 6.1-1.

6.1-1 Summary

1. A bed-topography model for a natural alignment has been developed with a satisfactory quality.
2. Bank-erosion models have been implemented and the results have been found to provide a satisfactory agreement with observation in nature and experiments.
3. A relationship between the velocities associated with the plane bed and the dune-covered bed for alluvial rivers has been introduced.
4. A model for roughness prediction which is based on this velocity relationship has been developed and the results found to be in satisfactory agreement with observations and other, theoretical results. In particular, the growth of the transition zone is represented very satisfactorily and can be simulated continuously.
5. A new grid mapping method has been proposed, tested and developed. The results are satisfactory.
6. A method to generate the grid over time has been proposed, tested and developed. The results are again satisfactory.

7. This type (of modular-modelling) of river plan-form movement is in a way a kind of monitoring system which controls and assembles the physically-based, independent modules.
8. The major factor that limits the maximum width of a river is the sediment carrying capacity of the alluvial channel and this is associated more with the features of a three-dimensional flow. However, the stable channel width or the optimum channel width can be determined with models of fewer dimensions, allowing the stable width or the optimum width to be decided for such rivers using reasonably economical numerical model simulations.
9. A meander could not exist if the banks were unerodible or if they were completely unstable. The meander pattern of melt water channels and incised meanders on ice are formed without any sediment load or point-bar construction by sediment deposition. Therefore bank erosion seems to be the only reason for meander formation. However, since a particular kind of meander pattern is in fact formed, the form itself is reinforced by the sediment transport mechanism. Therefore it can be said that the concept of an MTC channel width leads to a control of the width and this prevents the channel from being completely unstable.

6.1-2 Part A (Chapter 3)

The shear stress along a rough channel bank is an important phenomenon to be considered; the following conclusions concerning this phenomenon may be drawn from this study:

1. The roughness of the bank will decrease the longitudinal velocity, but increase the shear stress. If the effect of roughness change is combined with the effect of the secondary flow, a large bed shear stress at the toe of the bank is to be expected: hence the undermining of the bank.
2. The lateral momentum transfer both by the secondary flow and by turbulent shear are significant factors in shaping the cross-section of the channel. Therefore the suggestions of the authors upon whose work the present study has been founded are confirmed.

The model has been verified with flume experiments and observations of natural river situations. It has been proven to be reasonably accurate with regard to the depth-averaged flow field and the resulting bed topography.

Concerning the bed evolution process in river bends, it can be concluded that the point bar and pool configuration of the equilibrium bed in curved alluvial rivers have to be attributed to a transition in channel curvature. This fact is proven in the verification of the

model in the critical regions such as downstream of the entrance, the exit of a bend, and the region of the sudden change of the curvature or inflection points in the successive bend train. Only in a very long bend of constant curvature (eg. Fig. 3.34; Case 2), will there be a region (the fully-developed zone) where transitional effects have damped out and the *classical* theory of river bend morphology provides a good agreement with the simulated bed configuration. i.e. the transverse shear force due to the secondary flow is balanced by the downstream gravitational force, whereby the main flow and the sediment transport are parallel to the channel axis.

It has been found, concerning the treatment of the upstream condition without sediment input, differences occurred between nonequilibrium transport rates and comparable equilibrium capacity rates at a maximum near the beginning of the reach but diminishing towards the downstream end of the local scour hole. This spatial variation of the transport rate deficit exists because the flow requires a finite length of bed to erode sufficient bed material to satisfy its equilibrium transport capacity. Consequently, mathematical model performance will be poor in the local scour hole region.

6.1-3 Part B (Chapter 4)

The existence of the MTC channel width in straight rivers is well known in the literature. The present study shows that it also exists in meandering rivers. The advancement between the previous notion and the present notion is not only to considerations of the river plan-forms, but also the applied methods. The former is the analytical solution applied to straight rivers and the latter uses the simulation results of the numerical model to draw conclusion that apply to meandering rivers.

The following are the most important findings of the present study:

1. A velocity relationship for a river with two different regimes, corresponding to a plane bed and a dune-covered bed, both considered for constant discharge, slope and grain size, has been established.
2. The computing time is reduced by a factor of between 10 and 30 times.
3. The velocity relationship and proposed procedure provide a possible way to predict a more acceptable roughness factor in the transition zone.

An interesting debate concerning these matters is still continuing and appears to be developing in a positive direction. Among others, Julien and Simons, (1984) have drawn the following conclusions:

1. The hydraulic geometry of alluvial channels can be determined algebraically without the use of a sediment transport relationship, thus denying the very existence of an MTC channel.

- 2 Besides water discharge, sediment size is shown to be an important variable in defining the hydraulic geometry.

Nevertheless, the MTC hypothesis has a physical foundation. In our case, if the slope is predetermined, then the transport capacity increases with the reduction in width. However, the increase in transport capacity with width reduction is countered by the bank effects. Because of the lower shear stress along the banks, the banks contribute little or nothing to bed load transport.

According to the more basic hypotheses and theories, certain variational principles (extremum principles) can be used to solve the problems of dissipative mechanical systems in static or dynamic equilibrium conditions. The minimizing principle can be used independently or in tandem with the equations of motion to solve problems with a large degree of freedom. The equilibrium solution methodology thus obtained has been shown, however, to contain certain implicit assumptions.

We observe (Landau and Lifshitz, 1960) that in classical mechanics it may be shown that extremum principles provide viable alternatives to the better known mechanics based on Newton's laws. In fact, however, the equivalence is restricted within the context of a closed system. This is an unacceptable restriction when the problem considered cannot be regarded as a closed system. Fortunately in sediment transport mechanism it can be regarded as a closed system when sediment particles are flowing while not being emersed. On the other hand, the extremum principle might be applied most beneficially precisely to problems with large degrees of freedom, such as turbulence and river mechanics, for which the classical approach often fails to give a sufficient number of equations. Therefore it can be concluded that the optimum river width for meandering rivers clearly exists and it can be predicted from the sediment transport capacity.

6.1-4 Part C (Chapter 5)

A physical justification for such a simulation of river processes must still be firmly established. Physical understanding of the way in which channels become smaller is lacking. Not only do the phenomena appear to be random, but the two distinctive processes, enlargement and shrinkage, are of incomparable time scales. Therefore a constant width over the entire reach is assumed and an effort is made to understand the problem of the shifting movement of the plan-form.

Since the river channel is self-formed, the equilibrium channel geometry is so adjusted that it closely conforms to the flow pattern. Along a meandering channel consisting of bends (in bend train experiments) and crossovers, each bend apex, which approximately coincides with the zone of maximum curvature, is preceded and followed by transition curves. Helical motion is at the maximum strength near the apex and it is weak near the crossover. Therefore, the helical motion peaks, decays, reverses, and then grows between two consecutive apexes. This phenomenon is clearly expressed in terms of the simulated near-bank velocity excess. Correlation of this model with river data suggests that the meander

plan-form is related to the alternating flow development between the helical pattern and main flow (longitudinal flow). This in turn shows the applicability of the model, which in this case agrees with the theory of Rozovskii (1957).

Excess shear stress methodologies work best for cohesionless boundary materials. However a given flow can effect widely differing erosional responses. As Pizzuto and Meckelnburg (1989), observe: "for complex failure processes, simple correlations between erosion rate and near-bank velocity may not exist".

WRTC

Water, Research and
Training Centre

6.2 Discussions

The discussions cover three aspects, as following:- the physics, the mathematical formulation and the computational method.

6.2-1 The physics of natural rivers.

There are severe difficulties in applying the MTC channel width to natural streams. Briefly, these are as follows:

1. The explicit assumption is that the discharge is fixed while the width is considered a variable. Provided that the channel banks are sufficiently high to prevent over-bank flow, it is possible to vary the width while retaining a fixed dominant discharge. But in most natural alluvial channels there is an over-bank flow at stages that equal or exceed the dominant discharge. Thus, as the channel width is reduced, more of the high flow is wasted over-bank, and is not available for moving sediment along the bed of the channel. This implies a reduction of the dominant discharge with decreasing width, which proceeds against one of the initial assumptions.
2. The application becomes more complicated because nature's fluctuating discharges cannot be conveniently represented by a single dominant flow.

6.2-2 The mathematical formulation

The need of mathematical formulations for certain elements of the entire study calls for some attempts which are reported as followings.

6.2-2.1 Path of the sediment particle travelling along the river bend

An attempt is made to trace the path of the sediment transport along the individual stream lines as illustrated in Fig. 5.12. According to the experimental results, there are two possible paths for sediment to form a point bar which is located at the inner bend, downstream of the bend apex. The first one is that whereby material entrained from the concave bank is caught in the transverse component and carried towards the middle of the channel near the bed. The vigorous cross-currents near the bed in a bend can transport a

considerable amount of bed material toward the convex bank. This is a part of the mechanism of point-bar building. If the location from which the bed material was derived is far enough downstream in the bend, such material is not carried across the bed to the other side of the channel but moves into the crossover without having crossed the channel. Once into the reversed curve, it is drawn toward the same bank from which it started. To trace this phenomenon, the single bend and a series of bends are simulated with the same hydraulic characteristics and the same bed material properties. Unfortunately, the path of the sediment movement cannot be clearly explained from the results of the simulations. However, the cyclic order of curvature effect from the previous bend to the following bend is clearly noticed, see Fig. (3.36).

6.2-2.2 The secondary flow convection factor

The model shows that simulation results using the fixed secondary flow convection factor across the width of the river agree with the measurements along the outer wall while the transport is somewhat underestimated along the inner wall. On the other hand, if the simulated results fit with the measurements along the inner wall, they will differ from the measurements along the outer wall. The last and the most laborious trial was that of introducing the theoretical value of the secondary flow convection factor at the convex bank while introducing the double magnitude of the factor at the concave bank, and this was then introduced gradually over the river width from first value to the second. The results are promising, however to verify this factor needed more test runs.

6.2-3 The computational method

The present model yields satisfactory results in the case of bed configurations deviating from a flat bed. However, the influence of the side walls must be taken into account. The description of the flow field near the sidewalls raises many problems, both physical and mathematical. The physical problem is that of finding a suitable turbulent model and the other can be mentioned as that of the computation of laminar, axisymmetric flow.

The choice of grid size depends partly upon the amount of local geometry detail that is to be included, and partly upon the computing cost; often a compromise has to be made between these two factors.

6.3 Suggestions for the further study

6.3-1 Suggestions for part A

So far the simulation of the bed topography in an alluvial river bend gives satisfactory predictions and other information about the various sizes of river bend, including an infinitely long bend train. At this point, however, an important question arises. That is, on what basis one can say definitely that a river will change its plan-form? If it will change, in what way will it shift, and with which pattern (eg. lateral movement, downward movement, or a

combination of these). Of course, since we are concerned about the instability of the river, the inseparable phenomenon is the stability of the river. Strictly speaking, no flowing river is completely stable, but it does have an equilibrium condition, which is the result of a balance between different processes involving both erosion and deposition within the meso-scale time-span. This equilibrium condition can last momentary, or some years. If it may in certain singular cases endure for a couple of decades, this implies that the river is not actively changing its plan-form for a certain time-span. Therefore to be able to distinguish between these two is of prime important for the continuation of the present study.

As written earlier in this chapter, there is at present no satisfactory description of the mechanisms which determine the regime width of channels. The two available predictive methods are those of empirical regime theory and rational regime theory, both of which are based on an extremal hypothesis and both of which eschew any description of the physical processes involved. The other approaches only consider mechanisms for channel enlargement without taking account of the way in which the regime width is the result of a balance between different processes involving both erosion and deposition. A full description of the development of channel width may then require a knowledge of the distribution of the shear stress over the boundary of the channel.

Therefore the shear stress distribution for the bank line should be continued in a further study. Different sediment loading conditions, namely those of initial equilibrium, over-loading, under-loading and clear water need to be considered. The study should also be extended to cohesionless, fine-sediment bed forms in shallow flows.

6.3-2 Suggestions for part B

This study has assessed and applied exiting theories and has assembled them in an appropriate manner into specific problem areas in order to get nearer to a solution of the roughness-prediction problem. Some interesting points for further study are suggested here:-

1. general conclusions should be defined for meandering rivers for various sinuosity values, various bend angles, and various discharges. Some have been done already and can serve as working examples for the remaining areas of study.
2. the grain sorting effect is also attractive for further study. Sediment transport per size fraction can be calculated by size fraction formulae and the composition of the bed material can be changed as in nature. It will be interesting to see the interaction between local roughness and the bed material composition.

The relationship between this specific chapter and the river plan form movement simulation model could be further developed:-

1. The major deficiencies of the present mathematical model of river flow have been its failure to represent the dependence of friction factor on sediment discharge or concentration. Natural rivers adjust their hydraulic roughness in their own ways. Every beneficial feature of a physical system increases the complexity of its mathematical modelling in direct proportion to the value of the attendant benefits. Getting more insight into the physics and the ability to add more appropriate friction factors will help the simulation one step nearer to a reasonable prediction.
2. The shear stress is calculated from local flow and roughness conditions. Local shear stress is also calculated by dividing the river cross-section into a number of strips. Therefore, the local bank shear stresses of the inner and outer banks can be calculated from the two outer-most strips correspondingly. However, this is not really important for the case where the width-to-depth ratio is greater than 15. Moreover, although the local shear stresses are estimated, the critical bank shear stress is still unknown and indeed known not better than an empirical relationship, such as 0.75 times the bed shear stress. Therefore further research should be concentrated on both local and critical bank shear stresses.

6.3-3 Suggestions for part C

Since the RPM model is able to simulate both natural and hypothetical alluvial rivers in different sizes (within the limitation of its assumptions), the future study could be continue to investigate the most probable curvature of various sizes of rivers also within the limitation of its assumptions.

The RPM model is a kind of physically-based numerical model. The ambition for the future is to be able to demonstrate the sediment sorting process in the river bend in general and the pattern of river sediment deposits in the transverse direction in particular. In order to explain a clearer picture of this aim, let us consider one of the real cases in Muddy Creek. As Dietrich, 1989, describes it; "In the pool and along the steeper sloping surface of the point bar, the near-bed flow direction is strongly inward. At the edge of the bar top, the coarse sediment travels against this inward component of the secondary circulation by rolling, avalanching obliquely down from the crests of migrating dunes on the side or face of the point bar, and by being transported by trough-wise currents of obliquely oriented dunes. The finer sediment crosses the coarse sediment as it is carried inward from deeper water and up onto the downstream end of the bar by the inward directed boundary shear stress associated with the secondary circulation and flow in the lee of obliquely oriented bed-forms". If we add the non-uniform sediment transport process in the model, then we may be able to

simulate even this physical phenomenon. This implies, however, that the whole environment of the simulated flow field will be different because of the detailed account that will need to be taken of the dunes and bar formation and as a consequence the shear stress and the resistance to the flow and hence the velocity field, and so on. Thus it can be expected that this will provide a further deeper insight into the evolution of the river bed composition and structure and its associate bed features. From there, the corresponding migration rates and patterns which have been given in Chapter 5 will also however be changed.

The natural cut-off process is a following process of meander migration. The factors favourable to a small cut-off developing are that: (a) its channel should have at least three times the straight river's regime slope; and that (b) its upstream end should be taken off from a location where the parent's bed load has less than the average amount of coarse material from the downstream portion of the outside of a bend.

REFERENCES

- Andrews, E.D. 1980,
"Effective and bank-full discharges of streams in the Yampa river basin, Colorado and Wyoming",
J. of Hydro., Vol. 46, 1980, pp 311-330. (First method; computation)
- Ariathurai, R. and Arulanandan, K., 1978,
"Erosion rates of cohesive soils",
J. of Hyd. Div., ASCE, Vol. 104, No. HY2, February, pp. 279-283.
- Ascanio, M.F. and Kennedy, J.F. 1983,
"Flow in alluvial-river curves",
J. of Fluid Mech., Vol.33, 1983, pp 1-16.
- Ashida, K. and Michiue, M. 1973,
"Studies of bed-load transport rate in open channel flows",
International symposium on river mechanics 9-12 Jan. 1973 Bangkok, Thailand.
- Bagnold, R. A. 1966,
"An approach to the sediment transport problem from general physics",
U. S. Department of the Interior, Geological Survey Periodical paper. CBpr 514A
- Bathurst, J.C. 1988,
"Flow processes and data provision for channel flow models",
Modelling Geomorphological systems, Edited by M.G. Anderson, John Wiley & Sons Ltd., pp 127- 151.
- Bell, R.G. and Sutherland, A.J. 1983,
"Nonequilibrium bedload transport by steady flows",
J. of Hyd. Engg., Vol.109, No.3, March 1983, pp 351-367.
- Benson, M.A. and Thomas, D.M., 1966,
"A definition of dominant discharge",
Bulletin of the international association of scientific Hydrology, 11, 1966, pp 76.
- Bettess, R. and White, W. R.,
"Extremal hypotheses applied to river regime".
- Bettess, R. and White, W. R. 1983,
"Meandering and braiding of alluvial channels",
Proc.Instn Civ.Engrs, Part 2, 1983, 75, Sept. pp 525-538.

- Breusers, H. N. C. 1987,
"Lecture notes on sediment transport 1.", IHE, Delft, 1987.
- Brownlie, W. R. 1983,
"Flow depth in sand-bed channels",
J. of Hyd. Vol. 109, No. HY7, pp 959-989, July 1983.
- Burkham, D. E. 1980,
"General study of the modified Einstein method of computing total sediment discharge",
U. S. Department of the Interior, Geological Survey Periodical paper. CBpr 492F
- Callander, R. A. 1969,
"Instability and river channels",
J. of Fluid mech., 36, pp 465-480, 1969.
- Carson, M. A. and Griffiths, G. A. 1987,
"Influence of channel width on bed load transport capacity",
J. of Hyd. Vol.113, No. 2, Dec. 1987, pp 1489-1509.
- Chang, H. H. 1980,
"Stable alluvial canal design",
J. of Hyd. Vol. 106, No. HY5, May, 1980.
- Chang, H.H. 1983,
"Energy expenditure in curved open channels",
J. of Hyd. Engg., Vol.109, No.7, July 1983.
- Chang, H. H. 1984,
"Analysis of river meanders",
J. of Hyd. Vol.110, No. 1, Jan. 1984, pp 37-49.
- Chang, H.H. 1984,
"Regular meander path model"
J. of Hyd. Engg., Vol.110, No.10, Oct. 1984, pp 1398-1410.
- Chang, H.H. 1984,
"Variation of flow resistance through curved channels",
J. of Hyd. Engg., Vol.110, No.12, Dec. 1984, pp 1772-1782.
- Chang, H. H. 1985,
"Water and sediment routing through curved channels",
J. of Hyd. Vol.111, No. 4, April 1985, pp 644-658.

- Charles, C. S. et al. 1980,
"Minimum stream power : theory",
J. of Hyd. Vol. 106, No. HY9, Sept. 1980.
- Charles, C. S. et al. 1982,
"Discussion of Minimum stream power theory",
J. of Hyd. Vol. 108, No. HY7, July. 1982.
- Chin-lien Yen, 1970,
"Bed topography effect on flow in a meander",
J. of Hyd. Div., Vol.96, No.HY1, Jan. 1970, pp 57-73.
- Chow, V. T. 1981,
"Hydraulic Exponents",
J. of Hyd. Vol. 107, No. HY11, Nov. 1981.
- Davies, T. R. H. and Sutherland, A. J. 1983,
"Extremal hypotheses for river behavior",
Water resources research, Vol. 19, No. 1, pp 141-148, Feb. 1983.
- Deigaard, R. 1980,
"Longitudinal and transverse sorting of grain sizes in alluvial rivers",
Series paper 26. Inst. of Hydrodynamic and Hydraulic Engg., Tech. Univ. Denmark.
- Dietrich, W.E. and Smith, J.D. 1983,
"Influence of the point bar on flow through curved channels",
Water resources research, Vol.19, No.5, Oct. 1983, pp 1173-1192.
- Dietrich, W.E. and Whiting, P. 1989,
"Boundary shear stress and sediment transport in river meanders of sand and gravel",
Sediment transport in gravel-bed rivers, 1987, Editors; Thorne,C.R., Bathurst, J.C.
and Hey, R.D., pp 1-50.
- Druery et. al. and Leo C. van Rijn 1984,
"Discussions on shape and dimensions of stationary dunes in rivers",
J. of Hyd. Vol.110, No. 6, June 1984, pp 855-860.
- Edward, A. M. and Sabah Al-Nassri 1988,
"Uncertainty in suspended sediment transport curves",
J. of Hyd. Vol. 114, No. HY1, Jan. 1988.
- Engelund, F. and Hansen, E. 1966,
"Investigation of flow in alluvial streams",
ACTA Polytechnica Scandinavica, Civil engg. and building construction series No.
35, Copenhagen, 1966.

- Engelund, F. and Hansen, E. 1972,
"A nomograph on sediment transport in alluvial streams",
Technical press, Copenhagen, Denmark.
- Engelund, F. and Skovgaard, 1973,
"On the origin of meandering and braiding in alluvial streams",
J. of Fluid mech., 57, pp 289-302, 1973.
- Engelund, F. 1973,
"Steady transport of moderately graded sediment , part 1",
Prog. Rep. 35, pp 31-36, April, 1975, Tnst. Hydrodyn. and Hyd. Engg. Tech. Univ.
Denmark.
- Engelund, F. 1973,
"Steady transport of moderately graded sediment , part 2",
Prog. Rep. 29, pp 3-12, Aug. 1973, Tnst. Hydrodyn. and Hyd. Engg. Tech. Univ.
Denmark.
- Engelund, F. 1974,
"Experiments in curved alluvial channel : part1 and part 2",
Prog. Rep. 34, pp 31-36, Dec. 1974 and Prog. Rep. 38, pp 13-14, April 1976
Tnst. Hydrodyn. and Hyd. Engg. Tech. Univ. Denmark.
- Engelund, F. 1974,
"Flow and bed topography in channel bends",
J. of Hyd. Vol. 100, No. HY11, pp 1631-1648, Nov. 1974.
- Engelund, F. & Fredsøe, J. 1976,
"A sediment transport model for straight alluvial channels",
Nordic Hydrol. 7, 293.
- Engelund, F. 1981,
"The motion of sediment particles on an inclined bed",
Prog. Rep. 53, pp 15-20, April 1981, Tnst. Hydrodyn. and Hyd. Engg. Tech. Univ.
Denmark.
- Engelund, F. 1981,
"Transport of bed load at high shear stress",
Prog. Rep. 53, pp 31-35, April 1981, Tnst. Hydrodyn. and Hyd. Engg. Tech. Univ.
Denmark.
- Engelund, F. and Fredsøe, J., 1982,
"Hydraulic theory of alluvial rivers",
Advances in Hydroscience, Vol., 13., 1982.

- Fredsøe, J. 1978,
"Meandering and braiding of rivers",
J. of Fluid mech., 84, part 4, pp 609-624, 1978.
- Fredsøe, J. 1979,
"Unsteady flow in straight alluvial streams : modification of individual dunes",
J. of fluid mechanic, Vol. 91, part3, pp 497-512
- Fredsøe, J. 1982,
"Shape and dimensions of stationary dunes in rivers",
J. of Hyd. Vol. 108, No. HY8, Aug. 1982.
- Garde, R. J. and Raju, K. G. R. 1985,
"Mechanics of sediment transportation and alluvial stream problems",
second edition, 1985.
- Ghosh and Roy, 1970
Boundary shear distribution in open channel flow.
J. Hyd. Div. ASCE, 96(4), pp967-993, 1970.
- Gilbert, G.K., 1884
The sufficiency of Terrestrial Rotation for the Deflection of streams.
Nat. Acad. of Sci., Vol. 3, 1884. mentioned in Garde et al. 1985.
- Graf, W. L., 1984,
"A probabilistic approach to the spatial assessment of river channel instability",
Water resources research, Vol. 20, No. 7, July 1984, pp. 953-962.
- Griffiths, G. A. 1984,
"Extremal Hypotheses for River Regime : An Illusion of Progress",
Water Resources Research, Vol. 20, No. 1, pp 113-118, Jan. 1984.
- Guy, H. P. 1970,
"Fluvial sediment concepts",
Periodical paper, Source T. U. Delft Library, The Netherlands.
- Hansen, E. 1967,
"The formation of meander as a stability problem",
Hydraulic Lab. Tech. Univ. Denmark. Basic research prog. rep. No. 13.
- Hey, R. D. 1976,
"Geometry of river meanders",
Nature Vol. 262, Aug. 1976.

Hey, R. D., Bathurst, J. C. and Thorne, C. R. 1982,
"Gravel bed rivers",

Hicks, F.E., Jin, Y.C. and Steffler, P.M.,
"Flow near sloped bank in curved channel",
J. of Hyd. Engg., Vol.116, No.1, Jan. 1990, pp 55-70.

Hjulstrom, F., 1957
A study of the meander problem.
Institute of Hydraulics, Royal Institute of Technology, Stockholm, Bulletin No. 51,
1957.

Holtorff, G. 1982,
"Resistance to flow in alluvial channels",
J. of Hyd. Vol.108, No. 9, Sep. 1982, pp 1010-1027.

Hooke, J. M., 1979,
"An analysis of the processes of river bank erosion",
J. Hydrology. 42, pp. 39-62.

Hough, B. K., 1957,
"Basic soil engineering",
The Ronald Press Company, New York.

Ikeda, S. 1982,
"Incipient Motion of sand particles on side slopes",
J. of Hyd. Vol. 108, No. HY1, Jan. 1982.

Ikeda, S. et. al. 1990,
"Width and depth of self-formed straight gravel rivers with bank vegetation",
Water resources research, Vol. 26, No. 10, pp 2353-2364, Oct. 1990.

Jansen, Bendegom, Van Den Berg, De Vries and Zanen,
"Principles of river engineering the non-tidal alluvial river".

Johannesson, H. and Parker, G. 1987,
" Theory of river meanders",
University of Minnesota, St. Antony falls hydraulic laboratory, Project report No.
278. Nov. 1987.

Kalkwijk, J.P. and De Vriend, H.J. 1980,
"Computation of the flow in shallow river bends",
J. of Hyd. Research 18 (1980) No. 4, pp 327-342.

- Klaassen, G.J. et al., 1986,
"DHL-research on bedforms, resistance to flow and sediment transport" DHL
communication No. 362, July 1986.
- Klaassen et al., 1989,
"On cutoff ratios of curved channels"
XXIIth IAHR Congress, Otta, Canada, 21-25 August, 1989.
- Klaassen et al., 1992,
"Planform changes of a braided river with fine sand as bed and bank material",
5th International Symposium on River Sedimentation,
April 1992, Karlsruhe, F.R. of Germany.
- Knudsen, M. 1981,
"On the direction of the bed shear stress in channel bends",
Prog. Rep. 53, pp 3-7, April 1981, Tnst. Hydrodyn. and Hyd. Engg. Tech. Univ.
Denmark.
- Kuipers, J. and Vreugdenhil, C.B. 1973,
"Calculation of two-dimensional horizontal flow",
Report S163, part 1, Delft Hydraulics, October 1973.
- Lambe, T. W. and Whittman, R. V. 1969,
" Soil Mechanics",
John Wiley & Sons, Inc., New York.
- Lau, Y. L. 1983,
"Suspended sediment effect on flow resistance",
J. of Hyd. Vol. 109, No. HY5, pp 757-762, May, 1983.
- Lee, H. Y. and Odgaard, A. J. 1987,
"The dynamics of bends with nonuniform bed material",
Proceeding of IAHR Congress, 1987.
- Leopold, L. B. and Wolman, M. G. 1957,
"River channel patterns : braided, meandering and straight",
Geological survey prof. paper No. 282-B
- MacMurray, H.L. and Jaeggi, M.N.R 1990,
"Modelling erosion of sand and silt bed river",
J. of Hyd. Engg., Vol.116, No.9, Sept. 1990, pp 1080-1090.
- Maddock, T. 1970,
"Indeterminate hydraulics of alluvial channels",
J. of Hyd. Div. Vol. 96, No. HY11, pp2309-2323, Nov. 1970.

- Martin, N. R. J. 1980,
"Steepness of sedimentary dunes; Discussion",
J. of Hyd. Vol. 106, No. HY1, Jan., 1980.
- Melton, F.A., 1936,
"An empirical classification of flood-plain streams",
Geogr. Rev. Vol. 26, pp 593-609.
- Middleton, 1930,
"Properties of soils which influence soil erosion",
Technical Bulletin No. 178, U S Department of Agriculture, Washington, D.C.
- Murphy, P. J. 1981,
"A definition of bed load",
IAHR Workshop, April 6-8 1981.
- Myers, W. R. C. 1982,
"Flow resistance in wide rectangular channels",
J. of Hyd. Vol. 108, No. HY4, pp471-482, April, 1982.
- Naot, D. 1984,
"Response of channel flow to roughness heterogeneity",
J. of Hyd. Engg., Vol.110, No.11, Nov. 1984, pp 1568-1587.
- Neu, H.A., 1967
Transverse flow in a river due to Earth's Rotation.
J. of Hyd., Proc. ASCE, Vol. 93, No. HY-5, Sept. 1967.
- Newson, M., 1980,
"The geomorphological effectiveness of floods, a contribution stimulated by two recent events in Mid-Wales",
Earth surface processes, 5, 1980, pp 1-16.
- Nordin, Jr. C. F. 1964,
"Aspects of flow resistance and sediment transport studies of flow in alluvial channels",
U. S. Department of the Interior, Geological Survey Periodical paper. CBpr 492F
- Odgaard, A. J. 1981,
"Transverse bed slope in alluvial channel bends",
J. of Hyd. Vol. 107, No. HY12, Dec. 1981.
- Odgaard, A.J. 1982,
"Bed characteristics in alluvial channel bends",
J. of Hyd. Div., Vol.108, No.Hy11, Nov. 1982, pp 1268-1281.

- Odgaard, A. J., 1984,
"Flow and Bed Topography in alluvial channel bend",
J. of Hyd. Vol. 110, No.4 April 1984.
- Odgaard, A.J. 1986a,
"Meander flow model I: Development",
J. of Hyd. Engg., Vol.112, No.12, Dec. 1986, pp 1117-1136.
- Odgaard, A.J. 1986b,
"Meander flow model II: Applications",
J. of Hyd. Engg., Vol.112, No.12, Dec. 1986, pp 1137-1150.
- Odgaard, A.J. and Bergs, M.A. 1987,
"Flow in curved erodible channels",
IAHR congress, 1987, pp 136-141.
- Odgaard, A. J. and Mary, A. B. 1987,
"Flow in curved erodible channels", Institute of Hydraulic Research, The Univ. of Iowa, USA. Proceeding of IAHR Congress, 1987.
- Olesen, K.W. 1982a,
"Influence of secondary flow on meandering of rivers",
Report 1-82, Lab. of Fluid Mech., Dept. of Civil Engg., Delft Univ. of Tech., Delft, The Netherlands.
- Olesen, K.W. 1982b,
"Introduction of streamline curvature into flow computation for shallow river bends",
Report 5-82, Lab. of Fluid Mech., Dept. of Civil Engg., Delft Univ. of Tech., Delft, The Netherlands.
- Olesen, K.W. 1983,
"Alternate bars in and meandering of alluvial rivers",
Proc. ASCE Conference Rivers '83, New Orleans, pp 873.
Communications on Hydraulics 83-1, Dept. of Civil Engg., Delft Univ. of Tech., Delft, The Netherlands.
- Olesen, K.W. 1985,
"Flow and bed topography computation for shallow channel bends",
Communications on Hydraulics 85-1, Dept. of Civil Engg., Delft Univ. of Tech., Delft, The Netherlands.
- Olesen, K.W. 1987,
"Bed topography in shallow river bends",
Ph.D thesis, Delft Univ. of Tech., Delft, The Netherlands.

- Osman M. A. 1985,
"Channel width response to changes in flow hydraulics and sediment load",
Fort Collins, Colorado State Univ., dissertation, Feb. 1985.
- Pacheco-Ceballos, R. 1983,
"Energy losses and shear stresses in channel bends",
J. of Hyd. Engg., Vol.109, No.6, June 1983, pp 881-895.
- Parker, G. 1976,
"On the cause and characteristic scales of meandering and braiding in rivers",
J. of Fluid mech., 76, part 3, pp 457-480, 1976.
- Parker, G. 1978,
"Self-formed straight rivers with equilibrium banks and mobile bed : 1. The sand-silt river".
J. of Fluid mech., 89(1), 109-125, 1978a.
: 2. The gravel river", J. of Fluid mech., 89(1), 127-146, 1978b.
- Parker, G. et al. 1981,
"Bend theory of river meanders. part 1. Linear development",
J. of Fluid mech., Vol. 112, pp 363-377, 1981.
- Parker, G. et al. 1982,
"Bend theory of river meanders. part 2. Nonlinear deformation of finite-amplitude bends",
J. of Fluid mech., Vol. 115, pp 303-314, 1982.
- Phillips, B. C. and Sutherland, A. J. 1985,
"Numerical modelling of spatial and temporal lag effects in bed load sediment transport", 21st IAHR Congress, Melbourne, Australia, 19-23 August 1985.
- Pickup, G. and Warner, R. F., 1976,
"Effects of hydrological regime on magnitude and frequency of dominant discharge",
J. of hydro., Vol. 29, 1976, pp 51-77.(second method for effective Q)
- Ponce, V. M. et al. 1979.,
"Modelling Alluvial Channel Bed Transients",
J. of Hyd. Vol. 105, No. HY3, March, 1979.
- Proffitt, G. T. and Sutherland, A. J. 1983,
"Transport of non-uniform sediments",
J. of hydraulic research, Vol 21, No1 1983, pp 33-43

- Quraishy, M.S., 1943
River meandering and Earth's Rotation.
Current Science, Oct. 1943.
- Ramette, M. 1980,
"A theoretical approach on fluvial processes"
International symposium on river sedimentation, Beijing, China, March 1980.
- Rathbun, R. E. 1969,
"Response of a laboratory alluvial channel to changes of hydraulic and sediment transport variables", U. S. Department of the Interior, Geological Survey Periodical paper. CBpr 515A
- Raudikivi, A. J. and Witte, H. 1990,
"Development of bed features",
J. of Hyd. Vol.116, No. 9, Sep. 1990, pp 1063-1079.
- Richards, Keith 1982,
"Rivers, form and process in alluvial channels", Methuen & Co. Ltd.
- Rosso, M., Schiara, M. and Berlamont, J. 1990,
"Flow stability and friction factor in rough channels",
J. of Hyd. Engg., Vol.116, No.9, Sept. 1990, pp 1109-1118.
- Shen, H. W. and Kikkawa, H. 1980 (editors),
"Application of stochastic processes in sediment transport",
Water resources publication, Littleton, Colorado, USA.
- Shimizu, Y., Itakura, T. and Yamaguchi, H. 1987,
"Calculation of two-dimensional flow and bed deformation in rivers",
IAHR Congress, 1987, pp 201-206.
- Shimizu, Y., Yamaguchi, H. and Itakura, T. 1990,
"Three-dimensional computation of flow and bed deformation",
J. of Hyd. Engg., Vol.116, No.9, Sept. 1990, pp 1090-1105.
- Shrikrishna, V. C. 1970,
"River channel patterns",
J. of Hyd. Vol. 96, No. HY1, pp 201-221, Jan. 1970.
- Simons, D. B. and Şentürk, F., 1977,
"Sediment transport technology",

- Stavens, M. A. and Nordin, C. F. 1987,
"Critique of the regime theory for alluvial channels",
J. of Hyd. Vol.113, No. 11, Nov. 1987, pp 1359-1380.
- Struiksmā, N. et al. 1985,
"Bed deformation in curved alluvial channels",
J. of Hyd. Research, Vol.23, No.1, 1985, pp 57-79.
- Talmon, A. M. 1988,
"A theoretical model for suspended transport in river bends",
Delft Univ. of Tech. Rep. No. 2/88, July 1988.
- Taylor, D. W., 1948,
"Fundamentals of soil mechanics",
John Willey & Sons, New York.
- Thorne, C. R., 1982,
"Process and mechanisms of river bank erosion", Gravel-Bed rivers,
John Wiley & Sons, Ltd., London.
- Timothy, R. H. Davies, 1980,
"Bedform spacing and flow resistance",
J. of Hyd. Vol. 106, No. HY3, March, 1980.
- Timothy, R. H. Davies, 1982,
"Lower flow regime bedforms : Rational classification",
J. of Hyd. Vol. 108, No. HY3, March, 1982.
- Vriend, H.J. de and Geldof, H.J. 1983,
"Main flow velocity in short river bends",
J. of Hyd. Engg., Vol.1109, No.7, July 1983, pp 991-1011.
- Vriend, H.J. de and Struiksmā, N. 1983,
"Flow and bed deformation in river bends"
Publication No. 317, Delft Hydraulics Lab., Dec. 1983.
- Vries, de 1987,
"Engineering potamology",
IHE Lecture notes.
- Vries, M. de and Zwaard, J.J. van der, 1975,
"Movable-bed river-models",
Publication No. 156, Delft Hydraulics Lab., The Netherlands.

- Werner, P.W., 1951
On the origin of river meanders.
Trans. AGU, Vol. 32, No. 6, Dec. 1951.
- White, W.R. et.al. 1982,
"Analytical approach to river regime",
J. of Fluid mech., Vol.108, No. 10, Oct. 1982.
- Wijbenga, J. H. A. and Klaassen, G. J. 1981,
"Changes in bedform dimensions under unsteady flow conditions in a straight flume",
DHL Publication No.260 Dec. 1981.
- Williams, G. P. 1970,
"Flume width and water depth effects in sediment transport experiments",
U. S. Department of the Interior, Geological Survey Periodical paper. CBpr 515A
- Wolman, M. G. and Miller, J. P.,
"Magnitude and frequency of forces in geomorphic processes",
Journal of geology, 68, 1, 1960, pp54-74.
- Yalin, M. S. 1979,
"Steepness of sedimentary dunes",
J. of Hyd. Vol. 105, No. HY4, April, 1979.
- Yalin, M. S. et al., 1980,
"Steepness of sedimentary dunes", Closure of the discussion,
J. of Hyd. Vol. 106, No. HY10, Oct., 1980.
- Yang, C. T. et al. 1976,
"Applicability of unit stream power equation",
J. of Hyd. Vol. 102, No. HY5, May, 1976, pp 559 to 568.
- Yang, C.T. 1976,
"Minimum unit stream power and fluvial hydraulics",
J. of Hyd. Vol. 102, No. HY7, July 1976.
- Yang, C. T. 1979,
"Theory of minimum rate of energy dissipation",
J. of Hyd. Vol. 105, No. HY7, July, 1979.
- Yee-Chung Jin, Steffler, P.M. and Hicks, F.E 1990,
"Roughness effects on flow and shear stress near outer bank of curved channel",
J. of Hyd. Engg., Vol.116, No.4, April 1990, pp 563-577.

Yang, C. T. et al. 1982,
"Sediment transport and unit stream power function",
J. of Hyd. Vol. 108, No. HY6, June, 1982.

Yen, C. and Shin-ya Ho 1990,
"Bed evolution in channel bends",
J. of Hyd. Vol.116, No. 4, April 1990, pp 544-562.

Zhaohui, W. 1981,
"The deformation of a sand bed with a transverse slope",
Prog. Rep. 53, pp 9-14, April 1981, Tnst. Hydrodyn. and Hyd. Engg. Tech. Univ.
Denmark.

Zimmermann, C. and Kennedy, J. F. 1978,
"Transverse bed slope in curved alluvial streams",
J. of Hyd. Vol. 104, No. HY1, pp 33-47, Jan. 1978.

" Colloquium on The dynamics of alluvial rivers",
University of Genova, Italy. Genova June 25 to 26 1985.

"The main findings of sediment research, China",
International symposium on river sedimentation,
Beijing, China, March 1980.

LIST OF SYMBOLS

This list of symbol is made to have a quick look for the meaning of the symbols. However sometimes one symbol has different meanings and this happens because these particular symbols could not be renamed only for the sake of this thesis. The symbols come from the fundamental use of the different scientific fields and these names are fixed in their own field of science. The author felt that she has no right to change the well known and well established symbols. Therefore the meaning of symbols are always expressed in the text in each equation where they appeared.

A	=	an order-one scour factor parameterizing the role of secondary currents
A	=	catchment area
b	=	a power coefficient in the power law sediment transport formula
c	=	a power of flow depth in Manning's formula
C	=	local bend curvature
Ca	=	measure of Calcium ion
d	=	representative grain diameter
d_{50}	=	representative medium grain diameter
E	=	a dimensionless erosion coefficient
E_0	=	primary coefficient of bank erosion
e	=	secondary coefficient of bank erosion
e_v	=	the void ratio
F_s, F_n, F_z	=	friction terms in s-, n- and z- directions
f_0	=	a function to take account of the influence of the side walls
F_d	=	the particle densimetric Froude No.
g	=	acceleration due to gravity
H	=	reach-averaged depth
h	=	water depth
h_c	=	water depth at the river axis
h_p	=	water depth corresponding to the plane bed condition
I	=	hydraulic stability index
I	=	the longitudinal bed slope
I_a	=	agricultural intensity index
I_c	=	soil erodibility factor
i_s	=	the strength of the secondary flow
j	=	a position of the computation point in s direction
k	=	a position of the computation point in n direction
K_d	=	total roughness of dune-covered bed secondary flow intensity
$\mathcal{L}u_s$	=	shape of the longitudinal flow velocity
$\mathcal{L}u_n$	=	shape of the secondary flow velocity
L	=	length of the bank segment
m	=	local bed elevation
m	=	a factor depending on the bed roughness
m	=	a power of effective shear
M	=	an erosion rate constant

WRTC

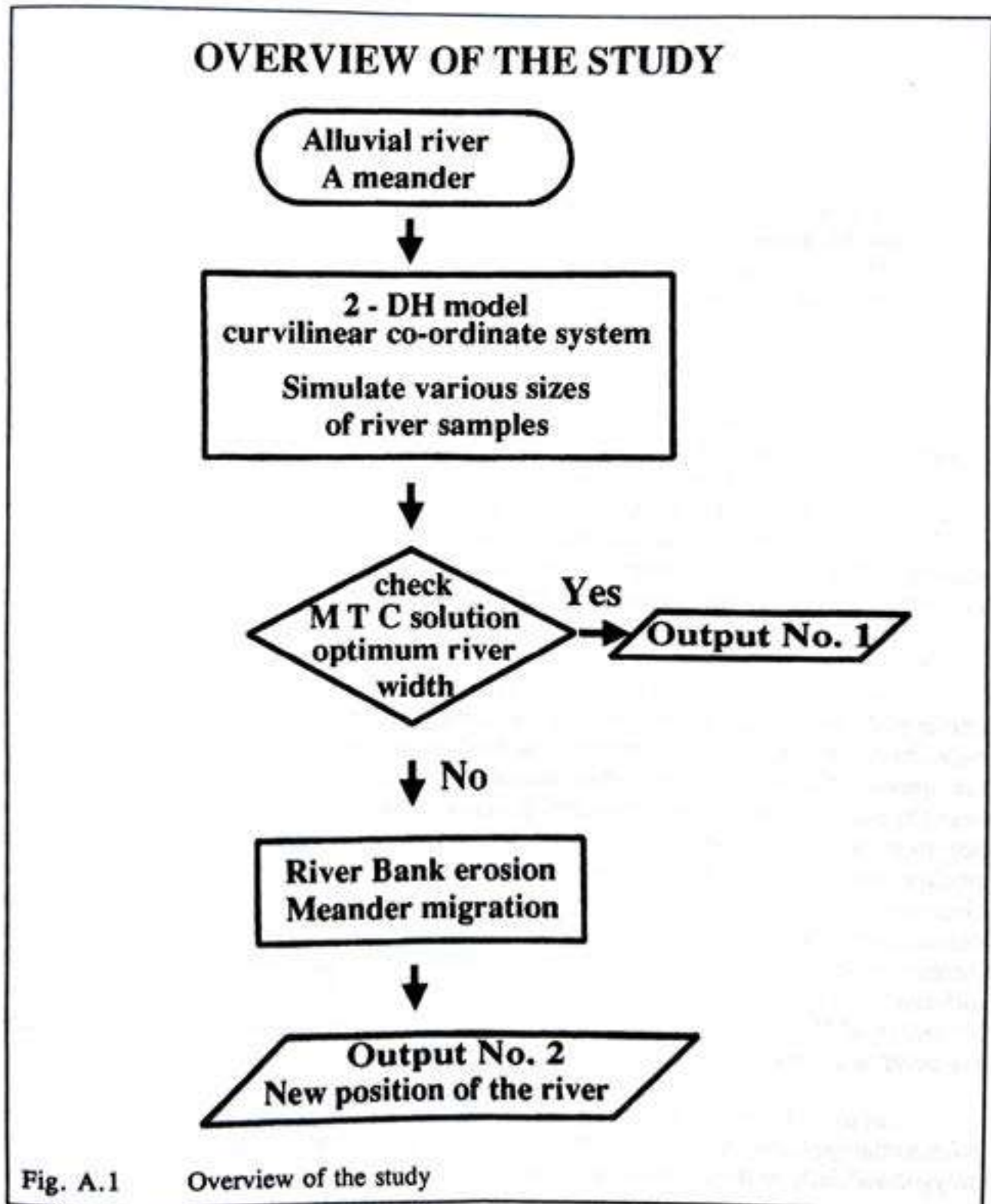
Water, Research and
Training Centre

Mg	=	measure of Magnesium ion
n	=	the cross-channel coordinate (n is orthogonal to s)
N	=	total number of trees in the segment
Na	=	measure of Sodium ion
p	=	the number of iterations
p and q	=	stream functions
P	=	total pressure
Q	=	the total discharge
R	=	local radius of curvature
R_c	=	the radius of curvature of the channel centre line
R_σ	=	radius of curvature of σ -axis
R_ψ	=	radius of curvature of ψ -axis
R_{st}	=	stream-line curvature
s	=	the longitudinal direction coordinate
S	=	river bed slope
SAR	=	Sodium adsorption ratio
S_c	=	the volumetric sediment transport flux
S_t	=	local transverse bed slope
S_{tc}	=	transverse bed slope at the river axis
U	=	local velocity
\bar{U}	=	reach-averaged mean velocity at bank-full discharge
U_b	=	near-bank velocity
U'_b	=	near-bank excess velocity
U_d	=	mean velocity of the dune-covered bed
U_{fp}	=	friction velocity due to the skin friction
U_s, U_n, U_z	=	velocity components in s-, n- and z- directions
W	=	width of the river
α	=	shape factor of the particle
α	=	a dimensionless roughness coefficient
β_f	=	the dynamic friction coefficient
ρ	=	mass density of the fluid
κ	=	the Von Kàrmàn constant
ξ	=	the rate of bank migration
Δn	=	a distance step in n direction
Δs	=	a distance step in s direction
Δt	=	a time step in numerical simulation
δ_s	=	bed shear stress direction angle
ψ	=	sediment transport direction angle
θ_c	=	the critical shear stress
τ_b	=	the bed shear stress
τ_n	=	the bed shear stress in n direction
τ_s	=	the bed shear stress in s direction
ρ	=	the density of the water (strictly speaking, the density of the fluid)
Δ	=	the specific gravity of the sediment
μ	=	the ripple factor
ϕ	=	the dynamic friction angle

θ_0	=	the bed shear stress for horizontally sloping bed
θ_{0h}	=	the bed shear stress value for horizontal bed
θ	=	Shield's parameter
Ω	=	a relaxation coefficient

APPENDICES

A.1 Overview of the study



A.2 Accuracy of the grid mapping

The accuracy of the grid mapping is considered from two aspects, the first being that of differential geometry and the other that of the physics of the stream flow. The first is concerned with the value of the angle through which an arc can maintain a constant radius and the second is concerned with a flow and bed material relaxation length. The first specification concerns the upper limit of arc that can be chosen for the largest value of the curvature encountered. In practice it is found that, the largest curvature can be taken as the radius of curvature that is less than or equal to four times the width of the river (see section, 3.12). The length of the computational cell in the s-direction is called Δs (the distance step) and it can be conveniently defined by the angle subtended at its centre of curvature. Experience in running this model has indicated that an upper limit for this angle for the largest curvature is approximately 0.062 radians. The second specification is effectively expressed through equation (3.64). The stability of the model can also be assured by these two specifications.

Here, the accuracy of the grid mapping by circular segments is explained. In order to prove that this method is applicable accurately enough in the sense of mathematics, the following explanation can be constructed. Let us consider a formula for the circumference of a circle, and the ancient problem of how to find the value of π (* - which of course, being irrational, cannot be determined exactly but only calculated with different degrees of accuracy). We begin by drawing a circle and two regular polygons, one inside the circle and the other outside, but both intersecting the circle only in a finite set of points. This is shown in Fig. A.2.

The polygon inside the circle is to have its corners just touching the circle, while the one outside has its sides just touching the circle; the former polygon, in other words, is 'inscribed', the latter 'circumscribed', in relation to the circle. Now it is clear that the circumference of our circle is greater than the perimeter of our inscribed polygon, but less than the perimeter of our circumscribed polygon. *If we increase the number of sides of the polygons, it is clear that the difference between the lengths of their perimeters becomes smaller and smaller as the number of sides is increased.* Since the circumference of our circle always lies between the length of our perimeters, we can find the circumference to any desired degree of accuracy by increasing the number of sides in our polygons indefinitely and thereby steadily reducing the difference between their perimeters, or *exhausting* that difference. Thus the distance between these circles, or the area between them, expressed as a function of the number of sides of the polygon, can serve as a *norm* for the adequacy of the polygon to represent the circle.

Let us pick out one side of the circumscribed polygon and joined its ends and its mid-point to the centre of the circle, as in Fig. A.2b; Fig. A.2c shows one side of the inscribed polygon similarly treated. Considered the diameter of the circle is 1 unit. From Fig. A.2b, the perimeter of our circle is a function of tangent (i) and according to Fig. A.2c, the perimeter of our circle is a function of sine (i) in which (i) is a half of the interior angle. If we take twelve-sided polygons inside and outside of the circle, the perimeter of the circle lies between 3.2148 and 3.1056. If we increase the number of sides to thirty six, the perimeter

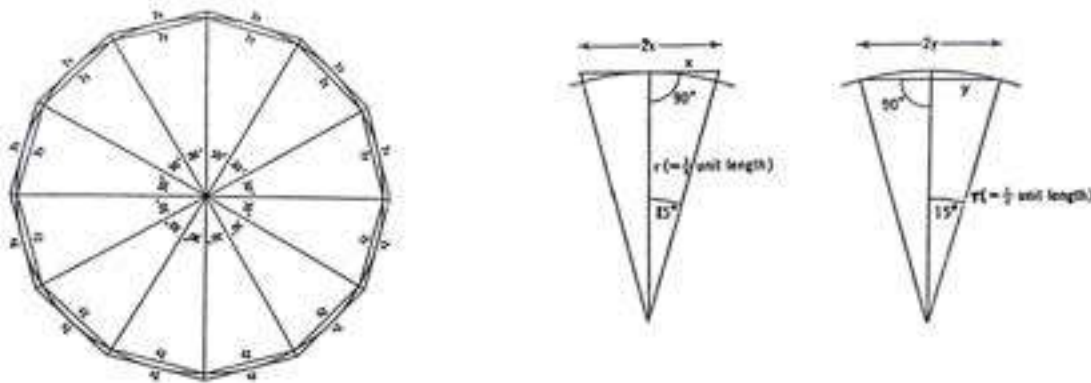


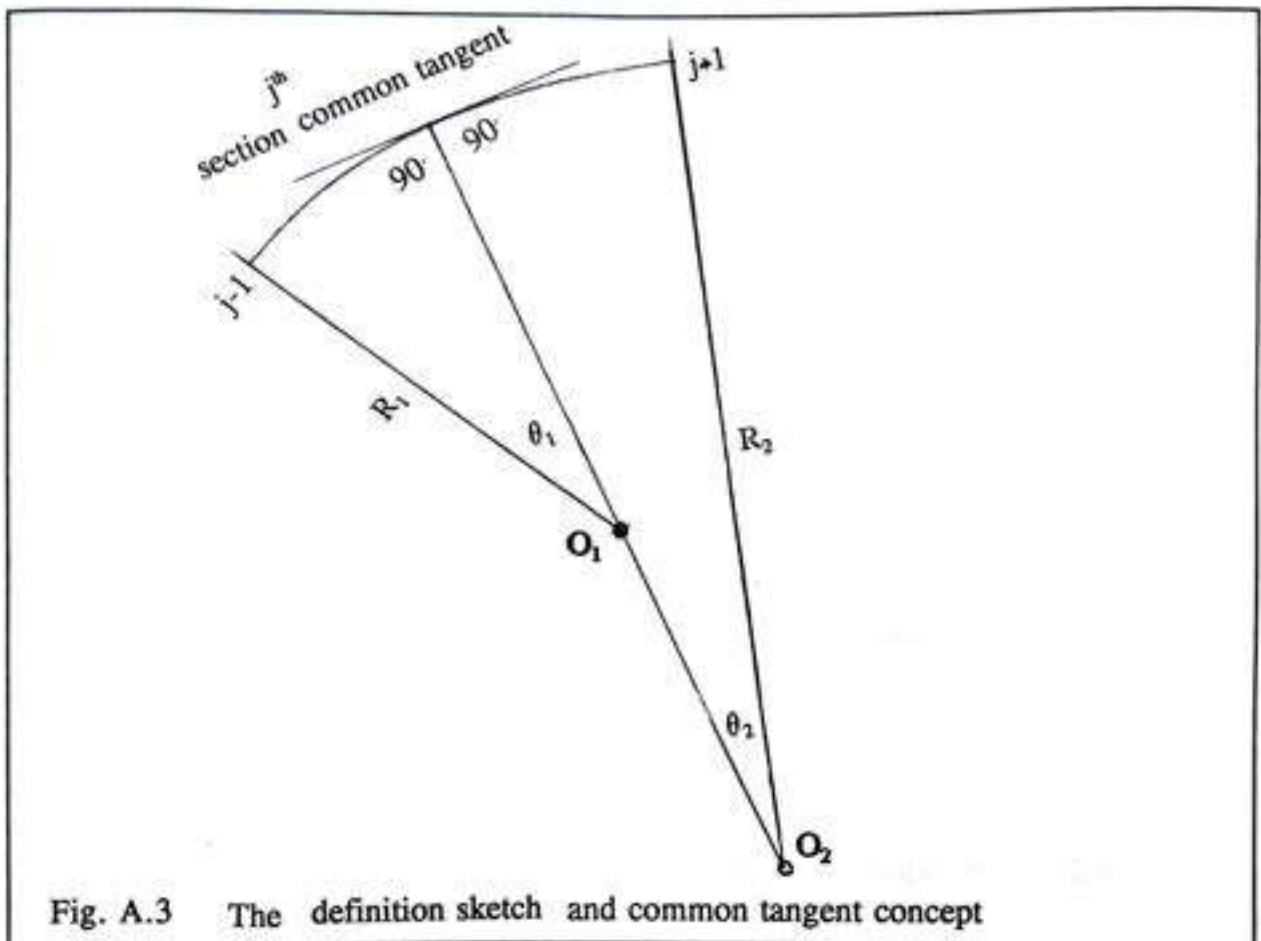
Fig. A.2 A circle with inscribed and circumscribed polygons and their corresponding segments

lies between 3.392 and 3.15. Of course, if we go on increasing the number of sides in the polygons 'to infinity', we arrive at π . Now that we have established that the value (circumference / diameter) may be found to any required degree of accuracy. Using this elementary (and ancient) construction in the set of formulae to set up the natural alignment of the river, provides the following criteria:

$$\begin{aligned}
 C_{TPj} &= 2\pi R_{TPj} \\
 S_{TPj} &= R_{TPj} \Theta_{TPj, rad} \\
 ARC_{TPj} &= S_{TPj} \text{ at the centre line of the river} \\
 \text{River Length} &= \Sigma ARC_{TPj}
 \end{aligned}$$

in which subscript TPj means (see Fig. A.3)

$$\begin{aligned}
 C_j &= \text{circumference of the corresponding circle "j"} \\
 S_j &= \text{circumference of the corresponding segment "j"} \\
 R_j &= \text{radius of the corresponding segment "j"} \\
 \Theta_{j, rad} &= \text{angle subtend at the centre of the corresponding segment "j"} \\
 ARC_j &= \text{an arc length along the centre line of the river at the corresponding segment "j"}
 \end{aligned}$$



- (1) The first step seems extremely simple, but by changing the angular measurements from sexagesimal measure to radians, this does provide a way to estimate the adequacy of the representation.
- (2) It shows how two consecutive segments should have a common tangent (see Fig. A.3b)
- (3) For a very strong curvature, say three to four times the width of the river, the angle $\theta < 0.062$ rad is suggested by the construction.
- (4) The definement of Δs also depends on the width-to-depth ratio of the river. It can only be achieved through experiencing the model; therefore some hints are presented in Chapter 3, section 3.11 and 3.12.

A.3 Derivation for bank-shear-stress value in a meandering river

Theory for meandering channel:- The presence of meandering channel introduces the complication of secondary current associated with the exchange of flow between the valley and the channel. This exchange is not constant, but is affected by a number of

variables, including the severity of the meander pattern and the relative depth of the flow in the channel to the flow in the valley. If one considers a meandering channel without flood plain, the exchange of flow between the valley and channel can be put aside but the secondary currents. For that reason, the cross-section is definitely non-prismatic.

If the cross-section is irregular, also referred to as a compound cross-section, application of Manning's, or Chezy's equation to the gross section will lead to a significant underestimate of the discharge. This arises because of the disproportionate effect on the hydraulic radius of the shallow flowing parts of the cross-section. These parts tend to increase the wetted perimeter relatively more than they increase the flow area. The calculated hydraulic radius is not a true representative of either the shallow part or the deep part of the cross-section. Therefore it seems reasonable to break a gross section up into a number of more or less regular sections and apply Manning's or Chezy's equation to each part separately. (Note. That is already done in the numerical model.) The total discharge is taken as the summation of the discharges of the parts. In this case the equations take the form

$$Q = \left(\frac{A_1 R_1^{2/3}}{n_1} + \frac{A_2 R_2^{2/3}}{n_2} + \dots \right) S^{1/2} \quad (\text{A.1})$$

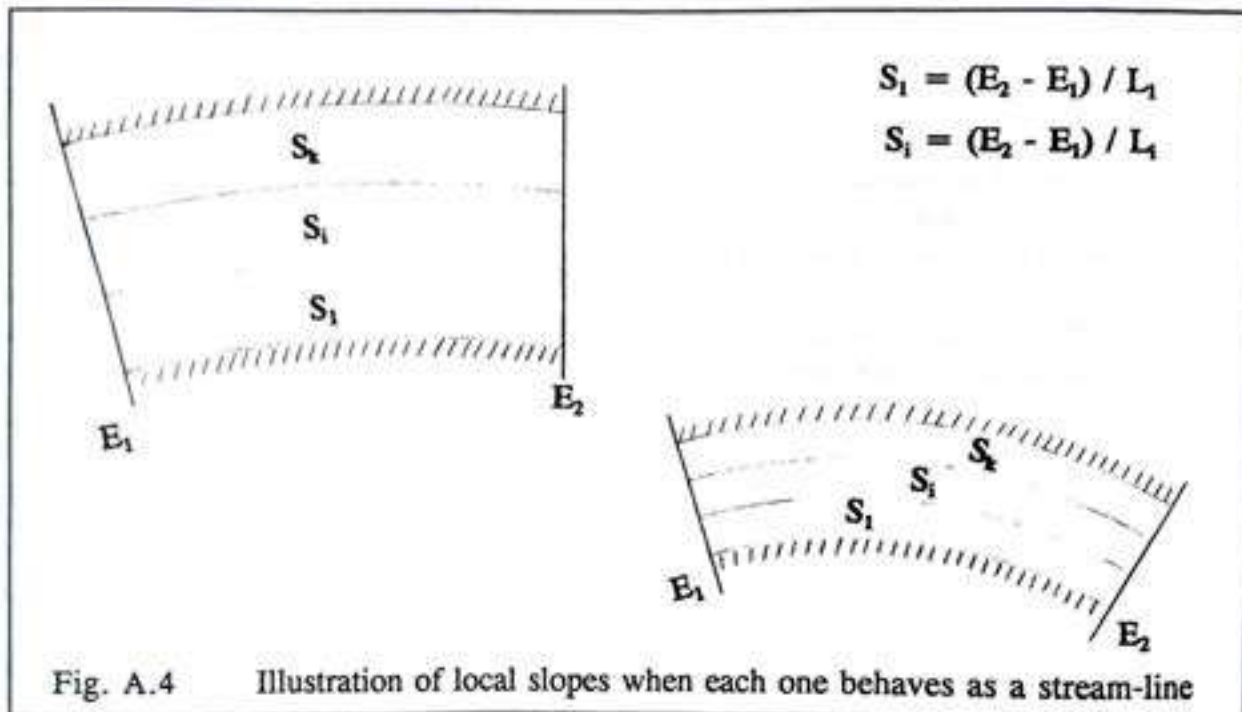
$$Q = (A_1 C_1 R_1^{1/2} + A_2 C_2 R_2^{1/2} + \dots) S^{1/2} \quad (\text{A.2})$$

An important feature of above equations is that it permits differences in roughness values in each part to be accounted for directly. In eqns. (A.1) and (A.2), the energy slope is the reach-averaged value. However different slopes S_k^l could be used for each sub-section by eqn. (A.3). For the time being the emphasis is place on the hydraulic radius and the roughness coefficient. Differences in roughness with respect to the water depth is more significant in laboratory flumes where the Reynold's numbers are in the lower range. In any case roughness decreases with an increase in water depth. This is attributed to the Reynold's numbers and relative roughness effect. Therefore variation in water depth, hydraulic radius and relative roughness lead to a way to develop an expression for bank-shear-stress.

$$S_k^l = \frac{|h_{y,k} - h_{j,k}|}{\sum_{j=1}^{y-1} \Delta S_{j,k}} \quad (\text{A.3})$$

To derive the bank-shear-stress in a meandering river, flow is firstly described as flow in a channel section with composite roughness. The following points are considered.

1. The roughness along the wetted perimeter may be distinctly different and the cross-section of a channel is composed of number of sub-sections (see Fig. A.**).
2. Mean flow velocity in each sub-section is different.
3. Bed and bank roughnesses are considered separately.



The force resisting the flow per unit area of the stream bed is proportional to velocity square. i.e. force $\propto V^2$

$$\therefore \text{force} = K V^2$$

in which K is the proportional constant. If surface area of contact can be expressed as PL (see Fig. A.**), then total force over this area is as follows:

$$\therefore \text{total force} = K V^2 P L$$

On the other hand total force can be the drag created by the flow of fluid,

$$\text{i.e. } C_d \rho V^2 P L / 2.$$

\therefore the magnitude of K can be expressed by coefficient of drag; $K = C_d \rho / 2$; in which ρ = density of water and C_d = coefficient of drag.

Assume total force resisting the flow (i.e. $K V^2 P L$) is equal to the sum of the forces resisting the flow developed in the subdivided areas. By this, equivalent roughness coefficient is

From the hydraulic condition, $n_1, n_2, \dots, n_i, \dots, n_N$ are known as equivalent roughness coefficients for each subsection. From fig. A.** the general equation for $n_1, n_2, \dots, n_i, \dots, n_N$ can be written as $n_1 = f(n_{w1}, n_{b1}), \dots, n_i = f(n_{wi}, n_{bi}), \dots$, and $n_N = f(n_{wN}, n_{bN})$ respectively. Let n_{wi} and n_{bi} be the roughness coefficients for bank and bed of sub-section "i" respectively. Then,

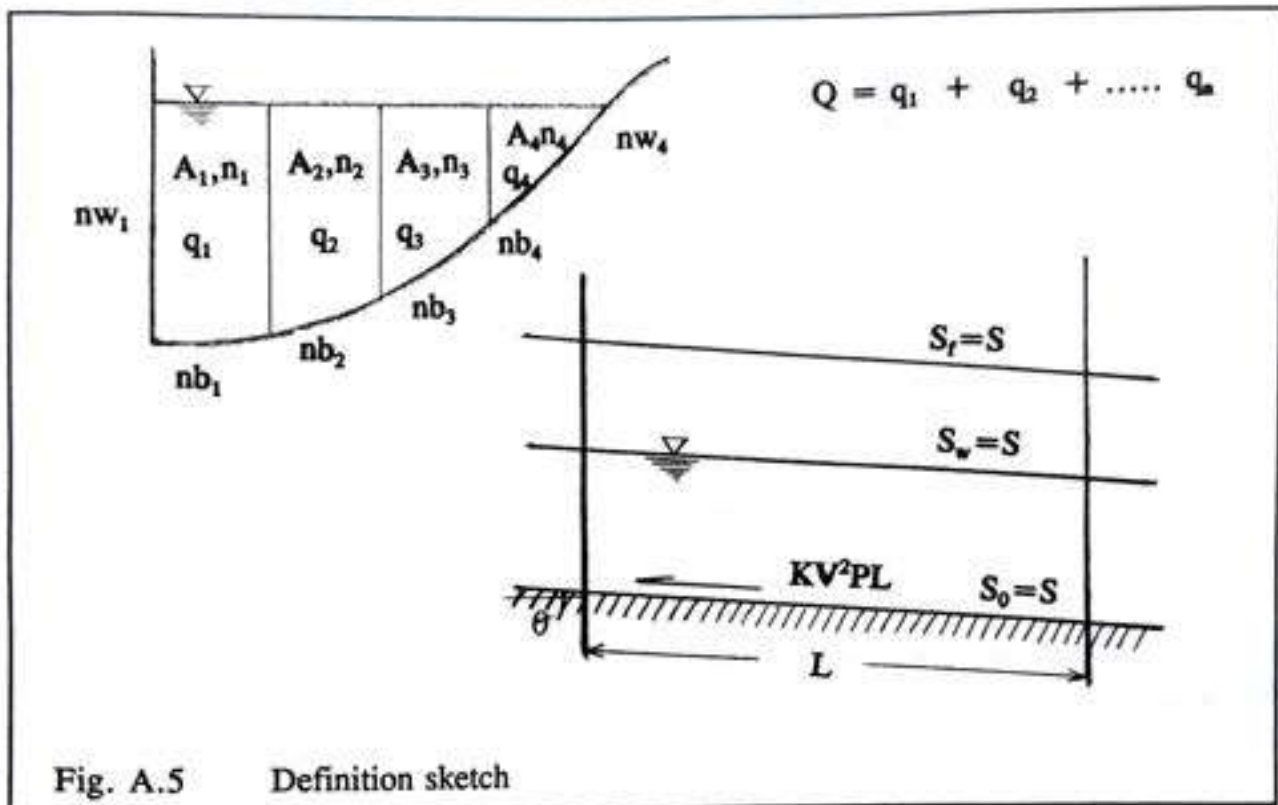


Fig. A.5 Definition sketch

$$n = \frac{\left[\sum_1^N (P_N n_N^2) \right]^{1/2}}{\sqrt{P}} \quad (\text{A.4})$$

wetted perimeter P_{wi} and P_{bi} for bank and bed should be defined appropriately. Thus the general equation for an equivalent roughness coefficient n_i might be useful to calculate the roughness coefficient of the bank portion. In order to develop a bank roughness coefficient relation from the certain hydraulic condition, assume that the total force resisting the flow is equal to the sum of the resisting force due to the channel bed and the bank. It can be expressed as follows:-

$$K V^2 L P = K_b V^2 L P_b + K_w V^2 L P_w \quad (\text{A.5})$$

Subscripts w refers to the bed and b refers to the bank respectively. From now on subscript i will be omitted for all the parameters would be refer to i^{th} subsection. The effective gravitational force component parallel to the bottom should also be considered and that is $\omega A L \sin \theta$.

in which

- ω = unit weight of water
- A = water area
- θ = bed slope angle

If we equate the two forces as below;

$$\omega A L S = K V^2 P L \quad (\text{A.6})$$

the velocity can be written as follows:-

$$V = \sqrt{\frac{\omega}{K} \frac{A}{P} S} \quad (\text{A.7})$$

$$V = \sqrt{\frac{\omega}{K} R S} \quad (\text{A.8})$$

from which one can exchanged $\sqrt{\omega/K}$ as Chézy coefficient and therefore eqn. (A.5) becomes

$$\frac{P}{C^2} = \frac{P_b}{C_b^2} + \frac{P_w}{C_w^2} \quad (\text{A.9})$$

Let the wetted perimeter $P_w = a P_b$ and substitute in eqn. (A.9), then

$$\frac{1+a}{C^2} = \frac{1}{C_b^2} + \frac{a}{C_w^2} \quad (\text{A.10})$$

For Manning roughness form, $C = R^{1/6}/n$ can be substituted in eqn. (A.10) and as a result eqn. (A.11) can be written as follows:-

$$\frac{(1+a)n^2}{R^{1/3}} = \frac{n_b^2}{R_b^{1/3}} + \frac{a n_w^2}{R_w^{1/3}} \quad (\text{A.11})$$

For the sake of convenience, both eqns. (A.10) and (A.11) are presented here where (A.10) is in the form of Chézy roughness and (A.11) is in the form of Manning roughness. Further assumed that the total hydraulic radius R is made up of two parts: the hydraulic radius R_b due to the channel bed and R_w to the bank; i.e. $R = R_b + R_w$.

Now let us assume that $\epsilon_b = R_b/R_w$ and $\epsilon_w = n_w/n_w$ eqn. (A.12) can be written as below.

$$(1+a) n^2 = n_w^2 \left(1 + \frac{1}{\varepsilon_b}\right)^{1/3} (\varepsilon_w^2 + a\varepsilon_b^{1/3}) \quad (\text{A.12})$$

For the condition of maximum discharge, Pavlovskii gave the following equation.

$$\frac{dn}{d\varepsilon_b} = 0 \quad (\text{A.13})$$

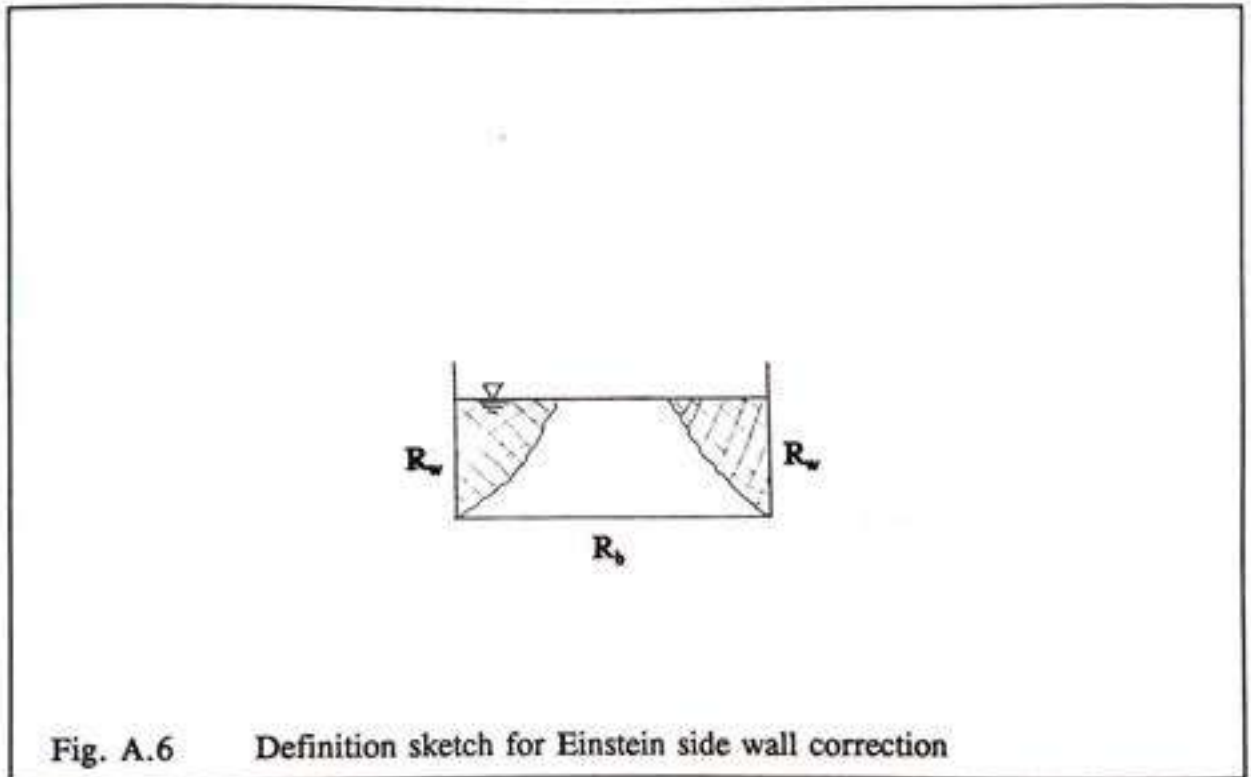
$$\varepsilon_w^2 = a \varepsilon_b^{4/3} \quad (\text{A.14})$$

Thus after some manipulations, the roughness coefficient for the channel bank can be written as below.

$$n_w = n \frac{\sqrt{1+a}}{(a^{3/4} + \varepsilon_w^{3/2})^{2/3}} \quad (\text{A.15})$$

In fact eqn.(A.15) can not be solved without any auxiliary condition equation because bank roughness n_w appears both sides of the equation. For this necessity Einstein (1934) side wall correction method is used as an auxiliary condition (presented in section A.6). Thus eqn.(A.15) is solved for any i^{th} sub-section (n is supposed to be n_i in this case) and hence the roughness coefficient n_w is calculated. In the same way Chézy coefficient for the side wall C_w can be calculated from the combination of eqn. (A.10) and Einstein side wall correction equations (A.16), (A.17), (A.18) and (A.19). There after the dimensionless shear stress for the side walls θ_w can be calculated. In other words θ_w is the bank-shear-stress value in a meandering river. The river cross section is composed of number of sub-sections and each section can be calculated in the same way under their respective conditions such as both side walls condition, one side wall condition and no side wall (middle sub-section) condition. Therefore the inner bank-shear-stress can be estimated from the calculation of innermost sub-section and the outer bank-shear stress can be estimated from the calculation of outermost sub-section. Moreover, by doing this calculation along the each grid point from the direction of upstream to the downstream, we have the spatial distribution of the bank-shear-stress value along the bank-line.

A.4 Einstein (1934) side wall correction



The side wall correction suggested by Einstein (1934) is used as an auxiliary condition for the previous section. This correction consists of the following equations.

$$\frac{q}{h} = C_w \sqrt{R_w S} = C_b \sqrt{R_b S} \quad (\text{A.16})$$

$$R_b = h \left(1 - 2 \frac{R_w}{W} \right) \quad (\text{A.17})$$

$$R_b = h \left(1 - \frac{R_w}{W} \right) \quad (\text{A.18})$$

$$C_w = 18 \log \frac{12 R_w}{k_w + \frac{3.48\nu}{\sqrt{gR_w S}}} \quad (\text{A.19})$$

in which

eqn. (A.17) = two side walls condition

eqn. (A.18) = one side wall condition

C_w = Chézy coefficient for the side walls

R_w = hydraulic radius of the side walls

R_b = hydraulic radius of the bed

S = energy slope

A.5 PROGRAM LISTING.....

THIS IS A SIMULATION PROGRAM FOR RIVER BED-TOPOGRAPHY WITH NATURAL ALIGNMENT IN ALLUVIAL RIVERS USING LOCAL ROUGHNESS (DUNE DIMENSIONS PRESENCE).

```

C *****
C * Program for meandering bed-topography model *
C *****
C * Four point scheme, Program Name = HYDHST.for *
C *****
C Radius of curvature is changing along the n,direction.
C
C DECLARATION OF VARIABLES
C
C$LARGE
PARAMETER (G=9.81,N=100,M=15,LL=10)
REAL QI, DN, RSC, DSC, CHE, EPS, RHS, MU, DM, DT, TOUC, DEL, BETA, TTIME,
& TOUP, H0, WIDTH, KSN, C, RSQS, DQ, EPS1, DIFF, DH, ERR, RSC1, DSC1, RSC2,
& DSC2, RSC3, DSC3, RSC4, DSC4, RSC5, DSC5, RSC6, DSC6, RSC7, DSC7, RSC8,
& DSC8, RSC9, DSC9
INTEGER I, JJ, KK, MM(M), VCOUNT, ITER, tp1, tp2, T, TT, PLOT, PTIME, OUT, CODE
& ,KKC, CORR, START, STOP, TP3, TP4, TP5, TP6, TP7, TP8, TP9, TP, L, JCRS
& ,NP, NP1, NP2, ITER2, IROUGH
REAL*8 w, d, ds, PERC, TH, LH
CHARACTER*50 TITLE
common /f1/CHE, SLOPE, RSC, DSC, RN, DN, JJ, KK, EQU, L, TP(LL), CHEL(N, M),
& RSCL(LL), DSCL(LL), HINIT(M), DPW(M), H(N, M), F(N, M),
& Q(N, M), P(N, M), QC(N)
common /f2/DSP(N, M), RSP(N, M), DSH(N, M), RSH(N, M), DSQ(N, M), RSQ(N, M),
& DNP(N, M), RNP(N, M), DNH(N, M), RNH(N, M), DNQ(N, M), RNQ(N, M),
& U(N, M), V(N, M), RSTP(N, M), RSTH(N, M), RSTQ(N, M)
common /f3/DT, TOUC, TOUS(N, M), DM, SS(N, M), SN(N, M), MU(N, M), TANS(N, M)
& ,DEL, TAND(N, M), ALSF(N, M), PLOT, TITLE
common /f4/BETA, GT(N, M), U0(M), HNP1(N, M), TTIME, TT, HCOUNT, TOUS0(M),
& SS0(M), MU0(M), TOUP(N, M)
DIMENSION RSQS(N), DQ(M), TEST(N), DIFF(N), EPS1(N), UB(N), w(N), d(N),
& ds(N), PERC(N), TH(N), LH(N)
C
C OPEN DATA INPUT
C
WRITE(*, *)'Please give me the START CODE'
READ(*, *) START
IF (START .EQ. 1) CALL READ1(OUT, CODE, H0, WIDTH, KSN, C, ITER)
IF (START .GT. 1) CALL READ2(OUT, CODE, H0, WIDTH, KSN, C, ITER)
CALL READ(NP, NP1, NP2, ITER2, w, d, ds, PERC, TH, LH)
C MAKE HEADING
OPEN(4, FILE='hyd.out', STATUS='new')
CALL PRT(WIDTH, KSN, C, ITER)
C
C CALCULATION OF GRID SIZES AND CURVATURE
I=0
CALL GRID(I, RSQS, DQ)
I=1

```

```

C   GOTO 808
C
C CALCULATION OF THE NO. OF TIME STEPS
  TT=TTIME/DT
C
C INITIAL STREAM-LINE CURVATURE
  DO 1 J=1,JJ
    DO 1 K=1,KK
      RSTH(J,K)=RSH(J,K)
      RSTP(J,K)=RSP(J,K)
      RSTQ(J,K)=RSQ(J,K)
    1 CONTINUE
C INITIAL WATER DEPTH
  IF (START .EQ. 1) THEN
    DO 11 J=1,JJ
      DO 11 K=1,KK
        H(J,K)=HINIT(K)
    11 CONTINUE
  ENDIF
C
C START CALCULATION
  PTIME = 0
  VCOUNT = 0
  IROUGH = 0
C INITIAL DISCHARGE CALCULATION AND U0(WEST BDY)
C BOUNDARY CONDITION  $dp/ds = 0$ 
  QI = 0.0
  DO 2 K=1,KK
    IF(START .EQ. 2) DPW(K)=P(1,K)
    IF(START .EQ. 3) THEN
      DPW(K)=P(JJ,K)
      H(1,K)=H(JJ,K)
    ENDIF
    QI = QI +DPW(K)*DNP(1,K)
    U0(K) = DPW(K)/H(1,K)
  2 CONTINUE
  DO 500 T=1,TT
    CORR=0
    IF(T .GT. 1) VCOUNT=1
  99 DO 300 J=1,JJ
    IF(J .EQ. 1) THEN
      CALL WBDY(G,J,QI,VCOUNT,DQ,WIDTH,KSN,C,RSQS,T,ITER)
    ELSE
      CALL SECTJ(G,J,QI,VCOUNT,DQ,WIDTH,KSN,C,RSQS,T,ITER)
    ENDIF
  300 CONTINUE
    IF(CORR .EQ. 1) THEN
      CORR=CORR+1
      CALL QQ
      GOTO 99
    ENDIF
    IF(CORR .EQ. 2) GOTO 700
    IF(VCOUNT .EQ. 1) GOTO 350

```



```

C
C CALCULATION OF TRANVERSE VELOCITIES
  CALL QQ
  IF(VCOUNT .EQ. 0)THEN
    VCOUNT=VCOUNT+1
    GOTO 99
  ENDIF
C STREAM-LINE CURVATURE CALCULATION
C
350  KKC=KK/2
360  IF(JUMP .LT. 20)THEN
  DO 400 J=1,JJ
    IF(KK .EQ. 2*KKC)THEN
      TEST(J)=RSTQ(J,KKC)
    ELSE
      TEST(J)=RSTH(J,KKC+1)
    ENDIF
400  CONTINUE
  CALL STRM
  JUMP=JUMP+1
  DO 401 J=1,JJ
    IF(KK .EQ. 2*KKC)THEN
      EPS1(J)= ABS(TEST(J)-RSTQ(J,KKC))
      DIFF(J)= .01*ABS(TEST(J))
    ELSE
      EPS1(J)= ABS(TEST(J)-RSTH(J,KKC+1))
      DIFF(J)= .01*ABS(TEST(J))
    ENDIF
    IF(EPS1(J) .GT. DIFF(J)) GOTO 360
401  CONTINUE
  ENDIF
  CORR=CORR+1
  GOTO 99
C NEAR BANK EXCESS VELOCITY
  CALL UBB(UB,JCRS)
C CALCULATION OF BED TOPOGRAPHY
700  CONTINUE
  IROUGH = IROUGH +1
  IF(IROUGH .EQ. 30) THEN
    CALL ROUGH(QI,H,U,DSH,DM,WIDTH,CHEL,JJ,KK,IROUGH,SLOPE,
&      NP,NP1,NP2,ITER2,w,d,ds,PERC,TH,LH)
    IROUGH=0
  ENDIF
  CALL BED(G,CODE,T,STOP)
  IF(STOP .EQ. 1) GOTO 800
  IF(T .EQ. 1) CALL LST(T,QI,H0,WIDTH,UB,JCRS)
C
C TABULATION OF RESULT
  PTIME = PTIME +1
  IF(PTIME .EQ. OUT)THEN
    CALL LST(T,QI,H0,WIDTH,UB,JCRS)
    CALL INTER(T)
    PTIME = 0

```

```

ENDIF
C
C INITIALIZATION FOR NEW TIME STEP
  DO 3 K=1, KK
    DO 3 J=1, JJ
      H(J,K)= HNP1(J,K)
    3 CONTINUE
  500 CONTINUE
  800 CALL LST(T,QI,H0,WIDTH,UB,JCRS)
    CALL INTER(T)
  808 CLOSE(4)
    STOP
    END

```

List of the attached subroutines

No1...SUBROUTINE FOR READING INPUT DATA

```

SUBROUTINE READ(NP,NP1,NP2,ITER2,w,d,ds,PERC,TH,LH)
PARAMETER(N=50)
REAL*8 w,d,ds,PERC,TH,LH
REAL A1,B1,C1,D1,E1,F1
INTEGER NP,NP1,NP2,MODEL,ITER2
DIMENSION w(N),d(N),ds(N),PERC(N),TH(N),LH(N)
C
  OPEN(3,FILE='IN',STATUS='OLD')
  CALL IREC
  READ(3,*)NP,NP1,NP2,ITER2
C
  CALL IREC
  DO 1 I=1,NP
    READ(3,*)A1,B1
    w(I)=A1
    d(I)=B1
  1 CONTINUE
C
  CALL IREC
  DO 2 I=1,NP1
    READ(3,*)C1,D1
    ds(I)=C1
    PERC(I)=D1
  2 CONTINUE
C
  CALL IREC
  DO 3 I=1,NP2
    READ(3,*)E1,F1
    TH(I)=E1
    LH(I)=F1
  3 CONTINUE
  CLOSE(3)
  RETURN
  END

```

No2...READING THE DATA FOR THE FIRST SIMULATION; TIME LEVEL ZERO


```

SUBROUTINE READ1(OUT, CODE, H0, WIDTH, KSN, C, ITER)
PARAMETER (N = 100, M = 15, LL = 10)
REAL QI, DN, RSC, DSC, CHE, EPS, RHS, MU, DM, DT, TOUC, DEL, BETA, TTIME,
& PTIME, TOUP, H0, WIDTH, KSN, C, ERR, CHE1, RSC1, DSC1, CHE2, RSC2,
& DSC2, CHE3, RSC3, DSC3, CHE4, RSC4, DSC4, CHE5, RSC5, DSC5, CHE6,
& RSC6, DSC6, CHE7, RSC7, DSC7, CHE8, RSC8, DSC8, CHE9, RSC9, DSC9,
& SI
INTEGER I, JJ, KK, MM(M), CODE, tp1, tp2, TT, HCOUNT, PLOT, OUT, START,
& TP3, TP4, TP5, TP6, TP7, TP8, TP9, ITER, L, TP
CHARACTER*50 TITLE
common /f1/CHE, SLOPE, RSC, DSC, RN, DN, JJ, KK, EQU, L, TP(LL), CHEL(N, M),
& RSCL(LL), DSCL(LL), HINIT(M), DPW(M), H(N, M), F(N, M),
& Q(N, M), P(N, M), QC(N)
common /f2/DSP(N, M), RSP(N, M), DSH(N, M), RSH(N, M), DSQ(N, M), RSQ(N, M),
& DNP(N, M), RNP(N, M), DNH(N, M), RNH(N, M), DNQ(N, M), RNQ(N, M),
& U(N, M), V(N, M), RSTP(N, M), RSTH(N, M), RSTQ(N, M)
common /f3/DT, TOUC, TOUS(N, M), DM, SS(N, M), SN(N, M), MU(N, M), TANS(N, M)
& DEL, TAND(N, M), ALSF(N, M), PLOT, TITLE
common /f4/BETA, GT(N, M), U0(M), HNP1(N, M), TTIME, TT, HCOUNT, TOUS0(M),
& SSO(M), MU0(M), TOUP(N, M)
C
C OPEN DATA INPUT
C
OPEN(3, FILE = 'HYD.IN', STATUS = 'OLD')
CALL IREC
READ(3, *) CHE, SLOPE, RSC, RN, DSC, DN, JJ, KK, EQU, ITER
CALL IREC
READ(3, *) L, (TP(I), I = 1, LL)
CALL IREC
READ(3, *) (DSCL(I), I = 1, L)
CALL IREC
READ(3, *) (RSCL(I), I = 1, L)
CALL IREC
READ(3, *) DT, TOUC, DM, DEL, BETA, TTIME, OUT
CALL IREC
READ(3, *) TITLE, PLOT, CODE, H0, WIDTH, KSN, C
CALL IREC
READ(3, *) (HINIT(K), K = 1, kk)
CALL IREC
READ(3, *) (DPW(K), K = 1, kk)
CLOSE(3)
RETURN
END

```

No3...READING THE DATA FROM THE INTERMEDIATE TIME LEVEL; TIME STEP=TT

```

SUBROUTINE READ2(OUT, CODE, H0, WIDTH, KSN, C, ITER)
PARAMETER (N = 100, M = 15, LL = 10)
REAL QI, DN, RSC, DSC, CHE, EPS, RHS, MU, DM, DT, TOUC, DEL, BETA, TTIME,
& PTIME, TOUP, H0, WIDTH, KSN, C, ERR, CHE1, RSC1, DSC1, CHE2, RSC2,
& DSC2, CHE3, RSC3, DSC3, CHE4, RSC4, DSC4, CHE5, RSC5, DSC5, CHE6,
& RSC6, DSC6, CHE7, RSC7, DSC7, CHE8, RSC8, DSC8, CHE9, RSC9, DSC9,
& SI

```

```

INTEGER I, JJ, KK, MM(M), CODE, TP1, TP2, TT, HCOUNT, PLOT, OUT,
& TP3, TP4, TP5, TP6, TP7, TP8, TP9, ITER, L, TP
CHARACTER*50 TITLE
common /f/CHE, SLOPE, RSC, DSC, RN, DN, JJ, KK, EQU, L, TP(LL), CHEL(N, M),
& RSCL(LL), DSCL(LL), HINIT(M), DPW(M), H(N, M), F(N, M),
& Q(N, M), P(N, M), QC(N)
common /f2/DSP(N, M), RSP(N, M), DSH(N, M), RSH(N, M), DSQ(N, M), RSQ(N, M),
& DNP(N, M), RNP(N, M), DNH(N, M), RNH(N, M), DNQ(N, M), RNQ(N, M),
& U(N, M), V(N, M), RSTP(N, M), RSTH(N, M), RSTQ(N, M)
common /f3/DT, TOUC, TOUS(N, M), DM, SS(N, M), SN(N, M), MU(N, M), TANS(N, M)
& DEL, TAND(N, M), ALSF(N, M), PLOT, TITLE
common /f4/BETA, GT(N, M), U0(M), HNP1(N, M), TTIME, TT, HCOUNT, TOUS0(M),
& SS0(M), MU0(M), TOUP(N, M)

```

C

```

OPEN(3, FILE='HYD.INT', STATUS='OLD')
CALL IREC
READ(3, *) CHE, SLOPE, RSC, RN, DSC, DN, JJ, KK, EQU, ITER
CALL IREC
READ(3, *) L, (TP(I), I=1, LL)
CALL IREC
READ(3, *) (DSCL(I), I=1, L)
CALL IREC
READ(3, *) (RSCL(I), I=1, L)
CALL IREC
READ(3, *) DT, TOUC, DM, DEL, BETA, TTIME, OUT
CALL IREC
READ(3, *) TITLE, PLOT, CODE, H0, WIDTH, KSN, C
CLOSE(3)

```

C

```

OPEN(2, FILE='INTER.IN', STATUS='OLD')
DO 10 J=1, JJ
READ(2, 70) (P(J, K), K=1, KK), (H(J, K), K=1, KK)
70 FORMAT (10E11.4, /, 10E11.4)
10 CONTINUE
CLOSE(2)
RETURN
END

```

No4...SUBROUTINE FOR GRID SIZE AND CURVATURE CALCULATION

```

SUBROUTINE GRID(I, RSQS, DQ)
PARAMETER(N=100, M=15, LL=10)
common /f/CHE, SLOPE, RSC, DSC, RN, DN, JJ, KK, EQU, L, TP(LL), CHEL(N, M),
& RSCL(LL), DSCL(LL), HINIT(M), DPW(M), H(N, M), F(N, M),
& Q(N, M), P(N, M), QC(N)
common /f2/DSP(N, M), RSP(N, M), DSH(N, M), RSH(N, M), DSQ(N, M), RSQ(N, M),
& DNP(N, M), RNP(N, M), DNH(N, M), RNH(N, M), DNQ(N, M), RNQ(N, M),
& U(N, M), V(N, M), RSTP(N, M), RSTH(N, M), RSTQ(N, M)
REAL CL, RN, DN, CHE, RSC, DSC, RSC1, DSC1, RSC2, DSC2, RSC3, DSC3, RSC4, DSC4
& RSC5, DSC5, RSC6, DSC6, RSC7, DSC7, RSC8, DSC8, RSC9, DSC9
INTEGER I, J, K, JJ, KK, TP1, TP2, TP3, TP4, TP5, TP6, TP7, TP8, TP9, TP, L
DIMENSION DSQS(N), RSQS(N), DQ(M), D(M)

```

C

C CALCULATION OF GRID CENTRE LINE


```

      CL = (KK+1.)*0.5
C FOR N,DIRECTION GRID AND CURVATURE
      DO 100 J=1,JJ
        DO 100 K=1,KK
          IF (I .EQ. 0) THEN
            CHEL(j,k)=CHE
          ENDIF
          dnp(j,k)=dn
          rnp(j,k)=rn
          dnh(j,k)=dn
          rnh(j,k)=rn
          dnq(j,k)=dn
          rmq(j,k)=rn
        100 CONTINUE
C FOR S,DIRECTION GRID AND CURVATURE
      TP1 = TP(1)
      IF(TP1 .GT. JJ) TP1=JJ+1
      DO 1 J=1,TP1-1
        dsqs(j)=dsc*(1+(0.5-cl)*dn*rsc)
        rsqs(j)=rsc/(1+(0.5-cl)*dn*rsc)
        DO 1 K=1,KK
          d(k)=(k-cl)*dn
          dsp(j,k)=dsc*(1+d(k)*rsc)
          rsp(j,k)=rsc/(1+d(k)*rsc)
          dsh(j,k)=dsp(j,k)
          rsh(j,k)=rsp(j,k)
          dq(k)=(k+0.5-cl)*dn
          dsq(j,k)=dsc*(1+dq(k)*rsc)
          rsq(j,k)=rsc/(1+dq(k)*rsc)
        1 CONTINUE
c after turning point 1
        IF(tp1 .GT. jj) goto 1111
        DSC=DSCL(1)
        RSC=RSCL(1)
        TP2=TP(2)
        IF(tp2 .gt. jj) TP2=JJ+1
        DO 2 J=TP1,TP2-1
          dsqs(j)=dsc*(1+(0.5-cl)*dn*rsc)
          rsqs(j)=rsc/(1+(0.5-cl)*dn*rsc)
          DO 2 k=1,KK
            dsp(j,k)=dsc*(1+d(k)*rsc)
            rsp(j,k)=rsc/(1+d(k)*rsc)
            dsh(j,k)=dsp(j,k)
            rsh(j,k)=rsp(j,k)
            dsq(j,k)=dsc*(1+dq(k)*rsc)
            rsq(j,k)=rsc/(1+dq(k)*rsc)
          2 CONTINUE
c after turning point 2
        IF(TP2 .GT. JJ) goto 1111
        DSC=DSCL(2)
        RSC=RSCL(2)
        TP3=TP(3)
        IF(TP3 .GT. JJ) TP3=JJ+1

```

```

DO 3 J = TP2, TP3-1
  dsqs(j) = dsc*(1 + (0.5-cl)*dn*rsc)
  rsqs(j) = rsc/(1 + (0.5-cl)*dn*rsc)
  DO 3 k = 1, KK
    dsp(j,k) = dsc*(1 + d(k)*rsc)
    rsp(j,k) = rsc/(1 + d(k)*rsc)
    dsh(j,k) = dsp(j,k)
    rsh(j,k) = rsp(j,k)
    dsq(j,k) = dsc*(1 + dq(k)*rsc)
    rsq(j,k) = rsc/(1 + dq(k)*rsc)
  3 CONTINUE
c after turning point 3
  IF(TP3 .GT. JJ) GOTO 1111
  DSC = DSCL(3)
  RSC = RSCL(3)
  TP4 = TP(4)
  IF(TP4 .GT. JJ) TP4 = JJ + 1
  DO 4 J = TP3, TP4-1
    dsqs(j) = dsc*(1 + (0.5-cl)*dn*rsc)
    rsqs(j) = rsc/(1 + (0.5-cl)*dn*rsc)
    DO 4 k = 1, KK
      dsp(j,k) = dsc*(1 + d(k)*rsc)
      rsp(j,k) = rsc/(1 + d(k)*rsc)
      dsh(j,k) = dsp(j,k)
      rsh(j,k) = rsp(j,k)
      dsq(j,k) = dsc*(1 + dq(k)*rsc)
      rsq(j,k) = rsc/(1 + dq(k)*rsc)
    4 CONTINUE
c after turning point 4
  IF(TP4 .GT. JJ) goto 1111
  DSC = DSCL(4)
  RSC = RSCL(4)
  TP5 = TP(5)
  IF(TP5 .GT. JJ) TP5 = JJ + 1
  DO 5 J = TP4, TP5-1
    dsqs(j) = dsc*(1 + (0.5-cl)*dn*rsc)
    rsqs(j) = rsc/(1 + (0.5-cl)*dn*rsc)
    DO 5 k = 1, KK
      dsp(j,k) = dsc*(1 + d(k)*rsc)
      rsp(j,k) = rsc/(1 + d(k)*rsc)
      dsh(j,k) = dsp(j,k)
      rsh(j,k) = rsp(j,k)
      dsq(j,k) = dsc*(1 + dq(k)*rsc)
      rsq(j,k) = rsc/(1 + dq(k)*rsc)
    5 CONTINUE
c after turning point 5
  IF(TP5 .GT. JJ) goto 1111
  DSC = DSCL(5)
  RSC = RSCL(5)
  TP6 = TP(6)
  IF(TP6 .GT. JJ) TP6 = JJ + 1
  DO 6 J = TP5, TP6-1
    dsqs(j) = dsc*(1 + (0.5-cl)*dn*rsc)

```



```

    rsqs(j) = rsc / (1 + (0.5-cl)*dn*rsc)
DO 6 k = 1, KK
    dsp(j,k) = dsc * (1 + d(k)*rsc)
    rsp(j,k) = rsc / (1 + d(k)*rsc)
    dsh(j,k) = dsp(j,k)
    rsh(j,k) = rsp(j,k)
    dsq(j,k) = dsc * (1 + dq(k)*rsc)
    rsq(j,k) = rsc / (1 + dq(k)*rsc)
6 CONTINUE
c after turning point 6
IF(TP6 .GT. JJ) goto 1111
DSC = DSCL(6)
RSC = RSCL(6)
TP7 = TP(7)
IF(TP7 .GT. JJ) TP7 = JJ + 1
DO 7 J = TP6, TP7-1
    dsqs(j) = dsc * (1 + (0.5-cl)*dn*rsc)
    rsqs(j) = rsc / (1 + (0.5-cl)*dn*rsc)
DO 7 k = 1, KK
    dsp(j,k) = dsc * (1 + d(k)*rsc)
    rsp(j,k) = rsc / (1 + d(k)*rsc)
    dsh(j,k) = dsp(j,k)
    rsh(j,k) = rsp(j,k)
    dsq(j,k) = dsc * (1 + dq(k)*rsc)
    rsq(j,k) = rsc / (1 + dq(k)*rsc)
7 CONTINUE
c after turning point 7
IF(TP7 .GT. JJ) GOTO 1111
DSC = DSCL(7)
RSC = RSCL(7)
TP8 = TP(8)
IF(TP8 .GT. JJ) TP8 = JJ + 1
DO 8 J = TP7, TP8-1
    dsqs(j) = dsc * (1 + (0.5-cl)*dn*rsc)
    rsqs(j) = rsc / (1 + (0.5-cl)*dn*rsc)
DO 8 k = 1, KK
    dsp(j,k) = dsc * (1 + d(k)*rsc)
    rsp(j,k) = rsc / (1 + d(k)*rsc)
    dsh(j,k) = dsp(j,k)
    rsh(j,k) = rsp(j,k)
    dsq(j,k) = dsc * (1 + dq(k)*rsc)
    rsq(j,k) = rsc / (1 + dq(k)*rsc)
8 CONTINUE
c after turning point 8
IF(TP8 .GT. JJ) GOTO 1111
DSC = DSCL(8)
RSC = RSCL(8)
TP9 = TP(9)
IF(TP9 .GT. JJ) TP9 = JJ + 1
DO 9 J = TP8, TP9-1
    dsqs(j) = dsc * (1 + (0.5-cl)*dn*rsc)
    rsqs(j) = rsc / (1 + (0.5-cl)*dn*rsc)
DO 9 k = 1, KK

```

```

dsp(j,k) = dsc*(1 + d(k)*rsc)
rsp(j,k) = rsc/(1 + d(k)*rsc)
dsh(j,k) = dsp(j,k)
rsh(j,k) = rsp(j,k)
dsq(j,k) = dsc*(1 + dq(k)*rsc)
rsq(j,k) = rsc/(1 + dq(k)*rsc)
9 CONTINUE

```

```

c after turning point 9
IF(TP9 .GT. JJ) GOTO 1111
DSC = DSCL(9)
RSC = RSCL(9)
DO 10 J = TP9, JJ
  dsqs(j) = dsc*(1 + (0.5-cl)*dn*rsc)
  rsqs(j) = rsc/(1 + (0.5-cl)*dn*rsc)
  DO 10 k = 1, KK
    dsp(j,k) = dsc*(1 + d(k)*rsc)
    rsp(j,k) = rsc/(1 + d(k)*rsc)
    dsh(j,k) = dsp(j,k)
    rsh(j,k) = rsp(j,k)
    dsq(j,k) = dsc*(1 + dq(k)*rsc)
    rsq(j,k) = rsc/(1 + dq(k)*rsc)
10 CONTINUE
1111 RETURN
END

```



No5...SUBROUTINE FOR CALCULATION AT WEST BOUNDARY

```

SUBROUTINE WBDY(G,J,QI,VCOUNT,DQ,WIDTH,KSN,C,RSQS,T,ITER)
PARAMETER(N=100,M=15,LL=10)
LOGICAL OLDM
common /f1/CHE,SLOPE,RSC,DSC,RN,DN,JJ,KK,EQU,L,TP(LL),CHEL(N,M),
& RSCL(LL),DSCL(LL),HINIT(M),DPW(M),H(N,M),F(N,M),
& Q(N,M),P(N,M),QC(N)
common /f2/DSP(N,M),RSP(N,M),DSH(N,M),RSH(N,M),DSQ(N,M),RSQ(N,M),
& DNP(N,M),RNP(N,M),DNH(N,M),RNH(N,M),DNQ(N,M),RNQ(N,M),
& U(N,M),V(N,M),RSTP(N,M),RSTH(N,M),RSTQ(N,M)
DIMENSION FNW(M),DQS(N),FP(N),QP(N),COEF1(M),COEF2(M),COEF3(M),
& COEF4(M),COEF5(M),COEF6(M),COEF62(M),COEF7(M),COEF8(M),
& COEF82(M),COEF9(M),COEF92(M),COEF10(M),COEF11(M),
& COEF12(M),COEF22(M),COEF13(M),COEF23(M),TM6(M),AA(M),
& AB(M),A32(M),COEFA1(M),COEFA2(M),COEFA3(M),DQ(M),RSQS(N)
C
REAL A1,A2,A3,RHS,TM1,TM2,TM3,TM4,TM5,TM6,TM7,QN1,QN2,QN3,
& QN4,PN1,X1,X2,A31,A32,HS1,HS2,P1,P2,P3,P4,P5,P6,
& P7,P8,P9,Q1,Q2,Q3,Q4,Q5,Q6,Q7,Q8,H2S1,H2S2,Q,KSN,KSNT1,
& KSNT2,H2S3,H2S4,H2S5,WIDTH,C,BB1,BB2,BB3
INTEGER I,II,J,K,VCOUNT,COUNT,T,ITER,TP,L
C
C WEST BOUNDARY ; DPW(K)=P(J-1,K); DQS(J)=Q(J,K-1)=0.
DQS(J) = 0.
COUNT = 0
DO 10 K=1,KK
  FNW(K) = DPW(K)*DPW(K)/H(J,K)

```



```

10 CONTINUE
C ASSUME F(J,K)
  IF (T .EQ. 1) THEN
    F(J,1)=FNW(1)
    P(J,1)=DPW(1)
  ENDIF
C START CALCULATION
  DO 40 K=1, KK-1
    HS1=(H(J,K)+H(J+1,K)+H(J,K+1)+H(J+1,K+1))/4
    HS2=(H(J,K)+H(J,K+1))/2
    COEF1(K)=1/H(j,k+1)+(dnq(j+1,k)+dnq(j,k))*
&      (RSTP(j,k+1)+RSTP(j,k))/(8*hs1)+
&      dsh(j,k+1)*rnh(j,k+1)/(2*H(j,k+1))
    COEF2(K)=g*dsh(j,k+1)/(che*che*H(j,k+1)*H(j,k+1)*2)
    COEF3(K)=-1/H(j,k)+(dnq(j+1,k)+dnq(j,k))*(RSTP(j,k+1)+
&      RSTP(j,k))/(8*hs1)-dsh(j,k)*rnh(j,k)/(2*H(j,k))
    COEF4(K)=g*dsh(j,k)/(che*che*H(j,k)*H(j,k)*2)
    COEF5(K)=FNW(K)/H(J,K)-FNW(K)*DSH(J,K)*RNH(J,K)/(H(J,K)*2)-
&      fnw(k+1)/H(j,k+1)+FNW(K+1)*DSH(J,K+1)*RNH(J,K+1)/
&      (H(J,K+1)*2)
    AA(K)= Q(J,K+1)*Q(J,K+1)+Q(J,K)*Q(J,K)
  IF (K .EQ. KK-1) THEN
    H2S3=H(J,K+1)*H(J,K+1)
  ELSE
    H2S3=(H(J,K+2)*H(J,K+2)+H(J,K+1)*H(J,K+1))/2
  ENDIF
  H2S4=(H(J,K+1)*H(J,K+1)+H(J,K)*H(J,K))/2
  BB1=(ABS(2*DQ(K))/WIDTH)**C
  IF(K .EQ. 1) THEN
    AB(K)= Q(J,K)*Q(J,K)+DQS(J)*DQS(J)
    H2S5=H(J,K)*H(J,K)
    BB2=(ABS(2*(DQ(K)-DN))/WIDTH)**C
    KSNT2=KSN/DNH(J,K)*(H2S4*RSTQ(J,K)*(1-BB1)
&      -H2S5*RSQS(J)*(1-BB2))
  ELSE
    AB(K)= Q(J,K)*Q(J,K)+Q(J,K-1)*Q(J,K-1)
    H2S5=(H(J,K-1)*H(J,K-1)+H(J,K)*H(J,K))/2
    BB2=(ABS(2*DQ(K-1))/WIDTH)**C
    KSNT2=KSN/DNH(J,K)*(H2S4*RSTQ(J,K)*(1-BB1)
&      -H2S5*RSTQ(J,K-1)*(1-BB2))
  ENDIF
  BA = (P(J,K+1)*P(J,K+1)+DPW(K+1)*DPW(K+1))
  BB = P(J,K)*P(J,K)+DPW(K)*DPW(K)
  BB3=(ABS(2*DQ(K+1))/WIDTH)**C
  KSNT1=KSN/DNH(J,K+1)*(H2S3*RSTQ(J,K+1)*(1-BB3)
&      -H2S4*RSTQ(J,K)*(1-BB1))
  COEFA1(K)=DSH(J,K+1)/(2*H(J,K+1)*H(J,K+1))*KSNT1
  COEFA2(K)=DSH(J,K)/(2*H(J,K)*H(J,K))*KSNT2
  COEFA3(K)=F(J-1,K+1)*COEFA1(K)-F(J-1,K)*COEFA2(K)
C
  A1=COEF1(K)+COEF2(K)*(1+AA(K)/BA)**0.5+COEFA1(K)
  A2=COEF3(K)-COEF4(K)*(1+AB(K)/BB)**0.5-COEFA2(K)
  A31=COEF5(K)-COEF4(K)*FNW(K)*(1+AB(K)/BB)**0.5+

```

```

& COEF2(K)*FNW(K+1)*(1+AA(K)/BA)**0.5
A32(K)=- (FNW(K+1)+FNW(k))*DNQ(J,K)
& *(RSTP(j,k+1)+RSTP(j,k))/(HS2*4)
A3=A31+A32(K)+COEFA3(K)
C
P1=(DPW(K+1)+P(J,K+1)+DPW(K)+P(J,K))/4
P4=(DPW(K+1)+DPW(K))/2
P6=(DPW(K)+P(J,K))/2
P7=(DPW(K+1)+P(J,K+1))/2
P8=(DPW(K+1)+DPW(K))/2
P9=(P(J,K+1)+P(J,K))/2
C
IF(VCOUNT .EQ. 0) THEN
P5=(P(J,K+1)+P(J,K))/2
ELSE
P5=(P(J+1,K+1)+P(J+1,K)+P(J,K+1)+P(J,K))/4
ENDIF
C
IF (K .EQ. KK-1) THEN
P3=(DPW(K+1)+P(J,K+1))/2
H3= H(J,K+1)
ELSE
P3=(DPW(K+2)+P(J,K+2)+DPW(K+1)+P(J,K+1))/4
H3=(H(J,K+2)+H(J,K+1))/2
ENDIF
IF(K .EQ. 1) THEN
P2=(DPW(K)+P(J,K))/2
ELSE
P2=(DPW(K-1)+P(J,K-1)+DPW(K)+P(J,K))/4
ENDIF
Q2=(Q(J,K+1)+Q(J,K))/2
Q3=Q(J,K)
Q4=(Q(J+1,K)+Q(J,K))/2
Q22=(Q(J,K+1)*Q(J,K+1)+Q(J,K)*Q(J,K))/2
Q23=Q(J,K)*Q(J,K)
Q24=(Q(J+1,K)*Q(J+1,K)+Q(J,K)*Q(J,K))/2
Q25=(Q(J,K+1)*Q(J,K+1)+Q(J,K)*Q(J,K))/2
Q27=(Q(J+1,K+1)*Q(J+1,K+1)+Q(J,K+1)*Q(J,K+1)+
& Q(J+1,K)*Q(J+1,K)+Q(J,K)*Q(J,K))/4
C
IF(K .EQ. 1) THEN
Q1=(DQS(J)+Q(J,K))/2
Q21=(DQS(J)*DQS(J)+Q(J,K)*Q(J,K))/2
Q26=(DQS(J)*DQS(J)+Q(J,K)*Q(J,K))/2
Q28=(DQS(J+1)*DQS(J+1)+DQS(J)*DQS(J)+
& Q(J+1,K)*Q(J+1,K)+Q(J,K)*Q(J,K))/4
ELSE
Q1=(Q(J,K-1)+Q(J,K))/2
Q21=(Q(J,K-1)*Q(J,K-1)+Q(J,K)*Q(J,K))/2
Q26=(Q(J,K-1)*Q(J,K-1)+Q(J,K)*Q(J,K))/2
Q28=(Q(J+1,K-1)*Q(J+1,K-1)+Q(J,K-1)*Q(J,K-1)+
& Q(J+1,K)*Q(J+1,K)+Q(J,K)*Q(J,K))/4
ENDIF

```



```

C
  H1=(H(J,K+1)+H(J,K))/2
  H4=H(J,K+1)
  H5=H(J,K)
  H6=(H(J,K+1)+H(J,K))/2
  H7=(H(J+1,K+1)+H(J+1,K))/2
  H8=(H(J+1,K+1)+H(J,K+1))/2
  H9=(H(J+1,K)+H(J,K))/2
  H2S1=(H(J+1,K+1)*H(J+1,K+1)+H(J+1,K)*H(J+1,K)+
&      H(J,K+1)*H(J,K+1)+H(J,K)*H(J,K))/4
  H2S2=(H(J,K+1)*H(J,K+1)+H(J,K)*H(J,K))/2
C
  IF(K .EQ. 1) THEN
    TM1= 1/H(J,K)*DSH(J,K)/DNH(J,K)*(P1*Q(J,K)/H1-P2*DQS(J)/
&      H(J,K))
  ELSE
    TM1= 1/H(J,K)*DSH(J,K)/DNH(J,K)*(P1*Q(J,K)/H1-P2*Q(J,K-1)*2/
&      (H(J,K-1)+H(J,K)))
  ENDIF
C
  COEF6(K)=2*Q1*DSH(J,K)*RSTH(J,K)/(H(J,K)*H(J,K))
  COEF62(K)=Q21*DSH(J,K)*RNH(J,K)/(H(J,K)*H(J,K))
  TM2=COEF6(K)*P6-COEF62(K)
  COEF7(K)=-1/H(J,K+1)*DSH(J,K+1)/DNH(J,K+1)
  TM3=COEF7(K)*(P3*Q(J,K+1)/H3-P1*Q(J,K)/H1)
  COEF8(K)=-2*Q2*DSH(J,K+1)/(H(J,K+1)*H(J,K+1))*RSTH(J,K+1)
  COEF82(K)=Q22*DSH(J,K+1)*RNH(J,K+1)/(H(J,K+1)*H(J,K+1))
  TM4=COEF8(K)*P7+COEF82(K)
  COEF9(K)=-((DNQ(J,K)+DNQ(J,K+1))/(DSP(J,K+1)+DSP(J,K))*HS2)
  COEF92(K)=P4*Q(J,K)/H4
  TM5=COEF9(K)*(P1*Q(J,K)/H1-COEF92(K))
  TM6(K)=-1/HS2*(Q25/H4-Q26/H5)-2*P8*Q3*(DNQ(J,K)+DNQ(J,K+1))/(2*
&      H2S2)*(RNP(J,K+1)+RNP(J,K))/2
  COEF10(K)=-Q23*(DNQ(J,K)+DNQ(J,K+1))/(2*H2S2)*(RSTQ(J,K)+
&      RSTQ(J,K+1))/2+1/HS1*(Q27/H8-Q28/H9)
  COEF11(K)=(DNQ(J+1,K)+DNQ(J,K))/(HS1*(DSP(J,K+1)+DSP(J,K)))
  TM7=COEF10(K)+COEF11(K)*(P5*Q(J+1,K)/H7-P1*Q(J,K)/H1)
  COEF12(K)=2*Q4*(DNQ(J+1,K)+DNQ(J,K))/(2*H2S1)*
&      (RNP(J,K+1)+RNP(J,K))/2
  COEF22(K)=Q24*(DNQ(J+1,K)+DNQ(J,K))/(2*H2S1)*
&      (RSTQ(J+1,K)+RSTQ(J,K))/2
  TM8=COEF12(K)*P9+COEF22(K)
  P21=(DPW(K+1)*DPW(K+1)+DPW(K)*DPW(K))/2
  P22=(P(J,K+1)*P(J,K+1)+P(J,K)*P(J,K))/2
  COEF13(K)=-G*DNQ(J,K)/(CHE*CHE*H2S2*HS2)
  COEF23(K)=G*(DNQ(J+1,K)+DNQ(J,K))/(2*CHE*CHE*H2S1*HS1)
  TM9=COEF13(K)*Q3*(Q23+P21)**0.5+COEF23(K)*Q4*(Q24+P22)**0.5
C
  RHS = TM1+TM2+TM3+TM4+TM5+TM6(K)+TM7+TM8+TM9
  F(J,K+1)=(RHS-A3-F(J,K)*A2)/A1
40 CONTINUE
  GOTO 110
C

```

C CORRECTION FOR F(J,1)

100 CONTINUE

IF (I .GT. 10) THEN

 OLDM = .FALSE.

 AUX = QP(I)-QP(I-1)

 IF (ABS(AUX/QI) .LT. .0001) THEN

 OLDM = .TRUE.

 ELSE

 F(J,1) = (FP(I)-FP(I-1))/AUX * (QI-QP(I)) + FP(I)

 IF (F(J,1) .LT. 0) OLDM = .TRUE.

 IF ((F(J,1)/FP(I)) .GT. 10) OLDM = .TRUE.

 ENDIF

ENDIF

IF ((I .LE. 10) .OR. (OLDM)) THEN

 F(J,1) = FP(I) * ((0.75 * QI + 0.25 * QP(I)) / QP(I))

ENDIF

P(J,1) = (F(J,1) * (H(J+1,1) + H(J,1)) / 2) * 0.5

C

DO 41 K=1, KK-1

 BA = P(J, K+1) * P(J, K+1) + DPW(K+1) * DPW(K+1)

 BB = P(J, K) * P(J, K) + DPW(K) * DPW(K)

 A1 = COEF1(K) + COEF2(K) * (1 + AA(K) / BA) ** 0.5 + COEFA1(K)

 A2 = COEF3(K) - COEF4(K) * (1 + AB(K) / BB) ** 0.5 - COEFA2(K)

 A31 = COEF5(K) - COEF4(K) * FNW(K) * (1 + AB(K) / BB) ** 0.5 +

& COEF2(K) * FNW(K+1) * (1 + AA(K) / BA) ** 0.5

 A3 = A31 + A32(K) + COEFA3(K)

C

P1 = (DPW(K+1) + P(J, K+1) + DPW(K) + P(J, K)) / 4

P6 = (DPW(K) + P(J, K)) / 2

P7 = (DPW(K+1) + P(J, K+1)) / 2

P9 = (P(J, K+1) + P(J, K)) / 2

H1 = (H(J, K+1) + H(J, K)) / 2

C

IF (VCOUNT .EQ. 0) THEN

 P5 = (P(J, K+1) + P(J, K)) / 2

ELSE

 P5 = (P(J+1, K+1) + P(J+1, K) + P(J, K+1) + P(J, K)) / 4

ENDIF

C

IF (K .EQ. KK-1) THEN

 P3 = (DPW(K+1) + P(J, K+1)) / 2

 H3 = H(J, K+1)

ELSE

 P3 = (DPW(K+2) + P(J, K+2) + DPW(K+1) + P(J, K+1)) / 4

 H3 = (H(J, K+2) + H(J, K+1)) / 2

ENDIF

IF (K .EQ. 1) THEN

 P2 = (DPW(K) + P(J, K)) / 2

ELSE

 P2 = (DPW(K-1) + P(J, K-1) + DPW(K) + P(J, K)) / 4

ENDIF

IF (K .EQ. 1) THEN

 TM1 = 1 / H(J, K) * DSH(J, K) / DNH(J, K) * (P1 * Q(J, K) / H1 - P2 * DQS(J) /


```

&      H(J,K))
ELSE
TM1 = 1/H(J,K)*DSH(J,K)/DNH(J,K)*(P1*Q(J,K)/H1-P2*Q(J,K-1)*2/
& (H(J,K-1)+H(J,K)))
ENDIF
TM2=COEF6(K)*P6-COEF62(K)
TM3=COEF7(K)*(P3*Q(J,K+1)/H3-P1*Q(J,K)/H1)
TM4=COEF8(K)*P7+COEF82(K)
TM5=COEF9(K)*(P1*Q(J,K)/H1-COEF92(K))
H7=(H(J+1,K+1)+H(J+1,K))/2
TM7=COEF10(K)+COEF11(K)*(P5*Q(J+1,K)/H7-P1*Q(J,K)/H1)
TM8=COEF12(K)*P9+COEF22(K)
P21=(DPW(K+1)*DPW(K+1)+DPW(K)*DPW(K))/2
P22=(P(J,K+1)*P(J,K+1)+P(J,K)*P(J,K))/2
TM9=COEF13(K)*Q3*(Q23+P21)**0.5+COEF23(K)*Q4*(Q24+P22)**0.5
RHS = TM1+TM2+TM3+TM4+TM5+TM6(K)+TM7+TM8+TM9
F(J,K+1)=(RHS-A3-F(J,K)*A2)/A1
41 CONTINUE
C
C CHECKING OF THE DISCHARGE (INTEGRATING OVER THE WIDTH)
110 DO 50 K=1, KK
P(J,K)=(F(J,K)*(H(J+1,K)+H(J,K))/2)**0.5
U(J,K)=P(J,K)*2/(H(J+1,K)+H(J,K))
50 CONTINUE
QC(J)=0.0
DO 60 K=1, KK
QC(J)=QC(J)+P(J,K)*DNH(J,K)
60 CONTINUE
EPS=ABS(QC(J)-QI)/QI
DIF=.0001
IF(EPS.GT.DIF)THEN
COUNT=COUNT+1
DO 200 I=COUNT
FP(I)=F(J,I)
QP(I)=QC(J)
200 CONTINUE
IF(COUNT.LT.ITER)GOTO 100
ENDIF
RETURN
END

```

No6...SUBROUTINE FOR CALCULATING J IN SECTION

```

SUBROUTINE SECTJ(G,J,QI,VCOUNT,DQ,WIDTH,KSN,C,RSQS,T,ITER)
PARAMETER(N=100,M=15,LL=10)
LOGICAL OLDM
REAL A1,A2,A3,RHS, TM1, TM2, TM3, TM4, TM5, TM6, TM7, TM8, QN1, QN2, QN3,
& QN4, PN1, X1, X2, A31, A32, HS1, HS2, Q1, Q2, Q3, Q4, H2S1, H2S2, QI, H2S5,
& p1, p2, p3, p4, p5, p6, p7, p8, p9, q21, q22, q23, q24, q25, q26, q27, q28,
& H1, H3, H4, H5, H6, H7, H8, H9, AA, AB, BB, BA, KSNT1, KSNT2, H2S3, H2S4,
& WIDTH, KSN, C, BB1, BB2, BB3
INTEGER I, II, J, K, KK, VCOUNT, COUNT, T, ITER, L, TP
DIMENSION DQS(N), FP(N), QP(N), COEF1(M), COEF2(M), COEF3(M), COEF4(M),

```

```

&      COEF5(M),COEF6(M),COEF62(M),COEF7(M),COEF8(M),COEF82(M),
&      COEF9(M),COEF92(M),COEF10(M),COEF11(M),COEF12(M),DQ(M),
&      COEF22(M),COEF13(M),COEF23(M),TM6(M),AA(M),AB(M),A32(M),
&      COEFa1(M),COEFa2(M),COEFa3(M),RSQS(N)
common /f/CHE,SLOPE,RSC,DSC,RN,DN,JJ,KK,EQU,L,TP(LL),CHEL(N,M),
&      RSCL(LL),DSCL(LL),HINIT(M),DPW(M),H(N,M),F(N,M),
&      Q(N,M),P(N,M),QC(N)
common /f2/DSP(N,M),RSP(N,M),DSH(N,M),RSH(N,M),DSQ(N,M),RSQ(N,M),
&      DNP(N,M),RNP(N,M),DNH(N,M),RNH(N,M),DNQ(N,M),RNQ(N,M),
&      U(N,M),V(N,M),RSTP(N,M),RSTH(N,M),RSTQ(N,M)
C
C   SOUTHERN BANK (DQS(J)=Q(J,K-1)=0)
      DQS(J)=0.
      count = 0
C ASSUME F(J,K)
      IF (T .EQ. 1) THEN
        F(J,1)=F(J-1,1)
        P(J,1)=P(J-1,1)
      ENDIF
C START CALCULATION
      DO 40 K=1,KK-1
        HS2=(H(J,K)+H(J-1,K)+H(J,K+1)+H(J-1,K+1))/4
        IF (J .EQ. JJ) THEN
          HS1=(H(J,K)+H(J,K+1))/2
          COEF1(K)=1/H(j,k+1)+dnq(j,k)*(RSTP(j,k+1)+
&          RSTP(j,k))/(4*hs1)+dsh(j,k+1)*
&          rnh(j,k+1)/(2*H(j,k+1))
          COEF3(K)=-1/H(j,k)+dnq(j,k)*(RSTP(j,k+1)+
&          RSTP(j,k))/(4*hs1)-dsh(j,k)*rnh(j,k)/(2*H(j,k))
        ELSE
          HS1=(H(J,K)+H(J+1,K)+H(J,K+1)+H(J+1,K+1))/4
          COEF1(K)=1/H(j,k+1)+(dnq(j+1,k)+dnq(j,k))*(RSTP(j,k+1)+
&          RSTP(j,k))/(8*hs1)+dsh(j,k+1)*
&          rnh(j,k+1)/(2*H(j,k+1))
          COEF3(K)=-1/H(j,k)+(dnq(j+1,k)+dnq(j,k))*(RSTP(j,k+1)+
&          RSTP(j,k))/(8*hs1)-dsh(j,k)*rnh(j,k)/(2*H(j,k))
        ENDIF
        COEF2(K)=g*dsh(j,k+1)/(che*che*H(j,k+1)*H(j,k+1)*2)
        COEF4(K)=g*dsh(j,k)/(che*che*H(j,k)*H(j,k)*2)
        COEF5(K)=F(J-1,K)/H(J,K)-F(J-1,K)*DSH(J,K)*RNH(J,K)/
&          (H(J,K)*2)-F(J-1,k+1)/H(j,k+1)+F(J-1,K+1)
&          *DSH(J,K+1)*RNH(J,K+1)/(H(J,K+1)*2)
        AA(K)=Q(J,K+1)*Q(J,K+1)+Q(J,K)*Q(J,K)
        IF (K .EQ. KK-1) THEN
          H2S3=H(J,K+1)*H(J,K+1)
        ELSE
          H2S3=(H(J,K+2)*H(J,K+2)+H(J,K+1)*H(J,K+1))/2
        ENDIF
        H2S4=(H(J,K+1)*H(J,K+1)+H(J,K)*H(J,K))/2
        BB1=(ABS(2*DQ(K))/WIDTH)**C
        IF (K .EQ. 1) THEN
          AB(K)=Q(J,K)*Q(J,K)+DQS(J)*DQS(J)
          H2S5=H(J,K)*H(J,K)

```



```

      BB2=(ABS(2*(DQ(K)-DN))/WIDTH)**C
      KSNT2=KSN/DNH(J,K)*(H2S4*RSTQ(J,K)*(1-BB1)
&      -H2S5*RSQS(J)*(1-BB2))
      ELSE
      AB(K)=Q(J,K)*Q(J,K)+Q(J,K-1)*Q(J,K-1)
      H2S5=(H(J,K-1)*H(J,K-1)+H(J,K)*H(J,K))/2
      BB2=(ABS(2*DQ(K-1))/WIDTH)**C
      KSNT2=KSN/DNH(J,K)*(H2S4*RSTQ(J,K)*(1-BB1)
&      -H2S5*RSTQ(J,K-1)*(1-BB2))
      ENDIF
      BA=P(J,K+1)*P(J,K+1)+P(J-1,K+1)*P(J-1,K+1)
      BB=P(J,K)*P(J,K)+P(J-1,K)*P(J-1,K)
      BB3=(ABS(2*DQ(K+1))/WIDTH)**C
      KSNT1=KSN/DNH(J,K+1)*(H2S3*RSTQ(J,K+1)*(1-BB3)
&      -H2S4*RSTQ(J,K)*(1-BB1))
      COEFA1(K)=DSH(J,K+1)/(2*H(J,K+1)*H(J,K+1))*KSNT1
      COEFA2(K)=DSH(J,K)/(2*H(J,K)*H(J,K))*KSNT2
      COEFA3(K)=F(J-1,K+1)*COEFA1(K)-F(J-1,K)*COEFA2(K)
C
      A1=COEF1(K)+COEF2(K)*(1+AA(K)/BA)**0.5+COEFA1(K)
      A2=COEF3(K)-COEF4(K)*(1+AB(K)/BB)**0.5-COEFA2(K)
      A31=COEF5(K)-COEF4(K)*F(J-1,K)*(1+AB(K)/BB)**0.5+
&      COEF2(K)*F(J-1,K+1)*(1+AA(K)/BA)**0.5
      A32(K)=-F(J-1,K+1)+F(J-1,K)*(DNQ(J-1,K)+
&      DNQ(J,K))/2*(RSTP(j,k+1)+RSTP(j,k))/(HS2*4)
      A3=A31+A32(K)+COEFA3(K)
C
      P1=(P(J-1,K+1)+P(J,K+1)+P(J-1,K)+P(J,K))/4
      P6=(P(J-1,K)+P(J,K))/2
      P7=(P(J-1,K+1)+P(J,K+1))/2
      P8=(P(J-1,K+1)+P(J-1,K))/2
      P9=(P(J,K+1)+P(J,K))/2
C
      IF(VCOUNT .EQ. 0) THEN
      P5=(P(J,K+1)+P(J,K))/2
      ELSEIF(J .EQ. JJ) THEN
      P5=(P(J,K+1)+P(J,K))/2
      ELSE
      P5=(P(J+1,K+1)+P(J+1,K)+P(J,K+1)+P(J,K))/4
      ENDIF
      IF (J .EQ. 2) THEN
      P4=(DPW(K+1)+P(J-1,K+1)+DPW(K)+P(J-1,K))/4
      ELSE
      P4=(P(J-2,K+1)+P(J-1,K+1)+P(J-2,K)+P(J-1,K))/4
      ENDIF
C
      IF (K .EQ. KK-1) THEN
      P3=(P(J-1,K+1)+P(J,K+1))/2
      H3=H(J,K+1)
      ELSE
      P3=(P(J-1,K+2)+P(J,K+2)+P(J-1,K+1)+P(J,K+1))/4
      H3=(H(J,K+2)+H(J,K+1))/2
      ENDIF

```

```

IF(K .EQ. 1) THEN
  P2=(P(J-1,K) + P(J,K))/2
ELSE
  P2=(P(J-1,K-1) + P(J,K-1) + P(J-1,K) + P(J,K))/4
ENDIF
Q2=(Q(J,K+1) + Q(J,K))/2
Q3=(Q(J-1,K) + Q(J,K))/2
Q22=(Q(J,K+1)*Q(J,K+1) + Q(J,K)*Q(J,K))/2
Q23=(Q(J-1,K)*Q(J-1,K) + Q(J,K)*Q(J,K))/2
Q25=(Q(J-1,K+1)*Q(J-1,K+1) + Q(J,K+1)*Q(J,K+1) +
& Q(J-1,K)*Q(J-1,K) + Q(J,K)*Q(J,K))/4
C
IF(K .EQ. 1) THEN
  Q1=(DQS(J) + Q(J,K))/2
  Q21=(DQS(J)*DQS(J) + Q(J,K)*Q(J,K))/2
  Q26=(DQS(J-1)*DQS(J-1) + DQS(J)*DQS(J) +
& Q(J-1,K)*Q(J-1,K) + Q(J,K)*Q(J,K))/4
ELSE
  Q1=(Q(J,K-1) + Q(J,K))/2
  Q21=(Q(J,K-1)*Q(J,K-1) + Q(J,K)*Q(J,K))/2
  Q26=(Q(J-1,K-1)*Q(J-1,K-1) + Q(J,K-1)*Q(J,K-1) +
& Q(J-1,K)*Q(J-1,K) + Q(J,K)*Q(J,K))/4
ENDIF
C
  H1=(H(J,K+1) + H(J,K))/2
  H4=(H(J-1,K+1) + H(J,K+1))/2
  H5=(H(J-1,K) + H(J,K))/2
  H6=(H(J-1,K+1) + H(J-1,K))/2
  H2S2=(H(J-1,K+1)*H(J-1,K+1) + H(J-1,K)*H(J-1,K) +
& H(J,K+1)*H(J,K+1) + H(J,K)*H(J,K))/4
C
IF(J .EQ. JJ) THEN
  Q4=Q(J,K)
  Q24=Q(J,K)*Q(J,K)
  Q27=(Q(J,K+1)*Q(J,K+1) + Q(J,K)*Q(J,K))/2
  IF(K .EQ. 1) THEN
    Q28=(DQS(J)*DQS(J) + Q(J,K)*Q(J,K))/2
  ELSE
    Q28=(Q(J,K-1)*Q(J,K-1) + Q(J,K)*Q(J,K))/2
  ENDIF
  H7=(H(J,K+1) + H(J,K))/2
  H8=H(J,K+1)
  H9=H(J,K)
  H2S1=(H(J,K+1)*H(J,K+1) + H(J,K)*H(J,K))/2
ELSE
  Q4=(Q(J+1,K) + Q(J,K))/2
  Q24=(Q(J+1,K)*Q(J+1,K) + Q(J,K)*Q(J,K))/2
  Q27=(Q(J+1,K+1)*Q(J+1,K+1) + Q(J,K+1)*Q(J,K+1) +
& Q(J+1,K)*Q(J+1,K) + Q(J,K)*Q(J,K))/4
  IF(K .EQ. 1) THEN
    Q28=(DQS(J+1)*DQS(J+1) + DQS(J)*DQS(J) +
& Q(J+1,K)*Q(J+1,K) + Q(J,K)*Q(J,K))/4
  ELSE

```



```

      Q28=(Q(J+1,K-1)*Q(J+1,K-1)+Q(J,K-1)*Q(J,K-1)+
&      Q(J+1,K)*Q(J+1,K)+Q(J,K)*Q(J,K))/4
      ENDIF
      H7=(H(J+1,K+1)+H(J+1,K))/2
      H8=(H(J+1,K+1)+H(J,K+1))/2
      H9=(H(J+1,K)+H(J,K))/2
      H2S1=(H(J+1,K+1)*H(J+1,K+1)+H(J+1,K)*H(J+1,K)+
&      H(J,K+1)*H(J,K+1)+H(J,K)*H(J,K))/4
      ENDIF
C
      IF(K .EQ. 1) THEN
        TM1= 1/H(J,K)*DSH(J,K)/DNH(J,K)*(P1*Q(J,K)/H1-P2*DQS(J)/
&      H(J,K))
      ELSE
        TM1= 1/H(J,K)*DSH(J,K)/DNH(J,K)*(P1*Q(J,K)/H1-P2*Q(J,K-1)*2/
&      (H(J,K-1)+H(J,K)))
      ENDIF
C
      COEF6(K)=2*Q1*DSH(J,K)*RSTH(J,K)/(H(J,K)*H(J,K))
      COEF62(K)=Q21*DSH(J,K)*RNH(J,K)/(H(J,K)*H(J,K))
      TM2=COEF6(K)*P6-COEF62(K)
      COEF7(K)= -1/H(J,K+1)*DSH(J,K+1)/DNH(J,K+1)
      TM3=COEF7(K)*(P3*Q(J,K+1)/H3-P1*Q(J,K)/H1)
      COEF8(K)= -2*Q2*DSH(J,K+1)/(H(J,K+1)*H(J,K+1))*RSTH(J,K+1)
      COEF82(K)=Q22*DSH(J,K+1)*RNH(J,K+1)/(H(J,K+1)*H(J,K+1))
      TM4=COEF8(K)*P7+COEF82(K)
      COEF9(K)= -(DNQ(J-1,K)+DNQ(J,K))/((DSP(J-1,K+1)+DSP(J-1,K))*HS2)
      COEF92(K)=P4*Q(J-1,K)/H4
      TM5=COEF9(K)*(P1*Q(J,K)/H1-COEF92(K))
      TM6(K)= -1/HS2*(Q25/H4-Q26/H5)-2*P8*Q3*(DNQ(J-1,K)+DNQ(J,K))/(2*
&      H2S2)*(RNP(J-1,K+1)+RNP(J-1,K))/2
      COEF10(K)= -Q23*(DNQ(J-1,K)+DNQ(J,K))/(2*H2S2)*(RSTQ(J-1,K)+
&      RSTQ(J,K))/2+1/HS1*(Q27/H8-Q28/H9)
C
      IF(J .EQ. JJ) THEN
        COEF11(K)=DNQ(J,K)/(HS1*(DSP(J,K+1)+DSP(J,K))/2)
        TM7=COEF10(K)+COEF11(K)*(P5*Q(J,K)/H7-P1*Q(J,K)/H1)
        COEF12(K)=2*Q4*DNQ(J,K)/H2S1*(RNP(J,K+1)+RNP(J,K))/2
        COEF22(K)=Q24*DNQ(J,K)/H2S1*RSTQ(J,K)
        COEF23(K)=G*DNQ(J,K)/(CHE*CHE*H2S1*HS1)
      ELSE
        COEF11(K)=(DNQ(J+1,K)+DNQ(J,K))/(HS1*(DSP(J,K+1)+DSP(J,K)))
        TM7=COEF10(K)+COEF11(K)*(P5*Q(J+1,K)/H7-P1*Q(J,K)/H1)
        COEF12(K)=2*Q4*(DNQ(J+1,K)+DNQ(J,K))/(2*H2S1)*
&      (RNP(J,K+1)+RNP(J,K))/2
        COEF22(K)=Q24*(DNQ(J+1,K)+DNQ(J,K))/(2*H2S1)*
&      (RSTQ(J+1,K)+RSTQ(J,K))/2
        COEF23(K)=G*(DNQ(J+1,K)+DNQ(J,K))/(2*CHE*CHE*H2S1*HS1)
      ENDIF
C
      TM8=COEF12(K)*P9+COEF22(K)
      P21=(P(J-1,K+1)*P(J-1,K+1)+P(J-1,K)*P(J-1,K))/2
      P22=(P(J,K+1)*P(J,K+1)+P(J,K)*P(J,K))/2

```

COEF13(K) = -G*(DNQ(J-1,K) + DNQ(J,K))/(2*CHE*CHE*H2S2*HS2)
 TM9 = COEF13(K)*Q3*(Q23 + P21)**0.5 + COEF23(K)*Q4*(Q24 + P22)**0.5
 RHS = TM1 + TM2 + TM3 + TM4 + TM5 + TM6(K) + TM7 + TM8 + TM9
 F(J,K+1) = (RHS - A3 - F(J,K)*A2)/A1

40 CONTINUE

GOTO 110

C

C CORRECTION FOR F(J,K)

100 CONTINUE

IF (I .GT. 10) THEN

OLDM = .FALSE.

AUX = QP(I) - QP(I-1)

IF (ABS(AUX/QI) .LT. .0001) THEN

OLDM = .TRUE.

ELSE

F(J,1) = (FP(I) - FP(I-1))/AUX * (QI - QP(I)) + FP(I)

IF (F(J,1) .LT. 0) OLDM = .TRUE.

IF ((F(J,1)/FP(I)) .GT. 10) OLDM = .TRUE.

ENDIF

ENDIF

IF ((I .LE. 10) .OR. (OLDM)) THEN

F(J,1) = FP(I) * ((0.75*QI + 0.25*QP(I))/QP(I))

c F(J,1) = FP(I) * QI / QP(I)

ENDIF

IF (J .EQ. JJ) THEN

P(J,1) = (F(J,1) * H(J,1)) ** 0.5

ELSE

P(J,1) = (F(J,1) * (H(J+1,1) + H(J,1)) / 2) ** 0.5

ENDIF

C

DO 41 K=1, KK-1

BA = P(J,K+1) * P(J,K+1) + P(J-1,K+1) * P(J-1,K+1)

BB = P(J,K) * P(J,K) + P(J-1,K) * P(J-1,K)

A1 = COEF1(K) + COEF2(K) * (1 + AA(K)/BA) ** 0.5 + COEFA1(K)

A2 = COEF3(K) - COEF4(K) * (1 + AB(K)/BB) ** 0.5 - COEFA2(K)

A31 = COEF5(K) - COEF4(K) * F(J-1,K) * (1 + AB(K)/BB) ** 0.5 +
 & COEF2(K) * F(J-1,K+1) * (1 + AA(K)/BA) ** 0.5

A3 = A31 + A32(K) + COEFA3(K)

C

P1 = (P(J-1,K+1) + P(J,K+1) + P(J-1,K) + P(J,K)) / 4

P6 = (P(J-1,K) + P(J,K)) / 2

P7 = (P(J-1,K+1) + P(J,K+1)) / 2

P9 = (P(J,K+1) + P(J,K)) / 2

H1 = (H(J,K+1) + H(J,K)) / 2

C

IF (VCOUNT .EQ. 0) THEN

P5 = (P(J,K+1) + P(J,K)) / 2

ELSEIF (J .EQ. JJ) THEN

P5 = (P(J,K+1) + P(J,K)) / 2

ELSE

P5 = (P(J+1,K+1) + P(J+1,K) + P(J,K+1) + P(J,K)) / 4

ENDIF

C


```

IF (K .EQ. KK-1) THEN
  P3=(P(J-1,K+1)+P(J,K+1))/2
  H3= H(J,K+1)
ELSE
  P3=(P(J-1,K+2)+P(J,K+2)+P(J-1,K+1)+P(J,K+1))/4
  H3=(H(J,K+2)+H(J,K+1))/2
ENDIF
IF(K .EQ. 1) THEN
  P2=(P(J-1,K)+P(J,K))/2
ELSE
  P2=(P(J-1,K-1)+P(J,K-1)+P(J-1,K)+P(J,K))/4
ENDIF
IF(K .EQ. 1) THEN
  TM1= 1/H(J,K)*DSH(J,K)/DNH(J,K)*(P1*Q(J,K)/H1-P2*DQS(J)/
& H(J,K))
ELSE
  TM1= 1/H(J,K)*DSH(J,K)/DNH(J,K)*(P1*Q(J,K)/H1-P2*Q(J,K-1)*2/
& (H(J,K-1)+H(J,K)))
ENDIF
TM2= COEF6(K)*P6-COEF62(K)
TM3= COEF7(K)*(P3*Q(J,K+1)/H3-P1*Q(J,K)/H1)
TM4= COEF8(K)*P7+COEF82(K)
TM5= COEF9(K)*(P1*Q(J,K)/H1-COEF92(K))
IF(J .EQ. JJ) THEN
  H7=(H(J,K+1)+H(J,K))/2
  TM7= COEF10(K)+COEF11(K)*(P5*Q(J,K)/H7-P1*Q(J,K)/H1)
ELSE
  H7=(H(J+1,K+1)+H(J+1,K))/2
  TM7= COEF10(K)+COEF11(K)*(P5*Q(J+1,K)/H7-P1*Q(J,K)/H1)
ENDIF
TM8= COEF12(K)*P9+COEF22(K)
P21=(P(J-1,K+1)*P(J-1,K+1)+P(J-1,K)*P(J-1,K))/2
P22=(P(J,K+1)*P(J,K+1)+P(J,K)*P(J,K))/2
TM9= COEF13(K)*Q3*(Q23+P21)**0.5+COEF23(K)*Q4*(Q24+P22)**0.5
RHS = TM1+TM2+TM3+TM4+TM5+TM6(K)+TM7+TM8+TM9
F(J,K+1)=(RHS-A3-F(J,K)*A2)/A1
41 CONTINUE
C
C CHECKING OF THE DISCHARGE (INTEGRATING OVER THE WIDTH)
110 DO 50 K=1, KK
  IF(J .EQ. JJ) THEN
    P(J,K)=(F(J,K)*H(J,K))**0.5
    U(J,K)=P(J,K)/H(J,K)
  ELSE
    P(J,K)=(F(J,K)*(H(J+1,K)+H(J,K))/2)**0.5
    U(J,K)=P(J,K)*2/(H(J+1,K)+H(J,K))
  ENDIF
50 CONTINUE
QC(J)=0.0
DO 60 K=1, KK
  QC(J)=QC(J)+P(J,K)*DNH(J,K)
60 CONTINUE
EPS= ABS(QC(J)-QI)/QI

```

```

DIF = .0001
IF(EPS .GT. DIF)THEN
  COUNT = COUNT+1
  DO 200 I = COUNT
    FP(I) = F(J,1)
    QP(I) = QC(J)
200 CONTINUE
C   write(*,*)'count2 in the sectj. for=',count
    IF(COUNT .LT. ITER) GOTO 100
  ENDIF
RETURN
END

```

No7...SUBROUTINE FOR Q-COMPONENTS

```

SUBROUTINE QQ
PARAMETER(N=100,M=15,LL=10)
common /f/CHE,SLOPE,RSC,DSC,RN,DN,JJ,KK,EQU,L,TP(LL),CHEL(N,M),
&   RSCL(LL),DSCL(LL),HINIT(M),DPW(M),H(N,M),F(N,M),
&   Q(N,M),P(N,M),QC(N)
common /f2/DSP(N,M),RSP(N,M),DSH(N,M),RSH(N,M),DSQ(N,M),RSQ(N,M),
&   DNP(N,M),RNP(N,M),DNH(N,M),RNH(N,M),DNQ(N,M),RNQ(N,M),
&   U(N,M),V(N,M),RSTP(N,M),RSTH(N,M),RSTQ(N,M)
dimension dqs(n)
C
DO 20 J=1,JJ
  DO 30 K=1,KK-1
    dqs(j)=0
C1
    IF(J .EQ. 1 .AND. K .EQ. 1) THEN
      Q(J,K) = (dpw(k)*dnp(j,k)-P(j,k)*dnp(j,k))/dsq(j,k)
      q(j,K)=0.
c
C2
    ELSEIF(J .EQ. 1) THEN
      Q(J,K) = (dpw(k)*dnp(j,k)-P(j,k)*dnp(j,k) + Q(j,k-1)*
&   dsq(j,k-1))/dsq(j,k)
      q(j,K)=0.
c
C3
    ELSEIF(K .EQ. 1) THEN
      Q(J,K) = (P(j-1,k)*dnp(j-1,k)-P(j,k)*dnp(j,k))/dsq(j,k)
      q(j,K)=0.
c
C4
    ELSE
      Q(J,K) = (P(j-1,k)*dnp(j-1,k)-P(j,k)*dnp(j,k) + Q(j,k-1)*
&   dsq(j,k-1))/dsq(j,k)
      q(j,K)=0.
c
    ENDIF
    V(J,K) = Q(J,K)*2/(H(J,K) + H(J,K+1))
30 CONTINUE
    Q(J,KK) = 0.
    V(J,KK) = 0.
20 CONTINUE
RETURN
END

```


No8.....SUBROUTINE FOR SEDIMENT TRANSPORTATION AND BED LEVEL CHANGES.

c This is $dz/dt=0$ at $J=1$ (Upstream treatment)

```

SUBROUTINE BED(G, CODE, T, STOP)
PARAMETER(N=100, M=15, LL=10)
common /f/CHE, SLOPE, RSC, DSC, RN, DN, JJ, KK, EQU, L, TP(LL), CHEL(N, M),
&    RSCL(LL), DSCL(LL), HINIT(M), DPW(M), H(N, M), F(N, M),
&    Q(N, M), P(N, M), QC(N)
common /f2/DSP(N, M), RSP(N, M), DSH(N, M), RSH(N, M), DSQ(N, M), RSQ(N, M),
&    DNP(N, M), RNP(N, M), DNH(N, M), RNH(N, M), DNQ(N, M), RNQ(N, M),
&    U(N, M), V(N, M), RSTP(N, M), RSTH(N, M), RSTQ(N, M)
common /f3/DT, TOUC, TOUS(N, M), DM, SS(N, M), SN(N, M), MU(N, M), TANS(N, M)
&    , DEL, TAND(N, M), ALSF(N, M), TITLE, PLOT
common /f4/BETA, GT(N, M), U0(M), HNP1(N, M), TTIME, TT, HCOUNT, TOUS0(M),
&    SS0(M), MU0(M), TOUP(N, M)
REAL MU, MU0, DM, DT, DEL, BETA, TTIME, a, a0, b, b0, C, TOUS, TOUP, TOUC, E,
&    ERR, DIFF, DH, C3
INTEGER J, JJ, K, KK, TT, PLOT, CODE, T, STOP, TP, L
DIMENSION G0(M), TOUP0(M)

```

```

c
DM = DM / 1000.
E = 4.0
IF(T .EQ. 1) THEN
  DO 1 K=1, KK
    TOUS0(K) = U0(K)*U0(K)/(CHEL(1, K)*CHEL(1, K)*DEL*DM)
    TOUP0(K) = TOUS0(K)*TOUS0(K)*0.4 + 0.06
1  CONTINUE
ENDIF
DO 10 J=1, JJ
  DO 11 K=1, KK
    TOUS(J, K) = U(J, K)*U(J, K)/(CHEL(J, K)*CHEL(J, K)*DEL*DM)
    TOUP(J, K) = TOUS(J, K)*TOUS(J, K)*0.4 + 0.06
11 CONTINUE

```

C1 This is power law

```

IF(CODE .EQ. 1) THEN
  E = 1.
  b = 5.0

```

```

IF(T .EQ. 1) b0 = 5.0

```

C2 This is EH formula (b=5.0)

```

ELSEIF(CODE .EQ. 2) THEN
  E = 1.
  ELSE
    goto 100
ENDIF
C3 = SQRT(DEL*G*DM)*DM
DO 21 K=1, KK
IF (TOUS (J, K) .LT. 0.06) THEN
  SS0(K) = 0.
  SS(J, K) = 0.
ELSE
  IF(T .EQ. 1) SS0(K) = 0.1*CHEL(1, K)*CHEL(1, K)/G*TOUS0(K)**2.5
  & *C3*(1 + E*(H(2, K)-H(1, K))/DSP(1, K))
  IF(J .LT. JJ) THEN

```

```

        SS(J,K) = 0.1*CHEL(J,K)*CHEL(J,K)/G*TOUS(J,K)**2.5*
&          C3*(1+E*(H(J+1,K)-H(J,K))/DSP(J,K))
        ELSE
        SS(J,K) = 0.1*CHEL(J,K)*CHEL(J,K)/G*TOUS(J,K)**2.5*
&          C3*(1+E*(H(J,K)-H(J-1,K))/DSP(J-1,K))
        ENDIF
    ENDIF
21 CONTINUE
    GOTO 200
C3
C MPM formula
100 DO 23 K=1, KK
    IF(T .EQ. 1) THEN
        MU0(K) = TOUP0(K)/TOUS0(K)
        b0 = 3*MU0(K)*TOUS0(K)/(MU0(K)*TOUS0(K)-TOUC)
        a0 = MU0(K)*TOUS0(K)-TOUC
        IF(a0 .LE. 0) THEN
            SS0(K)=0.
        ELSE
            SS0(K)=8.*SQRT(DEL*G*DM**3)*a**1.5*(1+E*(H(2,K)
&          -H(1,K))/DSP(1,K))
        ENDIF
    ENDIF
    MU(J,K) = TOUP(J,K)/TOUS(J,K)
    b = 3*MU(J,K)*TOUS(J,K)/(MU(J,K)*TOUS(J,K)-TOUC)
    E = TOUC/(MU(J,K)*TOUS(J,K)-TOUC)
    a = MU(J,K)*TOUS(J,K)-TOUC
    IF(a .LE. 0) THEN
        SS(J,K)=0
    ELSEIF(J .LT. JJ) THEN
        SS(J,K)=8.*SQRT(DEL*G*DM**3)*a**1.5*(1+E*
&          (H(J+1,K)-H(J,K))/DSP(J,K))
    ELSE
        SS(J,K)=8.*SQRT(DEL*G*DM**3)*a**1.5*(1+E*
&          (H(J,K)-H(J-1,K))/DSP(J-1,K))
    ENDIF
23 CONTINUE
C This is the calculation of bed shear stress direction model
200 DO 25 K=1, KK
    ALSF(J,K)=0.6 * H(J,K)*CHEL(J,K)/G**.5
C
C GT will be changed when tuning is necessary
C
    GT(J,K)=0.53/TOUS(J,K)**0.50
    G0(K)=0.53/TOUS0(K)**0.50
    IF(J .EQ. 1) THEN
        TAND(J,K)= -BETA * (H(J+1,K)+H(J,K))*(RSTH(J+1,K)+RSTH(J,K))
    ELSE
        TAND(J,K)=(TAND(J-1,K)*(ALSF(J,K)/DSH(J,K)-0.5)-BETA*H(J,K)*
&          RSTH(J,K))/(ALSF(J,K)/DSH(J,K)+.5)
    ENDIF
25 CONTINUE
C This is the calculation of sediment transport in transverse direction,

```



```

DO 30 K=1, KK-1
  IF(J .EQ. 1) THEN
    TANS(J,K)=V(J,K)*4/(U(J,K)+U(J,K+1)+U0(K)+U0(K+1))+
    & (TAND(J,K)+TAND(J,K+1))/2+(GT(J,K)+GT(J,K+1)+
    & G0(K)+G0(K+1))/4*(H(J,K+1)-H(J,K))/DNQ(J,K)
    SN(J,K)=TANS(J,K)*(SS(J,K)+SS(J,K+1)+SS0(K)+SS0(K+1))/4
  ELSE
    TANS(J,K)=V(J,K)*4/(U(J,K)+U(J,K+1)+U(J-1,K)+U(J-1,K+1))
    & +(TAND(J,K)+TAND(J,K+1)+TAND(J-1,K)
    & +TAND(J-1,K+1))/4+(GT(J,K)+GT(J-1,K)+GT(J,K+1)
    & +GT(J-1,K+1))/4*(H(J,K+1)-H(J,K))/DNQ(J,K)
    SN(J,K)=TANS(J,K)*(SS(J,K)+SS(J,K+1)+SS(J-1,K)+SS(J-1,K+1))/4
  ENDIF
30 CONTINUE
  SN(J, KK) = 0.
*****
C This is bed level calculation for no sediment input condition.
c Add this part only when s0=0 condition.
c DO 40 K=1, KK
c IF(J .EQ. 1 .AND. K .EQ. 1) THEN
c HNP1(J,K)=(SS(J,K)*DNP(J,K)+SN(J,K)*DSQ(J,K))/
c & (DSH(J,K)*DNH(J,K))*DT+H(J,K)
c ELSEIF(J .EQ. 1 .AND. K .GT. 1) THEN
c HNP1(J,K)=(SS(J,K)*DNP(J,K)+
c & (SN(J,K)*DSQ(J,K)-SN(J,K-1)*DSQ(J,K-1)))/
c & (DSH(J,K)*DNH(J,K))*DT+H(J,K)
c ELSEIF(J .GT. 1 .AND. K .EQ. 1) THEN
c HNP1(J,K)=((SS(J,K)*DNP(J,K)-SS(J-1,K)*DNP(J-1,K))+
c & (SN(J,K)*DSQ(J,K)))/
c & (DSH(J,K)*DNH(J,K))*DT+H(J,K)
c ELSE
c HNP1(J,K)=((SS(J,K)*DNP(J,K)-SS(J-1,K)*DNP(J-1,K))+
c & (SN(J,K)*DSQ(J,K)-SN(J,K-1)*DSQ(J,K-1)))/
c & (DSH(J,K)*DNH(J,K))*DT+H(J,K)
c ENDIF
c 40 CONTINUE
*****
C This is the bed level calculation for s0=EQUILIBRIUM condition
DO 40 K=1, KK
  IF(J .EQ. 1) THEN
    HNP1(J,K)=h(j,k)
  ELSEIF(J .GT. 1 .AND. K .EQ. 1) THEN
    HNP1(J,K)=((SS(J,K)*DNP(J,K)-SS(J-1,K)*DNP(J-1,K))+
    & (SN(J,K)*DSQ(J,K)))/
    & (DSH(J,K)*DNH(J,K))*DT+H(J,K)
  ELSE
    HNP1(J,K)=((SS(J,K)*DNP(J,K)-SS(J-1,K)*DNP(J-1,K))+
    & (SN(J,K)*DSQ(J,K)-SN(J,K-1)*DSQ(J,K-1)))/
    & (DSH(J,K)*DNH(J,K))*DT+H(J,K)
  ENDIF
40 CONTINUE
C
10 CONTINUE

```

RIVER PLAN-FORM MOVEMENT IN AN ALLUVIAL PLAIN

C To reduce the run-time this is one of the devices

```
STOP=0
IF(T.GT. 1) THEN
  DO 50 J=5,JJ
  DO 50 J=1,JJ
  DO 50 K=1,KK
    DH = ABS(HNP1(J,K)-H(J,K))/H(J,K)
    IF(DH.GT. EQU) GOTO 60
50 CONTINUE
STOP = 1
ENDIF
60 CONTINUE
DM = DM*1000.
RETURN
END
```

No9...SUBROUTINE FOR CALCULATION OF BEDLOAD BY JF METHOD

```
SUBROUTINE BEDLOAD(TETA,PHEB,DPHEB)
REAL*8 TETA,TETA2,TETAC,BETA,PI
REAL*8 PHEB,PHEB2,DPHEB,PFAC,PFAC2,CC
C
C CALCULATION OF P VALUE
C
PI=3.141592654
TETAC=0.047
BETA=0.65
CC=PI/6.*BETA/(TETA-TETAC)
PFAC=1./(1.+CC**4.)**0.25
C PHE-B
PHEB=5.*PFAC*(DSQRT(TETA)-0.7*DSQRT(TETAC))
C DPHE-B
TETA2=TETA+0.01
CC=PI/6.*BETA/(TETA2-TETAC)
PFAC2=1./(1.+CC**4.)**0.25
PHEB2=5.*PFAC2*(DSQRT(TETA2)-0.7*DSQRT(TETAC))
DPHEB=(PHEB2-PHEB)/0.01
RETURN
END
```

No10.....SUBROUTINE FOR DUNE DIMENSION

```
SUBROUTINE DUNE(PHEB,DPHEB,PHES,DPHES,TETA,h,d50,Wcr,Wsus,THpp,
& TH,LH,NP2)
PARAMETER(N=50)
REAL*8 PHES,DPHES,Wcr,Wsus,d50,h,LDH1,LDH2
REAL*8 DHh,PHEB,TETA,DPHEB,C1,C11,C2,Ubf
REAL*8 DELTh,DelDH,LDH,UUf,THpp,TH,LH
INTEGER NP2
DIMENSION TH(N),LH(N)
C CALCULATION
d50=d50/1000.
DHh= PHEB/(2*TETA*(DPHEB+DPHES))
C FOR SMALL VALUES OF TETA(THM), DIFFERENT EQUATION HAS TO BE USED
```



```

C INSTEAD OF EQUATION (4.2).
C CHECK FOR THE GREATER VALUE OF LDH IN THE CRITICAL REGION
  IF(TETA .LE. 0.2 .AND. TETA .GE. 0.047)THEN
    CALL INTEPO(I,TH,LH,TETA,LDH,NP2)
    LDH1=LDH
C CHECK POINT ; LHD FROM EQUATION
  C1 = h/(13*2*d50)
  Ubf = 8.3+2.5*DLOG(C1)
  C2 = Wcr/Wsus
  DELTh = C2*C2/13.*Ubf
  DelDH = DELTh/DHh
  LDH2 = (16.*PHEB+(16.+DelDH)*PHES)/(PHEB+PHES)
  IF(LDH1 .GE. LDH2) THEN
    LDH = LDH1
  ELSE
    LDH = LDH2
  ENDIF
ELSE
  C1 = h/(13*2*d50)
  Ubf = 8.3+2.5*DLOG(C1)
  C2 = Wcr/Wsus
  DELTh = C2*C2/13.*Ubf
  DelDH = DELTh/DHh
  LDH = (16.*PHEB+(16.+DelDH)*PHES)/(PHEB+PHES)
ENDIF
C11 = h/(2.*d50)
UUF = 6.+2.5*DLOG(C11)
THpp = 0.5*UUF*UUF*DHh/LDH
d50=d50*1000.
RETURN
END

```

No11....SUBROUTINE FOR LOCAL ROUGHNESS (variable roughness)

```

SUBROUTINE ROUGH(QI,H1,U1,DSH1,DM,W1,CHE1,JJ,KK,IROUGH,S1,
& NP,NP1,NP2,ITER2,w,d,ds,PERC,TH,LH)
PARAMETER (N=100,M=15)
REAL*8 PHES,PHES2,DPHES,Wcr,Wsus,Ufi,Wcr2,PERC2,dcr2,dsus2,
& dsus,wsus2,DEL,G
REAL*8 PHEB,DPHEB,CHE,FF,MANN,THE,TETA,TETAC,U,X,UUF,Uf,HYDR
REAL*8 RED,QS,Uf2,THpp,C1,C2,TH2,SLOPE,q,h,d50,WIDTH,TETA2
REAL*8 w,d,ds,PERC,TH,LH,FTILE,FT2,dcr,PERCR,Qn,hn,DIF
REAL QI,H1,U1,DSH1,DM,W1,CHE1,S1
INTEGER I,NP,NP1,NP2,MODEL,ITER2,IROUGH
DIMENSION w(N),d(N),ds(N),PERC(N),TH(N),LH(N),H1(N,M),U1(N,M),
& DSH1(N,M),CHE1(N,M)
C START CALCULATION
  q = QI/W1
  d50 = DM
  DEL = 1.65
  G = 9.81
C FIRST GUESS OF FRICTION VELOCITY Uf & TETA FOR PLANE BED
  DO 100 J = 1,JJ

```

```

DO 100 K = 1, KK
  IF(J .EQ. JJ) THEN
    SLOPE = (H1(J,K)-H1(J-1,K))/DSH1(J-1,K)
    IF(SLOPE .LE. S1) SLOPE = S1
  ELSE
    SLOPE = (H1(J+1,K)-H1(J,K))/DSH1(J,K)
    IF(SLOPE .LE. S1) SLOPE = S1
  ENDIF
  h = H1(J,K)
  U = U1(J,K)
C
DO 200 I=1, ITER2
  X = h/(2.*d50/1000.)
  Uuf = 6. + 2.5*DLOG(X)
  Uf = U/Uuf
  C1 = DEL*G*d50/1000.
  TETA = Uf*Uf/C1
C E&F
  IF(TETA .LE. 0.047) THEN
    THE = TETA
    GOTO 2000
  ENDIF
  CALL BEDLOAD(TETA, PHEB, DPHEB)
C .....
  Wcr = Uf
  CALL INTEPO(I, w, d, Wcr, dcr, NP)
  CALL INTEPO(I, ds, Perc, dcr, Percr, NP1)
  FTILE = Percr/2.
  CALL INTEPO(I, Perc, ds, FTILE, dsus, NP1)
  CALL INTEPO(I, d, w, dsus, Wsus, NP)
C CALCULATION OF SUSPENDED SEDIMENT
  CALL DIEG(Wcr, Wsus, h, d50, TETA, PHES)
C
C CALCULATION OF "DPHES"
  TETA2 = TETA + 0.01
  C2 = TETA2*C1
  Wcr2 = DSQRT(C2)
  CALL INTEPO(I, w, d, Wcr2, dcr2, NP)
  CALL INTEPO(I, ds, Perc, dcr2, Perc2, NP1)
  FT2 = Perc2/2.
  CALL INTEPO(I, Perc, ds, FT2, dsus2, NP1)
  CALL INTEPO(I, d, w, dsus2, Wsus2, NP)
C
  CALL DIEG(Wcr2, Wsus2, h, d50, TETA2, PHES2)
  DPHES = (PHES2-PHES)/0.01
  CALL DUNE(PHEB, DPHEB, PHES, DPHES, TETA, h, d50, Wcr, Wsus, THpp,
&          TH, LH, NP2)
  THE = TETA*(1. + THpp)
C CALCULATION OF ROUGHNESS COEFF FOR ALLUVIAL BED IN DUNE PHASE
2000 CONTINUE
  Uf2 = THE*C1
  Uf = DSQRT(Uf2)
C ROUGHNESS COEFFICIENTS
  FF = Uf*Uf*2./(U*U)

```



```

    Uuf = U/Uf
    CHE = DSQRT(2.*G/FF)
C
    hn = THE*del*d50/1000./SLOPE
    qn = CHE*DSQRT(hn*SLOPE)*hn
C
    DIF = DABS(q-qn)/q
    IF(DIF .GT. .0001) THEN
        h = 0.75*h + 0.25*hn
    ENDIF
200 CONTINUE
    CHE1(J,K) = CHE
C E-F
    IF(THE .LT. 0.047) THEN
        QS = 0.1E-09
    ELSE
        QS = (PHEB + PHES)*C3
    ENDIF
100 CONTINUE
    RETURN
    END

```

No12....SUBROUTINE FOR HOT START

C SUBROUTINE FOR INTERMEDIATE INPUT DATA COLLECTION

```

SUBROUTINE INTER(I)
PARAMETER(N=100,M=15,LL=10)
REAL QI, DN, RSC, DSC, CHE, EPS, RHS, MU, DM, DT, TOUC, DEL, BETA, TTIME, S
INTEGER I, JJ, KK, MM(M), VCOUNT, ITER, tp1, tp2, TT, HCOUNT, PLOT, TP, L
common /f/CHE, SLOPE, RSC, DSC, RN, DN, JJ, KK, EQU, L, TP(LL), CHEL(N, M),
& RSL(LL), DSCL(LL), HINIT(M), DPW(M), H(N, M), F(N, M),
& Q(N, M), P(N, M), QC(N)
common /f2/DSP(N, M), RSP(N, M), DSH(N, M), RSH(N, M), DSQ(N, M), RSQ(N, M),
& DNP(N, M), RNP(N, M), DNH(N, M), RNH(N, M), DNQ(N, M), RNQ(N, M),
& U(N, M), V(N, M), RSTP(N, M), RSTH(N, M), RSTQ(N, M)
common /f3/DT, TOUC, TOUS(N, M), DM, SS(N, M), SN(N, M), MU(N, M), TANS(N, M)
& , DEL, TAND(N, M), ALSF(N, M), PLOT, TITLE
common /f4/BETA, GT(N, M), U0(M), HNP1(N, M), TTIME, TT, HCOUNT, TOUS0(M),
& SS0(M), MU0(M), TOUP(N, M)
C
    OPEN(2, FILE = 'INTER.IN', STATUS = 'NEW')
    WRITE (2, 20) I
20 FORMAT('TIME STEP', I4)
    DO 10 J=1, JJ
        WRITE (2, 70) (P(J, K), K=1, KK), (HNP1(J, K), K=1, KK)
70 FORMAT (10E11.4, /, 10E11.4)
10 CONTINUE
    CLOSE(2)
    RETURN
    END

```

No13.... SUBROUTINE FOR SKIPS COMMENT CARDS IN INPUT DATA

```

C
SUBROUTINE IREC
CHARACTER*1 REC

```

RIVER PLAN-FORM MOVEMENT IN AN ALLUVIAL PLAIN

```
DO 10 I = 1,99
  READ (3,20) REC
  IF (REC .NE. 'C') GOTO 30
10 CONTINUE
20 FORMAT(A1)
30 RETURN
END
```

No14...SUBROUTINE FOR NEAR BANK VELOCITY EXCESS

```
SUBROUTINE UBB(UB,JCRS)
PARAMETER (G=9.81,N=100,M=15,LL=10)
common /f/CHE,SLOPE,RSC,DSC,RN,DN,JJ,KK,EQU,L,TP(LL),CHEL(N,M),
&  RSCL(LL),DSCL(LL),HINIT(M),DPW(M),H(N,M),F(N,M),
&  Q(N,M),P(N,M),QC(N)
DIMENSION UB(N),U(N,M)
INTEGER L2,JCRS
REAL CL,KKC,UCL

C
C NEAR BANK EXCESS VELOCITY
DO 700 J=1,JJ
  DO 700 K=1,KK
    U(j,k)=P(j,k)/H(j,k)
700 CONTINUE
C  CALCULATION OF CENTRE LINE VELOCITY
CL = (KK+1)*0.5
KKC=KK/2
JCRS=0
DO 750 J=1,JJ
  IF(KK .EQ. 2*KKC)THEN
    L2=CL+.5
    UCL=(U(J,L2)+U(J,L2-1))/2
  ELSE
    L2=CL
    UCL=U(J,L2)
  ENDIF
  UB(J)=U(J,KK)-UCL
  IF(J .GT. 10 .AND. UB(J) .LT. 0.)THEN
    IF(JCRS .EQ. 0) JCRS=J
    UB(J)=UCL-U(J,1)
  ENDIF
750 CONTINUE
RETURN
END
```

No15...SUBROUTINE FOR SUSPENDED SEDIMENT CONCENTRATION PROFILE

```
SUBROUTINE DIEG(Wcr,Wsus,h,d50,TETA,PHES)
REAL*8 Pfac,Wcr,Wsus,PHES
REAL*8 PI,BETA,C1,DELTA,Cb,z,ZETA,DELT,A1,A2,z1
REAL*8 C0,C01,C2,C3,C4,Qs,CC,A
REAL*8 TETA,TETAC,h,d50
C Calculation
PI= 3.141592654
```



```

TETAC=0.047
BETA=0.65
d50=d50/1000.
CC=PI/6.*BETA/(TETA-TETAC)
Pfac= 1./(1.+CC**4.)*0.25
C*Cb
C C1=ALUB
C1= (TETA-TETAC-PI/6.*BETA*Pfac)/0.027/TETA/2.65
IF(C1.LE.0) THEN
  PHES= 0
  GOTO 1000
ENDIF
DELTA= DSQRT(C1)
Cb= 0.65/(1.+1./DELTA)**3.
C*Uf,z,ZETA AND DELT
z= 2.5*Wsus/Wcr
ZETA= 13.*Wsus/Wcr
DELT= 0.192*h
A1= 2.*d50/h
A2= DELT/d50/2.
z1= 1.-z
C* Calculation
C1=8.5*A1/z1*(A2**z1-1.)+2.5*A1/z1*(A2**z1*(DLOG(A2)-1./z1)+1./z1)
C0= -0.808*ZETA
C01= A2**z
C2= (5.7+2.5*DLOG(A2))/C01*(1-DEXP(C0))/ZETA
C3= 16.1/C01*((1.+ZETA*0.192)/ZETA/ZETA-DEXP(C0)*(ZETA+1.)/ZETA**2)
C4= 8.05/C01*(0.192*0.192/ZETA+2*(1.+ZETA*0.192)/ZETA/ZETA
&      -DEXP(C0)*(3./ZETA+2./ZETA/ZETA) )
Qs= Wcr*Cb*h*(C1+C2+C3-C4)
C0= 1.65*9.81*d50**3.
PHES= Qs/DSQRT(C0)
1000 CONTINUE
C NOT TO MIX THE DIMENSION
d50=d50*1000.
RETURN
END

```

No16.... SUBROUTINE FOR INTERPOLATION OF THE FUNCTION

```

SUBROUTINE INTEPO(J,X,FX,X1,F1,IMAX)
PARAMETER(N=50)
INTEGER I,J,IMAX
REAL*8 X,FX,X1,F1
DIMENSION X(N),FX(N)
C
IF(X1 .LT. X(1))THEN
  F1=FX(1)
  GOTO 70
ELSEIF(X1 .GT. X(IMAX))THEN
  F1=FX(IMAX)
  GOTO 70
ELSE

```

```

DO 60 I=1,IMAX
  IF(X1 .GE. X(I) .AND. X1 .LT. X(I+1))THEN
    F1=(FX(I+1)-FX(I))/(X(I+1)-X(I))*(X1-X(I))+FX(I)
    GOTO 70
  ENDIF
60 CONTINUE
  ENDIF
70 CONTINUE
  RETURN
  END

```

No17... SUBROUTINE FOR TABULATION OF RESULT

```

SUBROUTINE LST(T,QI,H0,WIDTH,UB,JCRS)
PARAMETER(N=100,M=15,LL=10)
REAL QI, DN, RSC, DSC, CHE, EPS, RHS, MU, DM, DT, TOUC, DEL, BETA, TTIME, S
INTEGER T, JJ, KK, MM(M), VCOUNT, ITER, tp1, tp2, TT, HCOUNT, PLOT, L, TP, L2,
& JCRS
DIMENSION RH(N,M), RU(N,M), UB(N)
common /f1/CHE, SLOPE, RSC, DSC, RN, DN, JJ, KK, EQU, L, TP(LL), CHEL(N,M),
& RSCL(LL), DSCL(LL), HINIT(M), DPW(M), H(N,M), F(N,M),
& Q(N,M), P(N,M), QC(N)
common /f2/DSP(N,M), RSP(N,M), DSH(N,M), RSH(N,M), DSQ(N,M), RSQ(N,M),
& DNP(N,M), RNP(N,M), DNH(N,M), RNH(N,M), DNQ(N,M), RNQ(N,M),
& U(N,M), V(N,M), RSTP(N,M), RSTH(N,M), RSTQ(N,M)
common /f3/DT, TOUC, TOUS(N,M), DM, SS(N,M), SN(N,M), MU(N,M), TANS(N,M)
& DEL, TAND(N,M), ALSF(N,M), PLOT, TITLE
common /f4/BETA, GT(N,M), U0(M), HNP1(N,M), TTIME, TT, HCOUNT, TOUS0(M),
& SS0(M), MU0(M), TOUP(N,M)

```

C

```

OPEN(7, FILE='plt7.DAT', STATUS='NEW')
OPEN(8, FILE='plt8.DAT', STATUS='NEW')
OPEN(9, FILE='plt9.DAT', STATUS='NEW')
OPEN(10, FILE='plt10.DAT', STATUS='NEW')
OPEN(11, FILE='plt11.DAT', STATUS='NEW')
OPEN(12, FILE='plt12.DAT', STATUS='NEW')
OPEN(13, FILE='plt13.DAT', STATUS='NEW')
OPEN(14, FILE='plt14.DAT', STATUS='NEW')
OPEN(15, FILE='plt15.DAT', STATUS='NEW')
OPEN(16, FILE='plt16.DAT', STATUS='NEW')
OPEN(17, FILE='plt17.DAT', STATUS='NEW')
OPEN(18, FILE='plt18.DAT', STATUS='NEW')
OPEN(19, FILE='plt19.DAT', STATUS='NEW')
OPEN(20, FILE='plt20.DAT', STATUS='NEW')

```

C

```

WRITE (4,20) T,JCRS
20 FORMAT('TIME STEP',I4,10X,'CROSS-OVER SECT. No.=',I4)
DO 10 J=1,JJ
  WRITE (4,70) J,(P(J,K),K=1, KK),(Q(J,K),K=1, KK),
& (CHEL(J,K),K=1, KK),
& QI, QC(J), (-HNP1(J,K),K=1, KK),
& (SS(J,K),K=1, KK),(SN(J,K),K=1, KK)
70 FORMAT ('SECT.',I3,1X,'P (M2/S)',3E11.4,
& /,9X,'Q (M2/S)',3E11.4,/,8X,'CHE (M.5/S)',3E11.4,

```



```

&      /,10X,E11.4,'=INITIAL Q',
&      4X,E11.4,'=CALCULATED Q ',
&      /,9X,'Zn+1 (M)',3E11.4,/,9X,'SS(M2/S)',
&      3E11.4,/,9X,'SN(M2/S)',3E11.4,
&      /,159('-')
10 CONTINUE
C FOR PLOTTING THE CROSS-SECTIONS OF THE RIVER
  IF(PLOT .EQ. 1) THEN
    DO 71 J=1,JJ
      DO 71 K=1,KK
        WRITE(7,72)K,-HNP1(J,K)
72 FORMAT(4X,I2,1X,E11.4)
71 CONTINUE
C FOR PLOTTING THE BED LEVEL PROFILE
  ELSEIF(PLOT .EQ. 2) THEN
    DO 7 K=1,KK
      WRITE(19,77)K,-HNP1(JJ,K)
77 FORMAT(4X,I2,1X,E11.4)
7 CONTINUE
    DO 907 J=1,JJ
      s=(j-1)*dsc/1000.
      write(7,*)s,-HNP1(j,kk)
      write(8,*)s,-HNP1(j,kk-1)
      write(9,*)s,-HNP1(j,KK-2)
      write(10,*)s,-HNP1(j,KK-5)
      write(11,*)s,-HNP1(j,KK-7)
      write(12,*)s,-HNP1(j,1)
C
      write(13,*)s,U(j,KK)
      write(14,*)s,U(j,KK-1)
      write(15,*)s,U(j,KK-2)
      write(16,*)s,U(j,KK-5)
      write(17,*)s,U(j,KK-7)
      write(18,*)s,U(j,1)
C
      WRITE(20,*)S,UB(J)
907 CONTINUE
C FOR PLOTTING THE RELATIVE MAIN FLOW VELOCITY
  ELSEIF(PLOT .EQ. 3) THEN
    do 908 j=1,jj
      s=(j-1)*dsc/1000.
      write(7,*)s,U(j,KK)
      write(8,*)s,U(j,KK-1)
      write(9,*)s,U(j,1)
908 continue
C FOR STREAMLINE CURVATURE
  ELSEIF(PLOT .EQ. 4) THEN
    do 909 j=1,jj
      s=(j-1)*dsc/1000.
      write(7,*)s,RSTP(j,kk)
      write(8,*)s,RSTP(j,kk-1)
      write(9,*)s,RSTP(j,1)
909 continue

```

```

C FOR PLOTTING THE TRANSVERSE VELOCITY @ CENTRE LINE
ELSE
  do 910 j=1,jj
    s=(j-1)*dsc/1000.
    write(7,*)s,v(j,KK)
    write(8,*)s,v(j,KK-1)
    write(9,*)s,v(j,1)
910 continue
ENDIF
CLOSE(7)
CLOSE(8)
CLOSE(9)
CLOSE(10)
CLOSE(11)
CLOSE(12)
CLOSE(13)
CLOSE(14)
CLOSE(15)
CLOSE(16)
CLOSE(17)
CLOSE(18)
CLOSE(19)
CLOSE(20)
RETURN
END

```

No18.... SOUBROUTINE FOR OUTPUT HEADING

```

SUBROUTINE PRT(WIDTH,KSN,C,ITER)
PARAMETER(N=100,M=15,LL=10)
common /f1/CHE,SLOPE,RSC,DSC,RN,DN,JJ,KK,EQU,L,TP(LL),CHEL(N,M),
&      RSCL(LL),DSCL(LL),HINIT(M),DPW(M),H(N,M),F(N,M),
&      Q(N,M),P(N,M),QC(N)
common /f3/DT,TOUC,TOUS(N,M),DM,SS(N,M),SN(N,M),MU(N,M),TANS(N,M)
&      ,DEL,TAND(N,M),ALSF(N,M),PLOT,TITLE
common /f4/BETA,GT(N,M),U0(M),HNP1(N,M),TTIME,TT,HCOUNT,TOUS0(M),
&      SS0(M),MU0(M),TOUP(N,M)
REAL CHE,SI,RSC,RN,DIA,DSC,DN,TTIME,TTM,DT,DD,HINIT,DPW,WIDTH,
&      KSN,C,ERR
DIMENSION MM(M)
INTEGER JJ,KK,ITER,MM,TP1,TP2,TP3,TP4,TP5,TP6,TP7,TP8,TP9,TP,L
CHARACTER*50 TITLE
WRITE(4,60)TITLE
60 FORMAT(18X,'*****',
& /,18X,'* STEADY STATE FLOW COMPUTATION *',
& /,18X,'* Four point scheme *',
& /,18X,'*****',
& /,5x,'Transport formula.....',(A20))
DO 61 I6=1,KK
MM(I6)=I6

```



```

61 CONTINUE
  DD=DT/3600
  IF(TTIME .GE. 86400)THEN
    TTM=TTIME/86400
    WRITE (4,62) CHE,SLOPE,RSC,RN,DSC,DN,JJ,KK,L,ITER,DD,TTM,BETA,
    &      DM,WIDTH,KSN,C
62 FORMAT(5X,'INPUT DATA',/5X,10('-'),/5X,
  & 'Chezy coefficient (Initial) =',f7.2,'(m**0.5/s)',/5X,
  & 'Initial bed slope =',E11.4,/5X,
  & 'Centre line curvature =',E11.4,/5X,
  & 'Curvature in n-direction =',E11.4,/5X,
  & 'Centre line distance step =',f7.2,'(meter)',/5X,
  & 'Distance step on the n-axis =',f7.2,'(meter)',/5X,
  & 'No. of points in S-direction =',I4,'(points)',/5X,
  & 'No. of points in n-direction =',I4,'(points)',/5X,
  & 'No. of turning points =',I4,'(points)',/5X,
  & 'No. of iteration =',I4,'(times)',/5X,
  & 'Time step =',f7.2,'(hours)',/5X,
  & 'Total simulation time =',f7.2,'(days)',/5X,
  & 'Beta coefficient =',f7.2,/5X,
  & 'Sediment grain size diameter =',E11.4,'(meter)',/5X,
  & 'Width of the river =',f7.2,/5X,
  & 'ksn =',f7.2,/5X,
  & 'c ,power for steep bank =',f7.2)
  ELSE
    TTM=TTIME/3600
    WRITE (4,63) CHE,SI,RSC,RN,DSC,DN,JJ,KK,L,ITER,DD,TTM,BETA,
    &      DM
63 FORMAT(5X,'INPUT DATA',/5X,10('-'),/5X,
  & 'Chezy coefficient (Initial) =',f7.2,'(m**0.5/s)',/5X,
  & 'Initial bed slope =',E11.4,/5X,
  & 'Centre line curvature =',E11.4,/5X,
  & 'Curvature in n-direction =',E11.4,/5X,
  & 'Centre line distance step =',f7.2,'(meter)',/5X,
  & 'Distance step on the n-axis =',f7.2,'(meter)',/5X,
  & 'No. of points in S-direction =',I4,'(points)',/5X,
  & 'No. of points in n-direction =',I4,'(points)',/5X,
  & 'No. of turning points =',I4,'(points)',/5X,
  & 'No. of iteration =',I4,'(times)',/5X,
  & 'Time step =',f7.2,'(hours)',/5X,
  & 'Total simulation time =',f7.2,'(hours)',/5X,
  & 'Beta coefficient =',f7.2,/5X,
  & 'Sediment grain size diameter =',E11.4,'(meter)')
  ENDIF
c
  WRITE (4,64) (TP(I),I=1,L)
64 FORMAT(/5X,'Positions of the TP(L)',/5X,'J =',2x,I4,/5X,159('-'))
c
  WRITE (4,65) (CHEL(I),I=1,L)
65 FORMAT(/5X,'Chezy coeff. for different reaches',/5X,9F6.2,
  & /5X,159('-'))
c
  WRITE (4,66) (DSCL(I),I=1,L)

```

```
66 FORMAT(/,5X,'Centre line distance steps',/,5X,9F8.2,
& /,159('-'))
c
WRITE (4,67) (RSCL(I),I=1,L)
67 FORMAT(/,5X,'Centre line curvatures',/,5X,9E11.4,/,159('-'))
c
WRITE(4,68)(MM(I),I=1,KK)
68 FORMAT(/,5X,'[ K POINTS ]',11X,5I7)
WRITE (4,69) (HINIT(II),II=1,KK)
69 FORMAT (5X,97('-'),/,5X,'INITIAL WATER DEPTH [M]',3X,5F7.4)
WRITE (4,70) (DPW(II),II=1,KK)
70 FORMAT (5X,'FLUX AT WEST BOUNDRY [M2/S]',2X,5F7.4)
WRITE (4,71)(MM(I),I=1,KK)
71 FORMAT (/,35X,'TABULATION OF RESULTS ;P & Q OVER THE SECTION ',
& /,35X,47('-'),/, '[ K POINTS ]',5I11,/,159('-'))
RETURN
END
```


B.1 Roughness predictor model; Dune size calculation

This program is compatible with simulation model *HYDHST.FOR*.

```

PROGRAM ROUGH
PARAMETER (N=100)
REAL*8 PHES,PHES2,DPHES,Wcr,Wsus,Wcr2,PERC2,dcr2,dsus2,
& dsus,wsus2,DEL,G,RBD,UUfp,Qd,Up,Ufp,wsucr,Kd,bp,
& THPP1,THPP2,MANN,WSWCR2,THE,Re,Nu,UUf2,h2
REAL*8 PHEB,DPHEB,CHE,FF,TETA2,TEP,TETA,TETAC,U,X,UUf,Uf,HYDR,X1
REAL*8 QS,THpp,C1,C2,C3,TH2,SLOPE,Q,hd,d50,WIDTH,XX,A
REAL*8 w,d,ds,PERC,TH,LH,FTILE,FT2,dcr,PERCR,Qn,DIF,DHh,LDH,h
INTEGER I,J,NP,NP1,NP2,MODEL,ITER,PCODE,K
DIMENSION w(N),d(N),ds(N),PERC(N),TH(N),LH(N),h(N),Qn(N)
CHARACTER*12 NAME
C
OPEN(4,FILE='BST.DAT',STATUS='NEW')
OPEN(6,FILE='Tep.DAT',STATUS='NEW')
OPEN(7,FILE='depth.DAT',STATUS='NEW')
OPEN(5,FILE='TEST.INP',STATUS='OLD')
1 READ(5,'(5A)',ERR = 3000, END = 3000)NAME
C
OPEN(3,FILE=NAME,STATUS='OLD')
CALL READ(Q,SLOPE,d50,WIDTH,hp,NP,NP1,NP2,MODEL,ITER,PCODE,
& w,d,ds,PERC,TH,LH)
C START
DEL = 1.65
G = 9.81
C1 = DEL*G*d50/1000.
Nu = 1.1E-006
J = 2
C CALCULATION WITH PLANE BED
h(1) = hp
DO 60 I=1,ITER
UUfp = (6. + 2.5*DLOG(h(I)/(2.5*d50/1000.)))
Ufp = DSQRT(G*h(I)*SLOPE)
Up = UUfp*Ufp
Qn(I) = h(I)*WIDTH*Up
DIF = DABS(Q-Qn(I))/Q
WRITE(*,*)'DIF',DIF
HYDR = WIDTH*h(I)/(2.*h(I) + WIDTH)
RBD = HYDR/h(I)
C
C HINTS FOR CONVERGING PROCESS
C FOR IF R/h < 0.7 ,Q=f(h); IF R/h > 0.7 ,Q=f(h**1.5)
C
IF(DIF .GT. .00001 .AND. I .LE. 2) THEN
IF(RBD .LE. 0.7) THEN
h(I+1)=h(I)*Q/Qn(I)
ELSE
h(I+1)=h(I)*(Q/Qn(I))**.66667

```

```

        ENDIF
    ELSEIF(DIF .GT. .00001 .AND. I .GT. 2) THEN
        XX=(Q-Qn(I))*(Q-Qn(I-1))
        IF(XX .LT. 0.) THEN
            h(I+1)=(Q-Qn(I-1))/(Qn(I)-Qn(I-1))*(h(I)-h(I-1))
            &
            +h(I-1)
        ELSE
            C
            h(I+1)=h(I-2)*0.1+h(I-1)*0.75+h(I)*0.15
            h(I+1)=h(I-1)*0.5+h(I)*0.5
        ENDIF
        IF (I .EQ. ITER) THEN
            WRITE(*,*)'PLEASE IMPROVE YOUR GUESS'
            CLOSE(3)
            GOTO 1
        ENDIF
    ELSE
        hp=h(I)
        GOTO 600
    ENDIF
60 CONTINUE
600 TEP = hp*SLOPE/(DEL*d50/1000.)
C
C ROUGHNESS COEFFICIENTS FOR PLANE BED
C TWO CASES FOR PLANE ; 1 - DEFINED BY PHYSICS & 2 - DEFINED BY USER !
IF(TEP .GE. 2.5) PCODE = 1
IF (PCODE .EQ. 1) THEN
    FF = 2/(UUfp*UUfp)
    CHE = DSQRT(2.*G/FF)
    MANN = HYDR**0.1666666/CHE
    Kd = hp/DEXP((UUfp-6.)/2.5)
    hd = hp
    TETA = TEP
    GOTO 1000
ELSE
C CALCULATION FOR DUNE PHASE (Initial step)
    hd = 1.75*hp
    UUf = 0.43*UUfp
ENDIF
C
C CALCULATION FOR DUNE PHASE (WITH EXACT SOLUTION)
DO 50 I = 1,ITER
    HYDR = WIDTH*hd/(2.*hd+WIDTH)
    WRITE(*,*)'HYDR',HYDR
    WRITE(*,*)'HD 2-ITER',hd
    Uf = DSQRT(G*hd*SLOPE)
    WRITE(*,*)'Uf',Uf
    U = UUf*Uf
    WRITE(*,*)'U',U
    RBD = HYDR/hd
    WRITE(*,*)'RBD',RBD
C CALCULATION OF THETA
    TETA = hd*SLOPE/(DEL*d50/1000.)
    THPP1 = (TETA-TEP)/TEP

```



```

C
C ROUGHNESS COEFFICIENTS
  FF = 2/(UUf*UUf)
  CHE = DSQRT(2.*G/FF)
  MANN= HYDR**0.1666666/CHE
  Kd = hd/DEXP((UUf-6.)/2.5)
  IF(MODEL .NE. 3) GOTO 100
C
C THIS IS DUNE DIMENSION CALCULATION, FREDSOE METHOD.
C
  IF(pcode .EQ. 2) THEN
    CALL BEDLOAD(TETA,PHEB,DPHEB)
    Wcr=Uf
    CALL INTEPO(JJ,w,d,Wcr,dcr,NP)
    CALL INTEPO(JJ,ds,Perc,dcr,Percr,NP1)
    FTILE=Percr/2.
    CALL INTEPO(J,Perc,ds,FTILE,dsus,NP1)
    IF(J .EQ. 0) GOTO 700
    CALL INTEPO(JJ,d,w,dsus,Wsus,NP)
C CALCULATION OF SUSPENDED SEDIMENT DIEGAARD EQUATION!
    CALL DIEG(Wcr,Wsus,hd,d50,TETA,PHES,wsucr)
C
C CALCULATION OF "DPHES"
    TETA2= TETA+0.01
    h2=TETA2*DEL*d50/1000./SLOPE
    Wcr2= DSQRT(G*h2*SLOPE)
    CALL INTEPO(JJ,w,d,Wcr2,dcr2,NP)
    CALL INTEPO(JJ,ds,Perc,dcr2,Perc2,NP1)
    FT2=Perc2/2.
    CALL INTEPO(JJ,Perc,ds,FT2,dsus2,NP1)
    CALL INTEPO(JJ,d,w,dsus2,Wsus2,NP)
C
    CALL DIEG(Wcr2,Wsus2,h2,d50,TETA2,PHES2,wsucr2)
    DPHES= (PHES2-PHES)/0.01
    UUf2=U/Ufp
    CALL DUNE(J,PHEB,DPHEB,PHES,DPHES,TETA,hd,d50,Wcr,
&      Wsus,THpp,DHh,LDH,UUf2,TH,LH,NP2)
    THPP2 = THPP
    GOTO 222
C THIS IS A CASE FOR NO SUSPENDED SEDIMENT LOAD.
C THIS CASE CAN BE OCCURED WHEN SHIELDS PARAMETER < 0.2
700 CONTINUE
    DPHES = 0.
    PHES = 0.
    UUf2=U/Ufp
    CALL DUNE(J,PHEB,DPHEB,PHES,DPHES,TETA,hd,d50,Wcr,Wsus,THpp,
&      DHh,LDH,UUf2,TH,LH,NP2)
    THPP2 = THPP
222  dif = DABS(THPP2-THPP1)
    IF (DIF .GT. .0001)THEN
      K = ITER-10
      IF (I .GE. K) THEN
        X= 0.85*THPP1 + 0.15*THPP2

```

```

        ELSE
            X= 0.51*THPP1+0.49*THPP2
        ENDIF
        WRITE(*,*)'X',X
        UUf = (0.995194-1.39391*X+1.2904*X*X-0.7273*X*X*X
&          +0.216207*X*X*X*X-0.0256065*X*X*X*X*X)*UUfp
        hd = (X+1)*hp
        ELSE
            GOTO 2000
        ENDIF
        IF (I .EQ. ITER-1) A=X
        IF (I .EQ. ITER) THEN
            X=(A+X)/2.
            UUf = (0.995194-1.39391*X+1.2904*X*X-0.7273*X*X*X
&          +0.216207*X*X*X*X-0.0256065*X*X*X*X*X)*UUfp
            hd = (X+1)*hp
            TETA = hd*SLOPE/(DEL*d50/1000.)
            GOTO 2000
        ENDIF
    ENDIF
50 CONTINUE
C *CALCULATION OF ROUGHNESS COEFF. FOR ALLUVIAL DUNE COVERED-BED*
2000 Kd = hd/DEXP((UUf-6.)/2.5)
    Uf = DSQRT(G*hd*SLOPE)
    Qd = WIDTH*hd*UUf*Uf
    Re = Uf*d50/1000./Nu
    IF (Re .LT. 12.) THEN
        WRITE(*,*)'WARNING!! RIPPLES RATHER THAN DUNES'
    ENDIF
C SEDIMENT TRANSPORT
1000 C3 = DSQRT(C1)*d50/1000.
C MP & M
    IF(MODEL .EQ. 1) THEN
        IF(TETA .LT. 0.047) THEN
            QS= 0.1E-08
        ELSE
            X1= TETA - 0.047
            QS= 8.*X1**1.5*C3*WIDTH
        ENDIF
    ENDIF
C E-H
    IF(MODEL .EQ. 2) THEN
        TH2= (TEP-0.06)/0.4
        IF(TH2 .LT. 0. .OR. PCODE .EQ. 1) THEN
            TH2= TEP
        ELSE
            TH2= DSQRT(TH2)
        ENDIF
        IF(TH2 .LT. 0.047) THEN
            QS= 0.1E-08
        ELSE
            QS= 0.1/FF*TH2**2.5*C3*WIDTH
        ENDIF
    
```



```

ENDIF
C E-F
IF(MODEL .EQ. 3 .AND. PCODE .EQ. 1) THEN
    CALL BEDLOAD(TEP,PHEB,DPHEB)
    Wcr=Ufp
C
    CALL INTEPO(JJ,w,d,Wcr,dcr,NP)
    CALL INTEPO(JJ,ds,Perc,dcr,Percr,NP1)
    FTILE = Percr/2.
    CALL INTEPO(J,Perc,ds,FTILE,dsus,NP1)
    IF(J .EQ. 0) GOTO 777
    CALL INTEPO(JJ,d,w,dsus,Wsus,NP)
    CALL DIEG(Wcr,Wsus,hp,d50,TEP,PHES,wswcr)
    GOTO 888
777 PHES=0.
888 IF(TEP .LT. 0.047) THEN
    PHEB= 0.1E-10
    PHES= 0.1E-10
    QS= 0.1E-08
    ELSE
    QS= (PHEB+PHES)*C3*WIDTH
    ENDIF
ELSEIF(MODEL .EQ. 3 .AND. PCODE .EQ. 2) THEN
    QS= (PHEB+PHES)*C3*WIDTH
ENDIF
C PRINT OUT RESULTS DATA FILE
CALL OUTTEST(QS,WIDTH,tep,teta,Qd,hd)
CLOSE(3)
GOTO 1
3000 close(4)
CLOSE(5)
close(6)
close(7)
STOP
END

C SUBROUTINE FOR READING INPUT DATA

SUBROUTINE READ(Q,SLOPE,d50,WIDTH,h,NP,NP1,NP2,MODEL,ITER,PCODE,
& w,d,ds,PERC,TH,LH)
PARAMETER(N=100)
REAL*8 Q,SLOPE,d50,WIDTH,h,w,d,ds,PERC,TH,LH
REAL A,B,C,E,F,A1,B1,C1,D1,E1,F1
DIMENSION w(N),d(N),ds(N),PERC(N),TH(N),LH(N)
INTEGER NP,NP1,NP2,MODEL,ITER,PCODE
C
CALL IREC
READ(3,*)A,B,C,E,F
    Q=A
    SLOPE=B
    d50=C
    WIDTH=E

```

```

      h = F
C
      CALL IREC
      READ(3,*)NP,NP1,NP2,MODEL,ITER,PCODE
C
      CALL IREC
      DO 1 I=1,NP
        READ(3,*)A1,B1
        w(I) = A1
        d(I) = B1
1 CONTINUE
C
      CALL IREC
      DO 2 I=1,NP1
        READ(3,*)C1,D1
        ds(I) = C1
        PERC(I) = D1
2 CONTINUE
C
      CALL IREC
      DO 3 I=1,NP2
        READ(3,*)E1,F1
        TH(I) = E1
        LH(I) = F1
3 CONTINUE
      RETURN
      END

```

C SUBROUTINE FOR SKIPS COMMENT CARDS IN INPUT DATA

```

      SUBROUTINE IREC
      CHARACTER*1 REC
      DO 10 I = 1,99
        READ (3,20) REC
        IF (REC .NE. 'C') GOTO 30
10 CONTINUE
20 FORMAT(A1)
30 RETURN
      END

```

C
C SUBROUTINE FOR OUTPUT

```

      SUBROUTINE OUT(Q,Qd,h,d50,SLOPE,WIDTH,CHE,PHEB,PHES,MANN,FF,QS,
&      wswcr,MODEL,PCODE,TETA,TEP,U,Uf,UUf,DHh,LDH,Kd,
&      hp,UUfp,Up,Ufp,Re,TH2)
      REAL*8 Q,Qd,h,d50,SLOPE,WIDTH,CHE,PHEB,PHES,FF,QS,TEP,DHh,Re,
&      U,Uf,UUf,TETA,THPP,wswcr,hp,UUfp,Up,Ufp,LDH,MANN,Kd,TH2
      CHARACTER*10 FORM,REGM
      INTEGER MODEL,PCODE

```

```

C
      IF(MODEL .EQ. 1) FORM = 'MP&M'
      IF(MODEL .EQ. 2) FORM = 'E&H'
      IF(MODEL .EQ. 3) FORM = 'JF'

```



```

C
  WRITE(4,100)
100 FORMAT(10X,38('-'))
  WRITE(4,10)
10 FORMAT(10X,'PLANE BED FLOW FIELD & TETA-P')
  WRITE(4,100)
  WRITE(4,11)Q,bp,UUfp,Up,Ufp,TEP
11 FORMAT(/,9X,'DISCHARGE',2X,'DEPTH PB',6X,'U/Uf',10X,'U',10X,'Uf',
&      8X,'TEP',/,6X,6(E11.4),/)
C
  IF(PCODE .EQ. 1) REGM = 'PLANE BED'
  IF(PCODE .NE. 1) THEN
    REGM = 'DUNE PHASE'
    TETAPP=TETA-TEP
  ENDIF
C
  WRITE(4,100)
  WRITE(4,12)REGM,Re
12 FORMAT(10X,'HYDRAULIC CONDITION @',5X,(A10),/,15X,
&      'Reynolds No. =',E11.4)
  IF (Re .LT. 12) THEN
    WRITE(4,9)
9    FORMAT(10X,' WARNING! Ripples rather than Dunes')
  ENDIF
  WRITE(4,100)
  WRITE(4,13)Qd,h,d50,SLOPE,WIDTH
13 FORMAT(/,10X,'DISCHARGE',5X,'DEPTH',5X,'GRAIN SIZE',5X,'SLOPE',
&      5X,'WIDTH',/,9X,2(F10.3),2X,F10.3,3X,F10.7,1X,F10.2,/)
  WRITE(4,100)
c
  IF(PCODE .EQ. 1) THEN
    WRITE(4,14)
14 FORMAT(10X,'RESULT FILE FOR ROUGHNESS COEFFICIENTS (PLANE BED)')
    WRITE(4,100)
    ELSE
    WRITE(4,15)
15 FORMAT(10X,'RESULT FILE FOR ROUGHNESS COEFFICIENTS (JF METHID)')
    WRITE(4,100)
  ENDIF
  WRITE(4,16)CHE,FF,MANN,Kd,TEP,TETAPP,TETA
16 FORMAT(/,6X,'CHE COEFF.',3X,'C & W',2X,'MANNING',2X,
&      'Kd-PARAMETER',2X,'TETA-P',2X,'TETA-PP',2X,'TOTAL TETA',
&      /,6X,F7.3,6X,F5.4,2X,F5.4,5X,F6.4,7X,F6.4,2X,F6.4,4X,F6.4)
  IF(MODEL .EQ. 3) THEN
    WRITE(4,17)FORM,PHEB,PHEB,QS
17 FORMAT(/,6X,'FORMULA',4X,'BED LOAD',4X,'SUSPENDED',3X,
&      'TOTAL SED. TRANSPORT',/,17X,'DM-LESS',5X,
&      'DM-LESS',11X,'M**3/SEC',/,6X,(A7),2X,E11.4,1X,E11.4,6X,
&      E11.4,/)
  ELSEIF(MODEL .EQ. 2) THEN
    WRITE(4,18)FORM,QS,TH2
18 FORMAT(/,6X,'FORMULA',3X,'TOTAL SED. TRANSPORT (M**3/SEC)',
&      3X,'TOTAL THETA',/,6X,(A7),5X,E11.4,24X,F6.4,/)

```

```

ELSE
  WRITE(4,19)FORM,QS,TETA
19 FORMAT(/,6X,'FORMULA',3X,'TOTAL SED. TRANSPORT (M**3/SEC)',
  & 3X,'TOTAL THETA',/,6X,(A7),5X,E11.4,24X,F6.4,/)
  ENDIF
  IF(PCODE .EQ. 2) THEN
    WRITE(4,20)
20  FORMAT(10X,'A FLOW FIELD FOR A CERTAIN CONDITION')
    WRITE(4,100)
    IF(MODEL .EQ. 3) THEN
      WRITE(4,21)UUf,U,Uf,wswcr
21  FORMAT(/,9X,' U / Uf',6X,'MEAN VELOCITY',3X,
  & 'FRIC. VELOCITY',3X,'Wsus / Uf',/,6X,
  & F10.3,2X,F10.3,6X,F10.3,6X,F10.3)
      WRITE(4,22)DHh,LDH
22  FORMAT(/,8X,'DUNE HEIGHT / WATER DEPTH',2X,
  & 'DUNE SIZE (L/H)',/,14X,E11.4,9X,F9.4,/)
      WRITE(4,100)
    ELSE
      WRITE(4,23)UUf,U,Uf
23  FORMAT(/,9X,' U / Uf',6X,'MEAN VELOCITY',3X,
  & 'FRIC. VELOCITY',/,6X,F10.3,2X,F10.3,6X,F10.3)
      WRITE(4,100)
    ENDIF
  ENDIF
  RETURN
END

```

C SUBROUTINE FOR CALCULATION OF BEDLOAD BY FREDSSØE METHOD

```

SUBROUTINE BEDLOAD(TETA,PHEB,DPHEB)
REAL*8 TETA,TETA2,TETAC,BETA,PI,A
REAL*8 PHEB,PHEB2,DPHEB,PFAC,CC
C
C CALCULATION OF P VALUE
C
  PI=3.141592654
  TETAC=0.047
  BETA=0.65
  IF(TETA .LT. TETAC) THEN
    PHEB = 0.
    DPHEB = 0.
    GOTO 10
  ENDIF
C
C PHE-B
  CC=PI/6.*BETA/(TETA-TETAC)
  PFAC=1./(1.+CC**4)**0.25
  A=(DSQRT(TETA)-0.7*DSQRT(TETAC))
  PHEB = 5.*PFAC*A
C DPHE-B
  TETA2=TETA+0.01
  CC=PI/6.*BETA/(TETA2-TETAC)

```



```

PFAC=1./(1.+CC**4.)**0.25
A=(DSQRT(TETA2)-0.7*DSQRT(TETAC))
PHEB2 = 5.*PFAC*A
DPHEB=(PHEB2-PHEB)/0.01
10 RETURN
END

```

C SUBROUTINE FOR DUNE DIMENSIONS

```

SUBROUTINE DUNE(J,PHEB,DPHEB,PHES,DPHES,TETA,h,d50,Wcr,Wsus,
& THpp,DHh,LDH,UUf,TH,LH,NP2)
PARAMETER (N=100)
REAL*8 PHES,DPHES,Wcr,Wsus,d50,HYDR,LDH1,LDH2
REAL*8 DHh,PHEB,TETA,DPHEB,C1,C11,C2,Ubf,h
REAL*8 RHS,DELTh,DelDH,LDH,UUf,THpp,TH,LH
INTEGER J,NP2
DIMENSION TH(N),LH(N)
C CALCULATION
d50=d50/1000.
DHh = PHEB/(2*TETA*(DPHEB + DPHES))
IF(J .EQ. 0) THEN
  J = 2
  DelDH = 0.
  goto 100
ELSE
  C2 = Wcr/Wsus
ENDIF
C1 = h/(13*2.5*d50)
Ubf = 8.3+2.5*DLOG(C1)
DELTh = C2*C2/13.*Ubf
DelDH = DELTh/DHh
C FOR SMALL VALUES OF TETAP(THM)
C ***CHECK FOR THE GREATER VALUE OF LDH IN THE CRITICAL REGION***
100 IF(TETA .LE. 0.2 .AND. TETA .GE. 0.047)THEN
  CALL INTEPO(JJ,TH,LH,TETA,LDH,NP2)
  LDH1=LDH
C CHECK POINT ; LHD FROM EQUATION
LDH2 = (16.*PHEB+(16.+DelDH)*PHES)/(PHEB+PHES)
WRITE(*,*)'LDH2',LDH2
IF(LDH1 .GE. LDH2) THEN
  LDH = LDH1
ELSE
  LDH = LDH2
ENDIF
ELSE
  LDH = (16.*PHEB+(16.+DelDH)*PHES)/(PHEB+PHES)
ENDIF
THpp = 0.5*UUf*UUf*DHh/LDH
d50=d50*1000.
RETURN
END

```

RIVER PLAN-FORM MOVEMENT IN AN ALLUVIAL PLAIN

C SUBROUTINE FOR SUSPENDED SEDIMENT CONCENTRATION PROFILE

```

SUBROUTINE DIEG(Wcr,Wsus,h,d50,TETA,PHES,wsucr)
PARAMETER (N=100)
REAL*8 Pfac,Wcr,Wsus,PHES,wsucr
REAL*8 PI,BETA,C1,DELTA,b,Cb,z,ZETA,DELTA,A1,A2,z1
REAL*8 C0,C01,C2,C3,C4,Qs,CC,A
REAL*8 TETA,TETAC,h,d50
C Calculation
PI= 3.141592654
TETAC=0.047
BETA=0.65
d50=d50/1000.
CC=PI/6.*BETA/(TETA-TETAC)
Pfac= 1./(1.+CC**4.)**0.25
C*Cb
C C1=ALUB
C1= (TETA-TETAC-PI/6.*BETA*Pfac)/0.027/TETA/2.65
IF(C1.LE.0) THEN
  PHES= 0
  GOTO 1000
ENDIF
DELTA=b= DSQRT(C1)
Cb= 0.65/(1.+1./DELTA)**3.
C*Uf,z,ZETA AND DELT
wsucr=Wsus/Wcr
z= 2.5*Wsus/Wcr
ZETA= 13.*Wsus/Wcr
DELTA= 0.192*h
A1= 2.*d50/h
A2= DELTA/d50/2.
z1= 1.-z
C Calculation
C1=8.5*A1/z1*(A2**z1-1.)+2.5*A1/z1*(A2**z1*(DLOG(A2)-1./z1)+1./z1)
C0= -0.808*ZETA
C01= A2**z
C2= (5.7+2.5*DLOG(A2))/C01*(1-DEXP(C0))/ZETA
C3= 16.1/C01*((1.+ZETA*0.192)/ZETA/ZETA-DEXP(C0)*(ZETA+1.)/ZETA**2)
C4= 8.05/C01*(0.192*0.192/ZETA+2*(1.+ZETA*0.192)/ZETA/ZETA
& -DEXP(C0)*(3./ZETA+2./ZETA/ZETA) )
Qs= Wcr*Cb*h*(C1+C2+C3-C4)
C0= 1.65*9.81*d50**3.
PHES = Qs/DSQRT(C0)
1000 CONTINUE
C NOT TO MIX THE DIMENSION
d50=d50*1000.
RETURN
END

```


C SUBROUTINE G_CURVE finds the grain-curves from the LOG-NORMAL distribution,
C when D_{50} , D_{15} and D_{85} are specified.

```
SUBROUTINE GCURVE(D50,D85D15,Wcr,Wsusp)
REAL*8 D85D15,d50,WFALL(2),B(5),C(3),D(3),Wcr,Wsusp
REAL*8 PI,ALFA,BETA,dcr,Dgrain,X,X1,T,C1,PROC2,PROCENT,PROC22
REAL*8 C2,X2,ds
```

C CONSTANTS

```
WFALL(1)= 0.143077
WFALL(2)= -0.00915762
B(1)= 0.31938153
B(2)= -0.356563782
B(3)= 1.781477937
B(4)= -1.821255978
B(5)= 1.330274429
C(1)= 2.515517
C(2)= 0.802853
C(3)= 0.010328
D(1)= 1.432788
D(2)= 0.189269
D(3)= 0.001308
```

C CALCULATION

```
PI= 4.D+00*ATAN(1.)
ALFA= DLOG(d50)
BETA= 1./D85D15
```

C T is help variabel

```
dcr= (Wcr-WFALL(2))/WFALL(1)
Dgrain= dcr/1000.
X= (DLOG(Dgrain)-ALFA)/BETA
IF(X.LT.0) THEN
```

```
  X1= DABS(X)
  T= 1./(1.+0.2316419*X1)
  C1= -0.5*X1**2.
  PROC2= 1./SQRT(2.)/DSQRT(PI)*DEXP(C1)*
& (B(1)*T+B(2)*T*T+B(3)*T**3+B(4)*T**4+B(5)*T**5)
```

ELSE

```
  T= 1./(1.+0.2316419*X)
  C1= -0.5*X**2.
  PROCENT= 1./SQRT(2.)/DSQRT(PI)*DEXP(C1)*
& (B(1)*T+B(2)*T*T+B(3)*T**3+B(4)*T**4+B(5)*T**5)
  PROC2= 1.-PROCENT
```

ENDIF

```
PROC22= PROC2/2.
```

IF(PROC22.LE.0.5) THEN

```
  C1= 1./PROC22**2.
  C2= DLOG(C1)
  T= DSQRT(C2)
  X2= (C(1)+C(2)*T+C(3)*T*T)/(1.+D(1)*T+D(2)*T*T+D(3)*T**3)- T
```

ELSE

```
  C1= 1./(1.-PROC22)**2.
  C2= DLOG(C1)
  T= DSQRT(C2)
  X2= T - (C(1)+C(2)*T+C(3)*T*T)/(1.+D(1)*T+D(2)*T*T+D(3)*T**3)
```

```

ENDIF
C1 = X2*BETA + ALFA
ds = DEXP(C1)
Wsusp = WFALL(1)*ds*1000. + WFALL(2)
RETURN
END

```

C SUBROUTINE FOR INTERPOLATION OF THE FUNCTION

```

SUBROUTINE INTEPO(J,X,FX,X1,F1,IMAX)
PARAMETER(N=100)
INTEGER I,J,IMAX
REAL*8 X,FX,X1,F1
DIMENSION X(N),FX(N)
C
IF(X1 .LT. X(1))THEN
  J = 0
  F1 = FX(1)
  GOTO 70
ELSEIF(X1 .GT. X(IMAX))THEN
  J = 1
  F1 = FX(IMAX)
  GOTO 70
ELSE
  DO 60 I=1,IMAX
    IF(X1 .GE. X(I) .AND. X1 .LT. X(I+1))THEN
      F1 = (FX(I+1)-FX(I))/(X(I+1)-X(I))*(X1-X(I)) + FX(I)
      GOTO 70
    ENDIF
  60 CONTINUE
  ENDIF
70 CONTINUE
RETURN
END

```

C SUBROUTINE FOR DATA

```

SUBROUTINE OUTTEST(QS,W2,tep,teta,Qd,hd)
REAL*8 Qs,W2,tep,teta,Qd,hd
C1
WRITE(4,10)W2,QS
10 FORMAT(2(E11.4))
C2
WRITE(6,11)tep,teta
11 FORMAT(2(E11.4))
C3
WRITE(7,12)Qd,hd
12 FORMAT(2(E11.4))
C4
RETURN
END

```


B.2 Input data example for the dune size and roughness predictor model

C INPUT DATA FILE FOR ROUGH.FOR PROGRAM

C
 C Q(M3/S) SLOPE d50(mm) WIDTH(m) h(m) First Guess
 L -----
 5000. .00000969 .47 22. 85.

C
 C NP NP1 NP2 MODEL ITER PCODE
 L - - - - -
 34 100 8 3 20 2

C
 C RELATIONSHIP BETWEEN SIEVE-GRAIN DIAMETER AND FALL VELOCITY

C -----
 L w (m/s) (20 deg.C) d(mm) grain-diameter
 .0080 .0850
 .0130 .1291
 .0180 .1719
 .0230 .2134
 .0280 .2536
 .0330 .2926
 .0380 .3304
 .0430 .3670
 .0480 .4027
 .0530 .4375
 .0580 .4717
 .0630 .5054
 .0680 .5390
 .0730 .5725
 .0780 .6064
 .0830 .6410
 .0880 .6766
 .0930 .7136
 .0980 .7525
 .1030 .7936
 .1080 .8374
 .1130 .8844
 .1180 .9352
 .1230 .9902
 .1280 1.0502
 .1330 1.1157
 .1380 1.1873
 .1430 1.2657
 .1480 1.3517
 .1530 1.4459
 .1580 1.5491
 .1630 1.6621
 .1680 1.7857
 .1730 1.9208

C
 C

C -----
C GRAIN SIZE DISTRIBUTION CURVE
C -----

L	ds(mm)	% finer
	.1000	.8538
	.1100	.6186
	.1200	.4965
	.1300	.4888
	.1400	.5964
	.1500	.8192
	.1600	1.1566
	.1700	1.6076
	.1800	2.1706
	.1900	2.8434
	.2000	3.6235
	.2100	4.5080
	.2200	5.4934
	.2300	6.5763
	.2400	7.7525
	.2500	9.0179
	.2600	10.3680
	.2700	11.7980
	.2800	13.3032
	.2900	14.8783
	.3000	16.5183
	.3100	18.2179
	.3200	19.9717
	.3300	21.7744
	.3400	23.6204
	.3500	25.5043
	.3600	27.4208
	.3700	29.3644
	.3800	31.3298
	.3900	33.3117
	.4000	35.3049
	.4100	37.3044
	.4200	39.3052
	.4300	41.3025
	.4400	43.2917
	.4500	45.2683
	.4600	47.2281
	.4700	49.1668
	.4800	51.0806
	.4900	52.9659
	.5000	54.8190
	.5100	56.6369
	.5200	58.4165
	.5300	60.1551
	.5400	61.8501
	.5500	63.4992
	.5600	65.1006
	.5700	66.6523
	.5800	68.1530

.5900	69.6014
.6000	70.9965
.6100	72.3376
.6200	73.6243
.6300	74.8564
.6400	76.0338
.6500	77.1569
.6600	78.2263
.6700	79.2426
.6800	80.2068
.6900	81.1202
.7000	81.9841
.7100	82.8001
.7200	83.5700
.7300	84.2957
.7400	84.9794
.7500	85.6232
.7600	86.2296
.7700	86.8011
.7800	87.3401
.7900	87.8494
.8000	88.3316
.8100	88.7896
.8200	89.2261
.8300	89.6438
.8400	90.0455
.8500	90.4339
.8600	90.8117
.8700	91.1812
.8800	91.5450
.8900	91.9052
.9000	92.2639
.9100	92.6230
.9200	92.9841
.9300	93.3485
.9400	93.7172
.9500	94.0910
.9600	94.4703
.9700	94.8549
.9800	95.2443
.9900	95.6377
1.0000	96.0334
1.0100	96.4296
1.0200	96.8234
1.0300	97.2118
1.0400	97.5908
1.0500	97.9558
1.0600	98.3014
1.0700	98.6214
1.0800	98.9088
1.0900	99.1558

RIVER PLAN-FORM MOVEMENT IN AN ALLUVIAL PLAIN

C -----
C FOR SMALL VALUE OF SHEAR (TETAP) DUNE STEEPNESS SHOULD BE
C CALCULATED DIFFERENTLY FROM THE BIG-SHEAR-VALUES
C -----

L TH shear LH dune steepness

.047	50.
.06	42.
.07	36.
.08	32.
.10	28.
.12	26.
.14	24.
.20	23.

C.1 River Plan-form Movement Model

C.1-1 MAIN PROGRAM

```

C *****
C *   River Plan-Form Movement Model   *
C *****
C
C DECLARATION OF VARIABLES
C -----
C   PARAMETER (G=9.81,N=60,M=15)
C   REAL QI, DN, RSC, DSC, CHE, EPS, RHS, MU, DM, DT, TOUC, DEL, BETA, TTIME,
C   &   TOUP, H0, WIDTH, KSN, C, RSQS, DQ, EPS1, DIFF, DH
C   INTEGER I, JJ, KK, MM(M), VCOUNT, ITER, tp1, tp2, T, TT, HCOUNT, PLOT,
C   &   PTIME, OUT, CODE, KKC, CORR, START, STOP
C   CHARACTER*50 TITLE
C   common /f1/CHE, RSC, RN, DSC, DN, JJ, KK, ITER, tp1, tp2, CHE1, RSC1, RN1,
C   &   DSC1, DN1, CHE2, RSC2, RN2, DSC2, DN2,
C   &   HINIT(M), DPW(M), H(N, M), F(N, M), Q(N, M), P(N, M), QC(N)
C   common /f2/DSP(N, M), RSP(N, M), DSH(N, M), RSH(N, M), DSQ(N, M), RSQ(N, M),
C   &   DNP(N, M), RNP(N, M), DNH(N, M), RNH(N, M), DNQ(N, M), RNQ(N, M),
C   &   U(N, M), V(N, M), RSTP(N, M), RSTH(N, M), RSTQ(N, M)
C   common /f3/DT, TOUC, TOUS(N, M), DM, SS(N, M), SN(N, M), MU(N, M), TANS(N, M)
C   &   , DEL, TAND(N, M), ALSF(N, M), PLOT, TITLE
C   common /f4/BETA, GT(N, M), U0(M), HNP1(N, M), TTIME, TT, HCOUNT, TOUS0(M),
C   &   SS0(M), MU0(M), TOUP(N, M)
C   DIMENSION RSQS(N), DQ(M), TEST(N), DIFF(N), EPS1(N)
C
C OPEN DATA INPUT
C
C   CALL READ2(OUT, CODE, H0, WIDTH, KSN, C, START)
C MAKE HEADING
C   OPEN(4, FILE='hyd.out', STATUS='new')
C   CALL PRT(WIDTH, KSN, C)
C
C CALCULATION OF GRID SIZES AND CURVATURE
C   CALL GRID(RSQS, DQ)
C
C CALCULATION OF THE NO. OF TIME STEPS
C   TT=TTIME/DT
C
C INITIAL STREAM LINE CURVATURE
C   DO 1 J=1, JJ
C     DO 1 K=1, KK
C       RSTH(J, K)=RSH(J, K)
C       RSTP(J, K)=RSP(J, K)
C       RSTQ(J, K)=RSQ(J, K)
C   1 CONTINUE
C
C START CALCULATION

```

```

PTIME = 0
VCOUNT = 0
DO 500 T=START,TT
  CORR=0
  IF(T .GT. START) VCOUNT=1
C INITIAL DISCHARGE CALCULATION AND U0(WEST BDY)
  QI = 0.0
  DO 2 K=1,KK
    DPW(K) = 2*P(1,K)-P(2,K)
    QI = QI +DPW(K)*DNP(1,K)
    U0(K) = DPW(K)/H(1,K)
  2 CONTINUE
99 DO 300 J=1,JJ
  IF(J .EQ. 1) THEN
    CALL WBDY(G,J,QI,VCOUNT,DQ,WIDTH,KSN,C,RSQS,T,START)
  ELSE
    CALL SECTJ(G,J,QI,VCOUNT,DQ,WIDTH,KSN,C,RSQS,T,START)
  ENDIF
300 CONTINUE
  IF(CORR .EQ. 1) THEN
    CORR=CORR+1
    CALL QQ
    GOTO 99
  ENDIF
  IF(CORR .EQ. 2) GOTO 700
  IF(VCOUNT .EQ. 1) GOTO 350
C
C CALCULATION OF TRANVERSE VELOCITIES
  CALL QQ
  IF(VCOUNT .EQ. 0)THEN
    VCOUNT=VCOUNT+1
    GOTO 99
  ENDIF
C CORRECTION FOR STREAM LINE CURVATURE
C
350 KKC=KK/2
360 DO 400 J=1,JJ
  IF(KK .EQ. 2*KKC)THEN
    TEST(J)=RSTQ(J,KKC)
  ELSE
    TEST(J)=RSTH(J,KKC+1)
  ENDIF
400 CONTINUE
  CALL STRM
  DO 401 J=1,JJ
  IF(KK .EQ. 2*KKC)THEN
    EPS1(J) = ABS(TEST(J)-RSTQ(J,KKC))
    DIFF(J) = .01*ABS(TEST(J))
  ELSE
    EPS1(J) = ABS(TEST(J)-RSTH(J,KKC+1))
    DIFF(J) = .01*ABS(TEST(J))
  ENDIF
  IF(EPS1(J) .GT. DIFF(J)) GOTO 360

```



```

401 CONTINUE
   CORR = CORR + 1
   GOTO 99
C CALCULATION OF BED TOPOGRAPHY
700 CALL BED(G, CODE, T, STOP, START)
   IF(STOP .EQ. 1) GOTO 800
   IF(T .EQ. START) CALL LST(T, QI, H0, WIDTH)
C
C TABULATION OF RESULT
   PTIME = PTIME + 1
   IF(PTIME .EQ. OUT) THEN
     CALL LST(T, QI, H0, WIDTH)
     CALL INTER(T)
     PTIME = 0
   ENDIF
C Initialization to new time step
   DO 3 K=1, KK
     DO 3 J=1, JJ
       H(J, K) = HNP1(J, K)
     3 CONTINUE
500 CONTINUE
800 CALL LST(T, QI, H0, WIDTH)
   CALL INTER(T)
   CLOSE(4)
   STOP
   END

```

C.1-2 GRID GENERATION PROGRAM

```

PROGRAM GEN
PARAMETER(N=205, M=15, LL=9)
common /f/CHE, SLOPE, RSC0, DSC0, RN, DN, JJ, KK, EQU, L, TP(LL), CHEL(LL),
&   RSCL(LL), DSCL(LL), HINIT(M), DPW(M), H(N, M), F(N, M),
&   Q(N, M), P(N, M), QC(N), RSC(N), DSC(N)
common /f2/DSP(N, M), RSP(N, M), DSH(N, M), RSH(N, M), DSQ(N, M), RSQ(N, M),
&   DNP(N, M), RNP(N, M), DNH(N, M), RNH(N, M), DNQ(N, M), RNQ(N, M),
&   U(N, M), V(N, M), RSTP(N, M), RSTH(N, M), RSTQ(N, M)
REAL CL, RN, DN, CHE, RSC, DSC, CHE1, RSC1, DSC1, CHE2, RSC2, DSC2, CHE3, RSC3,
&   DSC3, CHE4, RSC4, DSC4, CHE5, RSC5, DSC5, CHE6, RSC6, DSC6, CHE7, RSC7,
&   DSC7, CHE8, RSC8, DSC8, CHE9, RSC9, DSC9, TTIME, RATE
INTEGER J, K, JJ, KK, TP1, TP2, TP3, TP4, TP5, TP6, TP7, TP8, TP9, TP, L
DIMENSION DSQS(N), RSQS(N), DQ(M), D(M), DB(N)
C
OPEN(3, FILE='GRID.IN', STATUS='OLD')
OPEN(9, FILE='GRID.OUT', STATUS='NEW')
CALL IREC
READ(3, *) DSC0, RSC0, RN, DN, JJ, KK, CHE, TTIME, RATE
CALL IREC
READ(3, *) L, (TP(I), I=1, LL)
CALL IREC
READ(3, *) (CHEL(I), I=1, L)

```

```

      CALL IREC
      READ(3,*) (DSCL(I),I=1,L)
      CALL IREC
      READ(3,*) (RSCL(I),I=1,L)
C INITIAL MAPPING
      CALL GRID(RSQS,DQ)

C DISTANT OF BANK EROSION
      CALL BANK(DB,TTIME,RATE,JJ)
C NEW CENTRE LINE POSITION
      CALL CLP(DB)
C NEW GRID MAPPING
      CALL GRID(RSQS,DQ)
C OUTPUT LISTING
      CALL WRIT2D(RSQ ,N,M,'RSQNEW' ,',9,JJ,KK)
      CALL WRIT2D(RSP ,N,M,'RSPNEW' ,',9,JJ,KK)
      CALL WRIT2D(RSH ,N,M,'RSHNEW' ,',9,JJ,KK)
      CLOSE(9)
      STOP
      END

C
      SUBROUTINE WRIT2D(ARRAY,JDIM,KDIM,TEXT,FOUT,JACT,KACT)
      DIMENSION ARRAY(JDIM,KDIM)
      INTEGER FOUT
      CHARACTER*8 TEXT
      WRITE(FOUT,*) 'TYPE ',TEXT
      DO 100 J=1,JACT
         WRITE(FOUT,1) J,(ARRAY(J,K),K=1,KACT)
1      FORMAT(1H ,I3,100E9.3)
100 CONTINUE
      RETURN
      END

C SUBROUTINE FOR BANK LINE DISPLACEMENT (DB(J))
      SUBROUTINE BANK(DB,TTIME,RATE,JJ)
      PARAMETER(N=205)
      REAL TTIME,RATE,S
      INTEGER JJ
      DIMENSION DB(N),UB(N)
C
      OPEN(3,FILE='plt19.DAT',STATUS='OLD')
      OPEN(4,FILE='DB.DAT',STATUS='NEW')
      DO 10 J=1,JJ
         READ(3,*)s,UB(j)
         DB(J)=UB(J)*RATE*TTIME
         WRITE(4,*)s,DB(j)
10 CONTINUE
      CLOSE(3)
      CLOSE(4)
      RETURN
      END

C
C SUBROUTINE FOR NEW CENTRE LINE POSITION

```



```

SUBROUTINE CLP(DB)
PARAMETER(N=205,M=15,LL=9)
common /f/CHE,SLOPE,RSC0,DSC0,RN,DN,JJ,KK,ERR,L,TP(LL),CHEL(LL),
&      RSCL(LL),DSCL(LL),HINIT(M),DPW(M),H(N,M),F(N,M),
&      Q(N,M),P(N,M),QC(N),RSC(N),DSC(N)
common /f2/DSP(N,M),RSP(N,M),DSH(N,M),RSH(N,M),DSQ(N,M),RSQ(N,M),
&      DNP(N,M),RNP(N,M),DNH(N,M),RNH(N,M),DNQ(N,M),RNQ(N,M),
&      U(N,M),V(N,M),RSTP(N,M),RSTH(N,M),RSTQ(N,M)
DIMENSION CSP(N),CNP(N),CSPN(N),CNP(N),RSCN(N),DSCN(N),DB(N)
C
CSP(1)=0.0
CNP(1)=0.0
DO 11 J=2,JJ
    CNP(J)=0.0
    CSP(J)=CSP(J-1)+DSC(J-1)
11 CONTINUE
C AFTER BANK EROSION
CSPN(1)=0.0
DO 20 J=1,JJ
    IF(J .LT. JJ) THEN
        DB(J)=(DB(J)+DB(J+1))/2
    ELSE
        DB(J)=DB(J-1)
    ENDIF
C THIS PART IS USED IF AN APPROACH CHANNEL EXISTS IN THE SIMULATION
IF(RSC(J) .EQ. 0) THEN
    RSCN(J)=RSC(J)
ELSE
C THIS IS FOR THE FOLLOWING BEND TRAIN
IF(RSC(J) .GT. 0 .AND. DB(J) .GT. 0) THEN
    RSCN(J)=1/(1/RSC(J)+DB(J))
ELSEIF(RSC(J) .LT. 0 .AND. DB(J) .LT. 0) THEN
    RSCN(J)=1/(1/RSC(J)+DB(J))
ELSE
    RSCN(J)=1/(1/RSC(J)-DB(J))
ENDIF
ENDIF
IF(RSCN(J) .EQ. 0) THEN
    DSCN(J)=DSC(J)
ELSE
    DSCN(J)=DSC(J)*RSC(J)/RSCN(J)
ENDIF
CSPN(J+1)=CSPN(J)+DSCN(J)
CNP(N)=CNP(J)+DB(J)
20 CONTINUE
C
OPEN(7,FILE='GEN.OUT',STATUS='NEW')
OPEN(8,FILE='NEWWSC.OUT',STATUS='NEW')
WRITE(7,*)'DSCN',(DSCN(J),J=1,JJ)
WRITE(7,*)'RSCN',(RSCN(J),J=1,JJ)
WRITE(7,*)'CSPN',(CSPN(J),J=1,JJ)
WRITE(7,*)'CNP(N),(CNP(N),J=1,JJ)
WRITE(7,*)'CSP',(CSP(J),J=1,JJ)

```

```

WRITE(7,*)'CNP',(CNP(J),J=1,JJ)
DO 30 J=1,JJ
  RSC(J)=RSCN(J)
  DSC(J)=DSCN(J)
30 CONTINUE
WRITE(8,*)'DSC',(DSC(J),J=1,JJ)
WRITE(8,*)'RSC',(RSC(J),J=1,JJ)
CLOSE(7)
CLOSE(8)
RETURN
ENDC

```

C SUBROUTINE FOR NEWGRID SIZE AND NEWCURVATURE CALCULATION

```

SUBROUTINE GRID(DSQS,DQ)
PARAMETER(N=205,M=15,LL=9)
common /f1/CHE,SLOPE,RSC0,DSC0,RN,DN,JJ,KK,EQU,L,TP(LL),CHEL(LL),
& RSC1(LL),DSC1(LL),HINIT(M),DPW(M),H(N,M),F(N,M),
& Q(N,M),P(N,M),QC(N),RSC(N),DSC(N)
common /f2/DSP(N,M),RSP(N,M),DSH(N,M),RSH(N,M),DSQ(N,M),RSQ(N,M),
& DNP(N,M),RNP(N,M),DNH(N,M),RNH(N,M),DNQ(N,M),RNQ(N,M),
& U(N,M),V(N,M),RSTP(N,M),RSTH(N,M),RSTQ(N,M)
REAL CL,RN,DN,CHE,RSC,DSC,CHE1,RSC1,DSC1,CHE2,RSC2,DSC2,CHE3,RSC3,
& DSC3,CHE4,RSC4,DSC4,CHE5,RSC5,DSC5,CHE6,RSC6,DSC6,CHE7,RSC7,
& DSC7,CHE8,RSC8,DSC8,CHE9,RSC9,DSC9
INTEGER J,K,JJ,KK,TP1,TP2,TP3,TP4,TP5,TP6,TP7,TP8,TP9,TP,L
DIMENSION DSQS(N),RSQS(N),DQ(M),D(M)

```

C

C CALCULATION OF GRID CENTRE LINE

$$CL = (KK + 1.) * 0.5$$

C FOR N,DIRECTION GRID AND CURVATURE

```

DO 100 J=1,JJ
  DO 100 K=1,KK
    dnp(j,k)=dn
    rnp(j,k)=rn
    dnh(j,k)=dn
    rnh(j,k)=rn
    dnq(j,k)=dn
    rnq(j,k)=rn

```

100 CONTINUE

C FOR S,DIRECTION GRID AND CURVATURE

```

TP1 = TP(1)
IF(TP1 .GT. JJ) TP1=JJ+1
DO 1 J=1,TP1-1
  dsqs(j)=dsc(J)*(1+(0.5-cl)*dn*rsc(J))
  rsqs(j)=rsc(J)/(1+(0.5-cl)*dn*rsc(J))
  DO 1 K=1,KK
    d(k)=(k-cl)*dn
    dsp(j,k)=dsc(J)*(1+d(k)*rsc(J))
    rsp(j,k)=rsc(J)/(1+d(k)*rsc(J))
    dsh(j,k)=dsp(j,k)
    rsh(j,k)=rsp(j,k)

```



```

      dq(k) = (k + 0.5-cl)*dn
      dsq(j,k) = dsc(J)*(1 + dq(k)*rsc(j))
      rsq(j,k) = rsc(J)/(1 + dq(k)*rsc(J))
1 CONTINUE
C
c after turning point 1
c
  IF(tp1 .GT. jj) goto 1111
  CHE = CHEL(1)
C   DSC = DSCL(1)
C   RSC = RSCL(1)
  TP2 = TP(2)
  IF(tp2 .gt. jj) TP2 = JJ + 1
  DO 2 J = TP1, TP2-1
    dsqs(j) = dsc(J)*(1 + (0.5-cl)*dn*rsc(J))
    rsqs(j) = rsc(J)/(1 + (0.5-cl)*dn*rsc(J))
    DO 2 k = 1, KK
      dsp(j,k) = dsc(J)*(1 + d(k)*rsc(J))
      rsp(j,k) = rsc(J)/(1 + d(k)*rsc(J))
      dsh(j,k) = dsp(j,k)
      rsh(j,k) = rsp(j,k)
      dsq(j,k) = dsc(J)*(1 + dq(k)*rsc(J))
      rsq(j,k) = rsc(J)/(1 + dq(k)*rsc(J))
2 CONTINUE
C
after turning point 2
c
  IF(TP2 .GT. JJ) goto 1111
  CHE = CHEL(2)
C   DSC = DSCL(2)
C   RSC = RSCL(2)
  TP3 = TP(3)
  IF(TP3 .GT. JJ) TP3 = JJ + 1
  DO 3 J = TP2, TP3-1
    dsqs(j) = dsc(J)*(1 + (0.5-cl)*dn*rsc(J))
    rsqs(j) = rsc(J)/(1 + (0.5-cl)*dn*rsc(J))
    DO 3 k = 1, KK
      dsp(j,k) = dsc(J)*(1 + d(k)*rsc(J))
      rsp(j,k) = rsc(J)/(1 + d(k)*rsc(J))
      dsh(j,k) = dsp(j,k)
      rsh(j,k) = rsp(j,k)
      dsq(j,k) = dsc(J)*(1 + dq(k)*rsc(J))
      rsq(j,k) = rsc(J)/(1 + dq(k)*rsc(J))
3 CONTINUE
c
c after turning point 3
c
  IF(TP3 .GT. JJ) GOTO 1111
  CHE = CHEL(3)
C   DSC = DSCL(3)
C   RSC = RSCL(3)
  TP4 = TP(4)
  IF(TP4 .GT. JJ) TP4 = JJ + 1

```

WR-6
 West. Research and
 Training Centre
 Training Centre

```

DO 4 J=TP3,TP4-1
  dsqs(j)=dsc(J)*(1+(0.5-cl)*dn*rsc(J))
  rsqs(j)=rsc(J)/(1+(0.5-cl)*dn*rsc(J))
  DO 4 k=1,KK
    dsp(j,k)=dsc(J)*(1+d(k)*rsc(J))
    rsp(j,k)=rsc(J)/(1+d(k)*rsc(J))
    dsh(j,k)=dsp(j,k)
    rsh(j,k)=rsp(j,k)
    dsq(j,k)=dsc(J)*(1+dq(k)*rsc(J))
    rsq(j,k)=rsc(J)/(1+dq(k)*rsc(J))
  4 CONTINUE

```

c

c after turning point 4

c

```

IF(TP4 .GT. JJ) goto 1111
  CHE=CHL(4)
C   DSC=DSCL(4)
C   RSC=RSCL(4)
  TP5=TP(5)
IF(TP5 .GT. JJ) TP5=JJ+1
DO 5 J=TP4,TP5-1
  dsqs(j)=dsc(J)*(1+(0.5-cl)*dn*rsc(J))
  rsqs(j)=rsc(J)/(1+(0.5-cl)*dn*rsc(J))
  DO 5 k=1,KK
    dsp(j,k)=dsc(J)*(1+d(k)*rsc(J))
    rsp(j,k)=rsc(J)/(1+d(k)*rsc(J))
    dsh(j,k)=dsp(j,k)
    rsh(j,k)=rsp(j,k)
    dsq(j,k)=dsc(J)*(1+dq(k)*rsc(J))
    rsq(j,k)=rsc(J)/(1+dq(k)*rsc(J))
  5 CONTINUE

```

c

c after turning point 5

c

```

IF(TP5 .GT. JJ) goto 1111
  CHE=CHL(5)
C   DSC=DSCL(5)
C   RSC=RSCL(5)
  TP6=TP(6)
IF(TP6 .GT. JJ) TP6=JJ+1
DO 6 J=TP5,TP6-1
  dsqs(j)=dsc(J)*(1+(0.5-cl)*dn*rsc(J))
  rsqs(j)=rsc(J)/(1+(0.5-cl)*dn*rsc(J))
  DO 6 k=1,KK
    dsp(j,k)=dsc(J)*(1+d(k)*rsc(J))
    rsp(j,k)=rsc(J)/(1+d(k)*rsc(J))
    dsh(j,k)=dsp(j,k)
    rsh(j,k)=rsp(j,k)
    dsq(j,k)=dsc(J)*(1+dq(k)*rsc(J))
    rsq(j,k)=rsc(J)/(1+dq(k)*rsc(J))
  6 CONTINUE

```

c

c after turning point 6


```

c
IF(TP6 .GT. JJ) goto 1111
  CHE = CHEL(6)
c   DSC = DSCL(6)
c   RSC = RSCL(6)
  TP7 = TP(7)
IF(TP7 .GT. JJ) TP7 = JJ + 1
DO 7 J = TP6, TP7 - 1
  dsqs(j) = dsc(J) * (1 + (0.5-cl) * dn * rsc(J))
  rsqs(j) = rsc(J) / (1 + (0.5-cl) * dn * rsc(J))
  DO 7 k = 1, KK
    dsp(j,k) = dsc(J) * (1 + d(k) * rsc(J))
    rsp(j,k) = rsc(J) / (1 + d(k) * rsc(J))
    dsh(j,k) = dsp(j,k)
    rsh(j,k) = rsp(j,k)
    dsq(j,k) = dsc(J) * (1 + dq(k) * rsc(J))
    rsq(j,k) = rsc(J) / (1 + dq(k) * rsc(J))
7 CONTINUE

```

c after turning point 7

```

c
IF(TP7 .GT. JJ) GOTO 1111
  CHE = CHEL(7)
c   DSC = DSCL(7)
c   RSC = RSCL(7)
  TP8 = TP(8)
IF(TP8 .GT. JJ) TP8 = JJ + 1
DO 8 J = TP7, TP8 - 1
  dsqs(j) = dsc(J) * (1 + (0.5-cl) * dn * rsc(J))
  rsqs(j) = rsc(J) / (1 + (0.5-cl) * dn * rsc(J))
  DO 8 k = 1, KK
    dsp(j,k) = dsc(J) * (1 + d(k) * rsc(J))
    rsp(j,k) = rsc(J) / (1 + d(k) * rsc(J))
    dsh(j,k) = dsp(j,k)
    rsh(j,k) = rsp(j,k)
    dsq(j,k) = dsc(J) * (1 + dq(k) * rsc(J))
    rsq(j,k) = rsc(J) / (1 + dq(k) * rsc(J))
8 CONTINUE

```

c after turning point 8

```

c
IF(TP8 .GT. JJ) GOTO 1111
  CHE = CHEL(8)
c   DSC = DSCL(8)
c   RSC = RSCL(8)
  TP9 = TP(9)
IF(TP9 .GT. JJ) TP9 = JJ + 1
DO 9 J = TP8, TP9 - 1
  dsqs(j) = dsc(J) * (1 + (0.5-cl) * dn * rsc(J))
  rsqs(j) = rsc(J) / (1 + (0.5-cl) * dn * rsc(J))

```

```

DO 9 k=1, KK
  dsp(j,k)=dsc(J)*(1+d(k)*rsc(J))
  rsp(j,k)=rsc(J)/(1+d(k)*rsc(J))
  dsh(j,k)=dsp(j,k)
  rsh(j,k)=rsp(j,k)
  dsq(j,k)=dsc(J)*(1+dq(k)*rsc(J))
  rsq(j,k)=rsc(J)/(1+dq(k)*rsc(J))
9 CONTINUE
c
c after turning point 9
c
IF(TP9 .GT. JJ) GOTO 1111
  CHE=CHL(9)
C   DSC=DSCL(9)
C   RSC=RSCL(9)
DO 10 J=TP9, JJ
  dsqs(j)=dsc(J)*(1+(0.5-cl)*dn*rsc(J))
  rsqs(j)=rsc(J)/(1+(0.5-cl)*dn*rsc(J))
  DO 10 k=1, KK
    dsp(j,k)=dsc(J)*(1+d(k)*rsc(J))
    rsp(j,k)=rsc(J)/(1+d(k)*rsc(J))
    dsh(j,k)=dsp(j,k)
    rsh(j,k)=rsp(j,k)
    dsq(j,k)=dsc(J)*(1+dq(k)*rsc(J))
    rsq(j,k)=rsc(J)/(1+dq(k)*rsc(J))
10 CONTINUE
1111 RETURN
END

```

C.1-3 GRAPHICAL PRESENTATION PROGRAM

This program has to be included for the necessity of graphical output result. Although the simulations and calculations have been done in s and n coordinate system, cartesian coordinate system has to be used to plot the graph on the printer or plotter. Therefore conversion of the numerical output to graphical output the following programs are developed and listed below.

```

C SUBROUTINE FOR THE CALCULATION OF X-Y AND S-N CO-ORDINATES
C INITIAL DATA MEANDER WAVE LENGTH AND A SINE CURVE
C SUBROUTINE COORD
PROGRAM COORD
PARAMETER(N=112,M=5,LL=9)
common /f1/CHE,SLOPE,RSC0,DSC0,RN,DN,JJ,KK,ERR,L,TP(LL),CHEL(LL),
&   RSCL(LL),DSCL(LL),HINIT(M),DPW(M),H(N,M),F(N,M),
&   Q(N,M),P(N,M),QC(N),RSC(N),DSC(N)
common /f2/DSP(N,M),RSP(N,M),DSH(N,M),RSH(N,M),DSQ(N,M),RSQ(N,M),
&   DNP(N,M),RNP(N,M),DNH(N,M),RNH(N,M),DNQ(N,M),RNQ(N,M),
&   U(N,M),V(N,M),RSTP(N,M),RSTH(N,M),RSTQ(N,M)

```



```

common /f4/X(N),Y(N),XN(N),YN(N),ALP(N),ALPN(N),DB(N),A,
&    CSP(N),CNP(N),CSPN(N),CNP(N),RSCN(N),DSCN(N)
REAL CL,RN,DN,CHE,RSC,DSC,CHE1,RSC1,DSC1,CHE2,RSC2,DSC2,CHE3,RSC3,
&    DSC3,CHE4,RSC4,DSC4,CHE5,RSC5,DSC5,CHE6,RSC6,DSC6,CHE7,RSC7,
&    DSC7,CHE8,RSC8,DSC8,CHE9,RSC9,DSC9,DSX,DSY,D2SX,D2SY,REACH,
&    PI,S1
INTEGER J,K,JJ,KK,TP1,TP2,TP3,TP4,TP5,TP6,TP7,TP8,TP9,TP,L
DIMENSION DSQS(N),RSQS(N),DQ(M),D(M),UB(N),S(N),RSCN1(N),RSCN2(N)
&    ,DSCN1(N),DSCN2(N),r0(n),r1(n),r2(n)
C
C NOTE HERE RSCN1(J)=X-Y COORDINATE ;RSCN2(J)=S-N COORDINATE
OPEN(3,FILE='COORD.IN',STATUS='OLD')
OPEN(4,FILE='DB.DAT',STATUS='OLD')
OPEN(9,FILE='XY.DAT',STATUS='NEW')
OPEN(10,FILE='XNYN.DAT',STATUS='NEW')
OPEN(11,FILE='CURV.OUT',STATUS='NEW')
OPEN(12,FILE='RSC.DAT',STATUS='NEW')
OPEN(13,FILE='R0.DAT',STATUS='NEW')
OPEN(14,FILE='R1.DAT',STATUS='NEW')
OPEN(15,FILE='R2.DAT',STATUS='NEW')
CALL IREC
READ(3,*) DSC0,RSC0,RN,DN,JJ,KK,A,REACH
DO 100 J=1,JJ
    READ(4,*) S1,DB(J)
100 CONTINUE
C CALL IREC
C READ(3,*) (X(J),J=1,JJ)
C X-Y CO-ORDINATES FOR THE INITIAL CENTER LINE
C STARTING FROM (DELTA S ) AND REACH LENGTH ; ASSUME Y=SIN(X)
DSC0=REACH/(JJ-1)
DO 1 J=1,JJ
    IF(J.EQ. 1) THEN
        X(J)=0.0
        DX=
        S(J)=SQRT(DX**2+SIN(DX)**2)
        REACH=S(J)*(JJ-1)
    ELSE
        x(j)=(j-1)*dx
    ENDIF
    Y(J)=A*SIN(X(J))
    ALP(J)=ATAN(A*COS(X(J)))
    S(J)=X(J)/SIN(ALP(J))
1 CONTINUE
C
C X-Y CO-ORDINATES FOR THE NEW CENTER LINE
PI=3.141592654
DO 2 J=1,JJ
C
C    RSC(J)=RSC0*COS(2*PI*S(J)/REACH)
RSC(J)=RSC0*Sin(2*PI*S(J)/REACH)
XN(J)=X(J)-DB(J)*SIN(ALP(J))
YN(J)=Y(J)+DB(J)*COS(ALP(J))
ALPN(J)=ATAN((Y(J+1)-Y(J))/(X(J+1)-X(J)))

```

RIVER PLAN-FORM MOVEMENT IN AN ALLUVIAL PLAIN

```

        if(rsc(j) .ne. 0.)then
          r0(j)=1/rsc(j)
        endif
      2 CONTINUE
C
C DSCN arc length of the new center line & RSCN new curvature
C USING X-Y COORDINATE
      DO 10 J=1, JJ-1
        DSC(J)=SQRT((X(J+1)-X(J))**2+(Y(J+1)-Y(J))**2)
        DSCN1(J)=SQRT((XN(J+1)-XN(J))**2+(YN(J+1)-YN(J))**2)
      10 CONTINUE
      DO 20 J=1, JJ-2
        DXS=((XN(J+1)-XN(J))/DSCN1(J)+(YN(J+2)-YN(J+1))/DSCN1(J+1))/2
        DYS=((YN(J+1)-YN(J))/DSCN1(J)+(XN(J+2)-XN(J+1))/DSCN1(J+1))/2
        D2XS=((XN(J+2)-XN(J+1))/DSCN1(J+1)-(XN(J+1)-XN(J))/DSCN1(J))/
        &      0.5*(DSCN1(J)+DSCN1(J+1))
        D2YS=((YN(J+2)-YN(J+1))/DSCN1(J+1)-(YN(J+1)-YN(J))/DSCN1(J))/
        &      0.5*(DSCN1(J)+DSCN1(J+1))
        RSCN1(J+1)=(DXS*D2YS-D2XS*DYS)/(SQRT(DXS**2+DYS**2))**3
        r1(j)=1/rscn1(j+1)
      20 CONTINUE
C
C CALCULATION FOR NEW CENTER LINE POSITION
C THIS IS S-N COORDINATE
      CSP(1)=0.0
      CNP(1)=0.0
      DO 11 J=2, JJ
        CNP(J)=0.0
        CSP(J)=CSP(J-1)+DSC(J-1)
      11 CONTINUE
C AFTER BANK EROSION
C BE ALWAYS CAREFUL FOR STRAIGHT CHANNEL
      CSPN(1)=0.0
      DO 22 J=1, JJ
        IF(J .LT. JJ) THEN
          DB(J)=(DB(J)+DB(J+1))/2
        ELSE
          DB(J)=DB(J-1)
        ENDIF
        IF(RSC(J) .GT. 0 .AND. DB(J) .GT. 0) THEN
          RSCN2(J)=1/(1/RSC(J)+DB(J))
        ELSEIF(RSC(J) .LT. 0 .AND. DB(J) .LT. 0) THEN
          RSCN2(J)=1/(1/RSC(J)+DB(J))
        ELSE
          RSCN2(J)=1/(1/RSC(J)-DB(J))
        ENDIF
        r2(j)=1/rscn2(j)
        DSCN2(J)=DSC(J)*RSC(J)/RSCN2(J)
        CSPN(J+1)=CSPN(J)+DSCN2(J)
        CNPN(J)=CNP(J)+DB(J)
      22 CONTINUE
C PRINT X-Y CO-ORDINATES
      DO 3 J=1, JJ

```



```

WRITE(9,*)X(J),Y(J)
WRITE(10,*)XN(J),YN(J)
3 CONTINUE
C1
WRITE(11,*)'DSC(J)'
WRITE(11,60)(DSC(J),J=1,JJ-1)
60 FORMAT(/,(7E11.4),/,(7E11.4),/,(7E11.4),/,(7E11.4),/,(7E11.4)
& ,(7E11.4),/,(7E11.4),/,(7E11.4),/,(7E11.4),/,(7E11.4),/
& ,(7E11.4),/,(7E11.4),/,(7E11.4),/,(7E11.4),/,(2E11.4),/)
C2
WRITE(11,*)'DSCN1(J)'
WRITE(11,70)(DSCN1(J),J=1,JJ-1)
70 FORMAT(/,(7E11.4),/,(7E11.4),/,(7E11.4),/,(7E11.4),/,(7E11.4)
& ,(7E11.4),/,(7E11.4),/,(7E11.4),/,(7E11.4),/,(7E11.4),/
& ,(7E11.4),/,(7E11.4),/,(7E11.4),/,(7E11.4),/,(2E11.4),/)
CC2
WRITE(11,*)'DSCN2(J)'
WRITE(11,72)(DSCN2(J),J=1,JJ-1)
72 FORMAT(/,(7E11.4),/,(7E11.4),/,(7E11.4),/,(7E11.4),/,(7E11.4)
& ,(7E11.4),/,(7E11.4),/,(7E11.4),/,(7E11.4),/,(7E11.4),/
& ,(7E11.4),/,(7E11.4),/,(7E11.4),/,(7E11.4),/,(2E11.4),/)
C3
WRITE(11,*)'RSC(J)'
WRITE(11,75)(RSC(J),J=1,JJ-1)
75 FORMAT(/,(7E11.4),/,(7E11.4),/,(7E11.4),/,(7E11.4),/,(7E11.4)
& ,(7E11.4),/,(7E11.4),/,(7E11.4),/,(7E11.4),/,(7E11.4),/
& ,(7E11.4),/,(7E11.4),/,(7E11.4),/,(7E11.4),/,(2E11.4),/)
C4
WRITE(11,*)'RSCN1(J)'
WRITE(11,80)(RSCN1(J),J=1,JJ-1)
80 FORMAT(/,(7E11.4),/,(7E11.4),/,(7E11.4),/,(7E11.4),/,(7E11.4)
& ,(7E11.4),/,(7E11.4),/,(7E11.4),/,(7E11.4),/,(7E11.4),/
& ,(7E11.4),/,(7E11.4),/,(7E11.4),/,(7E11.4),/,(2E11.4),/)
C5
WRITE(11,*)'RSCN2(J)'
WRITE(11,90)(RSCN2(J),J=1,JJ-1)
90 FORMAT(/,(7E11.4),/,(7E11.4),/,(7E11.4),/,(7E11.4),/,(7E11.4)
& ,(7E11.4),/,(7E11.4),/,(7E11.4),/,(7E11.4),/,(7E11.4),/
& ,(7E11.4),/,(7E11.4),/,(7E11.4),/,(7E11.4),/,(2E11.4),/)
C6
DO 111 J=1,JJ
WRITE(12,*)S(J),RSC(J)
111 CONTINUE
DO 112 J=1,JJ
WRITE(13,*)S(J),R0(J)
112 CONTINUE
DO 113 J=1,JJ
WRITE(14,*)S(J),R1(J)
113 CONTINUE
DO 114 J=1,JJ
WRITE(15,*)S(J),R2(J)
114 CONTINUE
CLOSE(9)

```

```

CLOSE(10)
CLOSE(11)
CLOSE(12)
CLOSE(13)
CLOSE(14)
CLOSE(15)
STOP
END

```

C CALCULATION FOR BANK DISPLACEMENT (DB(J))

```

PROGRAM BANK
PARAMETER(N=205)
REAL RATE, TTIME, S
INTEGER JJ
DIMENSION DB(N), UB(N)

```

```

C
OPEN(4, FILE='BANK.IN', STATUS='OLD')
OPEN(5, FILE='plt19.DAT', STATUS='OLD')
OPEN(6, FILE='BANK.OUT', STATUS='NEW')
CALL IREC
READ(4, *) RATE, TTIME, JJ
DO 10 J=1, JJ
  READ(5, *) S, UB(J)
  DB(J) = UB(J) * RATE * TTIME
  WRITE(6, *) S, DB(J)
10 CONTINUE
CLOSE(4)
CLOSE(5)
CLOSE(6)
STOP
END

```

```

C
SUBROUTINE IREC
CHARACTER*1 REC
DO 10 I = 1, 99
  READ (4, 20) REC
  IF (REC .NE. 'C') GOTO 30
10 CONTINUE
20 FORMAT(A1)
30 RETURN
END

```

C THE CALCULATION OF X-Y AND S-N CO-ORDINATES

C AFTER THE CENTER LINE MOVEMENT

C THIS IS FOR A SERIE OF CIRCULAR BENDS

```

PROGRAM PLAN
PARAMETER(N=112, M=5, LL=9)
common /f1/CHE, SLOPE, RSC0, DSC0, RN, DN, JJ, KK, ERR, L, TP(LL), CHEL(LL),
& RSCL(LL), DSCL(LL), HINIT(M), DPW(M), H(N, M), F(N, M),
& Q(N, M), P(N, M), QC(N), RSC(N), DSC(N)
common /f2/DSP(N, M), RSP(N, M), DSH(N, M), RSH(N, M), DSQ(N, M), RSQ(N, M),
& DNP(N, M), RNP(N, M), DNH(N, M), RNH(N, M), DNQ(N, M), RNQ(N, M),

```



```

&      U(N,M),V(N,M),RSTP(N,M),RSTH(N,M),RSTQ(N,M)
common /f4/X(N),Y(N),XN(N),YN(N),ALP(N),ALPN(N),DB(N),A,
&      CSP(N),CNP(N),CSPN(N),CNPN(N),RSCN(N),DSCN(N)
REAL CL,RN,DN,CHE,RSC,DSC,CHE1,RSC1,DSC1,CHE2,RSC2,DSC2,CHE3,RSC3,
&      DSC3,CHE4,RSC4,DSC4,CHE5,RSC5,DSC5,CHE6,RSC6,DSC6,CHE7,RSC7,
&      DSC7,CHE8,RSC8,DSC8,CHE9,RSC9,DSC9,DSX,DSY,D2SX,D2SY,REACH,
&      PI,S1
INTEGER J,K,JJ,KK,TP1,TP2,TP3,TP4,TP5,TP6,TP7,TP8,TP9,TP,L
DIMENSION DSQS(N),RSQS(N),DQ(M),D(M),UB(N),S(N),RSCN1(N),RSCN2(N)
&      ,DSCN1(N),DSCN2(N),r0(n),r1(n),r2(n),teta(n),ta(n),
&      dx(n),dy(n)
C
C NOTE HERE RSCN1(J)=X-Y COORDINATE ;RSCN2(J)=S-N COORDINATE
OPEN(3,FILE='DATA1.IN',STATUS='OLD')
OPEN(4,FILE='DATA2.IN',STATUS='OLD')
OPEN(5,FILE='DB.DAT',STATUS='OLD')
OPEN(9,FILE='XY.DAT',STATUS='NEW')
OPEN(10,FILE='XNYN.DAT',STATUS='NEW')
C
CALL IREC
READ(3,*) dsc0,RSC0,dsc1,rscl,dsc2,rscl2,RN,DN,JJ,KK
DO 100 J=1,JJ
  READ(4,*) S,DB(J)
100 CONTINUE
  do 101 j=1,jj
    dsc(j)=dsc0
    rsc(j)=rsc0
101 continue
C X-Y CO-ORDINATES FOR THE INITIAL CENTER LINE (Y=f(X))
C IT ALSO CAN BE ANY GIVEN POINTS (PREFERABLY IN TABULATED FORM)
PI=3.141592654
S(1)=0.
X(1)=0.
Y(1)=0.
TA(1)=0.
ALP(1)=PI/2-DSC(1)*RSC(1)/2
DX(1)=DSC(1)*COS(ALP(1))
DY(1)=DSC(1)*SIN(ALP(1))
DO 1 J=2,JJ
  TETA(J)=DSC(J)*RSC(J)
  TA(J)=TA(J-1)+TETA(J-1)
  ALP(J)=PI/2-TETA(J)/2-TA(J)/2
  DX(J)=DSC(J)*COS(ALP(j))
  DY(J)=DSC(J)*SIN(ALP(j))
  S(J)=S(J-1)+DSC(J-1)
  X(J)=X(J-1)+DX(J-1)
  Y(J)=Y(J-1)+DY(J-1)
1 CONTINUE
C
C X-Y CO-ORDINATES FOR THE NEW CENTER LINE
DO 2 J=1,JJ
  XN(J)=X(J)-DB(J)*SIN(ALP(J))
  YN(J)=Y(J)+DB(J)*COS(ALP(J))

```

```

        ALPN(J)=ATAN((Y(J+1)-Y(J))/(X(J+1)-X(J)))
        if(rsc(j) .ne. 0.)then
C         r0(j)=1/rsc(j)
        endif
    2 CONTINUE
C
C DSCN arc length of the new center line & RSCN new curvature
C USING X-Y COORDINATE
    DO 10 J=1, JJ-1
        DSC(J)=SQRT((X(J+1)-X(J))**2+(Y(J+1)-Y(J))**2)
C         DSC(J)=DSC0
        DSCN1(J)=SQRT((XN(J+1)-XN(J))**2+(YN(J+1)-YN(J))**2)
    10 CONTINUE
    DO 20 J=1, JJ-2
        DXS=((XN(J+1)-XN(J))/DSCN1(J)+(YN(J+2)-YN(J+1))/DSCN1(J+1))/2
        DYS=((YN(J+1)-YN(J))/DSCN1(J)+(XN(J+2)-XN(J+1))/DSCN1(J+1))/2
        D2XS=((XN(J+2)-XN(J+1))/DSCN1(J+1)-(XN(J+1)-XN(J))/DSCN1(J))/
        & 0.5*(DSCN1(J)+DSCN1(J+1))
        D2YS=((YN(J+2)-YN(J+1))/DSCN1(J+1)-(YN(J+1)-YN(J))/DSCN1(J))/
        & 0.5*(DSCN1(J)+DSCN1(J+1))
        RSCN1(J+1)=(DXS*D2YS-D2XS*DYS)/(SQRT(DXS**2+DYS**2))**3
C         r1(j)=1/rscn1(j+1)
    20 CONTINUE
C
C CALCULATION FOR NEW CENTER LINE POSITION
C THIS IS S-N COORDINATE
        CSP(1)=0.0
        CNP(1)=0.0
        DO 11 J=2, JJ
            CNP(J)=0.0
            CSP(J)=CSP(J-1)+DSC(J-1)
    11 CONTINUE
C AFTER BANK EROSION
C BE ALWAYS CAREFUL FOR STRAIGHT CHANNEL
        CSPN(1)=0.0
        DO 22 J=1, JJ
            IF(J .LT. JJ) THEN
                DB(J)=(DB(J)+DB(J+1))/2
            ELSE
                DB(J)=DB(J-1)
            ENDIF
            IF(RSC(J) .GT. 0 .AND. DB(J) .GT. 0) THEN
                RSCN2(J)=1/(1/RSC(J)+DB(J))
            ELSEIF(RSC(J) .LT. 0 .AND. DB(J) .LT. 0) THEN
                RSCN2(J)=1/(1/RSC(J)+DB(J))
            ELSE
                RSCN2(J)=1/(1/RSC(J)-DB(J))
            ENDIF
C         r2(j)=1/rscn2(j)
        DSCN2(J)=DSC(J)*RSC(J)/RSCN2(J)
        CSPN(J+1)=CSPN(J)+DSCN2(J)
        CNPN(J)=CNP(J)+DB(J)
    22 CONTINUE

```



```

C PRINT X-Y CO-ORDINATES
  DO 3 J=1, JJ
    WRITE(9,*)X(J),Y(J)
    WRITE(10,*)XN(J),YN(J)
  3 CONTINUE
C1
  WRITE(11,*)'DSC(J)'
  WRITE(11,60)(DSC(J),J=1, JJ-1)
60 FORMAT(/,(7E11.4),/, (7E11.4),/, (7E11.4),/, (7E11.4),/, (7E11.4)
& ,(7E11.4),/, (7E11.4),/, (7E11.4),/, (7E11.4),/, (7E11.4),/,
& ,(7E11.4),/, (7E11.4),/, (7E11.4),/, (7E11.4),/, (2E11.4),/)
C2
  WRITE(11,*)'DSCN1(J)'
  WRITE(11,70)(DSCN1(J),J=1, JJ-1)
70 FORMAT(/,(7E11.4),/, (7E11.4),/, (7E11.4),/, (7E11.4),/, (7E11.4)
& ,(7E11.4),/, (7E11.4),/, (7E11.4),/, (7E11.4),/, (7E11.4),/,
& ,(7E11.4),/, (7E11.4),/, (7E11.4),/, (7E11.4),/, (2E11.4),/)
CC2
  WRITE(11,*)'DSCN2(J)'
  WRITE(11,72)(DSCN2(J),J=1, JJ-1)
72 FORMAT(/,(7E11.4),/, (7E11.4),/, (7E11.4),/, (7E11.4),/, (7E11.4)
& ,(7E11.4),/, (7E11.4),/, (7E11.4),/, (7E11.4),/, (7E11.4),/,
& ,(7E11.4),/, (7E11.4),/, (7E11.4),/, (7E11.4),/, (2E11.4),/)
-3
  WRITE(11,*)'RSC(J)'
  WRITE(11,75)(RSC(J),J=1, JJ-1)
75 FORMAT(/,(7E11.4),/, (7E11.4),/, (7E11.4),/, (7E11.4),/, (7E11.4)
& ,(7E11.4),/, (7E11.4),/, (7E11.4),/, (7E11.4),/, (7E11.4),/,
& ,(7E11.4),/, (7E11.4),/, (7E11.4),/, (7E11.4),/, (2E11.4),/)
C4
  WRITE(11,*)'RSCN1(J)'
  WRITE(11,80)(RSCN1(J),J=1, JJ-1)
80 FORMAT(/,(7E11.4),/, (7E11.4),/, (7E11.4),/, (7E11.4),/, (7E11.4)
& ,(7E11.4),/, (7E11.4),/, (7E11.4),/, (7E11.4),/, (7E11.4),/,
& ,(7E11.4),/, (7E11.4),/, (7E11.4),/, (7E11.4),/, (2E11.4),/)
C5
  WRITE(11,*)'RSCN2(J)'
  WRITE(11,90)(RSCN2(J),J=1, JJ-1)
90 FORMAT(/,(7E11.4),/, (7E11.4),/, (7E11.4),/, (7E11.4),/, (7E11.4)
& ,(7E11.4),/, (7E11.4),/, (7E11.4),/, (7E11.4),/, (7E11.4),/,
& ,(7E11.4),/, (7E11.4),/, (7E11.4),/, (7E11.4),/, (2E11.4),/)
C6
  DO 111 J=1, JJ
    WRITE(12,*)S(J),RSC(J)
  111 CONTINUE
  DO 112 J=1, JJ
    WRITE(13,*)S(J),R0(J)
  112 CONTINUE
  DO 113 J=1, JJ
    WRITE(14,*)S(J),R1(J)
  113 CONTINUE
  DO 114 J=1, JJ
    WRITE(15,*)S(J),R2(J)

```

114 CONTINUE

 CLOSE(9)

 CLOSE(10)

 CLOSE(11)

 CLOSE(12)

 CLOSE(13)

 CLOSE(14)

 CLOSE(15)

 STOP

 END

C

C SUBROUTINE FOR SKIPS COMMENT CARDS IN INPUT DATA

C

 SUBROUTINE IREC

 CHARACTER*1 REC

 DO 10 I = 1,99

 READ (3,20) REC

 IF (REC .NE. 'C') GOTO 30

10 CONTINUE

20 FORMAT(A1)

30 RETURN

 END

C.2 Variety of bank erosion models

The most important programs for the calculation of bank erosion rates are presented in this section. There are nine different bank erosion rate programs available from the present study. The program codes which are not listed here are simple implementation of the empirical bank erosion rate formulas mentioned earlier in Chapter 5. The brief description of the available bank erosion rate modules result from the present study are as following.

Part 1

These three modules are written in the fortran 77 code, will be listed hereafter.

1. BANK1.FOR ; Ariathurai and Arulanandan Model, 1978. Based on the flume studies. Cohesive material with 30% illite.
2. BANK2.FOR ; Based on hydrodynamic forces. Derivation has been presented in section C.1.
3. BANK3.FOR ; Hasegawa Model, 1987. Based on hydrodynamic forces. Rederivation has been made by author which is not mentioned in the original paper.

Part 2

These two modules are also written in the fortran 77 code, but attached with simulation model, see sections C.2 and C.3.

9. BANK9.FOR ; Ikeda et. al Model, 1981
This model is directly attached to the subroutine of the bank line displacement.
10. BANK10.FOR ; Parker Model, 1983
This model is also directly attached to the subroutine of the bank line displacement.

Part 3

These modules are simple mathematical relations therefore details are not listed here. The corresponding names of the empirical formulas for these modules, bank4 to bank8 can be seen in Chapter 5.

1. BANK4.FOR
2. BANK5.FOR
3. BANK6.FOR
4. BANK7.FOR
5. BANK8.FOR

C.2-1 Bank erosion rate calculation for cohesive material

```

PROGRAM BANK1
C Bank erosion rate calculation ; for "Cohesive material"
C
  PARAMETER (G=9.81,TOUC=0.047,DEL=1.65,COE=.00165,PS=2650.,N=50)
  INTEGER J,JJ
  DIMENSION Q(N),H(N),U(N),S0(N),B(N),CEE(N)
  REAL LENGTH,SLOPE,DIA,DS,DT,H0,B0,CHE,TOUB,TOUS,D
C
  OPEN (3,FILE = 'BANK1.IN',STATUS = 'OLD')
  OPEN (6,FILE = 'BANK1.OUT',STATUS='NEW')
  CALL IREC
  READ (3,*) H0,SLOPE,CHE,B0,DIA,LENGTH,DS,DT
  WRITE (6,5)
  WRITE (6,6) LENGTH,B0,SLOPE,DIA,CHE,DS,DT
5 FORMAT (//,20X,'BANK EROSION RATE CALCULATION (BANK1.OUT)',
& /,20X,42('-'))
6 FORMAT (/,20X,'INPUT DATA INITIAL VALUES',
& /,20X,'-----',
& /,20X,'LENGTH OF THE RIVER',F10.2,' M',
& /,20X,'WIDTH OF THE RIVER ',F10.2,' M',
& /,20X,' BED SLOPE ',F10.4,
& /,20X,'GRAIN SIZE DIAMETER',E10.4,' M',
& /,20X,' CHEZY COEFF. ',F10.2,' M**0.5/S',
& /,20X,' DELTA S ',F10.2,' M',
& /,20X,' DELTA T ',F10.2,' S',/,20X,42('-')
& /,20X,29('-'),
& /,20X,'CEE = BANK EROSION RATE (M/S)',/,20X,29('-'))
C
C CALCULATE JJ = NUMBER OF NODES
  D = LENGTH/DS
  JJ = D + 1
C INITIALIZATION
  DO 10 I1= 1,JJ
    H(I1) = H0
    B(I1) = B0
    U(I1) = CHE * SQRT(SLOPE * H(I1))
    Q(I1) = U(I1) * H(I1) * B(I1)
  10 CONTINUE
C CALCULATION
  DO 30 J=1,JJ
    TOUS = U(J) * U(J) / (CHE*CHE*DEL*DIA)
    IF (TOUS .LE. TOUC) THEN
      S0(J) = 0.0
    ELSE
      S0(J) = 2.7* SQRT(DEL*G*DIA**3)*(TOUS-TOUC)**1.5
    ENDIF
    TOUB = 0.75*TOUS
    IF(TOUB .LE. TOUC) THEN

```



```

        CEE(J) = 0.0
    ELSE
        CEE(J) = COE*(TOUB/TOUC-1.)/(PS*100.*60.)
    ENDIF
30 continue
C TO MAKE THE OUTPUT FILE
    CALL WRITE(B,H,S0,CEE,JJ)
    CLOSE(3)
    CLOSE(6)
end
C
C SUBROUTINE FOR THE OUTPUT RESULTS
SUBROUTINE WRITE(B,H,S0,CEE,JJ)
REAL B(50),H(50),S0(50),CEE(50)
INTEGER J,JJ
    WRITE(6,21)
    WRITE(6,15) (B(J),J=1,8)
    WRITE(6,16) (H(J),J=1,8)
    WRITE(6,17) (S0(J),J=1,8)
    WRITE(6,18)(CEE(J),J=1,8)
    WRITE(6,20)
C
    WRITE(6,22)
    WRITE(6,15) (B(J),J=9,16)
    WRITE(6,16) (H(J),J=9,16)
    WRITE(6,17) (S0(J),J=9,16)
    WRITE(6,18)(CEE(J),J=9,16)
    WRITE(6,20)
C
    WRITE(6,23)
    WRITE(6,15) (B(J),J=17,JJ)
    WRITE(6,16) (H(J),J=17,JJ)
    WRITE(6,17) (S0(J),J=17,JJ)
    WRITE(6,18)(CEE(J),J=17,JJ)
    WRITE(6,20)
C
15 FORMAT (/,4X,'W',8E9.3)
16 FORMAT (4X,'H',8E9.3)
17 FORMAT (3X,'S0',8E9.3)
18 FORMAT (2X,'CEE',8E9.3)
20 FORMAT (1X,76('-'))
21 FORMAT (2X,'.....J=1 to J=8 .....')
22 FORMAT (2X,'.....J=9 to J=16 .....')
23 FORMAT (2X,'.....J=17 to J=24 .....')
    RETURN
    END
C
C SUBROUTINE SKIP
SUBROUTINE IREC
CHARACTER*1 REC
DO 10 I=1,30
    READ(3,20)REC
    IF (REC .NE. 'C') GOTO 30

```

```

10 CONTINUE
20 FORMAT(A1)
30 RETURN
END

```

C.2-2 Bank erosion rate calculation using force balance theory

```

PROGRAM BANK2
PARAMETER (G=9.81,TOUC=0.047,DEL=1.65,DMU=0.8,ALUB=0.4,N=50)
INTEGER J,JJ
DIMENSION Q(N),H(N),U(N),S0(N),B(N),TOUS(N),CEE(N),
& BNP1(N),SBP0(N),BS(N),AA(N),DIF(N),B2(N),X(N)
REAL LENGTH,SLOPE,DIA,DS,DT,H0,B0,CHE,YY,Y,XX,W,TETA,D
C Initialization
OPEN (3,FILE = 'BANK2.IN',STATUS = 'OLD')
OPEN (6,FILE = 'BANK2.OUT',STATUS='NEW')
CALL IREC
READ (3,*) H0,SLOPE,CHE,B0,DIA,LENGTH,DS,DT,TETA
WRITE (6,5)
    W = 2.* B0
WRITE (6,6) LENGTH,W,SLOPE,DIA,CHE,DS,DT
5 FORMAT (//,20X,'BANK EROSION RATE CALCULATION (BANK2.OUT)',
& /,20X,42('-'))
6 FORMAT (/,20X,'INPUT DATA INITIAL VALUES',
& /,20X,'-----',
& /,20X,'LENGTH OF THE RIVER',F10.2,' M',
& /,20X,'WIDTH OF THE RIVER ',F10.2,' M',
& /,20X,' BED SLOPE ',E10.4,
& /,20X,'GRAIN SIZE DIAMETER',E10.4,' M',
& /,20X,' CHEZY COEFF. ',F10.2,' M**0.5/S',
& /,20X,' DELTA S ',F10.2,' M',
& /,20X,' DELTA T ',F10.2,' S',/,20X,42('-')
& /,20X,29('-'),
& /,20X,'CEE = BANK EROSION RATE (M/S)',/,20X,29('-'))
C
C CALCULATE JJ = NUMBER OF NODES
D = LENGTH/DS
JJ = D+1
C INITIALIZATION
DO 10 I1= 1,JJ
H(I1) = H0
B(I1) = B0
U(I1) = CHE * SQRT(SLOPE * H(I1))
Q(I1) = U(I1) * H(I1) * B(I1) * 2.
10 CONTINUE
C
C CALCULATION
DO 30 J=1,JJ
TOUS(J) = U(J) * U(J) / (CHE*CHE*DEL*DIA)
IF (TOUS(J) .LE. TOUC) THEN
S0(J) = 0.0

```



```

ELSE
S0(J) = 2.7 * SQRT(DEL*G*DIA**3)*(TOUS(J)-TOUC)**1.5
ENDIF
SBP0(J) = S0(J)*H(J)/(B(J)*DMU)*(TOUC/TOUS(J))**0.5
C IF IT IS SEDIMENTATION, (+ VE)
Y = (1.- ALUB)*B(J)*H(J)*TETA*(1.-(1./(DMU*B(J))))
XX = SBP0(J)*DT*DMU*(TOUS(J)/TOUC)**0.5/Y
BS(J) = 1.0001
100 X(J) = BS(J)+BS(J)**3/3+BS(J)**5/5+BS(J)**7/7
YY = ABS(1-BS(J)*BS(J))
DIF(J) = XX-(2.*ABS(1-BS(J))**3*X(J)/YY)
BS(J) = BS(J) + DIF(J)
AA(J) = ABS(DIF(J))
IF(AA(J) .GT. 0.00001) GOTO 100
BNP1(J) = BS(J)*B(J)
CEE(J) = (BNP1(J) - B(J))/ DT
B2(J) = 2. * B(J)
30 continue
C TO MAKE THE OUTPUT FILE
CALL WRITE(B2,H,S0,SBP0,CEE,JJ)
CLOSE(3)
CLOSE(6)
end
C
C SUBROUTINE FOR THE OUTPUT RESULTS
SUBROUTINE WRITE(B2,H,S0,SBP0,CEE,JJ)
REAL B2(50),H(50),S0(50),SBP0(50),CEE(50)
INTEGER J,JJ
WRITE(6,21)
WRITE(6,15) (B2(J),J=1,8)
WRITE(6,16) (H(J),J=1,8)
WRITE(6,17) (S0(J),J=1,8)
WRITE(6,18)(SBP0(J),J=1,8)
WRITE(6,19)(CEE(J),J=1,8)
WRITE(6,20)
C
WRITE(6,22)
WRITE(6,15) (B2(J),J=9,16)
WRITE(6,16) (H(J),J=9,16)
WRITE(6,17) (S0(J),J=9,16)
WRITE(6,18)(SBP0(J),J=9,16)
WRITE(6,19)(CEE(J),J=9,16)
WRITE(6,20)
C
WRITE(6,23)
WRITE(6,15) (B2(J),J=17,JJ)
WRITE(6,16) (H(J),J=17,JJ)
WRITE(6,17) (S0(J),J=17,JJ)
WRITE(6,18)(SBP0(J),J=17,JJ)
WRITE(6,19)(CEE(J),J=17,JJ)
WRITE(6,20)
C
15 FORMAT (/,4X,'W',8E9.3)

```

```
16 FORMAT (4X,'H',8E9.3)
17 FORMAT (3X,'S0',8E9.3)
18 FORMAT (1X,'SBP0',8E9.3)
19 FORMAT (2X,'CEE',8E9.3)
20 FORMAT (1X,76('-'))
21 FORMAT (2X,'.....J=1 to J=8 .....')
22 FORMAT (2X,'.....J=9 to J=16 .....')
23 FORMAT (2X,'.....J=17 to J=24 .....')
  RETURN
  END
C
C SUBROUTINE SKIP
  SUBROUTINE IREC
  CHARACTER*1 REC
  DO 10 I=1,30
    READ(3,20)REC
    IF (REC .NE. 'C') GOTO 30
10 CONTINUE
20 FORMAT(A1)
30 RETURN
  END
```


C.2-3 Bank erosion rate calculation using near bank excess-velocity theory

```

PROGRAM BANK3
PARAMETER (G=9.81,touc=0.047,del=1.65,smu=1.0,dmu=0.8,ALUB=0.4,
&         N=50)
INTEGER J,JJ
DIMENSION H(N),U(N),B(N),CEE(N),BNP1(N),BB(N),CC(N),UB0(N),DB(N)
REAL U0,H0,LENGTH,SLOPE,DIA,RS,TETA,DS,DT,B0,CHE,S0,TOUS,AA,AP,
&     PSI,T,PHI,X
C Initialization
OPEN (3,FILE = 'BANK3.IN1',STATUS = 'OLD')
  CALL IREC
  READ (3,*) (U(I),I=1,12)
  CALL IREC
  READ (3,*) (U(I),I=13,24)
  CALL IREC
  READ (3,*) (H(I),I=1,12)
  CALL IREC
  READ (3,*) (H(I),I=13,24)
CLOSE(3)
OPEN (3,FILE = 'BANK3.IN2',STATUS = 'OLD')
  CALL IREC
  READ (3,*) U0,H0,SLOPE,CHE,B0,DIA,LENGTH
  CALL IREC
  READ (3,*) BETA,RS,TETA,DS,DT
CLOSE(3)
OPEN (6,FILE = 'BANK3.OUT',STATUS='NEW')
WRITE (6,5)
WRITE (6,6) LENGTH,B0,RS,SLOPE,CHE,DS,DT
5 FORMAT (//,20X,'BANK EROSION RATE CALCULATION',
&        /,20X,'-----')
6 FORMAT (/,20X,'INPUT DATA  INITIAL VALUES',
&        /,20X,'-----',
&        /,20X,'LENGTH OF THE RIVER',F10.2,'M',
&        /,20X,'WIDTH OF THE RIVER ',F10.2,'M',
&        /,20X,'RADIUS OF CURVATURE',F10.2,'M',
&        /,20X,'  BED  SLOPE ',E10.4,
&        /,20X,'  CHEZY COEFF. ',F10.2,'M**0.5/S',
&        /,20X,'  DELTA S   ',F10.2,'M',
&        /,20X,'  DELTA T   ',F10.2,'S',
&        /,20X,26('-'),
&        /,21X,'DB = BANK LINE DISPLACEMENT (M) OVER THE PERIOD DT'
&        /,22X,'H = WATER DEPTH (M)',
&        /,20X,'CEE = BANK EROSION RATE (M/S)',/20X,51('-'))
C
C CALCULATE JJ = NUMBER OF NODES
  X = LENGTH/DS
  JJ = X+1
C
C START CALCULATION

```

RIVER PLAN-FORM MOVEMENT IN AN ALLUVIAL PLAIN

C NEAR BANK EXCESS VELOCITY RATIO (HERE U(I1)=U(J, KK) FROM THE
C NUMERICAL SIMULATION MODEL HYDHST.FOR)

```

C
  DO 10 I1 = 1, JJ
    B(I1) = B0/2.
    UB0(I1) = U(I1)/U0-1.0
  10 CONTINUE
C
  CALL PARA(TOUS, PHI, S0, T, PSI, U0, H0, BETA, CHE, DIA, RS)
C
  ap = s0 /((1-alub)*h0)
  aa = ap*h0*3/(phi*teta)
  DO 25 i = 1, JJ
    bb(i) = (ap*slope/(phi*teta))*(ub0(i)+0.5)
    cc(i) = (ap*h0*(1+(3*ub0(i)/phi))*(T*teta-psi))/(phi*teta)
  25 continue
  DO 30 J = 2, JJ-1
    BNP1(J) = (AA*(UB0(J+1)-UB0(J-1))/(2*DS)-BB(J)
    &          + CC(J))*DT + B(J)
  30 continue
  BNP1(JJ) = (AA*(UB0(JJ)-UB0(JJ-1))/DS-BB(JJ) + CC(JJ))*DT + B(JJ)
  BNP1(1) = (AA*(UB0(2)-UB0(1))/DS-BB(1) + CC(1))*DT + B(1)
  DO 40 I4 = 1, JJ
    DB(I4) = BNP1(I4)-B(I4)
    IF(DB(I4) .LE. 0.) DB(I4)=0.
    CEE(I4) = DB(I4)/DT
  40 CONTINUE
  WRITE(6,19)
  WRITE(6,15) (DB(J), J=1,8)
  WRITE(6,16) (H(J), J=1,8)
  WRITE(6,17) (CEE(J), J=1,8)
  WRITE(6,18)
  WRITE(6,20)
  WRITE(6,15) (DB(J), J=9,16)
  WRITE(6,16) (H(J), J=9,16)
  WRITE(6,17) (CEE(J), J=9,16)
  WRITE(6,18)
  WRITE(6,21)
  WRITE(6,15) (DB(J), J=17, JJ)
  WRITE(6,16) (H(J), J=17, JJ)
  WRITE(6,17) (CEE(J), J=17, JJ)
  WRITE(6,18)
C
  15 FORMAT (2X, 'DB', 8E9.3)
  16 FORMAT (3X, 'H', 8E9.3)
  17 FORMAT (1X, 'CEE', 8E9.3)
  18 FORMAT (1X, 76('-'))
  19 FORMAT (4X, '.....J=1 to J=8 .....')
  20 FORMAT (4X, '.....J=9 to J=16 .....')
  21 FORMAT (4X, '.....J=17 to J=24 .....')
  CLOSE(6)
  END
C

```



```
c subroutine for parameters
  subroutine para(tous,phi,s0,t,psi,u0,h0,beta,che,dia,rs)
  parameter (g=9.81,del=1.65,touc=0.047,smu=1.0,dmu=0.8)
  REAL u0,tous,phi,s0,T,h0,psi
C
  tous = u0*u0/(che*che*del*dia)
  phi = (tous-touc)/tous
  if(tous .le. touc) then
    s0 = 0.0
  else
C
    s0 = 2.7 * SQRT(del*g*dia**3.)*(tous-touc)**1.5
  endif
    T = SQRT(touc/(smu*dmu*tous))
    psi = (-beta*h0/rs)
10 continue
  return
  end
C
C SUBROUTINE FOR SKIPS COMMENT CARDS IN INPUT DATA
C
  SUBROUTINE IREC
  CHARACTER*1 REC
  DO 10 I = 1,99
    READ (3,20) REC
    IF (REC .NE. 'C') GOTO 30
10 CONTINUE
20 FORMAT(A1)
30 RETURN
  END
```

*It is this we learn after so many failures,
The building of castles in sand, of queens in snow,
That we cannot make any corner in life or in life's beauty,
That no river is a river which does not flow.*

*Louis MacNeice
Autumn Journal, 1938*

WRTC
Water, Research and
Training Centre



Danish Hydraulic Institute

IHE and the Candidate thank the *Danish Hydraulic Institute* for the material and intellectual support that they have given to this project.

IHE 
D E L F T

P.O. Box 3015
2601 DA Delft
The Netherlands

Tel. : +31 (0)15 151715
Telex: 38099 ihe nl
Fax. : +31 (0)15 122921